THE UNIVERSITY OF MANITOBA

HYDRODYNAMICS AND HEAT TRANSFER IN TWO-PHASE TWO-COMPONENT FLOWS

by

Mohamed A. Aggour

A Thesis

Submitted to the Faculty of Graduate Studies

in Partial Fulfilment of the Requirements for the Degree of Doctor of Philosophy in Mechanical Engineering

Winnipeg, Manitoba

June, 1978

HYDRODYNAMICS AND HEAT TRANSFER IN TWO-PHASE TWO-COMPONENT FLOWS

BY

MOHAMED A. AGGOUR

A dissertation submitted to the Faculty of Graduate Studies of the University of Manitoba in partial fulfillment of the requirements of the degree of

DOCTOR OF PHILOSOPHY

© 1978

Permission has been granted to the LIBRARY OF THE UNIVERSITY OF MANITOBA to lend or sell copies of this dissertation, to the NATIONAL LIBRARY OF CANADA to microfilm this dissertation and to lend or sell copies of the film, and UNIVERSITY MICROFILMS to publish an abstract of this dissertation.

The author reserves other publication rights, and neither the dissertation nor extensive extracts from it may be printed or otherwise reproduced without the author's written permission.

ABSTRACT

A study was made of forced convective, co-current, two-phase, two-component (gas-water) flow in the thermal entry section of a vertical tube. Three gases (air, helium and Freon 12) were used to investigate the effect of gas density on the local and mean heat-transfer coefficients, frictional pressure drop and flow patterns.

The flow patterns were found to depend strongly on the relative superficial velocities of the two phases and slightly on the gas density. The frictional pressure drop and the heat-transfer coefficients were observed to depend strongly on the flow patterns. The gas-phase density was found to affect both the heat-transfer coefficients and the frictional pressure drop only at low water flow rates and moderate to high gas velocities.

The local heat-transfer coefficients were correlated by a modified form of the single-phase heat-transfer theory of Spalding; this was tested for generality by testing the theory against a wide range of data; excellent agreement was obtained (7.2% and 30.7% for the mean and rms deviations respectively).

A correlation of the two-phase mean heat-transfer coefficients, based on a simple model of single-phase liquid flow with a Reynolds number based on the actual mean velocity of the liquid in the two-phase flow, was developed and tested

against data covering a wide range of variables; satisfactory results were obtained. Further, the data were correlated in terms of the two-phase frictional pressure drop; a form of this correlation covering the widest range of variables studied so far was proposed.

A flow-visualization study, employing high-speed cine photography and both the hydrogen-bubble and dye-injection techniques, was made of air-water mixtures at low flow rates of the two phases where the local values of the heat transfer coefficient were observed to increase with increasing distance along the test section. Movie films of the motion of the liquid film at the walls were obtained, which clearly indicated the existence of downflow of the liquid at the wall in the bubble and slug flows under these flow conditions. The results qualitatively explained the observed behaviour of the local heat-transfer coefficients against the distance along the test section under these conditions.

Finally, a theoretical solution of pressure drop and holdup in horizontal stratified flow was developed. The theory was based on a simple model of co-current gas-liquid stratified flow between two wide horizontal parallel plates, taking into account the interfacial shear stress and considering a moving interface. The final results were presented in the form of simple, dimensionless algebraic equations which provided good predictions for flow in circular tubes and rectangular channels.

ACKNOWLEDGEMENTS

The author acknowledges his debt to Dr. G.E. Sims, the author's supervisor, whose continuing interest and guidance have contributed to make this investigation possible. Special thanks are due to Prof. R.E. Chant and Dr. G.K. Yuill for their helpful suggestions and continuing encouragement.

The author wishes to thank all the technicians in the Department of Mechanical Engineering at the University of Manitoba, particularly Mr. O. Tonn, Mr. F. Kapitoler, Mr. L. Wilkins, Mr. D. Schaldemose, Mr. H. Weiss and Mr. K. Tarte for their indispensable assistance.

Special thanks are due to Mr. A. Fathi who has diligently assisted in the reduction of the data and the preparation of the thesis. Thanks are also due to Miss C. Skelton, Miss M. Towers and Mrs. M. Wood for typing the manuscript.

The author acknowledges the financial support of the National Research Council of Canada.

I am especially grateful to my wife; without her continuing encouragement, patience, sacrifices and inspiration this thesis would have been impossible. My little son Tamir has indirectly contributed to this work by putting up with me all these years. My parents, brothers and sisters have also been a valuable source of inspiration.

TABLE OF CONTENTS

LIST OF FIGURES

LIST OF TABLES

NOMENCLATURE

a	Distance from the upper plate to the position of maximum gas velocity in Fig. 8.1	ft
A_C	Cross-sectional area of tube wall	ft^2
A_G	Flow area of the gas phase	ft^2
A_L	Flow area of the liquid phase	ft^2
A_M	Eigenvalues, Eq. (6.2)	-
A_T	Flow area of the tube	ft^2
A_1, A_2	Constants in various equations	
b	Distance from the interface to the position of maximum gas velocity, in Fig. 8.1	ft
B	Empirical coefficient, Eq. (E.39)	-
B_o, B, B_2, B_3	Constants appearing in Eq. (D.6)	-
C	Discharge coefficient for flow through an orifice plate	-
C_p	Specific heat	Btu/lbm^oF
C_1, C_2, C_3	Constants appearing in various equations	-
d	Diameter of orifice throat	ft
D	Inside diameter of the tube	ft
D_o	Outside diameter of the tube	ft
D_p	Diameter of the pipe connected to the orifice plate	ft
D^*	Parameter defined in Eq. (6.21)	ft
e	Local voltage of the heated tube	Volts
$\bar{e}$	Mean deviation defined in Eq. (5.1)	-
$\bar{e}'$	Root mean square deviation, Eq. (5.2)	-
e'	Constant in Eq. (E.23)	-

E	Total potential difference across the heated tube	Volts
E_{LG}, E_{UG}	Voltage drop across the lower and upper guard heaters respectively	Volts
f	Friction factor	-
f_{TP}	Two-phase friction factor as defined in homogenous theory, Eq. (E.29)	-
F	Velocity of approach factor, Eq. (D.60)	-
F_a	Thermal expansion factor of the orifice plate, Eq. (D.60)	-
Fr_{ED}	A dimensionless flow parameter, Eq. (2.28)	-
Fr_s	A dimensionless flow parameter, Eq. (2.29)	-
g	Acceleration due to gravity	ft/sec^2
g_c	Conversion factor	$lbmft/lb_f sec^2$
G	Conversion Factor = 3.41	Btu/Watt hr
G	Mass velocity	$lbm/hr\ ft^2$
G_{MIX}	Total mass velocity = $G_{SL} + G_{SG}$	$lbm/hr\ ft^2$
G_{SG}	Mass velocity of the gas phase as if it were flowing alone in the tube	$lbm/hr\ ft^2$
G_{SL}	Mass velocity of the liquid phase as if it were flowing alone in the tube	$lbm/hr\ ft^2$
h	Enthalpy per unit mass of fluid	Btu/lbm
$h, h(z)$	Local heat-transfer coefficient	$Btu/hr\ ft^2\ ^oF$
$\bar{h}$	Length - mean heat-transfer coefficient	$Btu/hr\ ft^2\ ^oF$
h'	Manometer reading	in.
$\bar{h}_{AG}$	Single phase gas heat-transfer coefficient based on actual mean velocity and cross-sectional area of the gas phase	$Btu/hr\ ft^2\ ^oF$
$\bar{h}_{AL}$	Same as $\bar{h}_{AG}$, defined for liquid	$Btu/hr\ ft^2\ ^oF$

h_w	Differential pressure across the orifice plate	$in.H_20$
H	Distance between the top and bottom plates in Fig. 8.1	ft
i	Axial current density	Amp/ft^2
I	Total current through the tube	Amp
k	Thermal conductivity	$Btu/hr\ ft^oF$
k_{MIX}	Thermal conductivity of mixture	$Btu/hr\ ft^oF$
k'_o, k_t	Thermal conductivity of tube material	$Btu/hr\ ft^oF$
K	Ratio of specific heats	-
K_W	Flow parameter in Eq. (2.3)	-
K_e	A parameter in Eq. (2.38)	-
L	Length of the heated test section	ft
L'	Calming length	ft
ΔL	Length used to calculate the length mean heat-transfer coefficient	ft
m	Variable defined in Eq. (D.11)	$^oF/ft^2$
$\dot{m}$	Mass flow rate	lbm/hr
n	Blasius exponent, or number of variables	-
n_1, n_2	Constants	-
Nu	Local Nusselt number - hD/k	-
$\overline{Nu}$	Mean Nusselt number	-
Nu_∞	Value of Nusselt when $Z \to \infty$	-
$\overset{*}{Nu}_{TP}$	Modified Nusselt number, Eq. (6.20)	-
P	Pressure	lb_f/in^2
P_a	Partial pressure of dry air	lb_f/in^2
P_F	Frictional component of pressure	lb_f/in^2

P_{FN}	P-function, Eq. (6.7)	-
P_g	Saturation pressure of vapour in air	lb_f/in^2
P_{MIX}	Average mixture pressure in the heated test section	lb_f/in
P_V	Partial pressure of vapour	lb_f/in^2
Pr	Prandtl number	-
Pr_T	Turbulent Prandtl number	-
ΔP	Pressure drop (total without the subscripts)	lb_f/in^2
$\Delta P/\Delta L$	Total pressure drop per unit length	lb_f/in^2
q	Heat flux	Btu/hr ft^2
q_v	Heat generated per unit volume of the heated tube	Btu/hr ft^3
q_w	Heat flux at the wall	Btu/hr ft^2
$(q_w)_{max}$	Maximum wall heat flux	Btu/hr ft^2
Q	Volumetric flow rate	ft^3/hr
r	Radial coordinate measured from the axis of the tube	ft
r_i	Radius of the gas-liquid interface	ft
R	Inside radius of the tube	ft
R	Gas constant	ft $lb_f/lbm\,^oF$
R_L	Liquid volume fraction or holdup	-
R_o	Outer radius of the tube	ft
R_t	Total resistance of test tube	Ohm
Re	Reynolds number	-
Re_d	Reynolds number based on orifice throat diameter	-
Re_L^*	A parameter in Eq. (2.36)	-
Re_M	Reynolds number of the mixture defined in Eq. (2.21)	-
Re_S	Reynolds number defined in Eq. (2.27)	-

Re_{SG}	Superficial gas Reynolds number	-
Re_{SL}	Superficial liquid Reynolds number	-
Re_2	$= Re_{SL} + Re_{SG}$ Eq. (2.16)	-
s	A parameter in Eq. (2.38)	-
S	Slip ratio, Eq. (D.52)	-
Sq	Spalding function, Eq. (6.4)	-
St	Local Stauton number = Nu/Re Pr	-
t	Wall thickness of the tube	ft
t_s	Variable in Eq. (2.38)	^oF
T	Temperature	^oF
T_{AVG}	Mean temperature of tube wall, Eq. (D.10)	^oF
T_L	Temperature of the liquid at the inlet to the mixer	^oF
T_c	Temperature as measured by the thermocouples on the heated tube	^oF
ΔT_W	Temperature drop across the tube wall	^oF
U*	Friction velocity, Eq. (2.33)	-
U^*_M	Mixture velocity	ft/sec
V	Velocity	ft/sec
V	Variable, in general	-
V_{EXP}	Experimental value of a variable	-
V_{MIX}	Mixture velocity, Eq. (2.10)	ft/sec
V_{THL}	Expected or theoretical value of V_{EXP}	-
V_S	Slip velocity, Eq. (2.24)	ft/sec
V*	Friction velocity = $(g_c\tau/\rho)^{1/2}$	ft/sec
V^+_z	Dimensionless velocity	-
W	Wattmeter reading	Watts
x	Flow quality = $\dot{m}_G/(\dot{m}_G + \dot{m}_L)$	-

x	Two-phase flow parameter	-
X^*	Dimensionless heat-transfer coefficient, Eq. (2.35)	-
X_{TT}	Martinelli parameter	-
y	Coordinate in general	ft
Y	Expansion factor, Eq. (D.61)	-
Y^*	A variable in Eq. (5.6)	-
Z	Axial coordinate measured from the commencement of heated section	in
Z^+	Variable defined in Eq. (6.6)	-
$\overline{Z}$	Variable defined in Eq. (6.1)	-
Z'	Variable defined in Eq. (6.3)	-

Greek Symbols

α	Void fraction	-
α'	Temperature coefficient of thermal conductivity of tube material	$(^{o}F)^{-1}$
β	d/DP, (Appendix D.4)	-
β'	Temperature - coefficient of electrical resistivity of tube material	$(^{o}F)^{-1}$
γ_M^2	Eigenvalues, Eq. (6.2)	-
$\varepsilon_H, \varepsilon_M$	Eddy diffusivity for heat and momentum transfer, respectively	-
ρ	Density	lbm/ft^3
$\rho', \rho_o', \overline{\rho}, \rho_t'$	Resistivities defined in Appendix D	ohm-ft
κ	Thermal diffusivity	ft^2/hr
μ	Dynamic viscosity	lbm/hr ft
ν	Kinematic viscosity	ft^2/hr
ξ	Constant in Eq. (2.33)	-
σ	Surface tension	lb_f/ft
τ	Shear stress	lb_f/ft^2
ϕ	Relative humidity	lb_f/ft^2

Φ^2	Pressure drop ratio	-
Φ^2_{LO}	Two-phase multiplier, Eq. (5.40)	-
Ψ^2	Ratio of two-phase to single-phase heat-transfer coefficients	-
$\overline{\Psi}$	Dimensionless temperature difference	-
ω	Uncertainty interval in a variable	-
ω	Mass of vapour/mass of dry gas	-

Subscripts

a	Dry air
B	Bulk, liquid or mixture
CW	Cooling water (heat exchanger)
EVAP	Evaporation
e	Effective
F	Generally frictional
G	Gas
G1,G2	At the inlet and outlet of orifice plate
GO	Gas-phase flowing alone at the same mass flow rate as the mixture
i	Location at which a thermocouple is attached to the wall; interfacial
IN,OUT	At the inlet and outlet of heated tube
L	Liquid
l	laminar
LO	Same as "GO", except refers to the liquid-phase
LS	Slug-liquid
MIX	Gas-liquid mixture
r	Radial component
S	Slip (e.g., slip velocity)
SG	Superficial gas
SL	Superficial liquid

SP	Single-phase (generally, liquid)
SPF	Single-phase frictional
SPG	Single-phase hydraulic
TP	Two-phase
TPF	Two-phase frictional
TPG	Two-phase hydraulic
t	Turbulent
v	Vapour
W	At the wall
WG	Gas at the wall
WL	Liquid at the wall (temperature)

CHAPTER 1

INTRODUCTION

1.1 Background

Two-phase flow, the simultaneous flow of a liquid and a gas (two-component) or a liquid and its vapour (single-component), with and without heat transfer is of great importance in many industrial applications, such as in nuclear reactors, rocket motors, oil and gas pipelines and many forms of chemical process equipment.

Although heat transfer in two-phase, single component flows (boiling and condensation) is more important in practical applications, it is a complex phenomenon affected by many variables. Because of this complexity, several investigators (e.g. [89,85,40]) have sought to improve the understanding of heat transfer in two-phase flow in general by investigating this phenomenon in two-component flows. Two-component systems are attractive mainly because, in contrast with one-component systems, the gas-phase rate of flow is independent of the rate of heat transfer and can be accurately controlled and measured (non-evaporating), the flow rates of the two phases do not change along the flow channel and because of the independent control of the properties of the two phases.

While a considerable volume of literature on the hydrodynamic aspects of two-phase flow exists [34,92] only a few investigators have dealt with heat transfer in two-phase, two-component flow in vertical tubes; among these only Vijay [90] has

dealt with local values in the sense of reporting the functional relationship between the local heat-transfer coefficient and the distance along the test section. Data on the effect of fluid properties on heat transfer are scanty; in fact the liquid viscosity is the only fluid property which has received extensive study of its effect on heat transfer [40,58,86-24,29,90].

The present investigation is a part of a larger program initiated at the University of Manitoba to investigate the effect of fluid properties and other geometrical parameters on pressure drop, flow patterns and both local and mean heat-transfer coefficients for two-phase, two-component (gas-liquid) flow in a vertical tube. The experiments described in the thesis are of forced-convention heat transfer. A major part of the investigation is a study of the effect of gas-phase density on flow patterns, pressure drop and local and mean heat-transfer coefficients. For this purpose, experiments were performed with three gas-water mixtures; the gases used were air, helium and Freon 12. Although different gases have different values for other properties, it is believed that among these properties only the density is the most effective in relation to the variables investigated. The flow-pattern and pressure drop results are discussed in Chapter 5 while the heat-transfer results are treated in Chapter 6. The experimental data are tabulated in Appendix H.

In an attempt to explain the earlier [90] local heat-transfer results obtained at low flow rates of the two phases for which the local values of the heat-transfer co-efficient increased with increasing distance along the test section (these results were confirmed in the present investigation) and to examine the theoretical model [90] developed for these conditions, a flow-visualization study of air-water flowing in a transparent test section, employing the hydrogen-bubble and dye-injection techniques, was performed. The results of this study are discussed in Chapter 8.

Although the thesis deals mainly with vertical flow, the problem of prediction of pressure drop and holdup in horizontal stratified flow has been considered here, firstly because of its well known importance in many engineering applications and secondly because the theory might be capable, with suitable modifications, of being extended to vertical annular flow. The present theory is based on a simple physical model of co-current gas-liquid stratified flow between two wide horizontal parallel plates, taking into account the interfacial shear stress and moving interface. The results are expressed in the form of simple algebraic equations which predict both pressure drop and holdup with good accuracy.

1.2 Purpose and Scope

In summary, the purpose of the present study is:

(i) to present experimental data on the effect of gas density on the flow patterns, frictional pressure drop and local and mean heat-transfer coefficients in vertical two-phase two-component flow;

(ii) to attempt a qualitative explanation of the effect of gas density on the variables stated above;

(iii) to correlate both local and mean heat-transfer coefficients and test the generality of the proposed correlations;

(iv) to study the motion of the liquid film in bubble and slug flows at low flow rates of the phases in an attempt to explain the earlier [90] local heat-transfer results obtained under these conditions;

(v) to present a theoretical solution of pressure drop and holdup in horizontal two-phase stratified flow.

With regard to the experimental work, the main dependent variables measured were the heat-transfer coefficients, pressure drop and flow patterns, the main independent variables were the water and gas flow rates and the gas density (through the use of different gases). The range of variables studied is given in Table 4.2.

1.3 Layout of the Thesis

A review of the literature on forced-convective heat-transfer in two-phase, two-component (gas-liquid) flow in

vertical tubes is presented in Chapter 2 and is summarized in Tables 2.2 and 2.3.

Chapter 3 describes the experimental facility with the detailed information given in Appendix A, while Chapter 4 presents the experimental procedure and conditions.

Chapter 5 presents the experimental data of the observed flow patterns (flow-pattern maps are shown in Figs. 5.6 and 5.7), and the frictional pressure drop data; the effect of gas density on frictional pressure drop is illustrated in Figs. 5.11 and 5.12.

Chapter 6 represents the main findings of this work; the raw heat-transfer data are shown in Figs. 6.5 to 6.10 with the effect of gas density on mean heat-transfer coefficients illustrated in Figs. 6.11 and 6.12. Figures 6.13 to 6.18 show the results of correlation of the local heat-transfer coefficients, while Figs. 6.26 and 6.29 give the results of correlation of the mean heat-transfer coefficients.

The flow-visualization study is presented in Chapter 7, and the stratified flow study in Chapter 8. Summary of the present work together with the main conclusion are presented in Chapter 9.

The number of each figure, table and equation in the thesis begins with the number of the Chapter, or the letter of the appendix in which it appears.

The variables appearing in the thesis are listed in the 'Nomenclature' together with the units employed.

CHAPTER 2

LITERATURE REVIEW

2.1. Introductory Remarks

As noted in the Introduction, the present investigation deals with three distinct subjects, namely, the forced convective two-phase, two-component flow and heat transfer in a vertical tube, the two-phase, two-component flow-visualization and the hydrodynamics of horizontal two-phase, two-component stratified flow. This chapter, however, is confined only to a review of the previous work in forced convective heat transfer in two-phase, two-component (gas-liquid) flow in vertical tubes. The literature on the other two topics as well as that pertaining to pressure drop, void fraction and flow patterns, relevant to the present investigation, will be discussed at appropriate points throughout the thesis.

An excellent review of the literature in forced convective heat transfer in two-phase, two-component flow in vertical tubes has recently been presented by Vijay [90]. The present review is similar in form to Vijay's although the initial work was done independently; similar detail is included here for the sake of completeness.

The literature review in this chapter is restricted to investigations relevant to the present study; these were selected on the basis of the following criteria:

1. The two-phase flow should be two-component (gas-liquid) with no change of phase; boiling and condensation are

therefore excluded.

2. The flow should be forced convective with independent control of the flow rates of both phases.

3. The flow should be co-current and confined to upward vertical* flow in circular tubes.

4. The flow patterns should be similar to those considered in the present investigation; the work of Perroud and de La Harpe [69] is therefore excluded.

2.2. Presentation

In the following subsections, the work of each of the authors reviewed is individually summarized, the data (as reported by the original authors) are presented and the correlations, if any, are stated. It should be noted that in most cases the data were extracted from the graphs presented in the original papers; this has, of course, resulted in some inaccuracies. The information pertaining to the experimental equipment of the investigators, fluids used, flow patterns observed and the measured coefficients of heat transfer are summarized in Table 2.2; the correlations proposed by each investigator together with the range of variables studied are listed in Table 2.3. These two tables appear at the end of this chapter.

---

* with the exception of the work of Fried [31] which was for horizontal flow; this is mainly because the correlation developed by the author was of such general nature that it could be extended to vertical flow.

2.2.1. Verschoor and Stemerding [89]

The authors measured average values of the coefficient of heat transfer for upward vertical flow of air-water mixtures in a circular tube and observed visually the flow patterns in a glass tube of the same size. The reported results are shown in Fig. 2.1 where the ratio of the two-phase mean heat-transfer coefficient $\bar{h}_{TP}$ to the single-phase (liquid) mean heat-transfer coefficient $\bar{h}_{SP}$ is plotted against the ratio of the superficial gas velocity to the superficial liquid velocity V_{SG}/V_{SL} with the liquid flow rate as a parameter. The values of $\bar{h}_{SP}$ were calculated from the following correlation:

$$\bar{N}u_{SP} = 0.024\ Re_{SL}^{0.8}\ Pr_L^{0.4} \qquad (2.1)$$

where

$\bar{N}u_{SP}$ is the single-phase mean Nusselt number $\equiv \bar{h}_{SP}D/k_L$,

D is the inside diameter of the tube,

k_L is the thermal conductivity of the liquid phase,

Re_{SL} is the superficial liquid Reynolds number $= \rho_L\ V_{SL}\ D/\mu_L$,

ρ_L is the liquid density,

μ_L is the liquid viscosity,

Pr_L is the liquid Prandtl number $\equiv C_{pL}\ \mu_L/k_L$,

C_{pL} is the specific heat of the liquid.

The authors observed that, for a constant liquid flow rate, $\bar{h}_{TP}$ increases with increasing the gas flow rate and

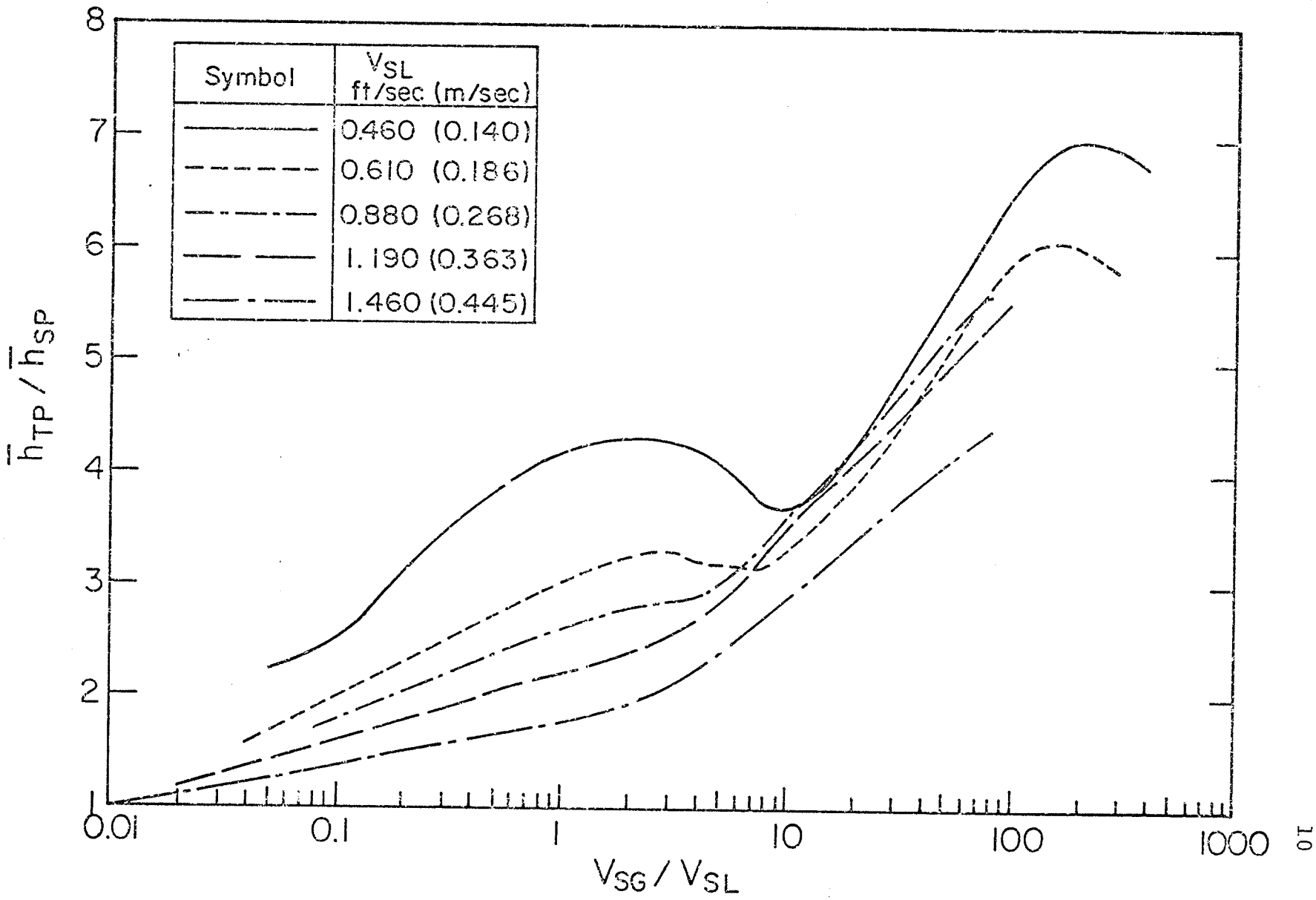

Fig. 2.1 Heat-Transfer Results of Verschoor and Stemerding

Fig. 2.1

that the introduction of the air was most effective in increasing the heat-transfer rate at the lower liquid flow rates. They also observed that $\bar{h}_{TP}$ values were dipped at $V_{SG}/V_{SL} = 2$ (see Fig. 2.1), and passed through a maximum at approximately $V_{SG}/V_{SL} = 200$; this behavior was attributed, by the authors, to the flow-regime transition from bubble to slug and from slug to annular flow respectively.

The authors were the first to observe the dependence of the two-phase heat-transfer coefficients on the flow patterns; however, in view of more recent evidence, the more likely transitions in flow pattern at the first and second maxima in $\bar{h}_{TP}$ would be from bubble to slug and from annular to mist flow respectively.

2.2.2. Ueda [85]

In this paper, the author reported the following for air-water flow in a vertical tube:

(i) Visual observations of the flow patterns and a flow-pattern map with the liquid flow rate $(\dot{m}_L)$ and the gas flow rate $(\dot{m}_G)$ as coordinates.

(ii) Measurements of the static pressure along the tube and predictions of the void fraction and relative velocity of the air.

(iii) A tentative correlation for the interfacial shear stress.

(iv) Measurements of the tube wall temperature, under a constant heat rate, for single-phase (water) and two-phase flow; the author concluded that $\bar{h}_{TP}$ values were

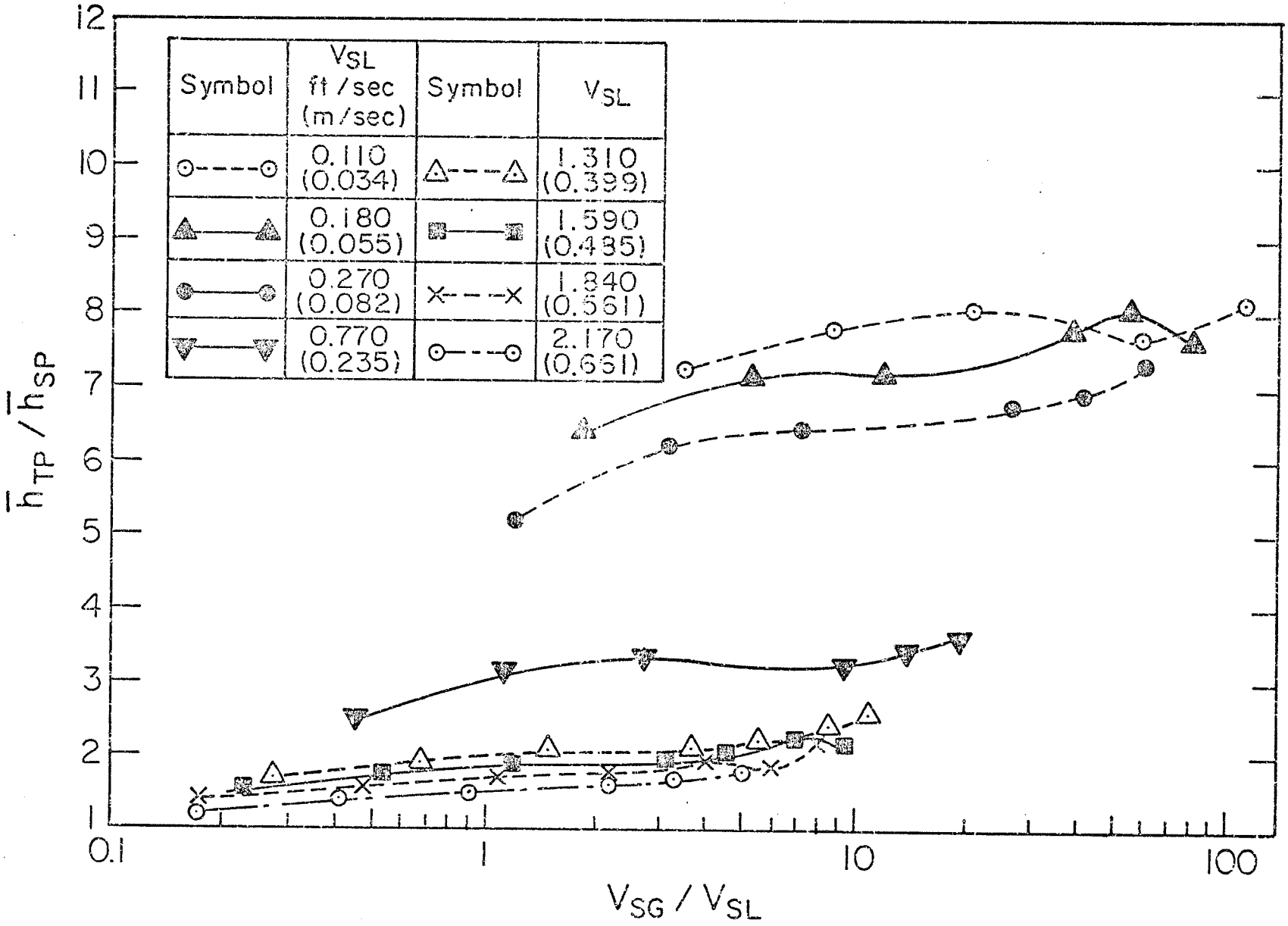

Fig. 2.2 Heat-Transfer Results of Ueda

Fig. 2.2

higher than $\bar{h}_{SP}$.

(v) The effect on heat-transfer of obstacles placed in the flow path; this had the effect of reducing $\bar{h}_{TP}$ values.

Figure 2.2 shows the author's data plotted as $(\bar{h}_{TP}/\bar{h}_{SP})$ versus (V_{SG}/V_{SL}), for a constant heat rate of 0.35×10^4 Btu/hr. ft^2. The data shown in the figure were calculated from the reported values of the temperature difference between the wall and the bulk. For the single-phase heat-transfer coefficient, the following correlation was used:

$$\bar{Nu}_{SP} = 0.036\ Re_{SL}^{0.8}\ Pr_L^{1/3}\ (\mu_L/\mu_W)^{0.14}\ (D/L)^{1/18} \qquad (2.2)$$

where

μ_W is the viscosity of the liquid evaluated at the wall temperature

L is the length of the heated test tube.

No correlation of the results was presented.

2.2.3. Katsuhara and Kazama [53]

The authors reported two-phase (air-water) heat-transfer data for upward flow in a vertical tube and presented an empirical correlation of their results. The reported data are shown in Fig. 2.3, where $\bar{h}_{TP}/\bar{h}_{SP}$ is plotted against the void fraction, α (defined below). The proposed correlation was in the form:

$$\frac{\bar{Nu}_{TP}}{Pr_{MIX}^{n}} = C\ K_W^{-0.5m}\ [Re_{MIX}\ (1 - \alpha)^{0.5}]^m \qquad (2.3)$$

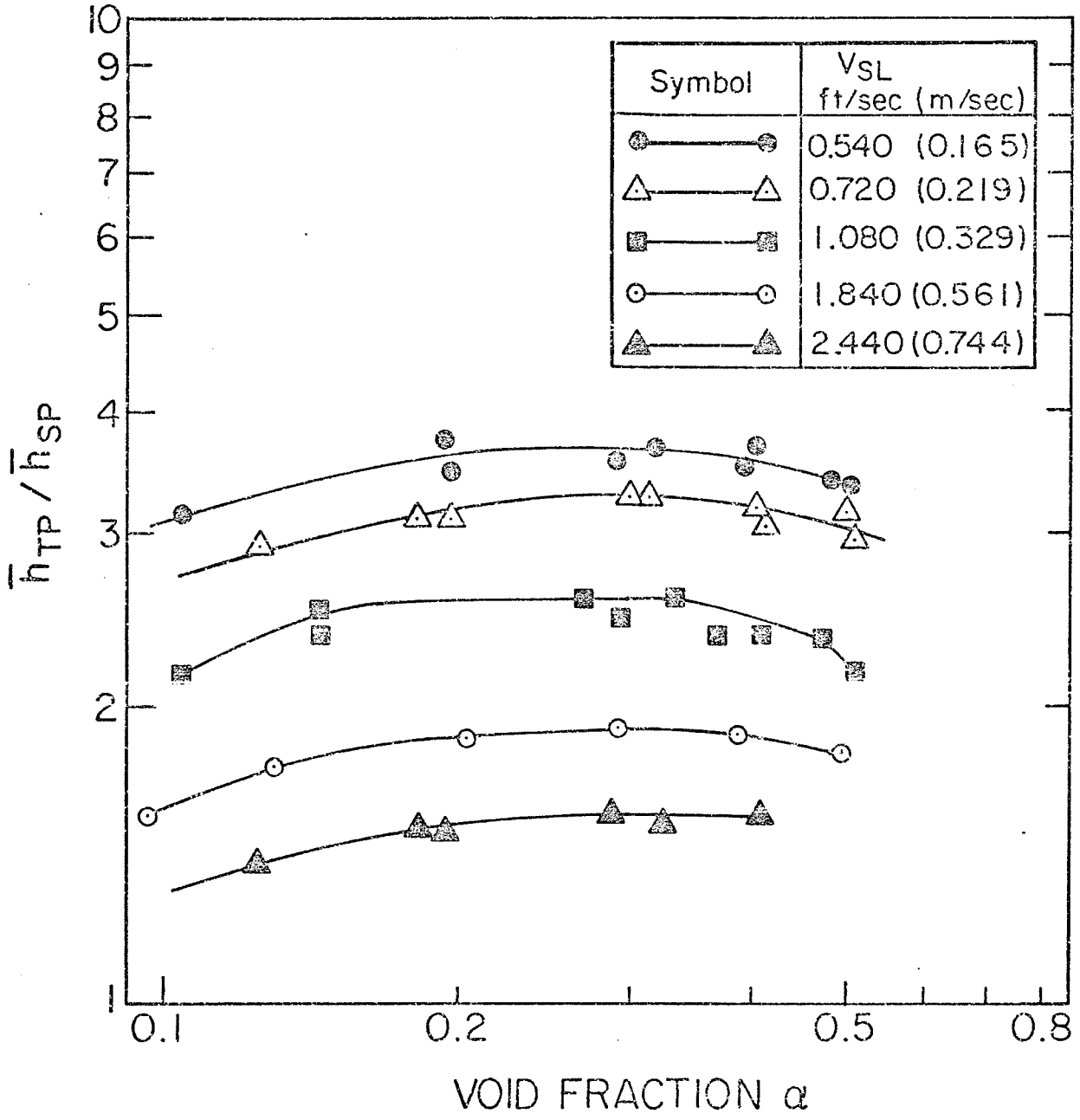

Fig.2.3 Heat-Transfer Results of Katsuhara and Kazama

where

n, m & C are constants,

K_W is a parameter which depends on the flow pattern,

α is the void fraction defined as the ratio of the volume of the tube occupied by the gas to the total volume of the tube; when a small length dZ of the tube is considered, α can be written as the ratio of the area of flow cross-section occupied by the gas (A_G) to the total cross-sectional area of the flow (A_T), i.e.,

$$\alpha = A_G/A_T \tag{2.4}$$

The liquid volume fraction R_L, usually referred to as the liquid holdup, is defined in a similar way as the ratio of the cross-sectional area of flow occupied by the liquid (A_L) to the total area, i.e.,

$$R_L = (1 - \alpha) = A_L/A_T$$

The variables in Eq. (2.3) are defined below with the subscript MIX referring to the two-phase mixture,

$$\bar{N}u_{TP} = \bar{h}_{TP}\, D/k_{MIX}\,, \tag{2.5}$$

$$k_{MIX} = \alpha \frac{\rho_G}{\rho_{MIX}} k_G + (1 - \alpha) \frac{\rho_L}{\rho_{MIX}} k_L \quad , \tag{2.6}$$

$$\rho_{MIX} = \alpha\, \rho_G + (1 - \alpha)\rho_L \quad , \tag{2.7}$$

$$Pr_{MIX} = \alpha \frac{\rho_G}{\rho_{MIX}} Pr_G + (1 - \alpha) \frac{\rho_L}{\rho_{MIX}} Pr_L \quad , \tag{2.8}$$

$$Re_{MIX} = V_{MIX}\, D/\nu_{MIX} \quad , \tag{2.9}$$

$$V_{MIX} = (\dot{m}_L + \dot{m}_G)/\rho_{MIX}\, A_T \quad , \tag{2.10}$$

$$\nu_{MIX} = \alpha \frac{\rho_G}{\rho_{MIX}} \nu_G + (1 - \alpha) \frac{\rho_L}{\rho_{MIX}} \nu_L \tag{2.11}$$

Within the range $0.08 < \alpha < 0.60$, the authors correlated their experimental results by the following expression:

$$\bar{N}u_{TP} = 8.70\, Pr_{MIX}^{0.4}\, (1 - \alpha)^{0.125}\, Re_{MIX}^{0.25} \tag{2.12}$$

The single-phase heat-transfer coefficients in Fig. 2.3 were obtained from the following correlation:

$$\bar{N}u_{SP} = 0.036\, Re_{SL}^{0.8}\, Pr_L^{1/3}\, (\mu_L/\mu_W)^{0.14}\, (D/L)^{0.1} \tag{2.13}$$

2.2.4. Groothuis and Hendal [40]

In this study, the heat transfer to two air-liquid mixtures was measured and the results were empirically correlated. The liquids used were water and gas-oil. The reported data are shown in Fig. 2.4. The authors reported that the tube-wall temperature influenced their results and that the $\bar{h}_{TP}$ values were recalculated for a wall temperatures of 140°F for air-water and 203°F for air-gas-oil.

The authors observed that the introduction of the first amount of air caused a rapid increase in $\bar{h}_{TP}$, but then the increase in $\bar{h}_{TP}$ was more gradual; further, the influence of air on the heat transfer rate was most pronounced at the lower liquid flow rates. A maximum in $\bar{h}_{TP}$ was observed for each liquid flow rate; the value of V_{SG}/V_{SL} at which the maximum

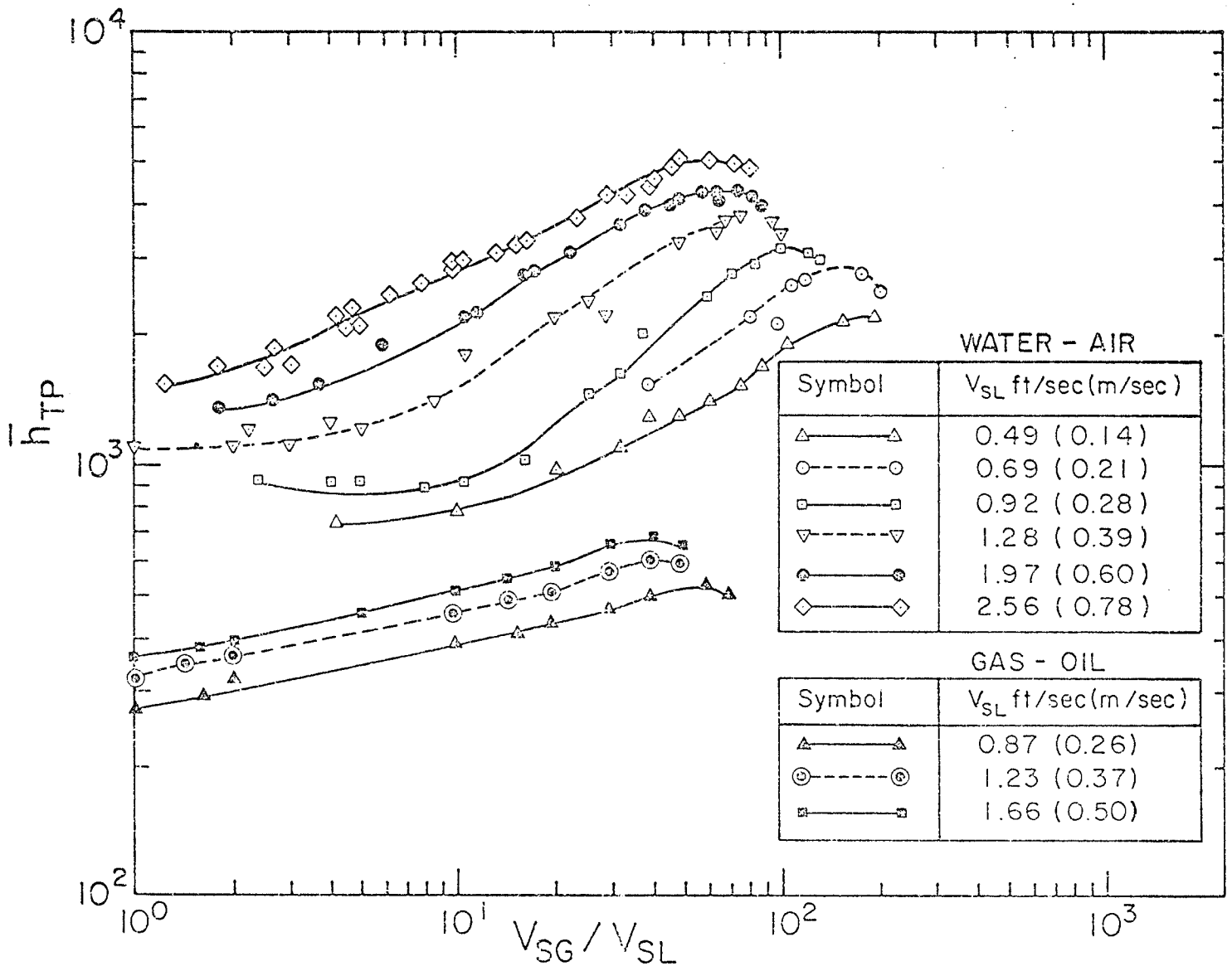

Fig. 2.4 Heat-Transfer Results of Groothuis and Hendal

occurred decreased as V_{SL} increased; further, the maxima, for air-gas-oil mixtures, occurred at considerably lower values of V_{SG}/V_{SL} than for air-water mixtures.

Satisfactory correlations of the results in the annular flow region (up to just below the maxima in $\bar{h}_{TP}$, Fig. 2.4) were obtained; these are as follows: for air-water

$$\bar{N}u_{TP} = \bar{h}_{TP} D/K_L = 0.029 \, Re_2^{0.87} \, Pr_L^{1/3} (\mu_L/\mu_W)^{0.14}$$

$$Re_{SL} > 5000, \; V_{SG}/V_{SL} > 1 \qquad (2.14)$$

for air-gas-oil

$$\bar{N}u_{TP} = 2.6 \, Re_2^{0.39} \, Pr_L^{1/3} \, (\mu_L/\mu_W)^{0.14} \qquad (2.15)$$

$$1400 < Re_{SL} < 3500, \; V_{SG}/V_{SL} > 1$$

where

$$Re_2 = Re_{SL} + Re_{SG} \qquad (2.16)$$

The authors correlated their single-phase results by the following expression:

$$\bar{N}u_{SP} = C \, Re_{SL}^{0.81} \, Pr_L^{1/3} \, (\mu_L/\mu_W)^{0.14} \qquad (2.17)$$

where

$C = 0.030$, for water $Re_{SL} > 5000$

$C = 0.028$, for gas-oil $Re_{SL} > 4000$

2.2.5. Knott, Anderson, Acrivos and Peterson [56]

Knott et al. measured the heat transfer to nitrogen-oil mixtures under constant heat flux. The authors' data are shown in Fig. 2.5 where $\bar{h}_{TP}/\bar{h}_{SP}$ is plotted against V_{SG}/V_{SL}. Very little increase in $\bar{h}_{TP}$ was observed up to a gas/liquid volumetric ratio of 0.2. As the gas flow was increased, for a fixed liquid flow rate, $\bar{h}_{TP}$ increased up to 200% of its liquid value (it should be noted that, in some cases, the authors obtained values of $\bar{h}_{TP}$ which were less than $\bar{h}_{SP}$).

The authors applied the single-phase heat-transfer theory to two-phase heat transfer and estimated $\bar{h}_{TP}$ from the equation of Sieder and Tate using a Reynolds number based on the mean velocity of the two phases ($\bar{V}_{TP}$). Although this method generally over-predicted the experimental values, it gave the approximate trends of the data.

Assuming that the bubbles had no effect on the boundary layer (in the bubble-flow region), the authors attributed the increase in $\bar{h}_{TP}$ to the increase in the mean velocity of the mixture, and, based on this assumption, they proposed the following correlation:

$$\bar{h}_{TP}/\bar{h}_{SP} = [1 + (V_{SG}/V_{SL})]^{1/3}, \qquad (2.18)$$

$$0.1 < V_{SG}/V_{SL} < 40$$

with $\bar{h}_{SP}$ calculated from the Sieder-Tate correlation.

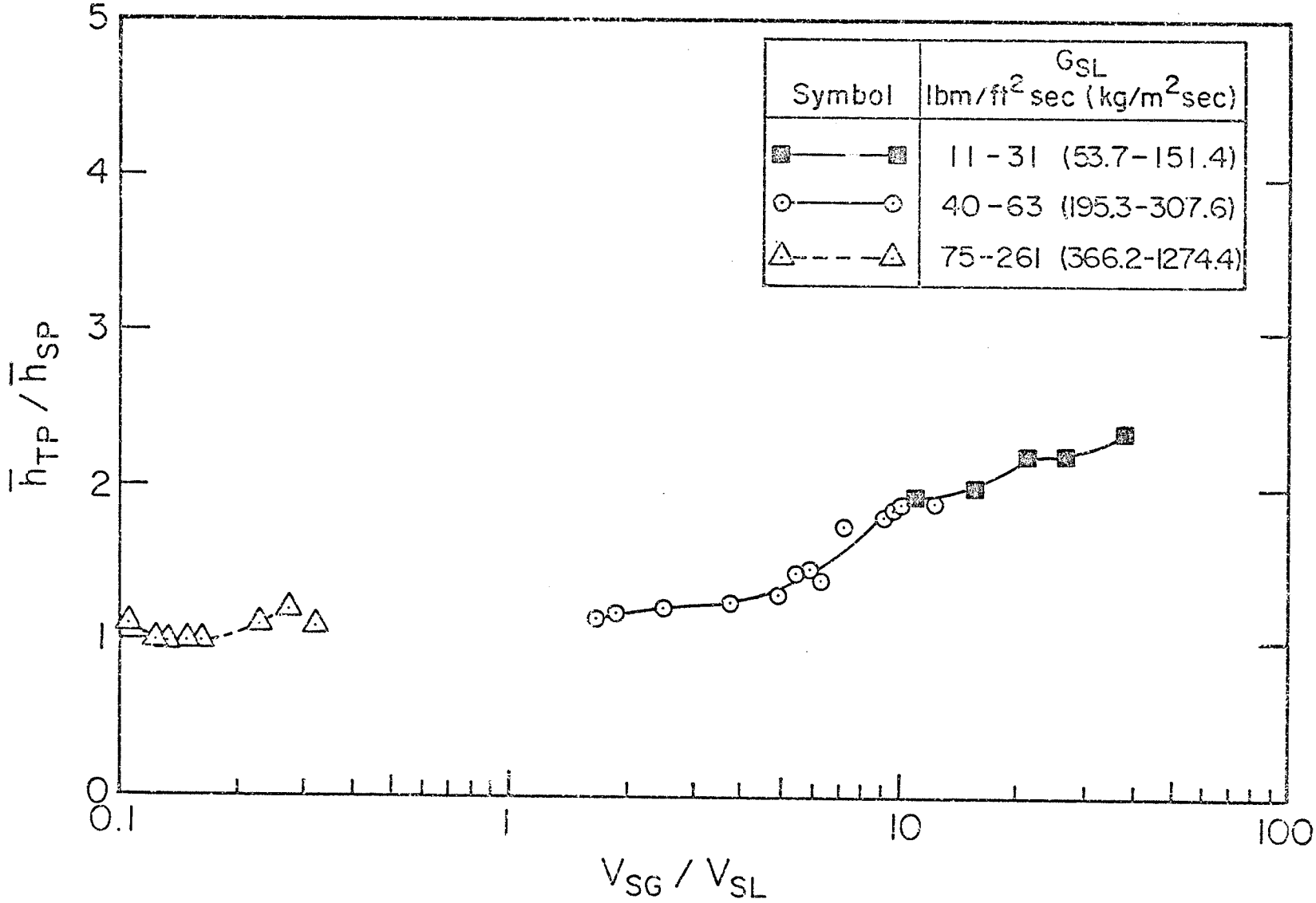

Fig. 2.5 Heat-Transfer Results of Knott et al.

2.2.6. Kudirka [58, 59]

In this study, Kudirka investigated some of the hydrodynamic aspects of boiling heat transfer in the low-quality range. The boiling process was simulated by bubbling air through the wall of a porous tube into water and ethylene glycol flowing upward inside the tube.

The author reported measurements of the void fraction (these were measured by means of gamma-ray attenuation technique and were correlated empirically), photographs of the flow patterns taken from a transparent tube following the heated test section, and measurements of the heat transfer to the two-phase mixtures with and without air injection. However, only the heat-transfer results with the air being injected through the section of the tube preceding the heated section are considered here; these were referred to by the author as the heat-transfer data with zero air-injection.

The reported data for the local heat-transfer coefficients at a location $Z = 15.8\ D$ are shown in Fig. 2.6, (Z is the distance measured from the start of the heated tube), where the ratio h_{TP}/h_{SP} is plotted against V_{SG}/V_{SL} with V_{SL} as a parameter. The local values of h_{SP} for water were calculated from the Sieder-Tate equation while actual test values were used for ethylene glycol.

The author correlated the heat transfer results, within $\pm$ 20%, with the following correlation:

$$Nu_{TP} = \frac{h_{TP}D}{k_L} = 125 \left(\frac{V_{SG}}{V_{SL}}\right)^{0.125} \left(\frac{\mu_G}{\mu_L}\right)^{0.6} Re_{SL}^{1/4}\ Pr_L^{1/3} \left(\frac{\mu_L}{\mu_W}\right)^{0.14} \tag{2.19}$$

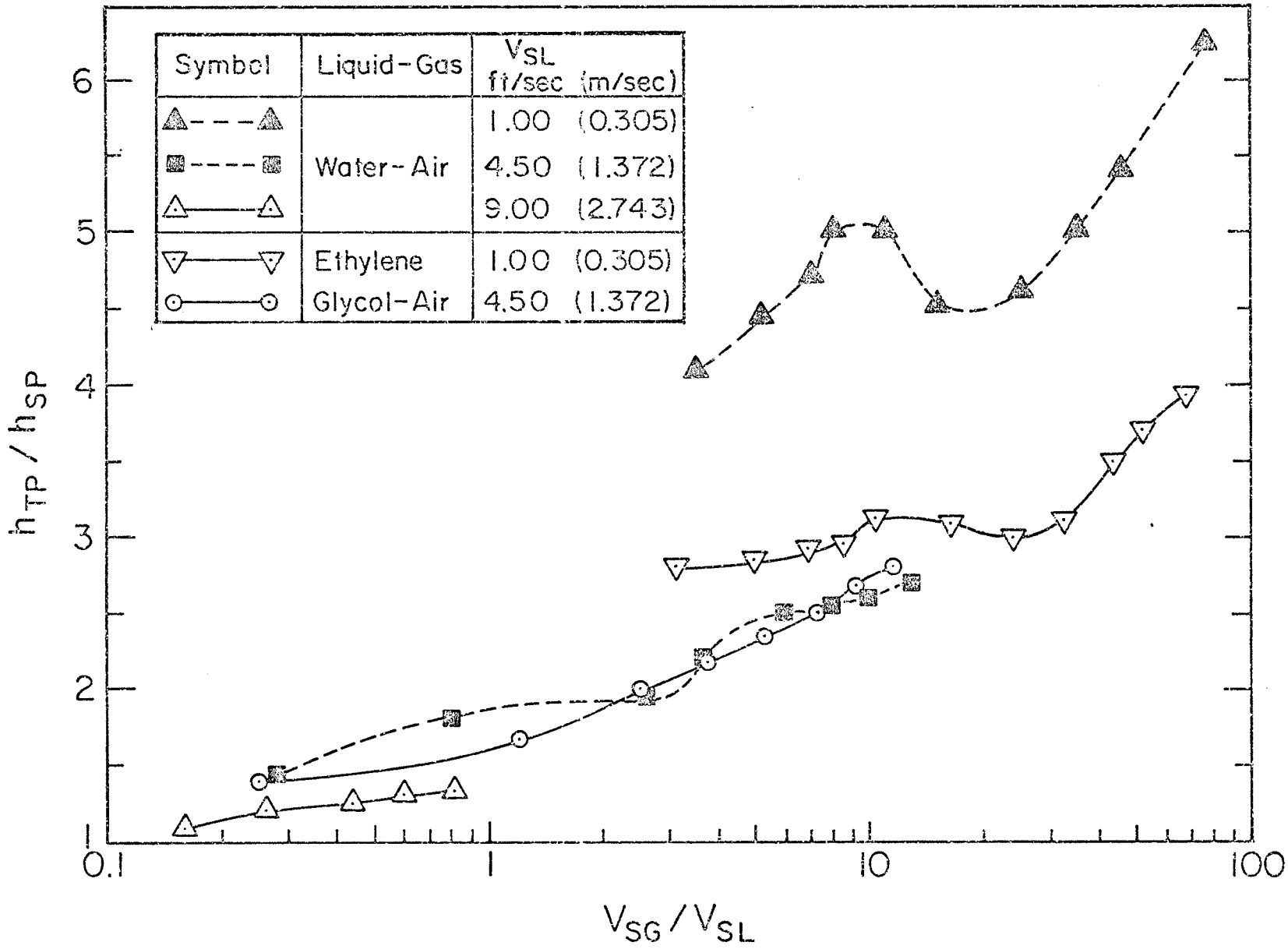

Fig. 2.6 Heat-Transfer Results of Kudirka

Fig. 2.6

As to the effect of liquid viscosity (viscosity of ethylene glycol was 17 times that of water) on the results, the author concluded the following:

(i) Under the same flow conditions, the higher the viscosity of the liquid, the lower the heat-transfer coefficients,

(ii) For the same liquid velocity, the transitions between the flow patterns for ethylene glycol-air flows occurred at lower values of V_{SG} than for water-air mixtures.

2.2.7. Ueda and Hanaoka [86]

In this investigation, the authors studied the effect on the average two-phase heat-transfer coefficient of the liquid Prandtl number by measuring the heat transfer to mixtures of air-water and air-water-solton solutions flowing in a vertical tube.

The reported data are shown in Fig. 2.7 where $\bar{h}_{TP}$ is plotted against the void fraction. The results showed that for low Pr_L, $\bar{h}_{TP}$ values were little affected by the variation of α at low V_{SG}/V_{SL}; at high values of V_{SG}/V_{SL}, $\bar{h}_{TP}$ increased sharply with increasing α. The data were correlated by the following expression:

$$\bar{Nu}_{TP} = \frac{\bar{h}_{TP}D}{k_L} = 0.075\ Re_M^{0.6}\ \frac{Pr_L}{1 + 0.035(Pr_L - 1)}\ , \qquad (2.20)$$

$$1500 < Re_M < 6 \times 10^4$$

where

$$Re_M = U_M^* D/\nu_L \qquad (2.21)$$

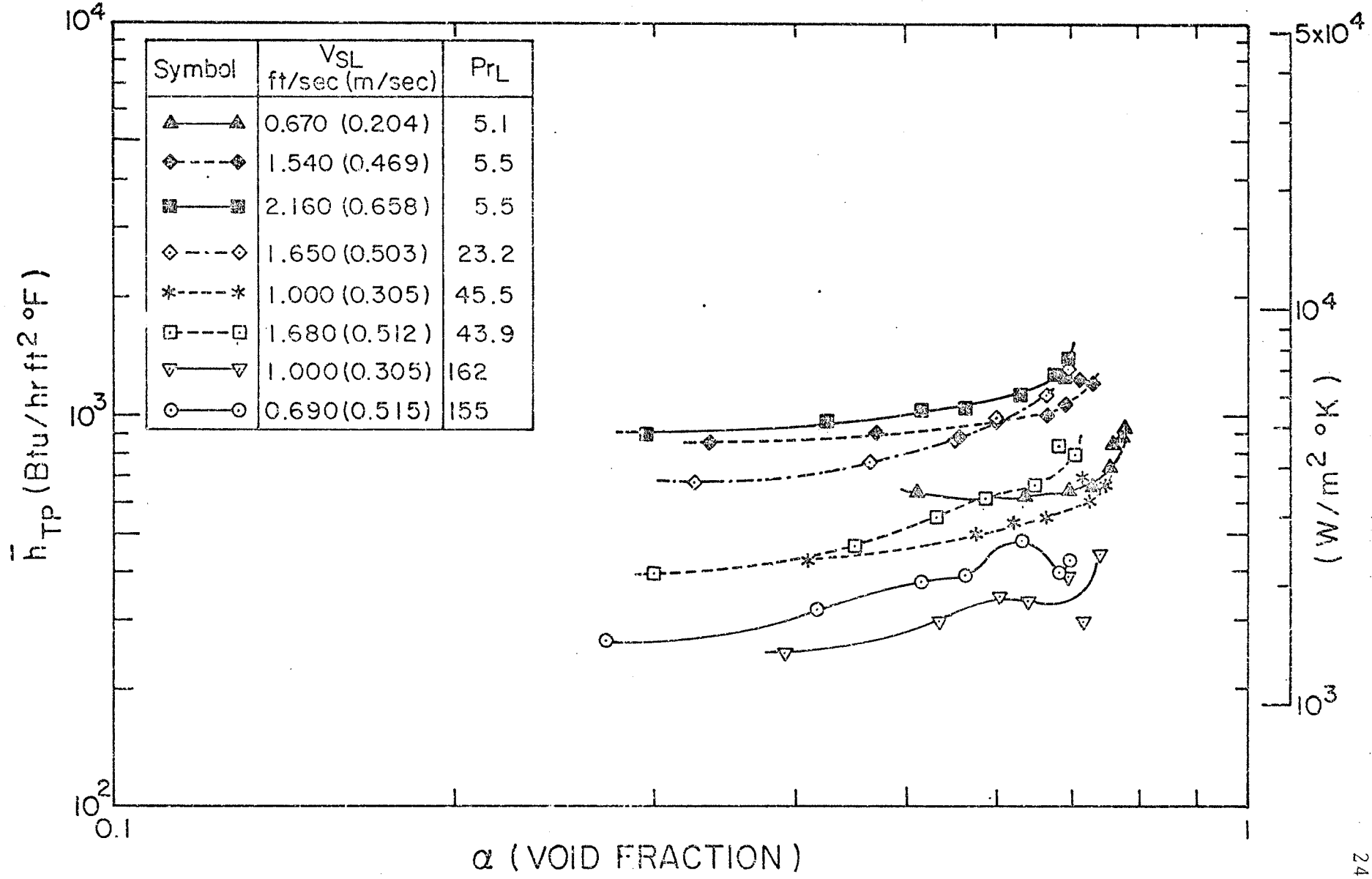

Fig. 2.7 Heat-Transfer Results of Ueda and Hanaoka

U_M^* was defined as the equivalent mean liquid velocity given by

$$U_M^* = V_L + 1.20\ Re_S^{-0.25}\ V_S - 12Fr_{ED}\ V_{ED} + 16Fr_S^{1.25}\ V_S \tag{2.22}$$

where

$$V_L = \text{mean velocity of the liquid} = V_{SL}/(1 - \alpha) \tag{2.23}$$

$$V_S = \text{slip velocity} = V_G - V_L\ , \tag{2.24}$$

$$V_G = \text{mean gas velocity} = V_{SG}/\alpha\ , \tag{2.25}$$

$$V_{ED} = V_{SL} + V_{SG}\ , \tag{2.26}$$

$$Re_S = V_S\ D(1 - \sqrt{\alpha})/\nu_L\ , \tag{2.27}$$

$$Fr_{ED} = g\ \alpha\ D(1 - \sqrt{\alpha})/V_{ED}^2\ , \tag{2.28}$$

$$Fr_S = g\ \alpha\ D(1 - \sqrt{\alpha})/V_S^2\ . \tag{2.29}$$

The authors presented an analytical solution for predicting the two-phase heat-transfer coefficient in the slug and annular flow region. In the derivation, it was assumed that the liquid film consisted of a laminar sublayer and a turbulent layer; in the laminar sublayer, the eddy diffusivity was assumed to be zero, while in the turbulent layer, the eddy diffusivity for momentum was assumed to be much greater than the kinematic viscosity, but equal to the eddy diffusivity for heat. The following relationships were used in the analysis:

$$\bar{h}_{TP} = q_W/(T_W - T_B) \quad , \tag{2.30}$$

$$T_B = \int_o^{y_i} V_L\, T\, dy \Big/ \int_o^{y_i} V_L\, dy$$

$$= \frac{\int_o^{\delta} V_L\, T\, dy + \int_{\delta}^{y_i} V_L\, T\, dy}{(\dot{m}_L/\pi D \rho_L\, g)} \tag{2.31}$$

where

V_L is the local velocity of the liquid,

y_i is the thickness of the liquid film,

δ is the thickness of the laminar sublayer of the liquid.

The authors solved Eq. (2.31) graphically and demonstrated good agreement between the theory and their experimental data.

In this work, the authors also reported data for the void fraction and frictional pressure drop for slug and annular flows. Based on the assumption of annular flow model and using the experimental data, they presented equations for predicting the following:

(i) the interfacial shear stress,

(ii) the flow state of the liquid film and the liquid-film thickness,

(iii) the frictional pressure drop; this was extended to predict the pressure drop in bubble flow,

(iv) the void fraction; this was derived from an empirical expression for the mean gas velocity.

2.2.8. Domanski, Tishin and Sokolov [24]

In this study, mean values of the coefficient of heat transfer were measured for the bubble flow of air-water, air-alcohol and air-glycerol solutions. The experimental results are shown in Fig. 2.8.

A correlation of the results was developed by assuming that the heat transfer process in the bubble flow regime is similar to isotropic turbulence; this was given by the following expression:

$$\bar{h}_{TP}\ \nu_L/k_L\ U_* = Pr_L/\bar{\psi} \qquad (2.32)$$

where

$\bar{\psi}$ is a dimensionless temperature difference

U_* is the friction velocity given by (for $V_{SL} < 0.33$),

$$U_* = [(\frac{\tau_W}{\rho_L})^2 + \xi^4\ \nu_L\ g\ V_S\ \alpha(1 - \alpha)^2]^{1/4} \qquad (2.33)$$

where

τ_W is the wall shear stress,

ξ is a proportionality factor.

A plot of $(Pr_L/\bar{\psi})$ as a function of $(U_*\ D/2\nu_L)$ with Pr_L as a parameter was presented. The authors showed that the above correlation, with $\xi = 1.9$, correlated their data within $\pm$ 12%.

2.2.9. Fedotkin and Zarudnev [29]

In this work, the heat transfer to air-water and air-

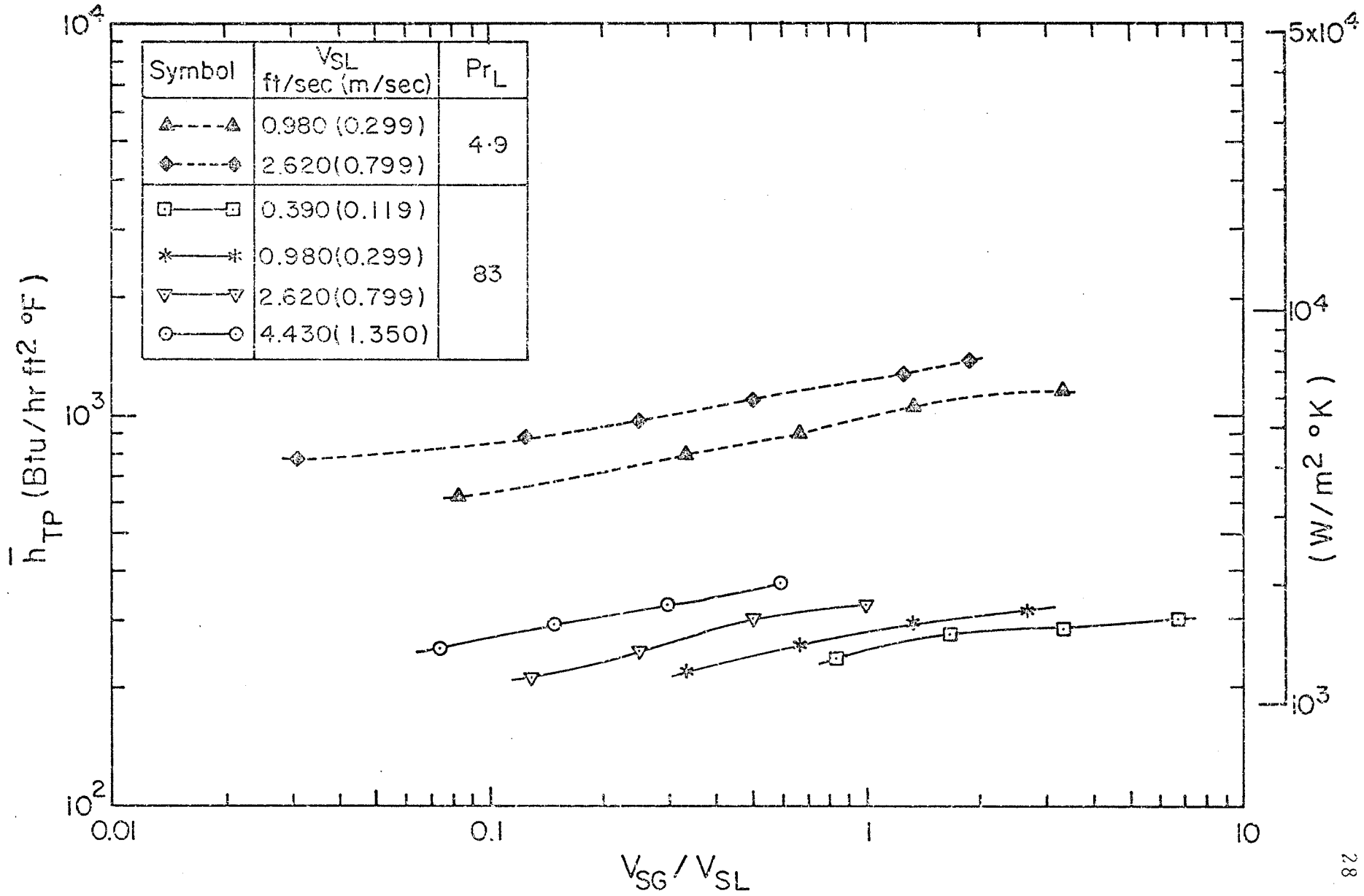

Fig. 2.8 Heat-Transfer Results of Domanski, Tishin and Sokolov

water solutions of different viscosities flowing in an elevator type (air-lift type) mixer, consisting of three chambers, placed one on top each other, was investigated. Measurements of wall temperature, pressure drop and void fraction were performed for each chamber, also, flow patterns were observed and photographed.

The authors presented correlations of the heat-transfer data for each of the observed flow patterns; these were reported as follows:

$$\bar{Nu} = \bar{h}_{TP}D/k_L = C_3 \, Re_2^n \, Pr_L^{0.43} (Pr_L/Pr_{WL})^{0.25} , \qquad (2.34)$$

$$1 < Pr_L < 200 \; ; \; 700 < Re_{SL} < 1.14 \times 10^4$$

where

Pr_{WL} is the liquid Prandtl number calculated at the wall temperature,

C_3 and n are constants, which were obtained from the authors' data for each observed flow pattern; these are given in Table 2.1.

It should be mentioned that, although the reported heat-transfer data were the average values for each chamber, they were referred to by the authors as the local values.

2.2.10. Ueda and Nose [87]

This investigation was devoted to the study of the heat transfer and hydrodynamics in annular and annular-mist flow. Data on local heat-transfer coefficients, pressure drop, mean liquid-film thickness, state of the gas-liquid interface and droplet entrainment were obtained for the developed film-flow

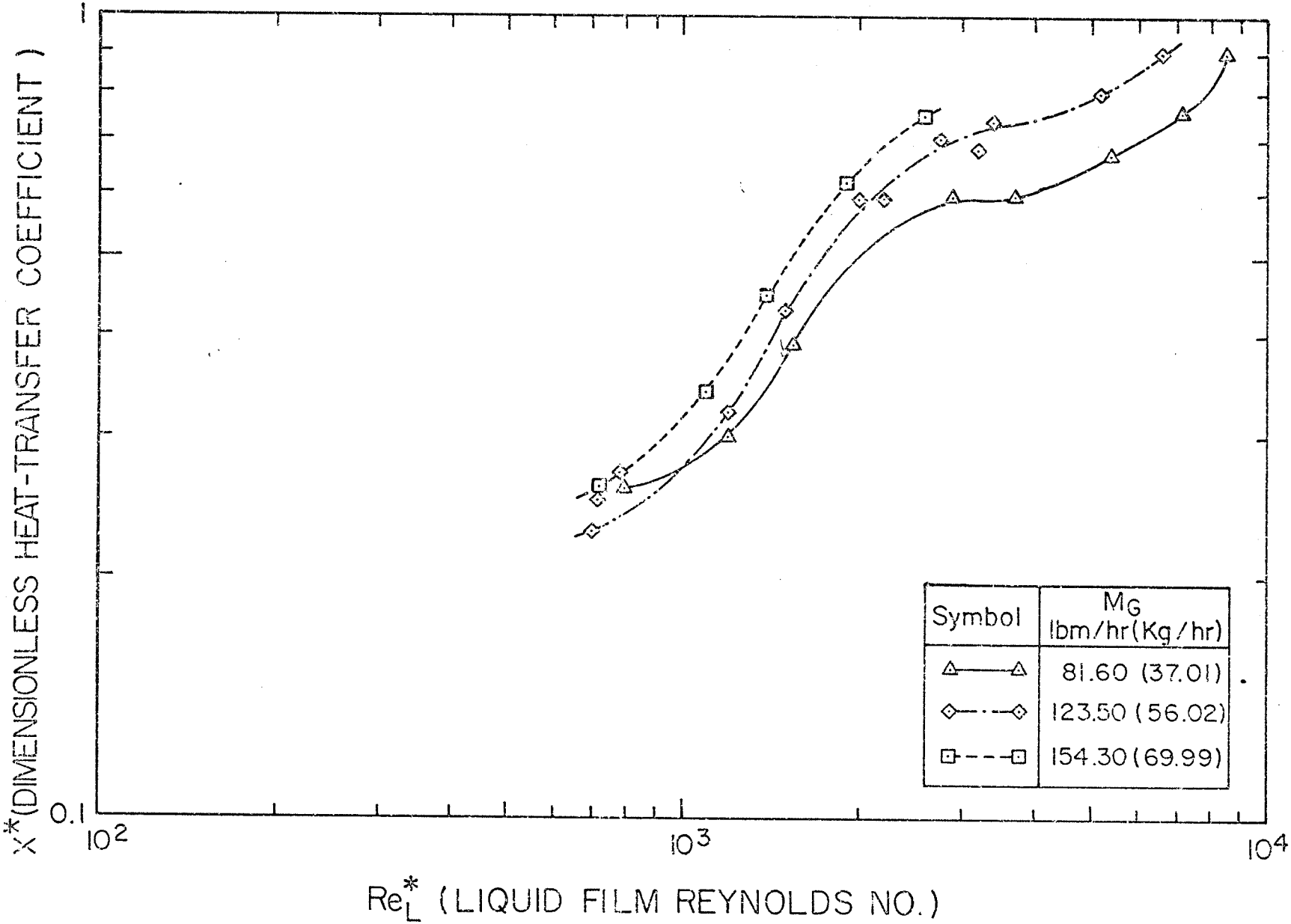

Fig. 2.9 Heat-Transfer Results of Ueda and Nose

TABLE 2.1

Values of C_3 and n in Eq. (2.34)

Liquid Flow	Flow Pattern	Section at 3.3 ft. from the Inlet		Section at 6.6 ft. from the Inlet	
		C_3	n	C_3	n
Laminar and Transition	Bubble	0.0702	0.702	0.0181	0.87
Laminar	Slug and Slug-Foam	4.455	0.410	3.450	0.267
		(1.18,0.39)*		(1.18)	
		2.18	0.175	5.40	0.148
		(0.85)		(0.85)	
	Annular	0.133	0.483	0.0764	0.610
Transition	Slug and Slug-Foam			0.059	0.750
	Annular			0.0224	0.785
	Bubble	0.059	0.090	0.084	0.720
		$3 \times 10^4 < Re_2 < 1.5 \times 10^5$			
Turbulent	Slug and Slug-Foam	0.0182	0.882	0.090	0.732
		$10^4 < Re_2 < 2 \times 10^5$			
	Annular	0.509	0.757	1.750	0.478
		(1.18)		(1.18)	
		0.0264	0.766	0.148	0.478
		(0.85)		(0.85)	
	Emulsion	0.0188	0.823	0.00564	1.000

* The tube diameter in inches.

regime.

The local heat-transfer data, measured at one location (Z = 32 D) were expressed in terms of a dimensionless heat-transfer coefficient, X*; these are plotted in Fig. 2.9 against the liquid-film Reynolds number, Re_L^*, where

$$X^* = (h_{TP}/k_L)(\nu_L^2/g)^{1/3} \tag{2.35}$$

$$Re_L^* = Re_F = 4\,\Gamma_F/\mu_L \tag{2.36}$$

and where

Γ_F is the mass flow rate in the liquid film.

The authors presented a theoretical analysis based on the assumption that the liquid film consisted of a laminar sub-layer and a turbulent layer. However, the equation obtained for the turbulent liquid film flow was not solved; instead, the authors used the theory proposed by Hewitt [46].

2.2.11. Kapinos, Slitenko, Chirkin and Povolotsky [52]

In this investigation, the authors studied the heat transfer in the entrance section of vertical tubes to air containing water droplets. Based on the measured mean heat-transfer coefficients in sixteen test sections of different L/D ratios, the authors concluded that the pipe length required for stabilizing the heat transfer was 30D.

The experimental results were correlated as follows: for L > 30D,

$$\bar{Nu}_{TP} = \bar{h}_{TP}\,D/K_G = 340\,Re_{SG}^{0.8}\,\tilde{G}^{0.15}\,K_\theta^{0.86}\,\tilde{q}^{0.82} \tag{2.37}$$

where

$\tilde{G}$ is the precentage ratio of the mass flow rate of the atomized water to the mass flow rate of the air,

$$K_\theta = \frac{S + (C_{PL})_W (t_S - \bar{T}_B)}{(G_{PG})_W (\bar{T}_W - \bar{T}_B)} , \qquad (2.38)$$

$$\tilde{q} = q_W / s \rho_L V_{SG} \qquad (2.39)$$

S and t_S were not defined; in addition the terms used in the paper were not clearly defined.

For $L < 30D$, the data were correlated by multiplying Eq. (2.39) by $[1 + 10.2/(L/D)^{1.74}]$.

2.2.12. Fried [31]

Although this investigation was for horizontal flow, it is considered here because the heat transfer correlation proposed by the author was so simple and general in nature that its extension to vertical flow seemed promising.

The author correlated his heat transfer results, within $\pm$ 30%, by plotting the ratio of the two-phase heat transfer coefficient to the single-phase heat transfer coefficient (ψ^2) against the two-phase frictional pressure drop ratio ϕ^2, defined below:

$$\psi^2 = \bar{h}_{TP}/\bar{h}_{SP} , \qquad (2.40)$$

$$\phi^2 = \Delta P_{TPF}/\Delta P_{SPF} \qquad (2.41)$$

where

ΔP_{TPF} is the two-phase frictional pressure drop,

ΔP_{SPF} is the single-phase frictional pressure drop of the liquid as if it were flowing alone in the tube.

2.2.13. Vijay [90]

This investigation presented the widest range of variables studied so far. The author studied the effect of the liquid Prandtl number, through changing the liquid viscosity, on the coefficients of heat transfer (both local and mean), the frictional pressure drop and the flow patterns. While air was always used as the gas phase, the author used water, a glycerine-water solution and glycerine for the liquid phase (Pr_L ranged from 5.6 to 6960).

Measurements of the local coefficients of heat transfer were taken at seven locations along the tube. These were correlated (within $\pm$ 50%) by modifying the Spalding [81] single-phase heat-transfer theory where the Spalding function $Sq(Z^+)$ and the dimensionless distance Z^+ were modified as follows:

$$Z^+_{TP} = Z/D^* \tag{2.42}$$

$$(Sq)_{TP} = h_{TP} D^*/k_{MIX} = Nu^*_{TP} \tag{2.43}$$

where

$$D^* = \mu_{MIX}/(g_c \tau_W \rho_{MIX})^{1/2} , \tag{2.44}$$

$$\tau_W = \frac{D}{4L} \Delta P_{TPF} \tag{2.45}$$

The author reported that the best agreement (within $\pm$ 50%)

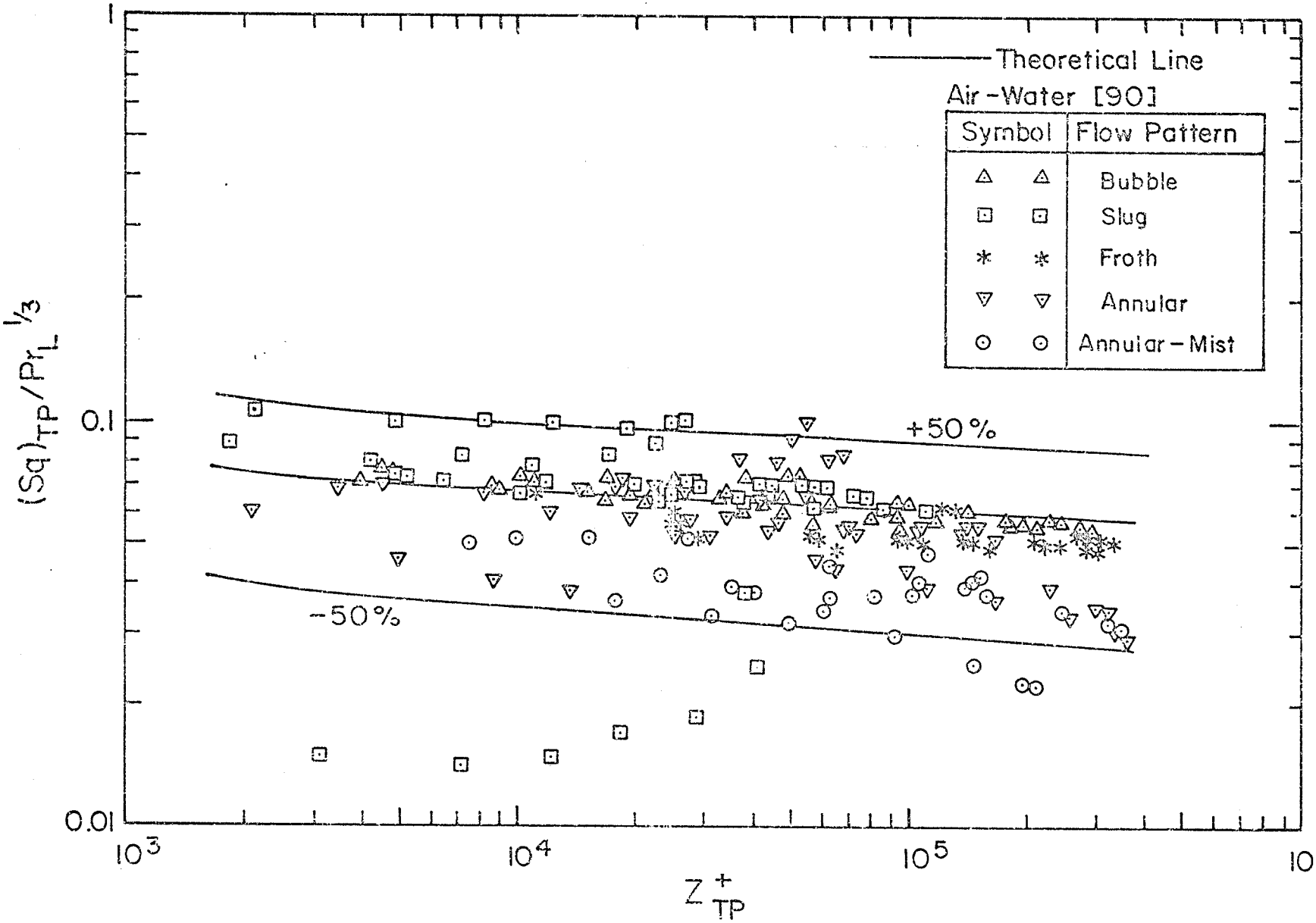

Fig. 2.10 Modified Spalding Correlation of Water-Air Local Heat-Transfer Data of Vijay

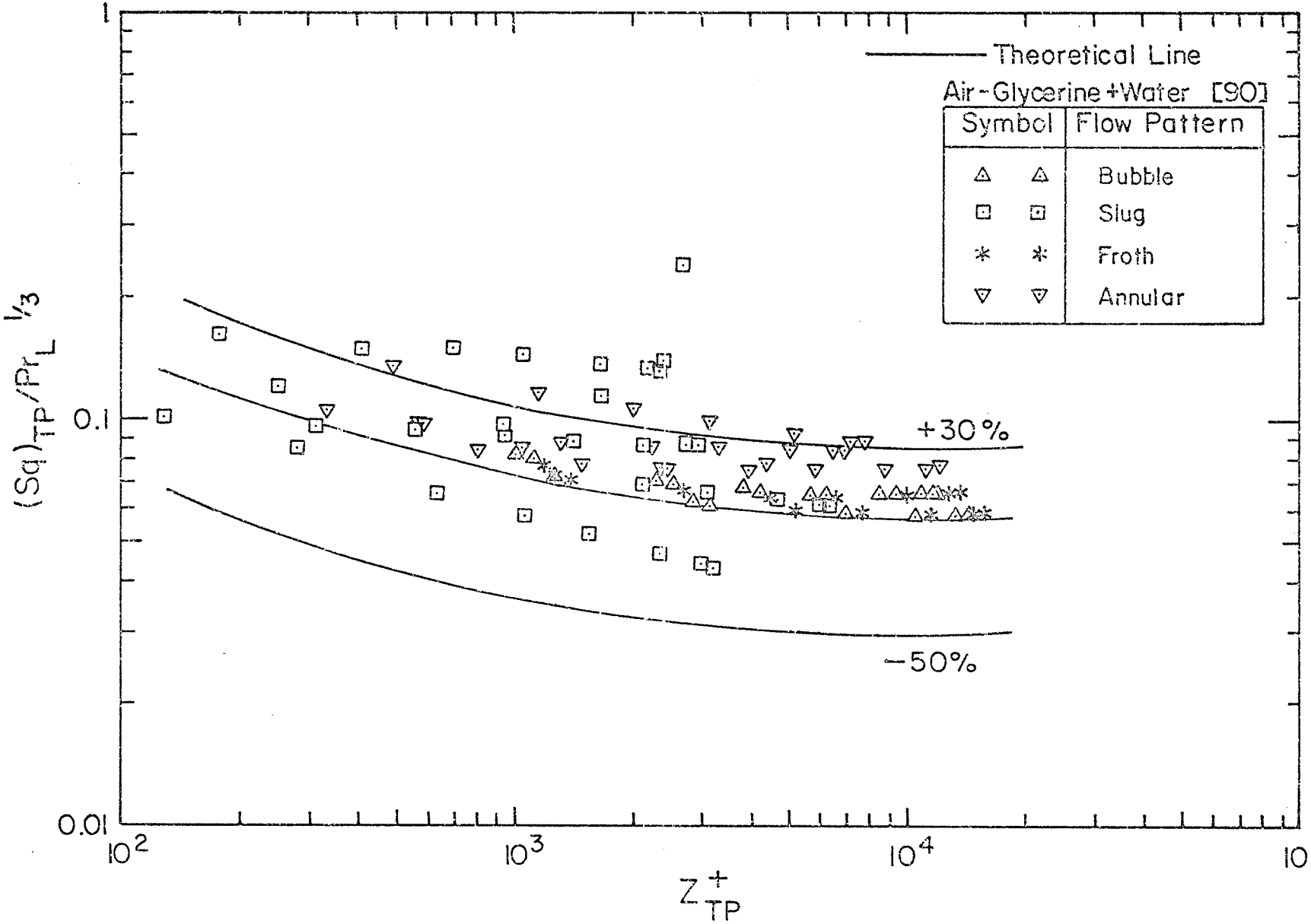

Fig. 2.11 Modified Spalding Correlation of Glycerine + Water-Air Data of Vijay

Fig.2.11

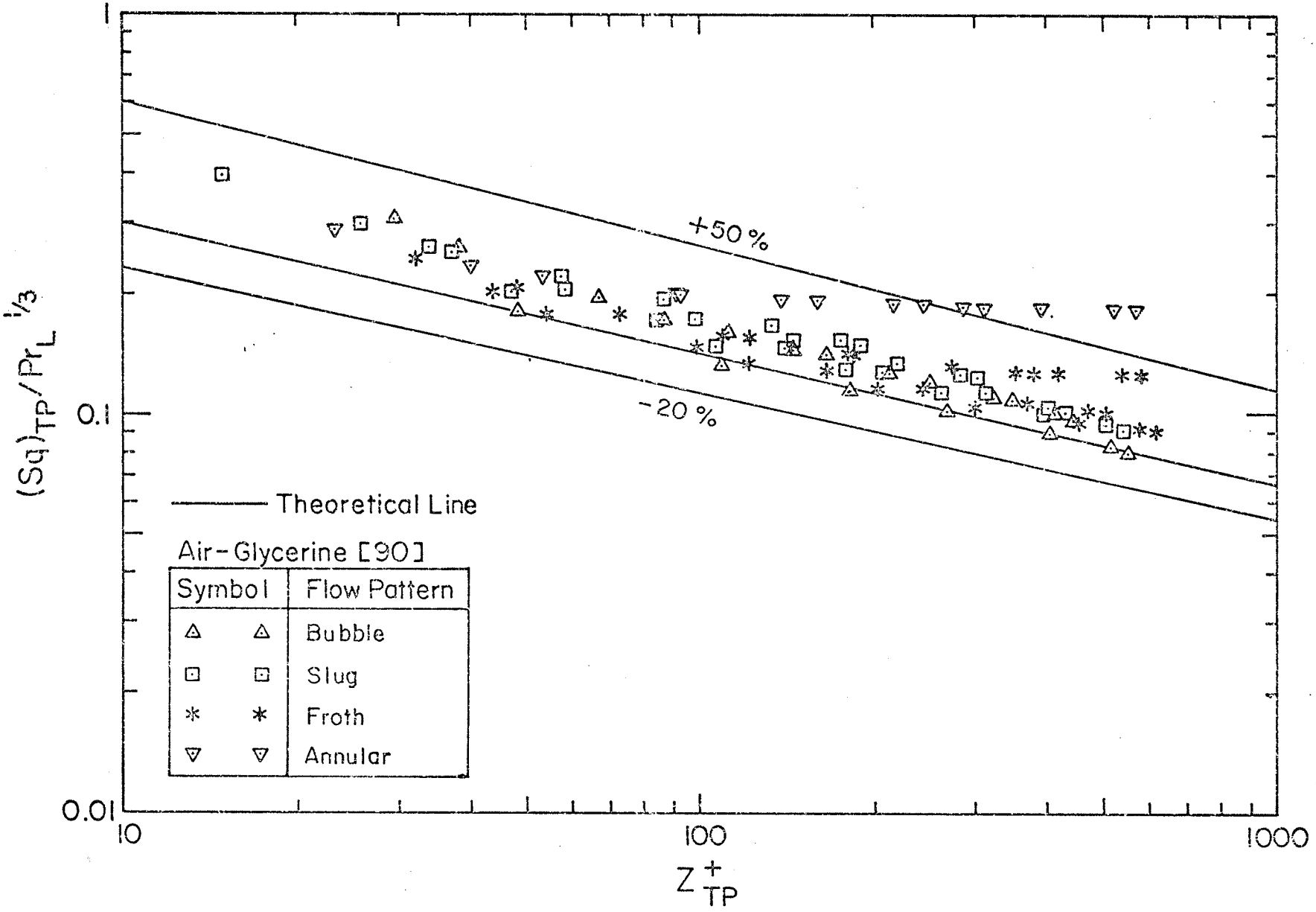

Fig. 2.12 Modified Spalding Correlation of Glycerine-Air Data of Vijay

between the experimental results and the theory was obtained when the liquid properties were used for the mixture. The results of the correlation, as given by the author, are shown in Figs. 2.10, 2.11 and 2.12 for water-air, glycerine + water - air and glycerine respectively.

In the bubble and bubble-slug flow regimes, at low liquid flow rates, the author observed that the values of $\bar{h}_{TP}$ increased with the distance along the tube. An approximate theory based on solving the classical Graetz problem for two-phase flow was developed which, qualitatively, explained these observations.

The author also reported measurements of the mean coefficients of heat transfer which were calculated from the local values; these are shown in Figs. 2.13, 2.14 and 2.15 for the three air-liquid combinations used. A simple correlation of $\bar{h}_{TP}$ data was proposed. This was based on a separated flow model in which the two phases were assumed to be flowing in two separate cylinders with the actual mean velocities of the phases (actual velocities here means the velocities calculated from the volume rates of flow and the cross-sectional areas occupied by each phase); these were determined from knowledge of the void fraction and that the cross-sectional areas of these cylinders add up to the total cross-sectional area of the actual tube; the author then proposed the following equation for $\bar{h}_{TP}$:

$$\bar{h}_{TP} = \bar{h}_{AL} + \bar{h}_{AG} \qquad (2.46)$$

where

$\bar{h}_{AL}$ is the single-phase liquid heat-transfer coefficient based on the actual mean velocity, defined earlier, and

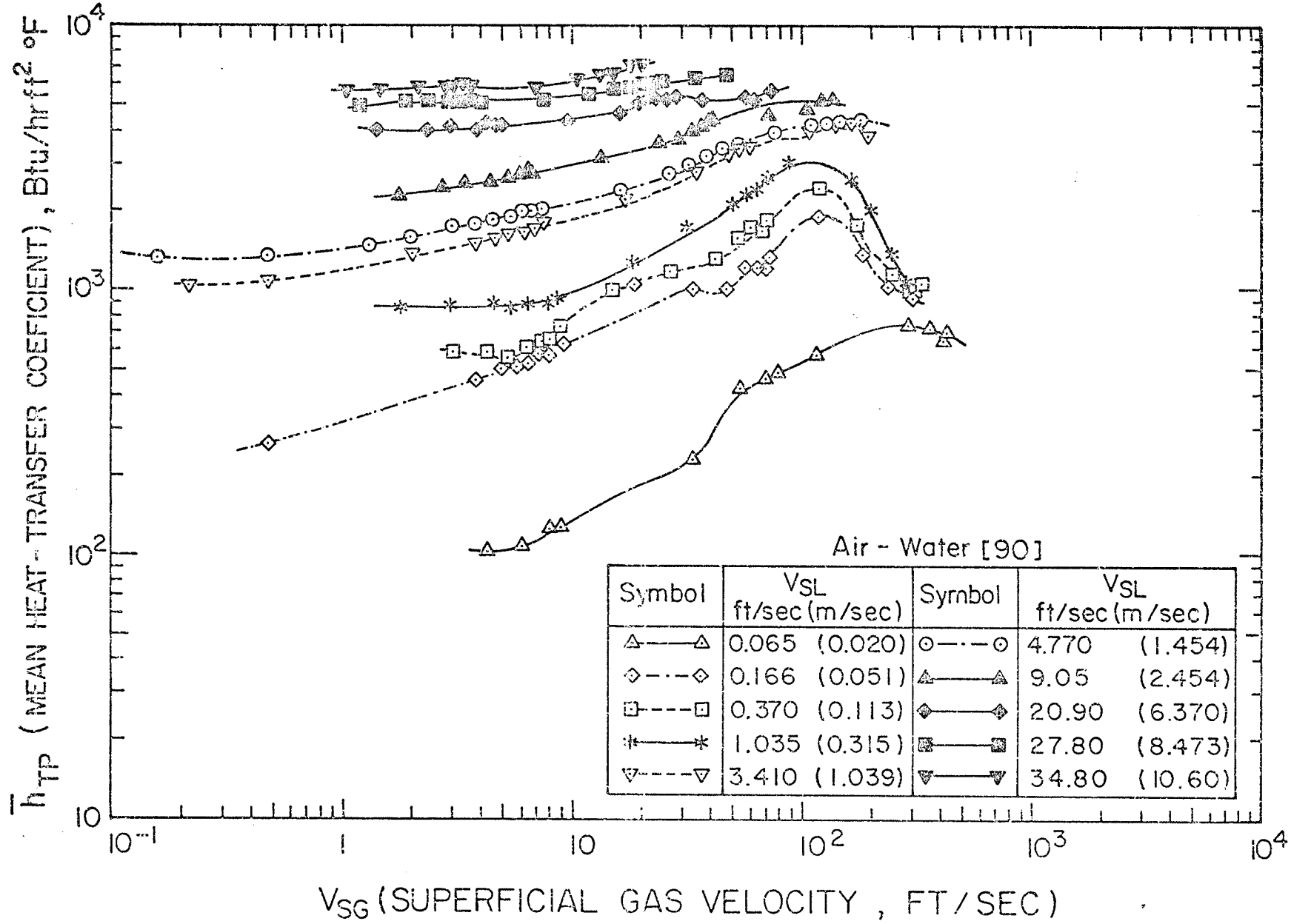

Fig. 2.13 Mean Heat-Transfer Data of Vijay, Water-Air

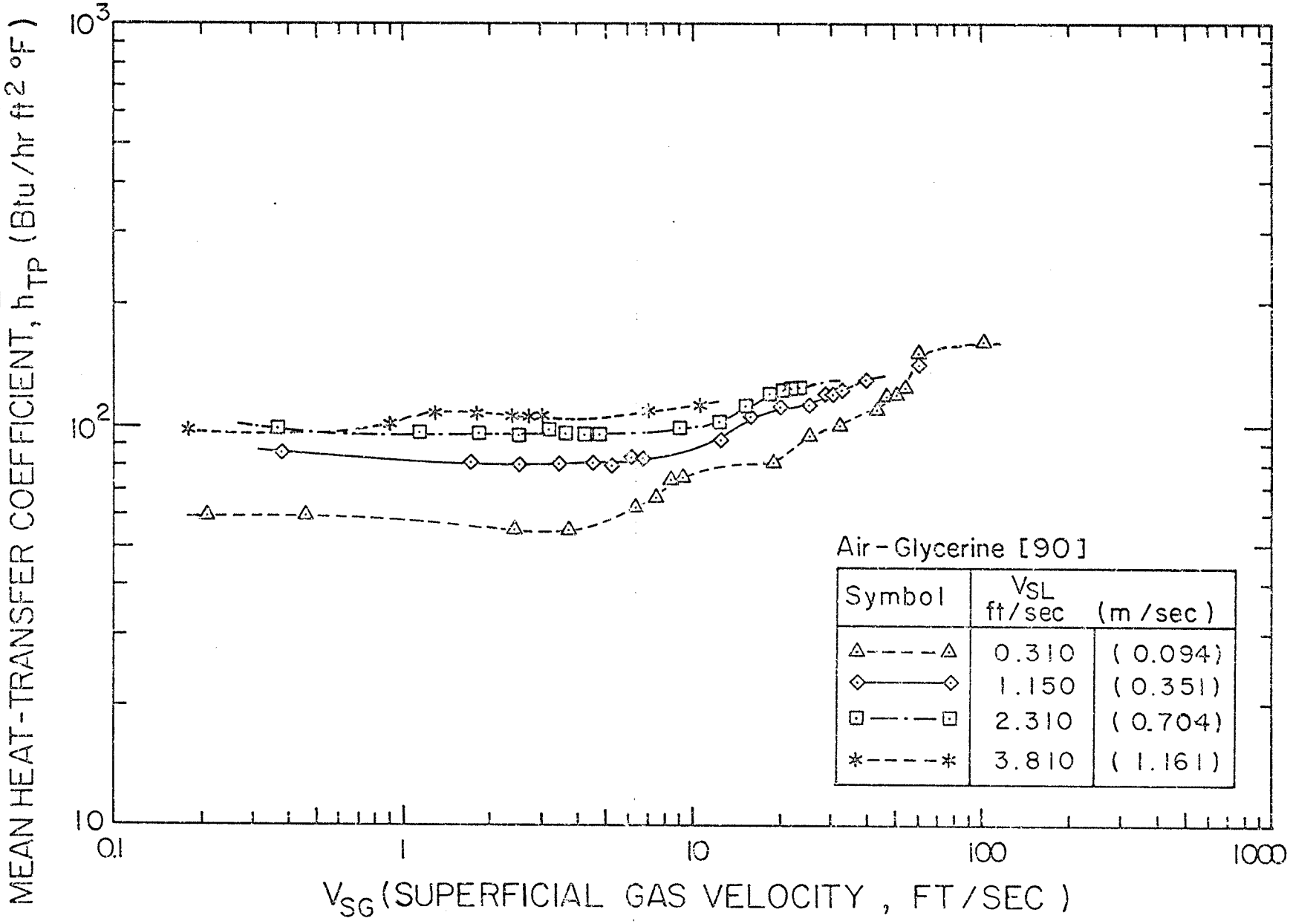

Fig. 2.14 Mean Heat-Transfer Data of Vijay, Glycerine + Water-Air

Fig. 2.14

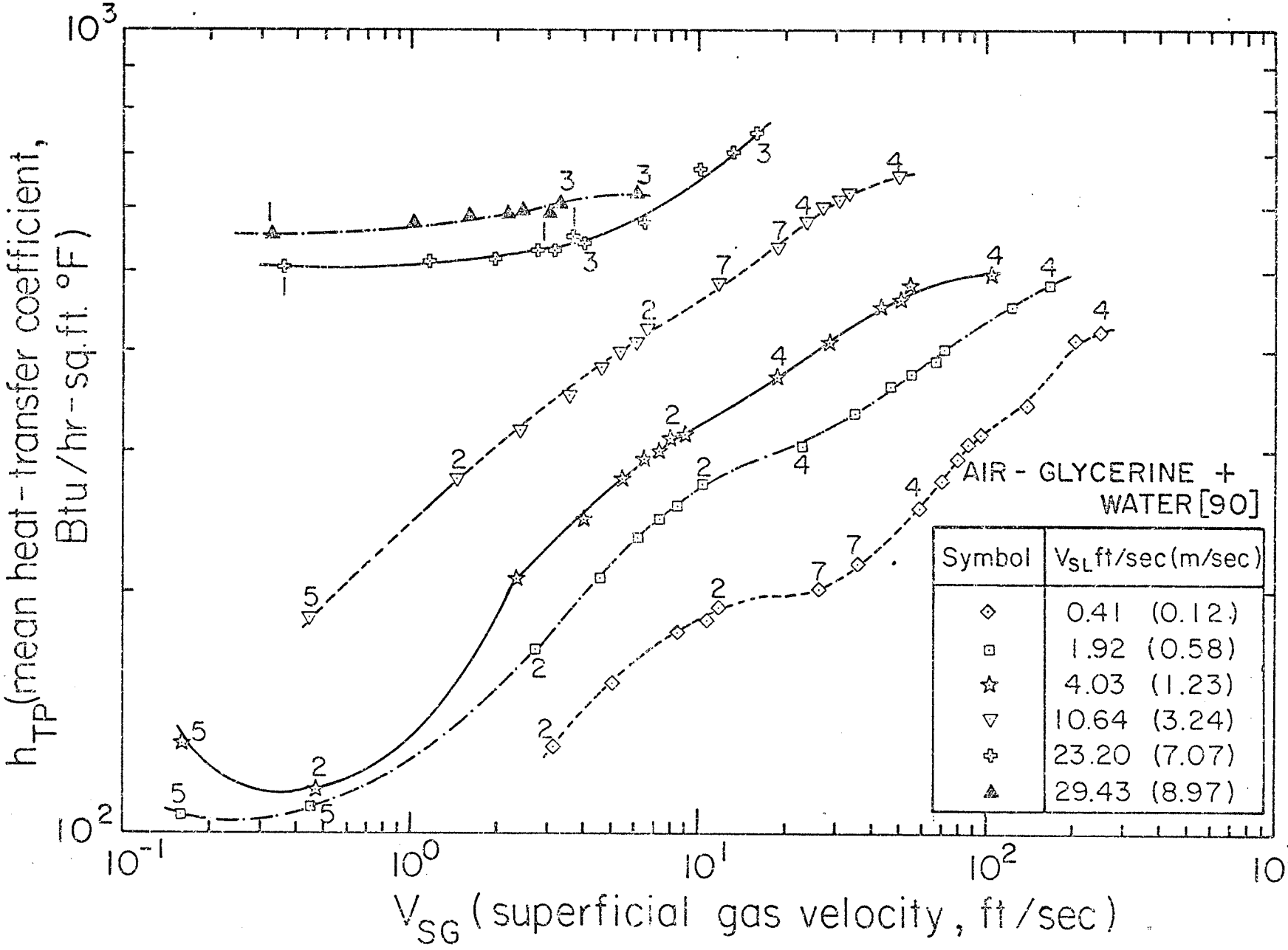

Fig. 2.15 Mean Heat-Transfer Data of Vijay, Glycerine - Air

actual flow cross-sectional area of the liquid,

$\bar{h}_{AG}$ is the single-phase gas heat-transfer coefficient based on the actual mean velocity and the actual flow cross-sectional area of the gas phase.

The single-phase coefficients of heat transer were calculated from the following expressions:

for laminar flow (both gas and liquid),

$$\bar{N}u_{SP} = 1.615[Re\ Pr(D/L)]^{1/3} \qquad (2.47)$$

for turbulent flow of water,

$$\bar{N}u_{SP} = 0.0155\ (Pr_L)^{0.5}\ (Re_L)^{0.83} \qquad (2.48)$$

for turbulent flow of glycerine and its solutions,

$$\bar{N}u_{SP} = 0.0118\ (Pr_L)^{0.3}\ (Re_L)^{0.9} \qquad (2.49)$$

for turbulent flow of air,

$$\bar{N}u_{SP} = 0.022\ (Pr_G)^{0.6}\ (Re_G)^{0.8} \qquad (2.50)$$

It should be noted, that in the above equations, actual values were used for Reynolds numbers and that the diameters used were those of the imaginary cylinders of the two-phases. This method correlated 87% of the authors data within $\pm$ 50%.

In addition, the author presented measurements of the frictional pressure drop, photographs of the flow patterns and flow-regime maps.

The following conclusions were reported:

(i) the effect of liquid viscosity on the flow patterns was insignificant,

(ii) the frictional pressure drop increased with increasing the liquid viscosity; this was, however, more pronounced at the lower liquid flow rates than at the higher rates,

THE UNIVERSITY OF MANITOBA LIBRARIES

(iii) the shape of the profiles of h_{TP} with distance along the tube was a function of the initial liquid velocity, the flow-pattern and the liquid viscosity,

(iv) the mean values of the heat-transfer coefficient were dependent on the initial liquid velocity, flow-pattern and liquid viscosity.

2.3. Conclusions

The following observations and conclusions are made from the papers and investigations reviewed in this chapter:

(i) The introduction of the gas phase into the liquid phase was observed to enhance the heat-transfer process and to result in higher coefficients of heat transfer than for the single phase at the same liquid flow rate; this effect was found to be more pronounced for the low liquid rates.

(ii) The two-phase heat-transfer coefficients were found to depend on the flow patterns, initial liquid velocity and liquid viscosity.

(iii) The liquid viscosity is the only fluid property which has received extensive study of its influence on the heat-transfer process. Information is lacking on the effect on the heat-transfer process of other fluid properties such as gas density and liquid surface tension.

(iv) The influence of liquid viscosity on two-phase flow and heat transfer was found to be as follows:

a - for the same flow rates, the higher the liquid

viscosity, the higher is the frictional pressure drop,

b - for the same gas and liquid flow rates, increasing the liquid viscosity reduces the coefficients of heat transfer,

c - the higher the value of viscosity, the lower the value of V_{SG}/V_{SL} at which the maxima in $\bar{h}_{TP}$ occurs (at the transition from annular to annular-mist flow),

d - the above mentioned effects are more pronounced at the lower liquid rates than the higher liquid rates,

e - no significant effect on the flow patterns of the liquid viscosity was observed.

(v) With the exception of Vijay [90], no extensive study of the local coefficients of heat-transfer was reported; more information on local h_{TP} is required.

(vi) Local values of h_{TP} and its variation with the distance along the tube were found to depend on the flow patterns, initial liquid velocity and liquid viscosity.

(vii) Fedotkin [29] and Vijay [90] showed that in some flow patterns under low liquid flow rates, h_{TP} increased with respect to Z; Vijay has presented a theory which qualitatively explained this behavior. This trend has been observed in the present investigation and has been explained through a flow-visualization study as shown later in the thesis.

(viii) In general, most of the correlations for $\bar{h}_{TP}$ presented in the previous work were empirical, obtained by extending the single-phase correlations. The only correlations

based on a physical model were attempted by Lunde [63], Vijay [90] (who used a sort of separated flow model), Ueda [86] and Domanskii [24] who used a turbulent flow model.

(ix) Attempts have been made by Domanskii [24], Fried [31] and Vijay [90] to correlate $\bar{h}_{TP}$ in terms of the frictional pressure drop and proved to be successful.

TABLE 2.2

Previous Work: General Observations

Reference	Test Section	Method of Heating ($q_{W,MAX}$, Btu/hr ft^2)	Method of Temperature Measurement	Fluids Used		h_{TP}		Effect Fluid Properties Studied	Flow Patterns Observed	Other Information
				Liquid	Gas	Local	Mean			
Verschoor and Stemerding [89]	Ambraloy 927 D=0.551 in. L=15.75 in. L/D=28.6	steam at atmospheric pressure $(q_W)_{MAX}$ = not given	Thermocouples soldered on to the tube wall. Fluids temps. were measured by thermometer	Water $\mu_L \approx 1$CP	Air		X	-----	Bubble, Slug & Annular	Calming length L' L' = 50D No correlation given
Ueda [85]	Steel D=2.01 in. L=3.94 in. L/D=1.96	D.C. electrical heating by means of external resistance wire (0.56×10^5)	Thermocouples inserted to the mid point of the tube wall thickness	Water $\mu_L \approx 1.5$CP	Air	X		-----	Bubble, Slug & Annular	L' = 23D No h_{TP} is reported only temperatures at two locations No correlation
Katsuhara and Kazama [53]	Copper D=1.18 in. L=10.63 in. L/D=9	Electric (Nichrome wire wound around the tube) $(q_W)_{MAX}$ not given	4 thermocouples attached on the outer surface. Mean used to calculate $\bar{h}_{TP}$	Water $\mu_L \approx 1$CP	Air		X	-----	Not reported (probably Bubble & Slug)	L' = 33D Empirical correlation for mean h_{TP}
Groothuis and Hendal [40]	Copper D=0.551 in. L=7.87 in. L/D=14.3 D_o=1.023 in.	Steam	B. Constantan wires were buried inside the wall to form together with the tube material 8 copper-constantan thermocouples. Mean used to calculate $\bar{h}_{TP}$. Accuracy 1°C	1.Water $\mu_L \approx 0.47$CP at 60°C 2.Gas-oil $\mu_L \approx 0.84$ at 97°C	Air Air		X	Viscosity Pr_L = 5 - 180	Not observed but observation of $\bar{h}_{TP}$ indicates. Bubble to annular-mist flow	L' = 86D semi-empirical correlation
Knott, Anderson, Acrivos & Petersen [56]	Type 304 Stainless steel D=0.506 in. L=60 in. L/D=118.6 D_o=0.562in.	A.C. electric heating (1.36×10^4)	6 No. 22 copper constantan thermocouples soldered on to the tube wall	Paraffin base petroleum oil $\mu_L \approx 10.86$CP at 210°F	Nitrogen		X	-----	Bubble	L' = 47D Integrated mean $(T_W - T_B)$ was used to calculate $\bar{h}_{TP}$. Empirical correlation.

Table 2.2 continued

Reference	Test Section	Method of Heating ($q_{W,MAX}$, Btu/hr ft^2)	Method of Temperature Measurement	Fluids Used		h_{TP}		Effect of Fluid Properties Studied	Flow Patterns Observed	Other Information
				Liquid	Gas	Local	Mean			
Kudirka [58,59]	Porous bronze D=0.625in. D_o=0.875in. L=11.0in. L/D=17.6	A.C. electric heating, using the tube as a resistor (7.13×10^4)	8 Cu-Con Thermocouples attached to the inner surface of the tube wall. Only one (9" from the start of the test tube) was used.	1.Water 2.Ethylene glycol μ_L=13CP at 100°F	Air Air	X		Viscosity Pr_L = 5 - 140	Bubble, Slug & Annular	L' = 0.0 The mixer was adjacent to the test section. Investigation was for boiling simulation. Empirical correlation.
Jeda and Hanaoka [86]	Brass D=0.766in. D_o=1.004in. L=51.20in. L/D=66.8	Hot water circulated through a jacket around the tube	3 pairs of thermocouples soldered on the outer surface of the tube. Mean used to calculate $\bar{h}_{TP}$	1.Water μ_L=0.6-0.8CP 2.Mixture of water and solton μ_L=0.35 to 8.4CP	Air Air	X	X	Viscosity Pr_L=4 to 155	Bubble, Slug & Annular	L' = 77.1D Only mean h_{TP} reported Empirical correlation for all flow patterns. Theoretical analysis of annular flow h_{TP}
Domanskii Tishin & Sokolov [24]	Copper D=1.260 L=39.37 L/D=31.25	Electrically by winding Nichrome strip around the tube	6 Cu-con thermocouples. Mean used to calculate $\bar{h}_{TP}$	1.Water 2.Alcohol 87% 3. Glycerol (54,65, 71,77,85%)	Air Air Air		X	Viscosity $Pr_L \approx$ 5 to 247	Bubble	No information about L'. Semi-empirical correlation.
Fedotkin and Zarudnev [29]	D=0.394, 0.846 & 1.19 in. L=39.4 & 98.4 in. (see section 2.2. 10)	Not given	Measured the wall temp. at 3 points in each chamber	Water and solutions of different μ_L	Air	X		Viscosity ν_L=0.116 to 1.085 ft^2/hr $1 < Pr_L < 200$	Bubble, Slug & Annular	L' = 6.4" Local here means h_{TP} calculated from the mean temperature of each individual chamber. Empirical correlations for each flow pattern. For both horizontal and vertical flow.

Table 2.2 continued

Reference	Test Section	Method of Heating ($q_{W,MAX}$, Btu/hr ft^2)	Method of Temperature Measurement	Fluids Used		h_{TP}		Effect of Fluid Properties Studied	Flow Patterns Observed	Other Information
				Liquid	Gas	Local	Mean			
Ueda and Nose [87]	Stainless steel D=1.177 in. D_o=1.256 in. L=51.2 in. L/D=43.5	A.C. electric heating of the tube	12 thermocoulpes attached on the outer surface at equal intervals	Water	Air	X		-----	Annular and mist	L' = 19.4D h_{TP} reported was at Z/C = 32 (4.2 ft downstream of test section inlet) No correlation
Kapinos et al. [52]	L/D=1.68 to 59.1	Not given (3.8×10^4)	Not given	Water	Air		X	-----	Mist (Fog) Flow	Empirical correlation for mean Nusselt number reported.
Fried [31]	Brass Horizontal tube D=0.737 in. L=183.4 in. L/D=256	Steam	24 thermocouples located on the outer surface of the tube Mean used for $\bar{h}_{TP}$	Water	Air		X	----	Not Specified	L' = 102 D Graphical correlation based on frictional pressure drop
Vijay [90]	Stainless steel 304 D=0.46 in. D_o=0.50in. L=24 in. L/D=52.2	A.C. electric heating using the tube as a resistor (1.06×10^5)	47 Cu-con (D=0.005") thermocouples were attached onto the outer surface of the tube by means of a scotch electric tape No. 27. 6 thermocouples were used for fluid temp. at inlet and outlet of the test section	1.Water 2.Water +glycerine 75% 3.Glycerine	Air Air Air	X X X	X X X	Liquid viscosity Pr_L = 5.6 to 6960	Bubble, Slug, Annular, Annular-Mist & Transition regimes observed and photographed.	L' = 130D Presented local h_{TP} as function of position. Correlated both local and mean h_{TP}. Also reported frictional pressure drop data, flow pattern maps and photographs of flow patterns.

TABLE 2.3

Previous Work: Range of Variables and Proposed Correlations

Reference	Range of $\dot{m}_L$ (lbm/hr)	Range of $\dot{m}_G$ (lbm/hr)	Range of Re_{SL}	Range of V_{SL} (ft/sec)	Range of V_{SG}/V_{SL}	Flow Patterns	Statement of Correlation and Limitations	Comments
Verschoor and Stemerding [89]	171 - 545	Not given	1960 to 6200	0.46 - 1.46	0.01 - 400	Bubble to Annular	No Correlation given	Plotted $\bar{h}_{TP}/h_{SP}$ against V_{SG}/V_{SL}
Ueda [85]	441 - 11025	0 - 99	138 - 3460	0.09 - 2.23	0.17 - 129	Bubble to Annular	No correlation	Plotted the mean (T_W-T_B) against liquid flow rate.
Katsuhara and Kazama [53]	915 - 4167	Not given		0.52 - 2.50	0.04 - 3.43	Bubble to Slug	$\frac{\bar{N}u_{TP}}{Pr_{MIX}^{0.4}} = 8.7(1-\alpha)^{0.125}(Re_{MIX})^{0.25}$ $0.080 \leq \alpha \leq 0.600$	Semi-empirical correlation. All variables are for the mixture defined in Eqs. (2.5) to (2.11).
Groothuis and Hendal [40]	1) 244-977 for water 2) 269-513 for gas-oil	Not given	1) 2794-11177 for water 2) 1440-3400 for gas-oil	1) 0.49-2.56 for water-air 2) 1440-3400 for gas-oil	1) 1-250 2) 0.6-80 2) 0.6-80	Bubble to Annular-Mist	1) For water-air: $\bar{N}u_{TP} = 0.029\, Re_2^{0.87} Pr_J^{1/3} (\mu_L/\mu_W)^{0.14}$, $[Re_{SL} > 5000, Re_{SG} > 0, V_{SG}/V_{SL} \geq 1]$, 2) For gas-oil-air: $\bar{N}u_{TP} = 2.6\, Re_2^{0.39} Pr_L^{1/3} (\mu_L/\mu_W)^{0.14}$, $[1400 \leq Re_{SL} \leq 3500, Re_{SG} < 0, V_{SG}/V_{SL} \geq 1]$	Empirical correlation. Data correlated within ± 15% $Re_2 = Re_{SL} + Re_{SG}$ All properties used are those of the liquid.
Knott et al. [56]	5.8 - 140*	0.22-6.90*	6.7 - 162	0.11-5.65*	0.106-39.4	Bubble	$\frac{\bar{h}_{TP}}{\bar{h}_{SP}} = [1 + (V_{SG}/V_{SL})]^{1/3}$ $0.1 < V_{SG}/V_{SL} < 40$ $\bar{h}_{SP}$ was obtained from the Sieder-Tate correlation.	Empirical correlation. Correlation overpredicted the authors data for $V_{SG}/V_{SL} > 0.3$ $126 < Re_{SG} < 3920$
Kudirka [58,59]	1) Water: 480-4320 2) Ethylene glycol: 540-2400	1) 0.83-68.50 2) 0-54.5	1) 5500-4.95×10^4 2) 380-1700	1) 1.0-9.0 2) 1.0-4.5	1) 0.16-75.0 2) 0.25-67.0	Bubble to Annular	$Nu_{TP} = 125 (Re_{SL})^{1/4} (Pr_L)^{1/3} \left(\frac{V_{SG}}{V_{SL}}\right)^{0.125} \times \left(\frac{\mu_G}{\mu_L}\right)^{0.6} \left(\frac{\mu_L}{\mu_W}\right)^{0.14}$ $2.6 \times 10^{-4} \leq x \leq 0.09$	Empirical correlation for local h_{TP}. Correlated data within ± 20% $Nu_{TP} = h_{TP} D/K_L$

* These figures were not given in the paper; these were calculated here, and, therefore, these values are only approximate.

Table 2.3 continued

Reference	Range of $\dot{m}_L$ (lbm/hr)	Range of $\dot{m}_G$ (lbm/hr)	Range of Re_{SL}	Range of V_{SL} (ft/sec)	Range of V_{SG}/V_{SL}	Flow Patterns	Statement of Correlation and Limitations	Comments
Ueda and Hanaoka [86]	1) Water: 229-1543 2) Mixtures of water & sol on: 697-1173	1) 1.10-13.43 2) 1.10-11.90	Re_M = 1.5 x 10^3 - 6 x 10^4	1) 0.322 - 2.156 2) 0.994 - 1.690	1) 0.58-50.30 2) 0.72-12.90	Slug and Annular	$\bar{Nu}_{TP}=0.075\ Re_M^{0.6}\ \frac{Pr_L}{1+0.035(Pr_L-1)}$, $Re_M = \rho_L U_M^* D/\mu_L$ U_M^* = equivalent mean velocity of the liquid phase, defined in Sec. 2.2.8 The authors also derived the following analytical expression for h_{TP}: $h_{TP} = q_W/(T_W-T_B)$, $T_B = \int_o^{y_i} V_L T\, dy / \int_o^{y_i} V_L\, dy$ Details are given in Sec. 2.2.8.	Semi-empirical correlation All liquid properties were calculated at the mean liquid temp. = $(T_{IN} + T_{OUT})/2$ The authors' data were in good agreement with the analytical solution.
Domanskii, Tishin & Sokolov [24]	Not given	Not given	Not given	0.328-7.22 for all liquids used	Range of V_{SG}: 0.082-4.92 ft/sec.	Bubble	$\frac{\bar{h}_{TP}\,\nu_L}{K_L\,U_*} = Pr_L/\bar{\psi}$ where U_* = friction velocity $\bar{\psi}$ = dimensionless temp. difference (see Sec. 2.2.9 for definitions)	Semi-empirical. Data were correlated within ± 12%. Liquid properties were taken at T_{BL}, $T_{BL} = (T_{IN} + T_{OUT} + T_W)/2$
Fedotkin and Zarudnev [29]	---	---	700 - 11400	---	---	Bubble to Annular-Mist	$\bar{Nu}_{TP} = C_3 Re_2^n\, Pr_L^{0.43} (Pr_L/Pr_W)^{0.25}$ C_3, n = constants Pr_W = Prandtl number calculated at the tube wall temp. $Re_2 = Re_{SL} + Re_{SG}$ $[700 \le Re_{SL} \le 11{,}400]$	Empirical correlation. C_3 & n depend on the flow regime, these are tabulated in Table 2.1.

Table 2.3 continued

Reference	Range of $\dot{m}_L$ (lbm/hr)	Range of $\dot{m}_G$ (lbm/hr)	Range of Re_{SL}	Range of V_{SL} (ft/sec)	Range of V_{SG}/V_{SL}	Flow Patterns	Statement of Correlation and Limitations	Comments
Ueda and Nose [87]	35.6-2505	81.6-154.4	Re_{LF} = liquid film Reynolds number: 190-13,700	0.021-1.476	Range of V_{SG}: 32.8-164 ft/sec	Annular & Annular-Mist	ANALYTICAL (Local) 1) For laminar liquid film flow: $\frac{h_{TP}}{K_L}\left(\frac{\nu_L^2}{g}\right)^{1/3} = X^* = Re_L^*/T^*$	Good agreement with the authors' data. Difficult correlation to use. See Sec. 2.2.10 for definition of each term.
							2) For turbulent liquid film flow: $q = \rho_L g\, C_{PL}\left(\frac{\nu_L}{Pr_L} + \varepsilon_n\right)\frac{dT}{dy}$, $h_{TP} = q_W/(T_W - T_{BF})$ T_{BF} = bulk mean temp. of the liquid film	No solution was presented for this case. The authors used theory developed by Hewitt [46].
Kapinos et al. [52]	Moisture content 2.7-15.3% by weight	Not given	----	----	V_{SG}=131 to 492	Mist or Fog Flow	$\bar{N}u_{TP} = 340 Re_{SG}^{0.8} \gamma^{0.15} K_B^{0.86} \gamma^{0.82}$ (L/D > 30) $\bar{N}u_{TP} = \bar{h}_{TP} D/K_G$ For L/D < 30, the above correlation should be multiplied by $\left[1 + \frac{10.2}{(L/D)^{1.74}}\right]$	Empirical correlation. The terms appearing in the correlation were not defined in the paper - see Sec. 2.2.11.
Fried [31]	1000-13,000	$2<Q_G<45$ S.C.F.M.	1.55×10^4 to 2.9×10^5	1.5 - 19.6	0.61 - 169 based on	Not specified	Empirical and graphical: $\bar{h}_{TP}$ were predicted by plotting against ϕ^2 where $\psi^2 = \bar{h}_{TP}/\bar{h}_{SP}$ $\phi^2 = \Delta P_{TPF}/\Delta P_{SPF}$	Data were correlated within + 30% correlation was for horizontal flow.

Table 2.3 continued

Reference	Range of $\dot{m}_L$ (lbm/hr)	Range of $\dot{m}_G$ (lbm/hr)	Range of Re_{SL}	Range of V_{SL} (ft/sec)	Range of V_{SG}/V_{SL}	Flow Patterns	Statement of Correlation and Limitations	Comments
Vijay [90]	1) Water: 16.7-8996 2) Glycerine + water 3) Glycerine	1) 0.042-214.3 2) 13.6-9119.5 3) 100.5-1242.6	1) 260-1.26 x 10^5 2) 8.0-4500 3) 1.80-21.0	1) 0.065-34.800 2) 0.044-29.427 3) 0.308-3.805	1) 0.030-6620.0 2) 0.013-6725.0 3) 0.048-329.70	1) Bubble to Annular Mist 2) Bubble to Annular 3) Bubble to Annular	Local h_{TP}'' By modifying Spalding [81] single-phase heat transfer theory as follows: $Sq = h_{TP} D^*/K_{MIX} = Nu^*_{TP}$ $= \{[\frac{Pr_{MIX}/Pr_T}{6.64(Z+/Pr_T)^{1/9} + P_{FN}}]^4 + [0.651(Z+/Pr_{MIX})^{1/3}]^{1/4}\}$ where $D^* = \mu_{MIX}/(g_c \tau_W \rho_{MIX})^{+/2}$ $Z+ = Z/D^*$ $P_{FN} = 11.570 [(Pr_{MIX}/Pr_T)^{3/4} - 1]$ Pr_T = turbulent Prandtl No. = 0.887 Mean h_{TP}: $\bar{h}_{TP} = \bar{h}_{AL} + \bar{h}_{AG}$ where, $\bar{h}_{AL}$ (or $\bar{h}_{AG}$) = single-phase liquid (or gas) heat-transfer coefficient based on actual mean velocity and actual cross-sectional are occupied by the liquid (or gas) phase. See Sec. 2.2.13 for details.	The author reported that the best agreement (± 50%) was obtained when the liquid properties were used for the mixture. This method correlated 87% of the author's data within ± 50%.

CHAPTER 3

EXPERIMENTAL APPARATUS

3.1 Introductory Remarks

As mentioned earlier, the present investigation was a continuation of the previous work [90] on investigating the effect of fluid properties on the heat transfer in two-phase, two-component flow in a vertical tube. The experimental facility used in the present study was essentially the same one used in [90], but with some modification. The major modifications were (i) the addition of an entirely transparent test section for flow-visualization study and (ii) the modification of the temperature measuring system. A detailed description of the apparatus is, however, presented in this chapter for the sake of completeness.

The most important components of the apparatus were:

(i) the heat-transfer test section, downstream of which, was a transparent section of the same inside diameter for visual observation and high-speed still photography of the flow patterns;

(ii) the flow-visualization test section for independent flow-visualization study and high-speed cine-photography of the flow.

The rest of the apparatus consisted of the following:

(i) the liquid-flow circuit,

(ii) the gas-flow circuit,

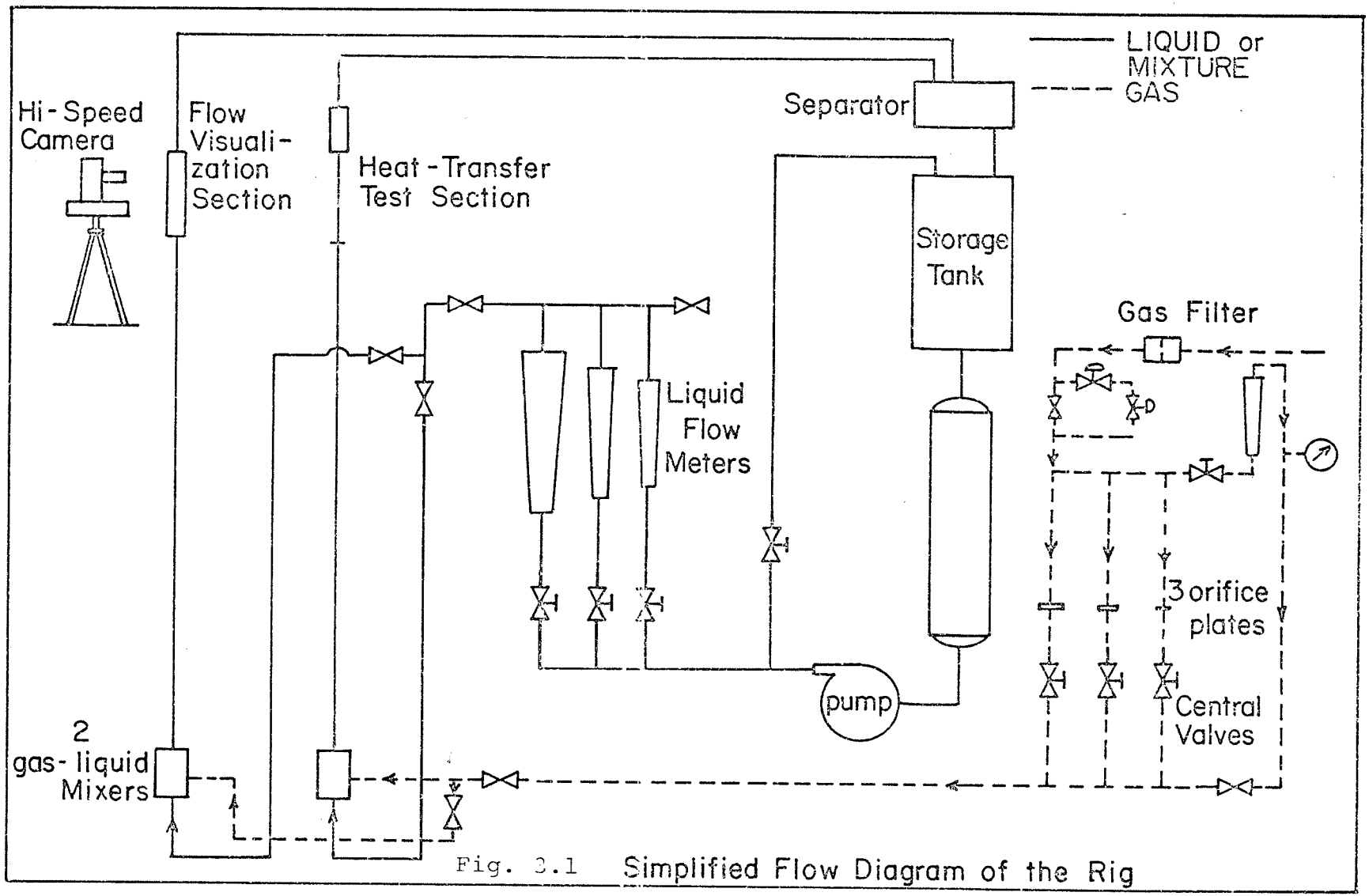

Fig. 3.1 Simplified Flow Diagram of the Rig

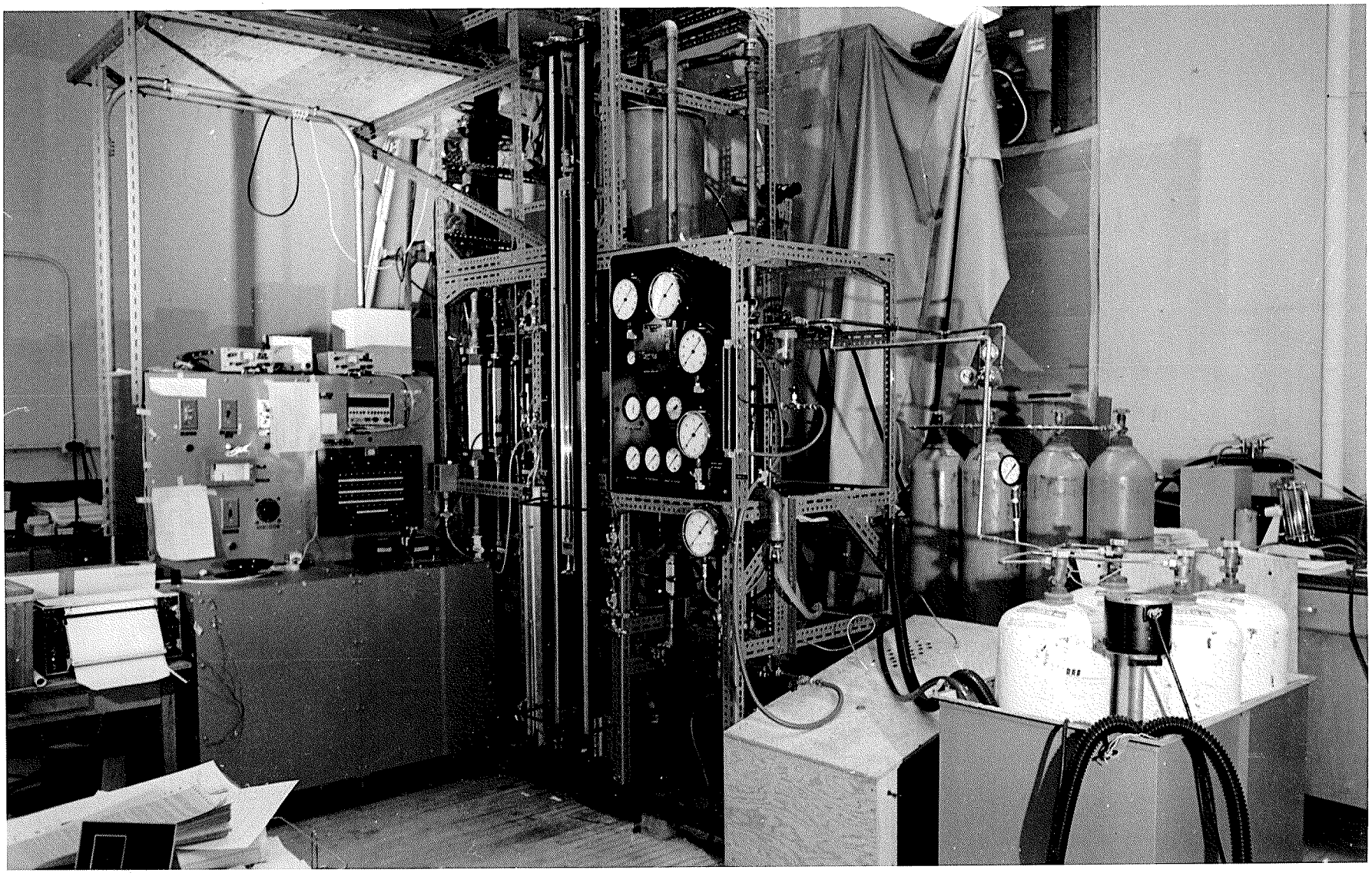

Fig. 3.2 General View of the Experimental Apparatus

(iii) the mixing chambers,

(iv) the power supply system,

(v) the measurement and control systems,

(vi) the photographic equipment.

A simplified flow diagram of the overall system is shown in Fig. 3.1 and a general view is shown in Fig. 3.2. The components of the apparatus are described briefly in this chapter while the details of the equipment are given in Table A.1. of Appendix A.

3.2 Heat-Transfer Test Section

3.2.1. General

The test section is shown in Fig. 3.3. It consisted of a gas-liquid mixing device downstream of which was a calming section 5 ft (1.524m) long (L = 130 D). This was followed by the heated tube and the transparent observation section, all having the same inside diameter.

3.2.2. Gas-Liquid Mixer

The details of the gas-liquid mixer are shown in Fig. 3.4. It consisted mainly of a grade B porous bronze tube, of the same inside diameter as the test tube, contained in a brass cylinder and equipped with a stainless steel strainer. The bottom flange was tapped for measurement of pressure in the mixing chamber.

Gas or liquid could be forced through the chamber radially or axially; however, in the present investigation the liquid

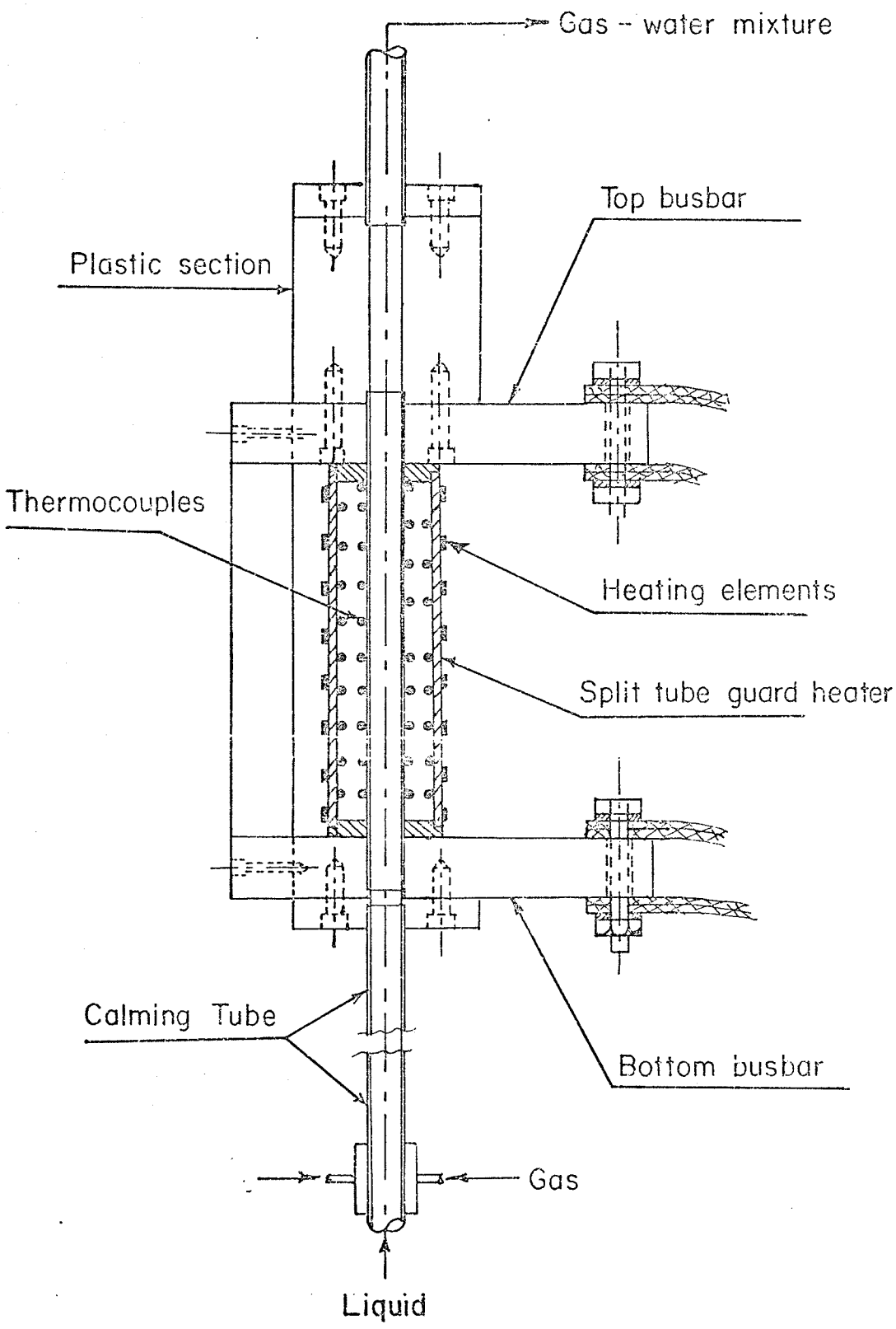

Fig. 3.3 Test Section

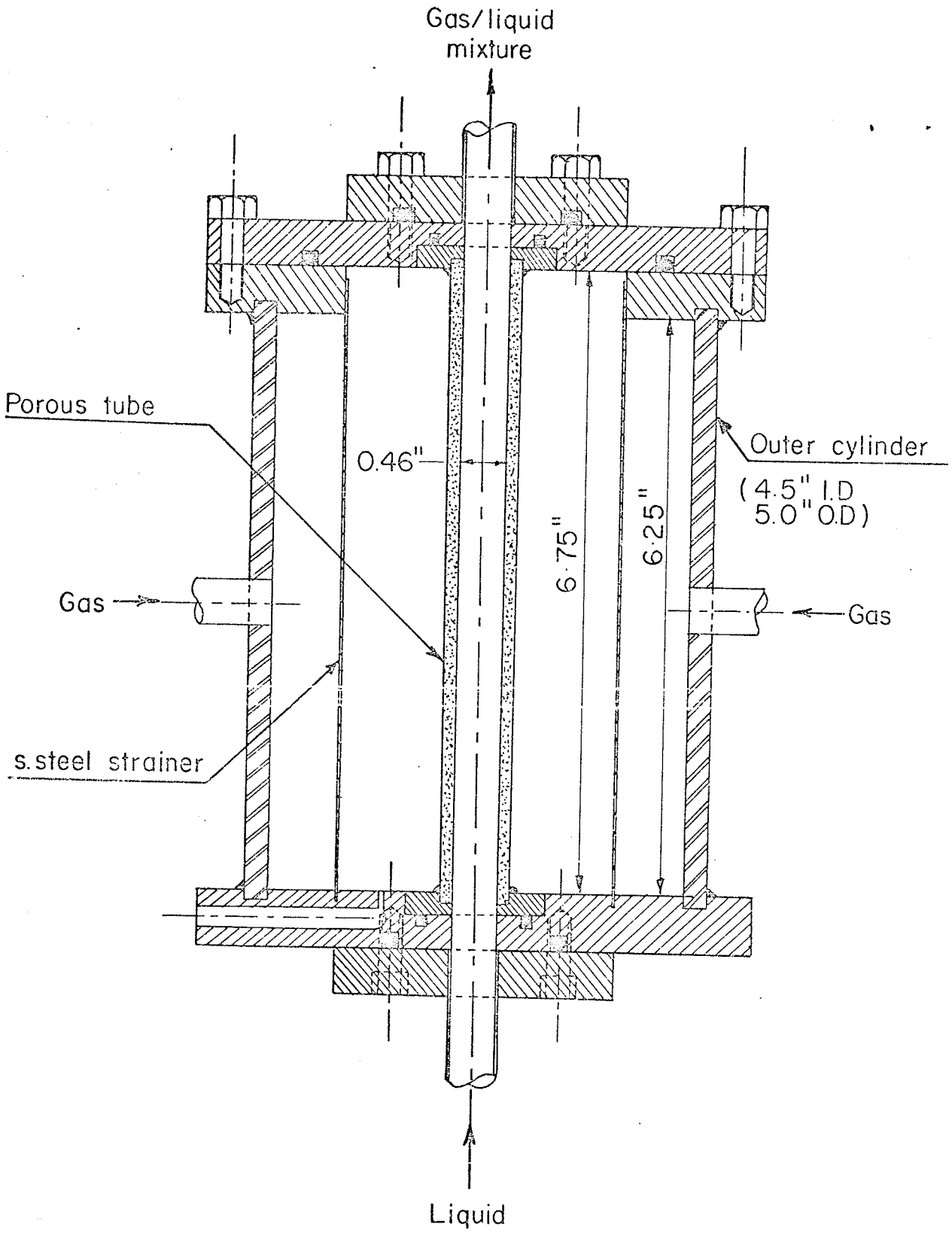

Fig.3.4 - The Mixer

flowed axially upwards while the gas was forced to diffuse through the porous tube.

3.2.3. Heated Test Section

The heated test section was made of type 304 stainless steel tube, 0.460 in. (1.168 cm) I.D., 0.500 in. (1.270 cm) O.D. and 2 ft (60.96 cm) long. The tube-wall thickness and the average roughness were measured [90] to be 0.02 $\pm$ 0.001 in. (0.508 $\pm$ 0.025 mm) and 40 $\pm$5μ in. ($\sim$ 1.016 x 10^{-4} cm) respectively. As shown in Fig. 3.3, two brass bus bars (for power supply) were silver soldered to the tube. A 1 in. x 1 in. x 2 ft. long (2.54 x 2.56 x 60.96 cm) Permali electrical insulator supporting bar was firmly attached to the bus bars (vertically between them) to avoid buckling of the heated tube due to the weight of the bus bars and the power cables.

Alternating-current electrical heating, using the tube as an electrical resistor, was employed because it offered a simple and accurate means of measuring and controlling the local heat flux.

A guard heater, made of a split copper tube (lower and upper guard heaters), was installed around the heated tube. Each guard heater was heated independently by a DC power supply using heating elements made of a Briskeat silicon rubber embedded heating tape 0.50 in (1.27 cm) wide. The purpose of the guard heater was to create a zero temperature gradient at the outer surface of the heated-tube wall mainly because this was the boundary condition used in estimating the inner surface tempera-

ture of the tube wall, and also to eliminate the heat losses from the heated test section to the surroundings. In order to create such a zero temperature gradient at the outer surface of the heated tube, the power supplied to each guard heater was adjusted so that the temperature of the inner surface of the guard heaters at any position along the axial direction would match approximately the temperature of the outer surface of the heated tube at the corresponding position. The criteria for adjusting the power supply to the guard heaters is discussed in detail in Chapter 4.

3.2.4 Observation Section

The observation section was made of a transparent cast acrylic rectangular block, 3 in. x 3 in. x 1 ft. long (7.62 x 7.62 x 30.48 cm). A precision, highly polished, hole of 0.45 in. (1.168 cm) I.D. (same I.D. as that of the heated test section) was drilled through the block. The block was placed above the heated section and was used for both visual observation and high-speed still photography of the flow patterns. It was assumed that the flow patterns observed were the same as those existing in the heated section. Clear observation and good photographs of the flow patterns were obtained with such a design of the observation section.

3.2.5 Temperature Measurement

A well-established method [19, 13, 57] was employed here to determine the inner wall temperature of the heated tube. In this method, the outer wall temperature was measured by means

of thermocouples (as explained below); the temperature drop across the tube wall was calculated from knowledge of the tube wall thickness, its properties and the electric current (this is discussed in detail in Appendix D); thus the inner wall temperature was determined.

Temperatures measured were those of the outer wall of the heated tube, the inner wall of the guard heater and the fluids. Copper-constantan AWG #36,0.005 in. (0.127 mm) diameter (T/G-36-DT) thermocouples were used on the heated test tube; and AWG #30(0.010 in. dia, T/G-30-DT) thermocouples were used for the guard heater and the fluids. The thermocouple wires, supplied by Thermoelectric Canada Ltd., were calibrated in the laboratory [90] over the temperature range involved in the present investigation; the details of this are given in Appendix B.

Forty-seven thermocouples were used to measure the tube wall temperature at 16 positions along the tube; 18 thermocouples were used to measure the guard heater wall temperature at nine positions. The location of thermocouples is shown in Fig. 3.5. The thermocouples sensing the fluids temperatures were used as follows: one for measuring the temperature of the gas at the inlet to the orifice meters, one for the liquid temperature at the inlet to the mixer, two for the mixture at the exit of the mixer and two at the outlet of the transparent section (note: these were used only for checking the heat balance, not for the heat transfer calculations).

Scotch electrical tape No. 27 was used to insulate the thermocouples from the tube and also to attach them to the tube

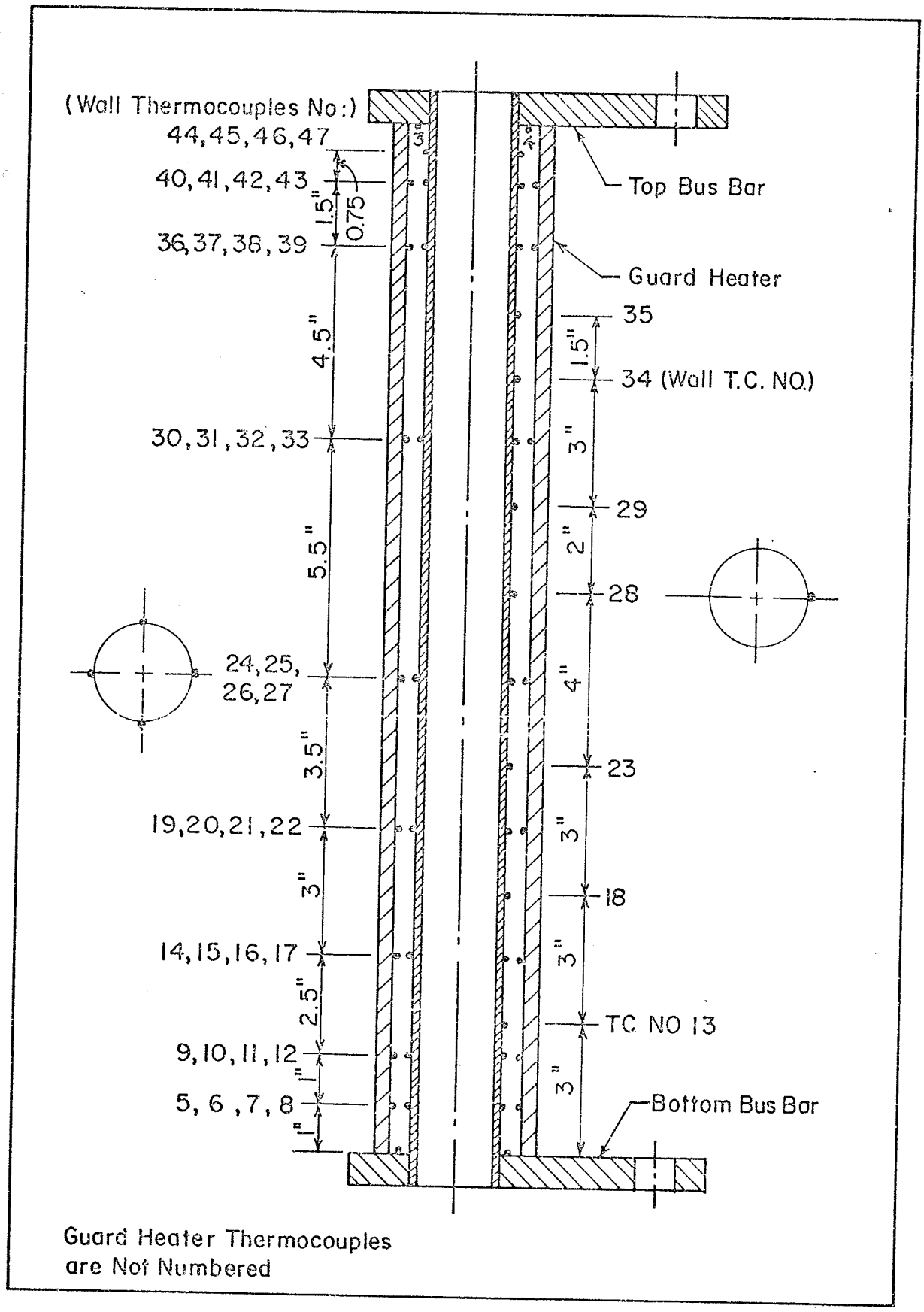

Fig. 3.5 Locations of Thermocouples

wall. At the desired location, a layer of the tape was wrapped around the tube, the thermocouple head was placed in position and 2 - 3 turns of the wire were wrapped around the tube in order to minimize the possible conduction error due to the temperature gradient along the wire.

3.3 Flow-Visualization Section

3.3.1 General

The flow-visualization test section was added to the original facility as a consequence of the local heat-transfer results obtained for the bubble and slug flow patterns at low liquid flow rates. Those heat-transfer results, as will be discussed in detail in a later chapter, could be explained by the presence of a downflow motion of the liquid film near the tube wall. The downflow of the liquid film is well known in the slug flow; however, no indication of such downflow has been reported for the bubble-flow pattern. Therefore, it was decided to examine the possibility of this downflow in the bubble flow and also to photograph (by means of high-speed cine photography) the motion of the liquid film in the slug-flow pattern using the hydrogen-bubble and dye-injection techniques.

A gas-liquid mixing chamber, exactly the same as the one described above for the heat-transfer test section, was built and the flow-visualization section was made entirely of transparent cast acrylic with approximately the same dimensions of the heat transfer section. It consisted of the same calming length of 5 ft. (1.524 m) cast acrylic tube of 0.50 in. (1.27)

cm) I.D. and 1.00 in. (2.54 cm) O.D., followed by a 2 ft. (60.96 cm) long visualization section. Downstream of the test section was another transparent tube, 1 ft. (30.48 cm) long, connected to a copper tube then to the discharge tube. High-speed cine photography together with both the hydrogen-bubble and dye-injection techniques were employed to observe the motion of the liquid film.

3.2.2. Flow-Visualization Test Section

The details of the flow-visualization test section are shown in Fig. 3.6. It consisted of a transparent cast acrylic block 1.75 in. x 1.75 in. x 2 ft. long (4.45 x 4.45 x 60.96 cm). A precision, highly polished, hole of 0.50 in. (1.27 cm) diameter was drilled through the block to simulate the heat-transfer test section. The diameter of 0.50 in. was chosen because it was the closest diameter to that of the heat-transfer test section for which transparent tubes (used as a calming length) were available. It should be mentioned, however, that the flow-visualization study was only a qualitative study; therefore, the small difference in diameter between the flow-visualization section and the heat-transfer section (0.1 cm) would not affect the purpose of this study as such a small difference is not expected to affect or change the flow patterns and the behavior of the liquid film from those existing in the heat-transfer test section. At three locations on the visualization section (4 in. (10.2 cm), 13 in. (33 cm) and 21.5 in. (54.6 cm) from the bottom) holes of 0.02 in. (0.5 mm) diameter were drilled,

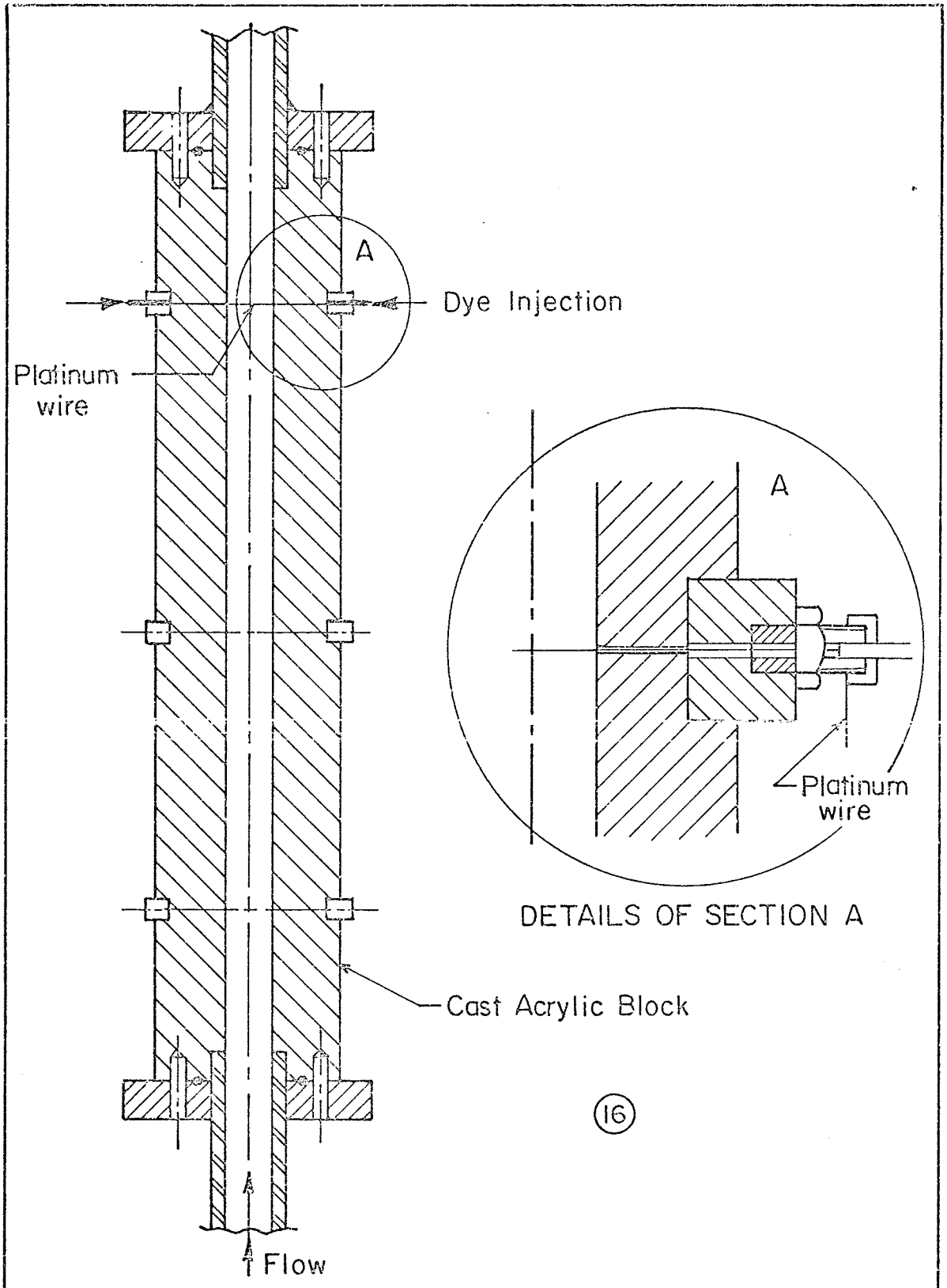

Fig. 3.6 Flow - Visualization Test Section

normal to the test tube wall, which were used for dye injection. A platinum wire of 0.003 in. (0.076 mm) diameter was inserted through the top holes (along the tube diameter), stretched and fixed at both ends. The platinum wire was used as a cathode for hydrogen bubble generation, while the discharge copper tube served as the anode.

3.3.3. Dye Injection System

The dye-injection system is shown in Fig. 3.7. It consisted of the following:

(i) a dye container; this was made of a clear plastic cylinder 2.5 in. I.D. and 2 ft. long, closed at both ends by two plastic discs. The bottom disc was equipped with a valve used for draining the container. A plastic tube was inserted into the container through a hole in the top disc, and was used to supply the dye to the injection points through two plastic hoses connected to it by means of a T-section,

(ii) a compressed air tank used to apply pressure on the dye in the container,

(iii) a pressure regulator used to adjust the pressure in the container to control the flow rate of the dye.

Milk and food coloring was used as a dye. The container pressure was adjusted so that the dye would enter the test tube with near-zero velocity.

3.3.4. Hydrogen-Bubble Generating Circuit

The hydrogen bubble generating circuit is shown in Fig.

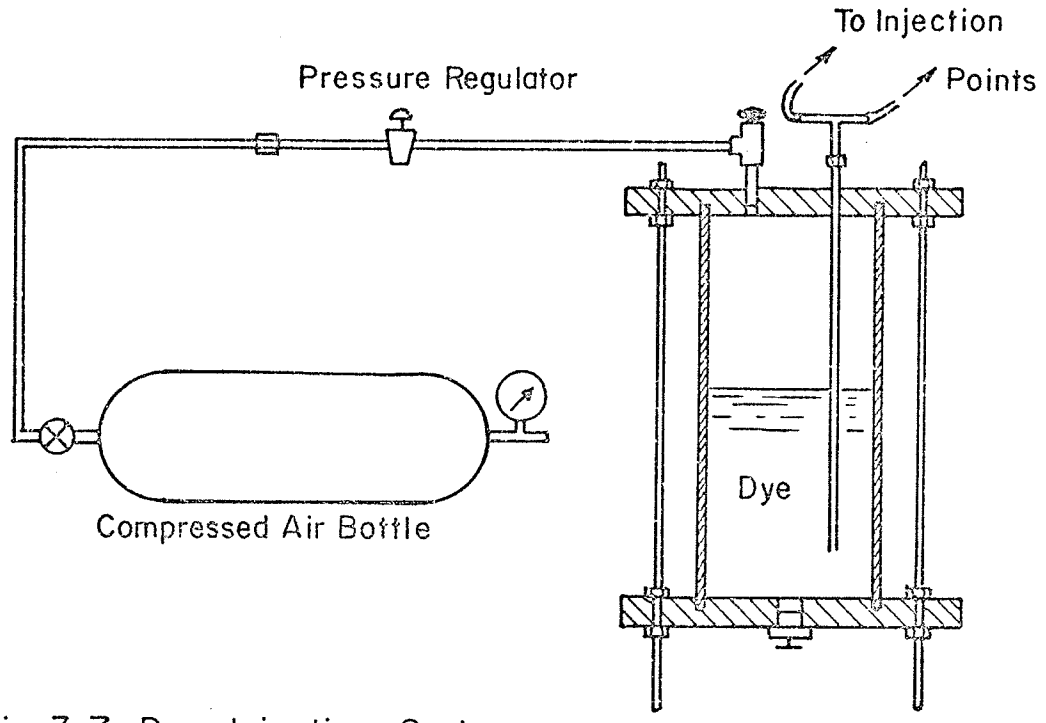

Fig. 3.7 Dye Injection System

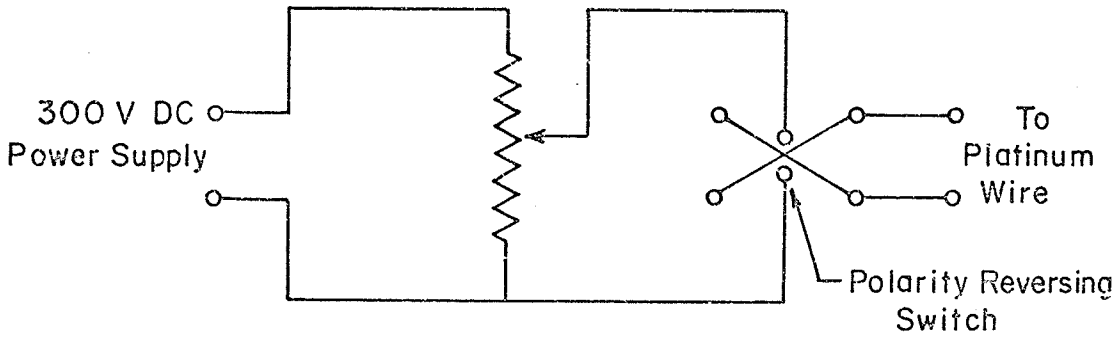

Fig. 3.8 Hydrogen Bubble Generating Circuit

Fig. 3.8

3.8. It consisted of the following:

(i) a DC power supply (model 890A, 0-320V, 0-0.6 amp, supplied by Harrison Laboratories),

(ii) a 0.003 in. (0.076 mm) diameter platinum wire serving as a cathode,

(iii) a copper tube, downstream of the test section, used as an anode,

(iv) a switching system which allowed reversing the polarity for cleaning the platinum wire of any accumulated deposits.

A combination of high potential difference (200 - 300V) and addition of sodium sulphate to the water was necessary to generate hydrogen bubble at an appreciable rate.

3.3.5. Photographic Equipment

The arrangement of the photographic section is shown in Fig. 3.9; it consisted of:

(i) a 16 mm high-speed movie camera (Hycam model K2004#, Red Lake Labs., Inc., Santa Clara, California),

(ii) two 650W (at 115V) Smith Victor quartz-bromine movie lights used for illumination.

Kodak Ektrachrome EF7242, and Kodak 4XR reversal 7277 films in 100 ft. (30.48 m) rolls were used. Developed films were projected using an LW motion analyzer model 900B.

3.4 Liquid-Flow Circuit

The details of the liquid-flow loops are shown in Fig. 3.10. It consisted of the following:

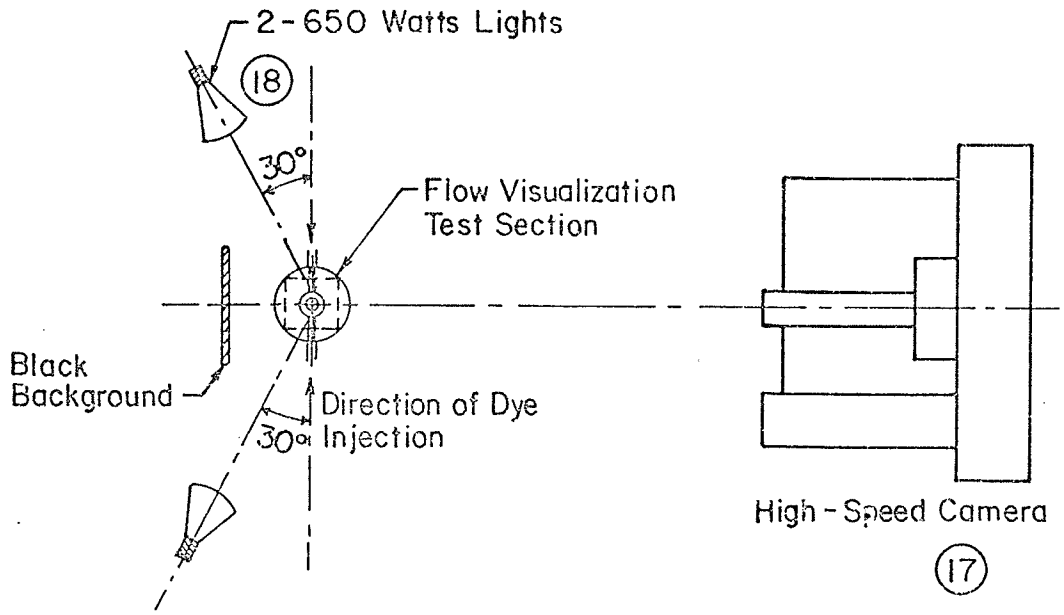

Fig. 3.9 Set-up of Flow-Visualization Photographic Equipment

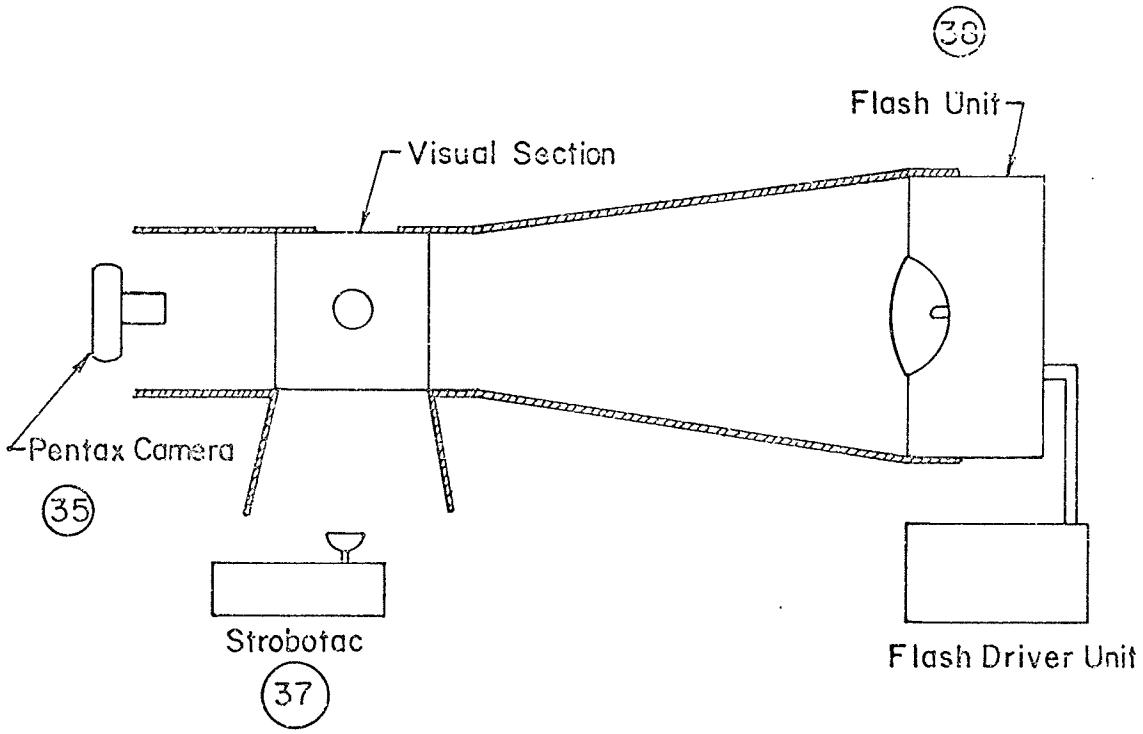

Fig. 3.14 Set-up of Observation and Still Photography Section

Figs. 3.9, 3.14

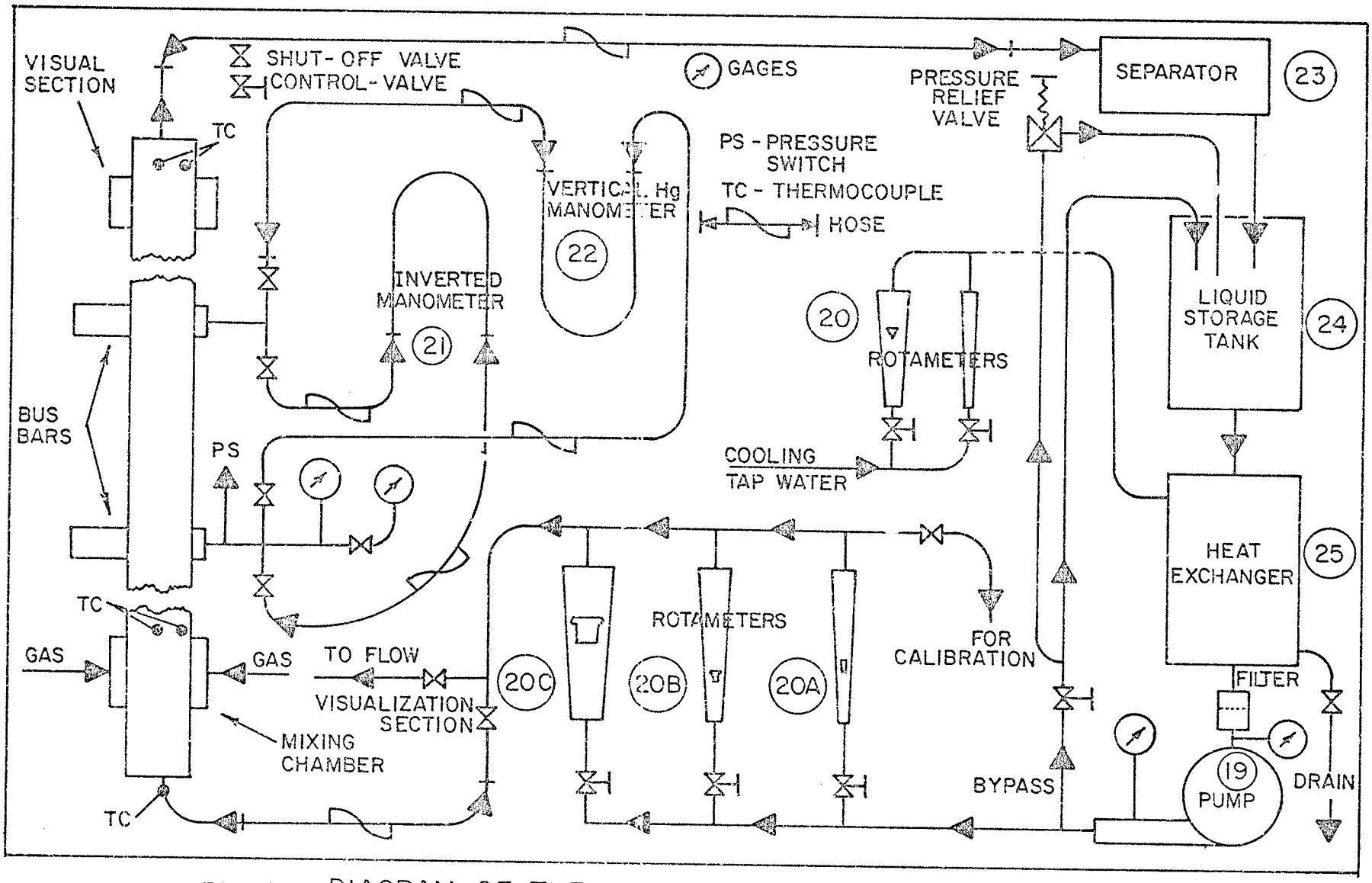

Fig. 3.10 DIAGRAM OF THE LIQUID FLOW LOOP

Fig. 3.10

(i) a stainless steel liquid storage tank of 40 U.S. gallons capacity;

(ii) a heat-exchanger to control the temperature of the liquid entering the test section;

(iii) a positive displacement gear pump;

(iv) a by-pass line (made of 1.5 I.D. copper tubing) with a control valve, used to set the required flow rate;

(v) three rotameters of different ranges with control valves in parallel, for measuring liquid flow rates;

(vi) the test section;

(vii) a liquid-gas separator consisting of an open tank which drained the liquid into the storage tank while discharging the gas to the atmosphere;

(viii) pressure gauges as shown in the diagram;

(ix) a vertical mercury manometer to measure the static pressure at the inlet to the heated test tube, a mercury manometer (for large pressure drop) to measure the total pressure drop across the heated test tube;

(x) a heat-exchanger cooling water system consisting of two parallel rotameters and control valves and using tap water.

The materials used in constructing the liquid circuit were stainless steel, brass and copper. All measuring devices were calibrated; this is discussed in Appendix C.

3.5. Gas-Flow Circuit

The details of the gas-flow loop are shown in Fig. 3.11.

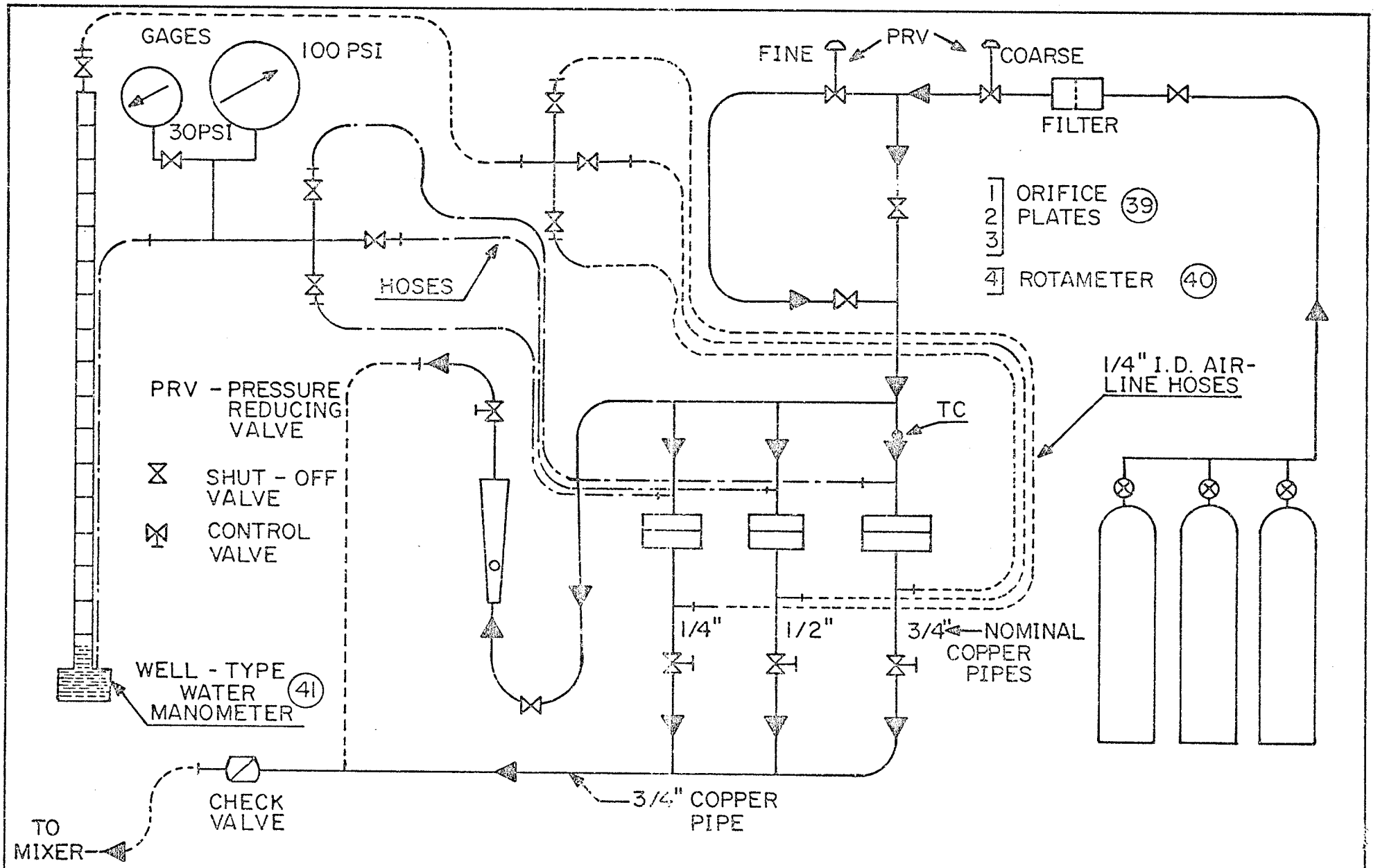

Fig. 3.11 DIAGRAM OF THE AIR FLOW LOOP

Fig. 3.11

Air, helium and Freon 12 vapour were used for the gas phase in the present investigation. For air, the central compressor in the Mechanical Engineering Laboratory was used; this was equipped with an automatic pressure switch for maintaining the air pressure constant at the required value. Helium was supplied from a system of four cylinders connected in parallel to a main manifold equipped with a two-stage pressure regulator. The Freon 12 vapour was supplied from a system of four cylinders connected in the same manner as the helium cylinders. The Freon cylinders, containing mixtures of saturated liquid and vapour, were placed in a water bath to control the temperature and pressure of the Freon. The Freon was throttled and the room temperature was maintained warm so that only superheated Freon vapour was flowing at any point in the apparatus.

The gas flow loop consisted of the following:

(i) a main gas-supply line equipped with a gas filter, a coarse pressure regulator, a by-pass line with a valve and a fine pressure regulator,

(ii) the air, helium and Freon lines which were connected to the main gas-supply line through three shut-off valves,

(iii) a system of three calibrated orifice plates and a rotameter connected in parallel, through four control needle valves, to the gas line leading to the mixing chambers; these were used to measure the gas flow rates,

(iv) a well-type water manometer for measuring the pressure drop across the orifice plates,

(v) a gas feed-line equipped with a check valve to prevent any water from entering the gas flow loop. This line was used to supply the gas to either of the two mixing chambers through a system of two shut-off valves,

(vi) pressure gauges for measuring the pressure at the inlet to the orifice plates (or rotameter), at the outlet of the rotameter, at the mixing chamber and the main gas line pressure.

3.6. Power Supply Circuit

A power system was constructed [90] to supply, control and measure the electric power to the stainless steel test section. The power supply circuit is shown in Fig. 3.12; it consisted of the following:

(i) a 240 volt, 100 amp, AC mains power source;

(ii) a power variac for control of the electrical power to the test section;

(iii) a 24 kVA transformer;

(iv) power measuring circuit consisting of a calibrated current transformer, a potential transformer, voltmeter, ammeter and wattmeter; the ammeter readings were used for the heat flux calculations while the voltmeter and wattmeter readings were used only as a check;

(v) the stainless steel test tube; this served as an electric resistor;

(vi) a pressure switch (sensing the pressure at the inlet to the test section) to shut off the power in case of flow

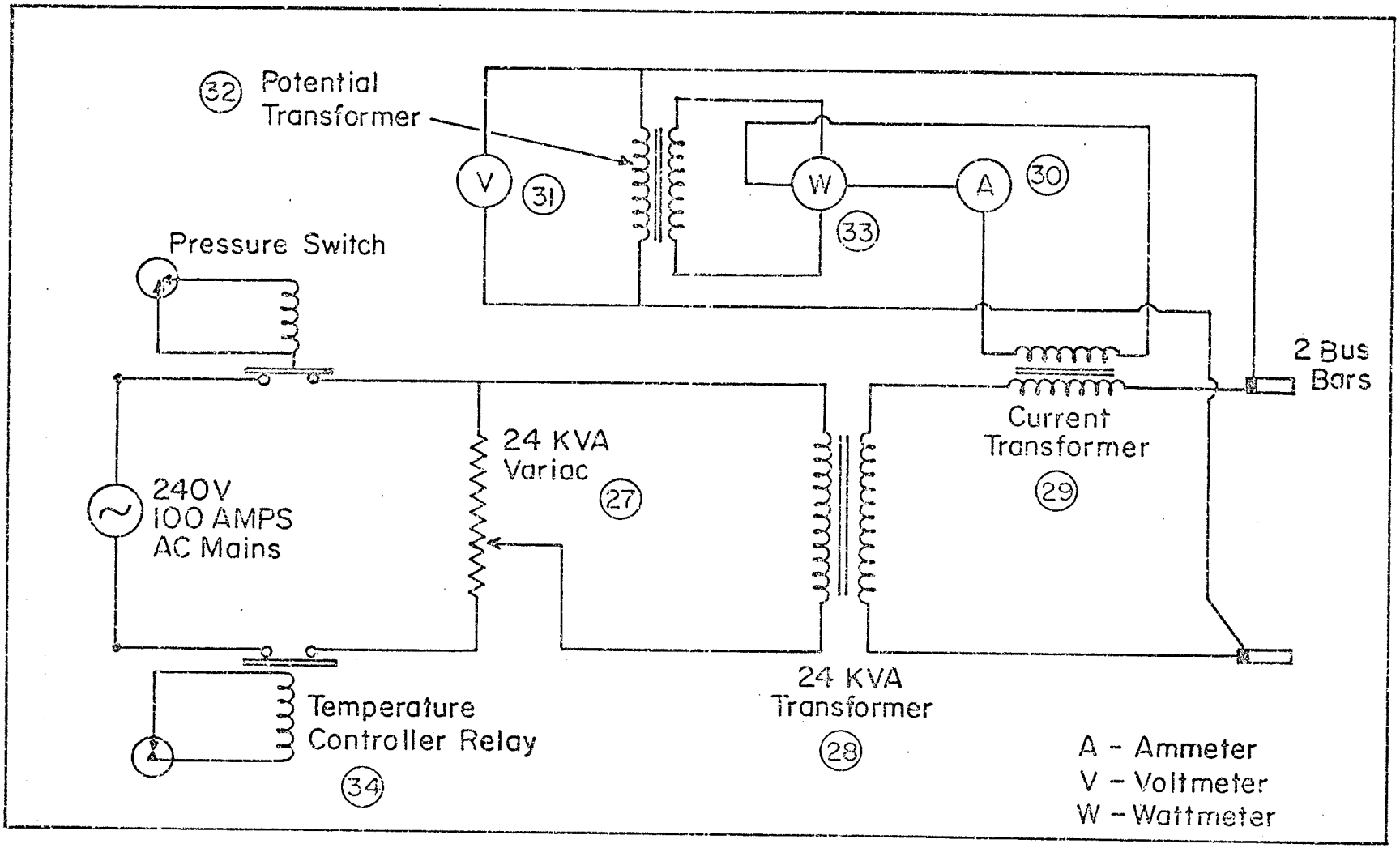

Fig. 3.12 Power Supply Circuit

Fig. 3.12

failure;

(vii) a temperature controller (sensing the temperature of the middle point on the test section) to shut off the power in case of accidental over-heating of the test section.

3.7. Temperature Measuring System

Temperatures of the test tube wall, the guard heater and the fluids were measured by means of copper-constantan thermocouples; this was described in detail in Section 3.2.5. In this section, the thermocouple emf measuring system is described and is shown in Fig. 3.13.

The original temperature measuring system [90] was as follows:

The wall and guard-heater thermocouples were connected to one bank of a multiple-point selector switch and all the fluid thermocouples were connected to another bank. Each bank had its own cold reference junction; both junctions were placed in an electronic ICELL (thermoelectric ice point reference unit) where the temperature was maintained at 32°F. The emf of the thermocouples was measured either by a Darcy 440 digital voltmeter or by a two-pen strip chart recorder by means of appropriate switches. With this system, a time of about 5 minutes was required to record the emf readings of the 71 thermocouples when the digital voltmeter was used; however, for unsteady flow conditions, e.g. slug flow, the fluctuations in the wall temperatures were large enough that it was difficult to use the digital voltmeter. In such cases, the output of

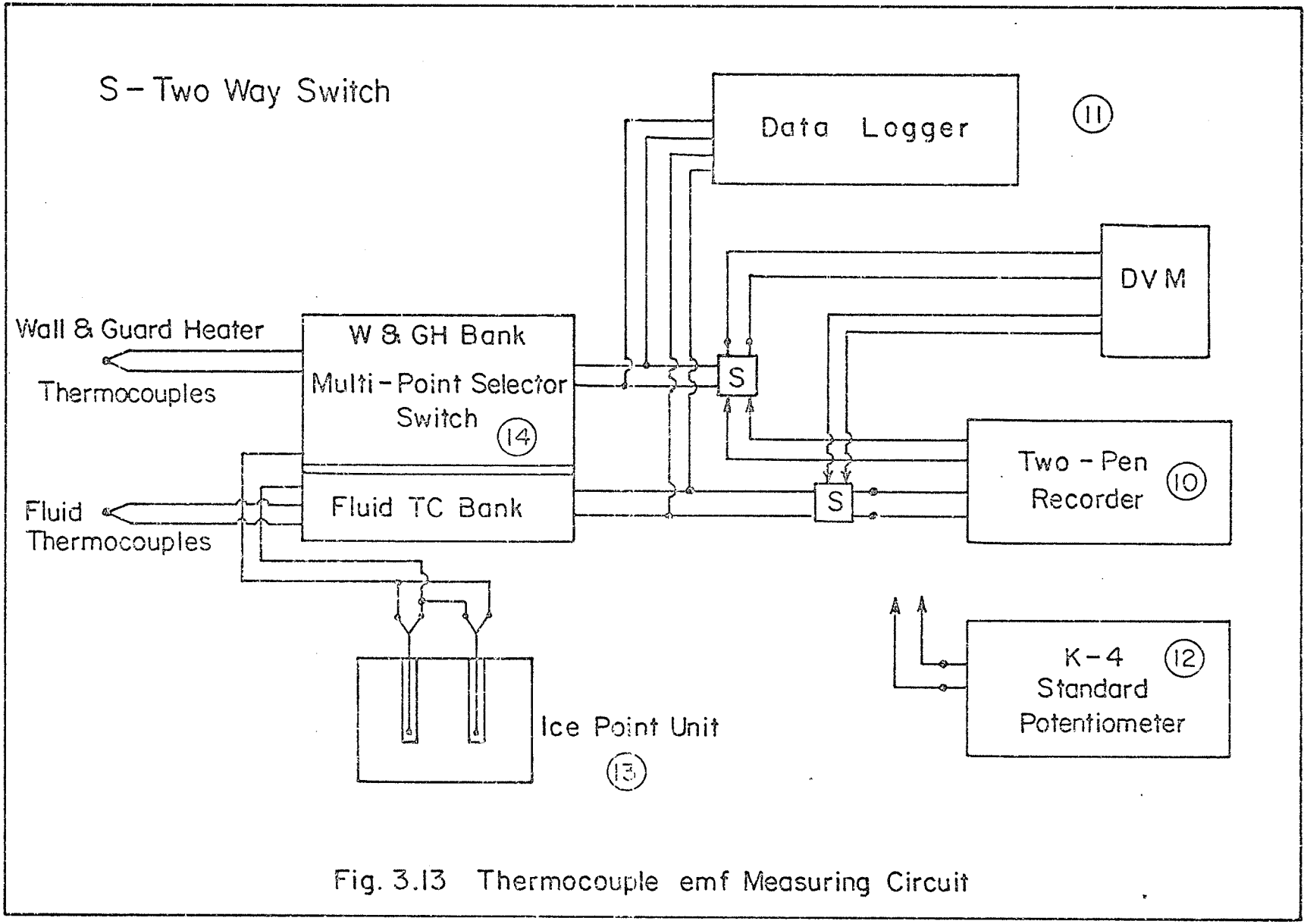

Fig. 3.13 Thermocouple emf Measuring Circuit

the wall thermocouples was recorded on the strip chart recorder which required between 10 and 15 minutes.

The measuring system was modified as follows: While the original system was left almost undisturbed (except that the two cold reference junctions were connected in parallel to form a single common reference junction for all thermocouples), a Fluke 2240A data logger with a 60-channel capacity and a scanning speed of up to 15 channels per second was connected in parallel with the original system. The first channel of the data logger was connected to a 1 mV standard potential source and was used to estimate the magnitude of the noise picked up by the data logger. The remaining 59 channels were used to measure the emf of all the wall and fluid thermocouples and 6 of the guard heater thermocouples; the emf of the rest of the guard-heater thermocouples was measured by the digital voltmeter.

The reliability of the new system was checked by repeating all the air-water experiments, which were performed with the original measuring system. The heat-transfer results were repeated within $\pm$ 1%. The modified system was, therefore, considered reliable, and all the results obtained with this system were considered to be comparable to the previously obtained results [90].

A high-precision K-4 potentiometer (Leeds & Northrup) was used to check and calibrate the DVM, the recorder and the data logger.

3.8. Photographic Equipment

The arrangement of the photographic equipment for high-speed still photography of the flow patterns is shown in Fig. 3.14. It consisted of the following:

(i) a Pentax Spotmatic camera equipped with super Takumar 50 mm/f-4 close-up lens;

(ii) an EG&G microflash electronic flash unit (0.5 μ sec flash duration), covered with a mylar diffuser;

(iii) a light guide made of cardboard lined with aluminum foil to diffuse and direct the light toward the visual section;

(iv) a General Radio type 1538-A strobotac electronic stroboscope.

Kodak Plus-X Pan (125 A.S.A.) films were used for all photographic work in this section.

CHAPTER 4

EXPERIMENTAL PROCEDURE

4.1. Introductory Remarks

This chapter describes the procedure used in the experiments. As mentioned in the introduction, the main independent variables in this investigation were the mass flow rate of the liquid $\dot{m}_L$, the mass flow rate of the gas $\dot{m}_G$ and the gas density. The main dependent variables were the local and mean heat-transfer coefficients h_{TP} and $\bar{h}_{TP}$ respectively, the two-phase frictional pressure drop ΔP_{TPF} and the flow patterns.

In conducting the experiments, various quantities were measured; these are shown in Fig. 4.1 in the circles and are listed and defined in Table 4.1. The procedure for calculating the heat-transfer coefficients and the hydrodynamic quantities is given in Appendix D. The calculations were performed on the University of Manitoba IBM 370 Computer.

4.2. Start-up Procedure

Two methods were employed in starting-up the rig with regard to the condition of the mixer. In one method, the test section and the mixer were drained and air was forced through the mixer to clear and dry the porous tube; the gas was first supplied, and then the water supply was turned on (tests taken with this method are referred to in the thesis as the "dry-mixer runs"). The other method did not involve the procedure of drying and clearing the porous tube in the mixer; in this

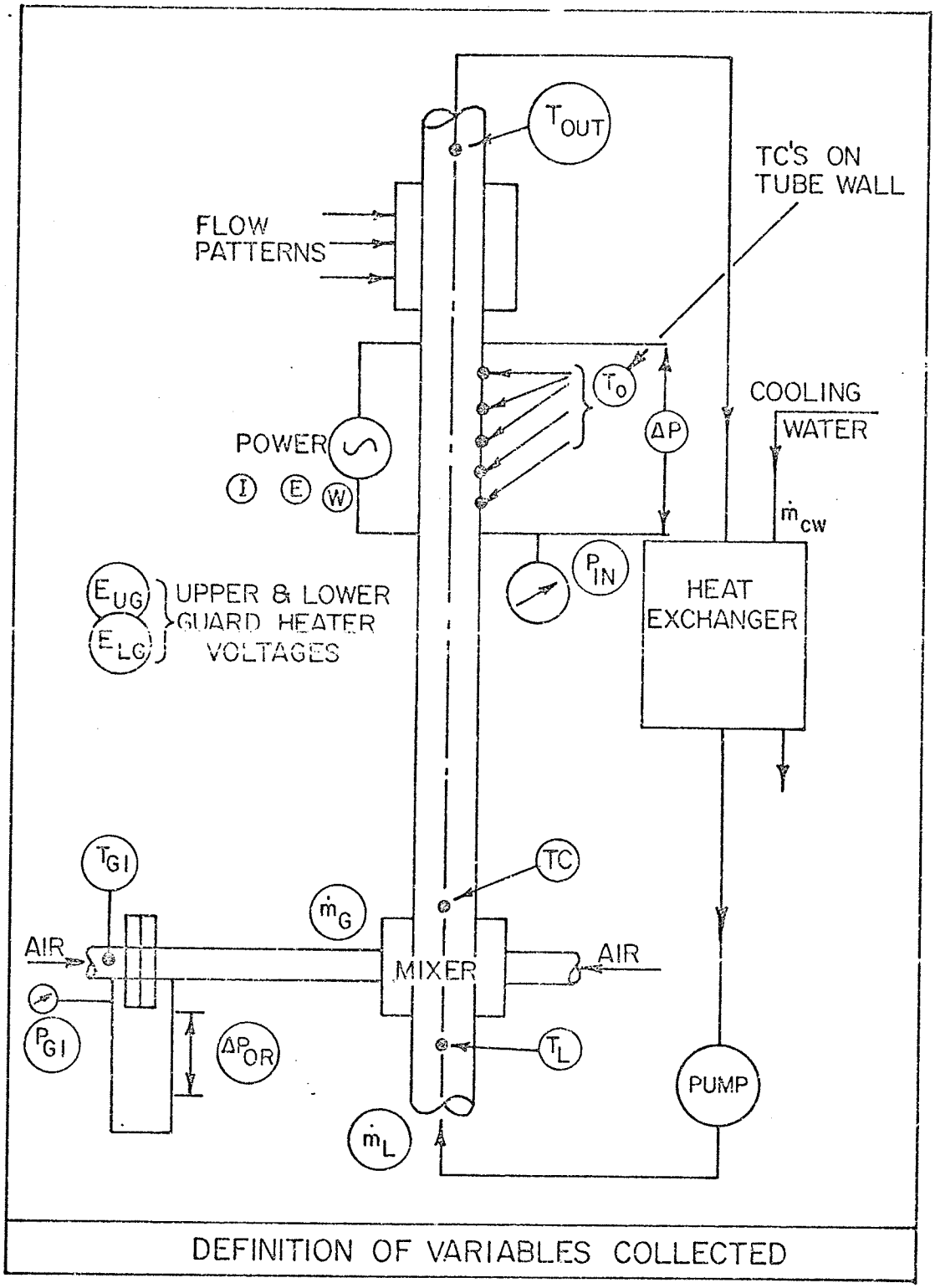
T_{OUT}
TC'S ON TUBE WALL
FLOW PATTERNS
T_0
ΔP
COOLING WATER
POWER
I
E
W
$\dot{m}_{cw}$
P_{IN}
HEAT EXCHANGER
E_{UG}
E_{LC}
UPPER & LOWER GUARD HEATER VOLTAGES
T_{GI}
TC
$\dot{m}_G$
AIR
MIXER
AIR
P_{GI}
ΔP_{OR}
T_L
PUMP
$\dot{m}_L$
DEFINITION OF VARIABLES COLLECTED

Fig. 4.1

Fig. 4.1

TABLE 4.1

Variables Measured in the Experiments

Power to Test Section			Power to Guard Heater		Water Flow Rate		Test Section Pressure	
(I) Ammeter Reading	(V) Voltmeter Reading	(W) Wattmeter Reading	E_{UG} volts	E_{LG} volts	Meter No.	Reading (%)	P_{IN}	ΔP
used to calculate the local heat flux	W and VI were used to check the power input to the test section		were adjusted to control the temperature of the guard heater		used with the calibration curves to calculate $\dot{m}_L$		Pressure at inlet to the test section	Total pressure drop across the test section

Gas Line Data			
O.P.N.	P_{G1}	ΔP_{OR}	P_{GL}
Orifice plate or Rotameter No.	Press. at inlet to the orifice or rotameter	Press. drop across the orifice plate or rotameter reading	Gas pressure in the supply line
used, together with the gas temperature at the inlet to the orifice plate assembly (T_{G1}), to calculate the gas flow rate ($\dot{m}_G$)			used to calculate the moisture content in the gas

Other Variables	
Barometric Pressure	measured 3 times during the course of the experiment
Flow Pattern	observed visually and photographed twice for each test

Thermocouple Readings	
TC No.	To measure the temperature of
1 to 47	the outer wall of the heated test tube (T_o)
48 to 65	the inner wall of the guard heater
66	the water at the inlet to the mixer (T_L)
67 & 68	the mixture at the outlet of the mixer
69 & 70	the mixture at the outlet of the test section (T_{OUT})
71	the gas at the inlet to the orifice plate assembly (T_{G1})

Table 4.1

method, tests were simply started by supplying the water first, and then the gas phase was introduced (tests taken with this method are referred to in the thesis as the "wet-mixer runs"). It should be mentioned that the mixer condition at the start of the run was just a minor independent variable in the present study; its effect on the above mentioned dependent variables is discussed in Appendix F. As discussed later in the thesis, the mixer condition did not affect the results except for a narrow range of variables, that is, at low liquid and gas flow rates. At low liquid flow rates and moderate to high gas flow rates, and at the higher liquid rates ($V_{SL} > 3.41$ ft/sec) and all gas flow rates, the results obtained were independent of the mixer condition. The results reported in the thesis are those obtained under the dry-mixer condition.

Prior to operating any of the flow circuits, the following checks were made: the gas circuit was tested for leaks; the leads from the orifice plates were checked to be clear of any water by allowing the gas to pass through them; the water level in the well-type manometer was checked and if necessary, adjusted; all manometer leads containing water were checked for the presence of gas and if necessary, purged (this was repeated as often as required during the running of the tests). The following steps were then taken:

(i) the cooling water to the heat exchanger was turned on;

(ii) the water pump was started with the by-pass fully opened;

(iii) the valve on the main gas supply line was opened and

the gas pressure at the inlet to the orifice-plate assembly was set at a constant value by adjusting the pressure regulators in the gas line;

(iv) the desired gas flow rate was set by controlling the needle valve at the outlet of the appropriate orifice plate or the rotameter;

(v) the water flow rate was then set at the desired value;

(vi) the power supply to the lower and upper guard heaters was switched on;

(vii) the power to the test section was then turned on;

(viii) the photographic equipment was prepared for proper operation.

The same start-up procedure, excluding steps (iii) and (iv), was employed for the single-phase water experiments. It should be mentioned that, as with other two-phase forced convection studies, it was found necessary to keep a large pressure drop across the control valves upstream of the water flow meters in order to prevent oscillations in the water flow rates.

The experimental procedure for the flow-visualization study is given in Chapter 7 when this topic is discussed.

4.3. Establishing Equilibrium Conditions

The criterion for equilibrium before any set of data was taken was that all instrument readings were constant over a time span of five minutes. It was necessary to monitor and control the following variables:

(i) the water temperature at the inlet to the mixer, T_L,

(ii) the voltage settings for the lower and upper guard heaters, E_{LG} and E_{UG} respectively;

(iii) the power supply to the test section.

4.3.1. Water Inlet Temperature

Since it was important to keep the fluid properties in the test section as constant as possible for all tests, it was necessary to maintain the mean temperature of the mixture in the test section constant. For this purpose, the practical way was to control both the water inlet temperature T_L and the test-section wall temperature. For each test, the mean mixture temperature was estimated from the temperatures at the inlet and outlet of the test section and accordingly, either the test-section wall temperature or T_L or both were adjusted.

The water inlet temperature and the test section wall temperature at the middle point of the test section were continuously recorded on the two-pen strip chart recorder. Thermal equilibrium conditions were deemed to prevail if the variations in these two temperatures, over a time span of five minutes, were not more than $\pm$ 0.2°F.

4.3.2. Power Input to Guard Heaters

Since the temperature of the heated test section increases almost linearly with distance, it was impossible to control the power input to the guard heaters to match exactly this linear rise in order to establish zero temperature gradients between the outer surface of the test section and the guard heaters. Preliminary tests performed [90] with single-phase water flow

showed that in the turbulent flow regime, the effect of the temperature difference between the outer surface of the test section and the inner surface of the guard heaters on the local values of the heat-transfer coefficient was almost negligible while in laminar flow, the effect was less than 2% even when the temperature difference was of the order of $\pm$ 4°F (in the present experiments, this temperature difference was typically $\pm$ 2.8°F; in the worst case, this was $\pm$ 3.2°F). On this basis, the power inputs to the guard heaters were controlled in such a way as to obtain the temperature profiles shown in Fig. 4.2. The emf readings of Thermocouple Numbers 5, 25, 40 on the test section and Numbers 48, 56 and 64 on the guard heaters were taken successively and used as a guide in controlling the power input the guard heaters.

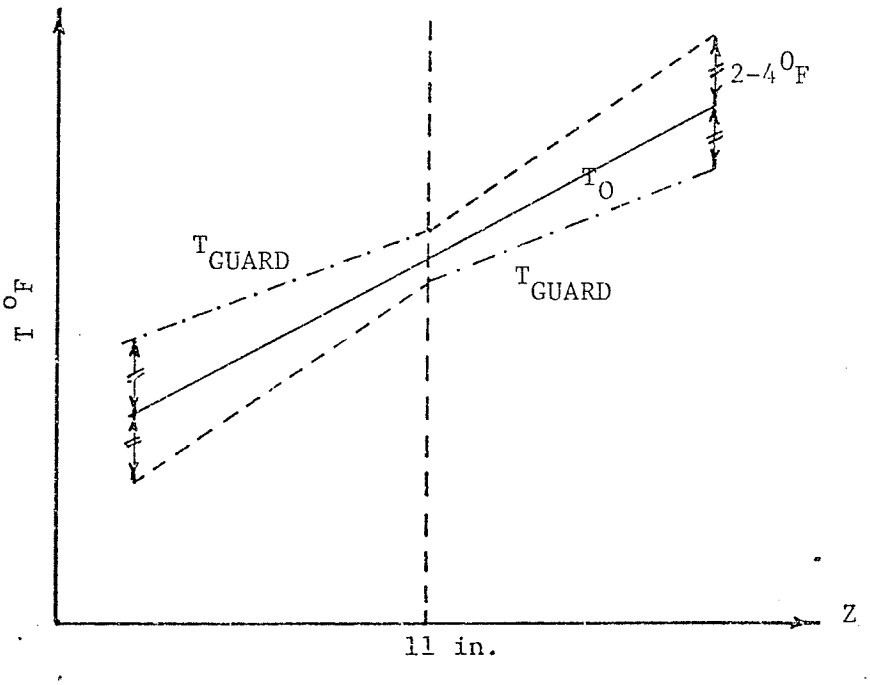

Fig. 4.2. Criterion for Guard Heater Power Setting

4.3.3 Power Input to the Test Section

In applying the power to the test tube, two considerations were of importance, these were: (i) the temperature difference between the tube wall and the bulk of the fluid should be a minimum in order to minimize the radial variation of fluid properties; (ii) this temperature difference, on the other hand, should be large enough to obtain accurate determination of the heat-transfer coefficients.

An estimated temperature difference $(T_W - T_B)$ of 15^oF was considered to be adequate to meet these requirements. The following procedure was used in adjusting the power to the test section:

(i) the outer wall temperature T_o at Z = 24D (Thermocouple No. 24), the water inlet temperature T_L and the outlet temperature of the mixture T_{OUT} were read from the recorder or the DVM;

(ii) the inner wall temperature T_W was estimated from a previously prepared table for the temperature drop across the wall ΔT_W as a function of the current I;

(iii) from T_L and T_{OUT}, an approximate value of T_B at the location Z = 24D was estimated;

(iv) the difference $(T_W - T_B)$ was then checked for the desired value and the power input was consequently adjusted if necessary.

An attempt was made to maintain a reasonably constant temperature difference for the entire series of experiments; the spread in $(T_W - T_B)$ was as follows:

Air - water:	$15^{o}F$	$^{+9.6}_{-9.1}$
Helium - water:	$15^{o}F$	$^{+5.5}_{-5.6}$
Freon 12 - water:	$15^{o}F$	$^{+2.7}_{-7.5}$

4.4. Taking of Data

After equilibrium conditions had been established, instrument readings were taken for all the variables listed in Table 4.1.

The thermocouple readings were taken last, in all the tests. If during the recording of all the thermocouple readings, the water inlet temperature varied by more than 0.2°F the data were rejected and the test was repeated.

The test conditions and the range of variables considered in the present investigation are listed in Table 4.2. Depending on the water flow rate, the gas flow rate was varied in order to obtain flow patterns from bubbly to annular-mist. It should be mentioned, however, that the maximum gas flow rate obtainable was limited by either the capacity of the gas supply system (as for air and helium), or by the thermodynamics properties (as for Freon 12 vapour).

4.5. Flow-Pattern Observation

High speed still photographs were taken of the flow patterns. For each test, the observation procedure was as follows:

(i) after the test conditions were set, the flow pattern was observed by the naked eye and with the aid of a strobo-

TABLE 4.2 Range of Variables Investigated

	Air - Water Experiments		Helium - Water Experiments		Freon - Water Experiments	
	Minimum	Maximum	Minimum	Maximum	Minimum	Maximum
m_L (lbm/hr)	267	8996	267	8996	267	3599
$\dot{m}_G$ (lbm/hr)	0.084	200.17	0.020	33.7	0.837	206.6
V_{SG} (ft/sec)	0.240	315	0.423	483.6	0.515	117.7
V_{SG}/V_{SL}	0.020	305.8	0.042	470	0.035	114
Re_{SG}	63.3	1.49×10^5	13.95	2.3×10^4	1894	2.09×10^5
q_W (Btu/hr)	3189	2.31×10^4	4297	2.4×10^4	3353	1.54×10^4
T_{IN} (^oF)	70.5	93.2	68.1	72.4	73.8	74.4
$\bar{T}_{MIX}$ (^oF)	75.6	95.3	70.6	78.9	76.6	79.6
ρ_G (lbm/ft^3)	0.0799	0.3276	0.0116	0.0375	0.3431	0.6034
Pr_G	0.709	0.709	0.6908	0.691	0.769	0.769

scope; the observations were recorded on the data sheet;

(ii) a photograph of the flow pattern was then taken;

(iii) after all data were taken, another photograph of the flow pattern was taken.

The photographs were taken, while the laboratory was totally darkened, using a Pentax camera and a microflash which photographically stopped the flow. The photographs and description of the flow patterns are presented in Chapter 5.

4.6. Shut-down Procedure

The following steps were taken to shut-down the rig:

(i) the power supply to the test section and the guard heaters was turned off;

(ii) the by-pass valve on the pump was fully opened and the control valves on the water flow meters were closed, then the pump was shutdown;

(iii) the cooling water to the heat exchanger was turned off;

(iv) the gas flow control valve closed and the main supply was shut off;

(v) finally, the test section and the mixer were drained and air was then supplied and was left flowing for at least one hour to dry the mixer.

In selecting the values of water flow rates (or V_{SL}) for the present experiments, it was advantageous to use the same values as in the earlier study performed with the present facility [90] in order to facilitate the comparison of the present results with those of [90]. Although the

present air-water experiments covered the whole range of water flow rate studies in [90], for the experiments with helium-water and Freon 12-water the lowest three water flow rates (V_{SL} = 0.065, 0.166 and 0.370 ft/sec) were excluded. At these water velocities, the conditions were highly unsteady resulting in large fluctuations in temperatures and pressure which made the taking of the data subject to large errors. The air-water experiments performed with these low water velocities were essentially to check the earlier [90] local heat-transfer results obtained for bubble and slug flows under the conditions where h_{TP} values were found to increase with increasing the distance Z along the test section. Similar results were obtained under the same conditions in the present study. Although these are not analyzed here, a sample of these data are shown in Fig. 6.5(A) when the present local data are presented, and in Fig. 7.1 where the flow-visualization study is discussed.

The water properties (surface tension and electric conductivity) were checked regularly during the course of the experiments. Neither of these properties were allowed to change by more than 5%.

CHAPTER 5

DISCUSSION OF FLOW PATTERNS AND PRESSURE DROP RESULTS

5.1 Introductory Remarks

The knowledge of the flow patterns is of great importance in two-phase flow investigations as these are known to affect both the pressure drop and heat transfer. As discussed in Chapter 4, the flow patterns were observed and photographed for all heat-transfer tests performed in the present study; samples of these photographs are presented in this chapter.

As indicated in Chapter 1, an attempt has been made to correlate the two-phase local and mean heat-transfer data in terms of the frictional pressure drop; this is discussed in the next chapter. The total pressure drops for all heat-transfer experiments were therefore measured, from which the frictional pressure drops were calculated and were used to correlate the heat-transfer data. The frictional pressure drop data for the three gas-water mixtures used in the present investigation are presented and discussed in this chapter because, as far as the author is aware, no report has been made of the effect of gas density on two-phase frictional pressure drop.

The flow-pattern data and the pressure drop data are tested by comparing them against the generally accepted flow regime map and pressure drop correlations respectively.

The calculation procedure for the reduction of the pressure drop data is given in Appendix D. The equations and correlations employed in testing the data are discussed in detail in Appendix E, while the data themselves are tabulated in Appendix H.

5.2 Single-Phase Pressure Drop

In two-phase flow investigations, the common procedure to test the reliability and performance of the experimental facility is to collect experimental data for single-phase flow and test these data against the well-established theories and correlations; if the data agree with the recommended correlations, the experimental facility is considered to be suitable for two-phase flow studies. Although the present facility has been checked for performance before [90], it was important to perform the present single-phase pressure drop and heat-transfer study to ensure the continued satisfactory performance of the rig (the single-phase heat-transfer study is discussed in Chapter 6).

In this section, the results of testing the experimental frictional pressure drop data for laminar and turbulent flow of water against the well-established correlations are presented. The degree of agreement between the experimental and the theoretical or empirical equations was determined by evaluating both the mean deviation $\bar{e}$ and the root mean square deviation $\bar{e}'$ defined below.

$$\bar{e} = \frac{1}{N} \Sigma \frac{(V_{EXPL} - V_{THL})}{V_{THL}} \quad ; \qquad (5.1)$$

$$\bar{e}' = \left| \frac{1}{N} \Sigma \left(\frac{V_{EXPL} - V_{THL}}{V_{THL}} \right)^2 \right|^{1/2} \qquad (5.2)$$

where

N is the number of data points,

V_{EXPL} is the experimental value of the variable under consideration,

V_{THL} is the theoretical (expected) value of the variable as determined from the equation under consideration.

The experimental data were tested against the well-accepted equations listed below.

For laminar flow ($Re_{SL}<2000$):

$$f_{SP} = 16/Re_{SL} \qquad (5.3)$$

For turbulent flow ($Re_{SL}>2000$):

$$f_{SP} = 0.079\ Re_{SL}^{-0.25}, \quad (2000<Re_{SL}<30,000)$$

and

$$f_{SP} = 0.046\ Re_{SL}^{-0.2}, \quad (Re_{SL}>30,000)$$

where f_{SP} is the single-phase flow friction factor.

The above equations are applicable to isothermal constant-property flows. For diabatic variable-property flows, there exist well-established correction factors [54] which accommodate for variations in fluid properties. However, as the property radial gradients in the present experiments were small (the temperature differences between the wall and the bulk were typically 15^{o}F), and therefore the effect of correcting the measured friction factors to "constant-property" values as recommended in [54] meant corrections of approximately 8% for laminar flow and not more than 1% for the more important case of turbulent flow, these corrections were neglected in plotting Fig. 5.1 where the data are tested against the above-listed correlations. The resulting deviations, however, are listed below for both the corrected and uncorrected data.

Table 5.1 Results of Testing the Single-Phase Pressure Drop Data Against the Existing Correlations.

	Laminar Flow		Turbulent Flow	
	$\bar{e}$	$\bar{e}'$	$\bar{e}$	$\bar{e}'$
Corrected Data	20.4%	21.2%	-1.8%	3.9%
Uncorrected Data	13.8%	15.7%	-2.2%	4.2%

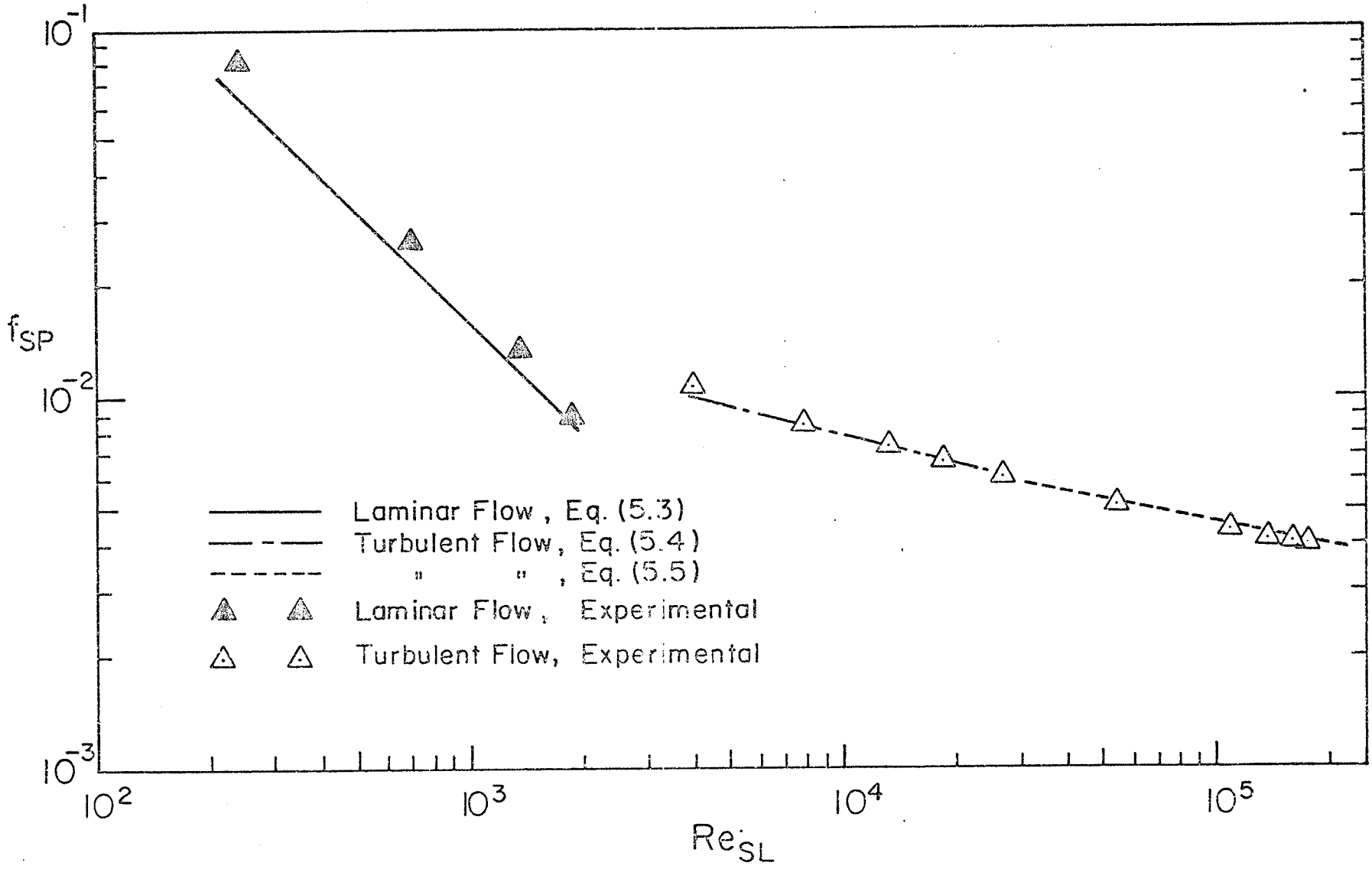

Fig. 5.1 Single-Phase Frictional Pressure Drop Results

Fig. 5.1

For turbulent flow the agreeement is excellent and for laminar flow it is reasonable. The large deviations encountered with laminar flow are mainly due to errors in reading the small deflections on the manometer.

5.3 Presentation and Discussion of Flow Pattern Data.

In this section, the basic flow patterns occurring in two-phase flow in vertical tubes are described; then, samples of the flow-pattern photographs from the present investigation are presented and, finally, the flow-pattern data are tested against the generalized flow-pattern map of Govier and Aziz [34].

5.3.1 Description of Flow Patterns

Although different terminology of the flow patterns is found in the literature [91], some attempts have been made recently to standardize the description and terminology of the flow patterns [34, 44, 92].

The basic flow patterns observed in the present study are shown in Fig 5.2, these are described generally in the order of increasing gas flow rate for a fixed liquid flow rate.

1. Bubble Flow: The liquid flows as a continuous phase with discrete gas bubbles dispersed in it.
2. Slug Flow: The gas flows as alternating large bullet-shaped bubbles which are surrounded by a thin liquid annulus and interspersed with slugs of liquid which may

or may not contain small bubbles of the gas. The thin liquid flim flows downward into the upward-moving liquid slug.

3. Froth Flow: This is also called "emulsion" flow. The gas and liquid phases flow in a highly turbulent, evenly dispersed mixture which has the appearance of an emulsion. This pattern was observed only at the high liquid flow rates where it occurred directly following the bubble flow.
4. Annular Flow: Here the gas flows in the central part of the tube and the liquid distributes itself between an upward moving annulus and coarse droplets carried in the continuous gas phase. The gas-liquid interface is always wavy with an amplitude which decreases as the gas flow rate increases.
5. Mist Flow: The liquid flows in the form of dispersed droplets carried along by a continuous gas phase.

The flow patterns described above do not generally occur in this order for all liquid flow rates. At the lower liquid flow rates in the present study, the froth flow has not been observed, the slug flow under these conditions was followed by annular flow through a slug-annular transition. It should be mentioned here that at the lowest superficial liquid velocity - 1.03 ft/sec (0.315 m/sec) - the observed flow patterns during the transition from slug to annular

flow (these are referred to here as "slug-annular") had such a nature that they could be also described as "churn flow." The churn flow pattern is characterized by its collapsing and pulsating nature and is generally considered as a transitional flow pattern between slug and annular flow. It should be noted that this flow pattern (churn) is similar to the froth flow defined by Govier and Aziz [34] and this is different from the froth flow defined here, which was observed only at high liquid flow rates and occurred after the bubble flow.

In the present investigation, as mentioned earlier, the flow patterns were observed visually with and without the aid of the stroboscope and were photographed by means of a still camera using a microflash for short exposure. On these bases, the flow patterns were classified as shown in Table 5.2. Each flow pattern is assigned a code letter for convenient identification throughout the thesis. The transitional flow patterns in the table (bubble-slug, slug-annular, etc.) are those which were difficult to classify or were of doubtful nature. The number of tests falling under each flow pattern is also listed in the table.

5.3.2. Presentation of Flow -Pattern Photographs.

A sample of photographs covering the flow patterns observed for each water flow rate considered in the present study are shown in Figs. 5.3 (A to G), 5.4 (A to D) and 5.5 (A to C) for air-water, helium-water and Freon-water respec-

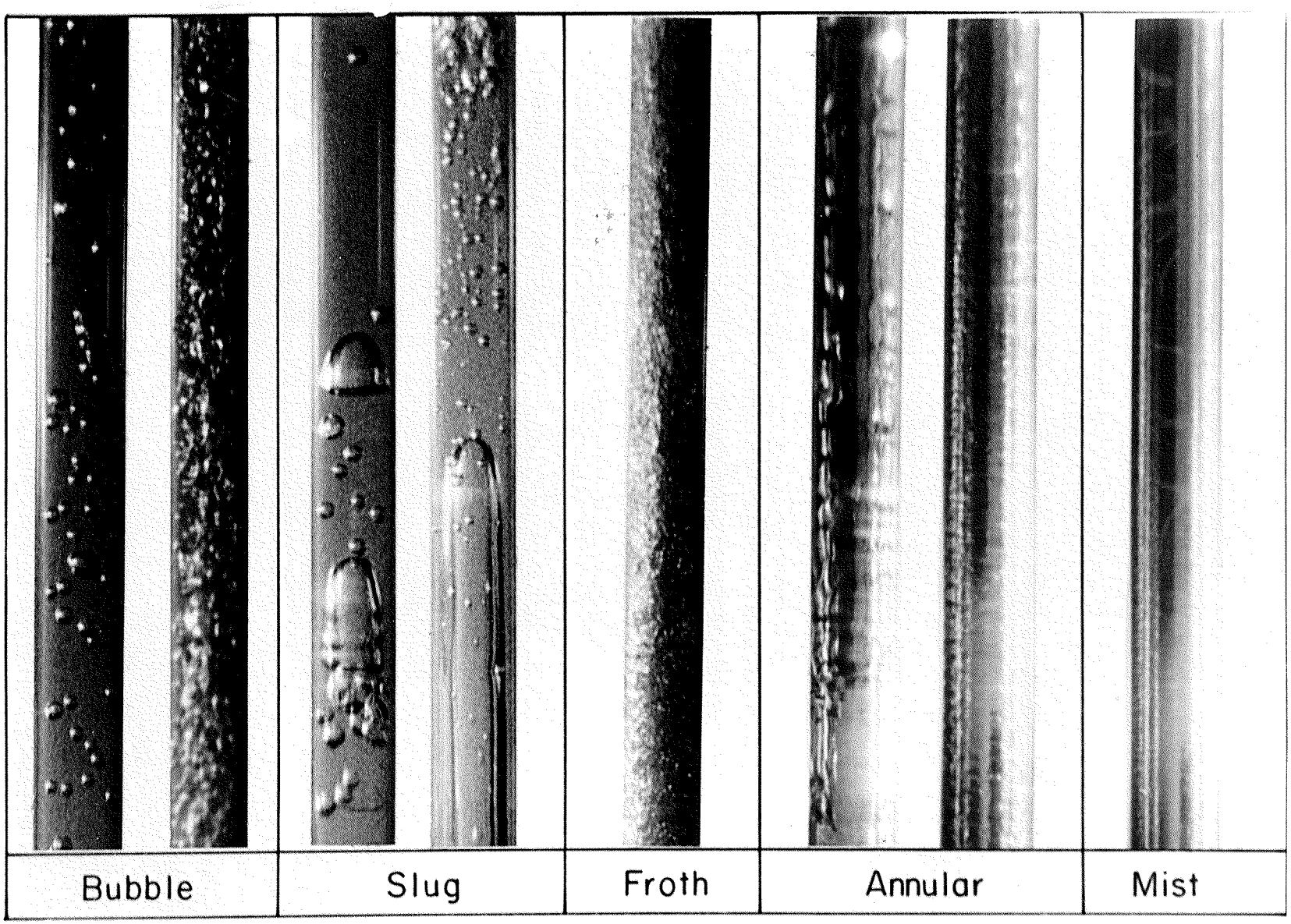

Fig. 5.2 Flow Patterns in Vertical Flow

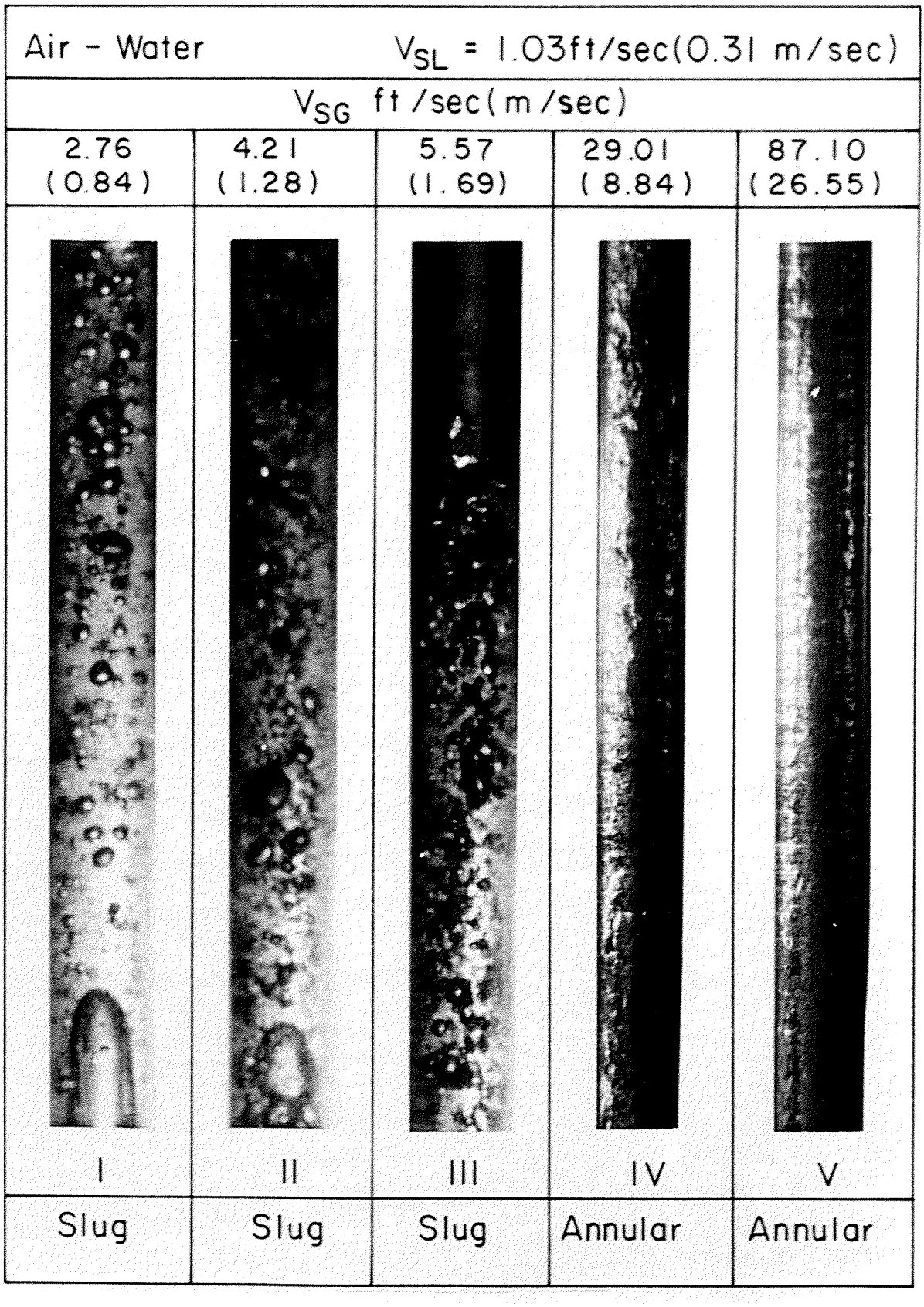
Air - Water
V_{SL} = 1.03ft/sec(0.31 m/sec)
V_{SG} ft/sec(m/sec)
2.76 (0.84)
4.21 (1.28)
5.57 (1.69)
29.01 (8.84)
87.10 (26.55)
I
II
III
IV
V
Slug
Slug
Slug
Annular
Annular

Fig. 5.3 (A)

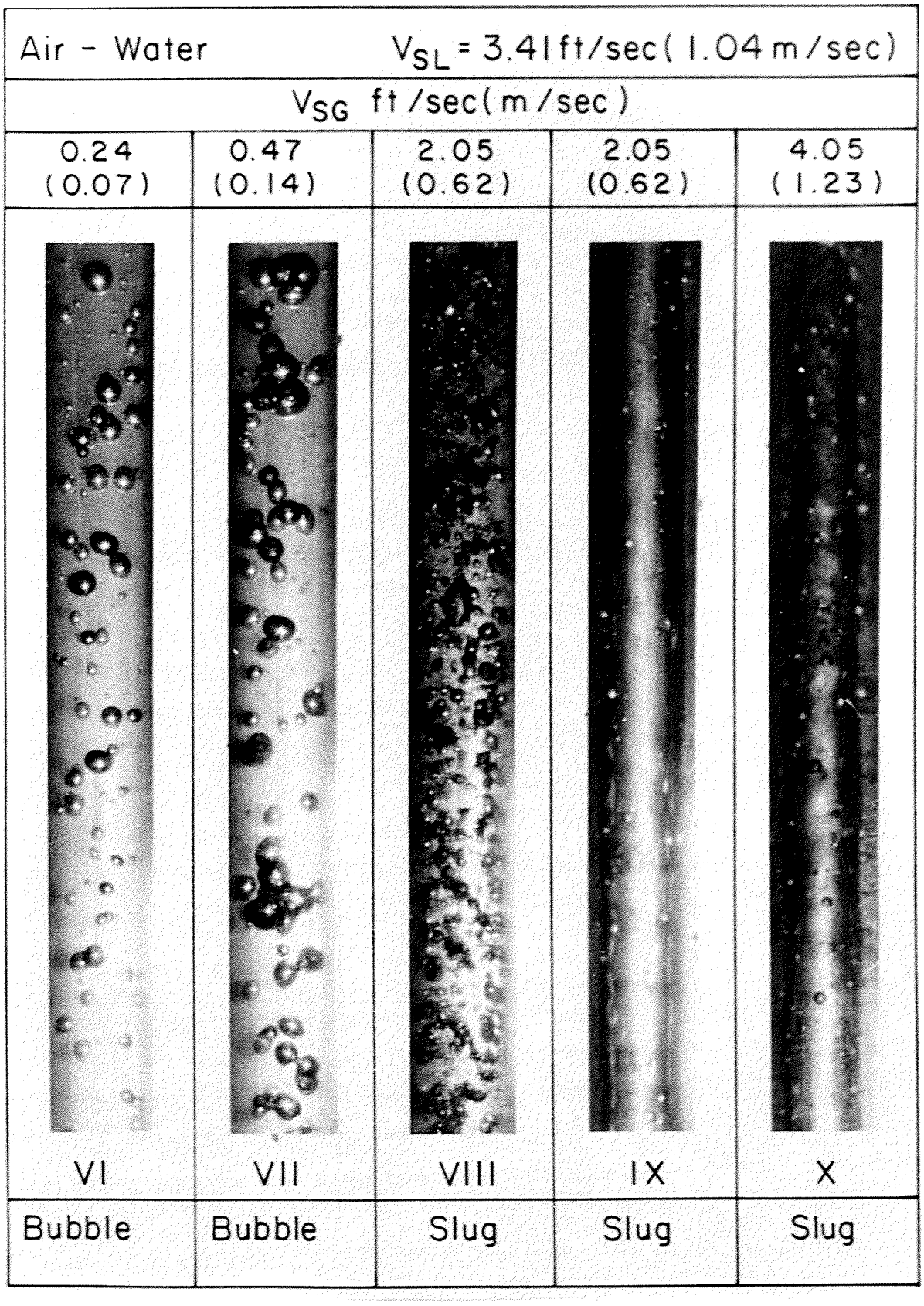
Air - Water
V_{SL} = 3.41 ft/sec (1.04 m/sec)
V_{SG} ft/sec (m/sec)
0.24 (0.07)
0.47 (0.14)
2.05 (0.62)
2.05 (0.62)
4.05 (1.23)
VI
VII
VIII
IX
X
Bubble
Bubble
Slug
Slug
Slug

Fig. 5.3 (B)

Air - Water	V_{SL} = 3.41 ft/sec (1.04 m /sec)			
V_{SG} ft /sec (m /sec)				
4.05 (1.23)	5.14 (1.57)	7.25 (2.21)	35.93 (10.95)	109.68 (33.43)
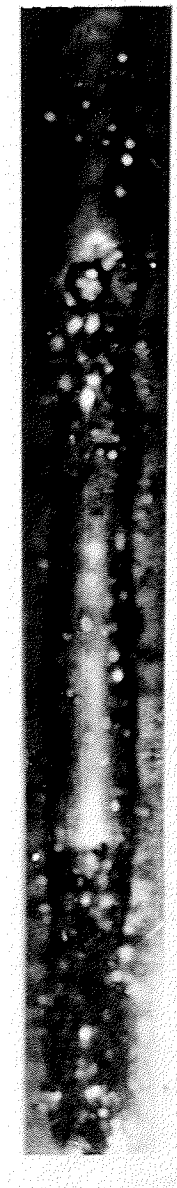				
XI	XII	XIII	XIV	XV
Slug	Slug	Slug - Annular	Annular	Annular

Fig. 5.3 (B) Continued

Air - Water	V_{SL} = 6.95ft/sec(2.12 m/sec)			
V_{SG} ft /sec (m /sec)				
1.13 (0.34)	3.45 (1.05)	5.12 (1.56)	7.21 (2.19)	104.68 (31.91)
			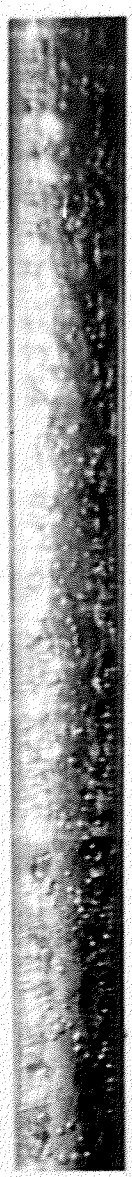	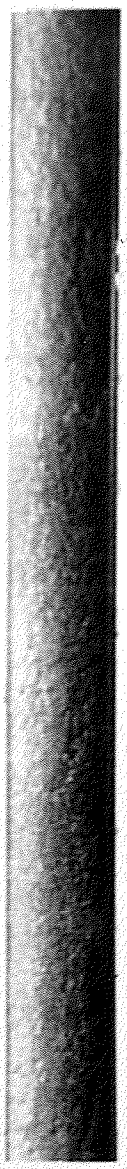
XVI	XVII	XVIII	XIX	XX
Bubble	Bubble - Slug	Slug	Froth Annular	Annular

Fig. 5.3 (C)

Air - Water	V_{SL} = 13.89 ft/sec (4.23 m/sec)			
V_{SG} ft/sec (m/sec)				
0.90 (0.27)	2.00 (0.61)	3.93 (1.20)	13.91 (4.24)	34.22 (10.43)
			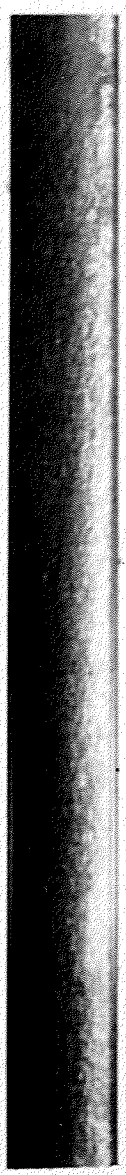	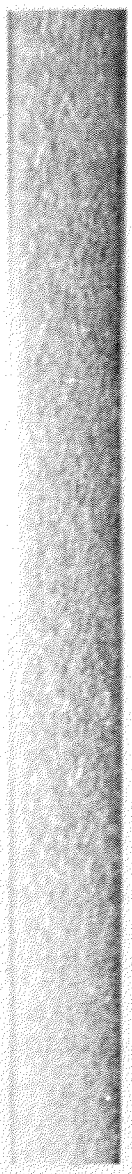
XXI	XXII	XXIII	XXIV	XXV
Bubble	Bubble	Bubble - Froth	Froth	Froth

Fig. 5.3 (D)

Air - Water	V_{SL} = 20.84 ft/sec (6.35 m/sec)			
V_{SG} ft/sec (m/sec)				
1.01 (0.30)	4.63 (1.41)	9.17 (2.80)	25.81 (7.87)	42.79 (13.04)
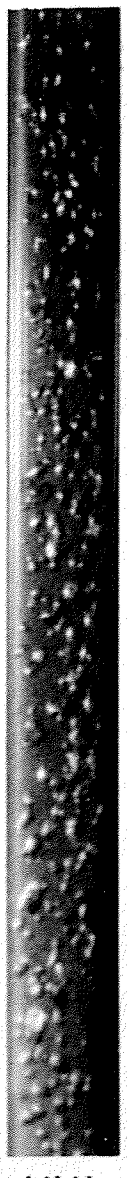	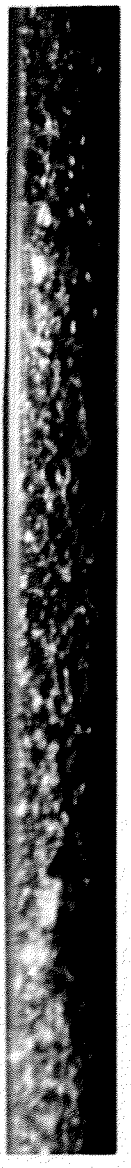	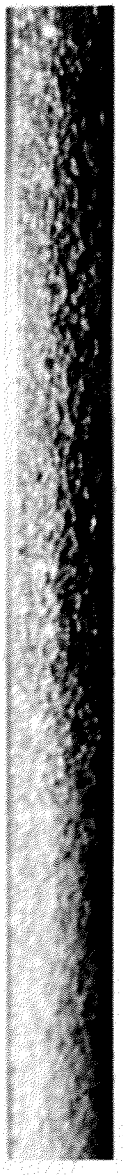	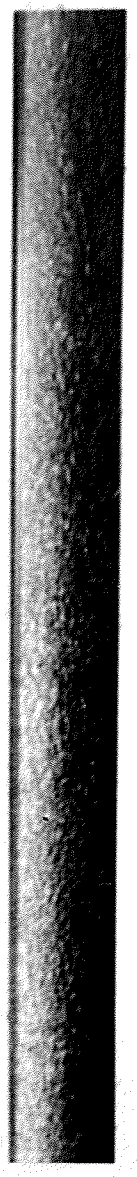	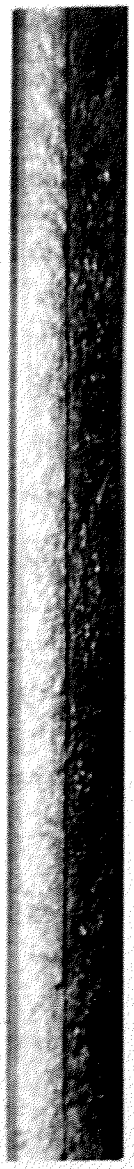
XXI	XXII	XXIII	XXIV	XXV
Bubble	Bubble	Bubble - Froth	Froth	Froth

Fig. 5.3 (E)

Air - Water	V_{SL} = 27.78 ft/sec (8.46 m/sec)			
V_{SG} ft/sec (m/sec)				
1.02 (0.31)	2.03 (0.61)	3.90 (1.18)	18.52 (5.64)	39.02 (11.89)
	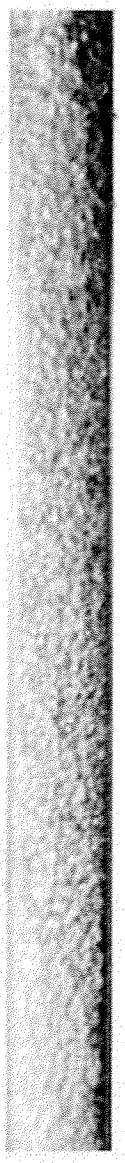	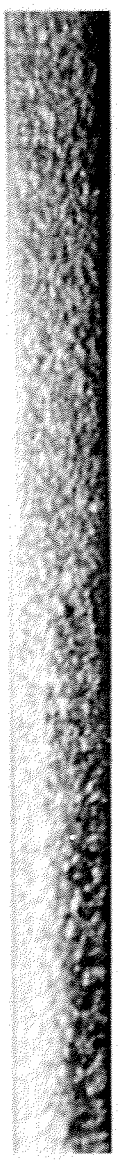	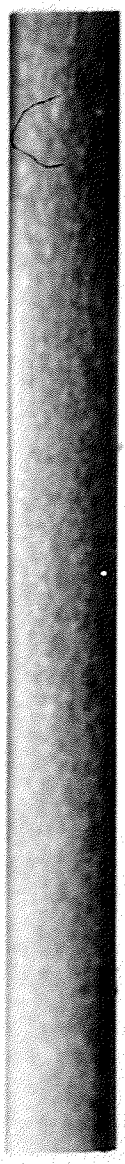	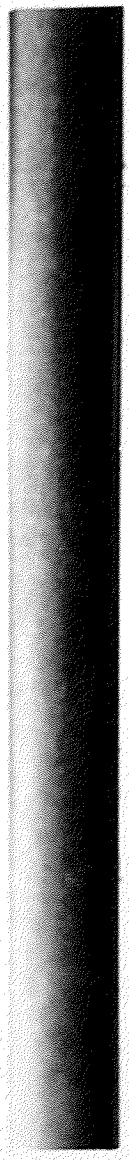
XXXI	XXXII	XXXIII	XXXIV	XXXV
Bubble	Bubble	Bubble	Froth	Froth

Fig. 5.3 (F)

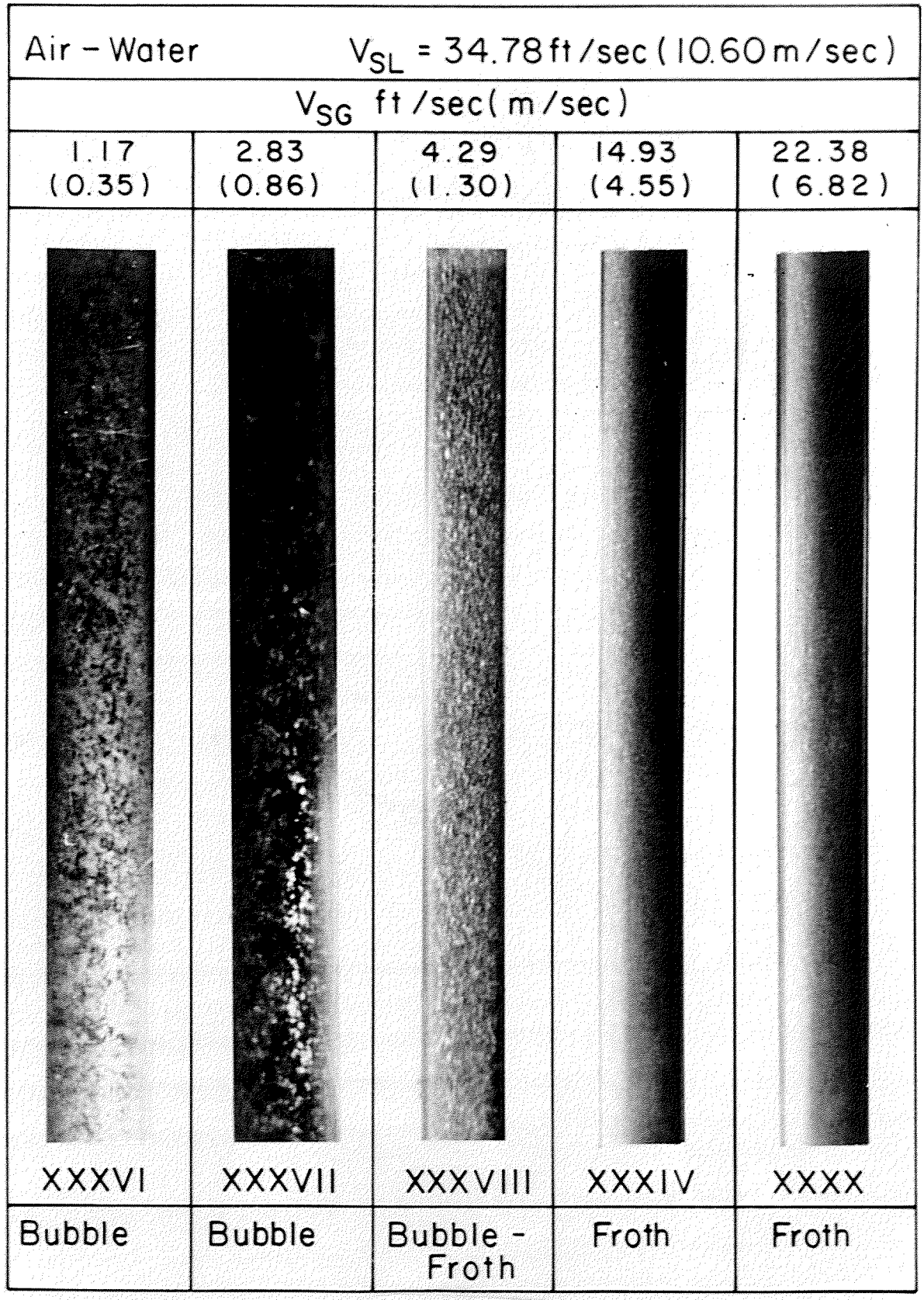
Air – Water
V_{SL} = 34.78 ft/sec (10.60 m/sec)
V_{SG} ft/sec (m/sec)
1.17 (0.35)
2.83 (0.86)
4.29 (1.30)
14.93 (4.55)
22.38 (6.82)
XXXVI
XXXVII
XXXVIII
XXXIV
XXXX
Bubble
Bubble
Bubble - Froth
Froth
Froth

Fig. 5.3 (G)

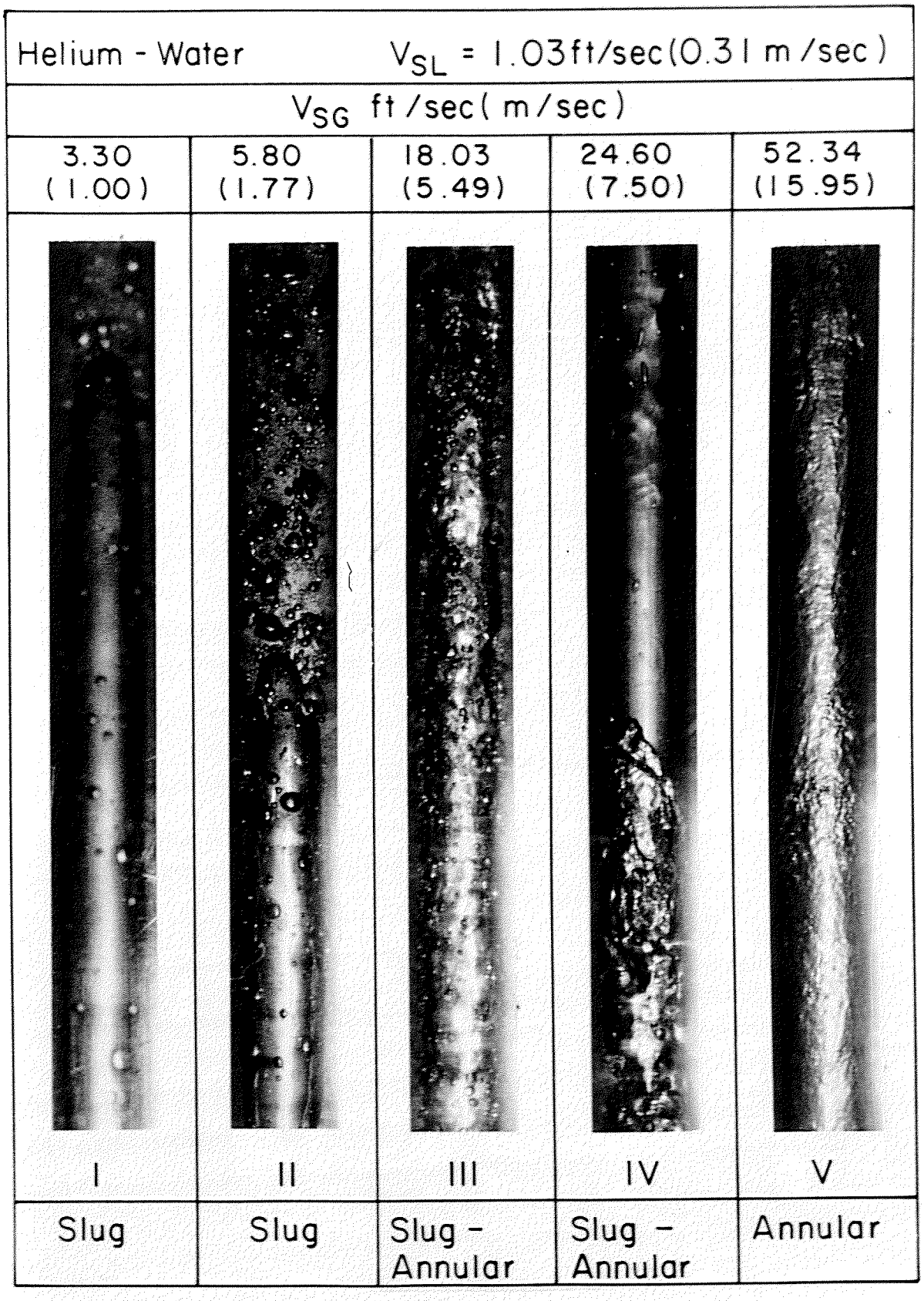
Helium - Water
V_{SL} = 1.03ft/sec(0.31 m/sec)
V_{SG} ft/sec(m/sec)
3.30 (1.00)
5.80 (1.77)
18.03 (5.49)
24.60 (7.50)
52.34 (15.95)
I
II
III
IV
V
Slug
Slug
Slug - Annular
Slug - Annular
Annular

Fig. 5.4 (A)

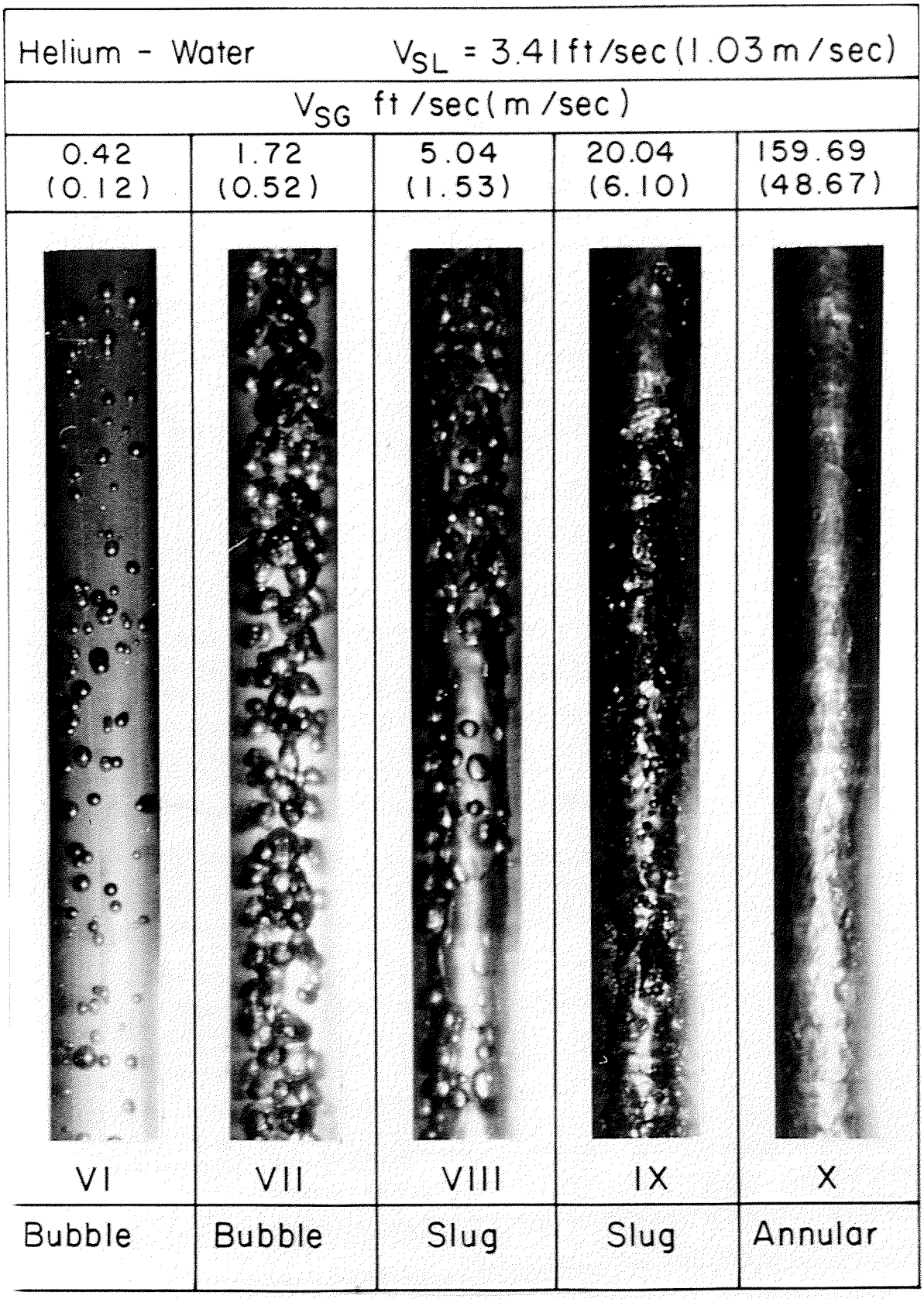
Helium - Water
V_{SL} = 3.41 ft/sec (1.03 m/sec)
V_{SG} ft/sec (m/sec)
0.42 (0.12)
1.72 (0.52)
5.04 (1.53)
20.04 (6.10)
159.69 (48.67)
VI
VII
VIII
IX
X
Bubble
Bubble
Slug
Slug
Annular

Fig. 5.4 (B)

Helium - Water	V_{SL} = 13.89 ft/sec (4.23 m/sec)			
V_{SG} ft/sec (m/sec)				
0.58 (0.17)	1.31 (0.39)	4.87 (1.48)	45.42 (13.84)	70.20 (21.39)
			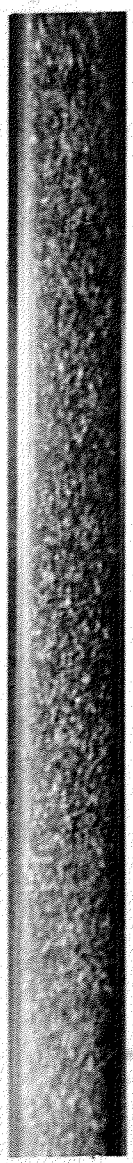	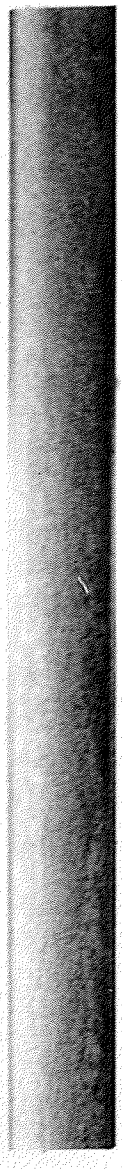
XI	XII	XIII	XIV	XV
Bubble	Bubble	Bubble - Froth	Froth	Froth

Fig. 5.4 (C)

Helium - Water	V_{SL} = 34.78 ft/sec (10.60 m/sec)			
V_{SG} ft/sec (m/sec)				
1.45 (0.44)	1.77 (0.54)	2.93 (0.89)	5.10 (1.55)	9.78 (2.98)
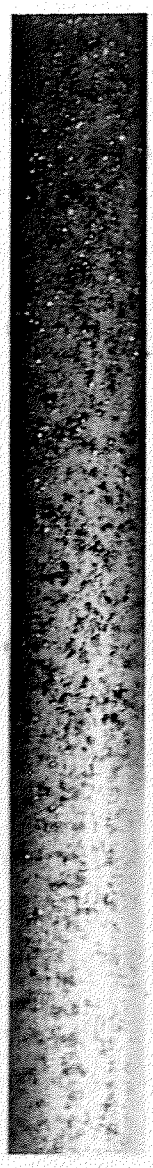		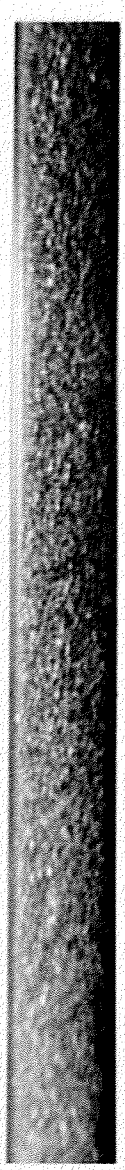	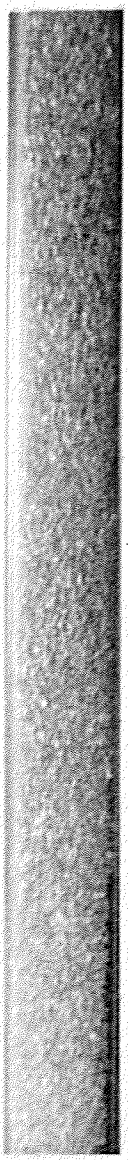	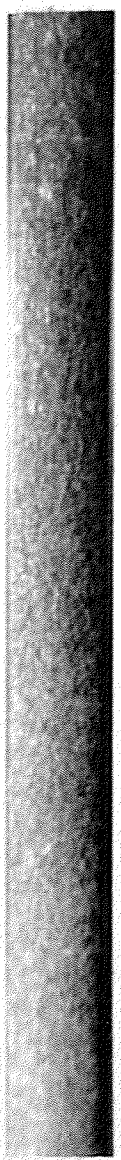
XVI	XVII	XVIII	XIV	XX
Bubble	Bubble	Bubble - Froth	Froth	Froth

Fig. 5.4 (D)

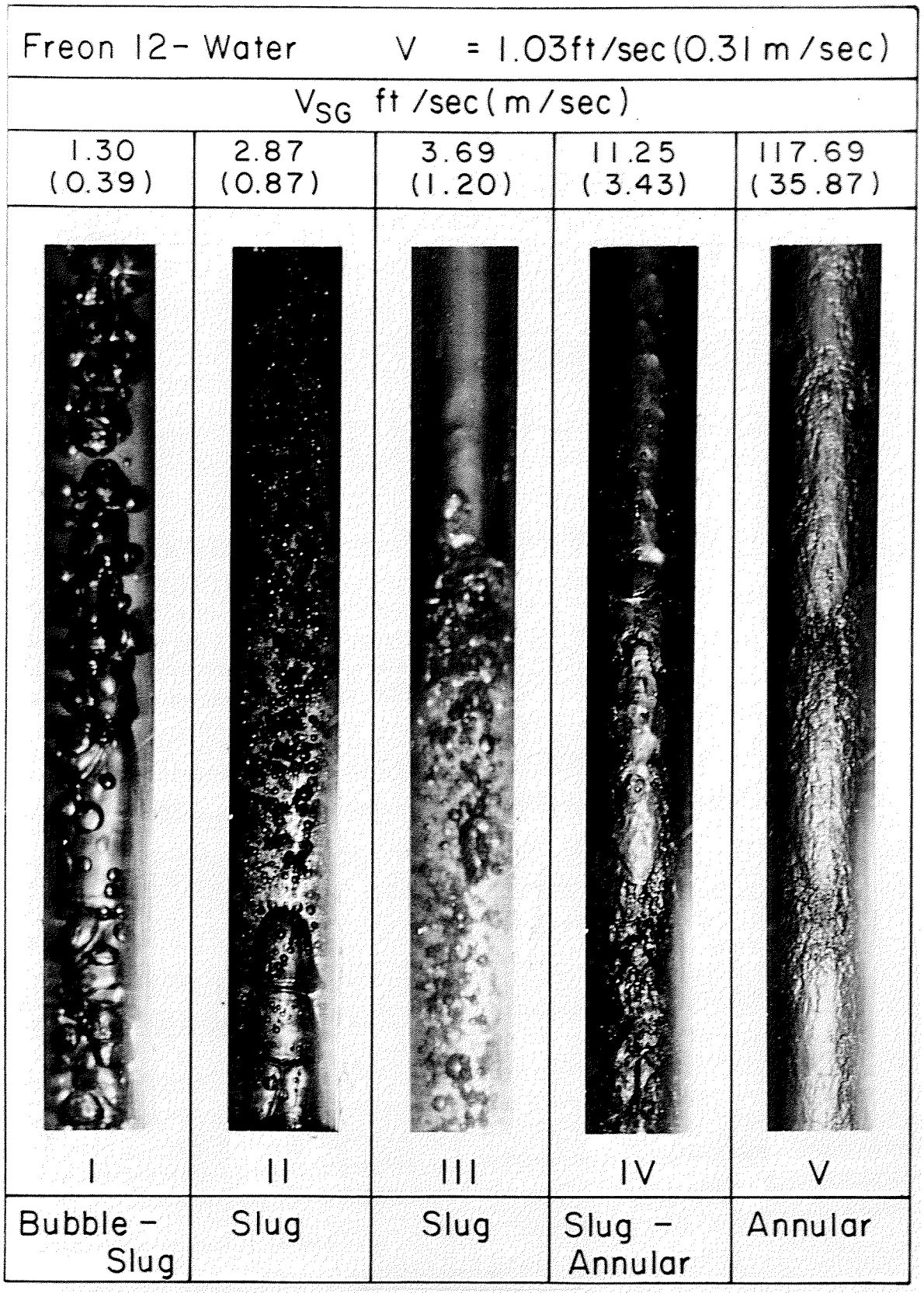
Freon 12- Water V = 1.03ft/sec(0.31 m/sec)
V_{SG} ft/sec(m/sec)
1.30 (0.39)
2.87 (0.87)
3.69 (1.20)
11.25 (3.43)
117.69 (35.87)
I
II
III
IV
V
Bubble - Slug
Slug
Slug
Slug - Annular
Annular

Fig. 5.5 (A)

Freon 12 - Water	V_{SL} = 3.41 ft/sec (1.03 m/sec)			
V_{SG} ft/sec (m/sec)				
0.69 (0.21)	1.60 (0.49)	3.69 (1.12)	5.17 (1.57)	34.95 (10.65)
				
VI	VII	VIII	IX	X
Bubble	Bubble	Bubble - Slug	Slug	Annular

Fig. 5.5 (B)

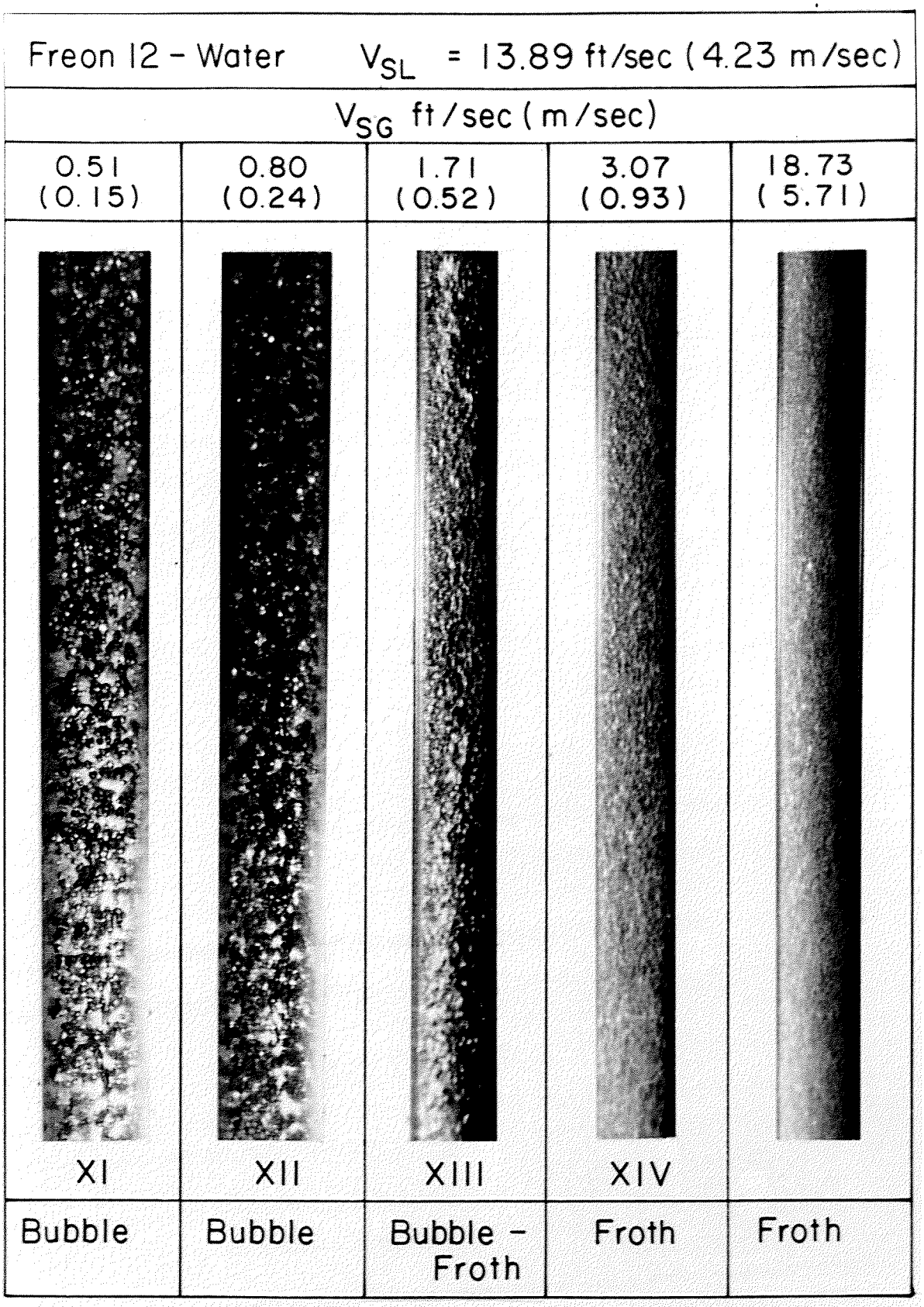
Freon 12 - Water V_{SL} = 13.89 ft/sec (4.23 m/sec)
V_{SG} ft/sec (m/sec)
0.51 (0.15)
0.80 (0.24)
1.71 (0.52)
3.07 (0.93)
18.73 (5.71)
XI
XII
XIII
XIV
Bubble
Bubble
Bubble - Froth
Froth
Froth

Fig. 5.5 (C)

Table 5.2 Flow-Pattern Classification in the Present Study.

Flow Pattern	Code Letter(s)	Number of Tests		
		Air-Water	Helium-Water	Freon-Water
Bubble	B	20	9	5
Slug	S	6	9	7
Froth	F	33	12	10
Annular	A	19	8	13
Bubble-Slug	BS	1	2	4
Bubble-Froth	BF	10	1	1
Slug-Annular	SA	2	4	2
Annular-Mist	AM	5	4	-

tively. For each water flow rate, the photographs are generally arranged in the order of increasing gas flow rate. Photographs marked with an asterisk were taken for the same test, i.e., same water and gas flow rates.

Although information with regard to the general description of the characteristics of flow patterns exist in the literature [34,44,91,92], some observations based on the photographs and visual observation of the flow patterns are given below.

(i) In the slug flow regime, the water film between the long bubble and the wall was observed to experience a downflow past the long bubble, this was highly perturbed by the large number of entrained bubbles. The flow here, was highly unsteady and accompanied by

large fluctuations in pressure and temperature in the test section.

(ii) In the annular flow regime, the liquid-gas interface was always wavy with an amplitude which decreased as the gas velocity was increased.

(iii) At high water and gas flow rates, it was difficult to identify the flow patterns as the mixture had the appearance of an emulsion. These were generally classified as froth flow.

(vi) The nature of a particular flow pattern is similar for all gas-liquid mixtures studied.

5.3.3 Flow-Pattern Maps

A flow-pattern map is simply a two-dimensional plot employed to predict the flow patterns and their transitions. Although theoretical expressions to predict flow-pattern transitions are emerging [71,82], all existing maps or correlations are, in general, empirical. Completely satisfactory maps of such kind have not yet been developed because of the extreme complexity of the flow mechanism and its changes with flow rate. Examination of the existing maps [34,64,67,68,91] shows that for any given fluid system the major factors in determining the flow pattern are the flow velocities. The fluid densities, viscosities and interfacial tension and the pipe diameter are the other factors. Duns and Ros [26] claim that the viscosities of the phases

are not important in determining the flow pattern, and that the effect of liquid density and interfacial tension is almost negligible. Vijay [90] observed no effect of liquid viscosity on flow regime transitions. The effect of the gas-phase density was shown [34] to be proportional to $(\rho_G)^{1/3}$ over a density range of 0.092 to 0.552 lbm/ft^3. The effect of the pipe diameter is claimed to be negligible [26].

A flow pattern map was constructed for the present data with the co-ordinates being the superficial gas and liquid velocities; this is shown in Fig. 5.6. The data are also shown in Fig 5.7 plotted on the generalized flow pattern map recommended by Govier and Aziz [34] where a modified superficial liquid velocity $Y^* V_{SL}$ and a modified superficial gas velocity $X^* V_{SG}$ are used as ordinate and abscissa respectively, where

$$Y^* = (\rho_L \sigma_{WA} / \rho_W \sigma_{LG})^{1/4}, \qquad (5.6)$$

$$X^* = Y^* (\rho_G / \rho_A)^{1/3} \qquad (5.7)$$

where

σ_{WA} is the interfacial tension of the water-air system at standard atmospheric conditions (taken as 60^{o}F and 14.65 psia),

σ_{LG} is the interfacial tension of the liquid-gas system at flowing conditions,

ρ_L is the density of liquid at flowing conditions,

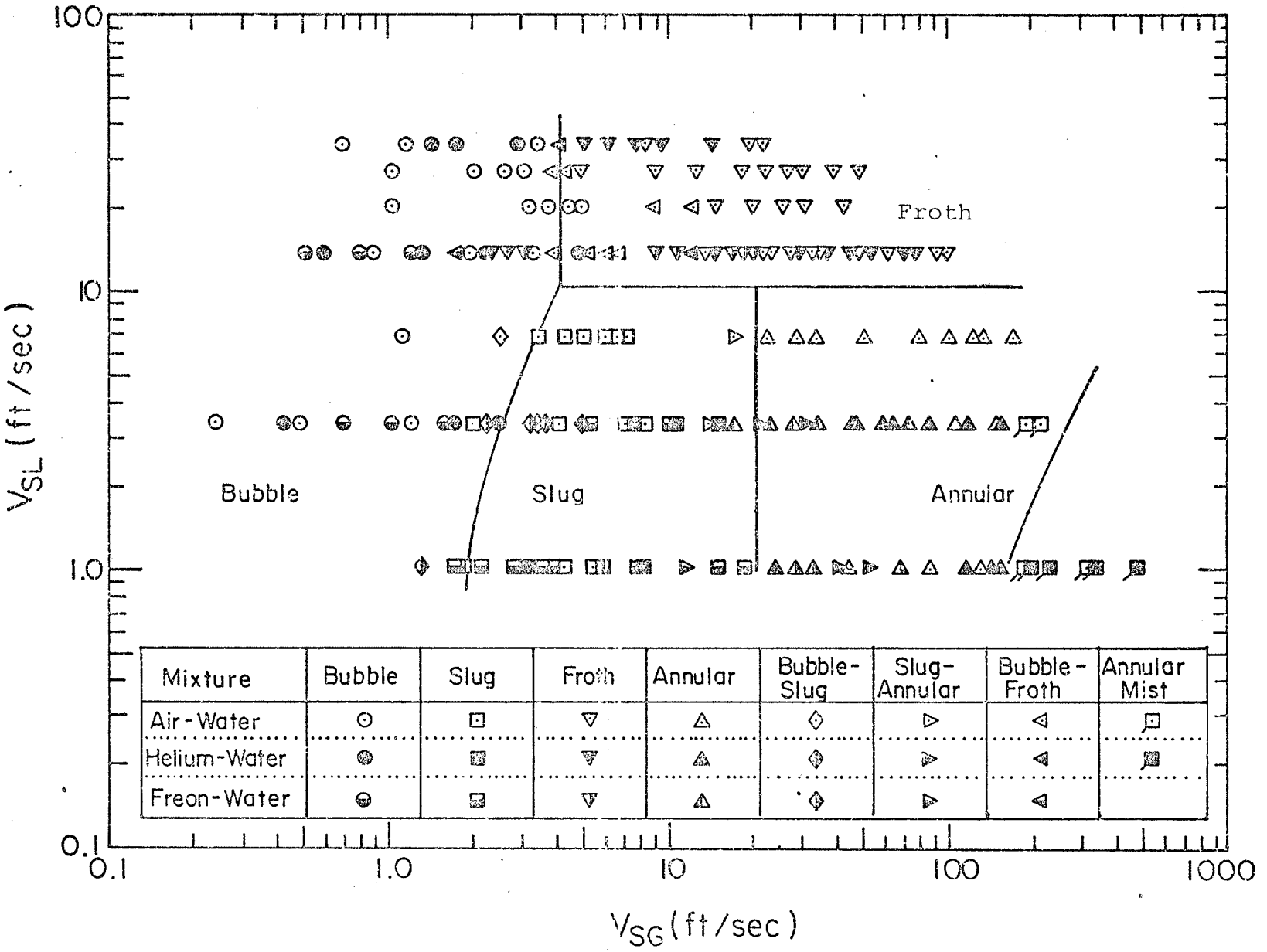

Fig. 5.6 Flow-Pattern Map Based on Superficial Velocities

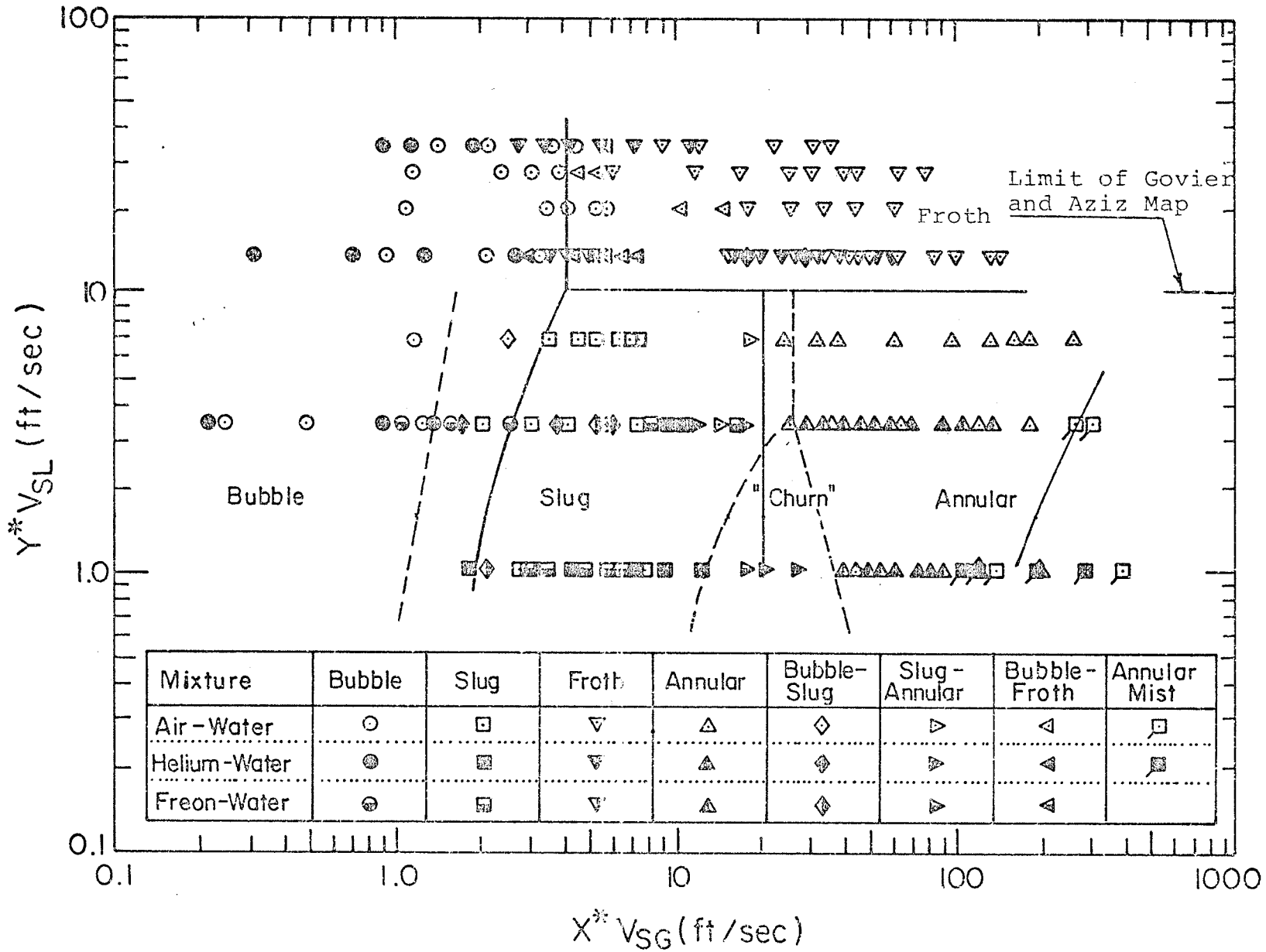

Fig. 5.7 Flow-Pattern Map: Govier and Aziz

ρ_W is the density of water at standard conditions,

ρ_G is the density of gas at flowing conditions,

ρ_A is the density of air at standard conditions.

This system of co-ordinates suggests that the liquid density and surface tension, and the gas density affect the flow pattern transitions.

The dashed lines in Fig. 5.7 represent the flow pattern boundaries as given by Govier and Aziz [34]; these are terminated at $Y^*V_{SL} = 10$ which is the upper limit of the ordinate on the original map. It should be noted that the "churn flow" region in Fig. 5.7 is replacing the "froth flow" region on the original map as the term "froth flow" here is used to describe a completely different flow pattern from that described by Govier and Aziz [34]; as mentioned earlier, the Govier and Aziz froth flow is similar to what is described here as churn or slug-annular flow. Also, in the original map, one region (labelled "annular-mist") was used for both annular and mist flows. The solid lines in the figure represent flow pattern boundaries based on the present data. Examination of Figs. 5.6 and 5.7 shows that they are, in general similar. The gas-density effect on flow-patterns is uncertain in that the gas-density correction of Govier and Aziz does not appear to work for all flow-pattern transitions as some of the boundaries are better defined when only V_{SL} and V_{SG} are used as coordinates. More data are still required in order to clearly determine the effect of gas density.

5.4 Presentation and Discussion of Frictional Pressure Drop Data

As mentioned earlier, the frictional pressure drop data discussed in this section were calculated from the measured total pressure drops as discussed in Appendix D. These data are presented and discussed here because, as far as the author is aware, no previous data on the effect of the gas-phase density on two-phase frictional pressure drop in vertical flow have been reported in the literature. The data are also tested against some of the existing correlations.

The total pressure drop ΔP_{TP} consists of three components: (i) the frictional pressure drop ΔP_{TPF}, (ii) the hydraulic or gravitational pressure drop ΔP_{TPG} and (iii) the accelerational pressure drop ΔP_{TPA}. The latter is usually assumed to be negligible and therefore,

$$\Delta P = \Delta P_{TPF} + \Delta P_{TPG} \qquad (5.8)$$

The hydraulic pressure drop is simply the static head and, in two-phase flow, it can be calculated from a knowledge of the void fraction and the densities of the phases. As discussed in Appendix D, the void fraction correlation of Chisholm [17] was employed to predict the void fractions, these were used to calculate the values of ΔP_{TPG}, and then Eq. (5.8) was employed to calculate ΔP_{TPF}.

5.4.1 Discussion of Experimental Data

The frictional pressure drop data are shown in Figs. 5.8, 5.9 and 5.10 for air-water, helium-water and Freon-water respectively. The data for all three gas-water mixtures are plotted in Fig. 5.11 in order to show the effect of gas density. In the figures, the frictional pressure drop is plotted against V_{SG} with V_{SL} as a parameter. At the lowest V_{SL} and low values of V_{SG} (where the mixture was in slug flow), the calculated values of ΔP_{TPF} were extremely low and in some cases were negative. Although the negative values of ΔP_{TPF} could be real as has been observed by other investigators [36,39,76,90] due to the downflow of the liquid film on the wall, these and other low values of ΔP_{TPF} were suspected to be in large error because under these conditions the fluctuations of the water levels in the inverted manometer were so high that it was difficult to read the total pressure drop with reasonable accuracy. On these basis, it was decided to exclude the data obtained under these conditions for which $\Delta P_{TPF} < 0.2$ in (0.51 cm) of water (approximately 0.01 psi). These data are not shown in Figs. 5.8 to 5.11 and were also excluded when the heat transfer data were correlated in terms of the frictional pressure drop as discussed in Chapter 6. The letters appearing next to the data points in the figures indicate the observed flow patterns (Table 5.2).

Examination of Figs 5.8, 5.9 and 5.10 shows that the

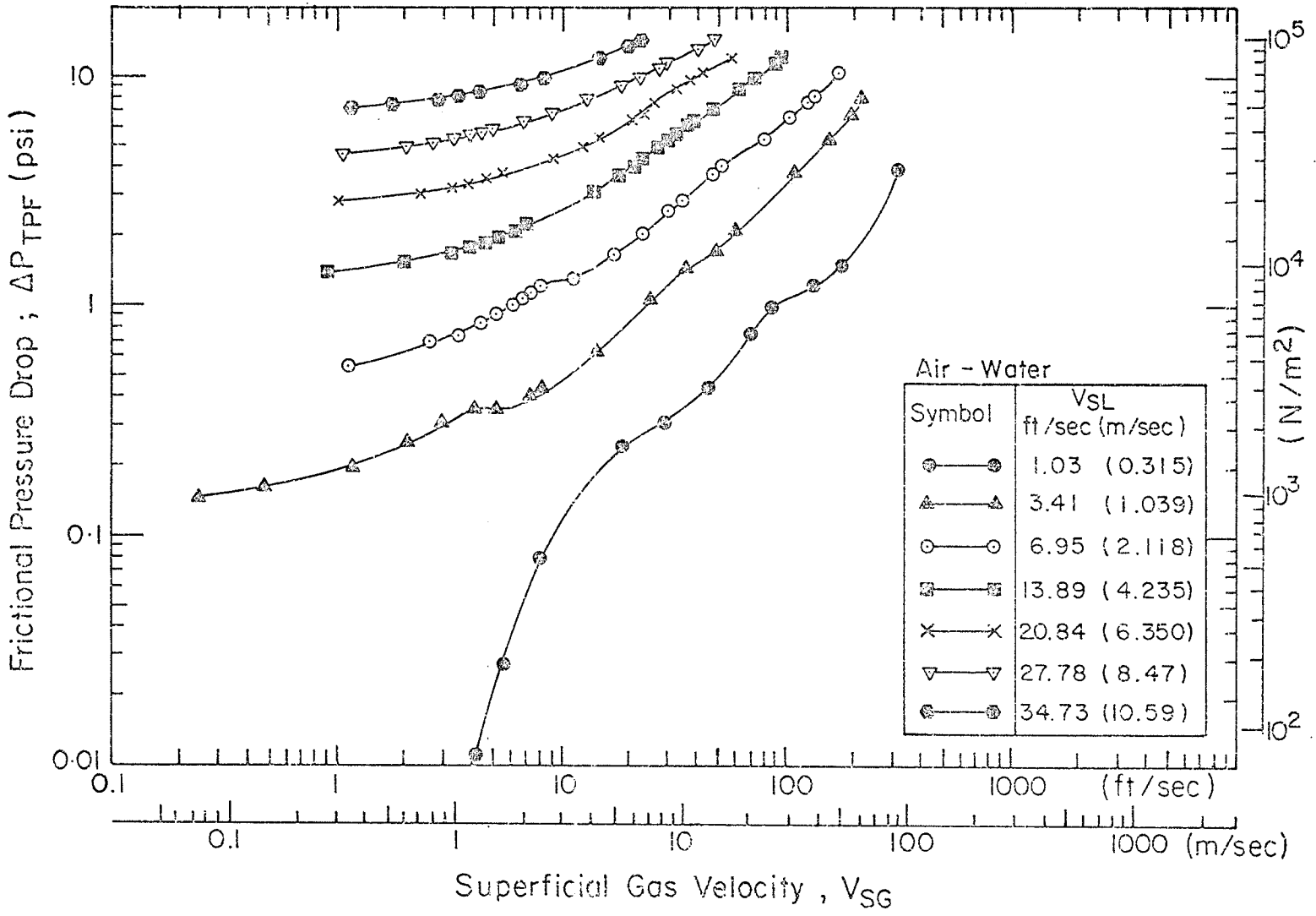

Fig. 5.8 Frictional Pressure Drop Results: Air-Water

Fig. 5.8

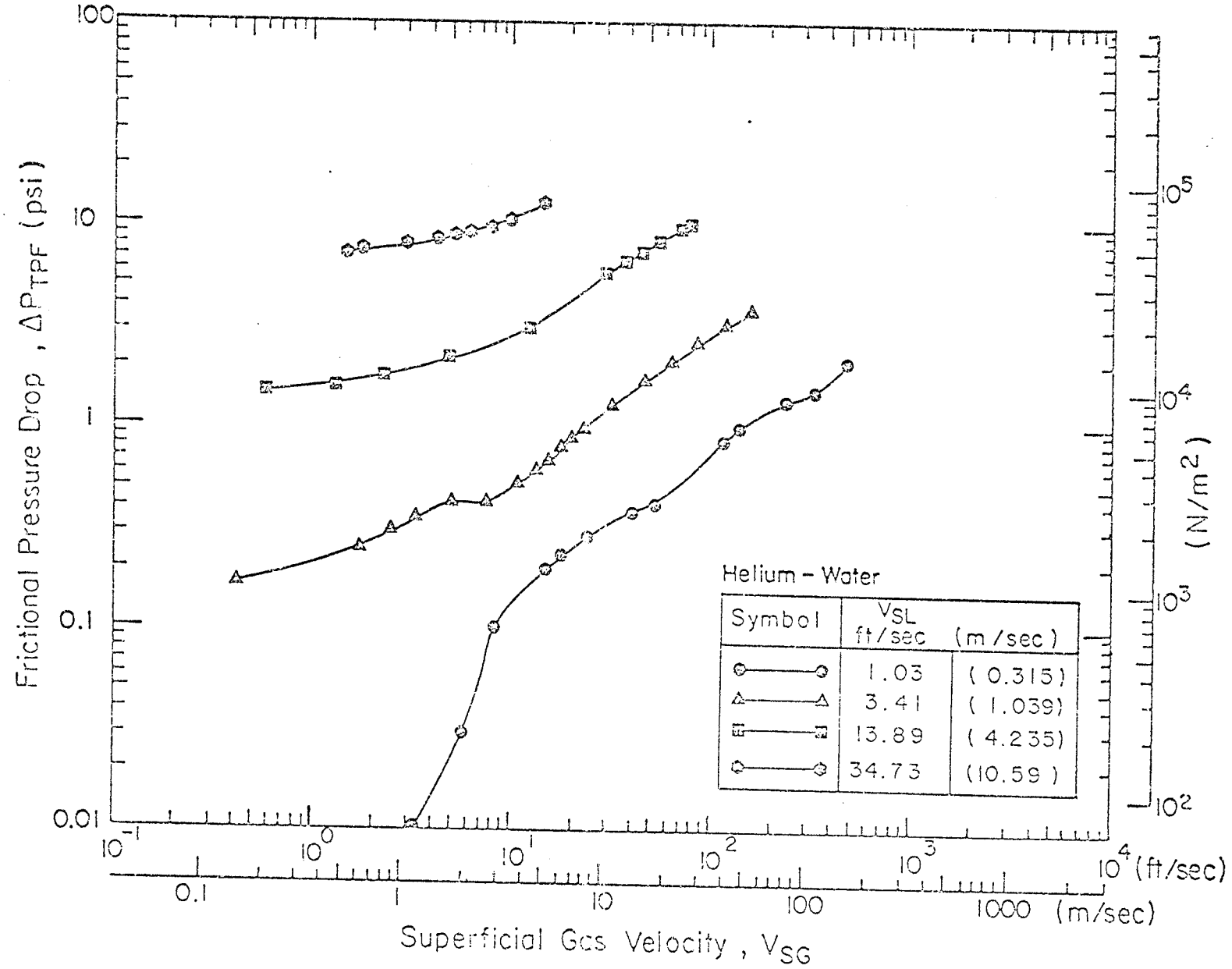

Fig. 5.9 Frictional Pressure Drop Results: Helium-Water

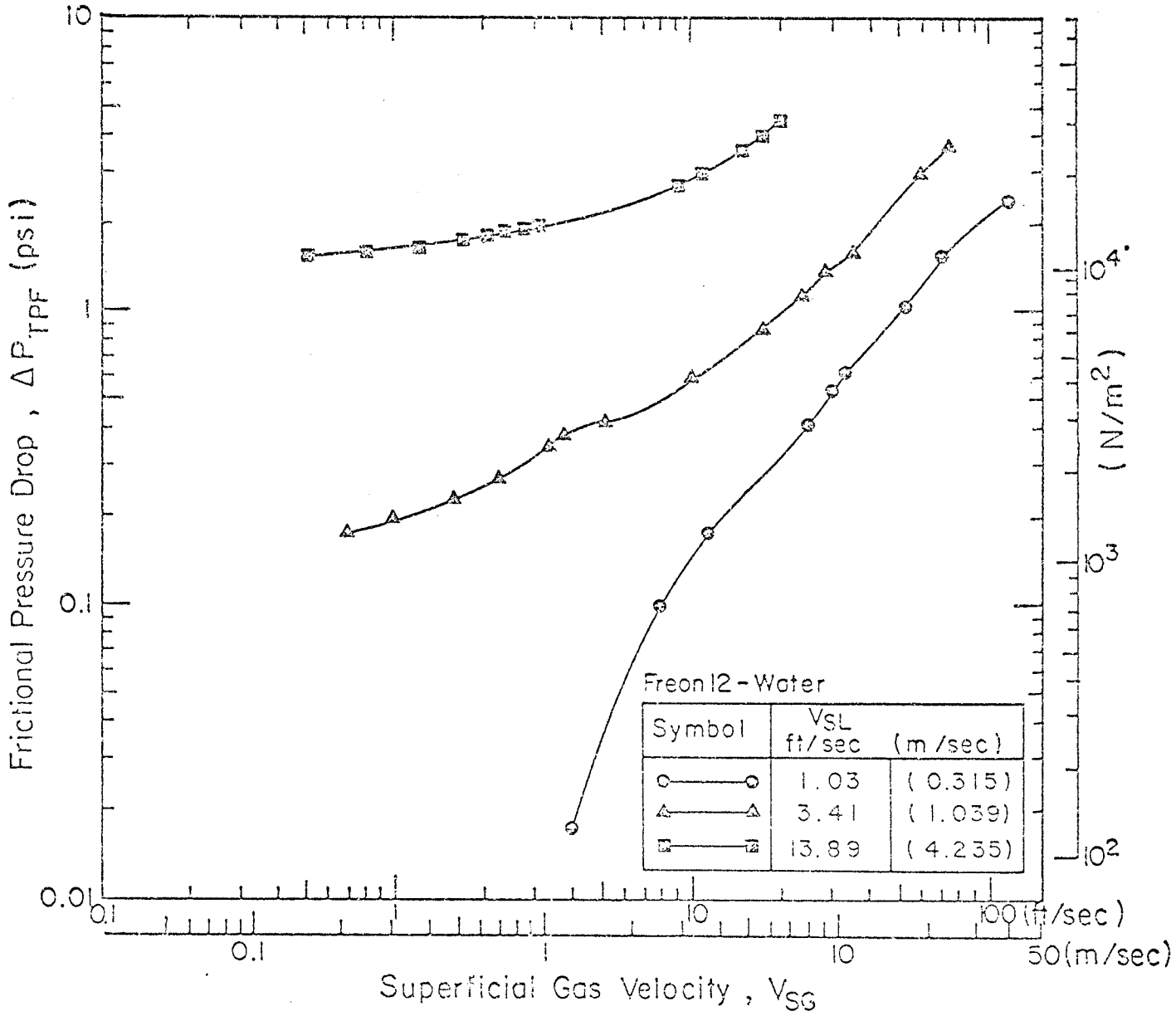

Fig. 5.10 Frictional Pressure Drop Results: Freon-Water

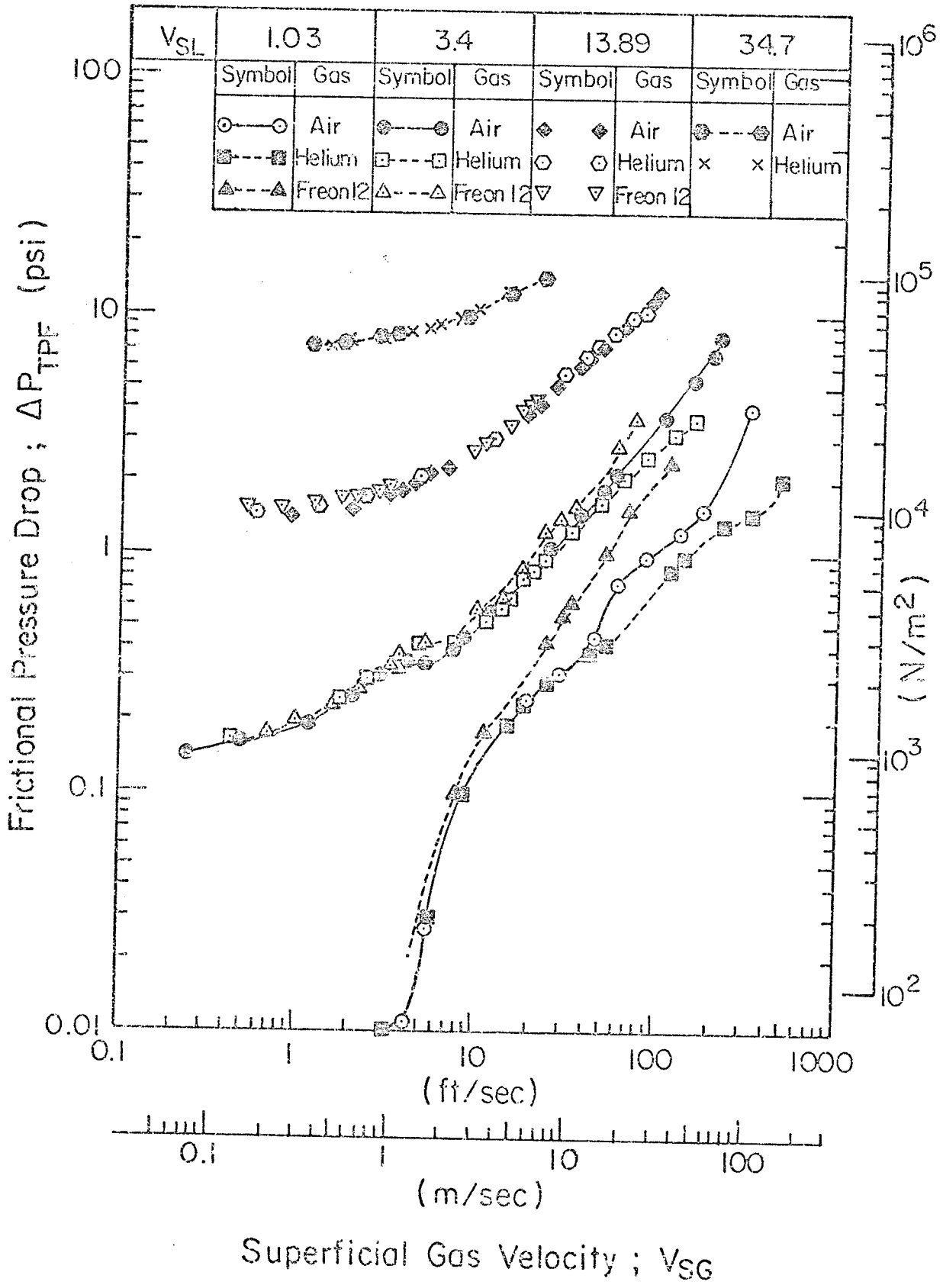

Fig. 5.11 Combined Plot of Frictional Pressure Drop Results for All Three Gas-Water Mixtures

$\Delta P_{TPF} \sim V_{SG}$ profiles are generally similar to those already reported [36,37]. The change in the slopes of the curves is usually associated with the flow pattern transitions. Since a large volume of literature on two-phase pressure drop exists, for example [5,34,92], the discussion presented below will be limited to observations with regard to the effect of gas density on ΔP_{TPF} as can be seen from Fig. 5.11.

- For the lower water velocities 1.03 ft/sec (0.314 m/sec) and 3.41 ft/sec (1.04 m/sec) and for superficial gas velocities up to about 5 ft/sec (1.52 m/sec), there is no apparent effect of the gas-phase density on ΔP_{TPF}.
- As the superficial gas velocity increases above 5ft/sec, some effect of ρ_G on ΔP_{TPF} is observed in such a way that for the same values of V_{SG}, the higher the gas density, the higher is the frictional pressure drop. Further, this effect appears to increase with increasing V_{SG}, for example, for V_{SL} = 1.03 ft/sec (0.314 m/sec) at V_{SG} value of about 50 ft/sec (15.24 m/sec), ΔP_{TPF} for Freon-water is about 73% higher than that for air-water and ΔP_{TPF} for helium-water is 28% lower than for air-water. As V_{SG} increases for the same V_{SL}, for example, at V_{SG} = 85 ft/sec.(30 m/sec), ΔP_{TPF} for Freon-water and helium-water become respectively about 89% higher and 32% lower than the air-water value.

- The above described effect is less pronounced at the higher values of V_{SL}. For example, for V_{SL} = 3.41 ft/sec (1.04m/sec) and V_{SG} = 50 ft/sec (15.24m/sec), ΔP_{TPF} for Freon-water is about 17% higher than the air-water value and ΔP_{TPF} for helium-water is about 7% lower as opposed to 73% and 28% respectively when V_{SL} = 1.03 ft/sec.
- For high water flow rates (V_{SL}>13.89 ft/sec), the effect of ρ_G on ΔP_{TPF} is not apparent.

In summary then, at low liquid flow rates and moderate to high gas flow rates, the gas phase density affects the two-phase frictional pressure drop in such a way that the higher the gas density the higher is the frictional pressure drop; further, this effect is more pronounced at the lower liquid rates and increases with increasing the superficial gas velocity. At high liquid flow rates, on the other hand, there is almost no such effect of ρ_G on ΔP_{TPF}.

From Fig. 5.11, it appears that it is not just the gas-phase density that affects the frictional pressure drop as it can be seen from the curves for low liquid flow rates, that there is almost no effect of the gas density on ΔP_{TPF} at the lower gas velocities; however for the same liquid flow rate and higher gas velocities, the effect is significant. The flow quality appears to be an important parameter in determining the onset of such effect. Considering all

data, no effect of ρ_G on P_{TPF} was observed for values of quality below approximately 0.001; further, the effect increased with increasing quality. A reasonable description of the variation of ΔP_{TPF} with gas density could probably be obtained by relating this variation to the density of the two-phase mixture (which is determined from the flow quality as given by Eq. (5.10)). If one considers the air-water mixture as a reference, a plot of the ratio of ΔP_{TPF} for a particular gas-water mixture to that for air-water at same V_{SL} and V_{SG} (these were taken from the smoothed curves in Fig. 5.11) against the ratio of the gas-water density to air-water density at the same conditions (same V_{SL} and V_{SG}), would appear as shown in Fig. 5.12.

Examination of Fig. 5.12 indicates that the density of the two-phase mixture is perhaps the important parameter affecting the frictional pressure drop. For all data at low V_{SL} and V_{SG}, and at high V_{SL} and all values of V_{SG}, the ratios of the mixture densities were equal or very close to one and so were the ratios of frictional pressure drops. For data at the two lower water rates and high values of V_{SG}, the density ratios differed from one and so did the ratios of ΔP_{TPF} (being higher than one for Freon-water and less than one for helium-water).

5.4.2 Comparison of ΔP_{TPF} Data with Some Correlations

A large number of correlations exist in the literature for the prediction of the frictional pressure drop in two-

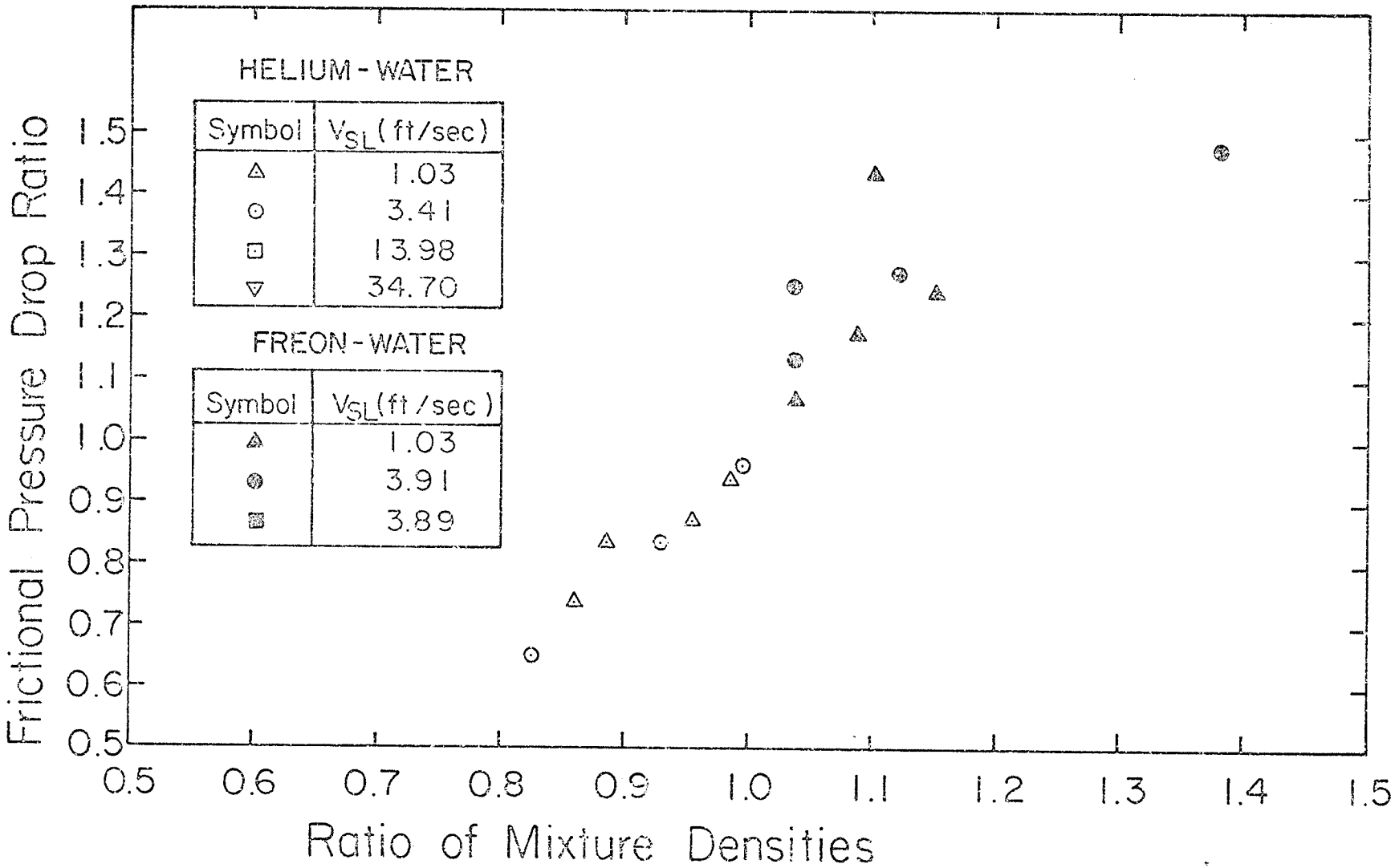

Fig. 5.12 Effect of Mixture Density on ΔP_{TPF}

phase flows. Govier and Aziz [34] recommend six correlations and claim that the Ros correlation [72,26] is probably the best general empirical correlation. In reference [5], on the other hand, eight methods for predicting P_{TPF} together with the criteria for selecting any one method are recommended. Many of the recommended methods are complicated multi-curve graphical correlations. In this section, the simplest three correlations recommended in the literature are tested against the present data. These are the method of the Homogeneous Flow Model [5] , the Lockhart-Martinelli correlation [62,45] and the Chisholm correlation [5,18]. The results of the test are given below. The correlations are discussed in detail and the calculation procedures are given in Appendix E.

(i) Homogeneous Flow Model [5]

In this model, the two phases are assumed to flow as a homogeneous mixture with a Reynolds number based on the total mass velocity, the tube diameter and the viscosity of the mixture. The frictional pressure drop can then be calculated in the same manner as for single-phase flow. Different expressions for the mixture properties have been tested [90], and the best agreement between the data and the predictions

was obtained when the expressions listed below for density and viscosity were used.

$$\mu_{MIX} = \mu_L \quad , \tag{5.9}$$

$$\rho_{MIX} = \left[\frac{x}{\rho_G} + \frac{(1-x)}{\rho_L}\right]^{-1} \tag{5.10}$$

The results of the comparison are shown in Fig. 5.13 and are summarized in Table 5.3.

(ii) Lockhart-Martinelli Correlation [62,45]

In this method, the authors [62] presented graphical correlations in the forms of plots of ϕ_G^2 and ϕ_L^2 against X^2 where:

$$\phi_G^2 = \Delta P_{TPF} \; / \; (\Delta P_{SPF})_G \quad , \tag{5.11}$$

$$\phi_L^2 = \Delta P_{TPF} \; / \; (\Delta P_{SPF})_L \quad , \tag{5.12}$$

$$X^2 = (\Delta P_{SPF})_L \; / \; (\Delta P_{SPF})_G \tag{5.13}$$

where $(\Delta P_{SPF})_L$ and $(\Delta P_{SPF})_G$ are the frictional pressure drops for the liquid and gas respectively if they were flowing alone in the tube. Hewitt et al. [45] fitted polynomial equations to the Lockhart-Martinelli correlations (these are given in Appendix E); these were used here to test the present data. The results of the test are shown in Fig. 5.14 and are summarized in Table 5.3.

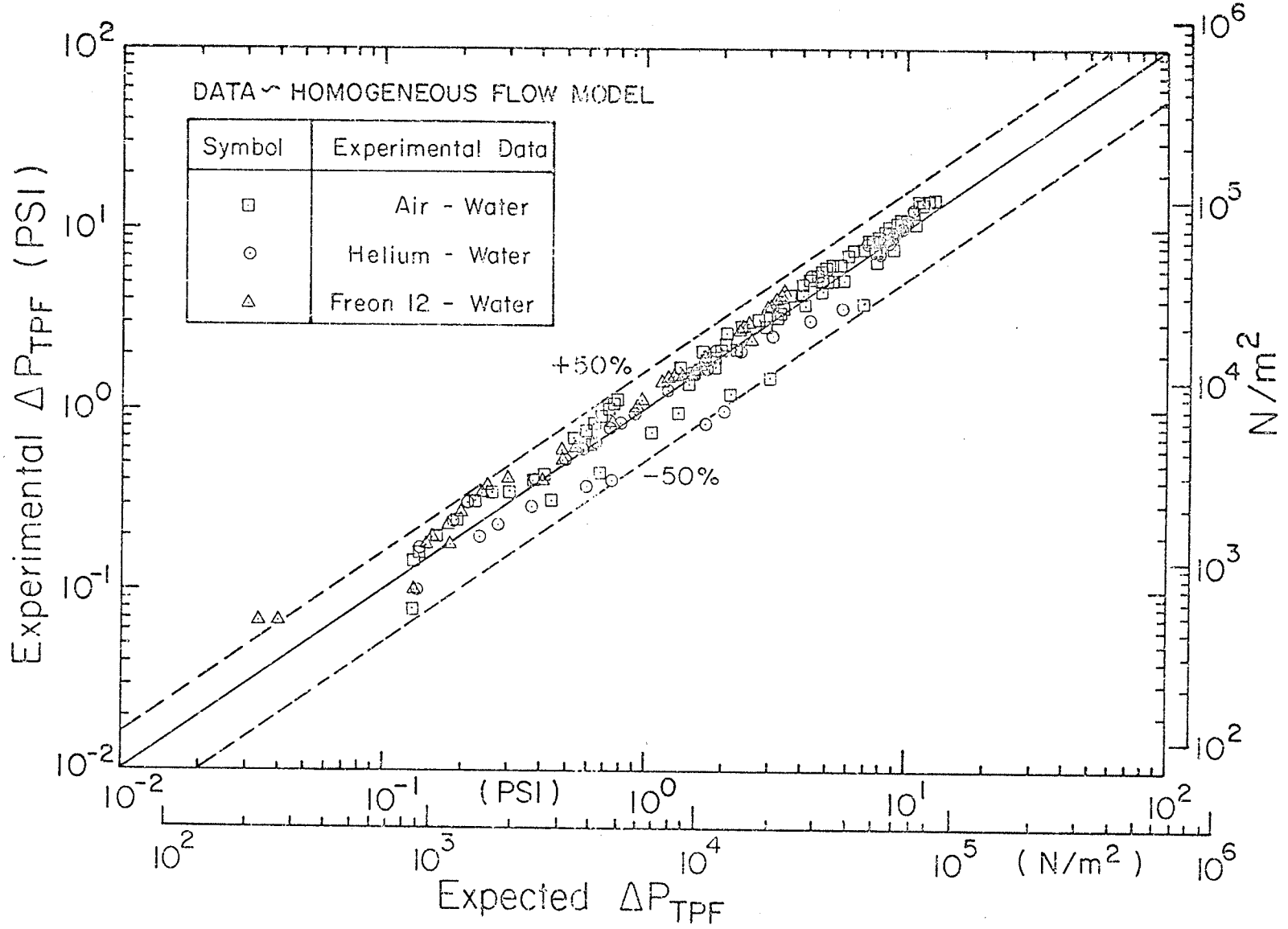

Fig. 5.13 Comparison of Experimental ΔP_{TPF} with the Homogeneous-Flow Model

Fig. 5.13

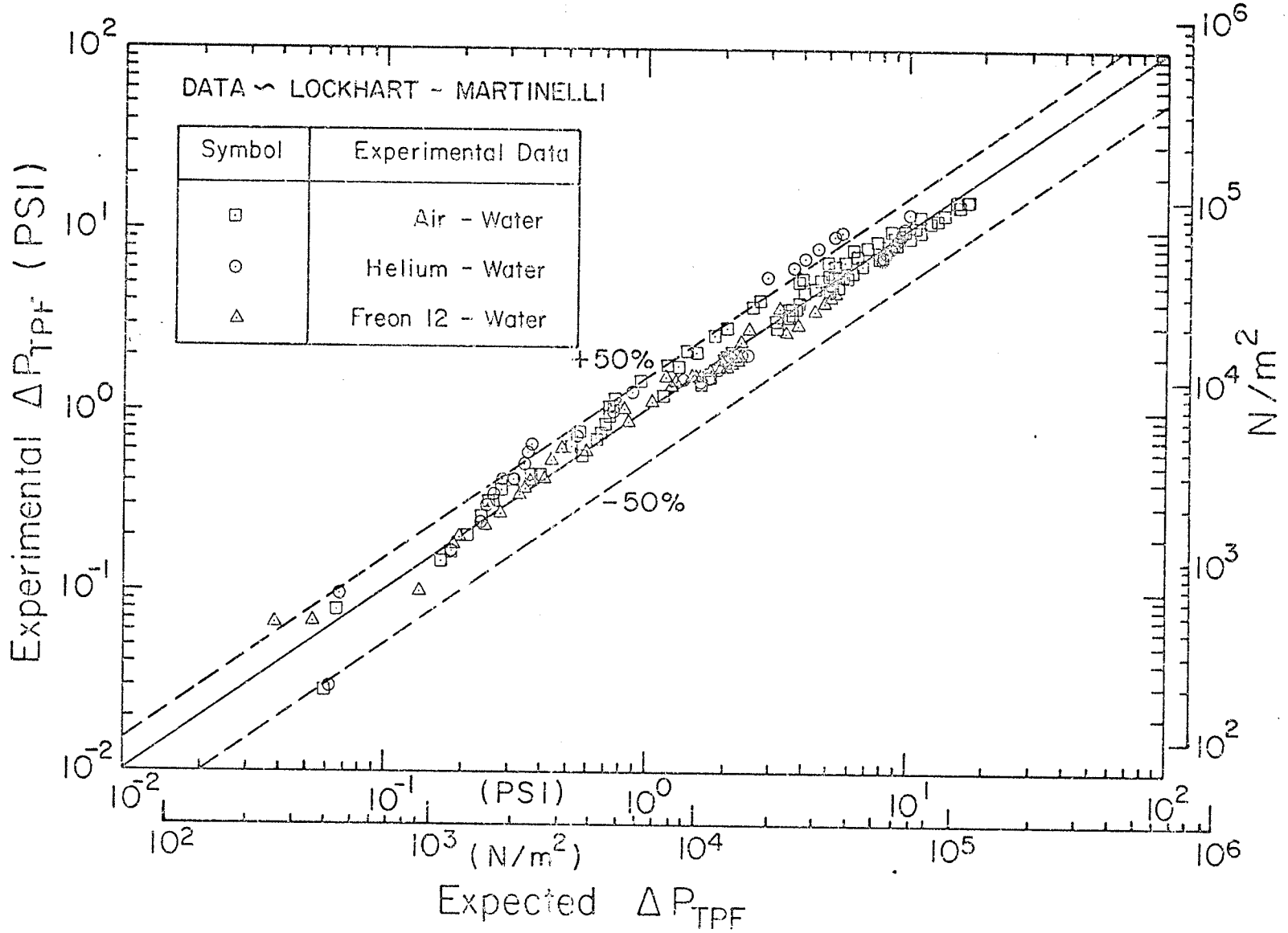

Fig. 5.14 Comparison of Experimental ΔP_{TPF} with the Lockhart-Martinelli Correlation.

(iii) Chisholm Correlation [5,18]

This correlation is a modification of the Lockhart-Martinelli correlation; the frictional pressure drop is given by

$$P_{TPF} = \phi^2_{LO} \left(P_{SPF} \right)_{LO} \qquad (5.14)$$

where the subscript "LO" refers to liquid phase flowing alone at a mass flow rate equals to the total mass flow rate of the two-phase mixture and ϕ^2_{LO} is defined in terms of a function similar to X^2 as given in Appendix E. The results of the comparison between the present data and Eq. (5.14) are shown in Fig. 5.15 and are summarized in Table 5.2.

Examination of Figs. 5.13, 5.14 and 5.15 and Table 5.3 with consideration that an impirical correlation for α was used which might influence the frictional pressure drop values, shows that the agreement between the data and the correlation is quite satisfactory. The homogeneous flow theory and the Lockhart-Martinelli correlation provided better predictions than the Chisholm Correlation as 96% and 87% of the data points agree within $\pm$50% with the first and second methods respectively.

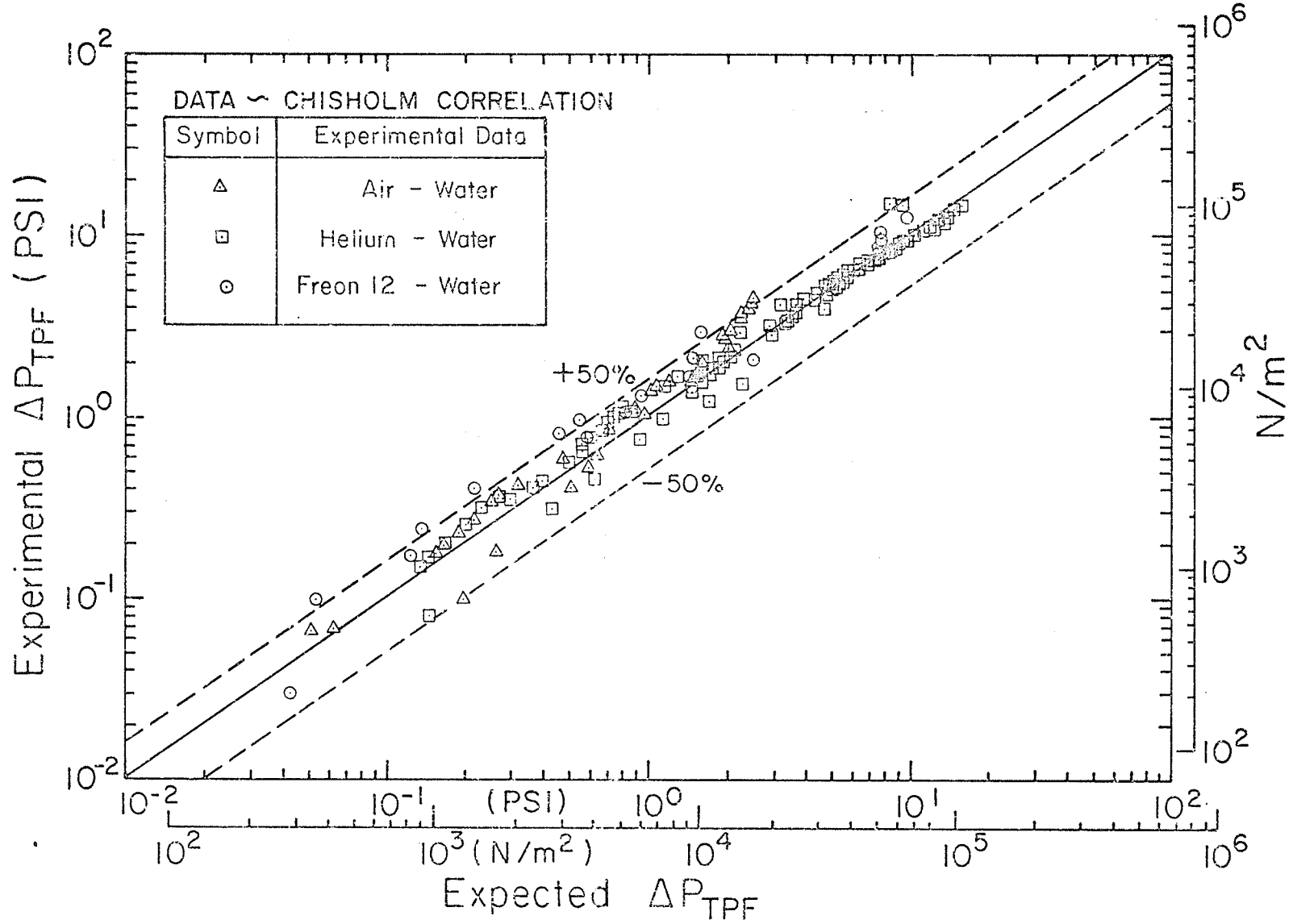

Fig.5.15

Fig.5.15 Comparison of Experimental ΔP_{TPF} with Chisholm Correlation

Table 5.3 Results of Correlation of Frictional Pressure Drop Data

Method of Correlation	Range of Deviations	Number of Data points (% of Total N) lying in the specified Range of Deviations				Comments
		Air-Water (N=105)	Helium-Water (50)	Freon-Water (37)	Complete Set (192)	
Homogeneous Flow Model	±20% ±30% ±40% ±50%	66.7 86.7 95.2 99	60 72 80 86	59.5 89.2 94.6 100	63.5 83.3 91.1 95.8	The agreement is excellent. $\bar{e}$ = 6.1% $\bar{e}'$=23.4%
Lockhart-Martinelli	±20% ±30% ±40% ±50%	75.2 81.9 91.4 99	32 38 46 50	78.4 100	64.6 74 81.3 86.5	The agreement is very good $\bar{e}$ = 20.2% $\bar{e}'$ = 51%
Chisholm	±20% ±30% ±40% ±50%	77.1 89.5 96.2 98.1	22 30 36 38	37.8 59.5 78.4 83.8	55.2 68.2 77.1 79.7	The agreement is fair $\bar{e}$ = 38.6% $\bar{e}'$ = 83.9%

CHAPTER 6

PRESENTATION AND DISCUSSION OF HEAT-TRANSFER RESULTS

6.1 Introductory Remarks

This chapter deals with the heat-transfer results of the present investigation. First, the single-phase results are presented and compared with the well-known theories and correlations. Then the two-phase heat-transfer data are presented and discussed. The local heat-transfer raw data are then correlated by means of the modified Spalding theory [81,90]. The mean heat-transfer data are then compared with some of the existing correlations. A simple method to correlate the mean heat-transfer data is then developed and tested for generaltiy. The mean heat-transfer data are then correlated in terms of the frictional pressure drop [31,90] and a general correlation of this nature is proposed. The data are then correlated in terms of the Martinelli parameter X_{tt} as proposed, for instance, by Collier and Pulling [21] for boiling. Finally there is a short discussion on possible future work.

The present data are tabulated in Appendix H. The equations and correlations employed in this chapter are discussed either in Appendix E or in Chapter 2. An error analysis of the results is given in Appendix I.

6.2 Single-Phase Heat-Transfer Results

In earlier work conducted on the present experimental facility [90], the apparatus was proven to be reliable. In the present investigation, however, it was necessary to ensure

that the apparatus continued to perform satisfactorily. This was effected in part by taking single-phase heat-transfer data and comparing them with the well-known theories and correlations, and in part by comparing the present two-phase, air-water results with the previous air-water results obtained from the same apparatus [90].

This section presents the results of the single-phase heat-transfer study. First the local data are presented and compared with the theories of Worsoe-Schmidt [95] and Seigel et al.[75] for laminar flow, and with the Spalding [81] theory for turbulent flow. Special attention is given to the theory of Spalding because a modified form of this theory was recommended [90] and is further tested here to correlate the two-phase local heat-transfer results. The mean heat-transfer data are then compared with the empirical correlation recommended by Kays [54] for turbulent flow, and with the semi-theoretical solution [6] for laminar flow.

6.2.1 Local Heat-Transfer Coefficients

As discussed in Appendix D, the local heat-transfer coefficients were measured at seven locations along the heated test section. The results are shown in Fig. 6.1 where h_{SP} is plotted as a function of the location Z with the water Reynolds number as a parameter. The h_{SP} - Z profiles shown in Fig. 6.1 have the same shapes as predicted by the theories.

The laminar-flow data were tested against the following theories:

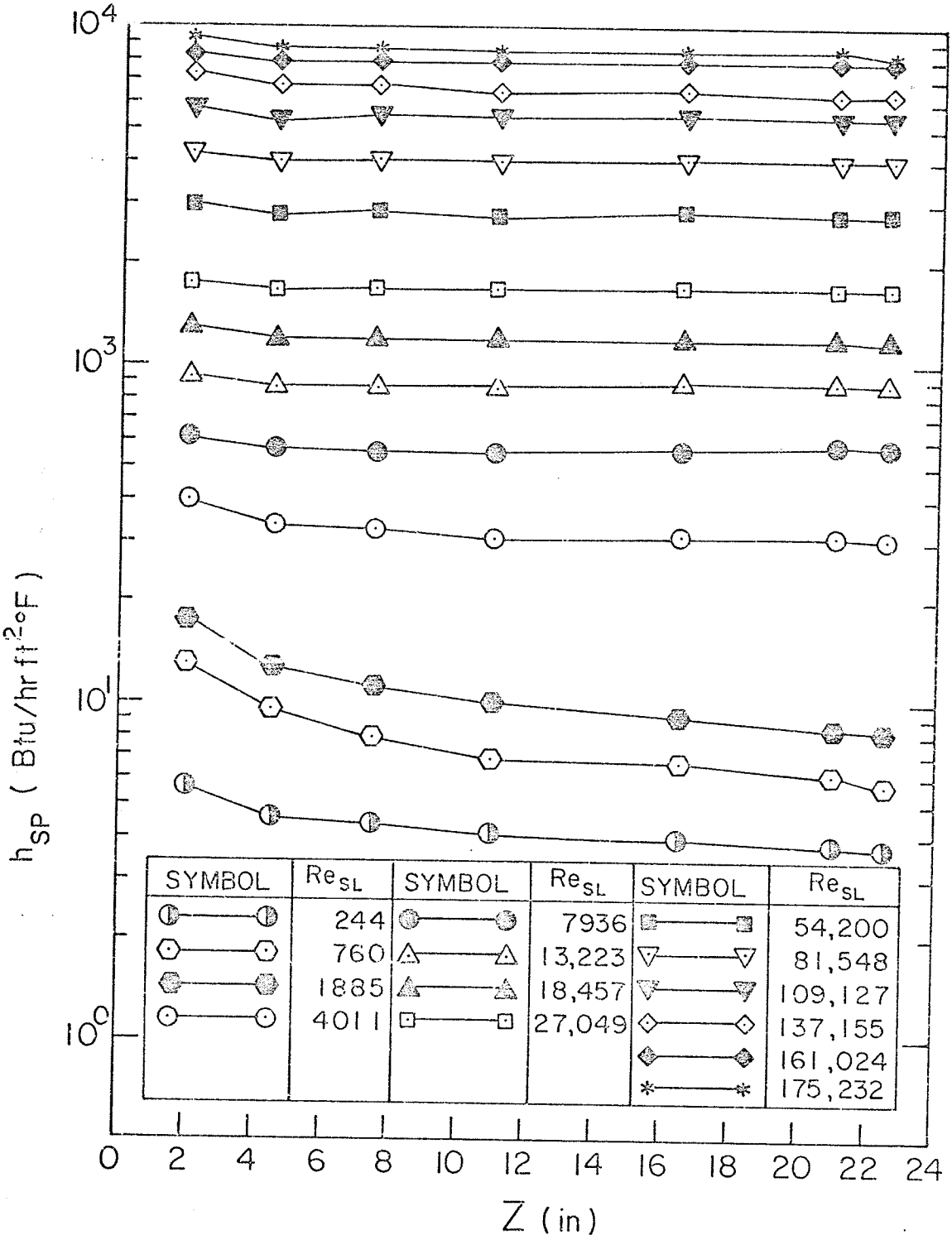

Fig. 6.1 Single-Phase Local Heat-Transfer Raw Data

(i) Worsoe - Schmidt [95]

The solution was performed numerically and was presented in the original paper in the form of tables listing the values of Nu_{SP} as a function of $\bar{Z}$, where

$$\bar{Z} = 4(Z/D)/Re_{SL}Pr_L \qquad (6.1)$$

(ii) Seigel et al. [75]

This solution was presented in the form of an infinite series as follows:

$$Nu_{SP}(Z') = [\frac{11}{48} - \frac{1}{2}\sum_{m=1}^{\infty} \frac{\exp(-\gamma_m^2 Z')}{A_m \gamma_m^4}] - 1 \qquad (6.2)$$

where Z' is a dimensionless axial distance given by

$$Z' = 2(Z/D)/Re_{SL}Pr_L = \bar{Z}/2; \qquad (6.3)$$

the values of A_m and γ_m are given in Appendix E (Table E.1).

For turbulent flow, the data were compared against the theory of Spalding [81] which may be represented by

$$S_q(Z^+) = \{[\frac{Pr_L/Pr_T}{6.64(Z^+/Pr_T)^{1/9} + P_{FN}}]^4 + [0.651\ (Z^+/Pr_L)^{-1/3}]^4\}^{1/4} \qquad (6.4)$$

where, $S_q(Z^+)$ is the Spalding function given by

$$S_q(Z^+) = Nu_{SP}(Z)/Re_{SL}(f_{SP}/2)^{1/2}, \qquad (6.5)$$

$$Z^+ = (Z/D)Re_{SL}(f_{SP}/2)^{1/2}, \qquad (6.6)$$

Pr_T is the turbulent Prandtl number recommended by Spalding to have the value 0.887;

P_{FN} is the P-function given by

$$P_{FN} = 11.570[(Pr_L/Pr_T)^{3/4}-1] \qquad (6.7)$$

The results of the comparison for both laminar and turbulent flow are shown in Fig. 6.2 and are summarized in Table 6.1. For turbulent flow, the agreement between the data and Eq. (6.4) is excellent; for laminar flow, the agreement is good. In Fig. 6.2, only the theoretical line of Worsoe-Schmidt is shown because it was difficult to distinguish between this line and that of Seigel et al.

TABLE 6.1

Comparison of h_{SP} Data with Existing Theories (81,75,95)

Type of Flow	Theory of	No. of Data Points	$\bar{e}$	$\bar{e}'$
Turbulent	Spalding, Eq.(6.4)	77	0.44	4.43
Laminar	Worsoe-Schmidt Seigel et al., Eq. (6.2)	28	3.01	13.22

It should be noted that the above theories were developed for isothermal constant-property flow; however, they were applied to test the present data without any modi-

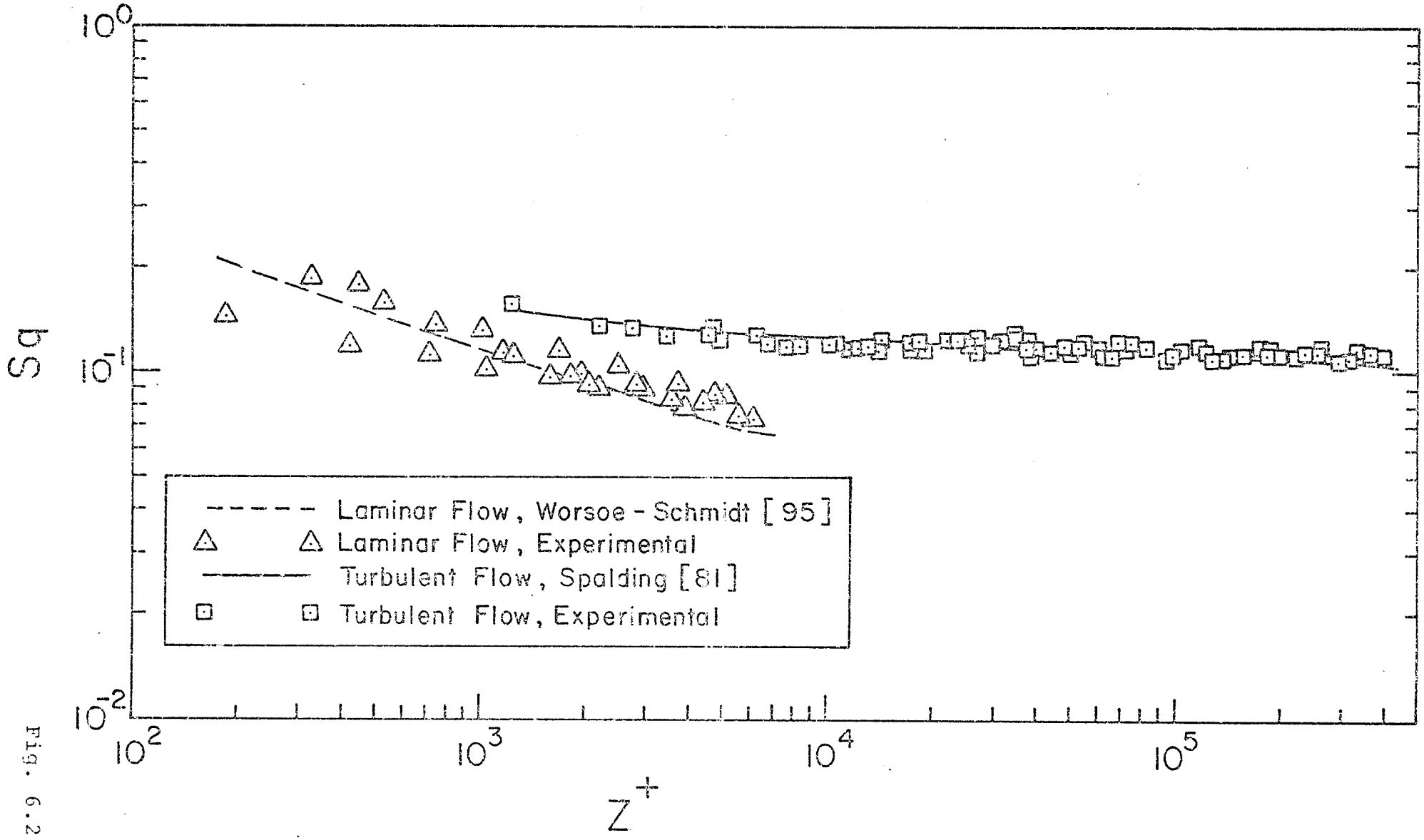

Fig. 6.2

Fig. 6.2 Comparison of Single-Phase Local Heat Transfer Data with Some Existing Theories

fication to accommodate the property variation. This is because the method of correction is not known (this correction has been done when the mean results were tested because the correction method in this case is well known). The property gradients in the present experiment, however, were small as the temperature differences between the wall and the bulk were of the order of 15°F.

6.2.2. Mean Heat-Transfer Coefficients

As discussed in Appendix D, the over-all length-mean heat-transfer coefficients were calculated from the measured local values using the following expression:

$$\bar{h}_{SP} = \frac{1}{\Delta L} \int_{L_1}^{L_2} h_{SP} \, dZ \tag{6.8}$$

where ΔL is the length of the heated test section over which the average heat-transfer coefficients are calculated.

The mean heat-transfer data were tested against the well-established correlations as discussed below.

(i) Laminar Flow

The following semi-theoretical correlation is recommended [6] to correlate the mean heat-transfer coefficients in laminar flow:

$$\bar{Nu}_{SP} = 1.615 \, (Re_{SL} \, Pr_L \, D/L)^{1/3} \tag{6.9}$$

Equation (6.9) is applicable for laminar flow of a constant-property fluid; in the present study, the variations

in the water properties in the radial direction were small (the temperature difference between the wall and the bulk was typically 15°F); however, Eq. (6.9) was modified to accommodate the property variation by using the well-known Sieder and Tate [78] type of viscosity correction term becoming

$$\bar{Nu}_{SP} = 1.615(Re_{SL}\ Pr_L\ D/L)^{1/3}\left(\frac{\mu_L}{\mu_W}\right)^{0.14} \tag{6.10}$$

The data were tested against Eq. (6.10); the results of the comparison are shown in Fig. 6.3; F^* in the ordinate of Fig. 6.3 is given by

$$F^* = (Pr_L\ D/L)^{1/3}(\mu_L/\mu_W)^{0.14} \tag{6.11}$$

The results are also summarized in Table 6.3 illustrating the good agreement between the data and Eq. (6.10).

TABLE 6.2

Comparison of Laminar Flow $\bar{h}_{SP}$ Data With Eq. (6.10)

Re_{SL}	Pr_L	$\left(\frac{\mu_L}{\mu_W}\right)$	$\bar{Nu}_{SP}$	
			Experimental	Eq. (6.10)
244	6.52	1.161	4.62	5.43
760	5.95	1.301	8.22	7.95
1371	6.54	1.202	11.22	9.71
1885	6.35	1.196	11.52	10.69
			$\bar{e}$	2.95%
			$\bar{e}'$	11.59%

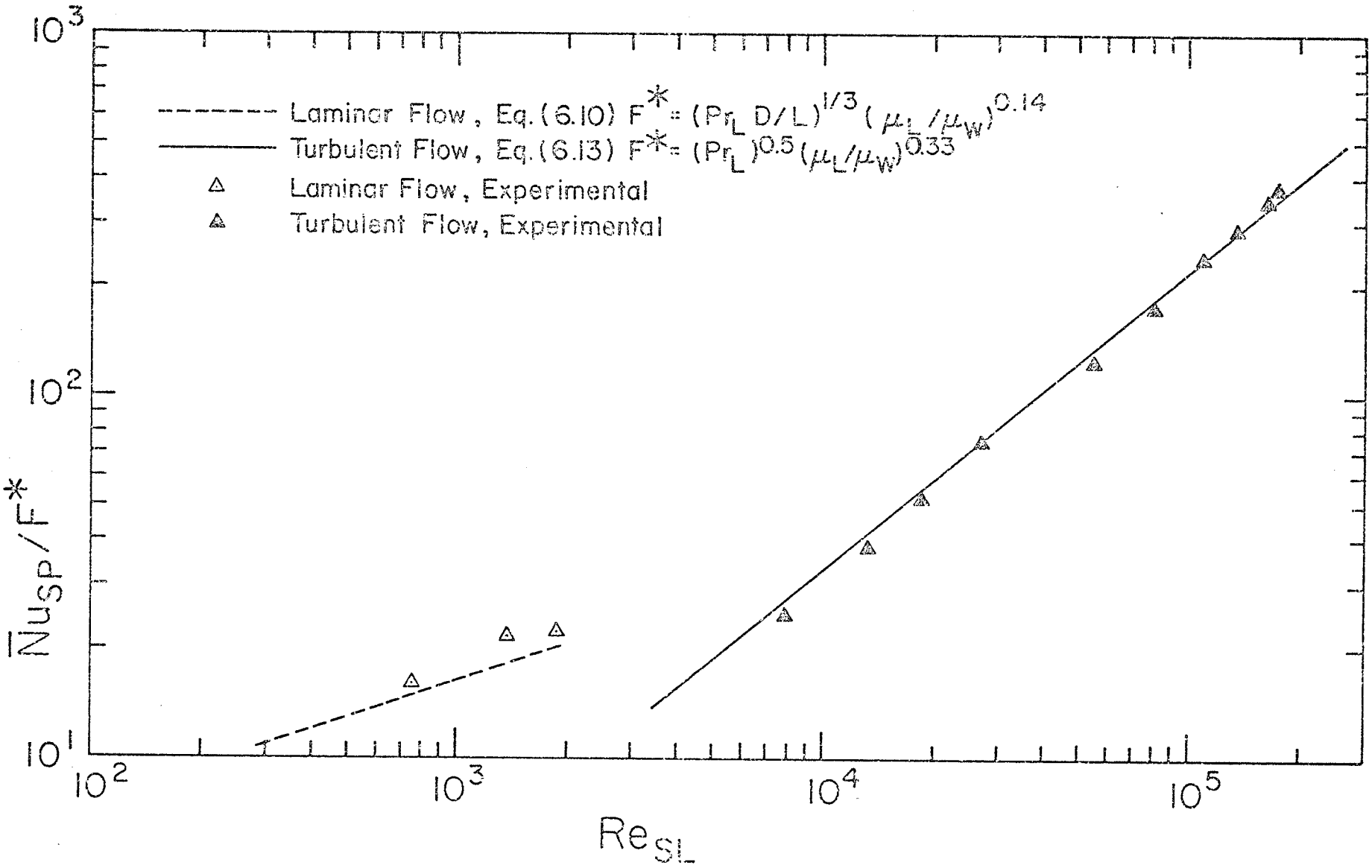

Fig. 6.3 Comparison of $\overline{h}_{SP}$ Data Against Some Existing Correlations

(ii) Turbulent Flow

The following correlation recommended by Kays [54] is applicable for turbulent flow of a constant-property fluid:

$$\bar{Nu}_{SP} = 0.0155(Re_{SL})^{0.83}\ (Pr_L)^{0.5} \tag{6.12}$$

As for laminar flow, Eq. (6.12) was modified to accommodate for the property variation as follows:

$$\bar{Nu}_{SP} = 0.0155(Re_{SL})^{0.83}(Pr_L)^{0.5}\left(\frac{\mu_L}{\mu_W}\right)^{0.33} \tag{6.13}$$

The data were compared with Eq. (6.13) and the results are shown in Fig. 6.3 where F^* is given by

$$F^* = (Pr_L)^{0.5}\ (\mu_L/\mu_W)^{0.33} \tag{6.14}$$

The deviations obtained are as follows:

$$\bar{e} = -5.89\%\ ,\ \bar{e}' = 7.97\%$$

From the material presented in this section, it is concluded that the apparatus continues to function properly and that the results obtained in the present investigation are reliable and comparable to the previous results obtained earlier from the same experimental facility [90].

6.3. Presentation of Two-Phase Heat-Transfer Results

In this section, the local and mean two-phase heat-transfer raw data of the present experiments are presented. As discussed earlier, it was necessary to check on the

repeatability of the results and the performance of the apparatus before collecting the new set of data, that is, the data with gases other than air. Therefore, the air-water experiments were performed first and the mean heat-transfer data of these experiments were compared with the data previously obtained from the same apparatus [90]. The results of the comparison are shown in Fig. 6.4 where $\bar{h}_{TP}$ is plotted against V_{SG} with V_{SL} as a parameter. The figure illustrates the good agreement between the present and the previous results for air-water flow (the previous results [90] are repeated with a maximum deviation of 9.30%).

From the above discussion and the material presented in Section 6.2, it is concluded that the results reported in this work are reliable; further, the previously reported results [90] and the present results can form together one set of data which cover the widest range of variables studied so far.

6.3.1. Local Heat-Transfer Data

The local values of the heat-transfer coefficient h_{TP} were calculated by the procedure discussed in Appendix D. The data are presented in Figs. 6.5(A to H), 6.6(A to D) and 6.7(A to C) for air-water, helium-water and Freon 12-water respectively. In each figure, h_{TP} is plotted as a function of the distance Z from the start of the heated tube for a fixed superficial water velocity with the superficial gas velocity as a parameter. It should be noted

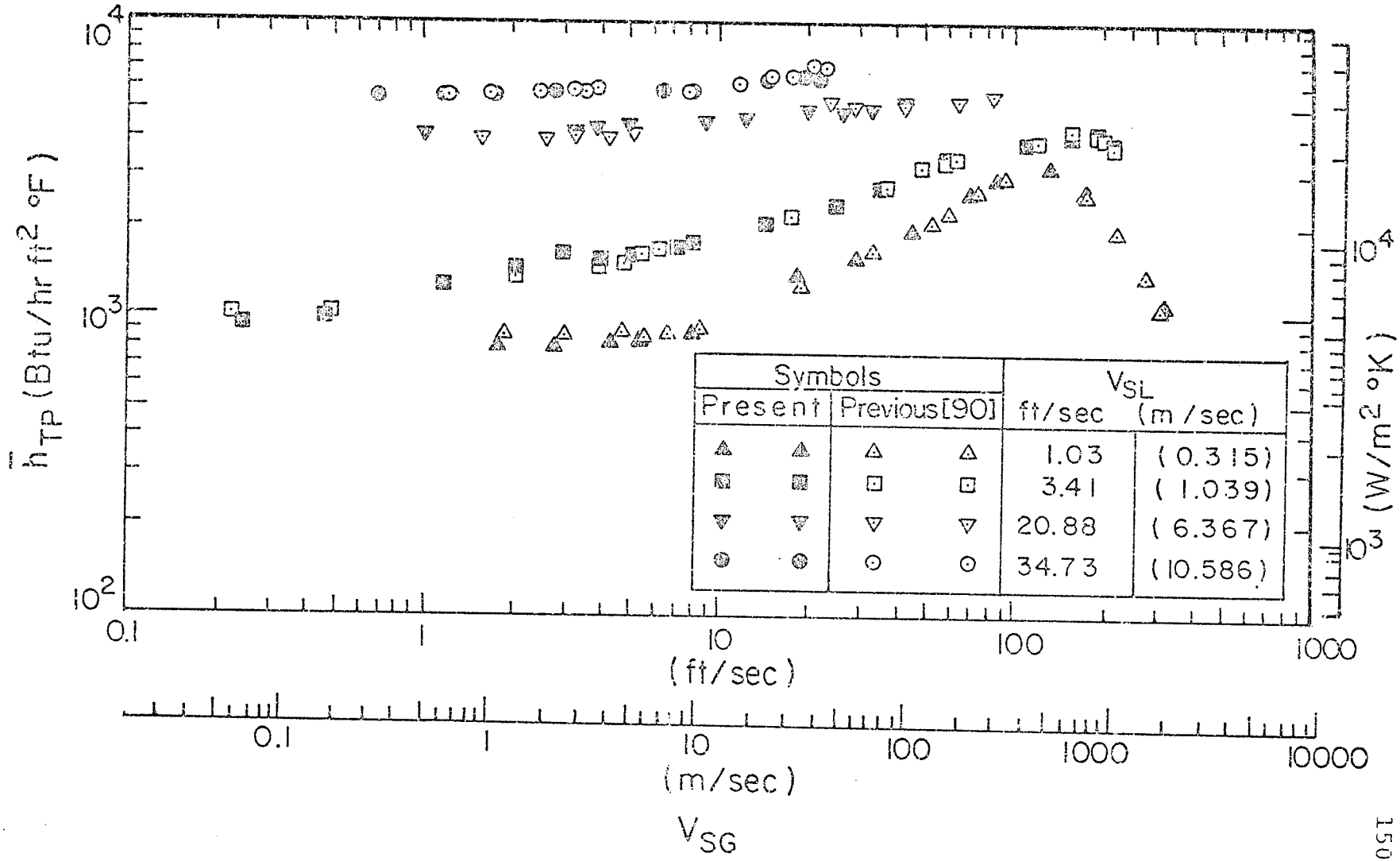

Fig. 6.4 Comparison of Air-Water $\bar{h}_{TP}$ Data with the Data of Vijay

Fig. 6.4

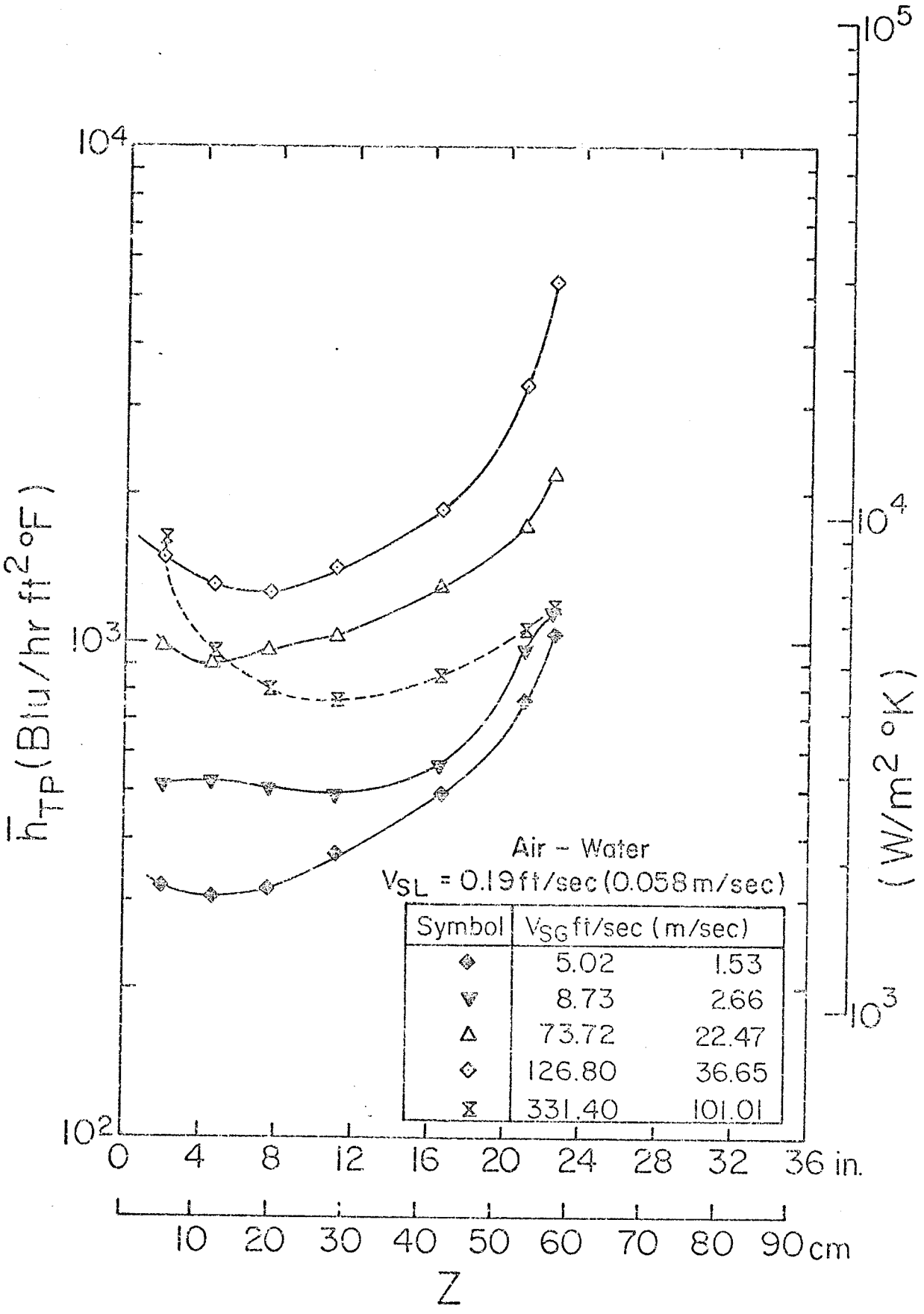

Fig.6.5A Two-Phase Air - Water Local Heat-Transfer Data

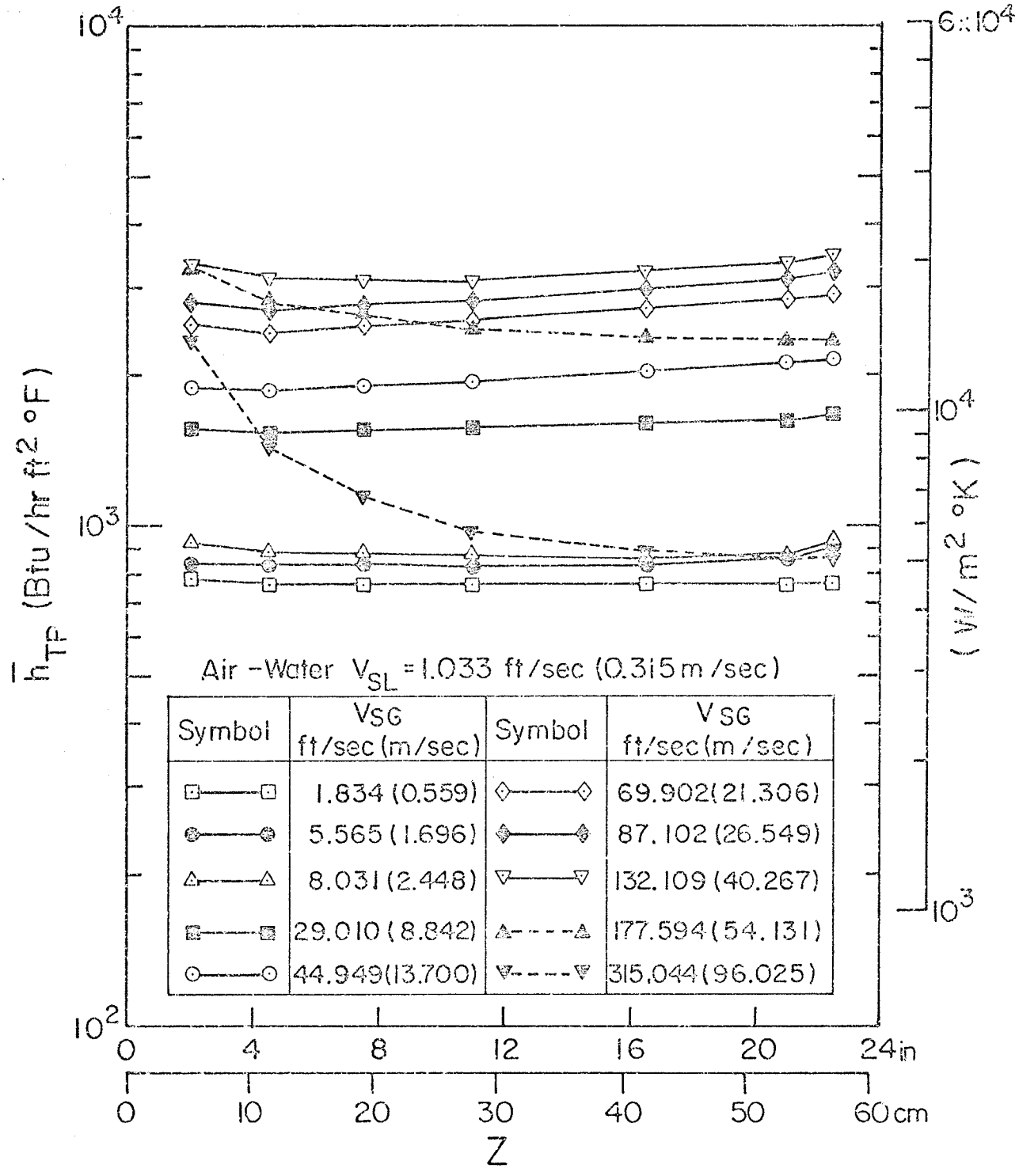

Fig. 6.5B Two-Phase Air-Water Local Heat-Transfer Data

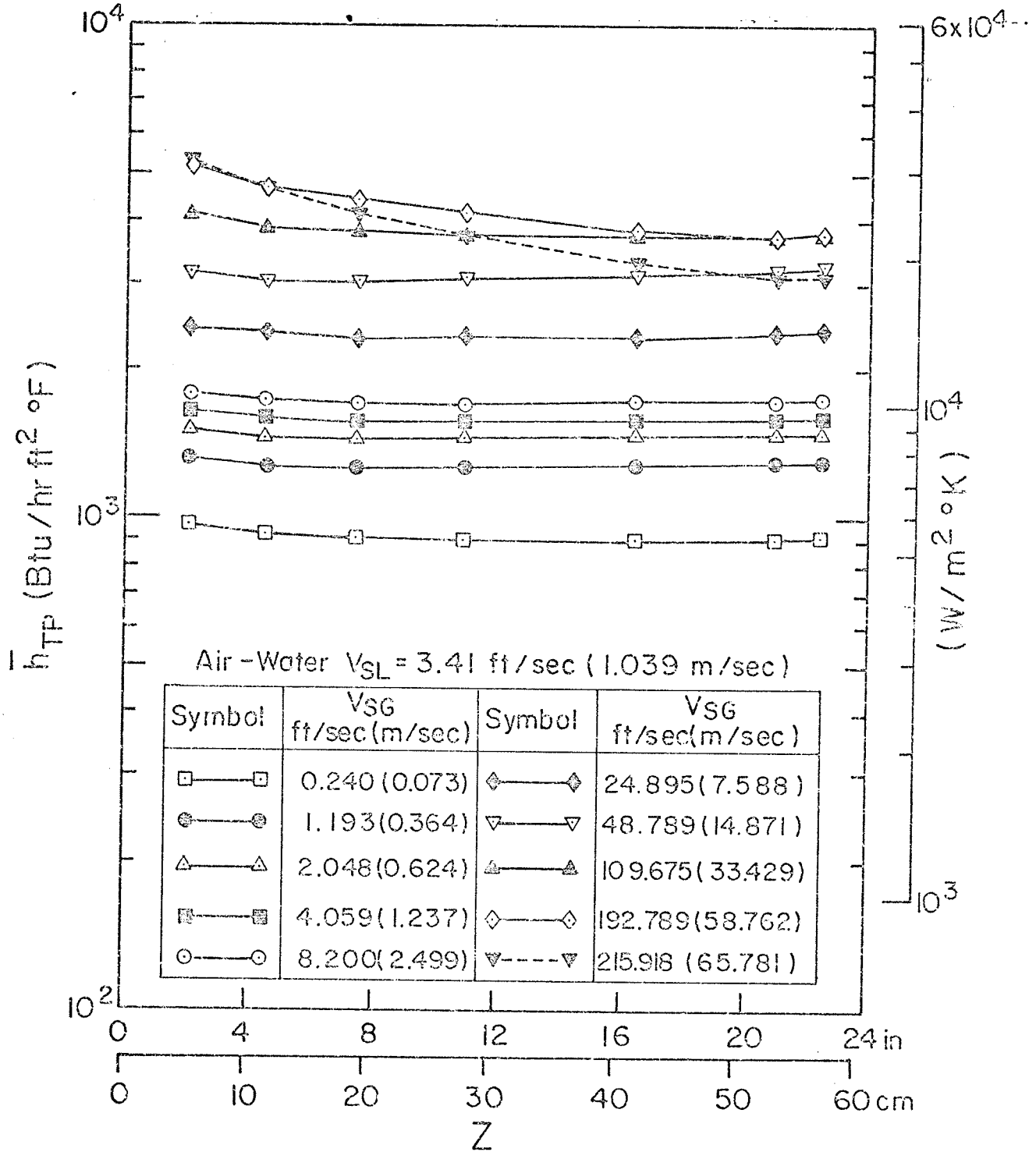

Fig.6.5C Two-Phase Air-Water Local Heat-Transfer Data

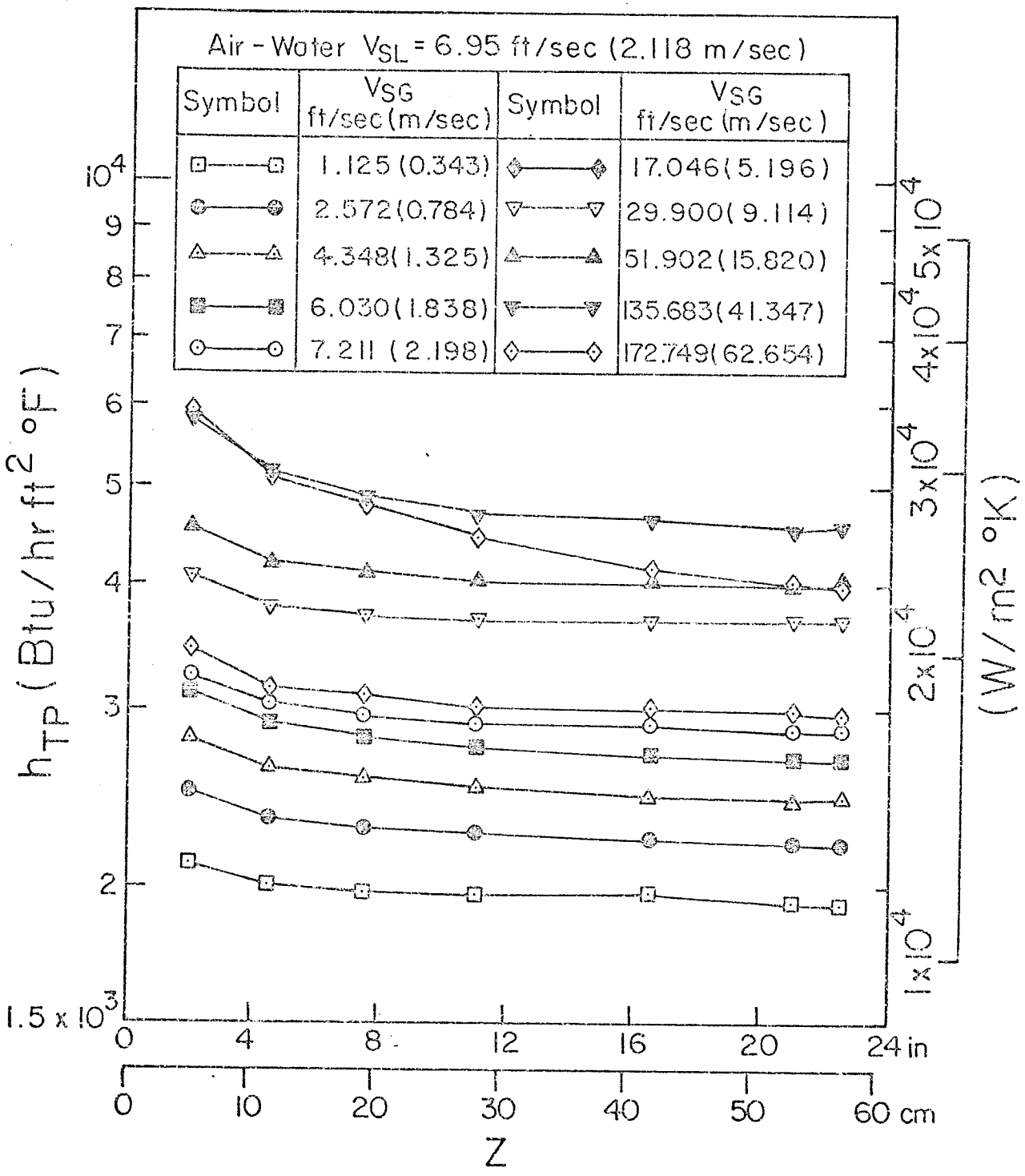

Fig. 6.5D Two-Phase Air-Water Local Heat-Transfer Data

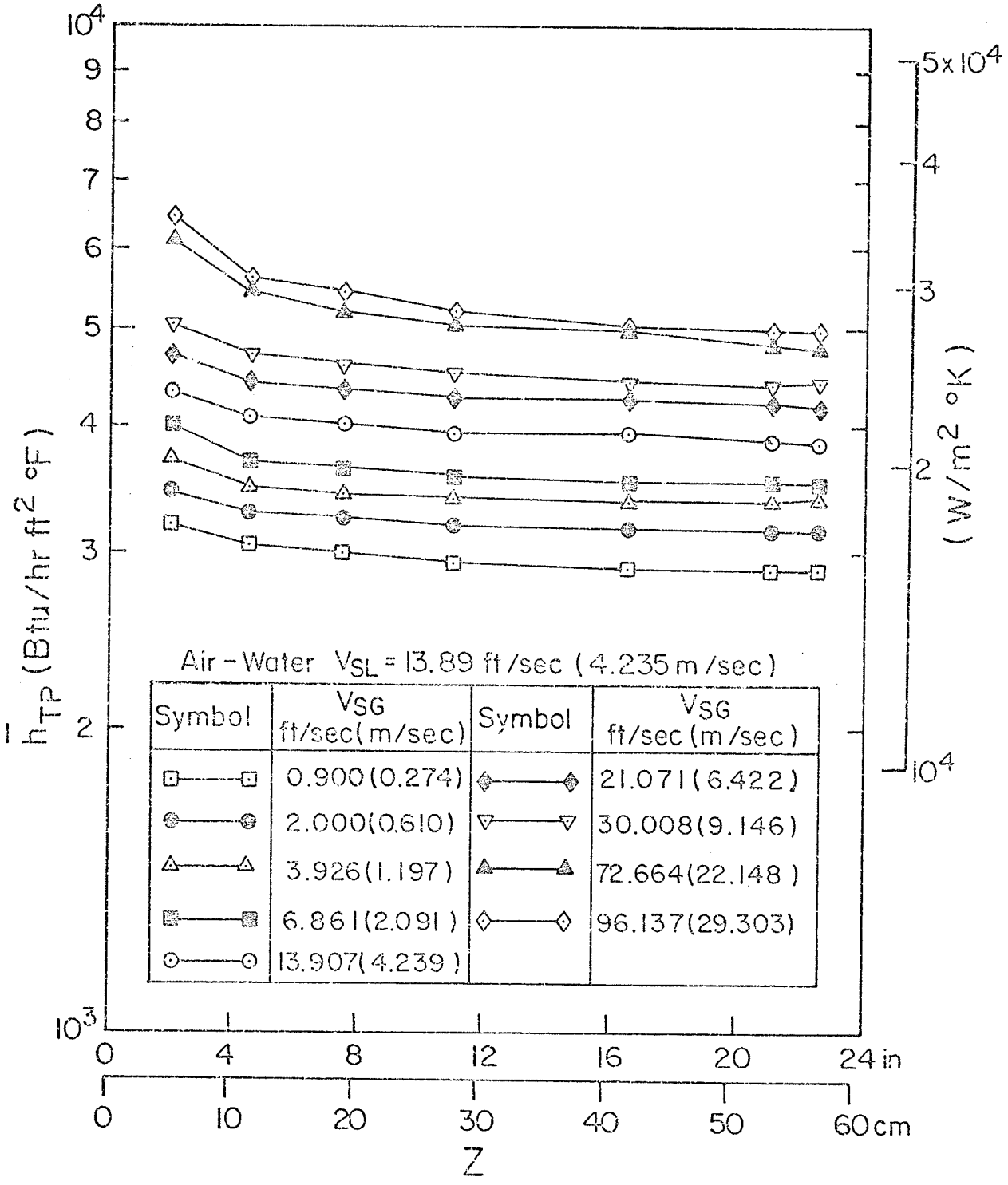

Fig. 6.5E Two-Phase Air-Water Local Heat-Transfer Data

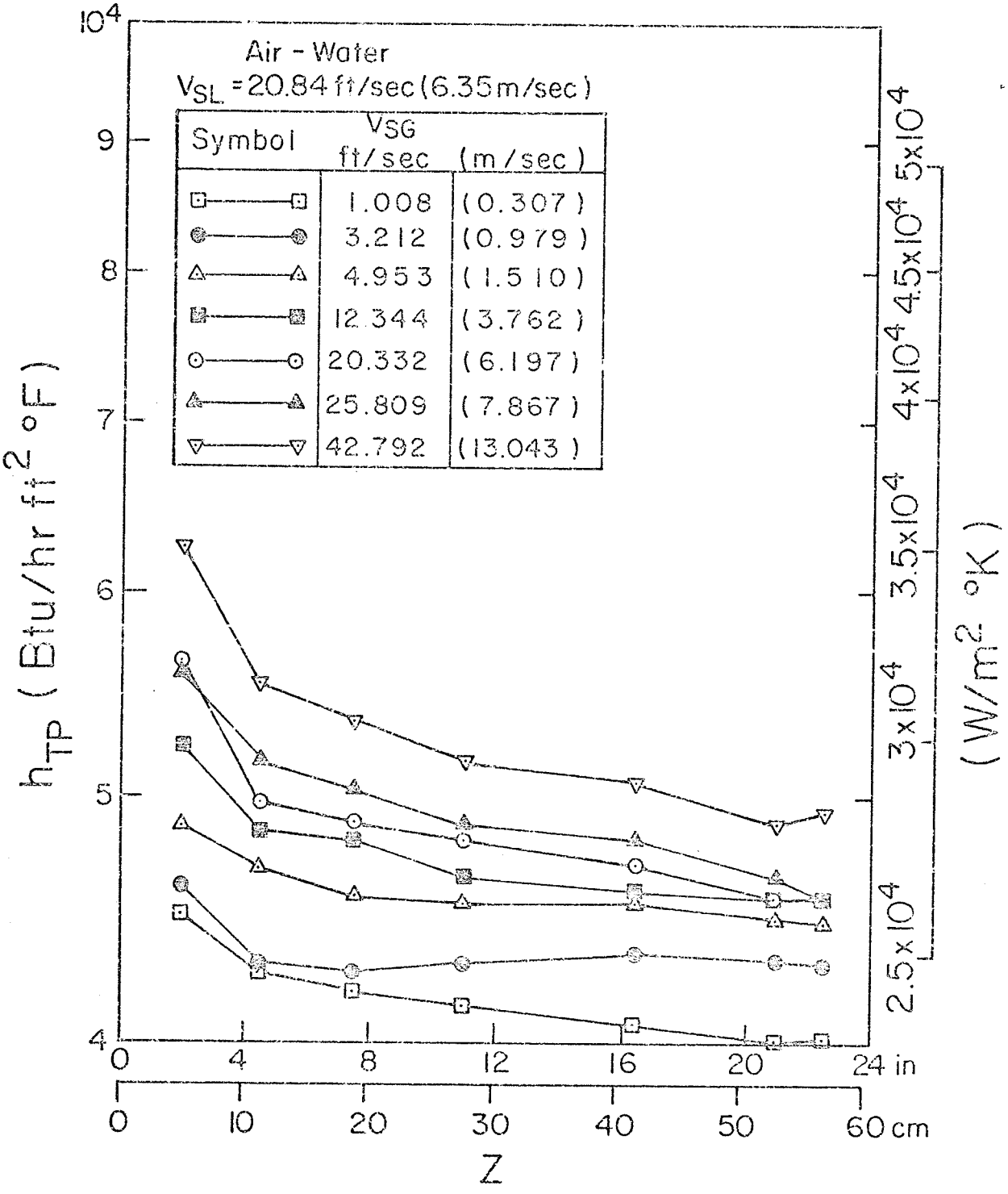

Fig. 6.5F Two-Phase Air Water Local Heat-Transfer Data

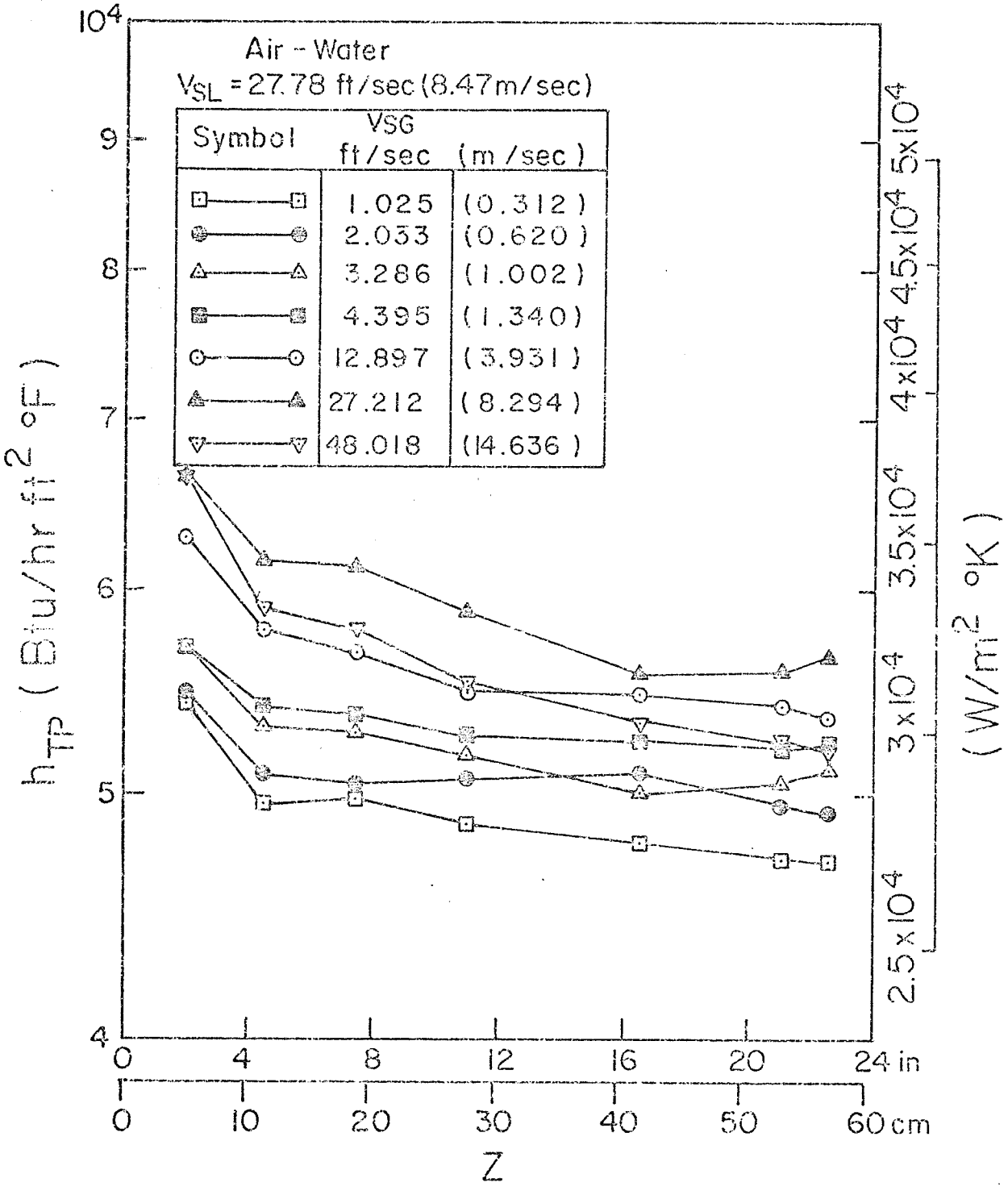

Fig. 6.5G Two-Phase Air-Water Local Heat-Transfer Data

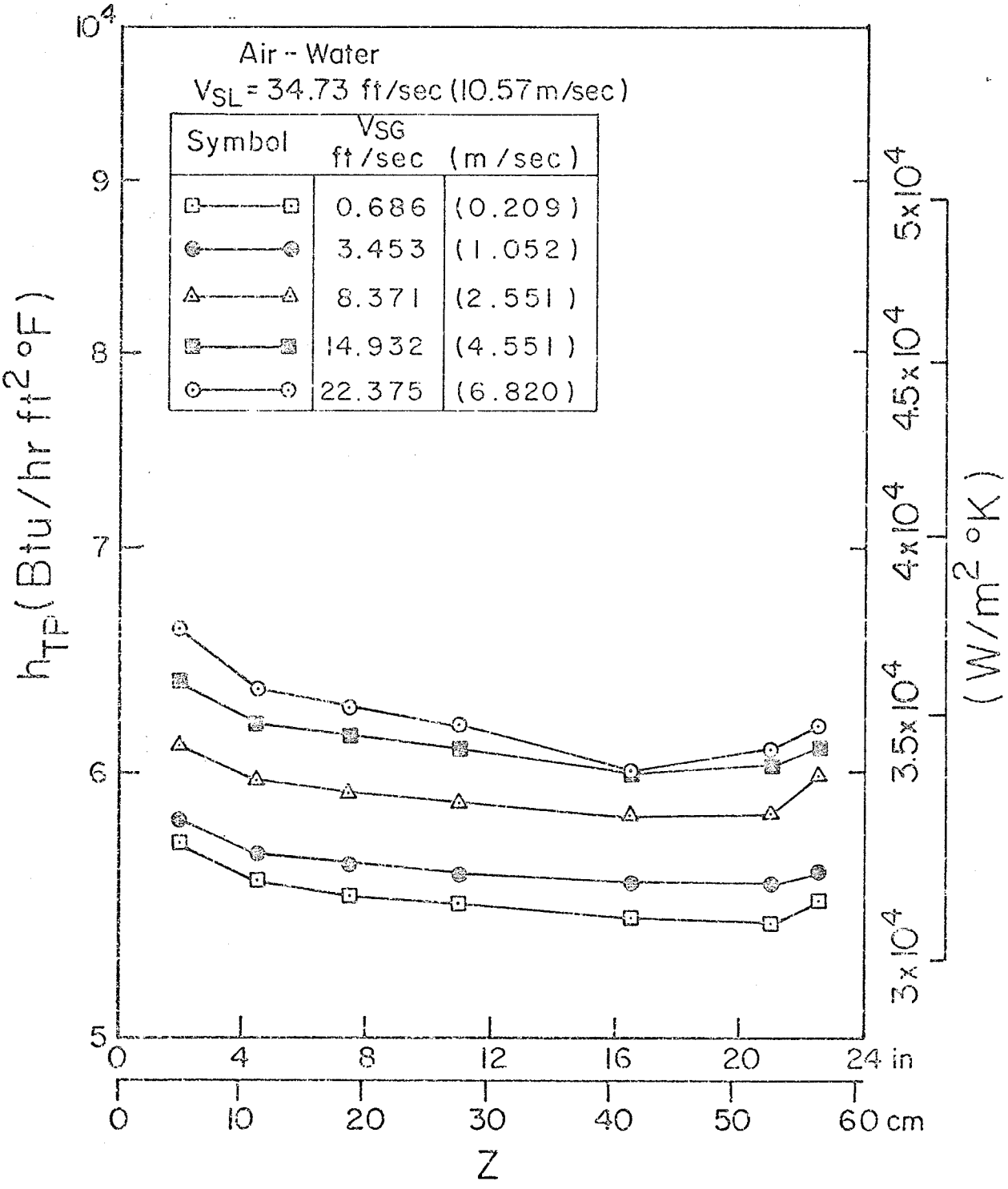

Fig.6.5H Two-Phase Air-Water Local Heat Transfer Data

Fig. 6.5H

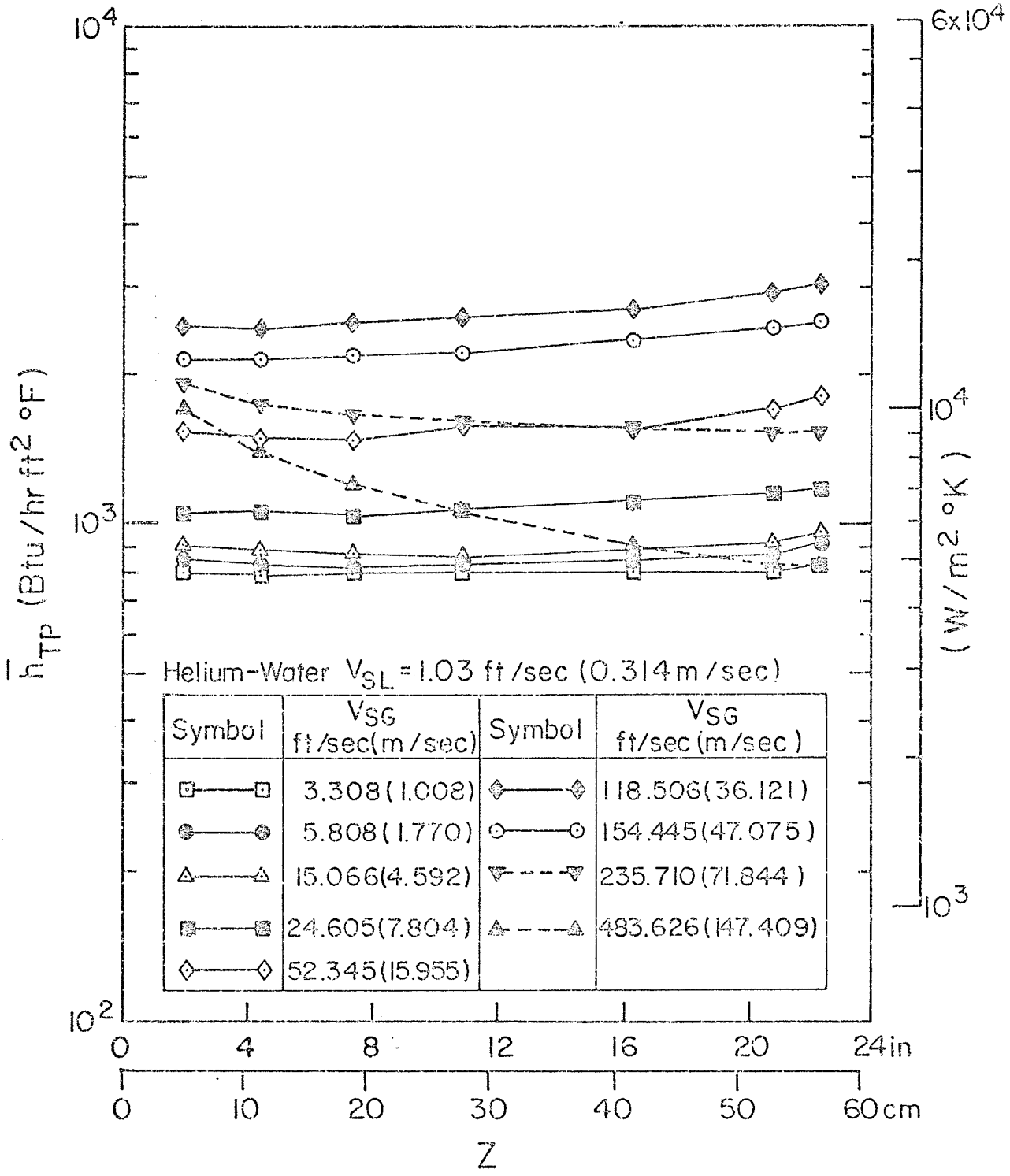

Fig. 6.6A Two-Phase Helium-Water Local Heat-Transfer Data

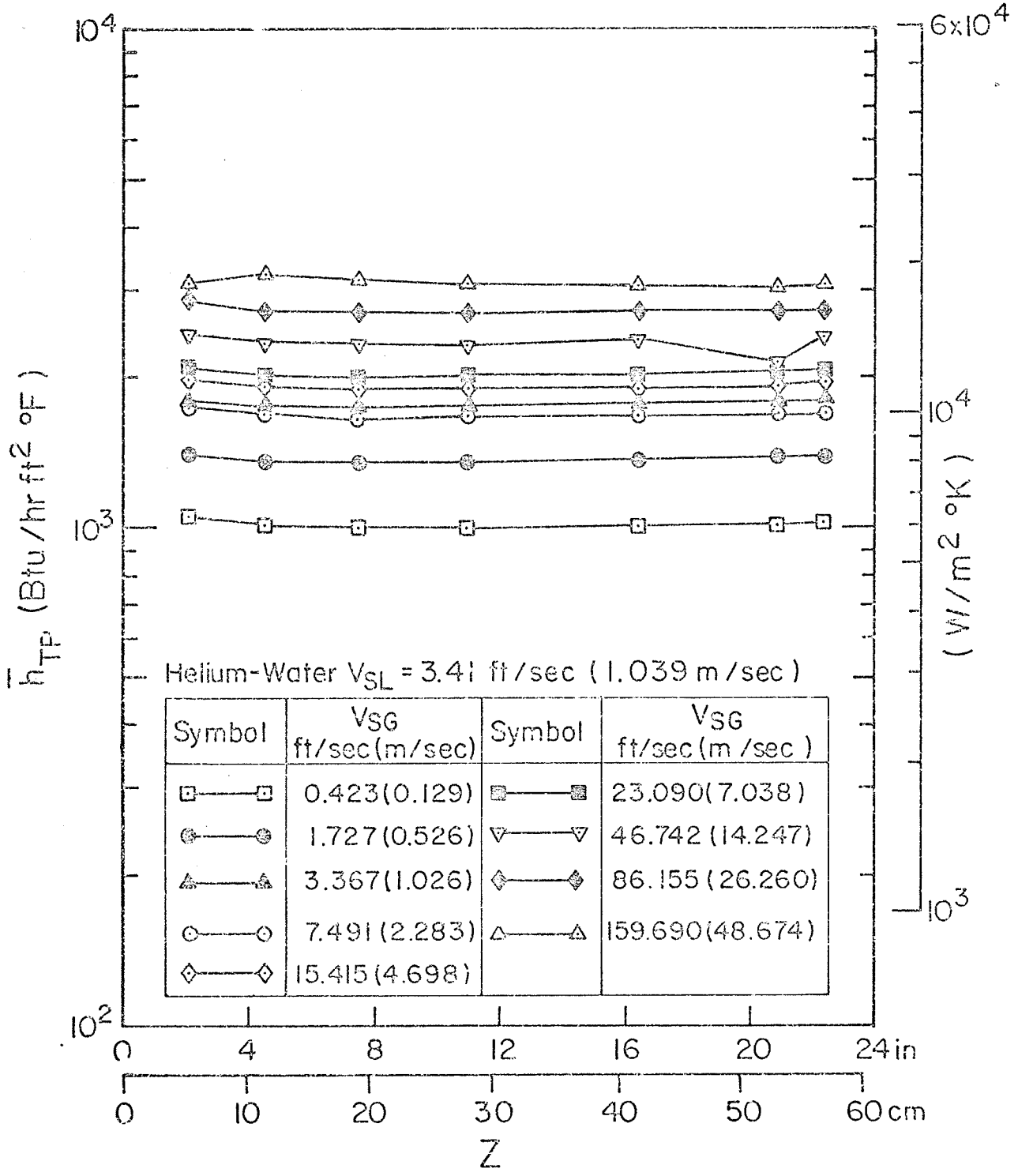

Fig. 6.6B Two-Phase Helium-Water Local Heat-Transfer Data

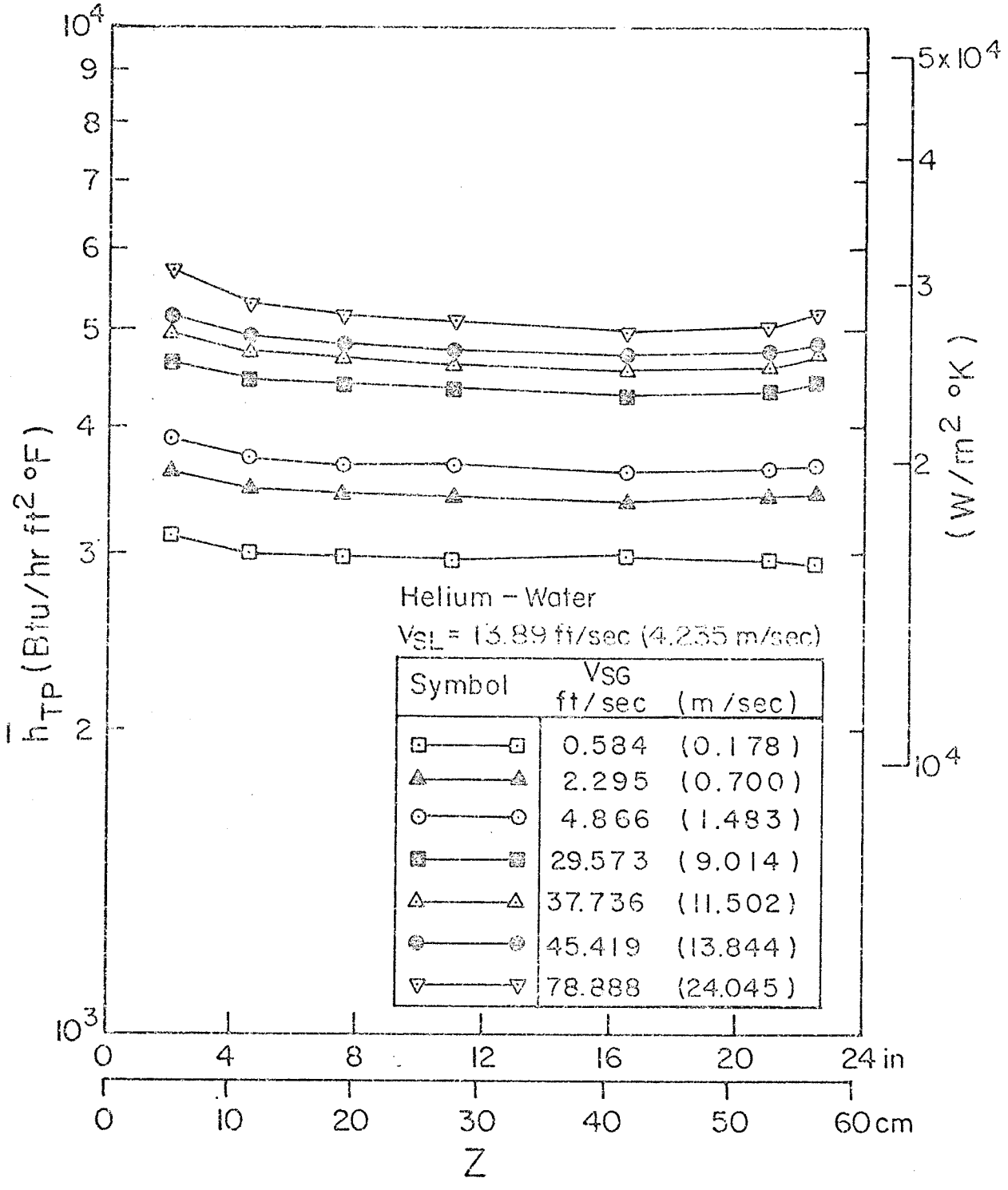

Fig. 6.6C Two-Phase Helium-Water Local Heat-Transfer Data

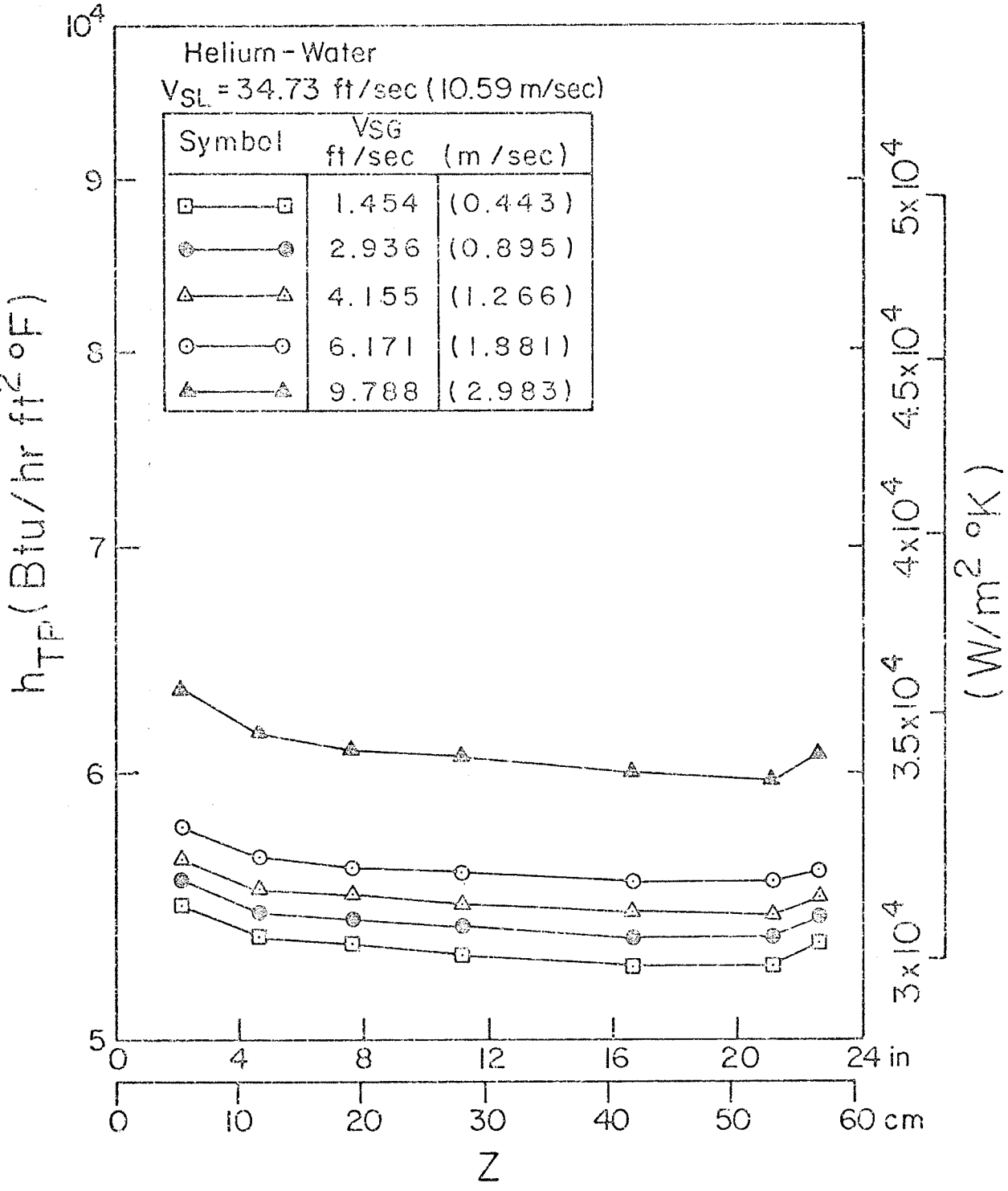

Fig. 6.6D Two-Phase Helium-Water Local Heat-Transfer Data

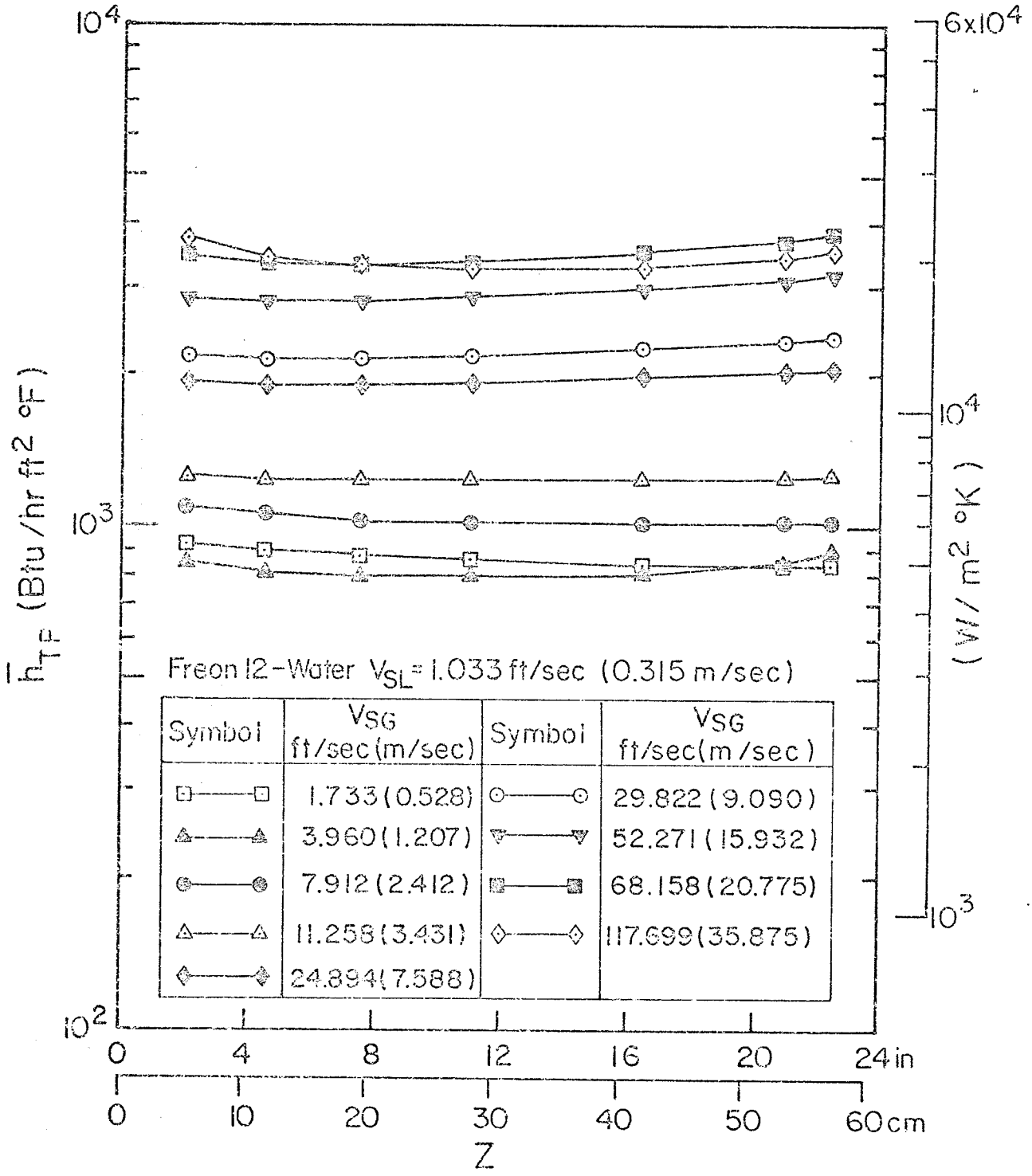

Fig.6.7A Two-Phase Freon-Water Local Heat-Transfer Data

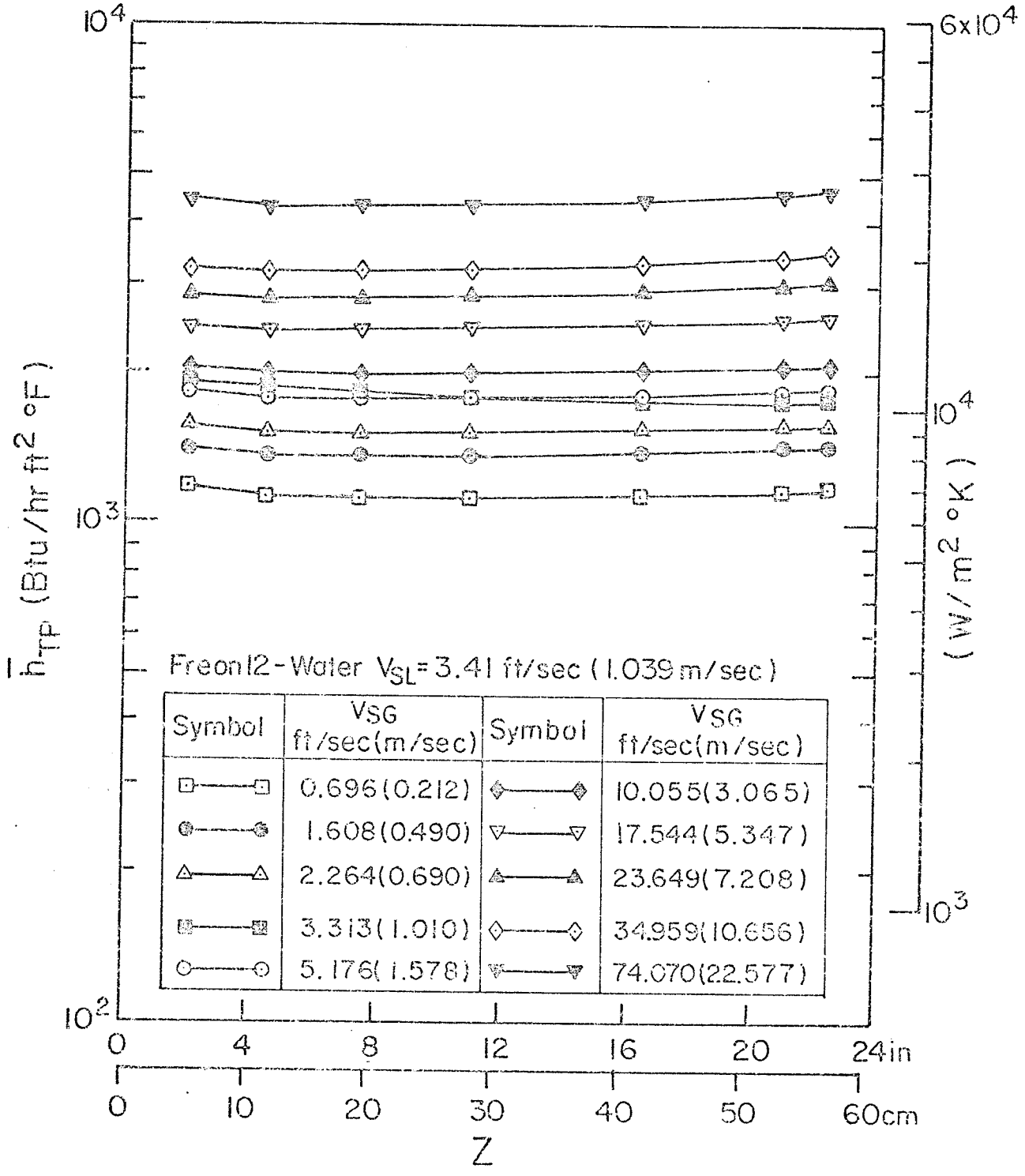

Fig.6.7B Two-Phase Freon-Water Local Heat-Transfer Data

Fig.6.7B

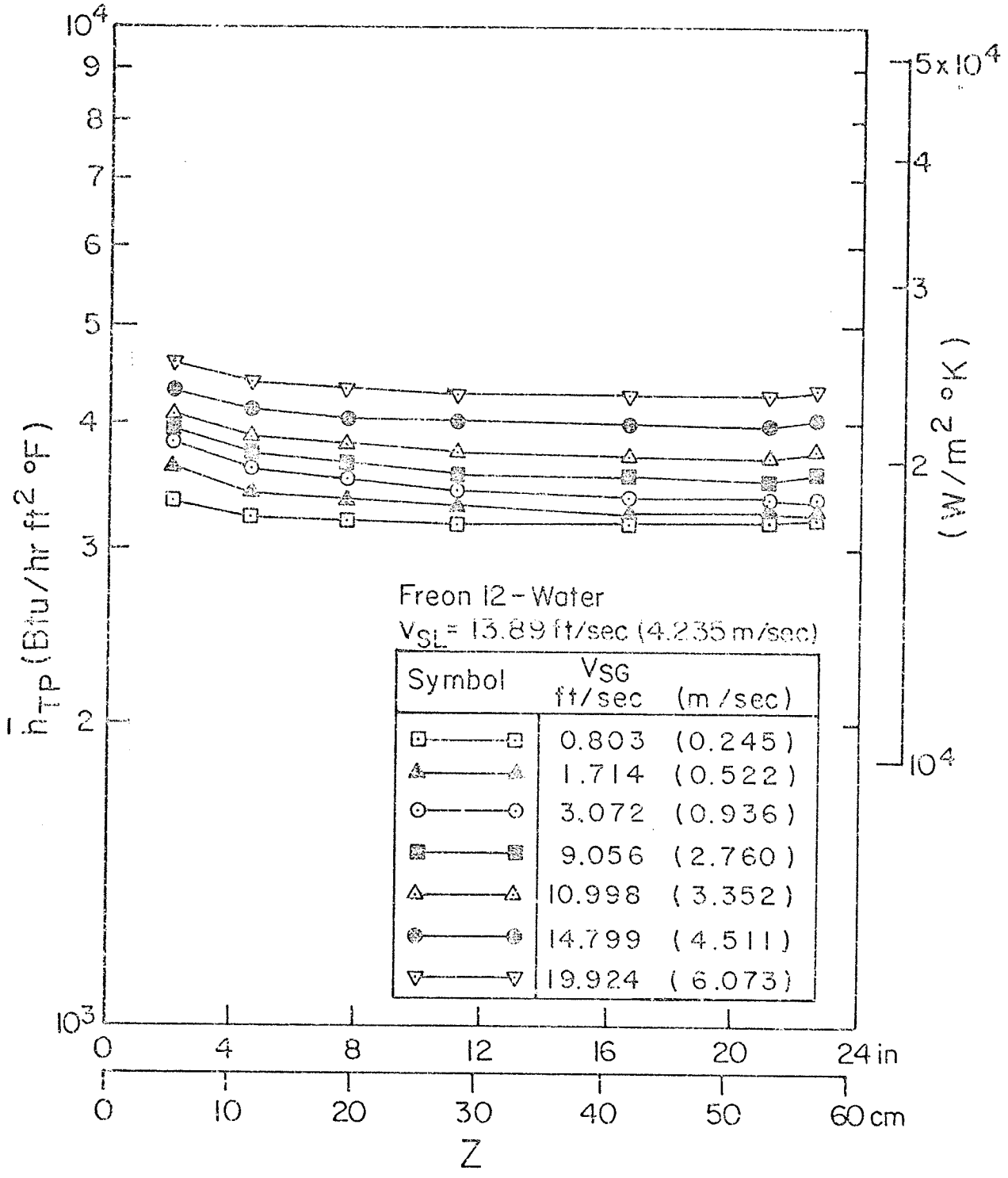

Fig.6.7C Two-Phase Freon-Water Local Heat-Transfer Data

that for some runs*, the number of tests* performed was as high as 23; in such cases only the data for some tests are shown in the figure for the sake of clarity. The data for all tests are, however, tabulated in Appendix H.

The $h_{TP} \sim Z$ profiles in the figures are generally similar to the $h_{SP} \sim Z$ profiles reported for single-phase flow in Fig. 6.1 with the exception of those in Fig. 6.5A at low mass flow rates of both phases. At these conditions, it is observed that h_{TP} tends to decrease first but then increases as Z increases. This reversed behavior of h_{TP} was not surprising because similar results have been reported in the literature. Fedotkin and Zarudnev [29] reported that for some flow regimes, the mean values of the heat-transfer coefficient were higher in the top section than they were in the bottom section of their test section; this could only happen if the local values of the heat-transfer coefficient increased with the axial distance along the test section. Frisk and Davis [32] reported, for horizontal air-water stratified flow in a rectangular channel, that at some point down-stream from the start of the heated

---

* The words "run" and "test" are used here in the following sense: A run is an experiment in which the water flow rate is fixed while the gas flow rate is varied; a test refers to an experiment with fixed water flow rate and fixed gas flow rate.

channel, the Nusselt number attained a minimum value then it increased with the distance along the channel; the authors attributed the increase in Nusselt number to the onset of natural convection. In the earlier work conducted with the present apparatus [90], similar results were also obtained. In reference [90], this behaviour was attributed to be due to any or a combination of the reasons listed below; a theory was developed which qualitatively explains this behaviour of h_{TP} with respect to Z. This behaviour of h_{TP} with respect to Z was observed for the slug, slug-annular and bubble flow patterns at low mass flow rates. The slug and slug-annular flows are associated with a downflow of the liquid film at the wall which could explain the increase of h_{TP} with Z. However, this downflow of the liquid film has not been observed before for the bubble flow. Therefore it was decided to investigate the existence of such downflow in the present investigation. This is discussed in detail in Chapter 7.

Listed below are other possible reasons for this observed behaviour of h_{TP} with respect to Z:

(i) In the bubble and slug flow patterns, the bubbles tend to grow in size as they rise from the inlet to the outlet of the test section due to the pressure gradient along the axis, coalescence of the bubbles and gradual heating of the fluid in the heated test section. Thus the bubble velocity increases dragging more liquid along the axis; this will cause, by reasons of continuity, a reduction

and ultimate reversal of the flow near the wall, together with a radial inward flow component. Cooler fluid will, therefore, be drawn towards the wall, thus increasing the heat-transfer rate.

(ii) The change in fluid properties, especially of the liquid, along the length of the heated test section results in an increasing heat-transfer rate with increasing Z.

For high liquid flow rates, the $h_{TP} \sim Z$ profiles are similar to those for single-phase flow (Figs. 6.5 B to H, 6.6 and 6.7). At these conditions, where the liquid flow is fully developed and highly turbulent, the liquid boundary layers are very thin [54] and therefore are not much perturbed by the introduction of the gas phase.

6.3.2. Mean Heat-Transfer Data

The mean heat-transfer coefficients were calculated by integrating the local values over the length of the heated test section as discussed in Appendix D. The data are presented in Figs. 6.8, 6.9 and 6.10 for air-water, helium-water and Freon 12-water respectively where the values of $\bar{h}_{TP}$ are plotted as a function of V_{SG} with V_{SL} as a parameter. The flow pattern observed for each test is indicated (by the flow pattern symbols given in Table 5.2) beside the data points in order to demonstrate the effect of flow pattern on $\bar{h}_{TP}$.

It is observed from Fig. 6.8, 6.9 and 6.10 that

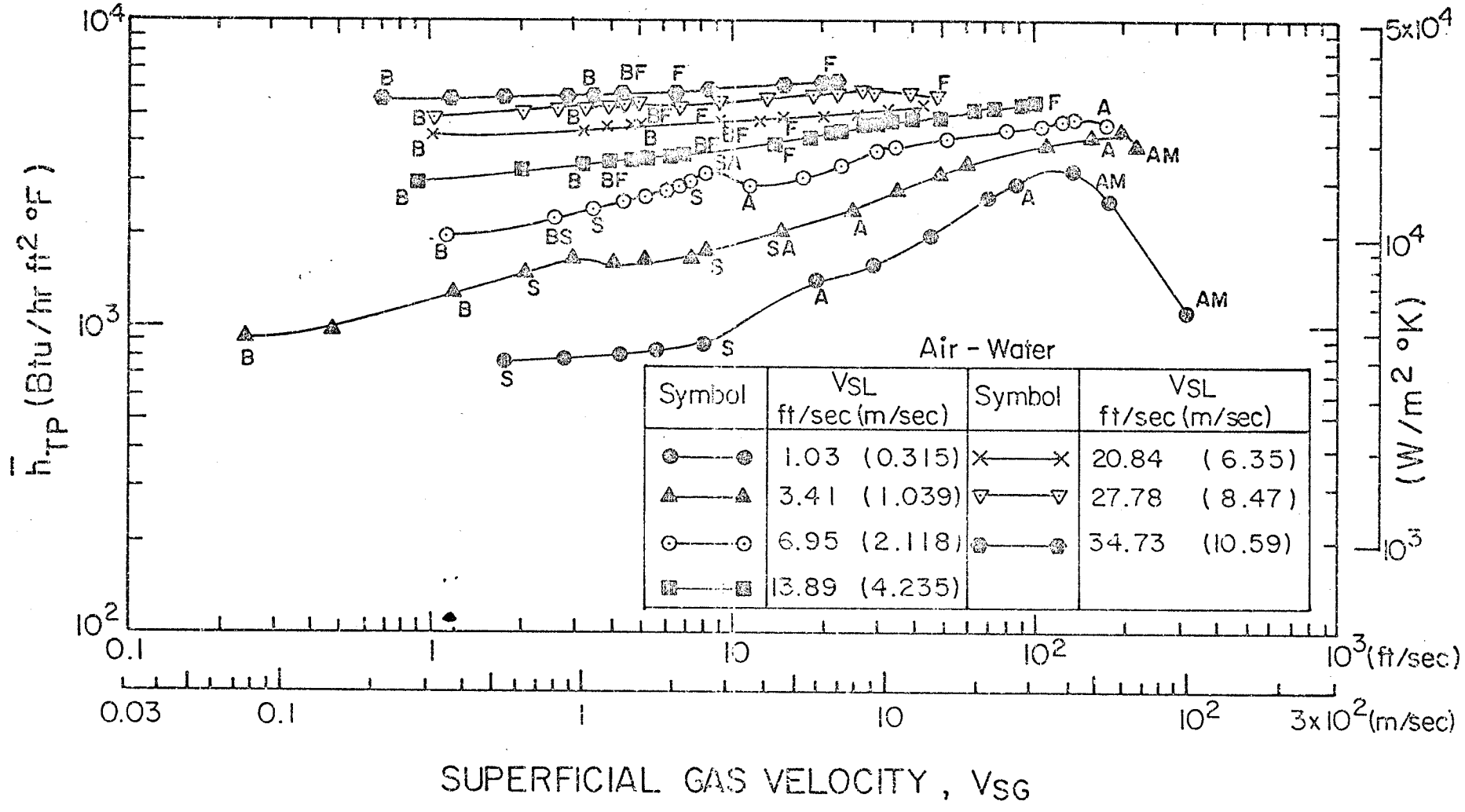

Fig. 6.8

Fig.6.8 Two-Phase Air-Water Mean Heat-Transfer Data

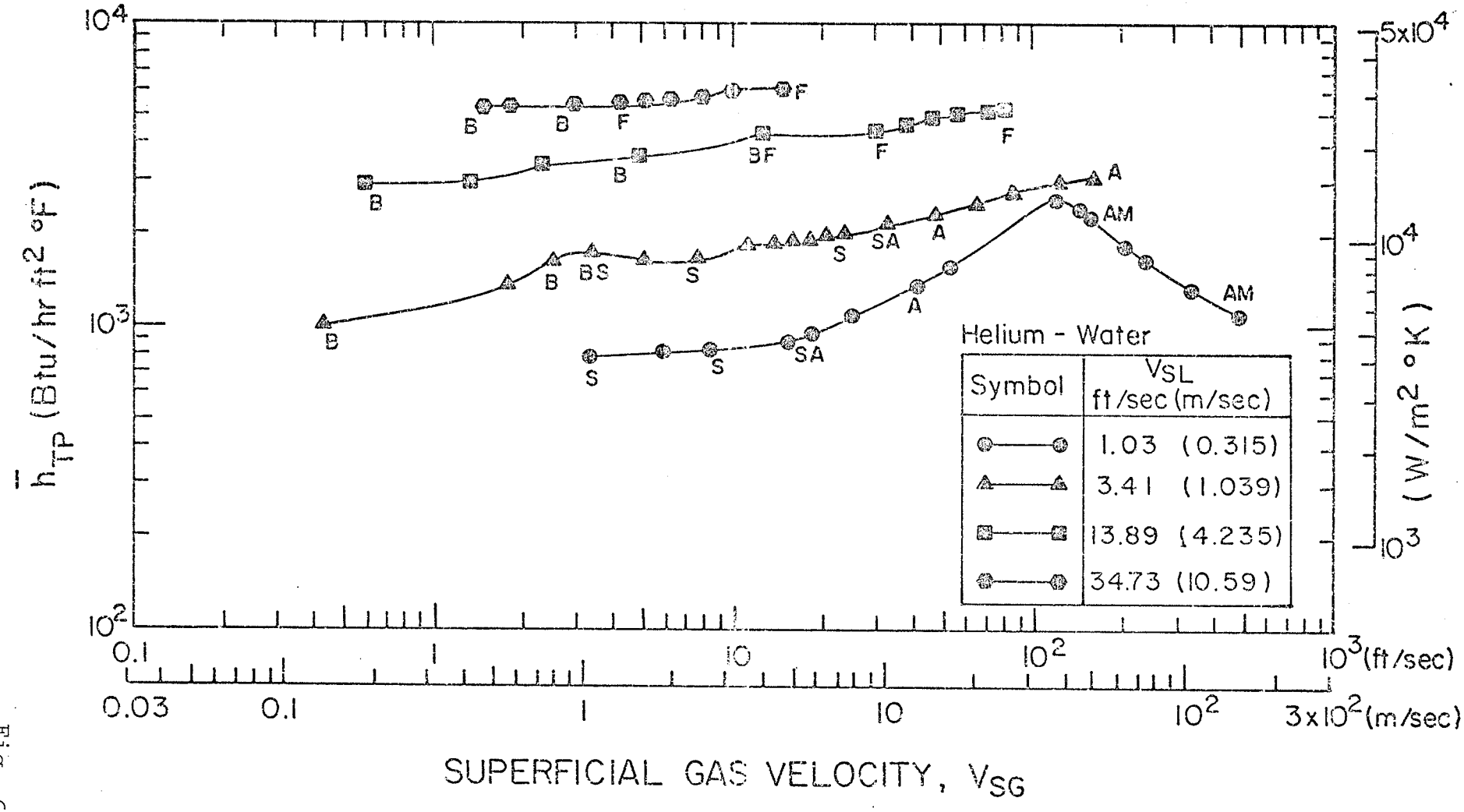

Fig. 6.9 Two-Phase Helium-Water Heat-Transfer Data

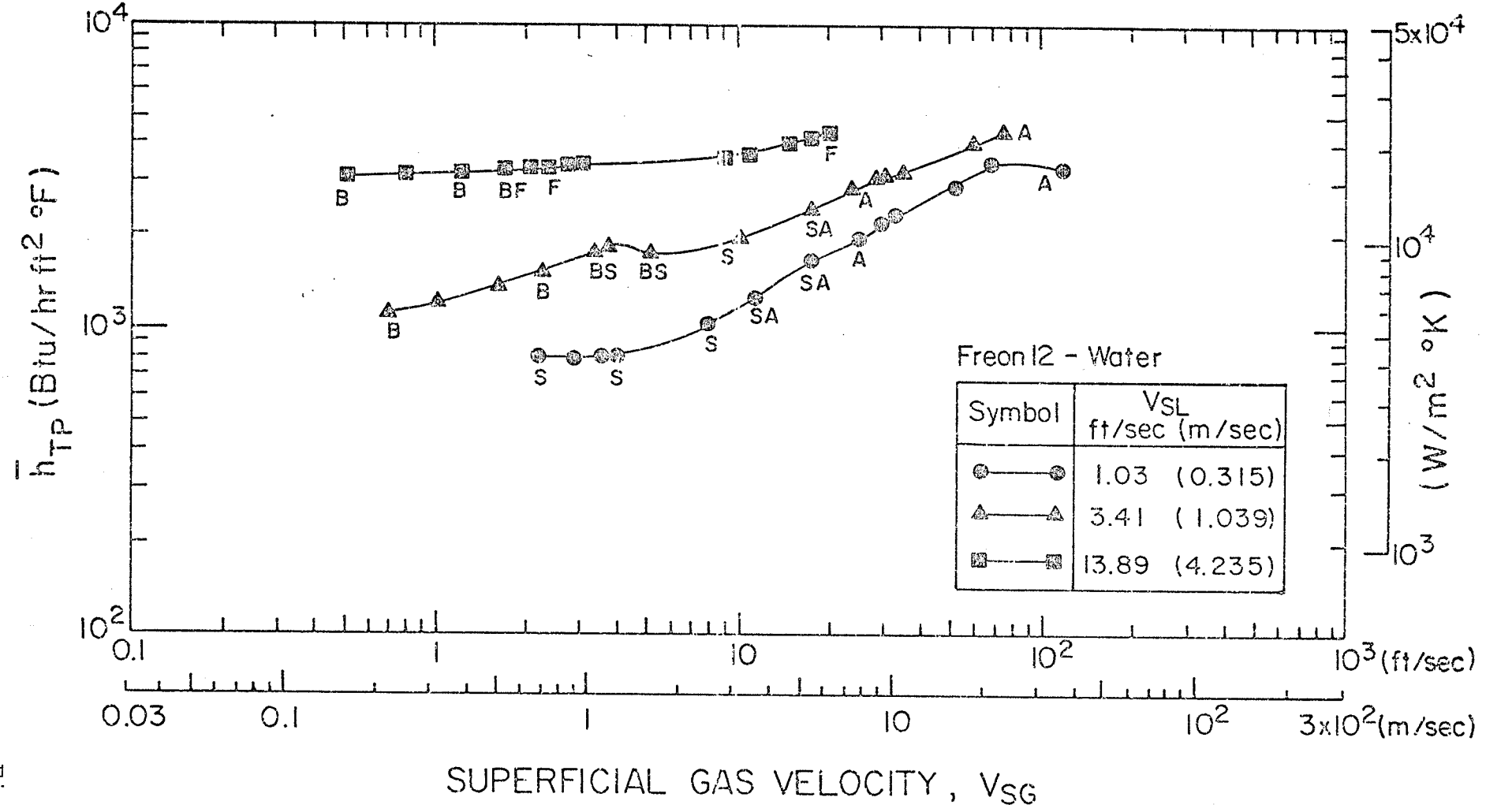

Fig. 6.10 Two-Phase Freon-Water Mean Heat-Transfer Data

for a given V_{SL}, $\bar{h}_{TP}$ generally increases with increasing V_{SG}; the rate of increase of $\bar{h}_{TP}$ with V_{SG} depends, however, on the value of V_{SL} as follows:

(i) For lower values of V_{SL}, high rates of increase of $\bar{h}_{TP}$ are obtained with increasing V_{SG} up to a maximum in $\bar{h}_{TP}$ where the transition to mist flow occurs, then $\bar{h}_{TP}$ decreases (for the reason discussed below).

(ii) For higher liquid flow rates, the rate of increase of $\bar{h}_{TP}$ with increasing the gas flow rate is smaller than that for the lower liquid flow rates.

The observed increase in $\bar{h}_{TP}$ with increasing V_{SG} may be mainly due to the increase in the mean velocity of the two phases (due to the reduction in the flow cross-sectional area of the two phases) which increases the turbulence levels of the flow and consequently enhances the heat-transfer rate. The introduction of the gas phase may also perturb the boundary layer reducing its thickness and, therefore, reduces the resistance to heat transfer. At high liquid flow rates, where the turbulence levels are initially high, the effect of V_{SG} on $\bar{h}_{TP}$ is less pronounced than at lower values of V_{SL}.

Figures 6.8, 6.9 and 6.10 also demonstrate the effect of flow pattern on $\bar{h}_{TP}$. In the regions of transition from one flow pattern to another, changes in the slope of the curves are generally observed and distinct maxima in $\bar{h}_{TP}$ occur for the lower liquid flow rates (V_{SL} = 1.03 and 3.41 ft/sec) at the transition from annular to mist flow. The existence of the maxima in $\bar{h}_{TP}$ may be attributed to the following mechanism: In the annular flow pattern, the heat transfer rate is determined by the thickness of the liquid film at the wall which represents the resistance to the heat transfer. As V_{SG} increases, the interfacial shear stress increases and acts to reduce the thickness of the liquid film by entraining more and more liquid droplets into the gas core; this results in a reduction in the resistance to heat transfer and consequently increases $\bar{h}_{TP}$. As more and more gas is introduced, the liquid film disintegrates until it entirely disappears resulting in the mist flow pattern, where the heat is transferred essentially to the gas resulting in a decrease in $\bar{h}_{TP}$.

In order to demonstrate the effect of gas density on $\bar{h}_{TP}$, the data for all three gas-water mixtures are plotted in Figs. 6.11 and 6.12. It should be noted that it was not possible to use Freon 12 for the entire range of V_{SG} and V_{SL} studied because of the thermodynamic limitations as discussed in Chapter 4. From Figs. 6.11 and 6.12, the following observations are made:

(i) For the two lower water flow rates, V_{SL} = 1.03

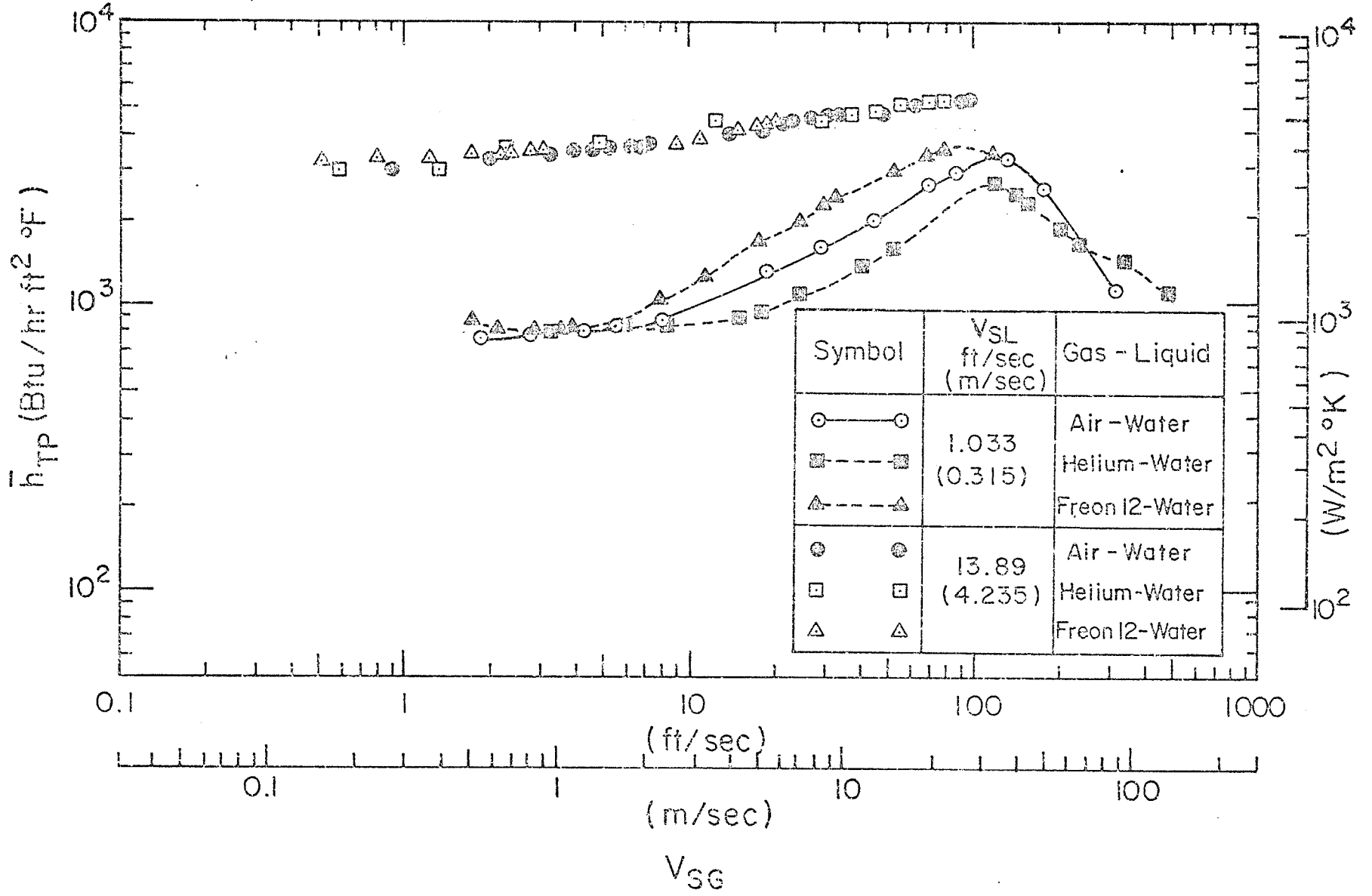

Fig. 6.11 Effect of Gas Density on $\bar{h}_{TP}$ Data

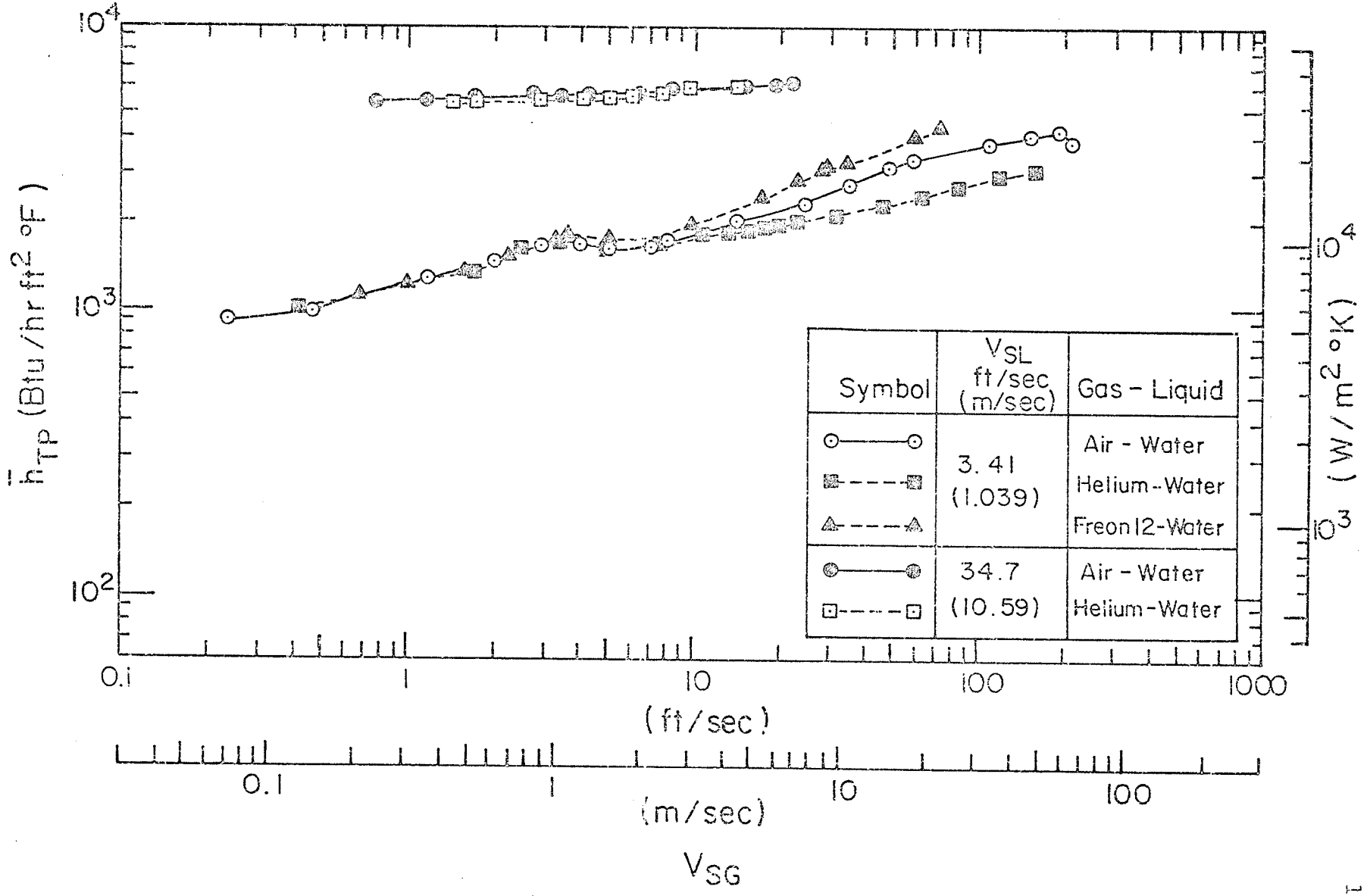

Fig. 6.12 Effect of Gas Density on $\bar{h}_{TP}$ Data

ft/sec (0.31 m/sec) and 3.41 ft/sec (1.04 m/sec), the gas density has almost no effect on $\bar{h}_{TP}$ up to a value of V_{SG} of about 5 ft/sec (1.52 m/sec); for higher V_{SG}, there is a direct relationship between $\bar{h}_{TP}$ and the gas density ρ_G; this is, for the same V_{SG} at a given V_{SL}, the higher the gas density the higher is the mean heat-transfer coefficient.

(ii) The effect of ρ_G on $\bar{h}_{TP}$ appears to decrease gradually as V_{SL} increases. For example, for V_{SL} = 1.03 ft/sec (0.31 m/sec) and V_{SG} = 30 ft/sec (9.14 m/sec), $\bar{h}_{TP}$ (helium-water) is 25.6% lower than $\bar{h}_{TP}$ (air-water) and $\bar{h}_{TP}$ (Freon-water) is 38.8% higher than $\bar{h}_{TP}$ (air-water); for the higher liquid velocity V_{SL} = 3.41 ft/sec (1.04 m/sec) and the same value of V_{SG}, the above figures drop to 16.6% and 26.5% respectively. At the higher water velocities, V_{SL} = 13.89 and 34.7 ft/sec (4.23 and 10.58 m/sec respectively), ρ_G has almost no effect on $\bar{h}_{TP}$ for all values of V_{SG}.

6.4 Correlation of Local Heat-Transfer

As discussed in Section 2.2.13 of Chapter 2, the Spalding [81] Correlation for single-phase heat-transfer was modified by Vijay [90] to correlate his two-phase local heat-transfer coefficients and proved to be successful as it correlated 84% of the data within ± 50%. Since the data of [90] were obtained from the same apparatus used in the present study and since the present air-water results repeated those of

[90] (Section 6.3), the two sets of data can be considered as one set of data obtained from the same apparatus, which covers the widest range of variables studied so far; that is, the widest range of flow rates, the widest range of liquid Prandtl number and the widest range of gas density. Therefore, the modified Spalding theory [90] was tested against the present data in an attempt to generalize that theory as discussed below.

As shown in [90], it is possible to employ single-phase heat-transfer theory [81], Eq. (6.4), to correlate the two-phase local heat-transfer coefficients if the two-phase mixture is assumed to be homogeneous. It is also assumed that the wall shear stress and the fluid properties are uniform with respect to Z. For two-phase flow, the variables S_q and Z+ could then be defined as follows [90]:

$$Z^+ = \int_o^Z \frac{1}{\nu_{MIX}} \left(\frac{g_c \tau_W}{\rho_{MIX}}\right)^{1/2} dZ \tag{6.15}$$

$$= Z(g_c \tau_W \rho_{MIX})^{1/2}/\mu_{MIX} \tag{6.16}$$

$$= Z/D^* \tag{6.17}$$

$$(S_q)_{TP} = \frac{Pr_{MIX} h_{TP}}{(C_P)_{MIX}(g_c \tau_W \rho_{MIX})^{1/2}} \tag{6.18}$$

$$= \frac{h_{TP}}{k_{MIX}} \cdot \mu_{MIX}/(g_c \tau_W \rho_{MIX})^{1/2} \tag{6.19}$$

$$= h_{TP} D^*/k_{MIX} = Nu^*_{TP} \tag{6.20}$$

where

$$D^* = \mu_{MIX} / (g_c \, \tau_W \, \rho_{MIX})^{1/2} , \qquad (6.21)$$

$$\tau_W = \frac{D}{4L} \cdot \Delta P_{TPF} \qquad (6.22)$$

and Nu^*_{TP} is a modified two-phase Nusselt number.

From the above equations, it is clear that a knowledge of the mixture properties is required to correlate the two-phase local heat-transfer data by Eq. (6.4). The problem of evaluating the mixture properties was examined in [90] where five different groups of mixture properties (with each group employing different combinations of expressions for μ, ρ, k and C_p) were tested. The best agreement between the data [90] and Eq. (6.4) was obtained when only liquid properties were used for the mixture. In the present study, however, another five groups of mixture properties, in addition to those tested in [90], were tested; this is discussed in detail in Section E.2.2 of Appendix E and the results are summarized in Table E.7 only for the new property groups which were not tested in [90] (the deviations obtained when the property groups tested in [90] were tested were larger than 100% which agrees with the results of [90] and therefore these groups were rejected). As shown in Section E.2.2, the use of only liquid properties for the mixture proved to be the best choice for correlating the two-phase local heat-transfer coefficients by Eq. (6.4). It should be mentioned that the use of only liquid properties was not

successful in the mist and mist-annular flow regime (the deviations from Eq. (6.4) of the data points in this flow regime were $> \pm 50\%$). This is expected because in the mist flow regime, the gas phase would be the main medium for transferring heat from the wall to the mixture. The gas properties would, therefore, be important in describing the mixture properties in this flow regime. Further study of the mixture properties in the mist and mist-annular flow regimes is, therefore, suggested. Since the data points lying in the mist and mist-annular flow regimes for both the tests reported in [90] and the present study were very few (2.6% of the total) compared with the total number of data points, it was decided to exclude these data in the final analysis of the correlation.

Examination of Eqs. (6.15) and (6.18) shows that the correlation of the data by Eq. (6.4) requires the knowledge of the wall shear stress; this was calculated from the measured pressure drop from Eq. (6.22). As discussed in Chapter 5, the frictional pressure drop data at low liquid and gas flow rates (mainly in the slug flow regime) were suspected to be in large error (the frictional pressure drops under these conditions were equivalent to a head of < 0.2 in. (0.51 cm) of water which was difficult to read on the inverted manometer with reasonable accuracy). These data were, therefore, excluded from consideration.

As discussed in Section 6.3, h_{TP} was observed to increase with Z at low liquid and gas flow rates. The

local heat-transfer data under these conditions did not agree with Eq. (6.4). This was expected because the theory does not accommodate such behavior of h_{TP}. The local heat-transfer data (both present and those of [90]) falling in this category were, therefore, excluded.

In summary then, the final results of the correlation presented below cover all the present data and those of [90] excluding the following:

(i) the data in the mist and mist-annular flow regimes,

(ii) the h_{TP} data which increase with Z,

(iii) the data with unreliable ΔP_{TPF} measurements (i.e., data with $\Delta P_{TPF} < 0.2$ in (0.51 cm) of water).

It should be noted that the air-water data of [90] are not considered in the present discussion because these were similar to the present data except that they contained data for lower water flow rates than those considered in the present study. Most of these later data, however, fall under one or more of the above restrictions; their exclusion is, therefore, justified.

As discussed in detail in Section E.2.2, different values of Pr_T exist in the literature; however, the value of 0.887 recommended by Spalding [81] was used in the present study mainly because the idea behind the present correlation of the two-phase local heat-transfer coefficients was to employ the Spalding [81] single-phase heat-transfer theory in the same form as presented by Spalding. However,

the experimental data were also tested against Eq. (6.4) with $Pr_T = 1$; the results of the test are summarized in Table E.6 which shows that the agreement between the data and the theory is not as good as it is when $Pr_T = 0.887$ is used (at least when the liquid properties are used for the mixture).

The present experimental data are compared with the theory in Figs. 6.13, 6.14 and 6.15 for air-water, helium-water and Freon-water respectively. In the figures, the experimental values of the ordinate $(Sq)_{TP}/(Pr_L/Pr_T)^{1/3}$ were calculated from Eq. (6.18) and the expected values from Eq. (6.4) taking $Pr_T = 0.887$. Figure 6.16 is a composite plot for all three gas-liquid mixtures together. The data of [90] are shown in Figs. 6.17 and 6.18 for air-glycerine +water and air-glycerine respectively. The two sets of data (present and [90]) are shown together in Fig. 6.19 illustrating the general nature of the correlation and its good prediction for such a wide range of variables (a quantitative analysis is given below).

A quantitative comparison of the two sets of data (present and [90]) with the theory is summarized in Table 6.3. The table shows that a majority of data agree with the theory within $\pm$30% and the 93% of the data agree with the theory within $\pm$50%. The agreement between the data and the theory is concluded to be excellent.

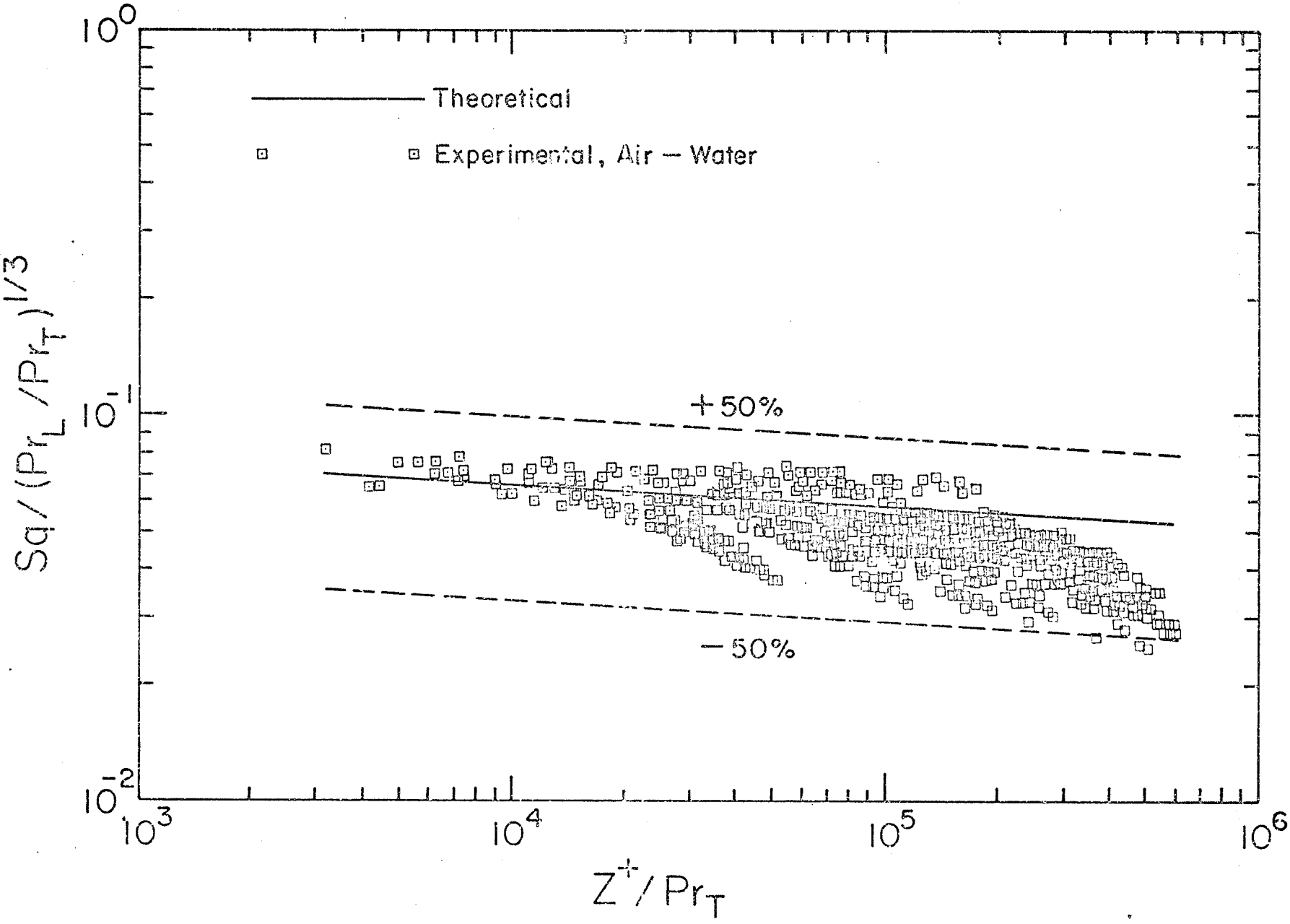

Fig. 6.13 Plot of Modified Spalding Function Against Z^+_{TP} (Air-Water)

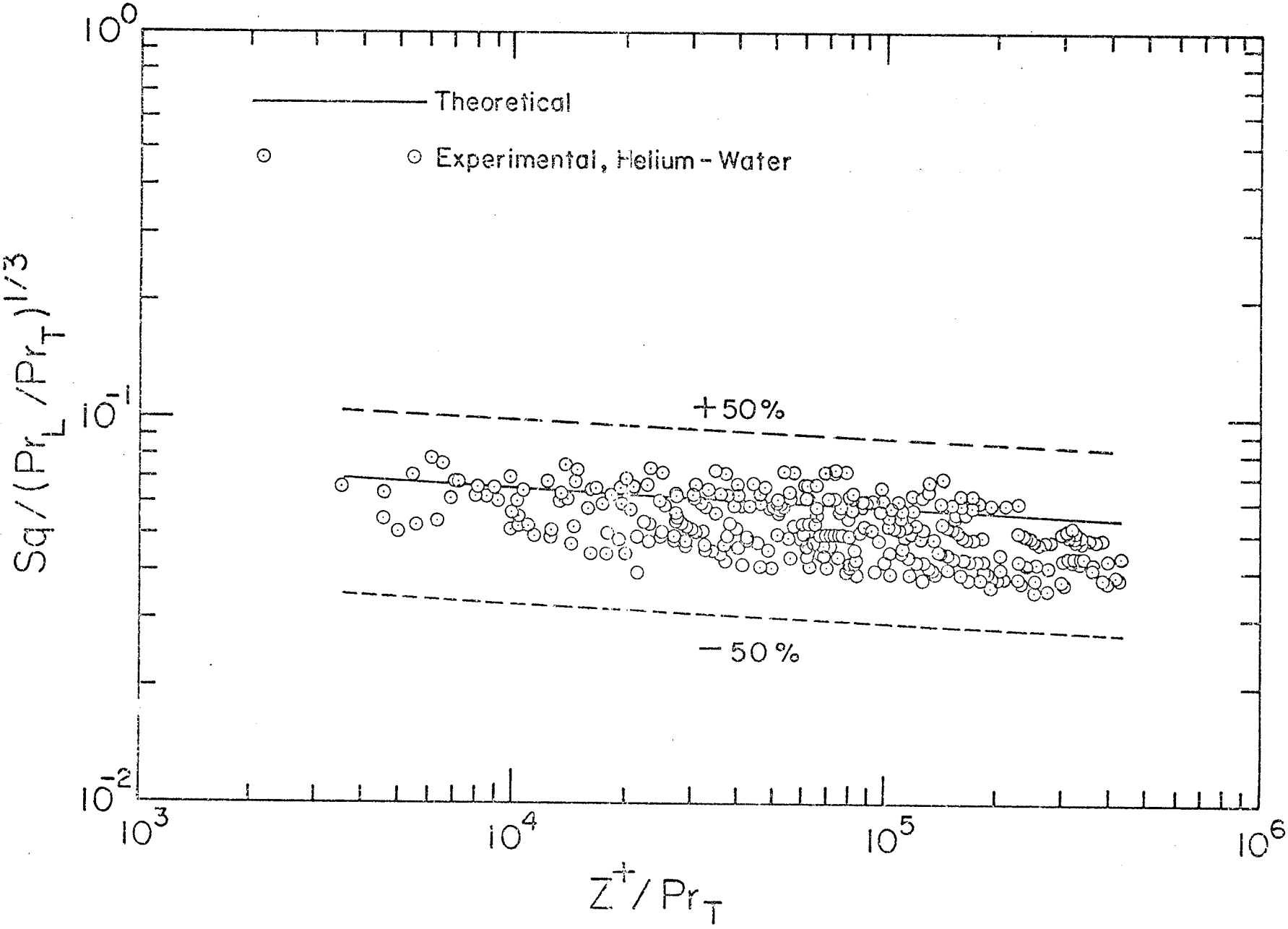

Fig. 6.14 Plot of Modified Spalding Function Against Z^+_{TP} (Helium-Water)

Fig. 6.14

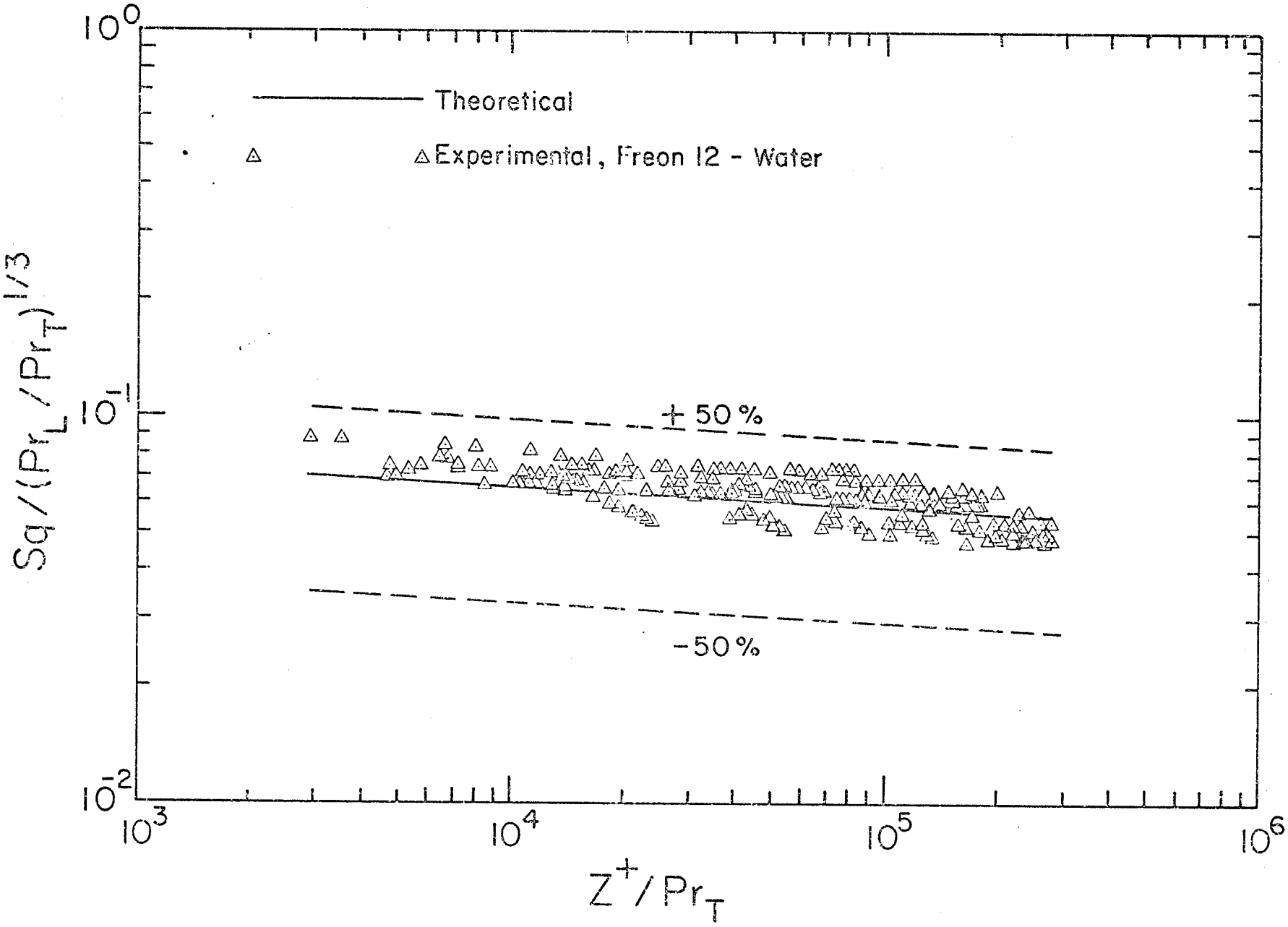

Fig. 6.15

Fig. 6.15 Plot of Modified Spalding Function Against Z^+_{TP} (Freon-Water)

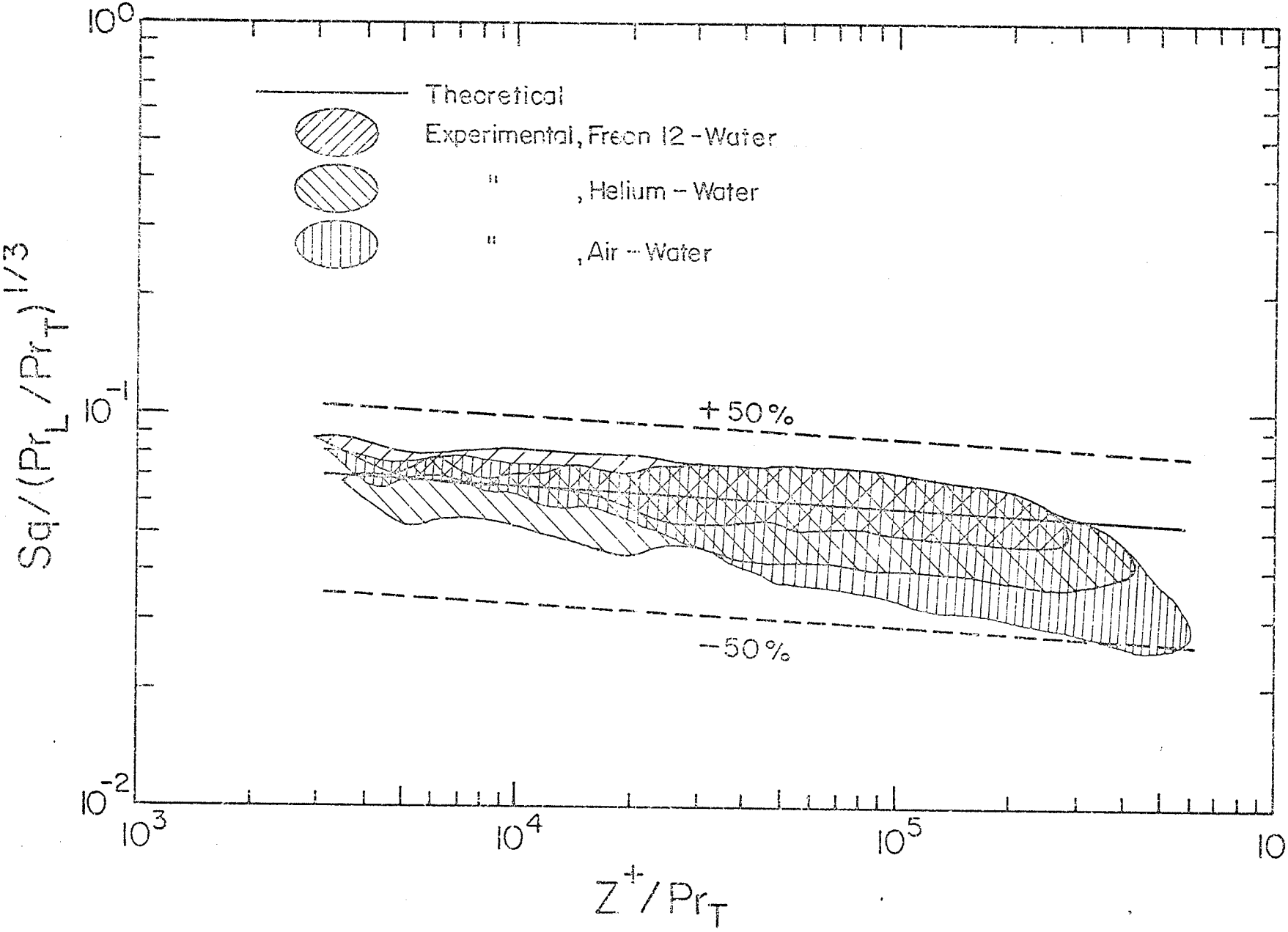

Fig. 6.16

Fig. 6.16 Plot of Modified Spalding Function Against Z^+_{TP} (all Present Data)

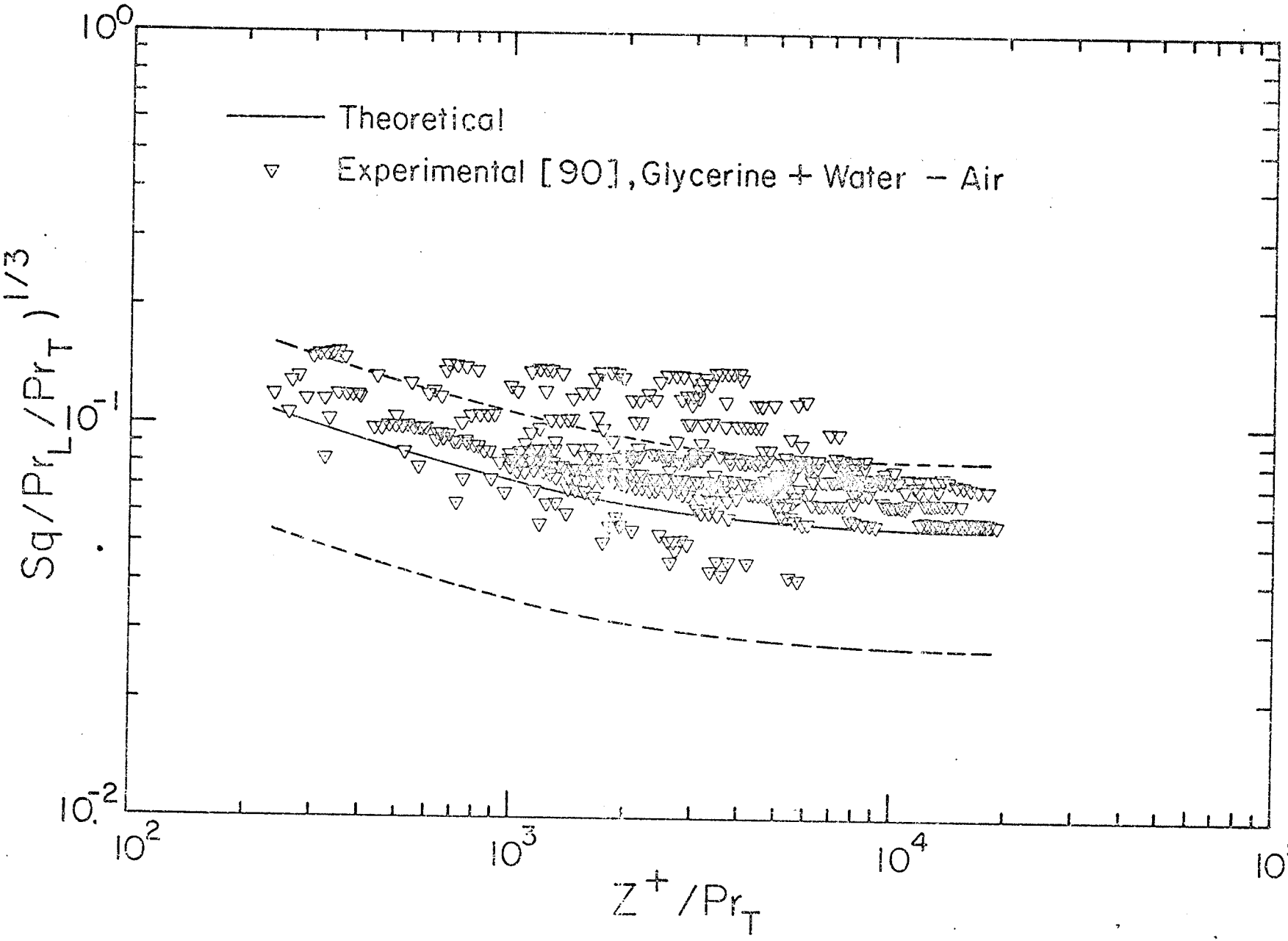

Fig. 6.17 Plot of Modified Spalding Function Against Z^+_{TP} (Air-Glycerine + Water) [90]

Fig.6.17

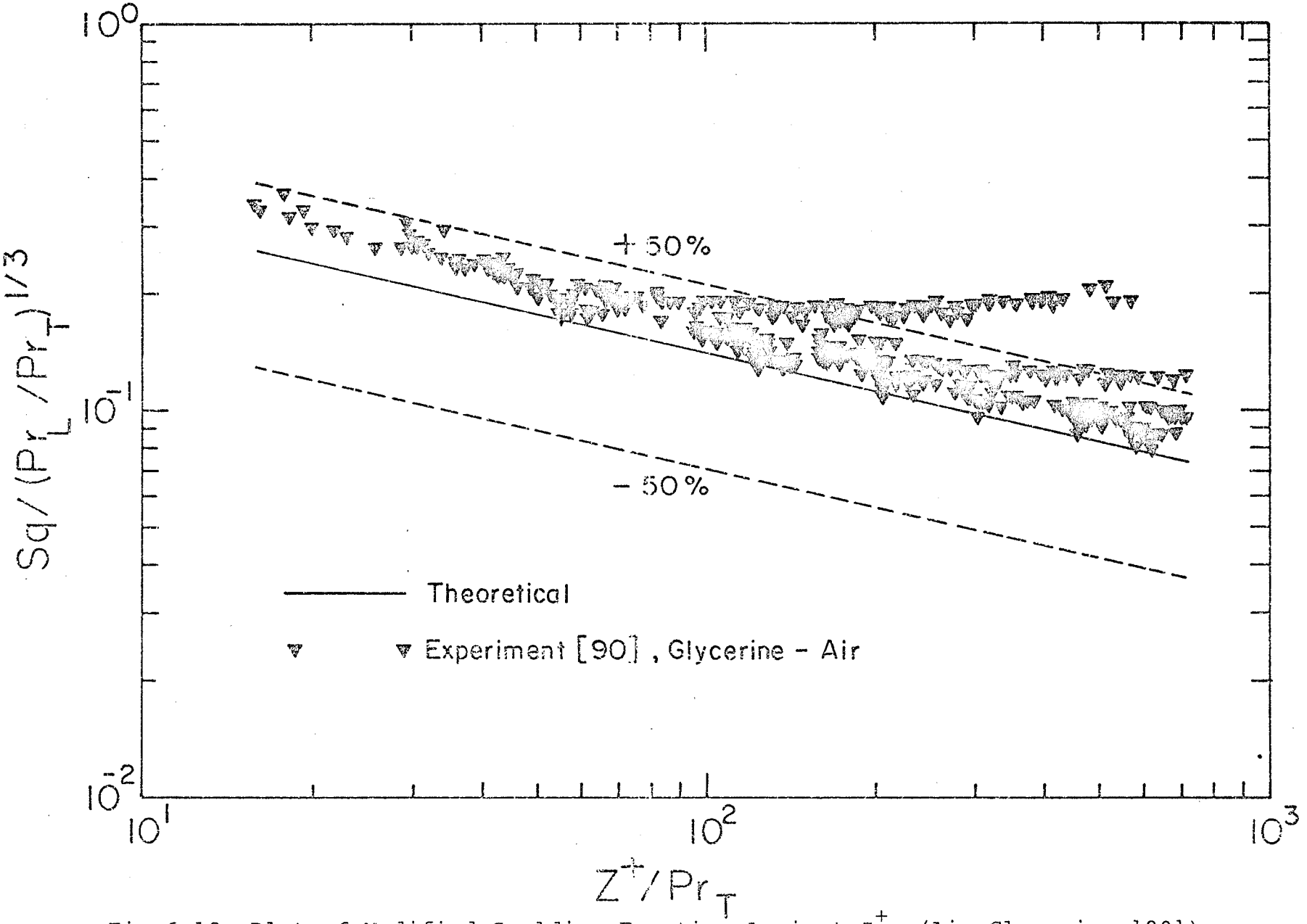

Fig. 6.18

Fig.6.18 Plot of Modified Spalding Function Against Z^+_{TP} (Air-Glycerine]90])

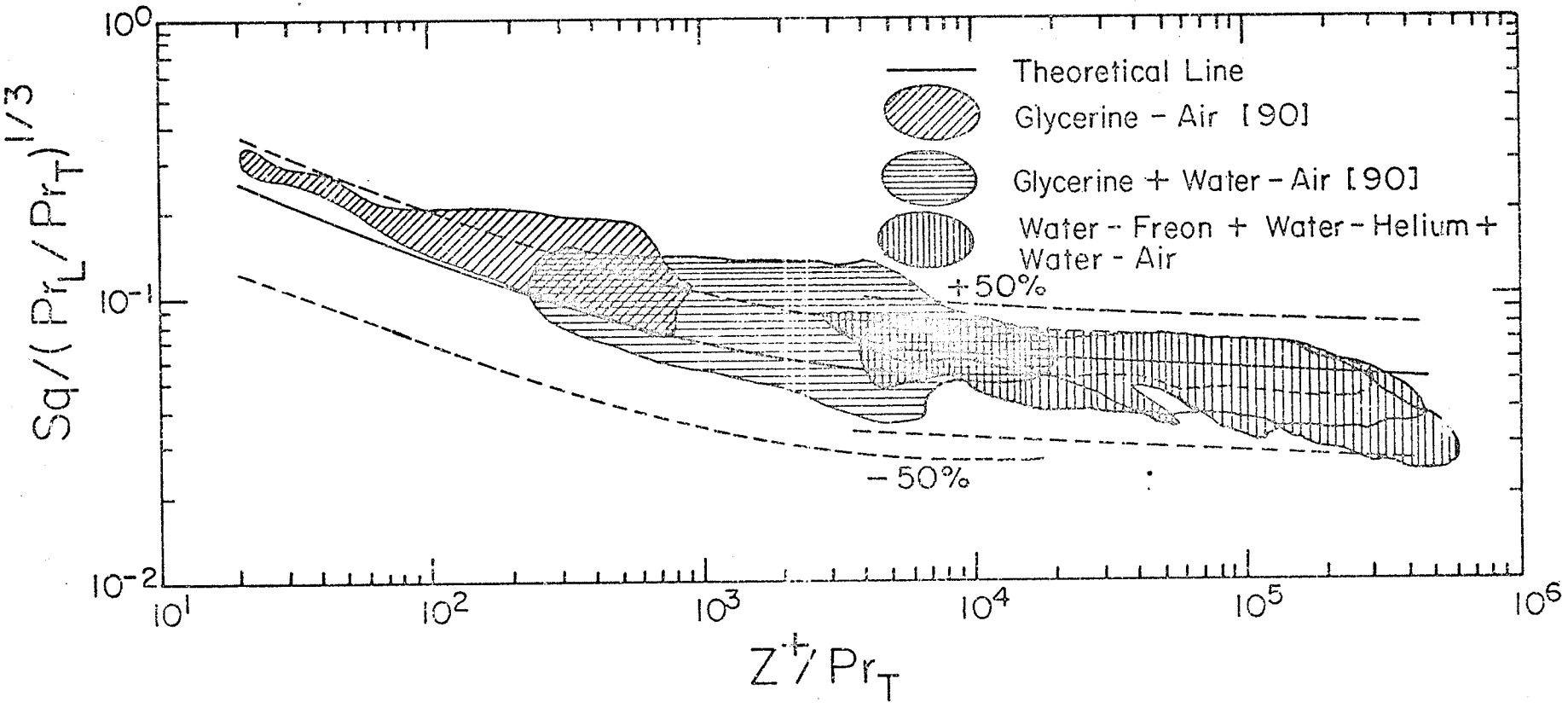

Fig. 6.19 Plot of Modified Spalding Function Against Z^+_{TP} (Present and Vijay's Data)

From the material presented in this section, the following remarks are made:

(i) The modified Spalding theory presented in this section is a successful means of correlation of the two-phase local heat-transfer coefficients for a wide range of variables (see Table 6.3).

(ii) The generality of the correlation is suggested, especially if the problem of the mixture properties is completely resolved.

(iii) The correlation of the two-phase local heat-transfer data in terms of the frictional pressure drop proved to be successful as it is for single-phase flow. Correlation of the two-phase mean heat-transfer data in terms of the frictional pressure drop is, therefore, suggested. This has been successfully tried before for horizontal [31] and vertical [90] flows and is extended here in Section 6.6.2.

TABLE 6.3

Summary of the Comparison Between the Two-Phase Local Heat-Transfer Data and Eq. (6.4)

Range of Deviations	Number of Data Points (% of Total N) Lying in the Specified Range of Deviations								
	Present Data				Data of [90]			Present and [90]	Range of Variables Covered
	Air-Water	Helium-Water	Freon-Water	Complete Set	Air Glycerine -- Water	Air-Glycerine	Complete Set		
±20%	58.95	64.88	93.23	68.13	42.67	45.57	43.93	57.61	Re_{SL} $(1.8\text{-}1.26\times10^5)$
±30%	79.15	88.39	100	86.29	61.14	70.20	65.09	77.08	Re_{SG} $(14\text{-}1.5\times10^5)$
±40%	93.43	100	100	96.70	73.71	79.56	76.26	87.82	Pr_L
±50%	99.51	100	100	99.75	81.71	85.96	83.57	92.72	(5.6-6960)
$\bar{e}$(%)	-15.48	-12.04	4.45	-10.14	30.27	29.11	29.76	7.20	ρ_L/ρ_G (103-5378)
$\bar{e}'$(%)	22.23	18.56	11.27	19.29	42.82	38.67	41.06	30.71	
N →	609	336	266	1211	525	406	931	2142	

6.5. Comparison of Mean Heat-Transfer Data Against Some Existing Correlations

This section presents the results of testing some of the existing correlations discussed in Chapter 2 against the present experimental data. The correlations tested here are those of Groothuis and Hendal [40], Knott et al. [56], Kudirka [58], Ueda and Hanaoka [86] and Vijay [90]. Although other correlations exists [24, 29, 52, 53, 63 and 87], they are not examined here because they either contained variables which were neither measured nor could be estimated from the variables measured in the present investigation [24, 52, 63, 87], or they correlated the data only flow-pattern wise [29, 53]; that is, different empirical constants were used for each flow pattern (in the present study, the data were correlated by a single correlation for all flow patterns).

It should be mentioned that with the exception of Ueda and Hanaoka [86] and Vijay [90], the correlations tested below are purely empirical. The pertinent empirical coefficients are, therefore, sensitive to the range and number of data points. However, these correlations are tested here for the total range of the present data. The real test of each correlation is, however, indicated by giving the degree of agreement between the correlation and the data in the range of applicability of the correlation.

6.5.1. Correlation of Groothuis and Hendal [40]

As discussed in Chapter 2, the authors presented

the following correlation for air-water flow:

$$\bar{Nu}_{TP} = 0.029\ Pr_L^{1/3}(\mu_L/\mu_W)^{0.14}Re_2^{0.087} \qquad (6.23)$$

Equation (6.23) is tested against the present data (only those lying in the range of Re_{SL} and V_{SG}/V_{SL} suggested by the authors) in Fig. 6.20. The results of the test are summarized in Table 6.4 for the data within the range suggested by the authors and for all data reported in the present study as well.

TABLE 6.4

Comparison of the Correlation of Groothuis and Hendal [40] with the Present Data

	Data in the range suggested by the Authors		Total range of Data	
	$\bar{e}$(%)	$\bar{e}'$(%)	$\bar{e}$(%)	$\bar{e}'$(%)
Air-Water	-29.11	17.03	-47.4	23.3
Helium-Water	5.03	18.98	-13.48	20.82
Freon-Water	-51.26	52.80	-51.55	54.24
All three mixtures	-25.16	29.44	-39.50	31.90

Table 6.4 shows that in the range of variables suggested by the authors [40], the agreement between Eq. (6.23) and the present data is fair for air-water and helium-water mixtures but poor for Freon-water. For the total range of the present data, however, the agreement is generally fair. As reported by Vijay [90], better agreement could be obtained if

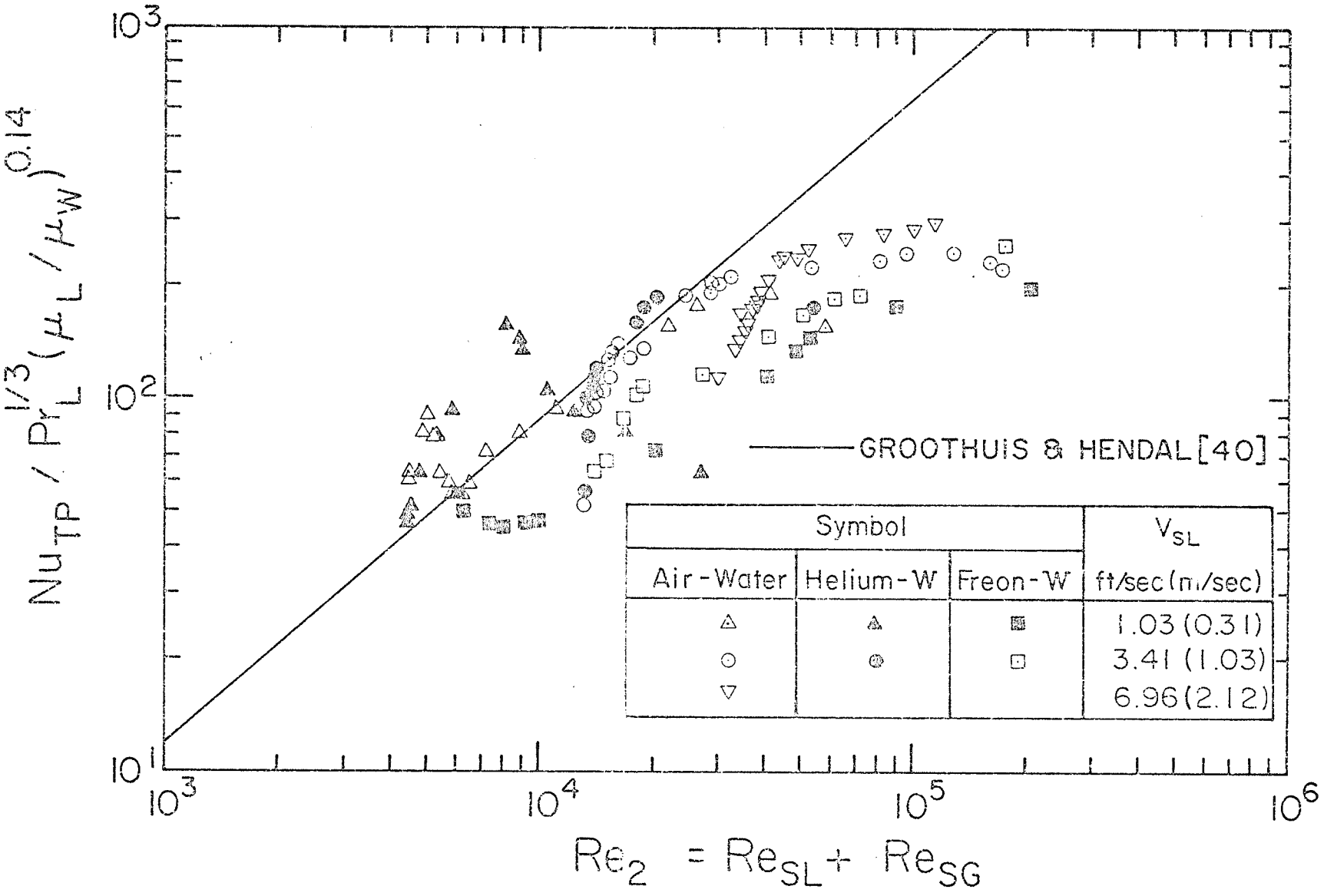

Fig. 6.20 Comparison of $\bar{h}_{TP}$ Data with the Correlation of Groothuis & Hendal

the data were analyzed flow-pattern wise; however, this would result in different equations for different flow patterns .

6.5.2. Correlation of Knott et al [56]

$$\frac{\bar{h}_{TP}}{\bar{h}_{SP}} = A\left(1 + \frac{V_{SG}}{V_{SL}}\right)^{n} \qquad (6.24)$$

where $A = 1.0$ and $n = 1/3$.

As discussed in Section 2.2.5, this correlation was based on a modification of the Sieder-Tate correlation for single-phase flow and was proposed for laminar liquid flow for the range of $0.1 \leq (V_{SG}/V_{SL}) \leq 40$.

The correlation was, however, extended here and tested against the present data which are all for turbulent liquid flow. This was done in two different ways. One way was to test the correlation with the same exponent $n = 1/3$, which was obtained from the laminar flow heat-transfer equation as discussed in Section 2.2.5, but to evaluate $\bar{h}_{SP}$ from the appropriate correlation; that is, from the turbulent flow correlation, Eq. (6.12). The results of this test are shown in Fig. 6.21 and are summarized in Table 6.5. The other way was to modify the above correlation for turbulent flow; that is, to obtain a new value of the exponent n in the same manner as done by the authors [40]. This was done by modifying Eq. (6.12) and, therefore, n was equal to 0.83. However, this method was not as successful as the first method described above as the deviations obtained were worse than those shown in Table 6.5.

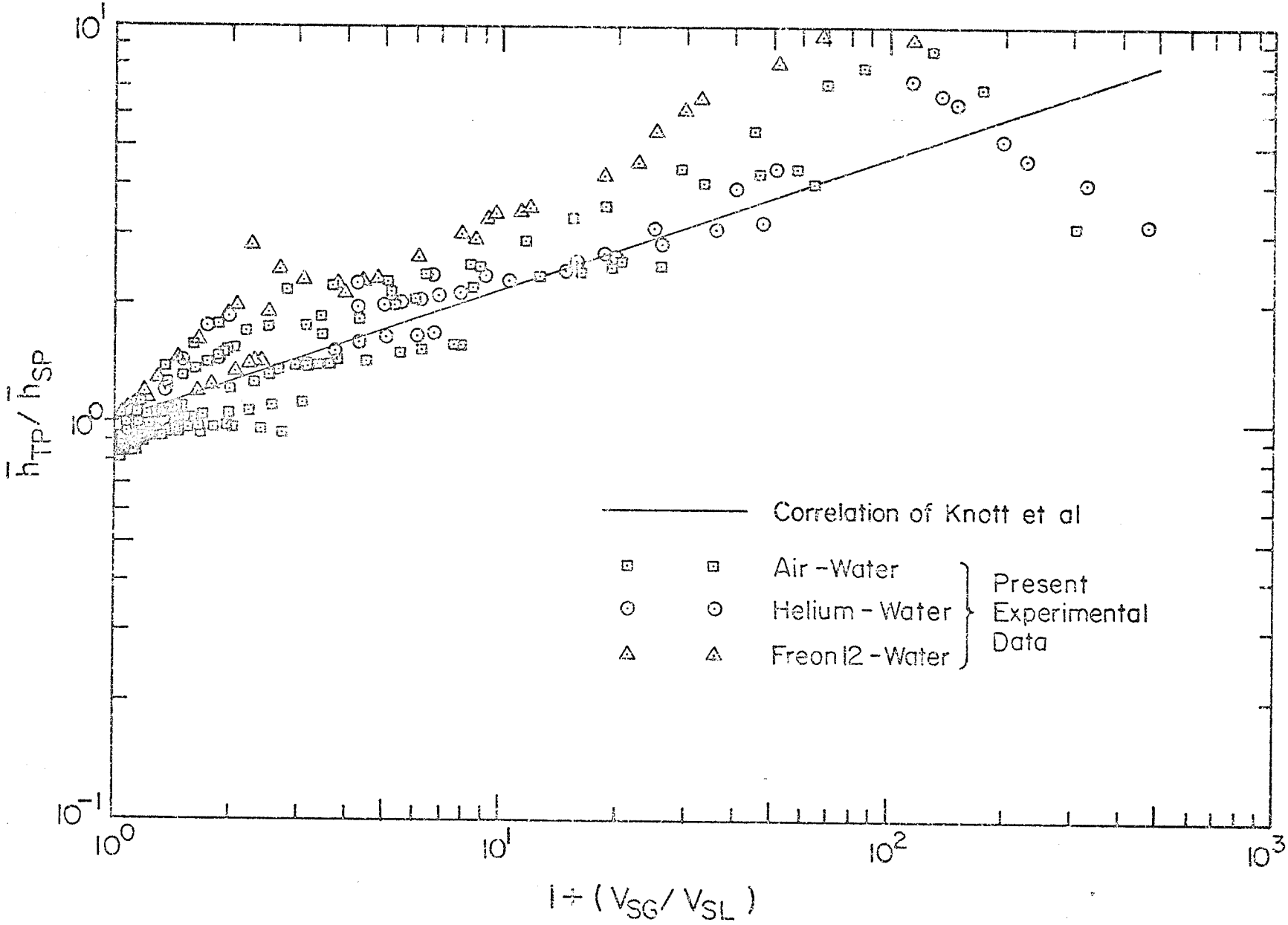

Fig. 6.21 Comparison of $\bar{h}_{TP}$ Data Against the Correlation of Knott et al.

Figure 6.21 shows that Eq. (6.24), with $\bar{h}_{SP}$ calculated from Eq. (6.12), correlates the present data reasonably well, especially in the range of V_{SG}/V_{SL} suggested by [56]; the worst deviations between the data and Eq. (6.24) are generally obtained for $V_{SG}/V_{SL} > 40$. If these data were excluded the agreement would greatly improve.

Table 6.5 shows that the agreement is reasonably good for air-water and helium-water mixtures, but poor for Freon-water. For the complete set of data, the correlation is generally good as it correlates 88% of the data within $\pm$ 50%.

6.5.3. Correlation of Kudirka [58]

$$\frac{\bar{Nu}_{TP}}{(\bar{Re}_{SL})^{1/4}\, Pr_L^{1/3} (\mu_G/\mu_L)^{0.6} (\mu_L/\mu_W)^{0.14}} = 125 \left(\frac{V_{SG}}{V_{SL}}\right)^{0.125} \tag{6.25}$$

This correlation was obtained to correlate the author's data (local data) at a single point on the heated test section for the range $1 \leq V_{SL} \leq 9$ ft/sec (0.305 to 2.7 m/sec), see Section 2.2.6.

The correlation is plotted in Fig. 6.22 where it is tested against the present data; the results are summarized in Table 6.6 below.

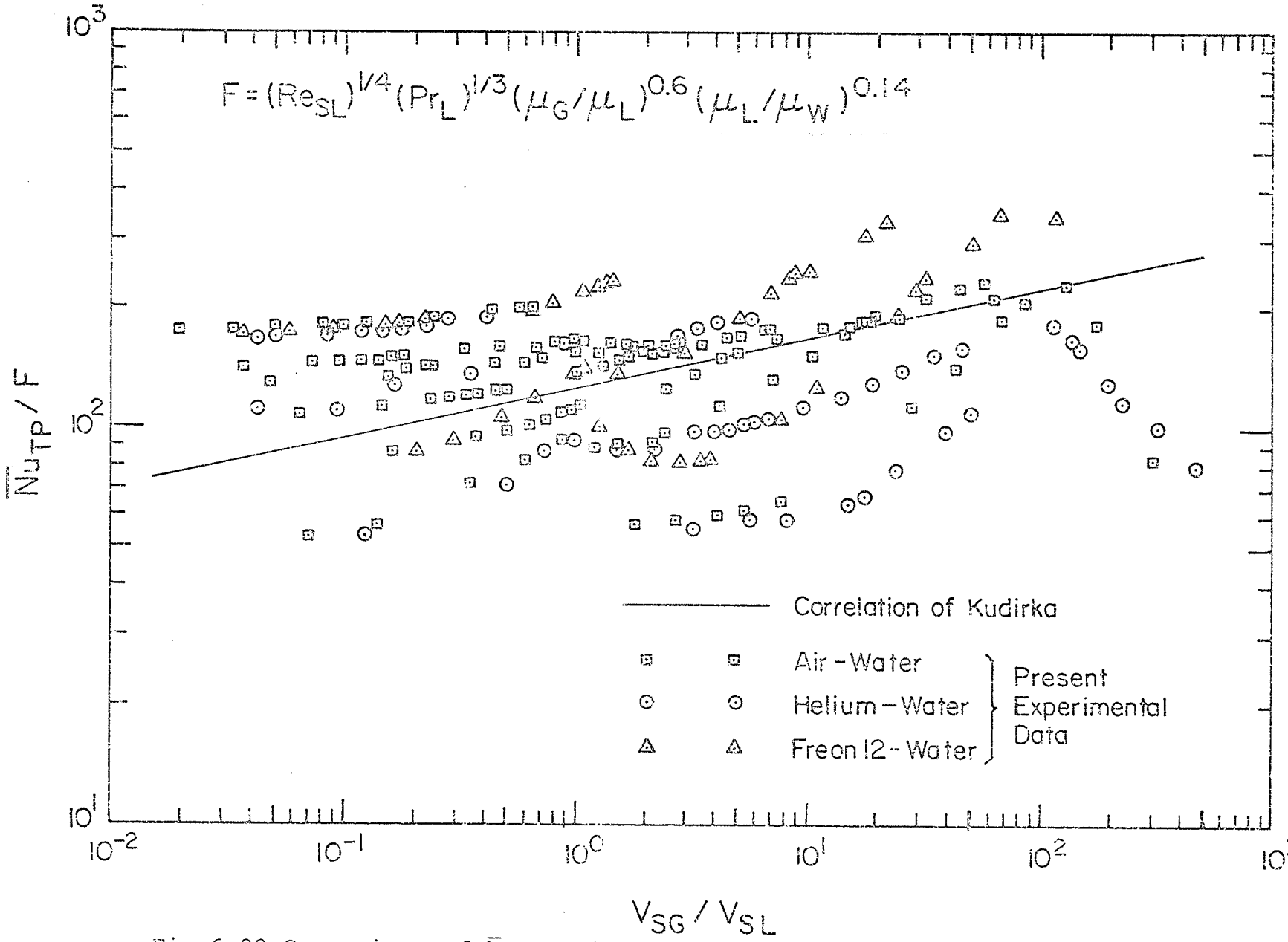

Fig. 6.22

Fig.6.22 Comparison of $\bar{h}_{TP}$ Against the Correlation of Kudirka

TABLE 6.5

Comparison of the Correlation of Knott et al. with the Present Data

Range of Deviations	Number of Data Points (% of Total N) Lying in the Specified Range of Deviations			
	Air-Water (N=109)	Helium-Water (53)	Freon-Water (43)	Complete Set (205)
±20%	69.72	75.47	36.36	64.08
±30%	87.16	86.79	38.64	76.70
±40%	91.74	90.57	50.00	82.52
±50%	94.50	98.11	61.36	88.35
> ±50%	5.50	1.89	38.64	11.65
$\bar{e}$(%)	1.65	3.01	42.64	10.76
$\bar{e}'$(%)	23.30	20.82	55.38	32.46

TABLE 6.6

Comparison of the Correlation of Kudirka [58] with Present Data

Range of Deviations	Number of Data Point (% of Total N) Lying in the Specified Range of Deviations			
	Air-Water (N=109)	Helium-Water (53)	Freon-Water (43)	Complete Set (205)
$\pm$20%	50.46	3.77	22.73	32.52
$\pm$30%	60.55	32.08	31.82	47.09
$\pm$40%	73.39	58.49	38.64	62.14
$\pm$50%	79.82	64.15	61.36	71.84
> $\pm$50%	20.18	35.85	38.64	28.16
$\bar{e}$(%)	12.20	- 6.79	31.74	11.49
$\bar{e}'$(%)	40.39	49.22	55.17	46.22

Figure 6.22 shows that the data spread widely around the correlation (data lie within the range 50-400 of the ordinate in the figure); it is therefore impossible to represent the data by a single line on the figure. The agreement between the data and Eq. (6.25) is generally poor as illustrated in Table 6.6. It should be noted, however, that in the range of applicability of the correlation, the agreement was good ($\bar{e}'$ = 18.5%).

6.5.4. Correlation of Ueda and Hanaoka [86]

$$\bar{Nu}_{TP} = 0.075(Re_M)^{0.6} \frac{Pr_L}{1 + 0.035(Pr_L - 1)} \qquad (6.26)$$

The correlation is compared against the present data in Fig. 6.23 and the results of the comparison are summarized in Table 6.7 below. Figure 6.23 shows a remarkably good agreement between the correlation and the data; only five data points (one for air-water and four for helium-water) deviate by more than 50% from the correlation. If these points, which are in the mist and mist-annular flow regimes, were excluded, the agreement would be excellent as can be seen from Table 6.7. Equation (6.26) is, therefore, accepted as a correlation for the present data up to the flow-pattern transition from annular to mist flow.

TABLE 6.7

Comparison of the Correlation of Ueda and Hanaoka [86] with Present Data

Range of Deviations	Number of Data Points (% of Total N) Lying in the Specified Range of Deviations			
	Air-Water (N=109)	Helium-Water (53)	Freon-Water (43)	Complete Set (205)
±20%	56.88	54.72	77.27	60.68
±30%	82.57	73.58	97.73	83.50
±40%	97.25	81.13	100.	93.69
±50%	98.17	92.45	100.	97.09
> ±50%	1.83	7.55	0	2.91
$\bar{e}$(%)	8.34	-13.72	4.36	1.81
$\bar{e}'$(%)	22.27	30.08	16.02	23.45

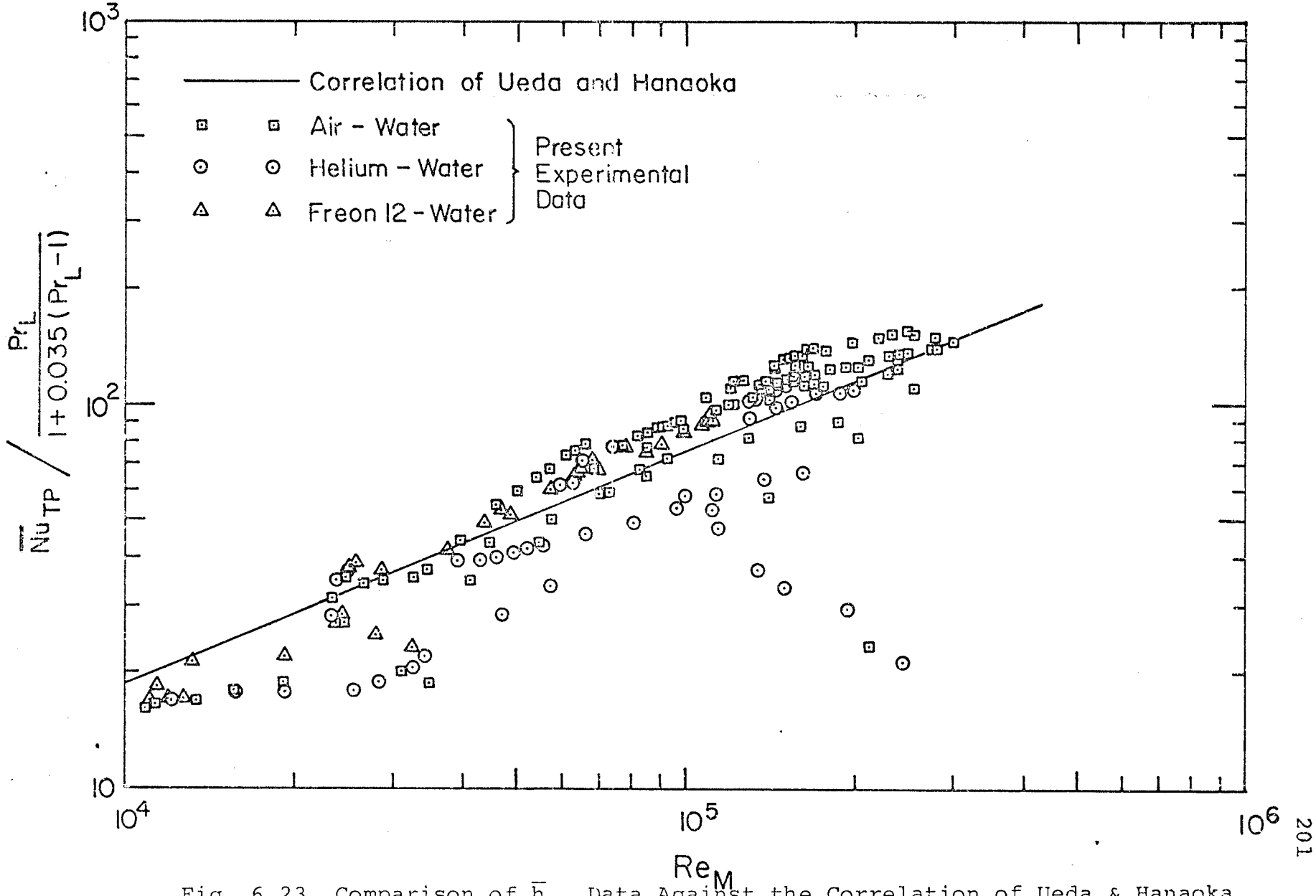

Fig. 6.23 Comparison of $\bar{h}_{TP}$ Data Against the Correlation of Ueda & Hanaoka

6.5.5. Correlation of Vijay [90]

$$\bar{h}_{TP} = \bar{h}_{AL} + \bar{h}_{AG} \qquad (6.27)$$

As discussed in detail in Section 2.2.13, Eq. (6.27) is based on a separated flow model, $\bar{h}_{AL}$ and $\bar{h}_{AG}$ are respectively the single-phase liquid and gas mean heat-transfer coefficients based on the actual mean velocity and the actual flow cross sectional area of the respective phases as calculated from Eqs. (2.47) to (2.50) and as explained in Section 2.2.13.

The correlation is tested in Fig. 6.24 where the experimental values of $\bar{h}_{TP}$ are plotted against the expected values calculated from Eq. (6.27). The results of the test are summarized in Table 6.8 below.

TABLE 6.8

Comparison of the Correlation of Vijay [90] with Present Data

Range of Deviations	Number of Data Points (% of Total N) Lying in the Specified Range of Deviations			
	Air-Water (N-109)	Helium-Water (53)	Freon-Water (43)	Complete Set (205)
±20%	44.04	32.08	81.82	49.03
±30%	66.97	54.72	97.73	70.39
±40%	83.49	79.25	97.73	85.44
±50%	96.33	90.57	97.73	95.15
> ±50%	3.67	9.43	2.27	4.85
$\bar{e}$(%)	-23.99	-27.34	- 2.37	-20.23
$\bar{e}'$(%)	28.55	33.53	14.71	27.69

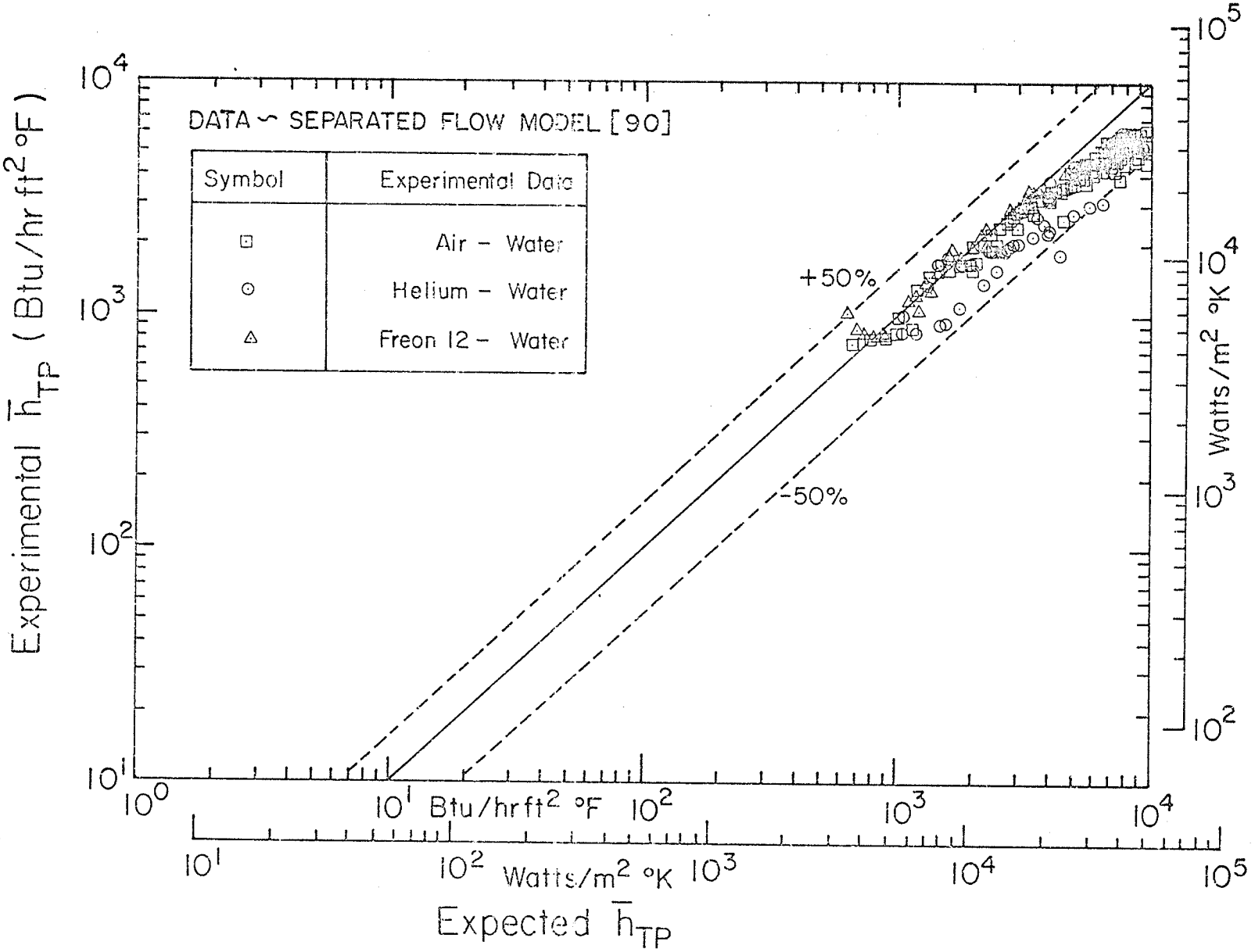

Fig. 6.24 Comparison of $\bar{h}_{TP}$ Data against the Correlation of Vijay

Figure 6.24 and Table 6.8 show that the agreement between the correlation and the data is excellent; however, it is clear that there is a general tendency for the correlation to overpredict the experimental data (this tendency was also observed for the data of [90]). Based on these observations, the correlation was studied in more detail where the contribution of each of $\bar{h}_{AL}$ and $\bar{h}_{AG}$ to $\bar{h}_{TP}$ was investigated considering both the present data and those of [90]. It was found that $\bar{h}_{AG}$ contributes but little to $\bar{h}_{TP}$ even at the lowest liquid flow rate and largest gas flow rate. It was also found that, for all data in general, $\bar{h}_{AL}$ alone would give better prediction of the experimental values than Eq. (6.27); that is, considering both the present data and the data of [90] which together form the widest range of data available, a better correlation of the data would take the form

$$\bar{h}_{TP} = \bar{h}_{AL} \tag{6.28}$$

Further discussion will be given in Section 6.6 where an attempt to develop a new correlation is made.

6.5.6. Summary of the Comparison

From the comparative discussion presented in the previous sections, it is concluded that the correlations of Ueda and Hanaoka [86] and Vijay [90] are the best among those existing in the literature. If one considers only the present data, the correlation of [86] would be superior over

that of [90] (compare Tables 6.7 and 6.8); on the other hand, when both the present data and those of [90] are considered (these form a very wide range of data), the correlation of Viday would be better. Although both correlations [86] and [90] depend strongly on the void fraction, the former is somewhat complicated and contains empirical constants which limits its range of applicability while the latter is very simple and does not contain any empirical constants. This correlation [90] is, therefore, recommended for predicting $\bar{h}_{TP}$; however, further study is required for improvement, e.g., using Eq. (6.28) as discussed above.

The correlation of Knott et al. [56] deserves special credit because of its simplicity and because it was possible to extend the correlation (which was developed for laminar liquid flow) to predict the present data (which were all for turbulent liquid flow) with faily good accuracy (see Table 6.4)

6.6 Development of Simple Correlations of the Mean Heat-Transfer Data

This section presents the results of correlating the mean heat-transfer data. Two different correlations are

developed for the present data; the first correlates the data in terms of a liquid-phase Reynolds number, which is a function of the mean liquid velocity and the actual tube diameter, and the liquid properties; the second correlation correlates the data in terms of the two-phase frictional pressure drop in a similar way to Fried's correlation [31] for horizontal flow. The two correlations are also tested against Vijay's data [90] which, together with the present data, cover the widest range of variables studied so far.

Further, the present data are correlated in terms of the Martinelli parameter as proposed, e.g., by Collier and Pulling [21] for boiling heat transfer.

6.6.1. Correlation of the Two-Phase Mean Heat-Transfer Data in Terms of a Single-Phase Liquid Flow Model

Detailed studies of the correlation proposed by Vijay [90] and tested in Section 6.5.5 above, showed that the correlation has a general tendency to overpredict the experimental data and that the gas-phase mean heat-transfer coefficient $\bar{h}_{AG}$ contributes but little to $\bar{h}_{TP}$. This suggested, as discussed earlier, that only $\bar{h}_{AL}$ may be used to predict the two-phase mean heat-transfer coefficients. Although $\bar{h}_{AL}$ provided better predictions of $\bar{h}_{TP}$ than Eq. (6.27), it did still generally overpredict the data. Based on these findings, the present model described below was developed.

It was assumed that the introduction of the gas

phase acts only to accelerate the liquid phase in the test section; further, the heat is transferred and carried away mainly by the liquid phase. The two-phase heat-transfer process can, therefore, be looked at as a heat-transfer to single-phase liquid flow with the liquid flowing with the actual mean, not the superficial, velocity in the test section. The liquid Reynolds number Re_L is therefore given by

$$Re_L \equiv \frac{\rho_L \, D \, V_L}{\mu_L} \tag{6.29}$$

where V_L is the mean liquid velocity in the two-phase flow and is given by

$$V_L = V_{SL}/(1 - \alpha) \tag{6.30}$$

The Reynolds number Re_L in Eq. (6.29) is similar to that defined by Lunde [63] and differs from that used by [90] in the diameter D. The heat-transfer coefficient can then be found from the well-established single-phase heat-transfer correlations in accordance with the type of flow (that is, laminar or turbulent) as determined by Re_L. From Eqs. (6.10) and (6.12), $\bar{h}_{TP}$ is, therefore, expressed as follows:

for laminar flow $(Re_L \leq 2000)$

$$\bar{h}_{TP} = 1.615 \left(\frac{k_L}{D}\right) (Re_L \, Pr_L \, D/L)^{1/3} \left(\frac{\mu_L}{\mu_W}\right)^{0.14} \tag{6.31}$$

$$= \bar{h}_{SP} \, (1 - \alpha)^{-1/3} \tag{6.32}$$

for turbulent flow $(Re_L > 2000)$

$$\bar{h}_{TP} = 0.0155 \left(\frac{k_L}{D}\right) Pr_L^{0.5} \, Re_L^{0.83} \tag{6.33}$$

$$\bar{h}_{TP} = \bar{h}_{SP}(1 - \alpha)^{-0.83} \qquad (6.34)$$

where $\bar{h}_{SP}$ is the single-phase liquid mean heat-transfer coefficient based on the superficial liquid Reynolds number. In general then

$$\bar{h}_{TP} = \bar{h}_{SP}(1 - \alpha)^{n} \qquad (6.35)$$

where $\bar{h}_{SP}$ is calculated from the appropriate single-phase correlation while $n = -1/3$ for laminar flow ($Re_{SL} < 1000$) and $n = -0.83$ for turbulent flow ($Re_{SL} > 2000$).

The results of the correlation are shown in Fig. 6.25 and are summarized in Table 6.9 below. The expected values of $\bar{h}_{TP}$ were calculated from Eq. (6.33) as all the present data were for turbulent liquid flow.

TABLE 6.9

Comparison of Eq. (6.35) with Present Experimental Data

Range of Deviations	Number of Data Points (% of Total N) Lying in the Specified Range of Deviations			
	Air-Water (N=109)	Helium-Water (53)	Freon-Water (43)	Complete Set (205)
±20%	54.13	43.40	79.07	56.59
±30%	77.06	77.36	93.02	80.49
±40%	92.66	90.57	97.67	93.17
±50%	99.08	94.34	97.67	97.56
> ±50%	0.92	5.66	2.33	2.44
$\bar{e}$(%)	-18.89	-20.81	6.52	-14.06
$\bar{e}'$(%)	24.47	27.45	17.40	24.01

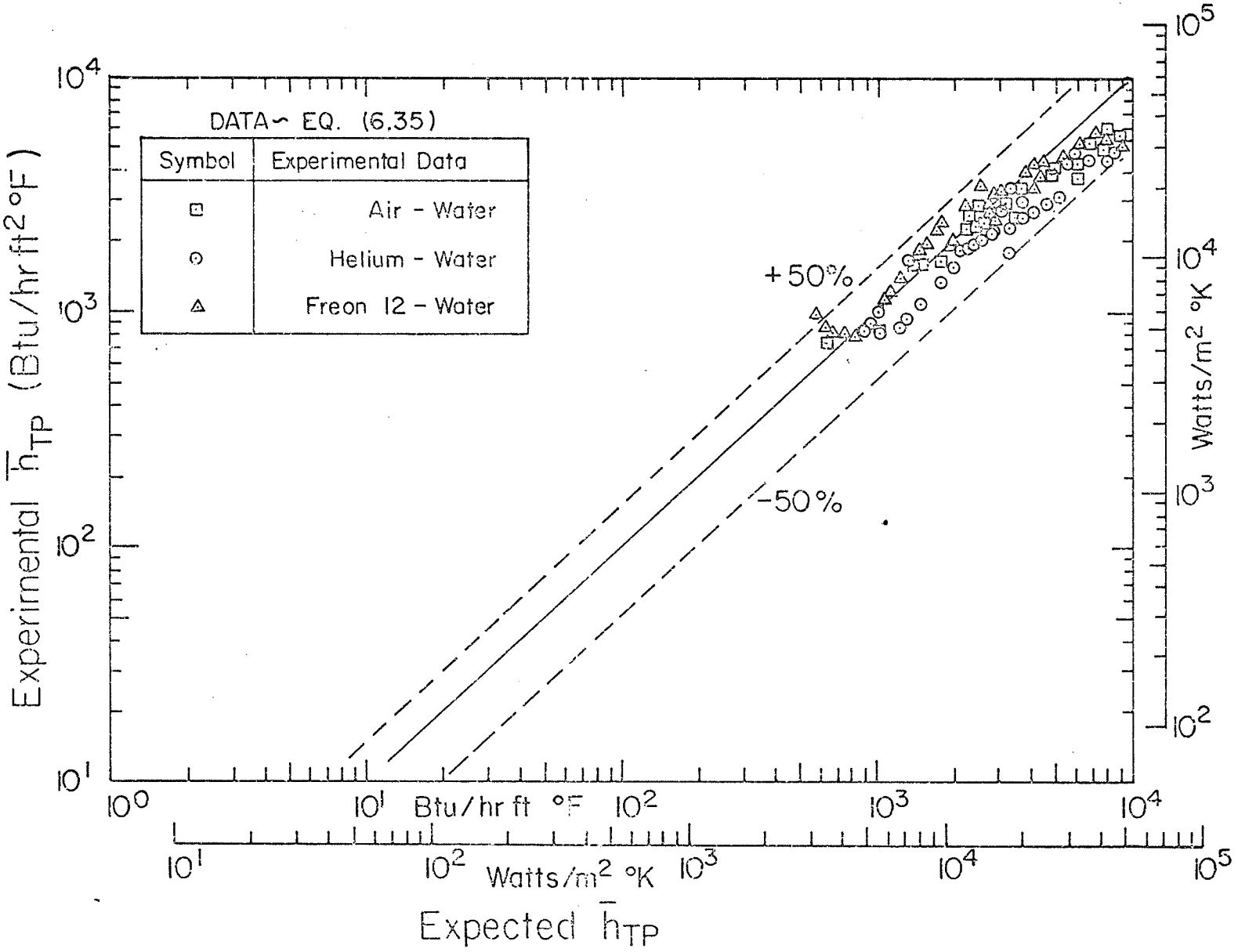

Fig. 6.25 Correlation of $\bar{h}_{TP}$ Data by Eq. (6.35)

Fig. 6.25

The conclusion from the figure and the above table is that the correlation is excellent as more than 80% and 97% of the data points fall within $\pm$30% and $\pm$50% of deviations respectively. The data with deviations > $\pm$50% represent only 2.33% of the data (five data points) which are all in the mist and mist-annular flow; this is expected because in these flow patterns the gas phase contributes more to the heat-transfer than the liquid phase does. If these five data points were excluded, that is, if the correlation were limited to be applicable only up to the transition to mist-annular flow, the agreement between the data and the correlation would be even better. A comparison between Table 6.9 and Table 6.8 shows that the present correlation is better than Eq. (6.27), as far as the present data is concerned.

To further test the present correlation, the data of Vijay [90] were compared against Eq. (6.35). The results of the comparison are shown in Fig. 6.26 and are summarized in Table 6.10 for the two sets of data (present and Vijay's). The data shown in Fig. 6.26 do not include the air-water data of Vijay as these were similar to the present air-water data. It should be noted that the data in the mist-annular flow were excluded from the comparison. Investigation of Fig. 6.26 and Table 6.10 shows excellent agreement between the data and the present correlation. As indicated in Table 6.10, the two sets of data (present and Vijay's) cover the widest range of variables studied so far; this suggests the generality of the correlation. However, the present

correlation is only a tentative suggestion which proved to work well for both the present data and Vijay's. Further testing of the correlation against other data is still required to examine its generality.

This section is concluded with the following remarks:

(i) It should be kept in mind that the present correlation requires the knowledge of the void fraction, this, however, was not measured in the present study; instead, it was calculated from the correlation of Chisholm.

(ii) The present correlation for laminar flow, Eq. (6.32) reduces to Knott's correlation [56], Eq. (6.24) for the case of no slip. The present correlation may be used as an extension of Knott's to include slip and to the turbulent flow case.

(iii) The present correlation is applicable to all flow patterns up to the transition to mist flow.

(iv) The excellent agreement between the correlation and the data considered here suggests its generality. However, further testing of the correlation against other data should be done before it is considered as being general.

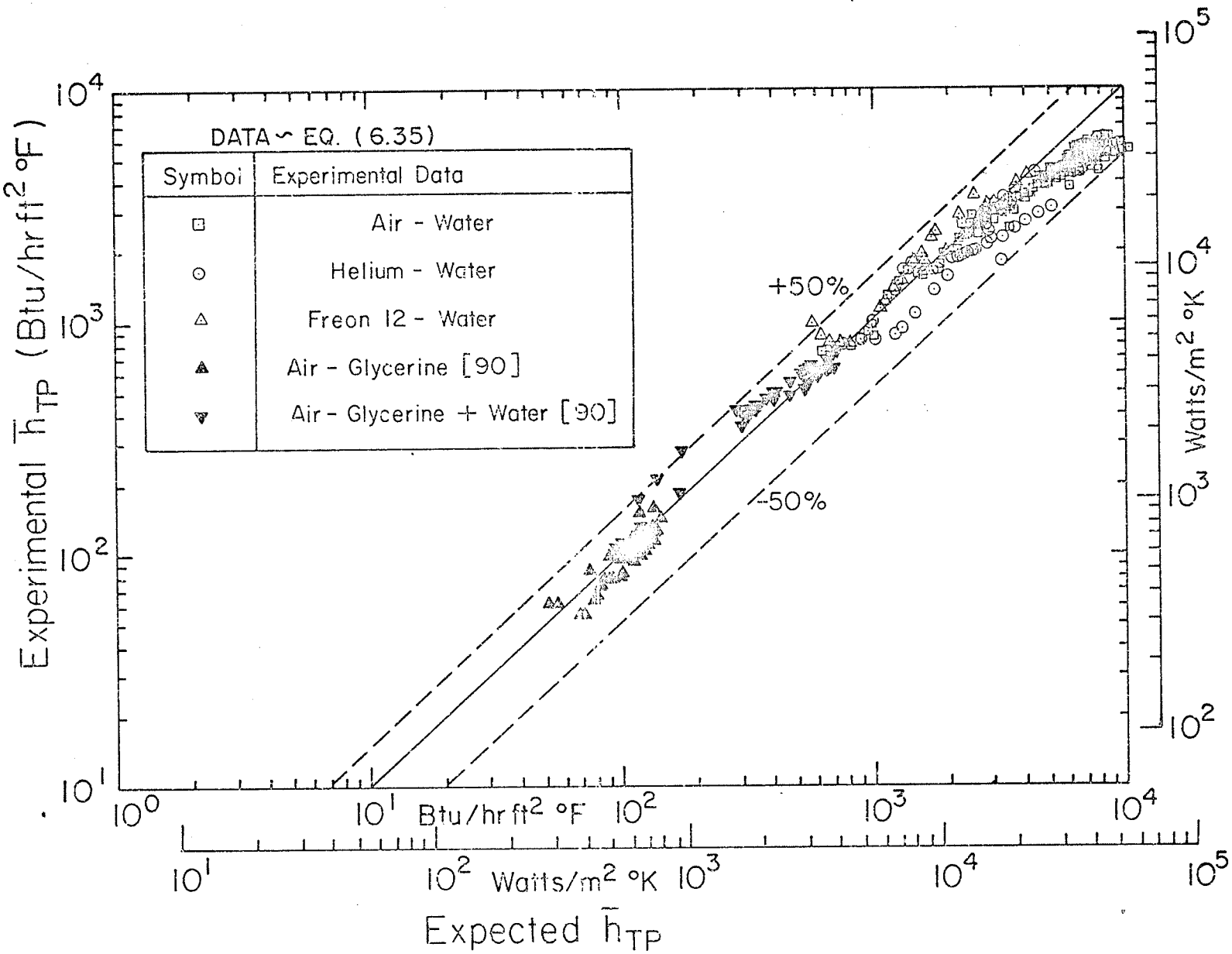

Fig. 6.26 Comparison of Eq. (6.35) Against Available Data

TABLE 6.10

Comparison of Eq. (6.35) Against the Present Data and Vijay's Data

Range of Deviations	Number of Data Points (% of Total N) Lying in the Specified Range of Deviations			Range of Variables
	Present Data (N=205)	Data of [90] (133)*	Complete Set (338)	
±20%	56.59	72.18	62.72	Re_{SL} (1.8-1.26x10^5)
±30%	80.49	78.20	79.59	Re_{SG} (14-1.6x10^5)
±40%	93.17	78.20	87.28	Pr_L (5.6-6960)
±50%	97.56	79.70	90.53	ρ_L/ρ_G (103-5378)
$\bar{e}$(%)	-14.06	18.17	- 1.38	
$\bar{e}'$(%)	24.01	43.83	32.84	

* Not including the air-water data

6.6.2. Correlation of the Mean Heat-Transfer Data in Terms of the Frictional Pressure Drop

This method of correlation was first attempted by Fried [31] for horizontal two-phase flow and was extended by Vijay [90] to vertical flow of different air-liquid mixtures covering a wide range of liquid Prandtl number (see Section 2.2.13). Since the correlation of the two-phase heat-transfer coefficients in terms of the frictional pressure drop was

accomplished for local values, through Spalding's theory (Section 6.4), and since the method has been tried [90] and was successful in correlating the mean heat-transfer data, it was natural to test this method of correlation for the present new range of data and to attempt a generalized form of this correlation for a wide range of data.

The variables involved in the correlation are:

$$\psi^2 = \bar{h}_{TP}/\bar{h}_{SP} \tag{6.36}$$

and

$$\phi^2 = \Delta P_{TPF}/\Delta P_{SPF} \tag{6.37}$$

While experimental values of $\bar{h}_{TP}$ and ΔP_{TPF} were used in evaluating ψ^2 and ϕ^2, $\bar{h}_{SP}$ and ΔP_{SPF} were calculated from the appropriate equations presented earlier (Eqs. (5.1) to (5.3) and Eqs. (6.10) and (6.12)).

The results of the correlation are shown in Figs. 6.27 and 6.28 for the present data and those of [90], respectively and are summarized in Table 6.11. No additional data of other investigators were considered because the information of ΔP_{TPF} were not generally reported. The data shown in the figures do not include those data where the pressure drop measurements were in large error (these were at low liquid rates as pointed out earlier); this is justified as the correlation depends on the frictional pressure drop. The factor $(Re_{SL})^{0.05}$ appearing in the ordinates of the figures was introduced [90] because of the dependence, though slight, on the liquid superficial Reynolds number which

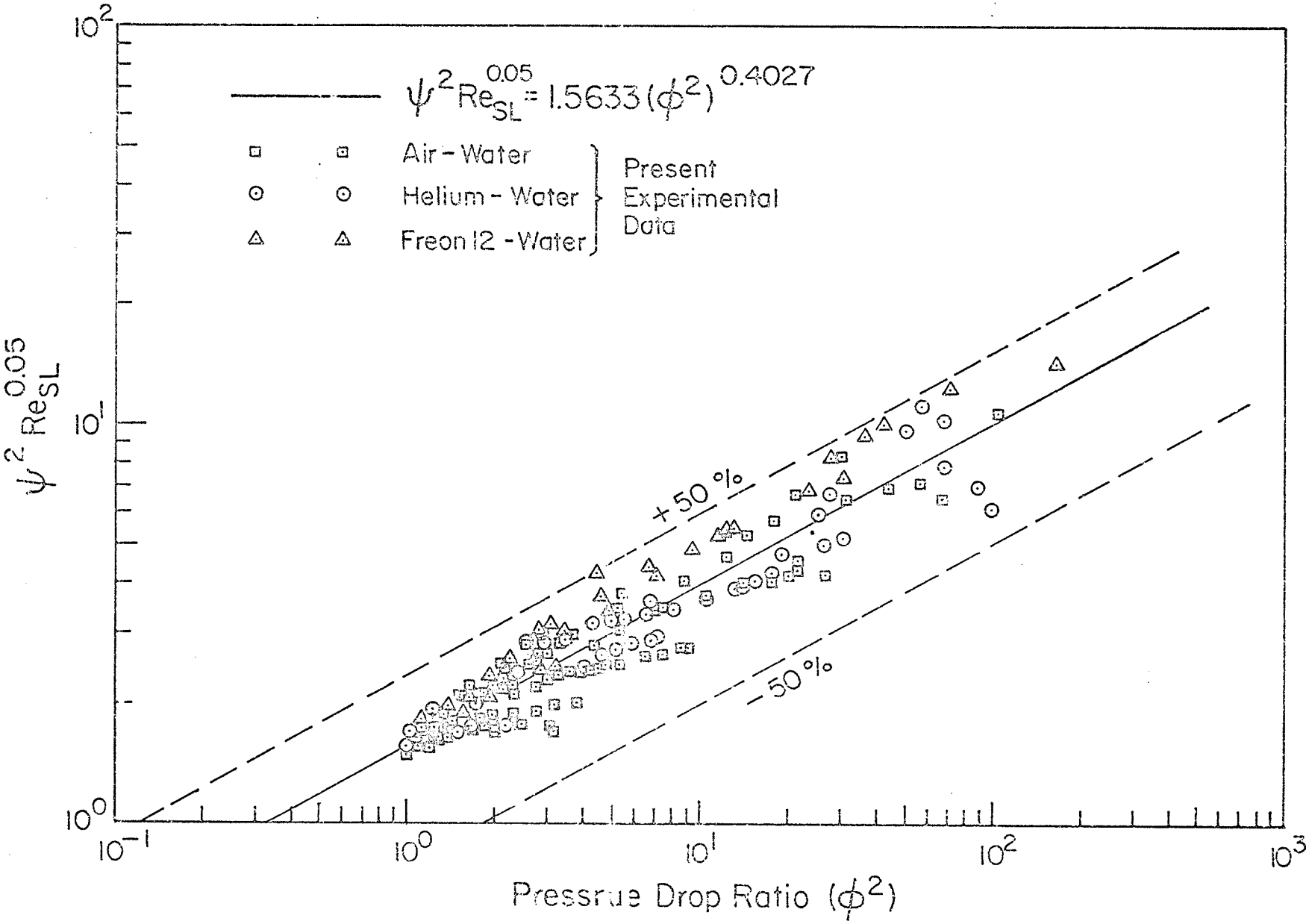

Fig. 6.27 Correlation of the Present P_{TP} Data in Terms of ΔP_{TPF} Eq. (6.38)

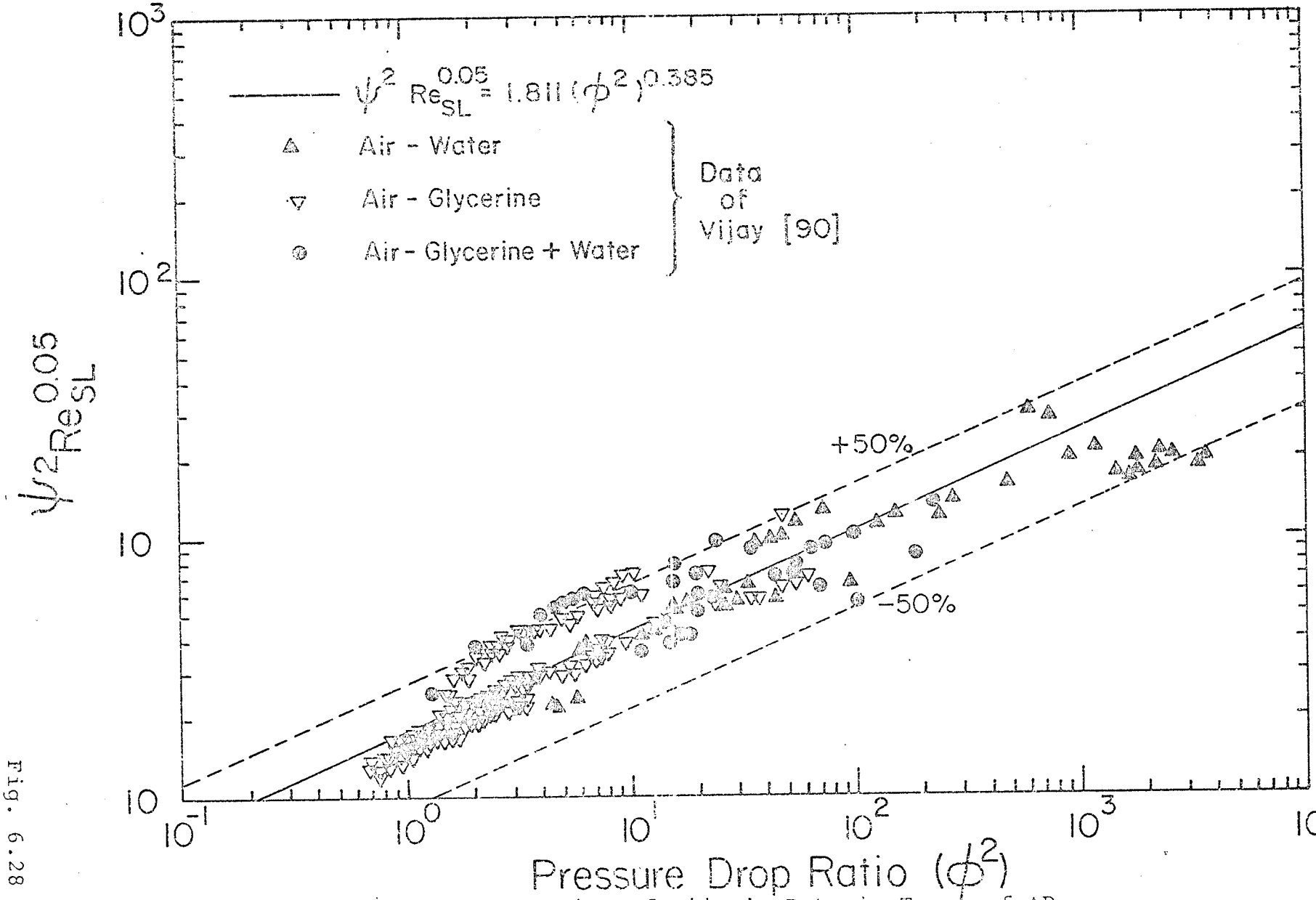

Fig. 6.28 Correlation of Vijay's Data in Terms of ΔP_{TPF}

was observed (in the present study and also in [90]) when the data were plotted as ψ^2 versus ϕ^2. The correlating equations, obtained by regression analysis, are given below.

$$\psi^2 (Re_{SL})^{0.05} = A(\phi^2)^n \tag{6.38}$$

where

$$A = 1.5633 \quad \text{and} \quad n = 0.4027 \tag{6.39}$$

for the present data (Fig. 6.27), and

$$A = 1.811 \quad \text{and} \quad n = 0.385 \tag{6.40}$$

for the data of [90] (Fig. 6.28).

TABLE 6.11

Results of Correlating the Mean Heat-Transfer Data in Terms of the Frictional Pressure Drop

Range of Deviations	Number of Data Points (% of Total N) Lying in the Specified Range of Deviations			Range of Variables Covered
	Present Data A = 1.5633 n = 0.4027 (N = 189)	Data of [90] A = 1.811 n = 0.385 (133)	Complete Set A = 1.594 n = 0.4357 (322)	
±20%	79.37	36.09	71.43	Re_{SL} $(1.8\text{-}1.26\times10^5)$
±30%	94.71	70.68	82.92	Re_{SG} $(14\text{-}1.5\times10^5)$
±40%	98.94	84.21	89.13	Pr_L (5.6-6960)
±50%	100.	91.73	93.79	ρ_L/ρ_G (103-5378)
$\bar{e}$(%)	1.22	4.00	2.30	
$\bar{e}'$(%)	15.79	29.07	22.88	

It is clear from the figures and Table 6.11 that this method provides an excellent means of correlation for both the present data and the data of [90]. Table 6.11 (last column) shows also that when both sets of data are combined together, they cover the widest range of variables studied so far; therefore, it is adequate to consider a correlation based on the complete set of data (i.e., present and [90]) as a general correlation of the two-phase mean heat-transfer coefficient.

The results of correlating the combined set of data are summarized in Table 6.11. The data are shown in Fig. 6.29 together with the correlating line as obtained by regression analysis. The correlating line is given by

$$\psi^2 (Re_{SL})^{0.05} = 1.594 (\phi^2)^{0.4357} \qquad (6.41)$$

As shown in Table 6.11 and Fig. 6.30, Eq. (6.41) is believed to be the best correlation of the mean heat-transfer data for the wide range variables listed in Table 6.11.

6.6.3. Correlation of the Mean Heat-Transfer Data in Terms of Martinelli Parameter (X_{TT})

A correlation of the data in terms of X_{TT} was attempted here because it has been successful in correlating the boiling heat-transfer coefficients [21, 23] and because of the simplicity and ease of calculating the parameter X_{TT}. The data are shown in Fig. 6.30 for all three gas-water mixtures together with the correlating line (obtained by regression

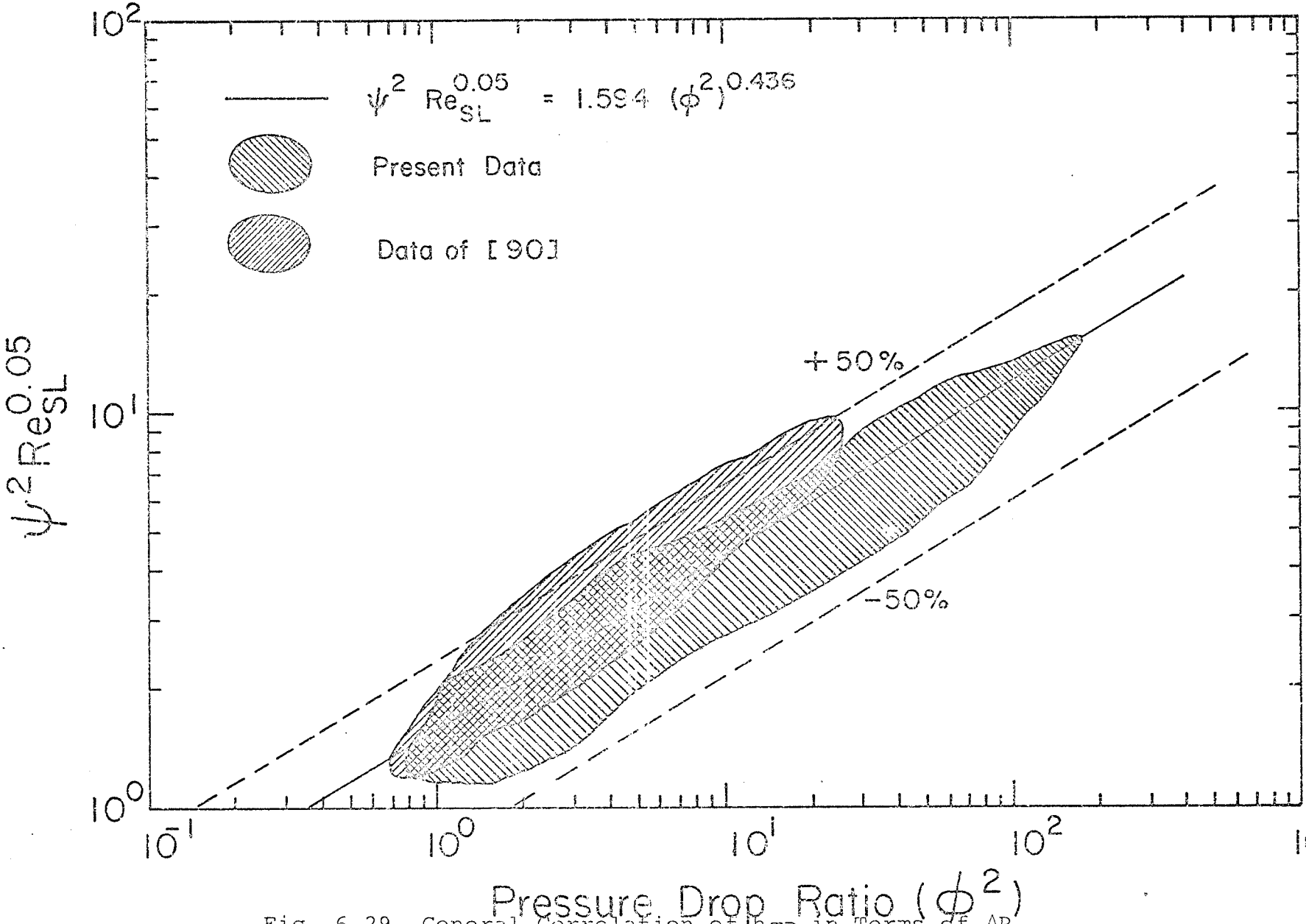

Fig. 6.29 General Correlation of h_{TP} in Terms of ΔP_{TPF}

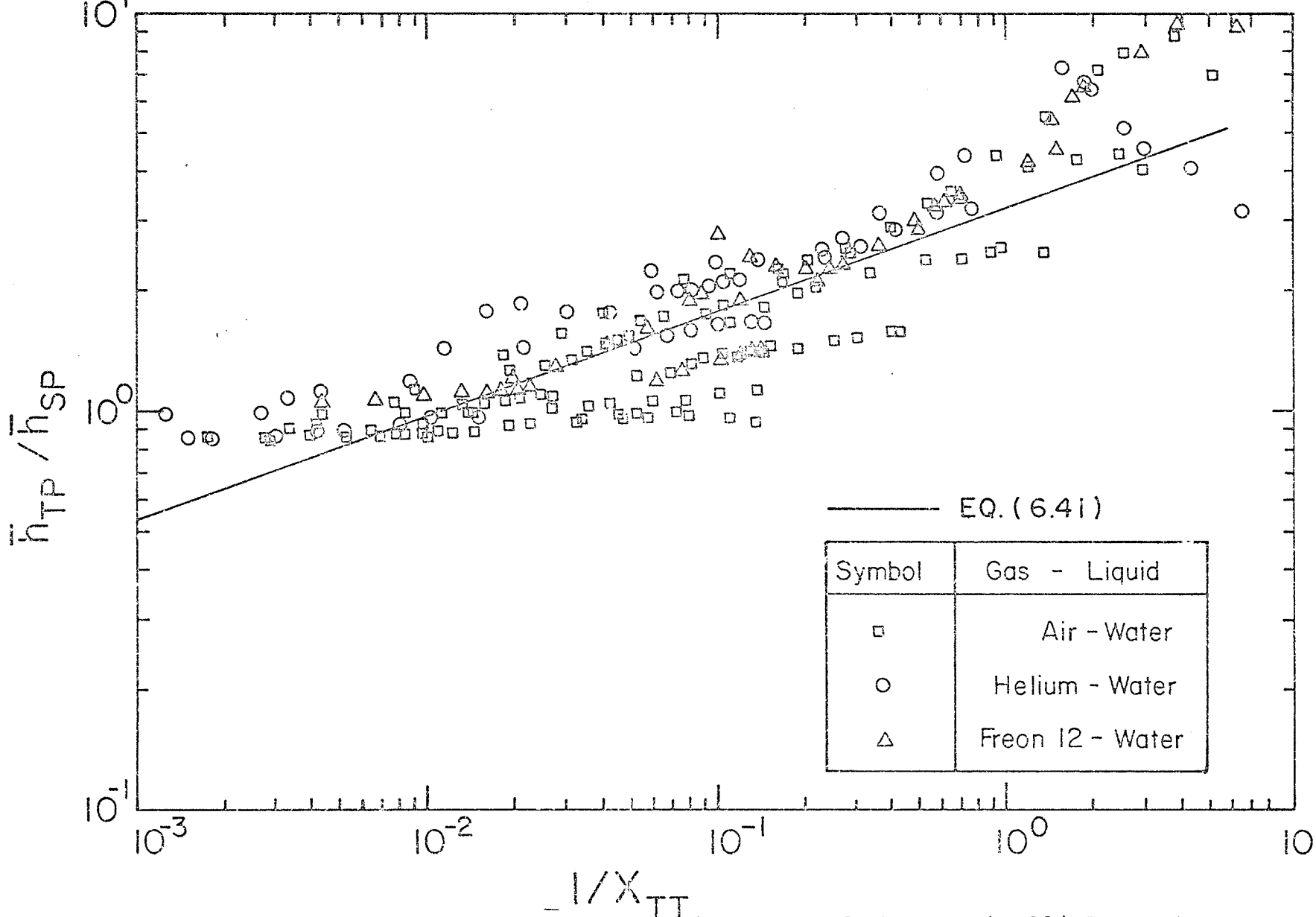

Fig. 6.30 Correlation of $\bar{h}_{TP}$ Data in Terms of the Martinelli Parameter

analysis of the data) given by

$$\frac{\bar{h}_{TP}}{\bar{h}_{SP}} = 3.353\left(\frac{1}{X_{TT}}\right)^{0.269} \qquad (6.41)$$

The percentage deviations between the data and Eq. (6.41) are summarized in Table 6.12 below.

TABLE 6.12

Summary of the Deviations Between the Mean Heat-Transfer Data and Eq. (6.41)

Range of Deviations (%)	±20	±30	±40	±50	> ±50
Number of Data Points (% of Total N) Lying in the Specified Range of Deviations	55.61	73.66	85.37	91.22	8.78
N = 205	$\bar{e}$ = 3.94			$\bar{e}'$ = 29.26	

Table 6.12 shows that the overall agreement between the data and Eq. (6.41) is good as 91% of the data fall within ±50% of deviations with a majority of data within ±30% deviations. However, Fig. 6.30 shows that the agreement is good only for moderate values of X_{TT} (0.1 to 100) while at very large or very small values of X_{TT}, the agreement is poor. This is expected as Eq. (6.41) would not hold for the extreme values of X_{TT} (0 and ∞).

Other forms of correlation, as suggested in the next section, may be more appropriate to correlate the data by this method.

It was not possible to generalize this correlation

in the form of Eq. (6.41) because it was not possible (as shown by [90]) to obtain one single equaltion from the entire set of data reported in [90], that is for all three air-liquid mixtures studied in [90].

6.7 Recommendations for Future Work

Based on the material presented up to this point of the thesis, a number of recommendations for future work can be made; these are listed below:

(i) In measuring the total pressure drop, pressure transducers should be used rather than the manometers in order to avoid the errors encountered due to rapid pressure fluctuations and the reading of small deflections on the manometers, especially at low flow rates of the phases.

(ii) It is recommended that void fractions be measured in future heat-transfer studies. This is especially so as some of the heat-transfer correlations (such as those proposed or tested in this chapter) are dependent on the void fraction. Employing void-fraction correlations to predict is not as good as using actual measurements.

(iii) Although the modified theory of Spalding has been successfully tested for general applicability as it was excellent in correlating the wide range of variables tested here, it should be tested for horizontal flows; further studies should be devoted

to resolve the problem of mixture properties especially for the mist and mist-annular flow patterns. It has been shown that the value of the turbulent Prandtl number recommended by Spalding for single-phase flow ($Pr_T = 0.887$) was more appropriate for correlating the two-phase heat-transfer data than the simplest value of one; however, further investigation of the significant and value of Pr_T for two-phase flow is required.

(iv) The correlations proposed in Sections 6.6.1 and 6.6.2 are of sufficiently general nature and deserve further study.

CHAPTER 7

FLOW-VISUALIZATION STUDY

7.1 Introductory Remarks

This chapter deals with the results of the flow-visualization experiments. As pointed out in Chapter 6, this study was initiated as a consequence of the two-phase local heat-transfer results at low flow rates of the phases which were first obtained by Vijay [90] and were confirmed in the present investigation. Under these conditions of low liquid and gas flow rates (where the observed flow patterns were bubble, slug, bubble-slug and slug-annular) the local values of the heat-transfer coefficient were found to generally increase with the distance Z along the test section. In reference [90], a theory was developed which qualitatively explained this behavior of the local heat-transfer coefficients. The theory is based on a bubble flow model in which it was assumed that the gas bubbles expand as they move from the inlet to the outlet of the test section due to the pressue drop across the test section and the heating of the fluid. The bubbles would, therefore, travel at higher velocities dragging more liquid along the centre line of the test section which, by reasons of continuity, would eventually result in an inward and downward flow of the liquid at the wall. Cooler liquid would then move

towards the wall resulting in an increase in the heat transfer rate. Although the downflow of the liquid film on the wall is well accepted for slug flow, no report of such downflow has been made for the bubble-flow regime.

Accepting the above described mechanism, the purpose of the present flow-visualization study was to examine the existence of such a downflow especially in the bubble flow regime, for which the theoretical work in [90] was developed, as a plausible explanation to the above-mentioned h_{TP}~Z relations.

As mentioned in Chapter 3, the flow-visualization experiments were performed with a transparent test section similiar in size to that used for the heat-transfer experiments. Both the dye-injection and the hydrogen-bubble techniques together with high-speed cine photography were employed to visualize the motion of the liquid film at the tube wall. The experiments were performed with air-water mixtures covering four superficial water velocities - 0.065 ft/sec (0.02m/sec), 0.166 (0.051), 0.070 (0.113) and 1.03 (0.315) for which heat-transfer experiments were performed in [90] and were repeated in the present investigation. The heat-transfer results for the first three liquid velocities, however, are not reported or analyzed in the thesis for the reasons given in Chapter 4; the experiments were performed here just to check and confirm the results of [90].

In this chapter, the flow-visualization techniques employed are discussed, then the experimental procedure is described; the results are then presented and discussed. It should be noted that the discussion presented here is purely qualitative.

7.2 Flow-Visualization Techniques

A flow-visualization technique is simply a means which enables the tracing of the motion of the particles of a moving fluid. Different techniques have been developed for single-phase flow [65]; however, no particular method has been recommended to visualize the motion of a two-phase mixture. Since the purpose of the present study was to visualize the motion of the liquid film at the wall, the flow-visualization methods developed for single-phase flow were deemed to be adequate. The dye-injection and the hydrogen-bubble techniques have long been popular methods of flow visualization; both were employed here and are described below.

7.2.1 The Dye-Injection Technique

In this method, the dye was released from small orifices which were drilled in the wall of the test section (see Chapter 3 for details of the test section). Since it is very important to avoid any disturbance of the boundary layer, the dye was released with almost no velocity component perpendicular to the wall. This was achieved by adjusting

the pressure on the free surface of the dye in the container. Having the dye released with practically zero velocity, its motion would therefore follow the motion of the liquid film near the wall of the test section. For successful visualization, the technique must fulfill several requirements: the dye should have an equal or at least very close density to that of the flowing water, the dye should have good reflective properties for high contrast and should be stable with respect to rapid diffusion. Since these properties are excellent in the case of milk, a dye mixture of milk and food colouring was used in the present experiments.

The dye injection system was prepared for operation as follows (see Fig. 3.7):

(i) The dye container and the leads carrying the dye to the injection points in the test section were checked for cleanliness.

(ii) The container was then half filled with the dye.

(iii) Air pressure was then applied on the free surface of the dye in the container and was adjusted (by means of the pressure regulator) so that the dye would be released into the flow with an extremely low velocity. It should be noted that it was difficult to maintain a uniform rate of dye flow into the test section for the slug flow regime due to the pressure fluctuations associated with this flow pattern.

(iv) After taking the photographic film, the dye flow was stopped by closing the valves on the leads carrying the dye, the pressure in the container was reduced, the container was emptied and the system was cleaned.

7.2.2 The Hydrogen-Bubble Technique

In this technique, the flow is visualized by tracing the motion of the hydrogen bubbles generated by the electrolysis of the flowing fluid provided that the fluid is an electrolytic conductor. Since ordinary tap water is an electrolytic conductor, it is therefore suitable for the application of this technique. If two electrodes are introduced into such a water flow and a DC voltage is applied between the electrodes, hydrogen bubbles are formed at the cathode and oxygen bubbles at the anode. Since the hydrogen bubbles develop with much smaller size than the oxygen bubbles, only the hydrogen bubbles are used as tracer particles as the rise rate of the bubbles (due to buoyancy) depends on the bubble size.

In the present experiments, a thin, fine platinum wire 0.003 in.(0.076mm) diameter was used as a cathode (the bubble size is of the order of the diameter of the generating cathode [65]) and was stretched along the diameter of the test section as described in Chapter 3. Sodium sulfate was added to the water at a concentration of 10mg/liter in order to increase its electrical conductivity. After establishing

the required experimental conditions, a DC voltage (200-300V) was applied between the cathode and the anode and was adjusted to obtain sufficient optical density of the hydrogen bubbles. The lighting was then adjusted and the photographic film was taken. It should be mentioned that the quality of the bubbles was observed to change after a few minutes of continuous operation, presumably as a result of the deposition of contaminating materials on the platinum wire; this was corrected by reversing the polarity in the electric circuit for about 30 sec (see Fig.3.8).

7.3 Experimental Procedure

The experiments were performed with air-water mixtures at room temperature and under adiabatic conditions. The air and water flow rates tested were those for which heat-transfer results are available in [90] (the heat-transfer experiments under these conditions were repeated here to confirm the results of [90] before conducting the flow-visualization experiments). The experimental procedure was, in general, similar to that described for the heat-transfer experiments; this is described below.

(i) The heat-transfer test section was isolated from the system and the flow was directed to the flow-visualization test section by means of the shut-off valves (see Chapter 3 for description of the apparatus).

(ii) The air pressure at the inlet to the orifice plate

assembly was set at the required value by means of the pressure regulator in the air line; the air flow rate was then set to the desired value by adjusting the appropriate needle valve.

(iii) The water pump was then started and the pump outlet pressure was set at a sufficiently high value so that a large pressure drop across the control valve was obtained on setting the water flow rate in order to avoid any fluctuations in the flow rates (necessary adjustments of the air and water flow rates were performed after the introduction of the water).

(iv) The high-speed movie camera was checked for proper film speed (500 to 2000 pictures per second depending on the flow velocities) at an aperture of f/5.6. The light intensity was then determined by a Spotmeter and adjusted through the variation of the input voltage to the two movie lights.

(v) The dye-injection system or the hydrogen-bubble generating circuit was put into operation and, finally, the photographic film was taken.

It should be noted that after each and every test employing the dye-injection technique, the apparatus was drained, flushed and recharged with fresh water in order to avoid over-contamination of the water with the dye.

Although the dye-injection method was successful for

all flow patterns observed in the experiments, it was possible to employ the hydrogen-bubble technique for tests only in the bubble flow regime.

In the next section, sample photographs of the films taken in this study are presented; however, the experimental conditions for all tests performed are summarized in Table 7.1.

7.4 Results and Discussion

As mentioned earlier, the purpose of this study is to test for presence of downflow at the walls as a possible explanation for the observed relationship between the local heat-transfer coefficients and the axial distance along the flow direction at low flow rates of the two phases; that is, the reasons for the increase of h_{TP} with Z under these conditions. This behavior has been observed before [29,32,90]; in reference [32] (which was dealing with horizontal stratified flow), the increase in h_{TP} with distance was attributed to the natural convection effects as the ratio of the Grashof number to the Reynolds number under these conditions was always larger than unity. In reference [90], the previously described theoretical model was developed and qualitatively explained this behavior.

In the present study, heat-transfer results for the flow conditions studied in [90] were obtained which confirmed the results of [90]. Some of these results are shown in

Table 7.1 Experimental Conditions

Re_{SL} (V_{SL}, ft/sec)	Re_{SG}	Flow Pattern	Method of Visualization	Film No.	Film Speed PPS
265 (0.065)	48	Bubble	Dye	B1	1500
	48	Bubble	H-Bubble	B2	1000
779 (0.166)	639	Slug	Dye	3B	500
	892	Slug		F3C	1000
	1655	Slug-Annular*		F1B	800
	1976	Slug-Annular*		5B	500
	13,370	Slug-Annular*		F4C	1000
	17,298	Annular with Liquid Bridging		F14C	2000
1400 (0.370)	479	Slug	Dye	1C	500
	1250	Slug		F7C	1000
	1520	Slug		2C	500
	2115	Slug		F8C	1000
	6629	Slug-Annular*		F9C	1000
	12,849	Slug-Annular*		F10C	1000
4090 (1.03)	1136	Slug	Dye+H-Bubble	F12C	2000
	1136	Bubble		F11C	1000
	16,265	Slug-Annular*	Dye	F13C	2000

* These could also be called Churn Flow.

Fig. 7.1 where the local values of the Nusselt number are plotted against the distance Z along the test section. Fig. 7.1 shows, in general, that Nu_{TP} first decreases with Z but then increases with increasing Z. The above mentioned possible reasons for this behavior [32,90] were examined here; however, the attribution of this Nu_{TP}~Z relation to natural convection effects was excluded as the calculated ratios of Grashof to the square of Reynolds numbers were less than unity for all tests performed. The explanation proposed in [90] was, therefore, accepted as it seems logical especially because the downflow of the liquid film at the wall is well accepted for slug flow and for annular flow under certain conditions [93,94]. However, no observations of such downflow have been reported for the bubble flow regime for which the theoretical model in [90] was developed. It was necessary, therefore, to check the existence of this downflow in the bubble flow regime in order to examine the validity of the model proposed in [90]. For this purpose, as mentioned earlier, high-speed movie films were taken to visualize the motion of the liquid film at the walls. Figure 7.2 is a reproduction of photographic Film Number B2 (see Table 7.1) which was taken for bubble flow at a low water flow rate (V_{SL} = 0.065 ft/sec (0.02m/sec)) and employing the hydrogen-bubble technique. Examination of the projected films (the one reproduced in Fig. 7.2 and Film Number B1 employing the

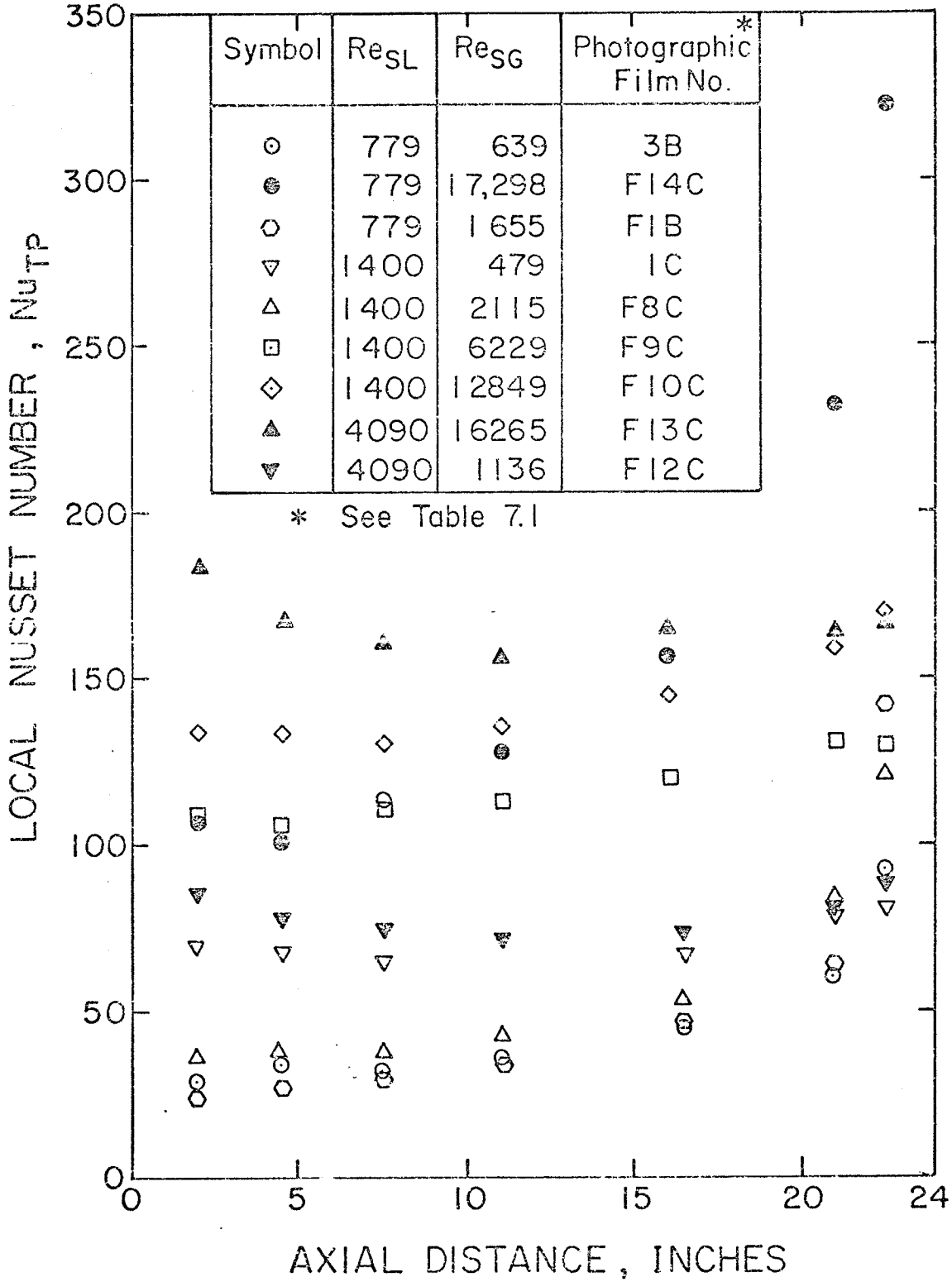

Fig. 7.1 Plot of Nu_{TP} Against Z

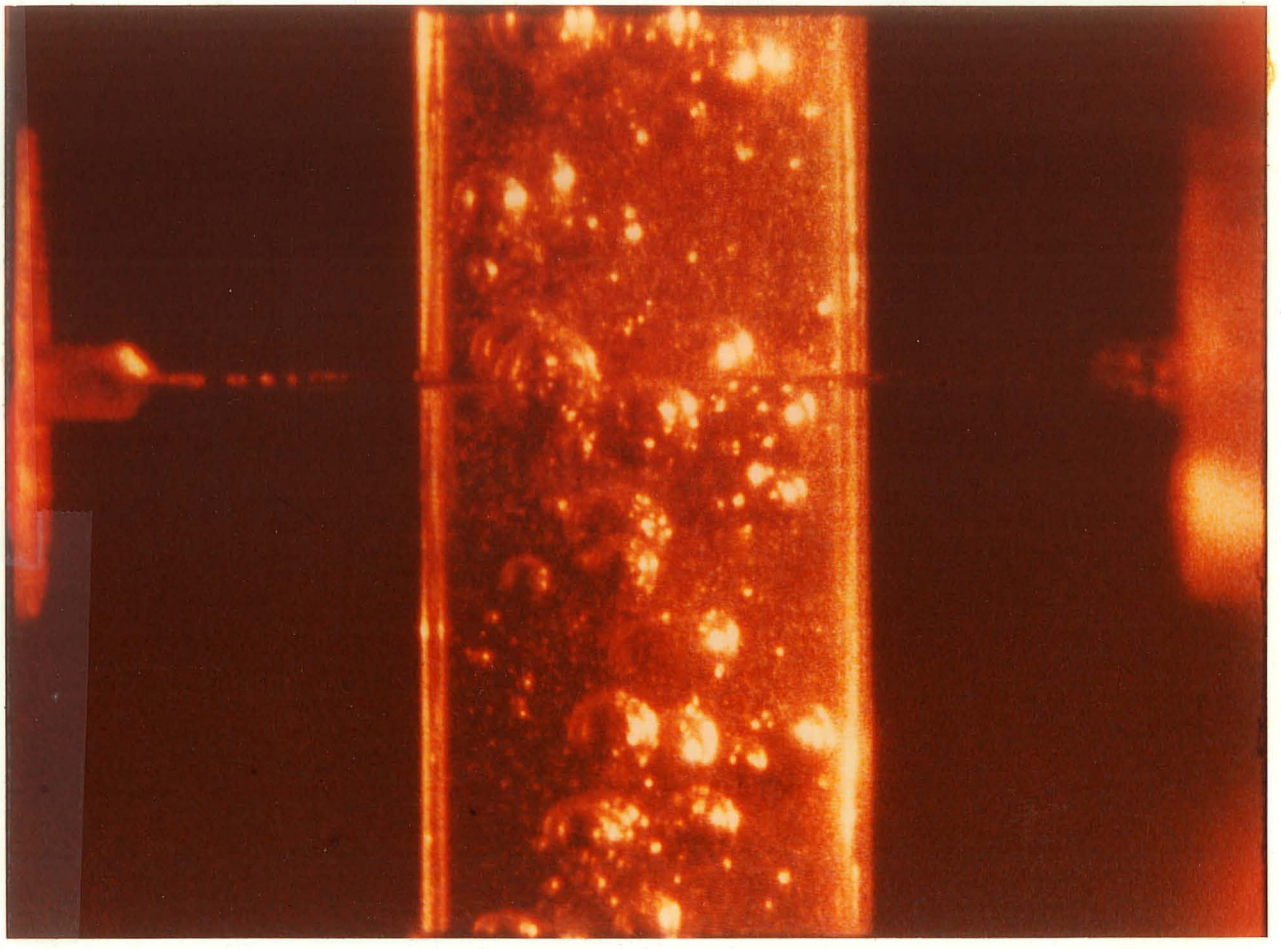

Fig. 7.2 Reproduction of Film No. B2

Notice the cloud of fine hydrogen bubbles below the wire.

dye injection technique) showed that:

(i) There is indeed downflow at the walls as the hydrogen bubbles generated near the walls or the injected dye were observed moving downwards (it should be noted that the static pictures, as those shown in Fig. 7.2, do not give the same dynamic impression of downflow as one can get from viewing the movie film. The downflow of the water film appears to extend along the tube walls as the hydrogen bubbles or the dye were observed at points about 1.5D below the wire or the injection points (the limits of field photographed).

(ii) The hydrogen bubbles or dye below the wire or points of injection has some inward movement which could support the theory [90] or be due to disruption of the flow near the wall by air bubbles in the vicinity of the wall, or both.

Figure 7.3 is a reproduction of photographic film number F8C. The following describes the motion of the liquid film as was observed from a fixed plane along the test section, for instance, the plane at which the dye was injected (see Fig. 7.3): before the long air bubble reaches the plane of observation, the flow is steady and totally upward; as the tip of the air bubble approaches the observation plane, initial deceleration of the liquid film occurs until its velocity becomes zero; thereafter, the liquid film reverses its

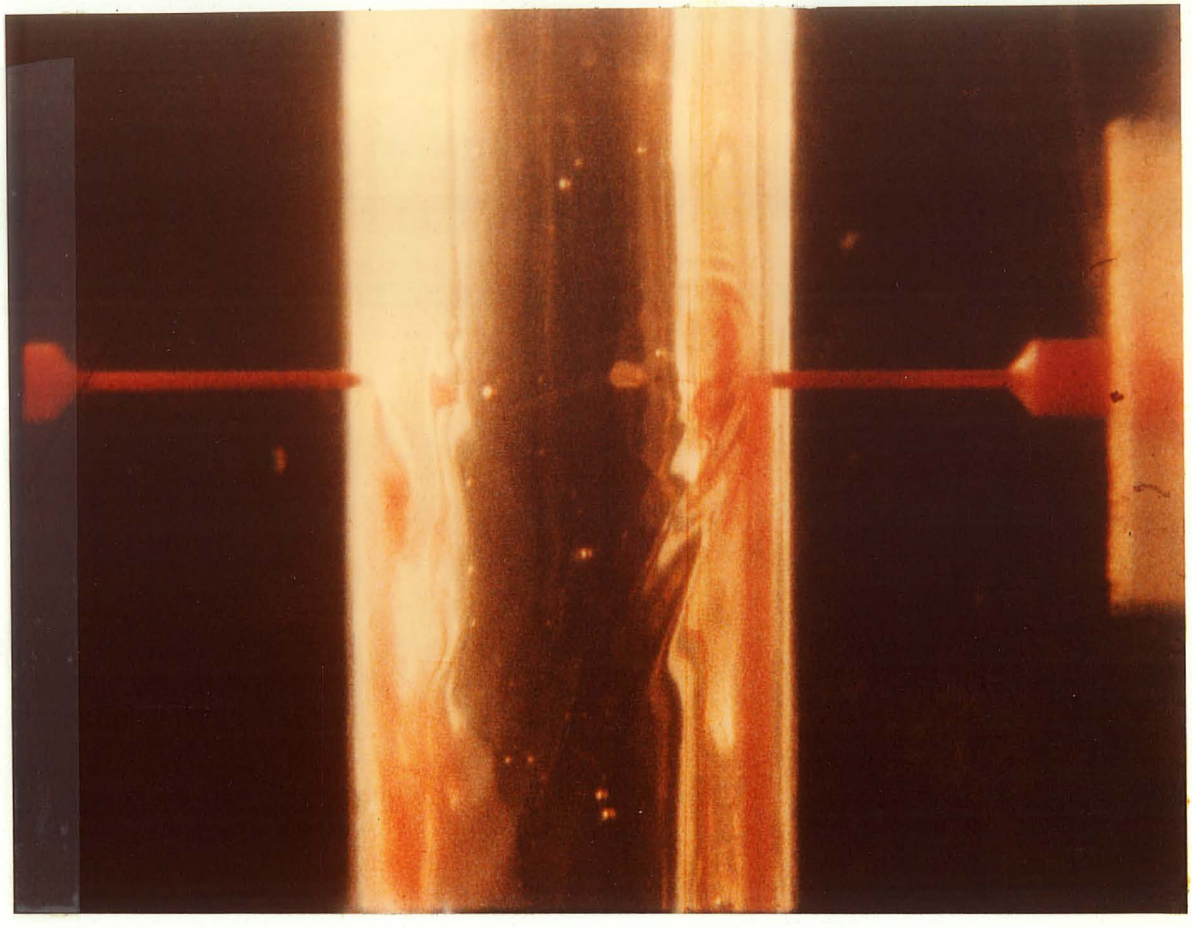

Fig. 7.3 Reproduction of Film No. F8C

See the pink colour of the dye below the injection points.

direction and accelerates downwards as long as the air bubble is moving upward until the water slug (which follows the long air bubble) reaches the plane of observation; then, the liquid film reverses its direction and moves upward with the moving water slug. The liquid in the falling film flows into the liquid slug downstream of the long air bubble and - by reasons of continuity - liquid from the slug upstream of the long air bubble will flow downward into the film, as illustrated in Fig. 7.4.. It should be noted that under the experimental conditions listed in Table 7.1 for slug flow, the air bubble was much longer in length than the water slug (typically the length of the air bubble was about six times that of the water slug) and longer than the length of the test section. On these bases, the flow could be regarded as a falling film flow with short periods of upward flow (air bubble is much longer than the water slug); this is a possible explanation of the observed behavior of h_{TP} with respect to Z.

Examination of Fig. 7.1 and Table 7.1 shows that the above described h_{TP} Z behavior was also oberved for annular flow at low liquid flow rates. However, it was difficult to observe a downflow in the liquid film from the photographic films taken under these conditions.

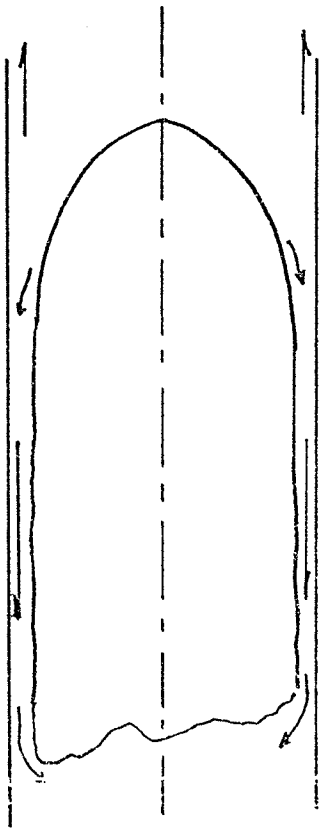

Fig. 7.4 Schematic of the Flow Direction of the Liquid Film in Slug Flow as Seen From a Stationary Point.

The existing theoretical work [93] suggests the existence of this downflow in the annular flow regime under the present experimental conditions. This, of course, would explain the h_{TP} - Z relation shown in Fig. 7.1.

From the material presented in this chapter, the following conclusion are drawn:

(i) The earlier heat-transfer results [90] for which h_{TP} increases with increasing Z are confirmed as

these have been repeated in the present study.

(ii) For bubble flow at low liquid flow rates, downflow of the liquid film at the wall has been observed; below the plane of hydrogen-bubble generation or dye injection there appears to be some inward movement of the liquid which could support the theory [90] or be due to disruption of the flow hear the wall by air bubbles in the vicinity of the wall.

(iii) The flow-visualization techniques used here (hydrogen-bubble and dye injection) are, in general, a successful means of flow visualization in two-phase flow.

CHAPTER 8

PREDICTION OF PRESSURE DROP AND HOLDUP IN HORIZONTAL TWO-PHASE STRATIFIED FLOW*

8.1 Introductory Remarks

This chapter presents a theoretical solution using a simple model of co-current stratified flow between two horizontal parallel plates, taking into account the interfacial shear stress and considering a moving interface, for predicting the pressure drop and holdup in each of the laminar-turbulent and turbulent-turbulent regimes for gas-liquid systems.

Although the major part of the thesis is dealing with vertical two-phase flow, the material presented in this chapter is included here firstly because the theory might be capable of being extended to vertical annular flow, and secondly because of the importance of this subject in many applications such as oil and gas pipelines, certain types of nuclear reactors and many chemical processes.

A brief review of the literature is first given, then the present theory is developed and the resulting equations are simplified. The theory is finally tested against available experimental data and is compared with existing correlations.

---

* The material presented in this chapter has been accepted for publication in the Proc. of the 1978 HTFMI and will be presented in the 26th HTFMI Conference, 26-28 June, 1978.

8.2 A Brief Review of the Literature

Although the Lockhart-Martinelli correlations [62] are well accepted as general correlations for predicting pressure drop and holdup for all flow patterns, experimental measurements [3,9,12,47] for stratified and wavy flows have shown large deviations from the Lockhart-Martinelli correlations. A number of different physical models exist in the literature which have improved on the Lockhart-Martinelli correlations for predicting pressure drop and holdup in horizontal stratified flow.

A simple trial and error method for calculating the pressure drop and holdup has been proposed by Etchells [28]; in this method, a value of the liquid holdup is first assumed and used as the basis for calculating the actual mean velocities and friction factors of the phases; the two-phase pressure drop is then calculated once from the velocity and friction factor of the liquid phase and once from the velocity and friction factor of the gas phase. The two values of ΔP_{TPF} are then compared, and if not equal, another value of the holdup is then assumed and the process is repeated (the pressure drop in the two phases must be the same and is equal to the two-phase pressure drop). Although this method gave better agreement with experimental data than the Lockhart-Martinelli correlations, it neglected the interfacial shear stress.

Dukler et al. [25] have presented a similarity analysis of the problem and shown that their "no-slip" method is better than the Lockhart-Martinelli correlation to predict the frictional pressure drop for stratified flow. In this method, the two-phase system is considered as a homogeneous single-phase fluid having properties equal to the volumetric averages of those of the two phases; the two phase pressure drop is then calculated from the mixture velocity ($V_{MIX}=V_{SL}+V_{SG}$) and a friction factor based on V_{MIX} and the mixture properties.

A simplified physical model for predicting ΔP_{TPF} and α has been suggested by Govier and Aziz [34]. This is basically the same as that presented by Etchells, except that the interfacial shear stress was taken into account (this was calculated from the empirical correlation proposed by Ellis and Gay [27]. However, in calculating the hydraulic diameter for the liquid phase they assumed that the interface was a stationary surface with respect to the liquid phase.

Agrawal et al. [3] modified the Govier and Aziz [34] model by considering the interface as a free surface with respect to the liquid phase and calculating the gas-friction factor from the Blasius equation. Although this model gave predictions which were somewhat higher than the experimental pressure drop values, it was more accurate than any of the Lockhart-Martinelli, Dukler et al., Govier and Aziz and Etchells models.

Johannessen [50] presented a theoretical solution for the Lockhart-Martinelli model for turbulent-turbulent flow in pipes. Although the interfacial shear stress was neglected in this model, it gave much better predictions of pressure drop and holdup than the Lockhart-Martinelli correlations, however, the solution was presented in a graphical form.

Russel et al. [73] presented a solution based on a two-dimensional analysis of the laminar velocity profile in the liquid phase, but arrived at no generalized dimensionless correlation.

Recently, Taitel and Dukler [82] presented a theoretical approach to the Lockhart-Martinelli correlation using the basic model proposed by Agrawal et al. They based their solution on the assumption that the gas-phase friction factor at the wall was equal to that at the interface, and showed that it agreed well with experimental measurements. They also concluded that the holdup and pressure drop are a unique function of the Martinelli parameter X provided that the ratio of the friction factor of the gas phase at the wall to that at the interface is constant.

In none of the above-mentioned works does one find the combination of the consideration of interfacial shear stress and a moving interface, and the obtaining of final results in the form of algebraic equations. Although there are other ways of obtaining relations for calculating pressure drop and

holdup for stratified flow (most notably using the separated flow model as described by Wallis [92]; this is discussed in detail later in this chapter), the development of comparatively simple relations among the variables based on models describing the main physical features of stratified flow is required.

8.3 Theoretical Analysis

In an effort to describe the main features of co-current, two-phase stratified flow in a plausible model, and to arrive at comparatively simple relations for predicting the pressure drop and holdup, the parallel plate geometry is used. The model, shown qualitatively in Fig. 8.1, is that of a co-current gas-liquid stratified flow between two wide horizontal parallel plates taking into account the interfacial shear stress τ_i and considering a moving interface. The velocity profile in the liquid phase is considered to be continuous from the bottom plate to the interface and is given by the one-seventh power law for turbulent flow or is derived from the momentum equation for laminar flow. In the gas-phase, however, the velocity profile is considered to consist of two parts; one part describes the velocity distribution (V_{G1} in Fig. 8.1) from the top plate to the position of maximum velocity V_{Gmax} and the second part (V_{G2} in Fig. 8.1) from the interface to the position of maximum velocity. In this latter part of the velocity profile, and in order to account

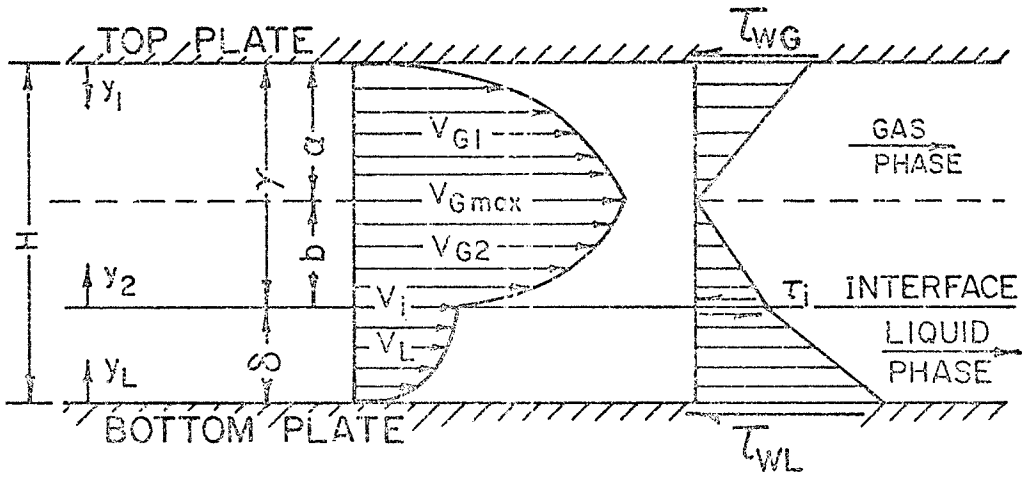

Fig. 8.1 The Physical Model of Horizontal Stratified Flow Between Parallel Plates

for the moving interface, superposition of velocity is used, i.e., the velocity is considered to be equal to that obtained considering the interface as a stationary surface with the wall shear stress being equal to the interfacial shear stress plus the interfacial velocity V_i. Throughout the analysis it is assumed that:

1. The flow is steady, adiabatic and one-dimensional.
2. The two-phases are incompressible with constant fluid properties.
3. The interface is smooth.
4. Both phases have equal velocities at the interface, i.e.,no slip.
5. The pressure drop in both phases is the same and is equal to the two-phase pressure drop.

8.3.1 Turbulent-Turbulent Flow

In this case, where both phases are in turbulent motion, the one-seventh power law is used in both phases for the velocity distribution. The velocity of the liquid phase is therefore given by

$$V_L = 8.7\ \nu_L^{-1/7}\ (\tau_{WL}/\rho_L)^{4/7}\ y_L^{1/7} \qquad (8.1)$$

where τ_{WL} is the shear stress on the bottom plate,

y_L is the vertical coordinate measured upward from the bottom plate in the liquid phase.

Integration of Eq. (8.1) from $y_L = 0$ to $y_L = \delta$ (the thick-

ness of the liquid phase) yields the volumetric rate of liquid flow per unit width as

$$Q_L = 7.6125\ \nu_L^{-1/7}\ (\tau_{WL}/\rho_L)^{4/7}\ \delta^{8/7} \qquad (8.2)$$

In the gas phase, the velocities V_{G1} and V_{G2} are given by

$$V_{G1} = 8.7\ \nu_G^{-1/7}\ (\tau_{WG}/\rho_G)^{4/7}\ y_1^{1/7},\ 0 \le y_1 \le a \qquad (8.3)$$

and

$$V_{G2} = 8.7\ \nu_G^{-1/7}\ (\tau_i/\rho_G)^{4/7}\ y_2^{1/7} + V_i,\ 0 \le y_2 \le b \qquad (8.4)$$

where τ_{WG} is the shear stress at the upper wall,

τ_i is the interfacial shear stress,

y_1 is the vertical coordinate measured downward from the top plate,

y_2 is the vertical coordinate measured upward from the interface.

Integration of Eqs. (8.3) and (8.4) after substituting for V_i from Eq. (8.1) with $y_L = \delta$, yields the volumetric rate of gas flow per unit width as

$$Q_G = 8.7\ \nu_L^{-1/7}(\tau_{WL}/\rho_L)^{4/7}\ \delta^{1/7}\ b + 7.6125\ \nu_G^{-1/7}(\rho_G)^{-4/7}[b^{8/7}\ \tau_i^{4/7} + \alpha^{8/7}\ \tau_{WG}^{4/7}] \qquad (8.5)$$

Equations (8.2) to (8.5), together with a force balance (Eqs. (I.7) to (I.10) in Appendix I) and the statement that $V_{G1} = V_{G2}$ at the position of maximum gas velocity,

are manipulated (details are given in Appendix I) yielding finally, the following dimensionless equations for the void fraction α and the pressure drop ratios ϕ_G^2 and ϕ_L^2

$$X_{tt}^2 = \left(\frac{1-\alpha}{\alpha}\right)^3 \left(1 + \frac{B_1}{1-\alpha}\right)(1+B_1)^{1/4} \cdot \left[1 - \frac{1}{7}\left(\frac{Q_L}{Q_G}\right)\left(\frac{\alpha}{1-\alpha}\right)\frac{B_1}{1+B_1}\right]^{7/4} \tag{8.6}$$

$$\phi_L^2 = 0.420\ (1 + B_1)/\left(1 + \frac{B_1}{1-\alpha}\right)(1-\alpha)^3 \tag{8.7}$$

$$\phi_G^2 = X_{tt}^2\ \phi_L^2 \tag{8.8}$$

Where ϕ_L, ϕ_G and X_{tt} are the Lockhart-Martinelli parameters and

$$B_1 = \left[1 - \frac{\alpha}{1-\alpha}\left(\frac{Q_L}{Q_G}\right)\right]^{7/5} \tag{8.9}$$

8.3.2 Laminar-Turbulent Flow

In this case, the liquid phase is considered to be in laminar motion and the gas phase is considered to be in turbulent motion. In the liquid phase, the momentum equation is solved for the velocity distribution to yield

$$V_L = \frac{1}{2\ \mu_L}\left(\frac{\Delta P}{\Delta L}\right)_{TPF}(2\ \delta\ y_L - y_L^2) + \frac{1}{\mu_L}\tau_i\ y_L \tag{8.10}$$

where $(\Delta P/\Delta L)_{TP}$ is the two-phase pressure drop per unit length. Integration of Eq. (8.10) over the liquid-film thickness gives

$$Q_L = \frac{1}{3\ \mu_L}\left(\frac{\Delta P}{\Delta L}\right)_{TPF}\delta^3 + \frac{1}{2\ \mu_L}\tau_i\ \delta^2 \tag{8.11}$$

In the gas phase, Eqs. (8.3) and (8.4) describe the velocity distribution as for the turbulent-turbulent case, and the volumetric rate of the gas flow per unit width can be shown to be

$$Q_G = \frac{1}{2\mu_L}\delta(\delta + 2b)\tau_i + 7.6125\ \nu_G^{-1/7}\rho_G^{-4/7}[a^{8/7}\tau_{WG}^{4/7} + b^{8/7}\tau_i^{4/7}] \qquad (8.12)$$

The above equations, together with a force balance and a statement that $V_{Gl} = V_{G2}$ at the position of maximum velocity, are manipulated in a similar way to the turbulent-turbulent case (details are given in Appendix I) with the final results expressed as follows:

$$X_{lt}^2 = 674.8\ \frac{(1-\alpha)^2}{\alpha}\left(\frac{1+B_2}{\alpha B_2}\right)^2\left[\frac{B_2}{(1-\alpha)+B_2}\cdot\frac{\alpha B_2 + (1-\alpha)(1+B_2)}{3\alpha B_2 + 2(1-\alpha)(1+B_2)}\right]^{3/4}$$

$$\times\ 0.0219\left[2(1-\alpha) + \frac{3\alpha B_2}{1+B_2}\right] - \left(\frac{Q_L}{Q_G}\right)\ \frac{1}{1+B_2}\ (0.066\alpha B_2 + 0.575\alpha)$$

$$\times\left[1 + \frac{2\alpha B_2}{(1-\alpha)(1+B_2)}\right]^{7/4} \qquad (8.13)$$

$$\Phi_L^2 = 1/2(1-\alpha)^2\left[2(1-\alpha) + \frac{3\ \alpha B_2}{1+B_2}\right] \qquad (8.14)$$

$$\Phi_G^2 = X_{lt}^2\,\Phi_L^2 \qquad (8.15)$$

where

$$B_2 = \left[1 - 5.25\left(\frac{Q_L}{Q_G}\right)\frac{\alpha}{(1-\alpha)(4-\alpha)}\right]^{7/5} \qquad (8.16)$$

8.3.3 A Simplified Form of the Theory

Equations (8.6) to (8.9) and (8.13) to (8.16) provide a means of predicting two-phase pressure drop and void fraction or holdup $(1-\alpha)$ in horizontal co-current stratified flow. These equations indicate that the two-phase pressure drop ratios and the void fraction depend on Q_L/Q_G as well as X. However, this dependence is extremely weak, indeed so weak that it would be difficult to establish this dependence experimentally. This dependence was examined by plotting the equations with Q_L/Q_G as a parameter (over the range of Q_L/Q_G values found in stratified flow) for the range of X appropraite for any particular Q_L/Q_G value. At any X the maximum difference in ϕ and holdup between the extreme values of Q_L/Q_G was of the order of 6 or 7%.

The form of the equations allow a marked simplification by neglecting certain terms compared with other terms. For turbulent-turbulent flow the term $[Q_L/Q_G][\alpha/(1-\alpha)]$ in B_1 is the inverse of the "slip ratio" and for stratified flow the literature indicates a maximum value of the order of 0.05 for this term. For laminar-turbulent flow, the literature indicates a maximum value of the term

$$5.25\ \left(\frac{Q_L}{Q_G}\right)\ \frac{\alpha}{(1-\alpha)(4-\alpha)}$$

in B_2 to be of the order of 0.06. Equations (8.6) to (8.9) and (8.13) to (8.16) may therefore be simplified by setting

B_1 and B_2 equal to 1 (this is the equivalent of setting the gas-side wall shear equal to the interfacial shear; see Eqs. (I.12) to (I.14) with $\gamma/\delta = \alpha/(1-\alpha)$, and Eq. (I.28). This yields, for turbulent-turbulent flow

$$X_{tt}^2 = 1.189\ (1-\alpha)^2(2-\alpha)/\alpha^3 \tag{8.17}$$

$$\Phi_L^2 = 0.841/(1-\alpha)^2(2-\alpha) \tag{8.18}$$

$$\Phi_G^2 = 1/\alpha^3 \tag{8.19}$$

and for laminar-turbulent flow

$$X_{\ell t}^2 = (1-\alpha)^2(4-\alpha)/\alpha^3 \tag{8.20}$$

$$\Phi_L^2 = 1/(1-\alpha)^2(4-\alpha) \tag{8.21}$$

$$\Phi_G^2 = 1/\alpha^3 \tag{8.22}$$

The values of Φ and $(1-\alpha)$ as calculated from the above equations are given in Table I.1 in Appendix I.

8.4 Comparison of Theory with Data and Correlations

The simplified theory as represented by Eqs. (8.17) to (8.22) is compared against available experimental data and existing correlations in Figs. 8.2 to 8.5. If the original equations (8.6) to (8.8) and (8.13) to (8.15) were plotted for appropriate values of Q_L/Q_G and X, for the turbulent-turbulent case (Figs. 8.2 and 8.3) the curves would be indistinguishable from those drawn; for the laminar-

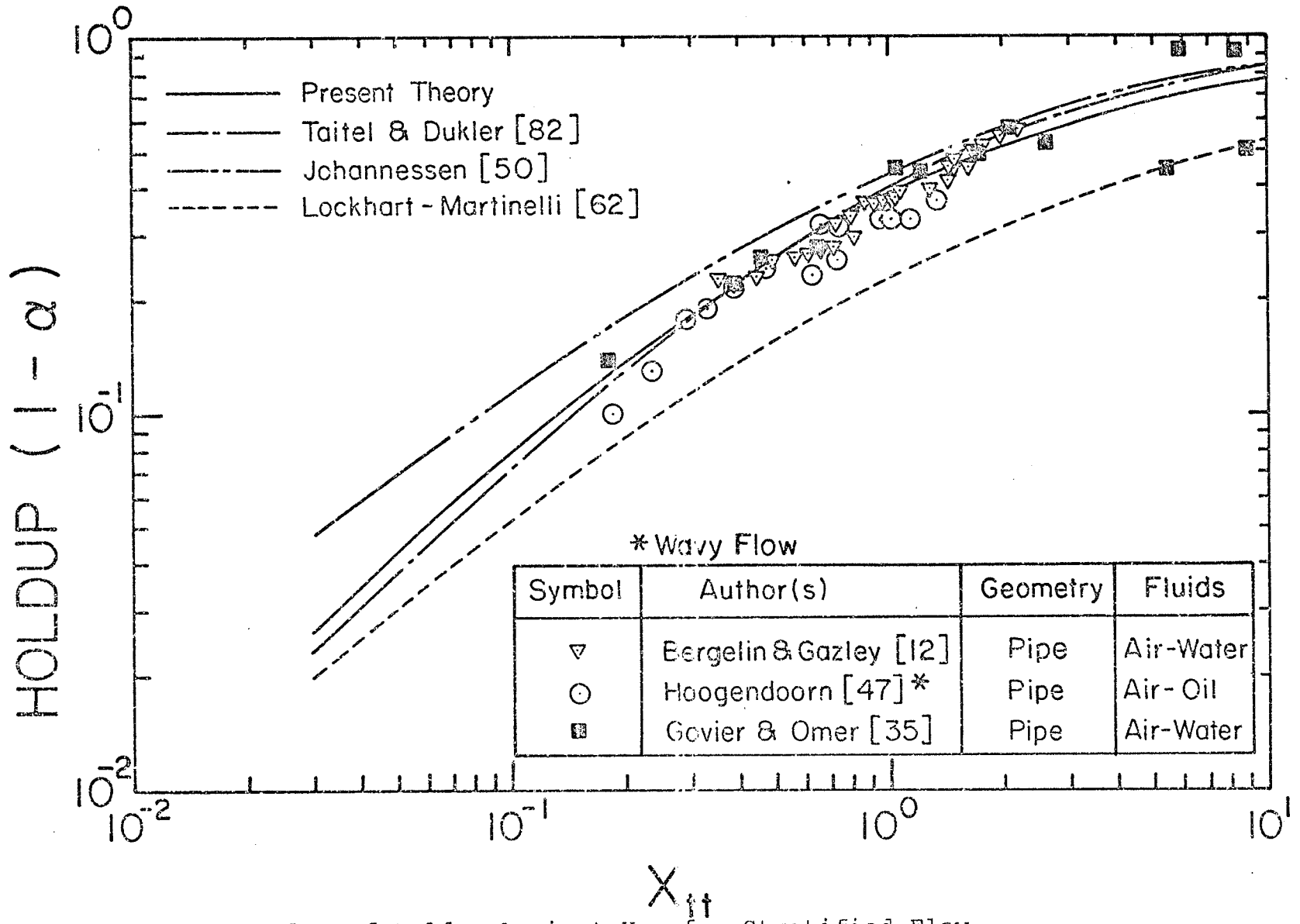

Fig. 8.2 Plot of Holdup Against X_{tt} for Stratified Flow

Fig. 8.2

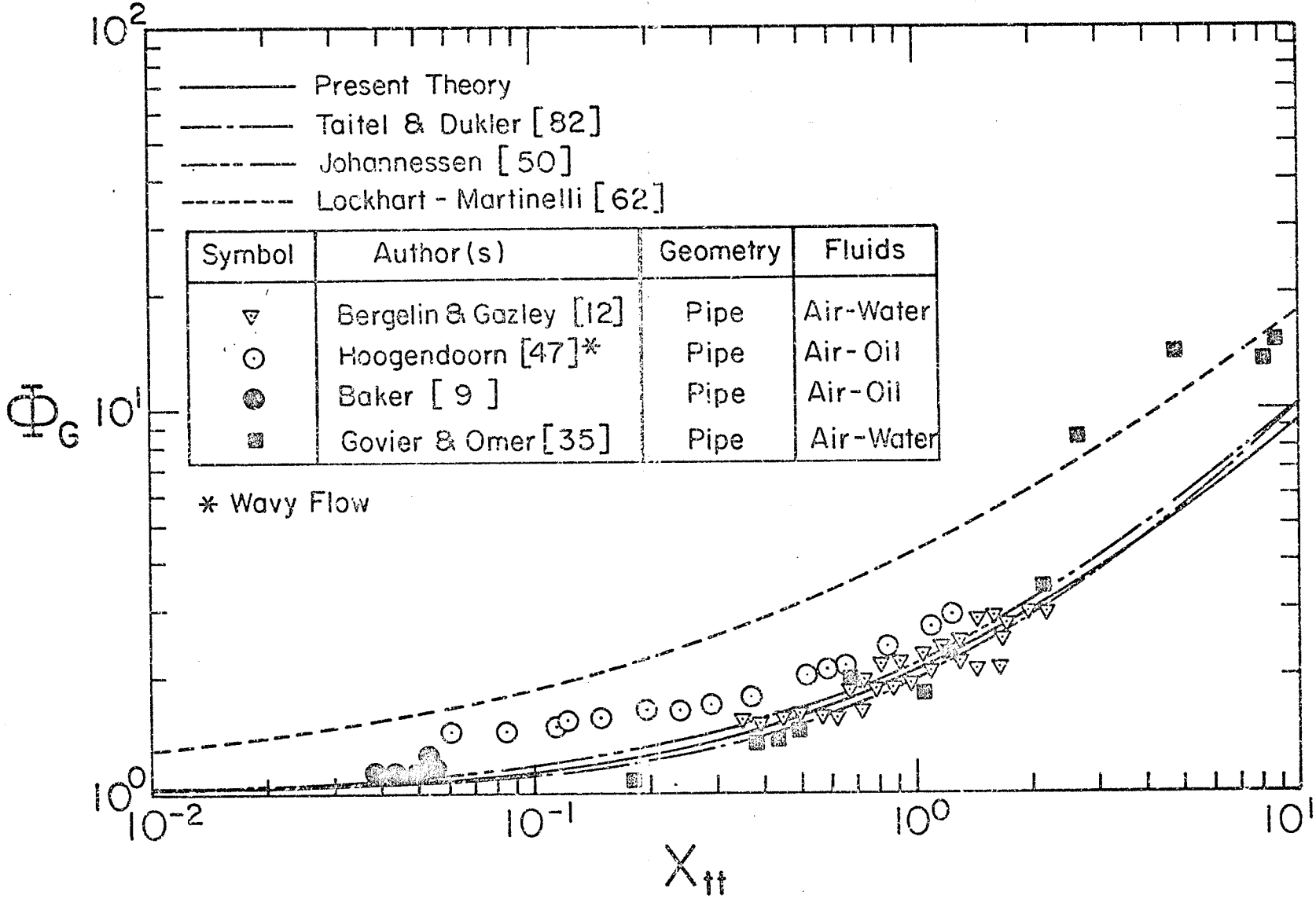

Fig. 8.3 Plot of ϕ_G Against X_{tt} for stratified flow.

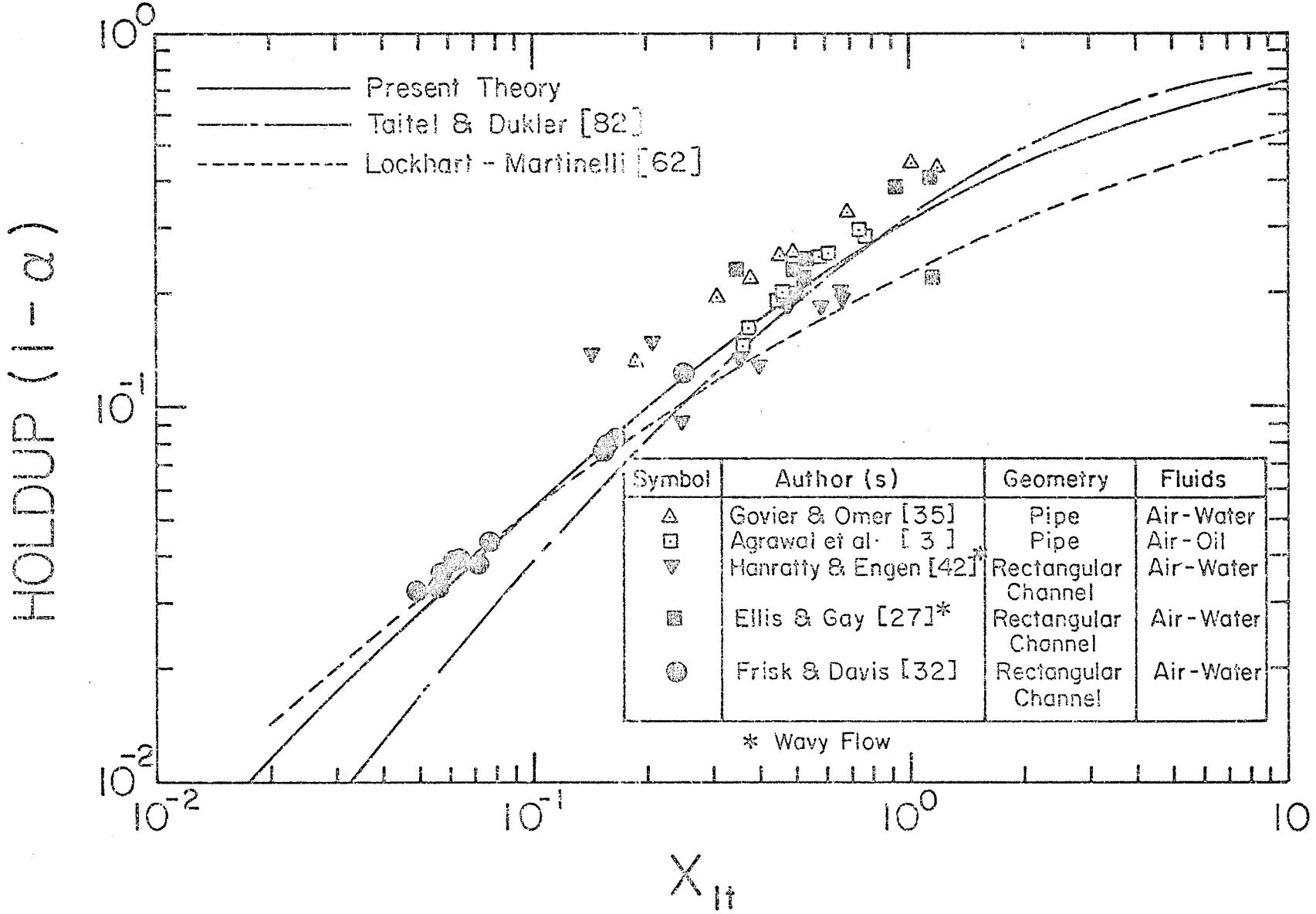

Fig. 8.4 Plot of Holdup Against X_{lt} for stratified flow

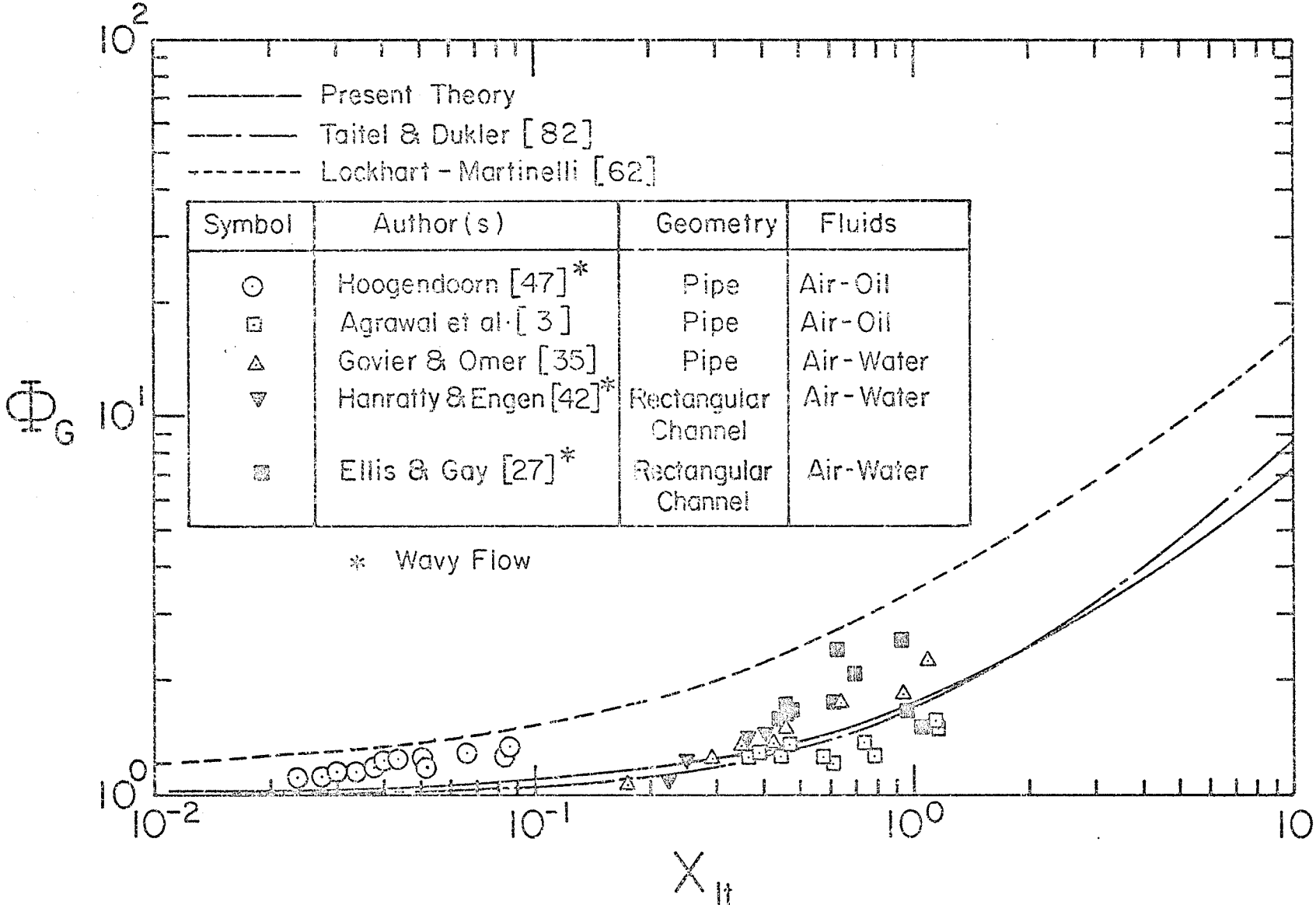

Fig. 8.5 Plot of ϕ_G Against X_{lt} for Stratified Flow

turbulent case (Figs. 8.4 and 8.5) the curves would be indistinguishable for $X_{\ell t} > 0.2$ while for $X_{\ell t} < 0.2$ the maximum differences from the curves appearing in the figures would be of the order of 8%.

In Figs. (8.2) and (8.3) the present theory for Φ_G and holdup $(1-\alpha)$ for turbulent-turbulent flow is tested against the experimental results of Baker [9], Govier and Omer [35], Bergelin and Gazley [12], and Hoogendoorn [47], for flow in pipes. The theory is also compared with the Lockhart-Martinelli [62] correlation and with the Johannessen [50] and the Taitel-Dukler [82] theories. In these figures, and in Figs. 8.4 and 8.5 discussed below, because of the paucity of data, both smooth-interface and wavy-interface data are shown. As regards holdup (Fig. 8.2), the agreement of the present theory with the data is good and is virtually the same as that of Taitel and Dukler while being somewhat better than that of Johannessen. For pressure drop (Fig. 8.3), the present theory and those of Johannessen and of Taitel and Dukler show approximately the same good agreement with the experimental data (generally the data lying above these theories are for a wavy interface [47]). The pressure drop data generally lie below, and the holdup data above, the Lockhart-Martinelli correlation; the exception to this is a few data points of Govier and Omer [35] in the X_{tt} range of 2.5 to 14 which lie slightly above the Lockhart-Martinelli line, or between it and the other theories discussed here.

In Figs. 8.4 and 8.5 the theory for laminar-turbulent flow is tested against the experimental pipe-flow results of Hoogendoorn [47], Govier and Omer [35], and Agrawal et al. [3] and against the experimental rectangular-channel data of Frisk and Davis [32] Hanratty and Engen [42] and Ellis and Gay [27]. In these last-mentioned cases, the aspect ratio was sufficiently high (of the order of 12) to approximate flow between parallel plates. The theory is also compared with the Lockhart-Martinelli correlation and the Taitel-Dukler theory. Over the range of $X_{\ell t}$ from 0.15 to 1.5 the present theory and that of Taitel and Dukler give approximately the same reasonable agreement with the holdup data (Fig. 8.4), although there may be a slight tendency for both to under-predict; at values of $X_{\ell t}$ less than 0.15, where only the rectangular-channel data of Frisk and Davis are shown, the agreement between the data and the present theory is somewhat better than with the Taitel-Dukler theory (which is for circular-tube geometry). The Lockhart-Martinelli correlation agrees well with the holdup data for $X_{\ell t} < 0.25$ while for larger values of $X_{\ell t}$ it tends to under-predict. As regards pressure drop (Fig. 8.5), over the range of the data the present and Taitel-Dukler theories are practically coincident; the agreement is very good for the smooth-interface data [7,35] while the data lying above the theory is generally for a wavy interface [27,47,42]. The data all lie below the Lockhart-Martinelli correlation.

It should be noted that the experimental data considered in the above comparison were in general classified as laminar-turbulent or turbulent-turbulent according to the criteria set by Lockhart and Martinelli unless otherwise stated in the original work; that is, the phase is considered to be in laminar motion if the superficial Reynolds number is less than 1000, and in turbulent motion if the Reynolds number is greater than 2000, any data lying between these limits were considered to be in turbulent flow. When different criteria were stated by authors of a particular investigation, the stated criteria were used.

There are other ways of obtaining relations among the variables Φ, α and X, most notably using the separated flow model as described by Wallis [92]. The simplest form of the equations is

$$\Phi_G = (X^{\frac{2}{n}} + 1)^{n/2}$$

$$1-\alpha = \frac{X^{2/n}}{1+X^{2/n}}$$

where for turbulent-turbulent flow n is in the range of 2.375 to 3.5. Within this range, n = 2.375 gives the closest representation of the data; Φ_G is predicted reasonably well with, for instance, predictions being of the order of 5-20% higher than the present theory over the range of interest (Fig. 8.3); holdup prediction is not so good, being slightly higher than the Johannessen theory (Fig. 8.2). However,

the simple form of the equations suggests an appealing means of fitting the data semi-empirically (as has been done in other circumstances [92]).

CHAPTER 9

SUMMARY AND CONCLUSIONS

The work presented here and the conclusions drawn may be summarized as follows:

1. Data for local and mean heat-transfer coefficients, frictional pressure drop and flow patterns were reported for a wide range of flow rates and gas densities in the forced convective flow of gas-water mixtures in a vertical tube.
2. The effect of gas density on the measured dependent variables was described; this may be summarized as follows:

(a) There appears to be a weak dependence of flow patterns on the gas density; this, however, was not clear. The gas-density correction suggested by Govier and Aziz [34] does not appear to work for all flow-pattern transitions as some of the transition boundaries were better defined when only superfacial velocities were used for the flow-pattern map coordinates. Additional data are required in order to clearly define the dependence of flow patterns on gas density.

(b) No effect was observed of the gas density on heat-transfer coefficients and frictional pressure drop for low water flow rates and low superficial gas velocities, and for high water flow rates and all values of superficial gas velocities examined in the experiments.

(c) For low water flow rates and moderate to high superficial gas velocities, there were significant effects of gas density on both heat-transfer coefficient and frictional pressure drop; for the same V_{SL} and V_{SG}, the higher the gas density, the higher is the heat-transfer coefficient and the frictional pressure drop.

3. The frictional pressure drop data were tested against some existing correlations in Figs. 5.13 to 5.15; the agreement was good as illustrated in Table 5.3.

4. The local heat-transfer coefficients were correlated in terms of the measured frictional pressure drop by the modified Spalding theory [81, 90], the agreement was excellent as 96.7% of 1211 data points agreed with the theory within ±40%. The correlation (theory) was tested for generality by testing a wide range of data (present and [90]); 93% of 2142 data points agreed with the theory within ±50%, for the whole of the data, the mean deviation and the rms deviations were 7.2% and 30.7% respectively.

5. Some of the existing correlations were tested against the present mean heat-transfer data and the results were generally good; the best agreement, however, was obtained with the correlations of Ueda and Hanaoka [86] and Vijay [90].

6. Simple correlation of the mean heat-transfer data was developed based on a simple model of single-phase liquid having a Reynolds number based on the actual mean velocity of the liquid in the two-phase flow; the final form of the correlation was

$$\bar{h}_{TP} = \bar{h}_{SP} \ (1-\alpha)^{n} \qquad (6.35)$$

where $\bar{h}_{SP}$ is the single-phase (liquid) mean heat transfer coefficient as calculated from the appropriate single-phase correlations (depending on Re_{SL}), while n = -1/3 for laminar flow and n = -0.83 for turbulent flow, and α is calculated from the Chisholm correlation. The proposed correlation was also tested against Vijay's data [90]. The two sets of data (present and Vijay's), which cover the widest range of variables studied so far, agreed very well with the correlation; 91% of 338 data points agreed with the correlation within ±50%; for the whole of the data the mean and rms deviations were -1.4% and 32.8 respectively.

7. A proposal was also made of a correlation of the mean heat-transfer coefficients in terms of the frictional pressure drop (this method was first employed by Fried [31] for horizontal flow and then by Vijay [90] for vertical flow). Excellent agreement between the correlation and the data for a wide range of conditions was obtained. (See Table 6.11).

8. A flow-visualization study was made of the air-water mixtures flowing in a transparent vertical tube at low flow rates of the two phases where the local values of the heat-transfer coefficient were observed to increase with increasing distance along the test section [90]. High-speed cine photography and both the hydrogen-bubble and the dye-injection techniques were employed. The movie films obtained of the motion of the liquid film at the wall in the bubble and slug flows clearly indicated the existence of downflow of the liquid film. The results of this study qualitatively explained the earlier results [90] of local heat-transfer coefficient under the above mentioned conditions.

9. Finally, a theoretical solution of pressure drop and hold-up in horizontal stratified flow was presented. The final results were obtained in the form of simple algebraic equations which accurately predicted both pressure drop and hold-up for both pipe flow and flow in rectangular channels.

REFERENCES

1. Abou-Sabe, A.A., Ph.D. Thesis, University of California, Berkeley, California, U.S.A. (1951).

2. Aggour, M.A. and Sims, G.E., A Theoretical Solution of Pressure Drop and Holdup in Two-Phase Stratified Flow, Proc. HTFMI (1978).

3. Agrawal, S.S., Gregory, G.A. and Govier, G.W., An Analysis of Horizontal Stratified Two-Phase Flow in Pipes, Can. J. Chem. Engng. 51, 280-286 (1973).

4. Alves, G.E., Chem. Eng. Progr. 50, 449-456 (1954).

5. Anon, The Frictional Component of Pressure Gradient for Two-Phase Gas or Vapour/Liquid Flow Through Straight Pipes, Engineering Sciences Data Item Number 76018, September (1976), Sponsored by I. Chem. E., and I. Mech. E., England, U.K.

6. Anon, Forced Convection Heat Transfer in Circular Tubes, Part II: Data for Laminar and Transitional Flows Including Free Convection Effects, Engineering Sciences Data, Item No. 68006, February (1968), Sponsored by I. Chem. E., and I. Mech. E., England, U.K.

7. Anon, Forced Convection Heat Transfer in Circular Tubes, Part III: Further Data for Turbulent Flow, Engineering Sciences Data, Item No. 68007, August (1968), Sponsored by I. Chem. E., and I. Mech. E., England, U.K.

8. Aziz, K., Govier, G.W., and Fogarasi, M., Pressure Drop in Wells Producing Oil and Gas, J. Can. Petrol. Technol. 11, 38, (1972).

9. Baker, O., Simultaneous Flow of Oil and Gas, Oil and Gas J. 53, 185-195 (1954).

10. Baroczy, C.J., A Systematic Correlation of Two-Phase Pressure Drop, Chem. Engng. Prog., Symp. Ser. 62 (64), 232-249 (1966).

11. Bennett, J.A.R., Two-Phase in Gas-Liquid Systems - A Literature Survey, UKAEA Report, AERE CE/R-2497, (1958).

12. Bergelin, O.P., and Gazley, C., Co-Current Gas-Liquid Flow in Horizontal Tubes, Proc. HTFMI 29, 5-18 (1949).

13. Bergles, A.E., and Rohsenow, W.M., Forced Convection Surface-Boiling Heat Transfer and Burout in Tubes of Small Diameter, Technical Report No. 8767-21, Massachusetts, Institute of Technology, May 25 (1962).

14. Bruzzi, S., Surface Temperature Measurement in Boiling Heat Transfer Experiments, Report BHT/TN/2, Imperial College of Science and Technology, London, U.K., October (1965).

15. Chapman, A.J., Heat Transfer, the MacMillan Company, N.Y. (1967).

16. Chenoweth, J.M., and Martin, M.W., Turbulent Two-Phase Flow, Petroleum Refinery, 34 (10), 151-155 (1955).

17. Chisholm, D., Research Note: Void Fraction During Two-Phase Flow, Jour. Mech. Eng. Sci. 15 (3), (1973).

18. Chisholm, D., Pressure Gradients due to Friction During the Flow of Evaporating Two-Phase Mixtures in Smooth Tubes and Channels, Int. J. Heat Mass Transfer 16, 347-358 (1973).

19. Clark, J.A., and Rohsenow, W.M., Local Boiling Heat Transfer to Water at Low Reynolds Numbers and High Pressures, Trans. ASME 76, 553-562 (1954).

20. Collier, J.G. Convective Boiling and Condensation, McGraw-Hill Book Co., N.Y. (1972).

21. Collier, J.G., and Pulling, D.J., Heat Transfer to Two-Phase Gas-Liquid Systems, UKAEA Report, AERE-R3809, England, U.K. (1962).

22. Collier, J.G., A Review of Two-Phase Heat Transfer (1935-1957), UKAEA Report, AERE CE/R-2496 (1958).

23. David, E.J., and David, M.M., Two-Phase Flow Gas Liquid Convection Heat Transfer - A Correlation, I & EC Fundamentals 3 (2), 111-118 (1964).

24. Domanskii, I.V., Tishin, V.B., and Sokolov, V.N., Heat Transfer During Motion of Gas-Liquid Mixtures in Vertical Pipes, Jour. of Applied Chemistry of the USSR 42 (4), 809-813 (1969).

25. Dukler, A.E., Wicks, M. and Cleveland, R.G., Frictional Pressure Drop in Two-Phase Flow: (B) An Approach Through Similarity Analysis, A.I.Ch. E. Journal 10, 44-51 (1964).

26. Duns, H., Jr., and Ros, N.C.J., Sixth World Petroleum Congress, Section 2, Paper No. 22, Frankfurt, Germany (1963).

27. Ellis, S.R. and Gay, B., The Parallel Flow of Two Fluid Streams: Interfacial Shear and Fluid-Fluid Interaction, Trans. Instn. Chem. Engrs. 37, 206-213 (1959).

28. Etchells, A.W., Ph.D. Thesis, University of Delaware (1970).

29. Fedotkin, I.M., and Zarudnev, L.P., Correlation of Experimental Data on Local Heat Transfer in Heating Air-Liquid Mixtures in Pipes, Heat Transfer - Soviet Research 2 (1), 175-181 (1970).

30. Fohrman, M.J., The Effect of Liquid Viscosity in Two-Phase, Two-Component Flow, Report ANL-6256, November (1960).

31. Fried, L., Pressure Drop and Heat Transfer for Two-Phase, Two-Component Flow, Chem. Eng. Prog. Symp. Series 50, 47-51 (1954).

32. Frisk, D.P., and Davis, E.J., The Enhancement of Heat Transfer by Waves in Stratified Gas-Liquid Flow, Int. J. Heat Mass Transfer 15, 1537-1552 (1972).

33. Golan, L.P., and Stenning, A.H., Two-Phase Vertical Flow Maps, Paper No. 14, Proc. Instn. Mech. Engrs. 184, 108-114 (1969-70).

34. Govier, G.W., and Aziz, K., The Flow of Complex Mixtures in Pipes, Van Nostrand Reinhold Company, New York (1973).

35. Govier, G.W. and Omer, M.M., The Horizontal Flow of Air-Water Mixtures, Can. J. Chem. Engng. 40, 93-104 (1962).

36. Govier, G.W., Radford, B.A., and Dunn, J.S.C., The Upwards Vertical Flow of Air-Water Mixtures, Effect of Air and Water Rates on Flow Pattern, Holdup and Pressure Drop, the Can. J. of Chem. Eng., 58-70, August (1957).

37. Govier, G.W. and Short, W.L., The Upward Vertical Flow of Air-Water Mixtures, Effect of Tubing Diameter on Flow Pattern, Holdup and Pressure Drop, The Can. J. of Chem. Eng., 195-202, October (1958).

38. Griffith, P., and Wallis, G.B., Two-Phase Slug Flow, J. Heat Transfer, Trans. ASME, Ser. C 83, 307 (1961).

39. Griffith, P., Two-Phase Flow in Pipes, Chp. 9, Developments in Heat Transfer, Ed., Rohsenow, W.M., The M.I.T. Press (1964).

40. Groothuis, H., and Hendal, W.B., Heat Transfer in Two-Phase Flow, Chem. Eng. Sci. 11, 212-220 (1959).

41. Hagedorn, A.R., and Brown, K.E., The Effect of Liquid Viscosity in Two-Phase Vertical Flow, J. Petroleum Technology, February (1964).

42. Hanratty, T.J. and Engen, J.M., Interaction Between a Turbulent Air Stream and a Moving Water Surface, A.I. Ch. E. Journal 3, 299-304 (1957).

43. Happel, J., and Brenner, H., Low Reynolds Number Hydrodynamics, Prentice-Hall, Inc., N.J., U.S.A. (1965).

44. Hewitt, G.F. and Semeria, R., Aspects of Two-Phase Gas-Liquid Flow, Chp. 12, Heat Exchangers: Design and Theory Source Book, Eds., Afgan, N. and Schlunder, Scripta Book Company, Washington, U.S.A. (1974).

45. Hewitt, G.F., King, R.D., and Lovegrove, P.C., Liquid Film and Pressure Drop Studies, Chemical and Process Engineering, 191-200, April (1964).

46. Hewitt, G.F., UKAEA Report No. AERE-R3680 (1961).

47. Hoogendoorn, G.J., Gas-Liquid Flow in Horizontal Pipes, Chem. Engng. Sci. 9, 205-217 (1959).

48. Hsu, Y.Y., and Graham, R.W., Transport Processes in Boiling and Two-Phase Systems, McGraw Hill Book Company, N.Y. (1976).

49. Isbin, H.S., Moen, R.H., and Mosher, D.R., Two-Phase Pressure Drops, USAEC Report No. AECU-2994 (1954).

50. Johannessen, T., A. Theoretical Solution of the Lockhart and Martinelli Flow Model for Calculating Two-Phase Flow Pressure Drop and Holdup, Int. J. Heat Mass Transfer 15, 1443-49 (1972).

51. Johnson, H.A., Trans. Am. Soc. Mech. Engrs. 77, 1257-1264 (1955).

52. Kapinos, V.M., Slitenko, A.F., Chirkin, N.B., and Povolotskiy, L.V., Heat Transfer in the Entrance Section of a Pipe with a Two-Phase Flow, Heat Transfer-Soviet Research 7, 126-128, March-April (1975).

53. Katsuhara, T. and Kazama, T., Heat Transfer in Two-Phase Flow of Mixtures of Air and Water, 2nd report - Vertical Channel, Trans. JSME 24 (144), 552-558 (1958).

54. Kays, W.M., Convective Heat and Mass Transfer, McGraw-Hill Book Company, N.Y. (1966).

55. King, C.D.G., M.Sc. Thesis, Univ. of California, Berkeley, California, U.S.A. (1952).

56. Knott, R.F., Anderson, R.N., Acrivos, A., and Peterson, E.E., Experimental Study of Heat Transfer to Nitrogen-Oil Mixtures, Ind. and Eng. Chemistry 51, 1369-1372 (1959).

57. Kreith, F., and Summerfield, M., Investigation of Heat Transfer at High Heat-Flux Densities: Experimental Study with Water of Friction Drop and Forced Convection with and without Surface Boiling in Tubes, Progress Report No. 4-68, Jet Propulsion Laboratory, California Institute of Technology, Pasadena, California, April 2, (1948).

58. Kudirka, A.A., Two-Phase Heat Transfer with Gas Injection Through a Porous Boundary Surface, U.S.A.E.C. Report ANL-6862 (1964).

59. Kudirka, A.A., Grosh, R.J., and McFadden, P.W., Two-Phase Heat Transfer in a Tube with Gas Injection from the Walls, ASME Paper No. 65-HT-47 (1965).

60. Lackme, C., Rapport TT No. 71, pp: 1-89, Service des Transfert Thermiques, GEA, GERN, Grenoble, France (1966).

61. Leveque, A., Les lois de la transmission de chaleur par convection, Annls Mines, Paris-Mem, Ser. 12, 13, 283-290 (1928).

62. Lockhart, R.W., and Martinelli, R.C., Proposed Correlation of Data for Isothermal Two-Phase Two-Component Flow in Pipes, Chem. Eng. Progr. 45, 39-48 (1949).

63. Lunde, K.E., Heat Transfer and Pressure Drop in Two-Phase Flow, Chem. Eng. Prog. Symp. Series 57 (32), 104-110 (1961).

64. Mandhane, M., Gregory, G.A., and Aziz, K., A Flow Pattern Map for Gas-Liquid Flow in Horizontal Pipes, Int. J. Multi-phase Flow 1, 537-553 (1974).

65. Merzkirch, W., Flow Visualization, Academic Press, 5-45 (1974).

66. Novosad, Z., Heat Transfer in Two-Phase, Liquid-Gas Systems, Collection Czechoslov. Cehm. Comm. 20, 477-498 (1955).

67. Oshinowo, T., and Charles, M.E., Vertical Two-Phase Flow, Part 1. Flow Pattern Correlations, The Can. J. Chem. Eng. 52, 25-35 (1974).

68. Oya, T., Upward Liquid Flow in Small Tube Into Which Air Streams, 1st Report, Experimental Apparatus and Flow Patterns, Bulletin of the JSME 14 (78), 1320-1329 (1971).

69. Perroud, P., and de LaHarpe, A., Transfert de chaleur part liquides entraines dans un ecoulement gazeux turbulent, Report CEA No. 1422, Commissariat a l'Energie Atomique, France.

70. Pletcher, R.H., and McManus, H.N., Jr., A Theory of Heat Transfer to Annular Two-Phase, Two-Component Flow, Int. J. Heat Mass Transfer 15, 2091-2096 (1972).

71. Quandt, E., Analysis of Gas-Liquid Flow Patterns, Chem. Eng. Progr. Symp. Ser. 61 (57), 128-135 (1965).

72. Ros, N.C.J., Simultaneous Flow of Gas and Liquid as Encountered in Well Tubing, J. Petroleum Technology, October (1961).

73. Russell, T.W.F., Etchells, A.W., Jensen, R.H. and Arruda, P.J. Pressure Drop and Holdup in Stratified Gas-Liquid Flow, A.I. Ch. E. Journal 20, 664-669 (1974).

74. Scheele, G.F., and Hanratty, T.J., Effect of Natural Convection on Stability of Flow in a Vertical Pipe, Jour. of Fluid Mechanics 14, Part 2, 244-256 (1962).

75. Seigel, R., Sparrow, E.M., and Hallman, T.M., Steady Laminar Heat Transfer in a Circular Tube with Prescribed Wall Heat Flux, Appl. Sci. Res. Ser. A. 7, (1958).

76. M. Shiba and Y. Yamazaki, A Comparative Study on the Pressure Drop of Air-Water Flow, Bulletin of JSME 10 (38), 290-298 (1967).

78. Sieder, E.N., and Tate, G.E., Heat Transfer and Pressure Drop of Liquids in Tubes, Ind. Eng. Chem. 28, 1429-1435, December (1936).

79. Sokolov, V.N., and Bushkov, M.D., Heat Transfer from Gas-Liquid Mixtures Moving in Vertical Tubes, Zh. Prikl. Khim. 37, 639-645, (1964). Translation available from Simon Carves Ltd., No. 1177 (1964).

80. Soo, S.L., Fluid Dynamics of Multiphase Systems, Blaisdell Publishing Company, Massachusetts, U.S.A. (1967).

81. Spalding, D.B., Contribution to the Theory of Heat Transfer Across a Turbulent Boundary Layer, Int. J. Heat Mass Transfer 7, 743-761 (1964).

82. Taitel, Y., and Dukler, A.E., A Model for Predicting Flow Regime Transitions in Horizontal and Near Horizontal Gas-Liquid Flow, AIChE Jour. 22 (1), 47-55 (1976).

83. Taitel, Y. and Dukler, A.E., A Theoretical Approach to the Lockhart-Martinelli Correlation for Stratified Flow, Int. J. Multi-phase Flow 2, 591-595 (1976).

84. Tong, L.S., Boiling Heat Transfer and Two-Phase Flow, John Wiley & Sons, Inc., N.Y. (1965).

85. Ueda, T., Studies on the Flow of Air-Water Mixtures: the Upward Flow in a Vertical Tube, Bull, JSME 1, 139-145 (1958).

86. Ueda, T., and Hanaoka, M., On The Upward Flow of Gas-Liquid Mixtures in Vertical Tubes: 1st Report - Experiment and Analysis of the Flow State; 2nd Report - Consideration of Frictional Pressure Drop and Void Fraction; 3rd Report - Heat Transfer Results and Analysis, Bull. JSME 10, 989-1015 (1967).

87. Ueda, T., and Nose, S., Studies of Liquid Film Flow in Two-Phase Annular and Annular-Mist Flow Regions, Bull. JSME 17, 614-624 (1974).

89. Verschoor, H., and Stemerding, S., Heat Transfer in Two-Phase Flow, General Discussion on Heat Transfer, 1951 ASME/I. Mech. E. Heat Transfer Conference, 201-203 (1951).

90. Vijay, M.M., Ph.D. Thesis, University of Manitoba (1978).

91. Vohr, J.H., Flow Patterns of Two-Phase Flow - A Survey of Literature, USAEC Report TID-11514 (1960).

92. Wallis, G.B., One-Dimensional Two-Phase Flow, Mcgraw-Hill Book Company, N.Y. (1969).

93. Wallis, G.B., Annular Two-Phase Flow, Part 1: A Simple Theory, Trans. ASME, Journal of Basic Engineering, 59-72, March (1970).

94. Wallis, G.B., Annular Two-Phase Flow Part 2: Additional Effects, Trans ASME, Journal of Basic Engineering, 73-82, March (1970).

95. Worsoe-Schmidt, P.M., Heat Transfer in the Thermal Entrance Region of Circular Tubes and Annular Passages with Fully Developed Laminar Flow, Int. J. Heat Mass Transfer 10, 541-551 (1967).

APPENDIX A

DETAILED INFORMATION ON EXPERIMENTAL EQUIPMENT

This appendix gives detailed information on the apparatus and measuring equipment including the fluid-properties measuring devices.

Table A.1 lists the manufacturer, model number, etc. of the equipment used; the numbers appearing in the table (the item number) corresponds with the circled numbers in Figs. 3.3 to 3.14 of Chapter 3.

Whenever possible, the important measuring instruments have been calibrated in the laboratory and are so stated in the table.

TABLE A.1

Information on the Components of the Experimental Facility

Part No. in Figs. 3.3 to 3.14	Name of the Component	Remarks
MIXING CHAMBER		
1	Stainless steel strainer	3.0 in. dia., 1/32 in. perforated stainless steel type 304 Sarco strainer. Sarco Canada Limited, Agincourt, Ontario, Canada.
2	Porosint bronze tube	0.460 in. I.D. x 0.740 in. O.D. x 8.0 in. 5 grades (A to E, coarse to fine); Sintered Products Limited, Sutton-in-Ashfield, Notts, England, U.K.
HEATED TEST SECTION:		
3	Heated test tube	Stainless steel type 304; 0.460 in. I.D. x 0.020 in. thick; Atlas Alloys, L = 2 ft.; Atlas Steels Limited, Welland Ontario, Canada.
4	Bus bars	Brass, 6.75 x 3.0 x 0.94 in.
5	Supporting bar	1.0 x 1.0 in. Permali insulating material; Permali (Canada) Limited, Toronto, Onatio, Canada.
6	Guard heater tube	1.5 in. I.D. x 0.0625 in. thick split copper tube retained by Permali rings.
7	Heating elements	Two Briskeat silicone rubber embedded heating tapes (0.5 in. wide x 8 ft. & 0.5 in. x 10 ft.); Briscoe Manufacturing Co., Columbus, Ohio, U.S.A.
OBSERVATION SECTION:		
8	Visual section	3.0 x 3.0 in. x 1 ft. cast acrylic rectangular prism with 0.460 in. precision bored hole.

Part No. in Figs. 3.3 to 3.14	Name of the Component	Remarks
TEMPERATURE MEASURING INSTRUMENTS:		
9	Digital voltmeter	The Darcy 440 Digital Multimeter, Model DM-440-2. Accuracy: ± 0.01% of reading ± 1 digit; Automatic ranging; Darcy Industries, Inc., Santa Monica, California, U.S.A. Calibrated in the laboratory regularly.
10	Strip recorder	Honeywell Two-Pen Electronik 104 Multi-Range Lab/Test Wide Chart Recorder, Model No. 104112-002-002); specified accuracy: span: ± 0.25% of span or 1 microvolt whichever is greater; zero position: ± (0.25 + 0.1 x suppression ratio)% of span or 1 microvolt whichever is greater; Honeywell Controls Ltd., Scarborough, Ontario, Canada. Calibrated in the laboratory regularly.
11	Data logger	Fluke data logger Model 2240A, 60 channel capacity (could be extended up to 1000 channels), scanning speeed up to 15 channel/sec., accuracy ± 0.1°C, programmable, equipped with a digital display and printer, displays and prints date, time (hour, min., sec.), channel no., reading (mV or °C) and units. John Fluke Mfg. Co., Inc., Mountlake Terrace, Washington, 98043.
12	Potentiometer	Leeds & Northrup Type K-4 Universal Guarded Potentiometer (Model 7554); calibrated accuracy: ± 0.005% of reading +0.5μv) on low range (-5μv to + 0.0161050 volt); Leeds & Northrup Co., Philadelphia, Pa., U.S.A. Used occasionally to check the accuracy and performance of the DVM and the recorder.
13	Ice bath	Thermo-Electric ICELL T.M. Ice Point Reference Unit; a completely automatized Ice Bath (Model 80020-6); Thermo Electric (Canada) Limited, Brampton, Ontario, Canada. Accuracy: 0.00°C to ± 0.05°C; Stability: ± 0.01° for any constant ambient.

Part No. in Figs. 3.3 to 3.14	Name of the Component	Remarks
14	Selector switch	Thermo-Electric Selector Switch; 96 points, 48 switches, custom key palladium contact switches, Model No. 33212. Double pole, double throw, centre OFF type.
15	Constant temperature bath	Gebruder Haake Model FS/FT Constant Temperature Bath; specified accuracy: ± 0.02°C; Gebruder Haake, Karlsruhe, W. Germany. Used for calibrating the thermocouples in the laboratory.
FLOW VISUALIZATION SECTION:		
16	Test section	1.75 x 1.75 in. x 2 ft. cast acrylic rectangular prism with 0.50 in. precision, highly polished bored hole. Three holes (at locations 3, 13 & 21.5 in. from the bottom) of 0.02 in. dia. were drilled normal to the vertical cylindrical hole surface; these were used for dye injection and for placing the platinum wire.
17	High-speed movie camera	A Hycam model K200rE, 16 mm high-speed movie camera. 100 to 11,000 PPS, frame rate control ± 1%, automatic servo brake, dual timing lights, films capacity up to 400 ft., Manufactured by Red Lake Laboratories, Inc., Santa Clara, California.
18	Movie lights	Smith Victor, quartz bromine movie lights, 650W at 115V.
LIQUID FLOW LOOP:		
18	Pump	Waukesha Positive Displacement Pump, Model No. 25 DO-1 1/2. All Nickel-Bronze construction (Waukesha Metal). Complete assembly supplied with a 5 hp (220 volt, DP) motor and a V-belt drive. Max. flow = 24 USGPM (water); Max. Pressure = 150 psi and Max. Temp. = 225°F. Buna-N seals; Waukesha Foundry Company, Waukesha, Wisconsin, U.S.A.

Part No. in Figs. 3.3 to 3.14	Name of the Component	Remarks
20	Flowmeters	
	A	Fischer & Porter Indicating Type Flowrator (Rotameter), Model No. 10A3537A, 316 stainless steel float (1/2 - GUSVT-40), Tube: FP=1/2-21-G-10/83, percent scale. Flowrate: Max. = 0.328 USGPM Liquid sp. gr. = 1.0.
	B	Model No. 10A3537A, 216 stainless steel float (3/4 27-G-10/83, % scale, Flowrate: Max. = 3.55 USGPM liquid sp. gr. = 1.0.
	C	Model No. 10A3537A, 316 stainless steel float (2-GSVGT-98), Tube: FP-2-27-G-10/83, % scale. Flowrate: Max. = 30 USGPM liquid sp. gr. 1.0.
	D	Model No. 10A3537P, 316 stainless steel float (NSVT-622), Tube: FP-1-60-P-8/83, % scale, Flowrate: Max. = 20 USGPM liquid sp. gr. = 1.0. (Used for measuring the cooling water rate in the heat exchanger). All flowrators were calibrated in the laboratory for all the liquids investigated Fischer & Porter (Canada) Ltd., Downsview, Ont.
21	Manometer (to measure ΔP)	1/4 in. I.D. inverted glass manometer. Designed and manufactured in the Mechanical Engineering Laboratory.
22	Manometer (to measure ΔP)	Meriam Model 20AA25TM, Range 100 in. U-type, mercury manometer. Equipped with standard scale and 303 stainless steel wetted parts. The Meriam Instrument Company, Cleveland, Ohio, U.S.A.
Not shown in the Fig.	Manometer (to measure inlet pressure)	1/4 in. I.D. Vertical U-type mercury manometer. Designed and built in the laboratory.
23	Gas-liquid separator tank	1 1/2 x 1.0 ft. stainless steel tank with 3 in. outlet in the cover plate and 1 1/2 in. drain; Greensteel Industries Limited, Winnipeg, Manitoba, Canada.

Part No. in Figs. 3.3 to 3.14	Name of the Components	Remarks
24	Liquid storage tank	1 1/2 x 3 ft. stainless steel tank with 3 holes in the cover plate (3 in. dia.) 1 1/2 in. drain and a side mounted 1/2 in. I.D. glass level indicator; Greensteel Industries Limited.
25	Heat exchanger	Liquid-to-liquid shell and tube type exchanger. All copper. 0.625 in. I.D. tubes by 4 ft. long shell dia. 2 ft. Automedic Instruments Limited, Winnipeg, Manitoba, Canada.
GAS FLOW LOOP:		
26	Compressor	7 x 7 in. double acting, single cylinder, type ES-1 and serial no. 14415; 1.375 in. diameter of piston rod; dual control; water cooled, single pass, conterflow; electrical drive, 15 hp, 220-440V, 3-phase, 1750 rpm motor; 92CFM capacity, at 300 rpm at 100 psi; Canadian Ingersoll Rand Co. Ltd., Canada.
POWER SUPPLY CIRCUIT:		
27	Variac	Powerstat variable Auto-transformer, Model No. P1156-4PS. Single-phase, 240 volt-100 amps-24 kvA. American Superior Electric Company, U.S.A.
28	Transformer	Single-phase Dry Type Distribution Transformer. Open-ventilated, class-F. Primary: 240 volt-100 amps, secondary: 1200 amps. Pioneer Electric Manitoba Limited, Winnipeg, Manitoba, Canada.
29	Current transformer	Weston Model 327, Type 2. Primary: 100 amps, secondary: 5 amps. Weston Electrical Instrument Corporation, Newark, N.J., U.S.A. Calibrated in the laboratory.
30 =	Ammeter	Weston A.C. Ammeter, Model 433 (25-500 cycles). Range: 5/2.5/1. Calibrated in the laboratory.

Part No. in Figs 3.3 to 3.14	Name of the Component	Remarks
31	Voltmeter	Weston A.C. R.M.S. Voltmeters. Range: 0 to 10 volts and 0 to 30 volts. Calibrated in the Laboratory.
32	Potential transformer	Weston Potential Transformer, Model 311, Type 1. 2300/1150: 115V, 15 VA, 25-133 CPS. Calibrated in the Laboratory.
33	Wattmeter	Weston Portable Wattmeter, Model 432. 5 amp. capacity. Voltage range: 75: 150: 300 v. Calibrated in the laboratory.
34	Temperature controller	Honewell Servotronik Temperature Controller, Model No. 5500101-2-05-02. Type T-couple. Range: 0 - 200°C.
PHOTOGRAPHIC SECTION:		
35	Camera	Pentax Spotmatic Single lens Reflex Camera equipped with Super-Takumar 50 mm/F4 Macro (close up) lens.
36	Camera	
37	Strobotac	General Radio Type 1538-A Strobotac Electronic Stroboscope. Flashing-rate range: 110 to 150,000 flashes per minute. Flash Duration: 0.5 to 3 μs. General Radio Company, West Concord, Massachusetts, U.S.A.
38	Flash unit	EG&G 549 Microflash System consisting of the Model 549-11 Flash Unit and the Model 549-21 Driver Unit. Flash Duration 0.5 μs; Peak light: 50 x 10^6 beam candle power. Edgerton, Germeshausen & Grier, Inc., Boston, Mass. U.S.A.
39	Ofifice plates	Three sharp-edged plates of 0.418, 0.141 and 0.046 in. dia., designed and manufactured in the Laboratory according to ASME Power Test Code. All orifice plates were calibrated in the Laboratory.

Part No. in Figs. 3.3 to 3.14	Name of the Component	Remarks
40	Rotameter	Tube No. 3-15-4; Glass Float; Brooks Instrument Co., Inc., Hatfield, Pennsylvania, U.S.A.
41	Manometer	Meriam Model 30EB25TM, Range 100", well-type manometer. Equipped with standard scale and 303 stainless steel wetted parts.
FLUID-PROPERTIES MEASURING EQUIPMENT:		
42	Surface tension analyzer	Fisher Model 215 Autotensiomat surface tension analyzer (operates on the principles of the du Nouy ring and Wilhelmy plate methods); analog panel meter readout (or potentiometric recorder); 0 to 100 dynes/cm range; 0.02 dynes/cm sensitivity; ± 2% relative accuracy; 0.02 dynes/cm resolution (on 0-5 dynes/cm range, using the recorder). Sample cup is made of a jacketed pyrex vessel to allow for temperature control of the liquid sample. Calibrated in laboratory before each measurements set, supplied by Fisher Scientific Canada Ltd.
43	Potentiometer recorder (accessory for surface-tension meter)	Fisher Recordall series 500, single-pen wide chart recorder, 1 MV to 10V range; 12 chart speeds; maximum error 0.1% of 1 MV full scale; repeatability + 0.01% of full scale. Houston Instrument, Austin, Texas. Calibrated regularly in Laboratory.
44	Viscometer	Haake Falling-Ball Viscometer Model B, used with a constant temperature circulator; for both gases and liquids; measuring range of 0.01 to 5 x 10^5 CP; accuracy of -0.1 to 0.5%; temperature range of -60 to +150°C. Supplied by Fisher Scientific Co., Ltd. Edm., Alta., Canada.

Part of the Figs. 3.3 to 3.14	Name of the Component	Remarks
45	Constant temperature circulator	Haake constant temperature circulator Model FS; temperature range up to 250°C; maximum accuracy of ± 0.004°C. Supplied by Fisher Scientific Co., Ltd.
MISCELLANEOUS:		
Not shown	Roughness meter	Bruel & Kjaer Roughness Meter, Type 6102 (used for measuring the roughness characteristics of the heated test section). Bruel & Kjaer, Naerum, Denmark.
Not shown	Conductivity meter	Conductivity Bridge Model RC-16B2. Industrial Instruments, Inc., U.S.A.
47	Pipes	All pipes used for connecting various components were standard copper, brass or stainless steel pipes. Sizes ranged from 1/2 to 1 1/2 in.
Not shown	Westphal balance	Used for measuring the specified gravity of the liquids.
Not shown	Saybolt universal viscosmeter	Precision Scientific Co., Chicago, Illinois, U.S.A. Used to measure the viscosity of liquids.
Noth shown	Deadweight tester	Ashcroft type 1305 Deadweight Tester for pressure gauge calibration. Manning, Maxwell & Moore of Canada Ltd., Galt, Ontario, Canada.
Not shown	Direct current comparator bridge	Direct current comparator bridge, Type 9920. Guildline Instruments Ltd., Smith Falls, Ontario, Canada. Used to measure the resistance of type 304 stainless steel tube as a function of temperature.

APPENDIX B

CALIBRATION OF INSTRUMENTS

B.1 Introductory Remarks

This appendix gives the results of the calibration of the measuring instruments and other sensing elements in the experimental facility. It should be noted that some components like thermocouples and the heat-transfer test section were calibrated only once before installation into the facility; for such components, the results presented here are taken from [90]; these are included here for the pupose of completeness. Other components such as electrical power measuring meters, fluid flow meters, temperature-measuring instruments, etc., were calibrated regularly (once in about 5 months) during the period of the present investigation and at the end of the experimental program. Throughout the appendix, sections dealing with results taken from the earlier work [90] are marked with an asterisk.

B.2 Calibration of Thermocouples*

Three rolls of thermocouple wire were obtained from the manufacturer. Samples of wire were cut from all the rolls for calibration to check continuity and uniformity of wires. The samples were inserted in hypodermic copper tubes and the tubes were immersed to a depth of 6 in. in a constant temperature oil bath (Gebruder Haake). Leeds and Northrup

potentiometer (7554 type K-4) and the Darcy Digital Multimeter were used to record the emf of the thermocouples. The temperature of the bath was read by a high precision mercury thermometer and a NBS calibrated Platinum Resistance Thermometer was used to read the temperature of the bath at the location where the thermocouples were immersed. The results are shown in Fig. B.1, where the measured emfs are compared with the tabulated values obtained from the NBS (National Bureau of Standards, U.S.A.). The maximum deviation between the NBS and the measured values were:

Roll 1: < 1.0%; Roll 2: < 1.25%; and

Roll 3: < 0.5%

In reducing the heat transfer data, NBS values were used with proper correction applied from the calibration data.

B.3 Calibration of the Resistivity of the Heat-Transfer Test Section*

The electrical resistivity of the stainless steel test section was measured as a function of temperature [90]. A direct current comparator bridge was used to measure the resistance between two probes (1.970±0.004 in apart) spot welded to a piece of tube. The tube was immersed in a constant temperature bath (Gebruder Haake) containing transformer oil. Measurements were also taken with the tube immersed in distilled water. The maximum deviation between the two sets of reading was less than 0.3%. The results are shown in Fig.

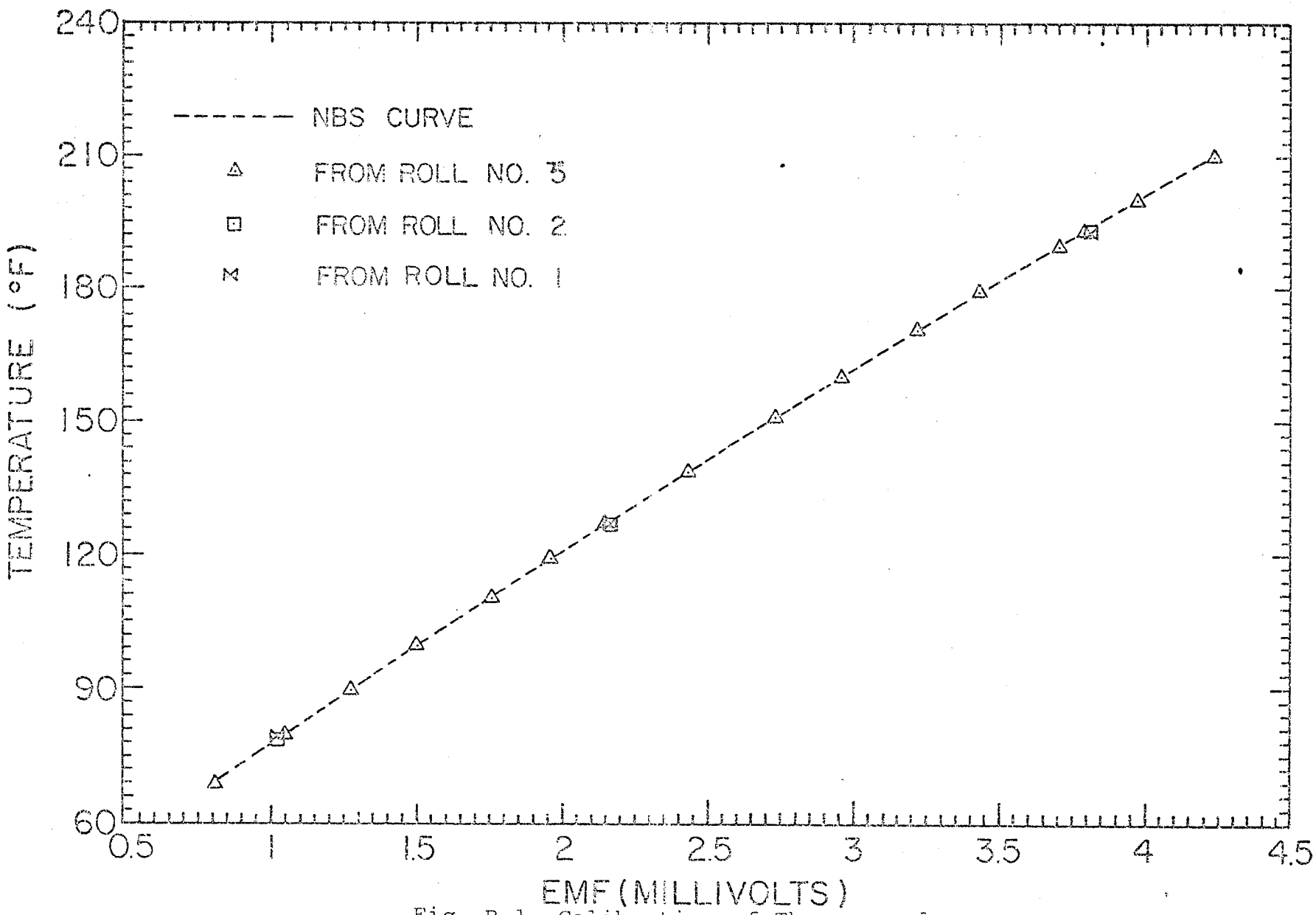

Fig. B.1 Calibration of Thermocouples

Fig. B.1

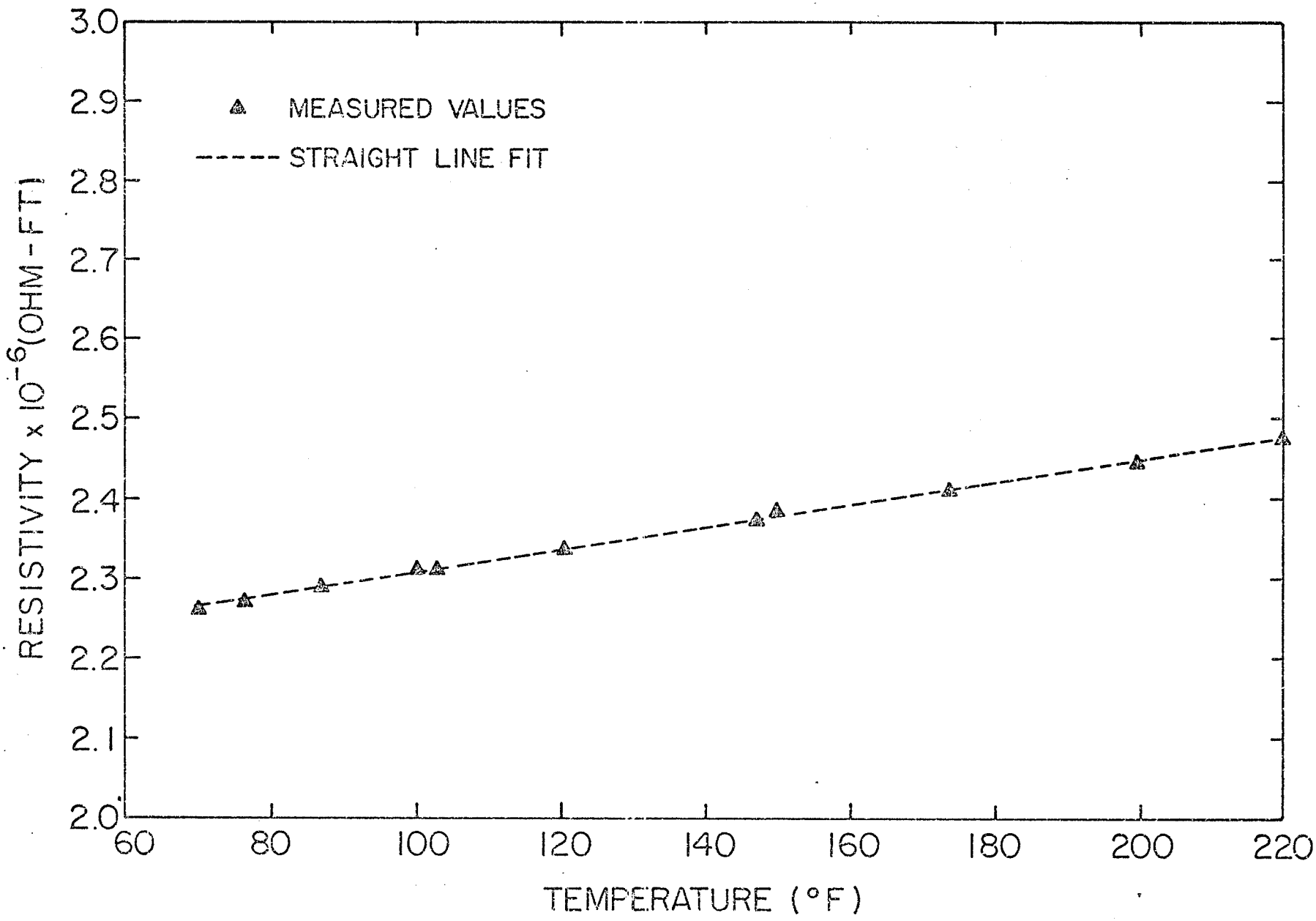

Fig. B.2 Resistivity of Test-Section Material

Fig. B.2

B.2 and the following equation was obtained by linear regression analysis.

$$\rho' = 0.216581 \times 10^{-5}(1+0.650408 \times 10^{-3}T) \quad (65 < T < 222\ ^{O}F \quad (B.1)$$

The maximum deviation between the value obtained from this equation and the measured value was less than 0.25%.

The results were compared with those reported by Bergles [13] and the data obtained from Sandvik Co. Bulletin. The maximum deviation was within 2.3% and 1.2% respectively.

B.4 Calibration of Power Measuring Instruments

B.4.1 Ammeter

The ammeter was calibrated regularly (once every six months) by means of a high precision Cambridge standard instrument. The results of the calibration, averaged over the total period of the investigation, are listed below.

Range (amps)	Max.Deviation (%)	Mean Deviation (%)
1-5	2.68	0.90
0.5-2.5	2.64	0.81
0.2-1.0	2.97	0.90

The current reading was corrected before any heat-transfer calculations were made.

B.4.2 Wattmeter

As mentioned in Chapter 4, the wattmeter reading was not used for the reduction of the heat-transfer data; it was only used to compare against the power obtained from the

current and resistance measurements. The maximum deviations between the standard and the wattmeter were in the order of 0.7% or less.

B.4.3 Voltmeter

The voltmeter reading together with the ammeter reading was used as another check on the power input to the test section. The maximum deviation obtained between the standard and the voltmeter was 1.12%.

B.4.4 Current Transformer*

The current transformer ratio was essential in calculating the local heat flux using the measured values of current and resistance. The C.T. was calibrated in the standards laboratory of Manitoba Hydro, Winnipeg, Manitoba, Canada. It was calibrated as a function of the secondary current (that is, at the input to the ammeter) and was found to vary from the value of 240 quoted by the manufacturer. The range of variation was as follows:

$$234.5 < \text{C.T. Ratio} < 250 \quad [242 \pm 3.1\%].$$

The value of 240 with the appropriate correction factor obtained from the calibration was used in calculating the heat flux.

B.4.5 Potential Transformer (P.T.)*

The potential transformer ratio was required in the calculation of power input to the test section from wattmeter measurements. The P.T. was calibrated in situ in the labora-

tory using two high impedance electronic voltmeters (D.V.M.) to measure the primary and secondary voltages. The ratio was obtained as a function of the ammeter reading. The range of variation found was as follows:

$$13.48 \leq \text{P.T. Ratio} \leq 15.1$$

or,

$$\text{P.T. Ratio} = 14.1^{+4.4\%}_{-7.1\%}$$

The value of 14.1 with the appropriate correction factor obtained from the calibration chart was used in calculating the power input from the wattmeter measurement.

B.5 Calibration of Pressure Gauges

All the pressure gauges used in the experimental apparatus were calibrated before installation [90], of those installed, only the gauges measuring the pressure at inlet to the test section and at inlet to the orifice plate assembly were calibrated frequently during the period of the investigation. The maximum deviations were not more than 0.5%.

B.6 Calibration of Water Flow Meters*

The Fischer and Porter rotameter used for water flow measurement were calibrated in the laboratory and the results were compared against the calibration curves supplied by the manufacturer as shown in Fig. B.3. The manufacturer's calibration curves were used for water flow rate calculations as the agreement between these curves and the measurements

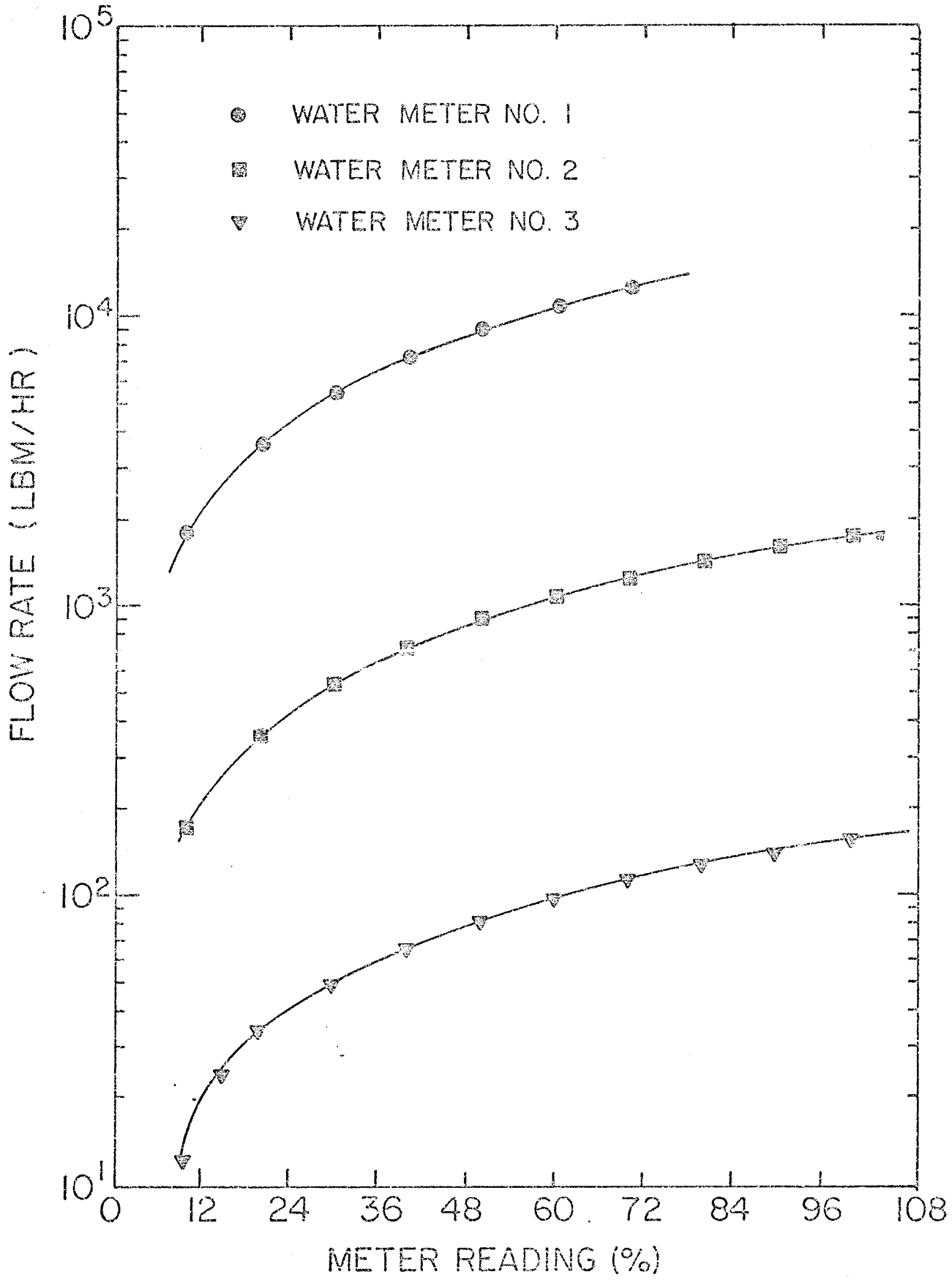

Fig. B.3 Calibration of Water Flow Meters

was excellent (within ±0.25% and 1.46% for Meter Number 1 and 2 respectively, and ±2.6% for Meter Number 3, for which no heat-transfer results are analyzed in the thesis).

B.7 Calibration of Orifice Plates and Rotameter for Gas Flow Rate

Three thin plate sharp edged orifice plates and a Brooks rotameter were used to measure the gas flow rates. The meters were calibrated in situ in the laboratory. The coefficient of discharge was a function of only the Reynolds number based on the orifice throat diameter Re_d. The results of the calibration are shown in Figs. B.4 and B.5 for the orifice plates and rotameter respectively.

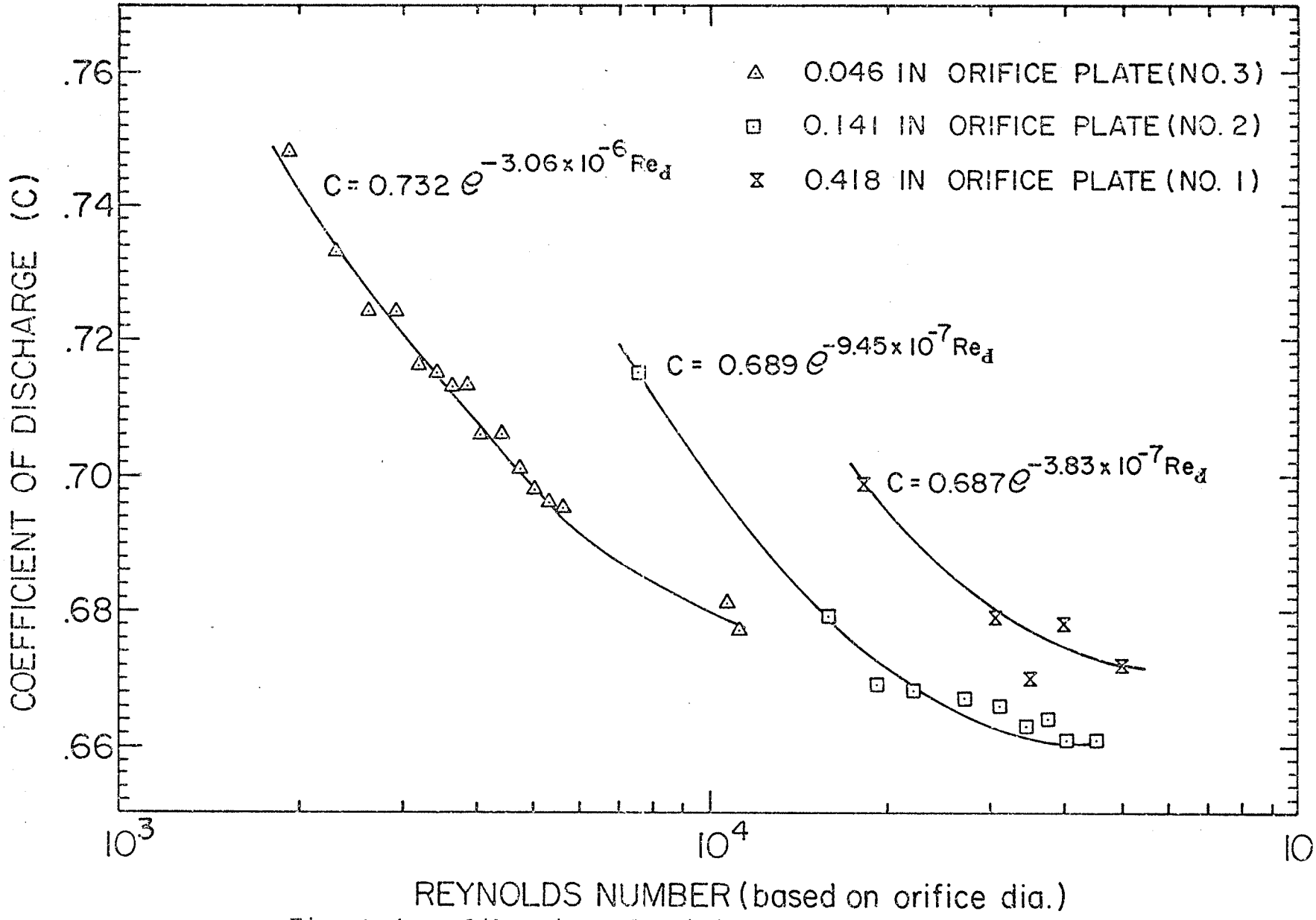

Fig. B.4 Calibration of Orifice Plates for Gas Flow

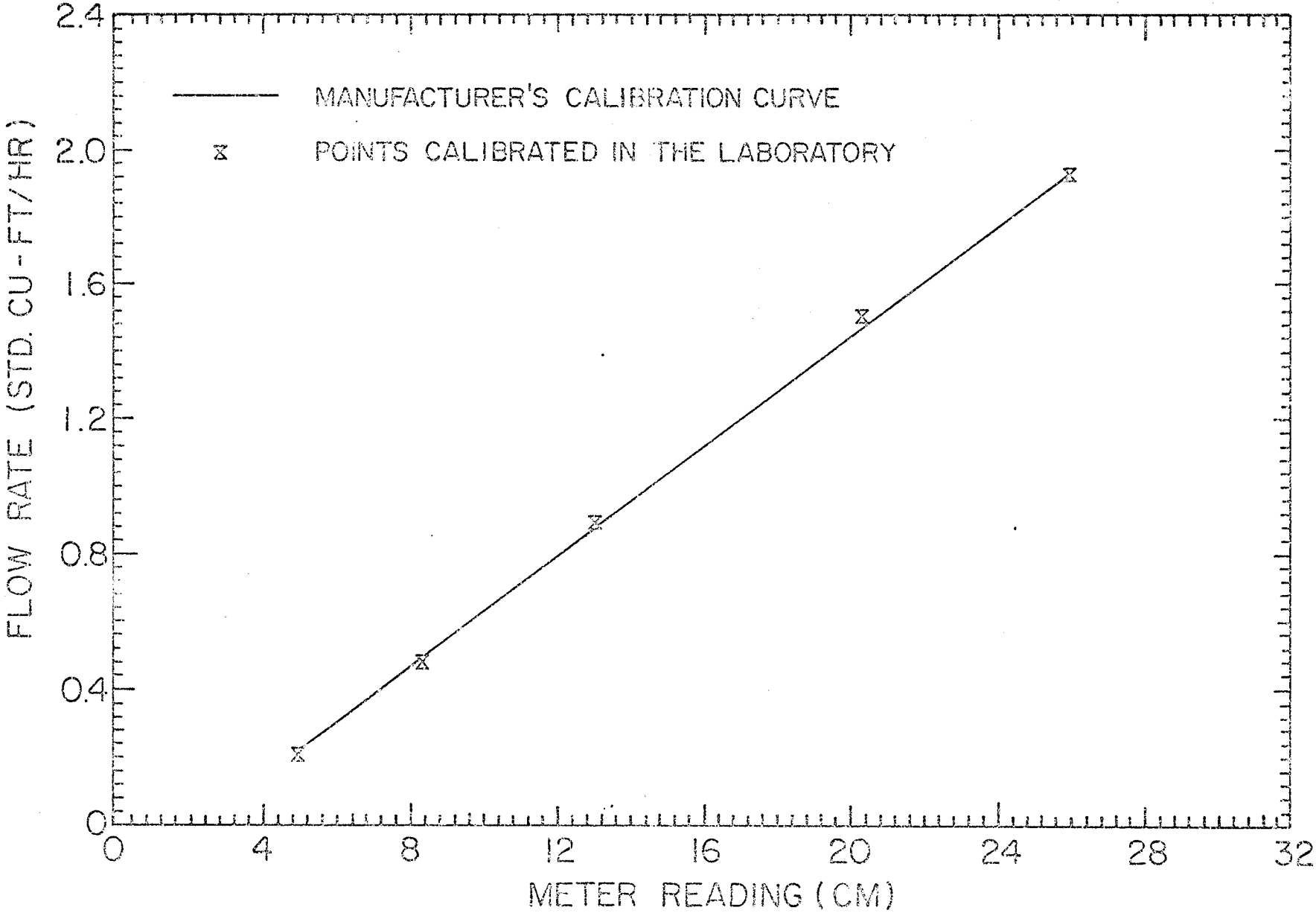

Fig. B.5 Calibration of Gas Flow Rotameter

Fig. B.5

APPENDIX C

PHYSICAL PROPERTIES OF THE FLUIDS

Knowledge of the physical properties of the fluids used in the experiments was necessary for the reduction of the heat-transfer data reported in the thesis. Since the reduction of the data was performed by computer, the physical properties were obtained from the equations describing them; these are given in Table C.1 together with the range of validity and the deviations between the value obtained from the equations and the tabulated and/or measured values. The equations for water and air were taken from [C.1] and [C.2]; the equations for Freon 12 were taken from [C.3] or were obtained by applying standard curve-fitting methods to tabulated or measured data; similarly the equations for helium were obtained. In obtaining the equations listed in the table, it was assumed that the pressure has no effect on viscosity, thermal conductivity and specific heat. Values of the properties at standard atmospheric conditions are given in Table C.2.

Table C.1 Physical Properties of Fluids

Water

Value or Equation For the Physical Property (T in ^{o}F)	Units	Range of Validity and Deviation
$\rho_L = [0.01602 - 1.303 \times 10^{-6}\ T + 2.101 \times 10^{-8}\ T^2]^{-1}$	lbm/ft^3	$32 \leq T \leq 212$ 0.1%
$C_{PL} = 1.018 - 3.374 \times 10^{-4}\ T + 1.337 \times 10^{-6}\ T^2$	$Btu/lbm^{o}F$	$32 < T < 212$ 0.3%
$\sigma_L = 5.346 \times 10^{-3} - 4.75886 \times 10^{-6}\ T - 8.05936 \times 10^{-9}\ T^2 + 5.52288 \times 10^{-12} T$	lbf/ft	$68 < T < 150$
$k_L = 0.3149 + 4.722 \times 10^{-4}\ T$	$btu/hrft^{o}F$	$32 < T < 176$ 0.2%
$\mu_L = [0.09461 + 3.863 \times 10^{-3}\ T + 1.207 \times 10^{-5}\ T^2]^{-1}$	lbm/ft hr	$32 < T < 212$ 1.0%

Table C.1 Physical Properties of Fluids

	Value or Equation For the Physical Property (T in ^{o}F)	Units	Range of Validity and Deviation
Air	$\rho_G = P/RT$ $P(lbf/ft^2)$, $T(^{o}R)$, R - 53.34 lbf-ft/lbm^{o}R	lbm/ft^3	Accurate in the range of pressure investigated
	$C_{PG} = 0.2401 + 7.540 \times 10^{-6} T$	$\frac{Btu/lbm}{^{o}F}$	$-10<T<242$ 0.2%
	$k_G = 0.01313 + 2.591 \times 10^{-5} T - 2.67 \times 10^{-9} T^2$	$\frac{Btu/hr}{ft\ ^{o}F}$	$-10<T<242$ 0.1%
	$\mu_G = 0.03936 + 6.819 \times 10^{-5} T$ $-2.673 \times 10^{-8} T^2$	lbm/fthr	same as above
Helium	$\rho_G = P/RT$, $T(^{o}R)$ R = 386	lbm/ft^3	accurate for present range of pressure
	$G_{PG} = 1.24$	$\frac{Btu/lbm}{^{o}F}$	$50<T<150$ 0.2%
	$k_G = 0.0784 + 12.333 \times 10^{-5} T$ $- 1.333 \times 10^{-7} T^2$	Btu/fthr	$50<T<150$ 0.2%

Table C.1 Physical Properties of Fluids - Freon 12

Value or Equation For the Physical Property (T in ^{O}F)	Units	Range of Validity and Deviation
ρ_G was determined from the relation $P = C_1T/b + (C_2 - C_3 T + C_4 e^{KTr})/b^2 + (C_5 - C_6T + C_7 e^{kTr})/b^3 - C_8/b^4 + (C_9T - C_{10}e^{KTr})/b^5$ where $b = (1/\rho_G) - 6.509 \times 10^{-3}$ $C_1 = 0.088734$, $C_2 = 3.409727$ $C_3 = 1.594348\times10^{-3}$, $C_4 = 56.767267$ $C_5 = 0.060239447$, $C_6 = 1.8796\times10^{-5}$ $C_7 = 1.311399$, $C_8 = 5.48737\times10^{-4}$ $C_9 = 3.468834\times10^{-9}$ $C_{10} = 2.54391\times10^{-5}$ $K = 5.475$, $T_r = T/693.3$ T in ^{O}R		ρ_G was obtained by a trial & error solution of the equation (0.5%)
$C_{PG} = 0.139 + 1.02 \times 10^{-4}T$	Btu/lbm^{O}F	0.3%
$K_G = 4.79 \times 10^{-3} + 7.615 \times 10^{-6} T^{1.11944}$	Btu/hrft^{O}F	50<T<150 0.2%
$\mu_G = 25.883 \times 10^{-3} + 8.458 \times 10^{-6} T^{0.90906}$	lbm/fthr	0<T<100 0.2%

Table C.2

Properties of Gases at
Standard Conditions ($70^{\circ}F$ and 1 atm)

	ρ_G lbm/ft^3	μ_G lbm/ft hr	C_{PG} $Btu/lbm^{\circ}F$	k_G $Btu/hrft^{\circ}F$
Air	0.075	0.0441	0.240	0.0149
Helium	0.0104	0.0481	1.24	0.0862
Freon 12*	0.3194	0.263	0.146	0.0057

* Saturation temperature at 1 atm = $-21.62^{\circ}F$

References for Appendix C

C.1 Greenland, R., Ph.D. Thesis, Mechanical Engineering Department, Imperial College of Science & Technology, University of London, London, England, U.K., 1963.

C.2 Gambil, W.R., Estimating Engineering Properties, Parts I to VI, Chemical Engineering 1957, 1958, 1959 and 1960.

C.3 McHarness, R.C., Eiseman, B.J., Jr., and Martin J.J., The New Thermodynamic Properties of "Freon 12", Refrigerating Engineering, 63, No. 9, 31-44, 1955.

APPENDIX D

CALCULATION PROCEDURE

This appendix gives the definition and procedure for calculating the heat-transfer coefficients and the hydrodynamic quantities of interest in the present investigation. It should be noted that the material presented in this appendix follows, in many ways, that represented in [90].

Because of the length of this appendix, the section headings are listed below in order to facilitate access to any desired material.

D.1. Definition of the Heat-Transfer Coefficients

The coefficients of heat transfer reported in the body of the thesis are both the local h and mean $\bar{h}$ heat-transfer coefficients; these are defined as follows:

(a) Local heat-transfer coefficient

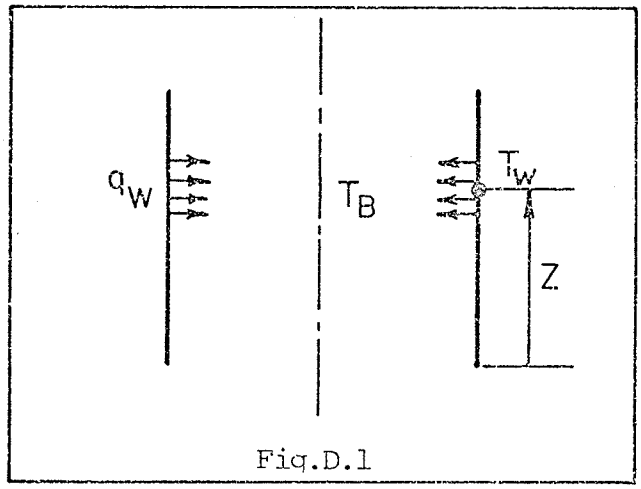

Fig.D.1

Referring to Fig. D.1 above, the local heat-transfer coefficient is defined as:

$$h(z) = \frac{q_w}{T_w - T_B} \qquad (D.1)$$

where

q_w is the heat flux at the wall at the location z,

T_w is the inner wall temperature at the location z,

T_B is the bulk fluid temperature at the location z,

$h(z)$ is the local heat-transfer coefficient.

(b) Mean Heat-Transfer Coefficient

Theoretically speaking, the mean heat-transfer coefficient can be calculated from the local values, provided that the

functional relationship between h and z is known, by the following expression:

$$\bar{h} = \frac{1}{L} \int_{o}^{L} h(Z)\, dz \qquad (D.2)$$

where L is the length of the heated test section.

For the present purpose, the $h \sim z$ relation was obtained by connecting linearly the local (h,Z) points as illustrated qualitatively in Fig. D.2; Eq. (D.2) was

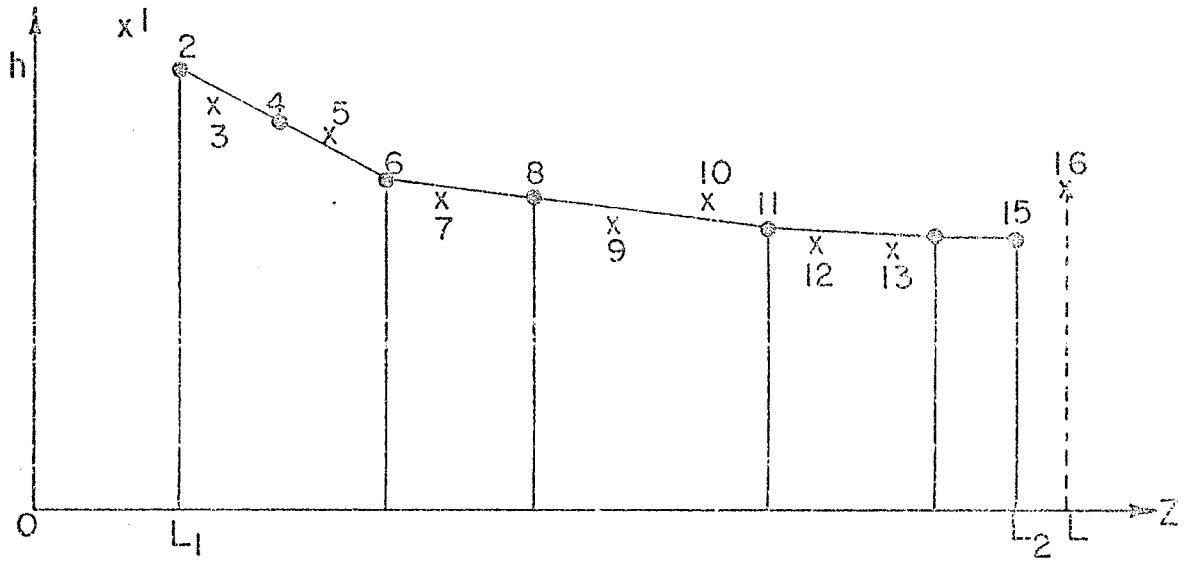

Fig. D.2. Sketch of $h \sim Z$ as used in Eq. (D.3).

modified to the practical form given by Eq. (D.3) to calculate $\bar{h}$ over a length $\Delta L = L_2 - L_1$ of the test section.

The values of h were measured at 16 planes along the test section, however, the values at the seven planes denoted by circles in Fig. D.2 only were used to calculate $\bar{h}$ for the following reasons:

1. Planes Number 1 and 16 (near the inlet and the outlet of the test section respectively) were close to the bus bars (these act as heat sinks) which were silver

soldered to the test section. The local heat flux and the output of the thermocouples at these planes were influenced by the presence of these materials in uncertain ways. Therefore, these two planes were excluded in all the subsequent calculations.

2. At the other seven planes shown by crosses in Fig. D.2 (these are planes Number 3, 5, 7, 9, 10, 12 and 13), there was only one thermocouple located at each plane while at the planes denoted by circles in Fig. D.2 there were four thermocouples placed around the circumference at each plane, the average of which was used to describe the local condition at that plane; i.e., at each of these planes four values of h were calculated from the local heat flux and the output of the four thermocouples; the average of the four values of h was then used as the local heat-transfer coefficient at that plane. At the same plane, the four values of h were found to differ from each other (in the worst case the difference was about 10%). This variation was proved, experimentally [90], to be due to the nonuniformity of the tube wall thickness around the circumference. Therefore, it was decided to exclude all planes having a single thermocouple in all subsequent calculations.

Equation (D.2) is, therefore, reduced to

$$\bar{h} = \frac{1}{\Delta L} \int_{L_1}^{L_2} h(Z)\, dZ \qquad (D.3)$$

where $\Delta L = L_2 - L_1$

Equation (D.3) was numerically integrated using the trapezoidal rule.

D.2. Calculation of the Local Heat Flux (q_W)

The local heat flux at the wall, which is also the net heat flux transferred to the fluid (the heat loss to the surroundings was negligible due to the presence of the guard heater and the insulation), is calculated from knowledge of

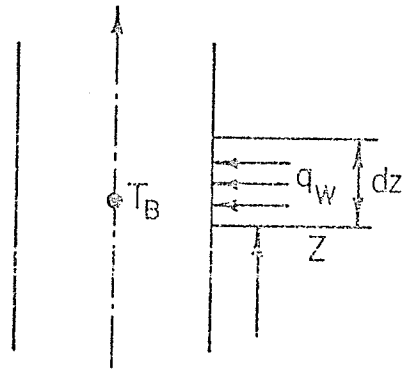

Fig. D.3

the local resistivity of, and the current flowing through the tube as follows:

Consider the elemental length dZ of the tube at location Z (Fig. D.3. above), the heat generated in this elemental length is given by

$$dq_W = GI^2 \, dR_t$$

where dR_t is the resistance of the elemental lenght dZ of the tube and is given by

$$dR_t = \overline{\rho'} \, dZ/A_C \ , \quad \text{ohm}$$

$\overline{\rho'}$ is the average resistivity of the tube at location Z,

A_C is the cross-sectional area of the tube wall,

I is the electric current flowing through the tube,

G is a conversion factor = 3.413 Btu/watt-hr.

Therefore

$$q_W = \frac{dq_W}{dA_s} = \frac{GI^2 \overline{\rho'} \, dZ}{A_C \, \pi \, D \, dZ}$$

where,

$dA_s = \pi \, D \, dZ$ is the elemental surface area of the tube,

Hence,

$$q_W = \frac{GI^2 \overline{\rho'}}{\pi \, D \, A_C} \quad \text{Btu/hr ft}^2 \qquad \text{(D.4)}$$

D.3. Calculation of the Inner Wall Temperature from the Measured Outer Temperature

In order to determine the local heat-transfer coefficient from Eq. (D.1), the local temperature T_W at the solid-fluid interface (inner wall temperature) is required. This was obtained by measuring the outer wall temperature T_o and calculating the temperature drop across the wall ΔT_W; that is,

$$T_W = T_o - \Delta T_W \quad ^\circ F \qquad \text{(D.5)}$$

ΔT_W was calculated using the method developed by Kreith and Summerfield [D.1] for the temperature distribution in an electrically heated resistor of tubular shape with total energy dissipated to a fluid flowing inside. The expression for ΔT_W

as given by the authors [D.1] is as follows:

$$\Delta T_W = B_o t^2 + B_1 t^3 + (B_2 + B_3) t^4 \quad °F \tag{D.6}$$

where

$t = (R_o - R)$ = wall thickness of the tube,

$B_o = m/(1 + \beta' T_o)(1 + \alpha' T_o)$,

$B_1 = 2m/3D_o(1 + \beta' T_o)(1 + \alpha' T_o)$,

$B_2 = m^2(3\alpha' + 4\alpha'\beta' T_o + \beta')/6(1 + \beta' T_o)^3(1 + \alpha' T_o)^3$,

$B_3 = m/D_o^2(1 + \beta' T_o)(1 + \alpha' T_o)$,

D_o is the outer diameter of the tube,

R_o is the outer radius of the tube,

R_i is the inner radius of the tube,

$$m = G(de/dZ)^2/2\ \rho_o'\ k_o', \tag{D.7}$$

β' is the temperature coefficient of resistivity of the tube material defined by

$$\rho' = \rho_o'(1 + \beta' T) \quad \text{ohm-ft},$$

ρ' is the electrical resistivity of the tube material,

α' is the temperature coefficient of thermal conductivity of the tube material defined by

$$k_t = k_o'(1 + \alpha' T) \quad \text{Btu/hr ft} \quad °F$$

k_t is the thermal conductivity of the tube material,

(de/dZ) is the voltage gradient in the tube.

In Eq. (D.7), m can be expressed in terms of the

measured current flowing through the tube in the following manner. For the elemental length dZ, the axial current density i may be expressed by

$$i = I/A_C = -\frac{1}{\rho'} \cdot \frac{\partial e}{\partial Z}$$

Hence,

$$m = \frac{G}{2\rho_o' k_o'} \cdot \rho'^2 \cdot \left(\frac{I}{A_C}\right)^2 \qquad (D.8)$$

In the calculations, ρ' was assumed to be constant, within the wall at any particular location, and equal to the average resistivity $\overline{\rho'}$ evaluated at the average temperature T_{AVG} of the tube wall at this particular location; that is ρ' becomes $\overline{\rho'}$ and is given by

$$\rho' = \overline{\rho'} = \rho_o'(1 + \beta' T_{AVG}) \quad \text{ohm-ft.} \qquad (D.9)$$

where

$$T_{AVG} = (T_o + T_W)/2 \quad °F \qquad (D.10)$$

Therefore, Eq. (D.8) can be rewritten as

$$m = \frac{G}{2\rho_o' k_o'} \cdot \overline{\rho'}^2 \cdot \left(\frac{I}{A_C}\right)^2 \quad °F/ft^2 \qquad (D.11)$$

Equation (D.6) was solved for ΔT_W (or T_W) by an iteration method as follows:

(i) a certain value was assumed for T_W (T_o was taken to start with)

(ii) $\overline{\rho'}$ and m were calculated from Eqs. (D.9) and (D.11)

(iii) T_W was then calculated from Eq. (D.6)

(iv) the new value of T_W (from step iii) was then used to calculate a new value for T_{AVG} and the above steps were repeated until two successive values of ΔT_W agreed within $\pm$ 0.0005°F.

The electric resistivity of the tube material was measured in the laboratory [90] and the following equation was used for ρ':

$$\rho' = 0.216581 \times 10^{-5}(1 + 0.650408 \times 10^{-3}\ T)\ \text{ohm-ft.} \tag{D.12}$$

The thermal conductivity of the tube material (type-304 stainless steel) was calculated from the equation reported by Bergles and Rohsenow [D.2], which agreed (in the temperature range of 75-150°F) within $\pm$2% with the data obtained from the manufacturer. This is given by

$$k_t = 8.46(1 + 0.000526T)\ \text{Btu/hr ft °F} \tag{D.13}$$

It should be mentioned that an alternative, much simpler, equation for ΔT_W was used to check ΔT_W obtained from Eq. (D.6). This is given by

$$\Delta T_W = \frac{q_v}{2k_t}\left[\frac{D_o^2}{4}\ \ell n\ \frac{D_o}{D} - \frac{(D_o^2 - D^2)}{8}\right]\ \text{°F} \tag{D.14}$$

where

$$q_V = \left(\frac{I}{A_C}\right)^2 \overline{\rho'}\ G\ \ \text{Btu/hr ft}^3 \tag{D.15}$$

is the volumetric heat generation rate. The difference in ΔT_W obtained from the two methods was 3.5% with a standard

deviation of $\pm$ 2.5%.

D.4. Calculation of the Local Bulk Temperature (T_B)

In deriving the equations for T_B, it was assumed that the mixture enters the heated test section fully saturated, that is, the saturation process takes place in the calming tube. Detailed calculations done by Sims [D.4] show that this assumption is valid.

Consider the elemental length of dZ of the heated tube (Fig. D.3), and let the temperature rise of the mixture in this length be dT_B. The amount of heat transferred to the fluid in dZ is given by

$$dq_t = q_W \, dA_s$$

Since the heat transfer is equal to the energy absorbed and converted by the fluid, therefore,

$$q_W \, dA_s = \dot{m}_L \, C_{PL} \, dT_B + \dot{m}_G \, C_{PG} \, dT_B \quad \text{Btu/hr}$$

Hence,

$$dT_B = \frac{q_W \, dA_s}{\dot{m}_L \, C_{PL} + \dot{m}_G \, C_{PG}} \quad °F \qquad (D.16)$$

To integrate Eq. (D.16) between two successive locations, the specific heats and the heat flux were assumed to remain constant in the interval between the two locations. With $dA_s = \pi \, D \, dZ = p dZ$, integration of Eq. (D.16) between Z_i and Z_{i+1} gives

$$\int_{z_i}^{z_{i+1}} dT_B = \frac{p \, q_W}{\dot{m}_L \, C_{PL} + \dot{m}_G \, C_{PG}} \int_{z_i}^{z_{i+1}} dZ$$

Therefore,

$$(T_B)_{i+1} - (T_B)_i = \frac{p\, q_W}{\dot{m}_L C_{PL} + \dot{m}_G C_{PG}} (Z_{i+1} - Z_i) \qquad (D.17)$$

Assuming that the temperature of the mixture at the inlet to the test section, T_{IN} is known (determination of T_{IN} is discussed in the next section), Eq. (D.17) was used to calculate T_B at plane 1 which in turn was used to calculate T_B at Plane 2 and so on.

D.5. Calculation of the Mixture Inlet Temperature (T_{IN})

The gas entering the mixing device is normally not saturated and generally becomes saturated in its passage through the calming tube [D.4] resulting in mass and heat transfer. Therefore, the temperature of the mixture at the inlet to the test section T_{IN} would generally be different from the temperature of the fluids at the inlet of the mixer (these were the measured temperature in the present experiments.) In this section, the equation for obtaining T_{IN} from the liquid and gas flow rates and temperature at the mixer inlet and the fluid properties is derived.

Consider the control volume shown by the dashed lines in Fig. D.4, the conservation of mass and energy yield:

$$\dot{m}_{L3} + \dot{m}_{G3} = \dot{m}_3 \qquad (D.18)$$

and

$$\dot{m}_{L1}\, h_{L1} + (\dot{m}h)_2 = (\dot{m}h)_3 \qquad (D.19)$$

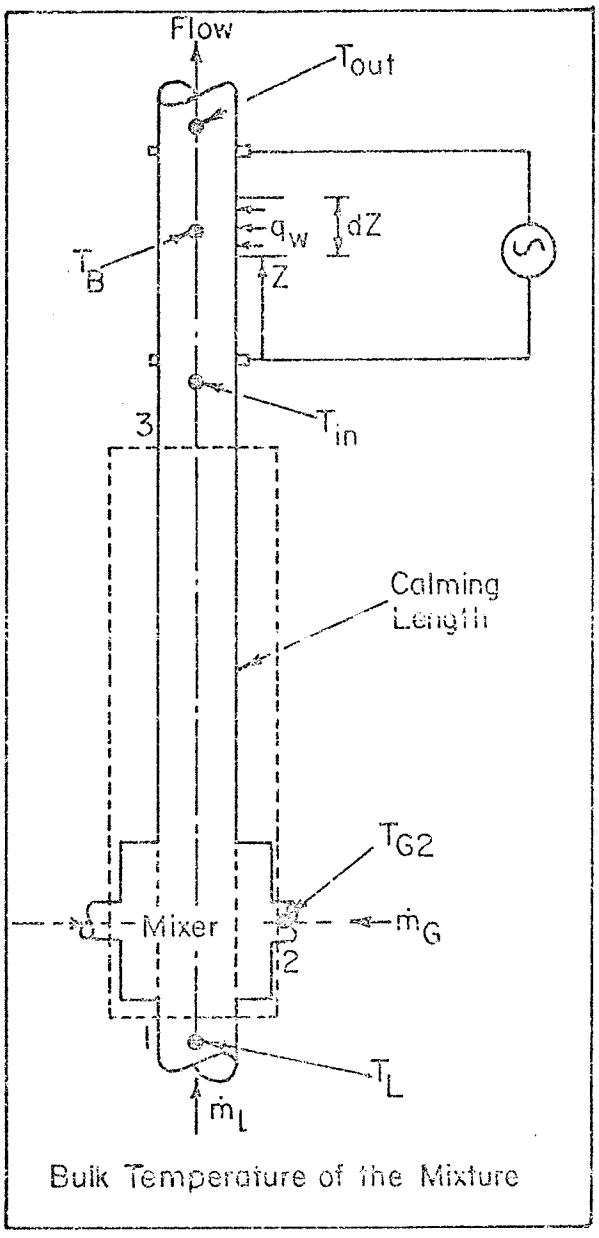

Fig. D.4 Control Volume for the Calculation of Mixture Inlet Temperature.

where

h is the enthalpay per unit mass of the fluid.

If the gas entering the mixer is not saturated, some of the liquid flashes into vapour to saturate the gas. Therefore,

$$\dot{m}_{L3} = \dot{m}_{L1} - \dot{m}_{L,EVAP}$$

where

$\dot{m}_{L,EVAP}$ is the mass of liquid evaporated to saturate the gas.

Further, suppose that the gas entering the mixer already contains some liquid vapor, $\dot{m}_{V2}$; that is,

$$\dot{m}_{G2} = \dot{m}_{DG2} + \dot{m}_{V2}$$

and

$$\dot{m}_{G3} = \dot{m}_{DG2} + \dot{m}_{V2} + \dot{m}_{L,EVAP}$$

where

$\dot{m}_{DG2}$ is the mass flow rate of dry gas = $\dot{m}_{DG3}$,

$\dot{m}_{V2}$ is the amount of liquid vapor already present in the gas entering the mixer.

$$\dot{m}_{V3} = \dot{m}_{V2} + \dot{m}_{L,EVAP}$$

$$(\dot{m}h)_2 = \dot{m}_{DG2}\, h_{G2} + \dot{m}_{V2}\, h_{V2}$$

$$(\dot{m}h)_3 = \dot{m}_{L3}\, h_{L3} + \dot{m}_{DG3}\, h_{G3} + \dot{m}_{V3}\, h_{V3}$$

Equation (D.19) now becomes

$$\dot{m}_{L1}\, h_{L1} + \dot{m}_{DG2}\, h_{G2} + \dot{m}_{LV2}\, h_{V2}$$

$$= \dot{m}_{L3}\, h_{L3} + \dot{m}_{DG2}\, h_{G3} + \dot{m}_{V3}\, h_{V3}$$

$$= (\dot{m}_{L1} - \dot{m}_{L,EVAP}) h_{L3} + \dot{m}_{DG2}\, h_{G3} + \dot{m}_{V3}\, h_{V3}$$

$$= [\dot{m}_{L1} - (\dot{m}_{V3} - \dot{m}_{V2})] h_{L3} + \dot{m}_{DG2}\, h_{G3} + \dot{m}_{V3}\, h_{V3}$$

Hence,

$$\dot{m}_{L1}(h_{L3} - h_{L1}) + \dot{m}_{DG2}(h_{G3} - h_{G2})$$

$$= (\dot{m}_{V3} - \dot{m}_{V2}) h_{L3} + \dot{m}_{V2}\, h_{V2} - \dot{m}_{V3}\, h_{V3} \qquad (D.20)$$

Dividing throughout by $\dot{m}_{DG2}$ and using $dh = C_p dT$ for both dry gas and liquid, Eq. (D.20) yields:

$$\frac{\dot{m}_{L1}}{\dot{m}_{DG2}} C_{PL}(T_{IN} - T_L) + C_{PG}(T_{IN} - T_{G2})$$

$$= (\omega_3 - \omega_2) h_{L3} + \omega_2 h_{V2} - \omega_3\, h_{V3} \qquad (D.21)$$

where

ω is the mass of liquid vapor per unit mass of dry gas

$$\omega = \dot{m}_V / \dot{m}_{DG} \qquad (D.22)$$

Equation (D.21) is solved for T_{IN} to give

$$T_{IN} = \frac{(\frac{\dot{m}_{L1}}{\dot{m}_{DG2}})\, C_{PL}\, T_L + C_{PG}\, T_{G2} + (\omega_3 - \omega_2) h_{L3} + \omega_2 h_{V2} - \omega_3 h_{V3}}{C_{PG} + (\frac{\dot{m}_{L1}}{\dot{m}_{DG2}})\, C_{PL}} \qquad (D.23)$$

which is the general equation for the inlet temperature of a gas-liquid mixture.

In Eq. (D.23), the quantities T_L, T_{G2}, $\dot{m}_{L1}$ and $\dot{m}_{DG2}$

are known from measurement; C_{PL}, C_{PG} and h can be found from property equations or thermodynamic tables; ω_2 and ω_3 are found as follows [D.5]:

$$\omega_2 = R_M \phi_2 P_{V2}/P_{Dg2} \tag{D.24}$$

and

$$\omega_3 = R_M \phi_3 P_{V3}/P_{Dg3} \tag{D.25}$$

where

R_M is the ratio of the molecular weight of the liquid to that of the dry gas,

ϕ is the relative humidity,

P_{V2} is the saturation pressure of liquid vapor in the gas at temperature T_{G2}, obtained from thermodynamic tables [D.5],

P_{Dg2} is the partial pressure of dry gas in the gas-liquid vapor mixture = $P_{G2} - P_{V2}$,

P_{G2} is the total pressure of the gas-liquid vapor mixture,

P_{V3} is the saturation pressure of the liquid vapor at T_{IN},

P_{Dg3} is the partial pressure of dry gas = $P_{IN} - P_{V3}$,

P_{IN} is the total pressure at the test section inlet (this was measured experimentally).

Of all the quantities above, only P_{V3} is a function of T_{IN}, that is, Eq. (D.23) has, in fact, two unknowns, T_{IN} and ω_3. It was solved by an iterative procedure on the computer.

In the present investigation, the liquid phase was always water, while three different gases were used, namely,

air, helium and a highly superheated freon-12 vapor. For each of the three gas-liquid mixtures, the above equations can be rewritten as follows:

(1) Air-Water

The air was supplied from a storage tank (at the outlet of the compressor) and was always saturated because of the presence of water at the bottom of the tank, that is, $\phi = 1.00$. As the air at the test section inlet was assumed to be saturated, ϕ_3 is also equal to 1. Therefore, for the air-water mixture the above equations take the following forms (after substituting with the subscript "a" for the dry air):

$$(\omega_2)_a = 0.622 (P_{V2}/P_{Da2}) \phi_2 \tag{D.26}$$

$$(\omega_3)_a = 0.622 \, P_{V3}/P_{Da3} \quad , \tag{D.27}$$

$$P_{a3} = P_{IN} - P_{V3} \tag{D.28}$$

$$T_{IN} = \frac{(\frac{\dot{m}_{L1}}{\dot{m}_{a2}}) \, C_{PL} \, T_L + C_{Pa} \, T_{G2} - (\omega_3)_a h_{fg3} + (\omega_2)_a (h_{V2} - h_{L3})}{C_{Pa} + (\frac{\dot{m}_{L1}}{\dot{m}_{a2}}) \, C_{PL}} \tag{D.29}$$

where

$$h_{fg3} = h_{V3} - h_{L3}$$

(2) Helium-Water

In this case the helium was supplied from a set of compressed helium cylinders as dry gas, and since it was

assumed to be saturated at the test section inlet, therefore,

$$(\omega_2)_{He} = 0 \tag{D.30}$$

$$(\omega_3)_{He} = 4.5\ P_{V3}/P_{He3} \tag{D.31}$$

$$T_{IN} = \frac{(\frac{\dot{m}_{Ll}}{\dot{m}_{He2}})\ C_{PL}\ T_L + C_{PHe}\ T_{G2} - (\omega_3)_{He}\ h_{fg3}}{C_{PHe} + (\frac{\dot{m}_{Ll}}{\dot{m}_{He2}})\ C_{PL}} \tag{D.32}$$

(3) Freon-12-Water

The Freon was supplied at the mixer as a dry, highly superheated vapor, while it was considered to be saturated with water vapor at the test section inlet. Therefore,

$$(\omega_2)_{Fr} = 0 \tag{D.33}$$

$$(\omega_3)_{Fr} = 0.148883\ P_{V3}/P_{Fr3} \tag{D.34}$$

$$T_{IN} = \frac{(\frac{\dot{m}_{Ll}}{\dot{m}_{Fr2}})\ C_{PL}\ T_L + V_{PFr}\ T_{G2} - (\omega_3)_{Fr}\ h_{fg3}}{C_{PFr} + (\frac{\dot{m}_{Ll}}{\dot{m}_{Fr2}})\ C_{PL}} \tag{D.35}$$

D.6. Summary of the Calculation Procedure for the Heat-Transfer Coefficients

In this section, the calculation procedure for the heat-transfer coefficient is summarized, the important equations used in the calculation are listed in Table D.1 together with an indication of where in the text the definitions of

the

the symbols may be found.

In connection with the calculation of the heat-transfer coefficient, the following quantities were measured: I (electric current flowing through the tube), T_o (outer wall temperature at 16 planes, T_o at seven planes only were used), T_L (liquid temperature at inlet to the mixer), T_{G2} (gas temperature at the mixer inlet), $\dot{m}_{L1}$ and $\dot{m}_{G2}$ (liquid and gas flow rates respectively) and P_{IN} (pressure at inlet to the test section).

The calculation procedure was as follows:

(i) The local values of the heat flux (q_w) were calculated from Eq. (D.4),

(ii) The local values of the inner wall temperature (T_w) were calculated from Eq. (D.6) as explained in section D.3,

(iii) The mixture temperature at the test section inlet (T_{IN}) was calculated from Eqs. (D.26) to (D.35), (see section D.5),

(iv) The local values of the bulk temperature (T_B) were then calculated from Eq. (D.17),

(v) Finally, Eqs. (D.1) and (D.3) were used to calculate the local and mean values of the heat-transfer coefficient, respectively.

D.7. Calculation of the Frictional Pressure Drop

In the experiments, the total pressure drop across the test section was measured by means of manometers. Two

TABLE D.1

Summary of the Important Equations Used in the Calculation of the Heat-Transfer Coefficient

Equation No.	Equation	Places where symbols are defined
D.4	$q_W = GI^2 \overline{\rho'}/\pi\, DA_C$ with $\overline{\rho'}$ from Eq. A.12	Section D.2
D.6	$T_W = T_o - [B_o t^2 + B_1 t^3 + (B_2+B_3) t^4]$	Below Eq. (D.6)
D.23	$T_{IN} = \dfrac{(\dfrac{\dot{m}_{L1}}{\dot{m}_{DG2}}) C_{PL} T_L + C_{PG} T_{G2} + (\omega_3 - \omega_2) h_{L3}}{C_{PG} + (\dfrac{\dot{m}_{L1}}{\dot{m}_{DG2}})\, C_{PL}} + \dfrac{\omega_2 h_{V2} - \omega_3 h_{V3}}{C_{PG} + (\dfrac{\dot{m}_{L1}}{\dot{m}_{DG2}})\, C_{PL}}$	Fig. D.4; below Eq. (D.19); Eqs. (D.24) and (D.25) and below Eq. (D.25).
D.17	$(T_B)_{i+1} = (T_B)_i + \dfrac{p\, q_w}{\dot{m}_L C_{PL} + \dot{m}_G C_{PG}} (Z_{i+1} - Z_i)$	Fig. D.3
D.1	$h(Z) = \dfrac{q_w}{(T_W - T_B)}$	Below Eq. (D.1)
D.3	$\bar{h} = \dfrac{1}{\Delta L} \int_{L_1}^{L_2} h(Z)\, dZ$	

manometers were used for this purpose, one upright mercury manometer and one inverted manometer using the test liquid; these are shown in Figs. D.5a and b. The measured total pressure drop was used to calculate the frictional pressure drop in the manner described below.

D.7.1. Inverted Manometer

Consideration of the balance of forces acting on the plane XX, allows the following equation to be obtained:

$$P_{IN} - P_{OUT} = \frac{g}{g_c} \rho_L L + \frac{g}{g_c} (\rho_L - \rho_a) h' \qquad (D.36)$$

where

g = acceleration due to gravity

= 32.174 ft/sec,

g_c = conversion factor = $32.174 \frac{\text{lbm ft}}{\text{lbf sec}^2}$,

ρ_L = density of water,

ρ_a = density of air in the manometer.

Since $\rho_a << \rho_L$, Eq. (D.36) reduces to

$$P_{IN} - P_{OUT} = \frac{g}{g_c} \rho_L L + \frac{g}{g_c} \rho_L h' \qquad (D.37)$$

(i) Single-Phase Flow

For single-phase liquid flow, the total pressure drop consists of:

$$\Delta P = P_{IN} - P_{OUT} = \Delta P_{SPG} + \Delta P_{SPA} + \Delta P_{SPF} \qquad (D.38)$$

where

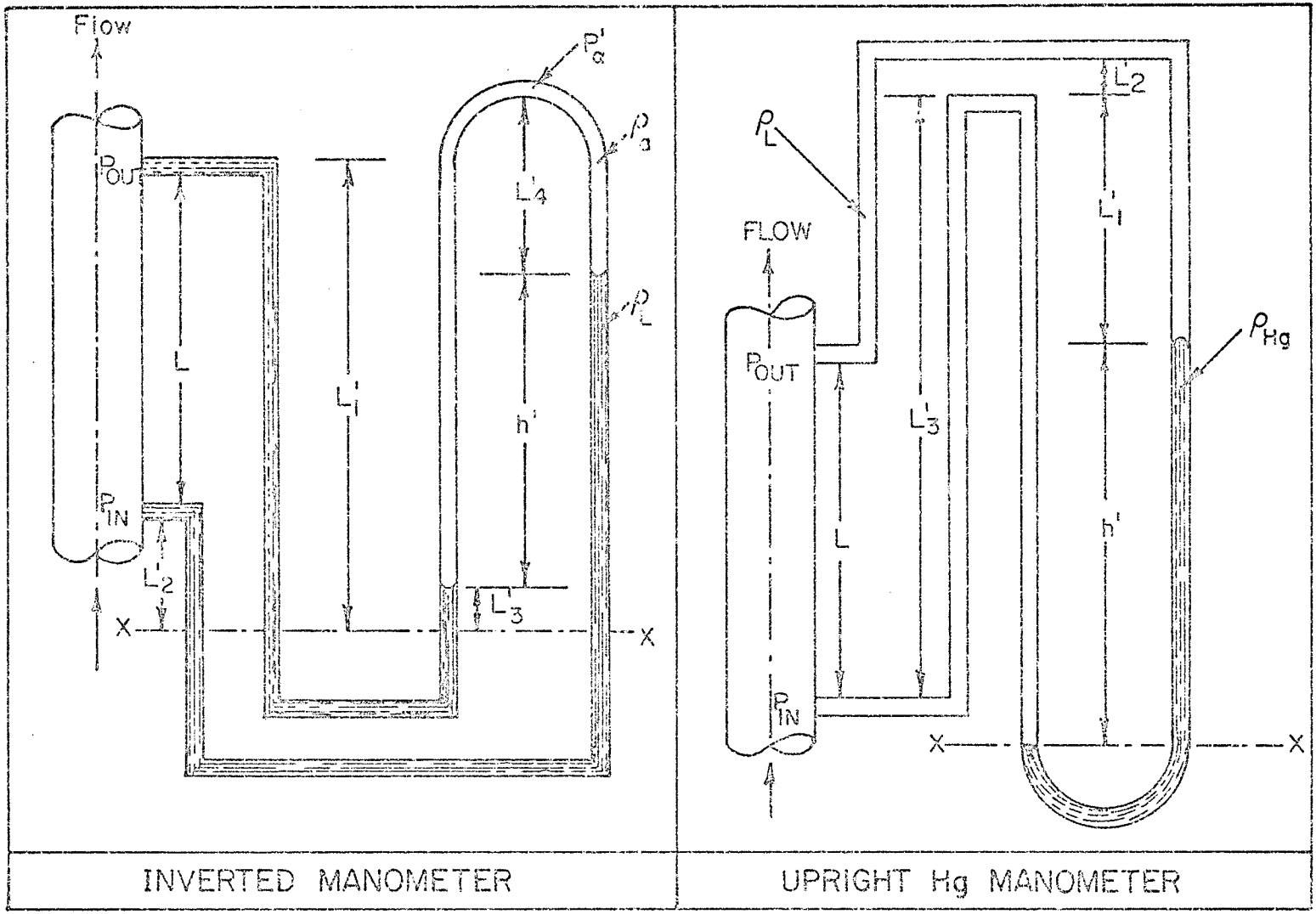

Fig. D.5a

Fig. D.5b

Figs. D.5a & D.5b

ΔP_{SPG} = single-phase hydraulic gradient

ΔP_{SPA} = single-phase accelerational pressure drop ≈ 0 for all the tests and

ΔP_{SPF} = single-phase frictional pressure drop.

The hydraulic pressure gradient is simply the head of liquid in the test section and is given by

$$\Delta P_{SPG} = \frac{g}{g_c} \rho_L L \tag{D.39}$$

Therefore,

$$\Delta P_{SPF} = \Delta P - \Delta P_{SPG}$$

$$= \frac{g}{g_c} \rho_L h' \tag{D.40}$$

(ii) Two-Phase Flow

In this case, neglecting the accelerational pressure drop again, the frictional pressure drop is given by

ΔP_{TPF} = Two-phase frictional pressure drop

= Total pressure drop − hydraulic pressure drop

= $\Delta P - \Delta P_{TPG}$

where

$$\Delta P_{TPG} = \frac{g}{g_c} L \rho_{MIX}$$

$$\rho_{MIX} = (1 - \alpha) \rho_L + \alpha \rho_G \tag{D.41}$$

= mixture density

where α is the void fraction.

Therefore,

$$\Delta P_{TPF} = \frac{g}{g_c} \rho_L L + \frac{g}{g_c} \rho_L h' - \frac{g}{g_c}[(1-\alpha)\rho_L + \alpha\rho_G]L$$

$$= \frac{g}{g_c} \rho_L h' + \frac{g}{g_c} L \alpha(\rho_L - \rho_G) \qquad (D.42)$$

If $\rho_G << \rho_L$ which was true for all the tests carried out, then Eq. (D.42) reduces to

$$\Delta P_{TPF} = \frac{g}{g_c} \rho_L (h' + \alpha L) \qquad (D.43)$$

The above equations are based on the assumption that the density of the liquid in the manometer is equal to the density of the liquid in the test section.

D.7.2. Upright Manometer

In this case, consideration of the balance of forces acting on the plane XX yields the following equation:

$$P_{IN} - P_{OUT} = \frac{g}{g_c}(\rho_{Hg} - \rho_L)h' + \frac{g}{g_c} \rho_L L \qquad (D.44)$$

where ρ_{Hg} is the density of mercury in the manometer. By the arguments given for the inverted manometer, the equations for the frictional pressure drop are as follows:

(i) Single-Phase Flow

$$\Delta P_{SPF} = \frac{g}{g_c} (\rho_{Hg} - \rho_L)h' \qquad (D.45)$$

(ii) Two-Phase Flow

$$\Delta P_{TPF} = \frac{g}{g_c}(\rho_{Hg} - \rho_L)h' + \frac{g}{g_c}(\rho_L - \rho_{MIX})L$$

$$= \frac{g}{g_c}(\rho_{Hg} - \rho_L)h' + \frac{g}{g_c}\alpha(\rho_L - \rho_G)L \qquad (D.46)$$

D.8. Calculation of the Mean Pressure and Temperature in the Test Section

The mean pressure in the test section was calculated as follows:

$$P_{MIX} = (P_{IN} + P_{OUT})/2 \qquad (D.47)$$

Since P_{IN} and the total pressure drop were measured, this equation was modified to the following form:

$$P_{MIX} = P_{IN} - (\Delta P/2) \qquad (D.48)$$

The mean temperature of the mixture, $\overline{T}_{MIX}$, was calculated from,

$$\overline{T}_{MIX} = (T_{IN} + T_{OUT})/2 \qquad (D.49)$$

where, T_{OUT} is the bulk temperature at the tube outlet.

A.9. Calculation of the Void Fraction

As shown in Section D.7, a knowledge of the void fraction α was required to calculate the pressure gradient and hence the frictional pressure drop. The void fraction was also required to correlate the two-phase mean heat-transfer coefficients as discussed in Chapter 6. The void-fraction correlation proposed by Chisholm [17] was chosen because it is well accepted, simple to use and it was the best in correlating the heat-transfer data. The void fraction was, therefore, calculated in the manner described below.

The ratio of the mean velocities of the two-phases,

usually known as the slip ratio, is given by

$$S = V_G/V_L \tag{D.50}$$

From the definition of the flow quality and void fraction, it can be shown that

$$R_L = \frac{S(1-x)/\rho_L}{(x/\rho_G) + S(1-x)/\rho_L} \tag{D.51}$$

where

$R_L = (1 - \alpha)$ is the liquid volume fraction,

$X = \dot{m}_G/(\dot{m}_G + \dot{m}_L)$ is the flow quality.

In the paper [17], the author showed that S can be approximated by

$$S \approx (\rho_L/\rho_{MIX})^{1/2} \tag{D.52}$$

where

$$\frac{1}{\rho_{MIX}} = \frac{(1 - x)}{\rho_L} + \frac{x}{\rho_G} \tag{D.53}$$

Since X, ρ_G and ρ_L were known, ρ_{MIX} and S were calculated from Eqs. (D.53) and (D.52) respectively, and the void fraction was then evaluated from Eq. (D.51).

D.10. Calculation of the Liquid and Gas Flow Rates and Superficial Velocities

D.10.1. Water Flow Rate and Superficial Velocity

(i) Flow Rate: The water flow rate was measured by means of three rotameters which were calibrated in situ. The water

flow rate was determined as follows:

- for meter number 1 (high flow range);

$$\dot{m}_L = 0.2742856 + 179.9142\ R_m \qquad (D.54)$$

- for meter number 2 (medium flow range);

$$\dot{m}_L = 4.1487510 + 17.560450\ R_m \qquad (D.55)$$

- for meter number 3 (low flow range);

$$\dot{m}_L = 1.0562240 + 1.565065\ R_m \qquad (D.56)$$

where

R_m is the meter reading (%).

(ii) Superficial Velocity (V_{SL})

By definition, the superficial water velocity was calculated from the following equation:

$$V_{SL} = \dot{m}_L/\rho_L\ A_T \qquad (D.57)$$

where

$A_T = (\pi/4)D^2$ is the cross sectional area of the tube.

D.10.2 Gas Flow Rate and Superficial Velocity

(i) Flow rate:

The gas flow rate was measured by means of three orifice plates and a Brooks rotameter; these were calibrated in the laboratory. The following equations were used for the calculation of the gas flow rate [90]:

- for the rotameter (lowest flow range);

$$\dot{m}_G = 0.27364 \ (\rho_{Gl})^{1/2} \ Q_o \qquad (D.58)$$

where

$$Q_o = -0.1825 + 0.0813 \ R_G \ , \qquad (D.59)$$

is the volumetric flow rate of the gas at standard conditions (in ft^3/hr), as obtained from the calibration curve, ρ_{Gl} is the gas density at the rotameter inlet, R_G is the meter reading.

Equation (A.60) follows directly from the basic equations for calculating the gas flow rates through rotameter [D.8].

The mass flow rate through the orifice plates was calculated from the following equation [D.9]:

$$\dot{m}_G = 359.052 \ d^2 \ F \ Y \ C \ F_a (\rho_{Gl} h_W)^{1/2} \qquad (D.60)$$

where

d is the orifice throat diameter,

$F = (1-\beta^4)^{-1/2}$ is the velocity of approach factor,

$\beta = d/D_p$ is the ratio of orifice throat diameter to pipe diameter,

Y is the expansion factor given by [A.9]

$$Y = 1 - (0.41 + 0.35\beta^4) \ \frac{\Delta P_{OR}}{k \ P_{Gl}} \ , \qquad (D.61)$$

F_a is the thermal expansion faction = 1.00, in the temperature range involved in the experiments,

h_W is the pressure drop across the orifice plate (in H_2O),

k is the ratio of specific heats,

ΔP_{OR} is the pressure drop across the orifice plate,

C is the coefficient of discharge which was determined (from the calibration chart) as a function of the Reynolds number, Re_d, based on the orifice throat diameter, i.e.,

$$Re_d = 4\dot{m}_G/\pi d\ \mu_G \qquad (D.62)$$

The following equations, for C, were obtained from the calibration chart [90]:

Orifice plate no.	Throat diameter (in)	C
1	0.418	$0.687\ EXP(-3.83 \times 10^{-7}\ Re_d)$
2	0.141	$0.689\ EXP(-9.45 \times 10^{-7}\ Re_d)$
3	0.048	$0.732\ EXP(-3.06 \times 10^{-6}\ Re_d)$

The procedure for calculating $\dot{m}_G$ was as follows:

1. From the measured values of P_{G1} and T_{G1}, ρ_{G1} was calculated assuming an ideal gas, i.e.

   $$\rho_{G1} = P_{G1}/R\ T_{G1}$$

   with R being the characteristic gas constant.

2. Y was calculated from Eq. (D.61) (ΔP_{OR}, the pressure drop across the orifice plate was measured).

3. An arbitrary value for C was chosen (0.6 to start with), and Eq. (D.60) was used to determine $\dot{m}_G$.

4. Re_d was then evaluated and a new value for C was determined, then a new value of $\dot{m}_G$ was calculated.

5. The procedure was repeated until two successive values of $\dot{m}_G$ agreed within $\pm$ 0.1%.

(ii) Superficial Velocity (V_{SG})

The superficial gas velocity is given by

$$V_{SG} = \dot{m}_G/\rho_G A_T \qquad (D.63)$$

The gas density changes along the length of the heated test tube due to changes in temperature and pressure. Therefore, local values of V_{SG} were calculated by assuming a linear drop in the total pressure across the test tube; and using local values of T_B the mean value of V_{SG} ($\bar{V}_{SG}$) was then calculated from the relation

$$\bar{V}_{SG} = \frac{1}{L} \int_o^L V_{SG}\, dZ$$

References for Appendix D

D.1. Kreith, F. and Summerfield, M., Investigation of heat transfer at high heat-flux densities: experimental study with water of friction drop and forced convection with and without surface boiling in tubes, Progress Report No. 4-68, Jet Propulsion Laboratory, California Institute of Technology, Pasadena, California, April 2, 1948.

D.2. Bergles, A.E. and Rohsenow, W.M., Forced convection surface-boiling heat transfer and burnout in tubes of

small diameter, Technical Report No. 8767-21, MIT, May 25, 1962.

D.3. Heineman, J.B., An experimental investigation of heat transfer to superheated steam in round and rectangular channels, ANL-6213, 1960.

D.4. Sims, G.E., Forced convection heat transfer to water with air injection through one porous heated wall of a rectangular duct, Ph.D. Thesis, Imperial College of Science and Technology, University of London, London, U.K., 1969, P. 239.

D.5. Van Wylen, G.J. and Sonntag, R.E., Fundamentals of classical thermodynamics, John Wiley & Sons, Inc., New York, U.S.A., 1973.

D.6. Chisholm, D., Research note: void fraction during two-phase flow, Jour. Mech. Eng. Sci., 15(3), P. 235, (1973).

D.7. Butterworth, D., A comparison of some void-fraction relationships for co-current gas-liquid flow, Int. J. Multiphase Flow, 1, 845-850 (1975).

D.8. Head, V.P., Coefficients of float-type variable-area flowmeters, Trans. ASME, 851-862 (1954).

D.9. ASME Power Test Codes, Instruments and Apparatus, Chapter 4, Flow Measurement, Part 5, Measurement of Quality of Materials, February 1959.

APPENDIX E

DISCUSSION OF PRESSURE DROP AND HEAT TRANSFER EQUATIONS AND CORRELATIONS

E.1. Single-Phase Flow

This section presents a discussion of the frictional pressure drop and local heat-transfer correlations and equations which have been used in the single-phase flow study presented in Sections 5.2 and 6.2. The main purpose is to summarize the relevant equations without deriving them; the derivations can be found in the references listed in the bibliography.

E.1.1. Frictional Pressure Drop

The basic equations of fluid mechanics for the steady axisymmetric flow of an incompressible constant property fluid in circular tube are given below [54].

The continuity equation:

$$\frac{\partial V_Z}{\partial Z} + \frac{\partial V_r}{\partial r} + \frac{V_r}{r} = 0 \qquad \text{(E.1)}$$

where V_Z and V_r respectively are the axial and radial velocities (see Fig. E.1).

The momentum equation:

The momentum equation is deduced from the Navier-Stokes equation using the boundary layer approximations, this is given by

$$V_Z \frac{\partial V_Z}{\partial Z} + V_r \frac{\partial V_Z}{\partial r} + \frac{g_c}{\rho} \frac{\partial P_F}{\partial Z} = \frac{\nu}{r} \frac{\partial}{\partial r}\left(r \frac{\partial V_Z}{\partial r}\right) \qquad \text{(E.2)}$$

For a fully developed flow:

$$V_r = 0 \ ;$$

$$\frac{\partial V_Z}{\partial Z} = 0$$

Therefore, Eq. (E.2) becomes:

$$\frac{\mu}{r}\frac{d}{dr}\left(r\frac{dV_Z}{dr}\right) = g_c\frac{dP_F}{dZ} \quad (E.3)$$

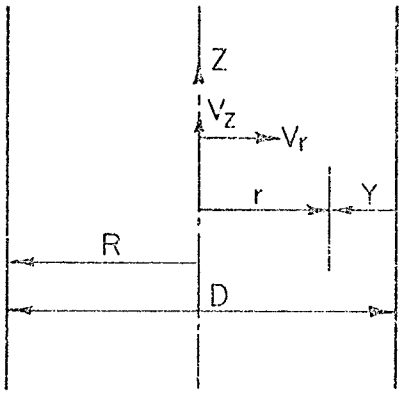

Fig. E.1 Coordinates for Flow in Circular Tube

By performing a force balance on a cylindrical element of the fluid of length dZ and radius R, it can be shown that

$$\tau_W = \frac{D}{4}\frac{dP_F}{dZ} \quad (E.4)$$

where τ_W is the wall shear stress.

τ_W is also expressed in terms of the mean velocity of the flow "V" and the friction factor "f" as follows:

$$\tau_W = f\,\rho\,V^2/2g_c \quad (E.5)$$

Equations (E.4) and (E.5) are combined to yield the following expression for the frictional pressure drop over a length L of the tube "ΔP_F", thus

$$\Delta P_F = \frac{2L}{g_c D}\cdot\frac{G^2}{\rho}\cdot f \quad (E.6)$$

where $G = \rho V$ is the mass velocity.

Equations (E.4) and (E.6) are applicable to both laminar and turubulent flow; Eq. (E.6) can be applied to both single-and two-phase flow (depending on how f and G are

defined).

For laminar flow, Eq. (E.3) is solved for the velocity gradient at the wall which is related to the wall shear stress as follows:

$$\tau_W = \frac{\mu}{g_c}\left(\frac{dV_Z}{dr}\right)_{r=R} , \tag{E.7}$$

the friction factor in this case is given by:

$$f = 16/Re \tag{E.8}$$

For turbulent flow, Eq. (E.2) is not applicable unless other terms are introduced to take into account the fluctuating nature of the velocity component. A simpler approach has been taken where a total apparent shear stress is defined as follows:

$$\tau\left(\frac{g_c}{\rho}\right) = (\nu + \varepsilon_M)\left(\frac{\partial V_Z}{\partial Y}\right) \tag{E.9}$$

where ε_M is the eddy diffusivity for momentum.
The solution of this equation is obtained in the form:

$$V_Z^+ = f(Y^+) \tag{E.10}$$

where

$$V_Z^+ = V_Z/(g_c\ \tau_W/\rho)^{1/2} \tag{E.11}$$

and

$$Y^+ = Y(g_c\ \tau_W/\rho)^{1/2}/\nu \tag{E.12}$$

Many expressions have been developed for the velocity distribution, Eq. (E.10), depending on the assumptions made re-

garding ε_M; however, the equations for "f" obtained from these expressions are not easy to use for direct determination of f. The following simple expression, recommended by Kays [54] to be valid in the range $30,000 < Re < 10^6$, was used in the present study:

$$f = 0.046/Re^{0.2} \tag{E.13}$$

For the range $5000 < Re < 30,000$, the Blasius equation was employed; this is given by

$$f = 0.079/Re^{0.25} \tag{E.14}$$

E.1.2. Heat-Transfer Coefficients

(i) Laminar Flow

The general differential equation of the heat-transfer for a steady laminar flow, neglecting the energy terms arising from the normal and shear stresses and the body forces, is given by:

$$(\nabla \cdot \bar{V})T = \alpha_T \nabla^2 T \tag{E.15}$$

where $\alpha_T = K/\rho C_P$ is the thermal diffusivity. For the hydrodynamically fully developed axisymmetric flow in a circular tube where the axial conduction is negligible, Eq. (E.15) reduces to:

$$\frac{1}{r}\frac{\partial}{\partial r}\left(r\frac{\partial T}{\partial r}\right) = \frac{V_Z}{\alpha_T}\frac{\partial T}{\partial Z} \tag{E.16}$$

Equation (E.16) was solved numerically by Worsoe-

Schmidt [95] for the local Nusselt number in the thermal entry length; the solution was presented in form of tables listing the values of Nu_{SP} against the dimensionless distance $\bar{Z}$ defined by

$$\bar{Z} = 4(\frac{Z}{D})/Re\ Pr \qquad (E.17)$$

Equation (E.16) was also solved analytically by Seigel et al [75]; the solution was presented in the following form:

$$Nu_{SP} = [\frac{1}{Nu_\infty} - \frac{1}{2}\sum_{1}^{\infty} \frac{\exp(-\gamma_m^2\ \bar{Z}/2)}{A_m\ \gamma_m^4}]^{-1} \qquad (E.18)$$

where $Nu_{SP} \to Nu_\infty = 48/11$ as $Z \to \infty$,

A_m and γ_m are the eigenvalues, listed in Table E.1 below.

TABLE E.1

Values of A_m and γ_m in Eq. (E.18)

m	A_m	γ_m
1	7.630×10^{-3}	25.68
2	2.058×10^{-3}	83.86
3	0.901×10^{-3}	174.20
4	0.487×10^{-3}	296.50
5	0.297×10^{-3}	450.90
for larger m:	$\gamma_m = 4m + 4/3$; $A_m = 0.358\ \gamma_m^{-2.32}$	

The above two solutions [75, 95] were employed to test the present experimental data in Section 6.2.1 where good agree-

ment was obtained. The two solutions are compared in Table E.2 which shows that both solutions give almost identical results. In Table E.2, the values of $\bar{Z}$ and Nu_{SP} are expressed in terms of Z^+ and $Sq(Z^+)$ respectively, where

$$Z^+ = \frac{1}{4} \bar{Z} \, Pr \, Re^2 (f/2)^{1/2} \tag{E.19}$$

$$= \left(\frac{Z}{D}\right) Re \, (f/2)^{1/2} \tag{E.20}$$

and

$$Sq(Z^+) = Nu_{SP}/Re(f/2)^{1/2} \tag{E.21}$$

TABLE E.2

Comparison of the Solutions of Seigel et al and Worsoe-Schmidt

Z^+	Sq.	
	Worsoe-Schmidt [95]	Seigel et al [75]
175	0.2100	0.2098
351	0.1697	0.1696
702	0.1392	0.1390
3525	0.0789	0.0788
7051	0.0667	0.0666

(ii) Turbulent Flow

Because of the fluctuations in the velocity and temperature in turbulent flow, Eqs. (E.15) and (E.16) are not applicable here. An approach similar to that discussed for the momentum equation has been taken by Spalding [E.1] who derived the following differential equation for the heat-transfer in turbulent flow:

$$\frac{\partial T}{\partial Z^+} = \frac{1}{V_Z^+ \varepsilon_V^+} \frac{\partial}{\partial V_Z^+} \left(\frac{\varepsilon_H^+}{\varepsilon_V^+} \frac{\partial T}{\partial V_Z^+}\right) \tag{E.22}$$

where

$$\varepsilon_V^+ = 1 + \frac{K'}{e'}\left[e^{K'V_Z^+} - 1 - K'V_Z^+ - \frac{(K'V_Z^+)}{2!} - \frac{(K'V_Z^+)}{3!}\right] \tag{E.23}$$

$$K' = 0.407 \quad , \quad e' = 10.09 \ ,$$

$$\varepsilon_H^+ = 1/Pr + \varepsilon_V^+ - 1 \ , \tag{E.24}$$

$$V_Z^+ = V_Z/(\tau_W/\rho)^{1/2}$$

Equation (E.22) was originally solved by Smith and Shah [F.2] for the boundary condition of constant heat flux by using the numerical integration technique. The solution was later generalized by Spalding [81]; this was expressed in terms of Sq, Eq. (E.21), a function which is generally referred to as the Spalding function [E.3], as follows:

$$Sq(Z^+) = 0.651\ (Z^+/Pr)^{-1/3} \ , \ Z^+ \leq 100 \tag{E.25}$$

$$Sq(Z^+) = \frac{Pr}{Pr_T}\left[6.64(Z^+/Pr_T)^{1/9} + P_{FN}\right]^{-1} \ Z^+ \geq 10^4 \tag{E.26}$$

$Pr_T = 0.887$ = Turbulent Prandtl Number,

P_{FN} = P-Function

$$= 11.570\left[(Pr/Pr_T)^{3/4} - 1\right] \tag{E.27}$$

It should be noted that Eq. (E.25), which applies to laminar flow, corresponds to the equation originally derived by Lévêque [61].

Further, the following equation was proposed to be valid for all values of Z^+:

$$Sq(Z^+) = \{ \left[\frac{Pr/Pr_T}{6.64(Z^+/Pr_T^{1/9} + P_{FN}} \right]^4 + [0.651(Z^+/Pr)^{-1/3}]^4 \}^{1/4} \quad \text{(E.28)}$$

Though Eq. (E.26) is more accurate for large values of Z^+, Eq. (E.28) was employed to test the present experimental results as idscussed in Chapter 6 where excellent agreement was obtained.

E.2. Two-Phase Flow

E.2.1. Frictional Pressure Drop Correlations

The frictional pressure drop correlations employed in Chapter 5 to test the present pressure drop data are discussed in this section.

Although many correlations exist for predicting the two-phase frictional pressure drop, only the three methods recommended in [5] were used to test the present data; these were:

(i) The Homogeneous Flow Model [5]

(ii) The Lockhart-Martinelli Correlations [62,5]

(iii) The Chisholm Correlation [5,18]

In the following, the three methods are described and the calculation procedure for each is given.

(i) The Homogeneous Flow Model [5,92]

In this model, the two-phase mixture is treated as a single fluid with suitably averaged properties to represent

the mixture; the single-phase flow equations are then applied to the mixture. The two-phase frictional pressure drop is therefore given by:

$$\Delta P_{TPF} = \frac{2L}{g_c D} \frac{G_{MIX}^2}{\rho_{MIX}} f_{TP} \qquad (E.29)$$

where

$$G_{MIX} = (\dot{m}_L + \dot{m}_G)/A_T = G_{SL} + G_{SG} \qquad (E.30)$$

$$f_{TP} = f(Re_{MIX}) ,$$

is the two-phase friction factor,

$$Re_{MIX} = G_{MIX} D/\mu_{MIX} , \qquad (E.31)$$

ρ_{MIX} and μ_{MIX} are the density and viscosity of the mixture. The following expressions were recommended [90] for ρ_{MIX} and μ_{MIX}:

$$\frac{1}{\rho_{MIX}} = \frac{x}{\rho_G} + \frac{(1 - x)}{\rho_L} \qquad (E.32)$$

and

$$\mu_{MIX} = \mu_L \qquad (E.33)$$

where X is the flow quality.

The calculation procedure was as follows:

(a) From the known fluid properties and the measured mass flow rates, G_{MIX}, ρ_{MIX} and μ_{MIX} were calculated from Eqs. (E.30), (E.32) and (E.33) respectively.

(b) Re_{MIX} was calculated from Eq. (E.31) and depending on its value (i.e., whether the flow is laminar or

turbulent) the two-phase friction factor "f_{TP}" was obtained from Eqs. (E.8), (E.13) or (E.14).

(c) Finally, ΔP_{TPF} was calculated from Eq. (E.29) and was then compared with the experimental value.

(ii) The Lockhart-Martinelli Correlation [5, 62, 92]

The correlation proposed by Lockhart-Martinelli is based on the separated flow model in which the two phases are assumed to flow separately with differing velocities and properties. A detailed treatment of this subject is given by Wallis [92].

The following dimensionless parameters, generally referred to as the Martinelli parameters, were used in presenting this correlation:

$$\phi_L^2 = \Delta P_{TPF} / (\Delta P_{SPF})_L \ , \qquad (E.34)$$

$$\phi_G^2 = \Delta P_{TPF} / (\Delta P_{SPF})_G \qquad (E.35)$$

and

$$X^2 = \phi_G^2 / \phi_L^2 = (\Delta P_{SPF})_L / (\Delta P_{SPF})_G \qquad (E.36)$$

where

$(\Delta P_{SPF})_L$ is the single-phase liquid frictional pressure drop when the liquid flows alone at the same flow rate,

$(\Delta P_{SPF})_G$ is the single-phase gas frictional pressure drop when the gas flows alone at the same flow rate.

The correlation was presented in graphical forms where curves were plotted for ϕ_L^2 and ϕ_G^2 against X^2 for the possible four combinations given in Table E.3 below.

TABLE E.3

Combinations of Flow Regimes

Type of Flow / Reynolds Number	Laminar*-Laminar	Laminar-Turbulent	Turbulent-Laminar	Turbulent-Turbulent
Re_{SL}	<1000	<1000	>2000	>2000
Re_{SG}	<1000	>2000	<1000	>2000

* The flow conditions are given for the liquid phase first, then for the gas phase.

It should be noted that the authors did not define the type of flow for the range 1000 < Re < 2000. In the present study, however, laminar flow was assumed to exist for Re_{SL}, $Re_{SG} < 2000$.

Hewitt et al. [45] fitted polynomial equations to the four correlations, these are given in Table E.4 and were used in the calculation of the frictional pressure drop as follows:

(a) Knowing the mass flow rates, fluids properties and the tube diameter, Re_{SL} and Re_{SG} were evaluated.

(b) Depending on the values of Re_{SL} and Re_{SG}, f_{SP} values were calculated from Eqs. (E.8), (E.13) or (E.14) and then $(\Delta P_{SPF})_L$ and $(\Delta P_{SPF})_G$ were obtained from Eq. (E.29); and X^2 was calculated from Eq. (E.36).

(c) Depending on the type of flow, ϕ_G^2 was obtained from the equations given in Table E.3.

(d) ΔP_{TPF} was then calculated from Eq. (E.35), and was compared with the experimental value as given in Chapter 6.

(iii) The Chisholm Correlation [5,18]

This correlation was originally developed [18] for two-phase, single-component evaporating flows; it was then modified and extended to two-phase, two-component flows [5].

In this method, ΔP_{TPF} is assumed to be given by:

$$\Delta P_{TPF} = \frac{2L}{g_c D} \frac{G_{MIX}^2}{\rho_L} \phi_{LO}^2 f_{LO} \qquad (E.37)$$

$$= \phi_{LO}^2 (\Delta P_{SPF})_{LO} \qquad (E.38)$$

where

$$\phi_{LO}^2 = 1 + (\Gamma^2 - 1) x^{(2-n)/2} [B(1-x)^{(2-n)/2} + x^{(2-n)/2}], \qquad (E.39)$$

$$\Gamma^2 = (\Delta P_{SPF})_{GO} / (\Delta P_{SPF})_{LO} , \qquad (E.40)$$

$(\Delta P_{SPF})_{LO}$ is the single-phase liquid frictional pressure drop if the liquid were flowing alone with the total mass flow rate of the mixture,

$(\Delta P_{SPF})_{GO}$ is the single-phase gas frictional pressure drop defined similarly as above,

$$n = \log_{10}(\Gamma^2 \rho_G / \rho_L) / \log_{10}(\mu_G / \mu_L) \qquad (E.41)$$

n above is the Blasius exponent obtained on the basis of a turbulent-turbulent flow, i.e., the correlation is applicable

TABLE E.4

Lockhart-Martinelli Correlation: Coefficients of Fitted Polynomial Equations

Equations	Cofficients
$\underline{(\phi_G)_{LL}}$ $Ln(\phi_G)_{LL} = \sum_{n=0}^{5} e_n (Ln\ X)^n$	$e_0 = 9.7950655 \times 10^{-1}$ $e_1 = 5.6919828 \times 10^{-1}$ $e_2 = 9.5809158 \times 10^{-2}$ $e_3 = 5.2155316 \times 10^{-3}$ $e_4 = 1.4334631 \times 10^{-3}$ $e_5 = 1.0692395 \times 10^{-4}$
$\underline{(\phi_G)_{LT}}$ $Ln(\phi_G)_{LT} = \sum_{n=0}^{5} C_n (Ln\ X)^n$	$c_0 = 1.2386656$ $c_1 = 5.3137894 \times 10^{-1}$ $c_2 = 7.1746540 \times 10^{-2}$ $c_3 = -4.3863795 \times 10^{-3}$ $c_4 = -6.9122899 \times 10^{-4}$ $c_5 = 1.1996845 \times 10^{-4}$
$\underline{(\phi_G)_{TL}}$ $Ln(\phi_G)_{TL} = \sum_{n=0}^{5} d_n (Ln\ X)^n$	$d_0 = 1.2502036$ $d_1 = 5.5586231 \times 10^{-1}$ $d_2 = 6.6838261 \times 10^{-2}$ $d_3 = -5.1185552 \times 10^{-3}$ $d_4 = -5.7824134 \times 10^{-4}$ $d_5 = 1.1641920 \times 10^{-4}$
$\underline{(\phi_G)_{TT}}$ $Ln(\phi_G)_{TT} = \sum_{n=0}^{5} b_n (Ln\ X)^n$	$b_0 = 1.4450574$ $b_1 = 4.0572147 \times 10^{-1}$ $b_2 = 5.7617506 \times 10^{-2}$ $b_3 = -1.1699323 \times 10^{-3}$ $b_4 = -4.2882670 \times 10^{-4}$ $b_5 = 3.1502187 \times 10^{-5}$

only for this type of flow. The constant B in Eq. (E.30) is an empirical coefficient which is a function of Γ and G_{MIX} as shown in Table E.5 below.

TABLE E.5

The values of "B" in Eq. (E.39)

Γ	G_{MIX} (lbm/ft^2 hr)	B
≤ 9.5	$\leq 9.59 \times 10^4$	4.8
	$> 9.59 \times 10^4$	$1493.48\ G_{MIX}^{0.5}$
$9.5 < \Gamma < 28$	$\leq 4.42 \times 10^5$	$1.412 \times 10^4/\Gamma\ G_{MIX}^{0.5}$
	$> 4.42 \times 10^5$	
≥ 28	Any value	$r.073 \times 10^5/\Gamma^2 G_{MIX}^{0.5}$

ΔP_{TPF} was calculated as follows:

(a) Knowing D, the mass flow rates and fluid properties, G_{MIX}, X, Re_{LO} and Re_{GO} were calculated, where

$$Re_{LO} = G_{MIX}\ D/\mu_L \qquad (E.42)$$

and

$$Re_{GO} = G_{MIX}\ D/\mu_G \qquad (E.43)$$

(b) From the values of Re_{LO} and Re_{GO}, f_{LO}, f_{GO}, $(\Delta P_{SPF})_{LO}$ and $(\Delta P_{SPF})_{GO}$ were obtained from the single-phase flow equations (Section E.1.1).

(c) Eqs. (E.40), (E.41) and Table E.5 were then used to calculate Γ, n and B.

(d) ϕ^2_{LO} was then calculated from Eq. (E.39) and ΔP_{TPF} obtained from Eq. (E.37).

E.2.2. Two-Phase Heat-Transfer Correlations

(i) Local Heat-Transfer Coefficients

As discussed in Chapter 6, the local heat-transfer data were correlated by the modified theory of Spalding [81] which was first employed by [90]. In this model, the two-phase mixture is treated as a homogeneous mixture, the single-phase heat-transfer theory developed by Spalding is then applied for predicting the local heat-transfer coefficients. A knowledge of the mixture properties is, therefore, required. In reference [90], five different combinations for the mixture properties were tested (these are given in Table E.6) and the best agreement between the theory and the data of [90] was obtained when the liquid properties were used for the mixture. This result was based on testing two-phase data for a wide range of liquid Prandtl number.

In the present study, the same combinations of the mixture properties used in [90] were tested for the whole range of gas density studied and the same conclusion was obtained; that is, the use of liquid properties for the mixture offered the best agreement between the experimental data and the theory. However, additional combinations for the mixture properties were tested in the present study and

TABLE E.6

Combinations of the Mixture Properties Tested in [90]

Group No.	ρ_{MIX}	μ_{MIX}	C_{PMIX}	k_{MIX}	Comments
1	ρ_L	μ_L	C_{PL}	k_L	Provided the best agreement
2	$[\frac{x}{\rho_G} + \frac{(1 - x)}{\rho_L}]^{-1}$	μ_L	C_{PL}	k_L	Typically, more than 50% of the data points were in the range of deviations > $\pm$50%. $\bar{e}'$ was between 200 and 630%
3	$[\frac{x}{\rho_G} + \frac{(1 - x)}{\rho_L}]^{-1}$	μ_L	$x\, C_{PG} + (1 - x)C_{PL}$	k_L	
4	$(1 - \alpha)\rho_L + \alpha\rho_G$	μ_L	C_{PL}	k_L	
5	$(1 - \alpha)\rho_L + \alpha\rho_G$	μ_L	$x\, C_{PG} + (1 - x)C_{PL}$	k_L	

and the degree of agreement between the data and the theory obtained with these combinations was, in some cases, similar or slightly better than that obtained when only liquid properties were used. The results of this exercise are summarized in Table E.7 for air-water data. Similar results, however, were obtained for helium-water and Freon-water data. The mixture properties were those of the liquid or were calculated from either of the expressions listed below as indicated in Table E.7.

$$P_{MIX} = x\, P_G + (1 - x) P_L \qquad (E.44)$$

or

$$P_{MIX} = \alpha\, P_G + (1 - \alpha) P_L \qquad (E.45)$$

where P stands for property (ρ, μ, k and C_p).

Table E.7 shows that the second, fourth and fifth groups of mixture properties give slightly better agreements than that of the first group (all liquid properties). However, the excellent agreement obtained when only liquid properties were used, with the considerations of the simplicity and convenience of using only liquid properties and the conclusions of [90] with regard to this subject, suggest that the use of only liquid properties for the mixture is most acceptable to correlate the present data in terms of the modified Spalding theory. This, however, is not applicable to data in the mist or annular-mist flows as the deviations obtained under these conditions were generally higher than ±50%. Further study of the mixture properties especially at

high void fractions is required for possible improvements.

In comparing the data with Eq. (E.25) the value of the turbulent Prandtl number was required. For single-phase heat-transfer, different values of Pr_T have been used by different investigators [E.3, 81]; however, the significance and value of Pr_T for two-phase flow have not been investigated. In the present study, the value of 0.887 recommended by Spalding [81] for single-phase flow was used for the analysis of the two-phase heat-transfer data. However, the data were also analyzed taking $Pr_T = 1$ [F.3] and the results were compared with those obtained with $Pr_T = 0.887$. The results of the comparison are shown in Table E.8, illustrating that the agreement between the data and the theory was slightly better when Pr_T was set equal to 0.887. This value of Pr_T should not be considered as the recommended value; further study of this problem is, of course, required.

It is important here to stress again on the range of applicability of the modified Spalding theory in the form proposed here. The theory is applicable to all flow patterns with the exception of mist and annular-mist flow regimes, However, the data of [90] for which the local values of the heat-transfer coefficients increase with distance along the test section are excluded; these are data obtained in the bubble and slug flows at low liquid flow rates. A criterion to define the conditions under which such data are obtained is not available at the moment; the development of such a criterion, however, is in progress at the University of

TABLE E.7

Comparison of Air-Water Local Heat-Transfer Data Against Eq. (E.25) for Different Combinations of Mixture Properties

Mixture Properties	Number of Data Points (% of Total N) Lying in the Specified Range of Deviations						
	±20%	±30%	±40%	±50%	>±50%	$\bar{e}$ (%)	$\bar{e}'$ (%)
(1) All liquid properties	58.9	79.1	93.4	99.5	0.5	-15.48	22.23
(2) μ_L, C_{PL}, k_L ρ from Eq. (E.44)	58.3	80.5	95.4	100	-	-14.88	22.02
(3) C_{PL}, k_L ρ and μ from Eq. (E.44)	58.6	79.1	93.4	99.5	0.5	-15.58	22.26
(4) ρ_L, μ_L C_p & k from Eq. (E.44)	57.6	80.5	95.73	100	-	-14.33	21.92
(5) All from Eq. (E.44)	57.6	80.8	95.7	100		-14.40	21.90
(6) C_{PL}, k_L ρ and μ from Eq. (E.45)	58.9	84.1	97.7	98.5	1.5	-12.40	21.85

Data points do not include those in the mist-annular flow

Manitoba. For the present purpose, the conditions under which these data were obtained is summarized in Table E.9 below.

TABLE E.8

Results of Correlation of Local Heat-Transfer Data by Eq. (E.25) for Different Values of Pr_T

Range of Deviations	Number of Data Points (% of Total N) Lying in the Specified Range of Deviations		Remarks
	$Pr_T = 0.887$	$Pr_T = 1$	
±20	68.13	69.12	Number of data points considered = 1211 points. This does not include mist and annular-mist flow data.
±30	86.29	83.51	
±40	96.70	94.61	
±50	99.75	98.20	
$\bar{e}$	-10.14	-12.43	
$\bar{e}'$	19.29	21.15	

TABLE E.9

Range of Data Not Included in the Correlation of Local Heat-Transfer Coefficients

Gas-Liquid Mixture	Re_{SL}	Range of Re_{SG}
Air-Water	263	$1000 - 1.53 \times 10^5$
	760	$118 - 9.19 \times 10^4$
	1460	$730 - 7.45 \times 10^4$
Air-Glycerine + Water	8.2	$1200 - 1.14 \times 10^5$

References for Appendix E

E.1. Spalding, D.B., Heat-Transfer to a Turbulent Stream from a Surface with a Step-Wise Discontinuity in Wall Temperature, Intl. Develop. in Heat Trans., ASME, Boulder, Colorado, U.S.A., Part II, pp. 439-446, 1961.

E.2. Smith, A.G. and Shah, V.L., The Calculation of Wall and Fluid Temperatures for the Incompressible Turbulent Boundary Layer with Arbitrary Distribution of Wall Heat Flux, Int. J. Heat Mass Transfer 5, 1179-1189, 1962.

E.3. Kestin, J. and Persen, L.N., Application of Schmidt's Method to the Calculation of Spalding's Function and of the Skin-Friction Coefficient in Turbulent Flow, Int. J. Heat Mass Transfer 5, 143-152, 1962.

APPENDIX F

EFFECT OF MIXER CONDITIONS ON FLOW PATTERNS AND HEAT TRANSFER

As mentioned in Chapter 4, the conditions in the mixer before starting the apparatus (whether wet or dry) have some effect on the flow patterns and heat transfer. These effects were investigated in the present study; the results are summarized in this appendix. Experimental heat-transfer and flow pattern data were obtained with the mixer initially soaked in water and were compared with data obtained with the mixer initially dry (the data reported in the thesis were all obtained under dry-mixer conditions). The experiments covered four water flow rates (V_{SL} = 1.03, 3.41, 13.89 and 34.7 ft/sec) and all possible air flow rates. Only the results for the lowest water flow rate, however, are shown in Fig. F.1 as no significant effect was observed for the higher water flow rates. The data points shown in the figure are those obtained with the mixer initially wet while the solid curve is for data with initially dry mixer for the same V_{SL}.

It is clear from the figure that, for this water flow rate (V_{SL} = 1.03 ft/sec), the mixer conditions have a significant effect on $\bar{h}_{TP}$ for superficial gas velocities below about 9 ft/sec, the shape of the $\bar{h}_{TP}$~V_{SG} profile dramatically

changes according to the initial wet or dry condition of the mixer. However, at higher values of V_{SG} no such effect is observed. In fact, the changes in the shape of the $\bar{h}_{TP}$~V_{SG} curve is a reflection of the flow patterns; while slug flow was observed for the "dry-mixer" curve up to V_{SG} = 10 ft/sec, bubble and bubble-slug flows were observed under the "wet mixer" condition. It should be noted that the shape of the curve for wet mixer results is similar to those reported by Verschoor and Stemerding [89] and Kudirka [58]. At higher values of V_{SL} (not shown in the figure) no effect was observed for all values of V_{SG}.

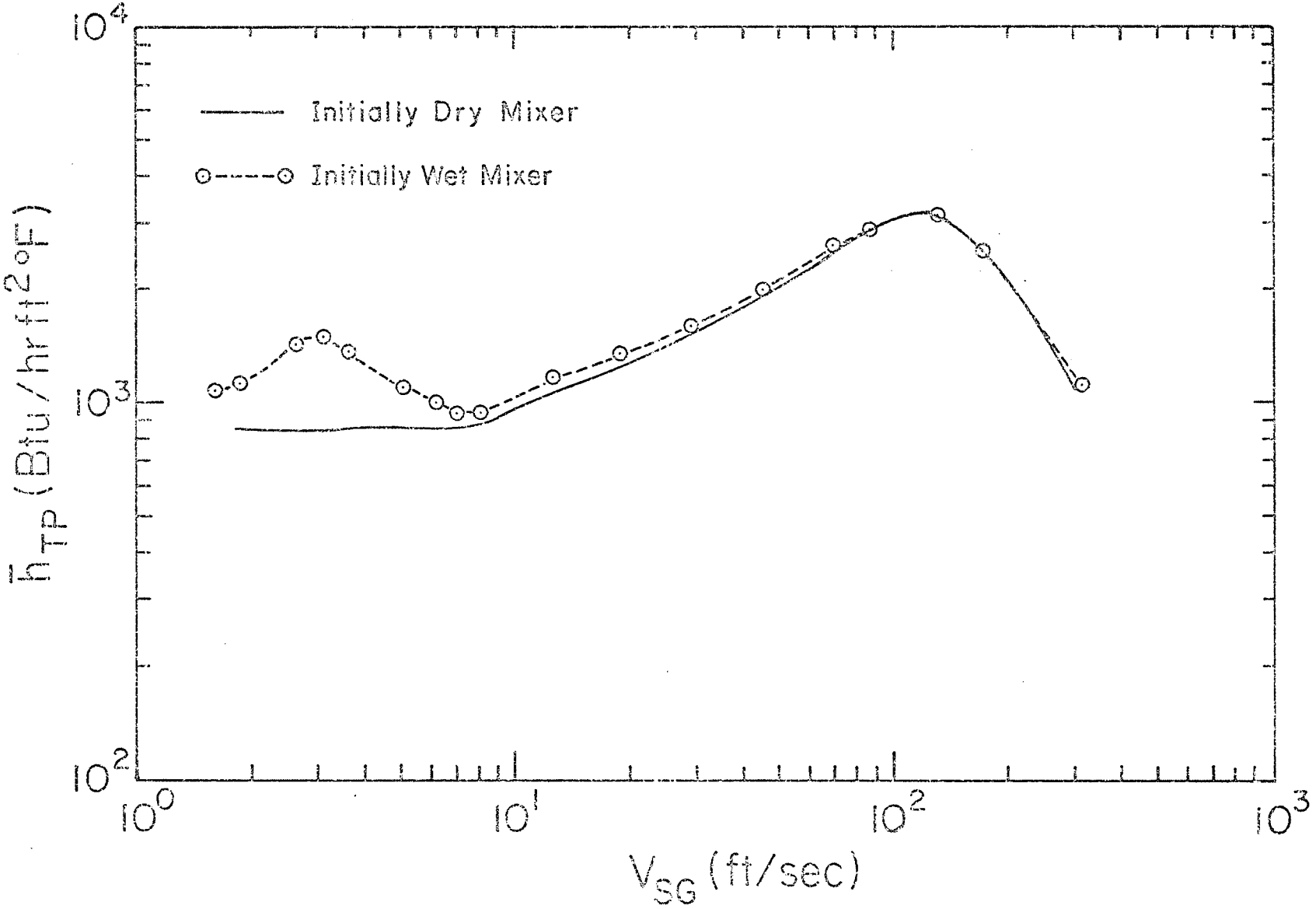

Fig. F.1 Effect of Mixer Condition on $\bar{h}_{TP}$

APPENDIX G

ERROR ANALYSIS AND REPEATABILITY

G.1 Error Analysis

The accuracy of the measured quantities and of the calculated results was estimated according to the method of Kline and McClintok [G.1] The authors [G.1] conclude that, where a "result" R is a function of variables $V_1, V_2, \ldots V_n$ and the "uncertainty interval* "w_i in any variable V_i is known, or estimated, based on certain "odds", then the uncertainty interval W_R in the results should be obtained from

$$W_R = \left[\left(\frac{\partial R}{\partial V_1} W_1\right)^2 + \left(\frac{\partial R}{\partial V_2} W_2\right)^2 + \cdots + \left(\frac{\partial R}{\partial V_n} W_n\right)^2\right]^{1/2} \qquad (G.1)$$

or

$$\frac{W_R}{R} = \left\{\left[W_1 \frac{\partial}{\partial V_1}(\ln R)\right]^2 + \left[W_2 \frac{\partial}{\partial V_2}(\ln R)\right]^2 + \cdots + \left[W_n \frac{\partial}{\partial V_n}(\ln R)\right]^2\right\}^{1/2} \qquad (G.2)$$

The "odds" mentioned above are the odds that the experimenter is willing to wager that any given reading lies with $\pm W_i$ of the true value. The estimated errors in the main measured variables and the calculated results are summarized in Table G.1.

---

* In the terminology of [G.1], "uncertainty" is the possible value the "error" might have; the "error" is the difference between the true and observed value for a single observation. In the present appendix, however, as is common usage, the term "error" is used synonymously with "uncertainty."

G.2 Repeatability of the Results

Although the present air-water results repeated the earlier [90] results obtained from the same experimental facility (with a maximum deviation of 9.3% and rms deviation of 5.3%), a total of 62 tests (44, 10 and 8 with air-water, helium-water and Freon-water respectively) were repeated during the experimental program and 11 air-water tests at the end of the experimental program. The degree of repeatability was in general satisfactory as the maximum deviation obtained (at the lowest water flow rate studied) was 8.3% and the rms deviation, 5.4%.

TABLE G.1

Summary of Estimated Errors in the

Main Measured Variables and Results

Variable	Error (±)
Current I	1.4%
Wall thickness of the tube, t	5.0% [90]
Outer Wall temperature	0.2°F
Inlet temperature T_{IN}	1.2°F
Bulk temperature T_B	1.8° F
Inside Wall temperature T_W	0.3°F
Heat Flux	1-5.7%
Heat-transfer coefficients	4-16%
m_L	5.7%
m_G	7-9%
V_{SL}	4-7%
V_{SG}	7-9%
ΔP	0.15-0.5%
ΔP_{TPF}	1-19%

APPENDIX H

TABULATED DATA

This appendix reports the two-phase experimental data. The air-water data are given in Table H.1, the helium-water data in Table H.2 and the Freon-water data in Table H.3. The data for each gas-water mixture are given in the order of increasing gas flow rate for each water mass flow rate. For each test the data are tabulated in the following order:

- The first two lines give the average values of the following quantities:

ML=	water mass flow rate	lb/hr
MG=	gas mass flow rate	lb/hr
QFLUX=	average heat flux	Btu/hr ft^2
NUTP=	average Nusselt number	
HTP=	average two-phase heat-transfer coefficient	Btu/hr ft^2F
PDT=	total pressure drop	$lb_f/in.^2$
PDF=	frictional pressure drop	$lb_f/in.^2$
ALFA=	void fraction	
XTT=	Martinelli parameter	
WE=	Weber number	
FR=	Froude number	

- The next three lines give respectively the inlet, outlet and mean values of the foll0wing quantities:

TMIX=	mixture temperature	F
RESL=	superficial liquid Reynolds number	
RESG=	superficial gas Reynolds number	
P=	pressure	$lb_f/in.^2$

PRL= liquid Prandtl number

PRG= gas Prandtl number

VSL= superficial liquid velocity ft/sec

VSG= superficial gas velocity ft/sec

- Then, the local values of the quantities listed below are given at seven locations (Z in.) along the test section.

RESL= superficial liquid Reynolds number

VSG= superficial gas velocity ft/sec

TBULK= bulk temperature of the mixture F

(T_W-T_B)= temperature difference between wall and bulk F

NUTP= two-phase Nusselt number

HTP= two-phase heat-transfer coefficient Btu/hr ft^2F

It should be noted that in calculating the value of V_{SL} at the inlet to the test section, the water density was assumed to be the same for all experiments and equal to 62.3 lbm/ft^3. The local values of V_{SL}, however, were calculated using density values evaluated from the equation given in Appendix C. This resulted, for those cases where the outlet temperatures of the mixture were lower than the temperature corresponding to a density of 62.3 lbs/ft^3, in an outlet V_{SL} slightly lower than the inlet value as can be seen in Tests A7.1 to A7.11 and H4.1 to H4.9.

Table H.1 Air-Water Data

TEST NO.: A1. 1 FLOW PATTERN:SLUG

ML= 267 MG= 0.61 QFLUX= 11876 NUTP= 82.9 HTP= 760 PDT= 0.427

PDF= 0.013 ALFA=0.513 XTT= 12.60 WE= 16.1 FR= 0.87

	TMIX	RESL	RESG	P	PRL	PRG	VSL	VSG
INLET	72.41	3890	458.3	16.1	6.50	0.710	1.03	1.79
OUTLET	83.10	4436	451.3	15.7	5.67	0.708	1.03	1.87
MEAN	77.76	4163	454.8	15.9	6.08	0.709	1.03	1.83

Z	RESL	VSG	TBULK	(TW-TB)	NUTP	HTP
2.0	3935	1.80	73.30	15.18	85.5	779.0
4.5	3990	1.81	74.41	15.56	83.4	761.0
7.5	4058	1.82	75.74	15.61	83.1	759.0
11.0	4137	1.83	77.30	15.62	82.9	759.0
16.5	4262	1.85	79.76	15.63	82.7	760.0
21.0	4366	1.87	81.77	15.78	81.8	754.0
22.5	4401	1.87	82.44	15.61	82.6	762.0

TEST NO.: A1. 2 FLOW PATTERN:SLUG

ML= 267 MG= 0.91 QFLUX= 12002 NUTP= 85.2 HTP= 781 PDT= 0.365

PDF= 0.007 ALFA=0.580 XTT= 8.75 WE= 16.1 FR= 0.87

	TMIX	RESL	RESG	P	PRL	PRG	VSL	VSG
INLET	72.31	3885	685.7	16.0	6.51	0.710	1.03	2.70
OUTLET	83.11	4436	675.1	15.7	5.67	0.708	1.03	2.81
MEAN	77.71	4161	680.4	15.9	6.08	0.709	1.03	2.76

Z	RESL	VSG	TBULK	(TW-TB)	NUTP	HTP
2.0	3930	2.71	73.20	14.93	87.9	801.0
4.5	3986	2.72	74.33	15.13	86.7	791.0
7.5	4054	2.73	75.67	15.42	85.0	777.0
11.0	4134	2.75	77.25	15.29	85.6	784.0
16.5	4261	2.78	79.73	15.53	84.1	773.0
21.0	4366	2.80	81.76	15.53	84.0	774.0
22.5	4401	2.81	82.43	15.31	85.2	786.0

TEST NO.: A1. 3 FLOW PATTERN:SLUG

ML= 267 MG= 1.38 QFLUX= 12129 NUTP= 87.0 HTP= 798 PDT= 0.316

PDF= 0.011 ALFA=0.642 XTT= 6.00 WE= 16.1 FR= 0.87

	TMIX	RESL	RESG	P	PRL	PRG	VSL	VSG
INLET	72.24	3882	1037.0	15.9	6.52	0.710	1.03	4.13
OUTLET	83.15	4438	1021.6	15.6	5.67	0.708	1.03	4.29
MEAN	77.69	4160	1029.7	15.7	6.09	0.709	1.03	4.21

Z	RESL	VSG	TBULK	(TW-TB)	NUTP	HTP
2.0	3927	4.14	73.14	15.43	86.0	783.0
4.5	3984	4.16	74.28	15.38	86.2	786.0
7.5	4053	4.18	75.64	15.34	86.4	789.0
11.0	4133	4.20	77.23	15.15	87.3	800.0
16.5	4261	4.24	79.74	15.25	86.6	796.0
21.0	4367	4.27	81.79	14.97	88.1	812.0
22.5	4403	4.28	82.47	14.49	90.9	838.0

TEST NO.: A1. 4 FLOW PATTERN:SLUG

ML= 267 MG= 1.80 QFLUX= 12767 NUTP= 91.0 HTP= 835 PDT= 0.301

PDF= 0.027 ALFA=0.679 XTT= 4.69 WE= 16.1 FR= 0.87

	TMIX	RESL	RESG	P	PRL	PRG	VSL	VSG
INLET	73.09	3924	1349.0	15.7	6.44	0.710	1.03	5.45
OUTLET	84.57	4513	1327.5	15.4	5.57	0.708	1.03	5.67
MEAN	78.83	4218	1338.6	15.5	5.99	0.709	1.03	5.56

Z	RESL	VSG	TBULK	(TW-TB)	NUTP	HTP
2.0	3972	5.47	74.04	15.14	92.1	840.0
4.5	4032	5.49	75.23	15.28	91.2	833.0
7.5	4105	5.52	76.67	15.27	91.2	835.0
11.0	4190	5.56	78.34	15.56	89.4	820.0
16.5	4325	5.61	80.98	15.39	90.2	830.0
21.0	4438	5.65	83.14	15.04	92.1	850.0
22.5	4475	5.66	83.86	14.14	97.9	905.0

TEST NO.: A1. 5 FLOW PATTERN:SLUG

ML= 267 MG= 2.58 QFLUX= 12794 NUTP= 95.4 HTP= 876 PDT= 0.315

PDF= 0.079 ALFA=0.723 XTT= 3.38 WE= 16.1 FR= 0.87

	TMIX	RESL	RESG	P	PRL	PRG	VSL	VSG
INLET	73.22	3930	1934.0	15.6	6.43	0.709	1.03	7.86
OUTLET	84.71	4520	1902.8	15.3	5.56	0.708	1.03	8.19
MEAN	78.96	4225	1918.7	15.4	5.98	0.709	1.03	8.03

Z	RESL	VSG	TBULK	(TW-TB)	NUTP	HTP
2.0	3978	7.89	74.17	13.81	101.2	923.0
4.5	4039	7.93	75.37	14.39	97.0	886.0
7.5	4111	7.97	76.80	14.51	96.1	880.0
11.0	4197	8.02	78.48	14.71	94.7	869.0
16.5	4333	8.09	81.12	14.95	93.0	857.0
21.0	4445	8.16	83.28	14.66	94.7	874.0
22.5	4483	8.18	84.00	14.01	99.0	915.0

TEST NO.: A1. 6 FLOW PATTERN:ANNULAR

ML= 267 MG= 9.52 QFLUX= 21741 NUTP=170.9 HTP=1577 PDT= 0.443

PDF= 0.307 ALFA=0.840 XTT= 1.05 WE= 16.2 FR= 0.87

	TMIX	RESL	RESG	P	PRL	PRG	VSL	VSG
INLET	72.13	3876	7161.0	16.1	6.50	0.710	1.03	28.09
OUTLET	91.55	4884	6965.6	15.6	5.11	0.707	1.03	29.88
MEAN	81.84	4380	7063.4	15.9	5.77	0.708	1.03	29.01

Z	RESL	VSG	TBULK	(TW-TB)	NUTP	HTP
2.0	3957	28.24	73.74	13.86	171.0	1560.0
4.5	4058	28.43	75.76	14.14	167.4	1531.0
7.5	4182	28.66	78.18	13.97	169.3	1553.0
11.0	4327	28.92	81.01	13.90	169.7	1563.0
16.5	4560	29.35	85.47	13.61	172.8	1600.0
21.0	4754	29.70	89.12	13.54	173.2	1612.0
22.5	4819	29.82	90.34	13.24	176.9	1649.0

TEST NO.: A1. 7 FLOW PATTERN:ANNULAR

ML= 267 MG= 14.85 QFLUX= 23824 NUTP=213.2 HTP=1970 PDI= 0.552

PDF= 0.439 ALFA=0.869 XTT= 0.71 WE= 16.2 FR= 0.87

	TMIX	RESL	RESG	P	PRL	PRG	VSL	VSG
INLET	72.36	3888	11166.0	16.3	6.47	0.710	1.03	43.31
OUTLET	93.54	4992	10835.2	15.7	4.99	0.707	1.03	46.51
MEAN	82.95	4440	11000.8	16.0	5.69	0.708	1.03	44.95

Z	RESL	VSG	TBULK	(TW-TB)	NUTP	HTP
2.0	3976	43.58	74.12	12.53	207.2	1891.0
4.5	4087	43.91	76.32	12.73	203.7	1865.0
7.5	4222	44.32	78.96	12.51	206.8	1899.0
11.0	4381	44.79	82.05	12.33	209.4	1931.0
16.5	4636	45.55	86.91	11.78	218.4	2027.0
21.0	4849	46.19	90.89	11.40	224.8	2098.0
22.5	4921	46.40	92.22	11.21	228.4	2136.0

TEST NO.: A1. 8 FLOW PATTERN:ANNULAR

ML= 267 MG= 23.76 QFLUX= 27147 NUTP=282.0 HTP=2610 PDI= 0.840

PDF= 0.749 ALFA=0.894 XTT= 0.47 WE= 16.3 FR= 0.87

	TMIX	RESL	RESG	P	PRL	PRG	VSL	VSG
INLET	71.97	3868	17874.0	16.9	6.49	0.710	1.03	66.62
OUTLET	95.91	5122	17277.1	16.1	4.85	0.707	1.03	73.05
MEAN	83.94	4495	17575.6	16.5	5.63	0.708	1.03	69.90

Z	RESL	VSG	TBULK	(TW-TB)	NUTP	HTP
2.0	3968	67.15	73.96	10.68	276.9	2527.0
4.5	4093	67.82	76.44	11.16	264.5	2422.0
7.5	4245	68.62	79.42	10.87	270.8	2489.0
11.0	4426	69.58	82.91	10.64	276.1	2549.0
16.5	4716	71.11	88.41	10.07	290.5	2702.0
21.0	4958	72.40	92.92	9.68	301.1	2818.0
22.5	5040	72.83	94.42	9.51	306.2	2871.0

TEST NO.: A1. 9 FLOW PATTERN:ANNULAR

ML= 267 MG= 30.31 QFLUX= 28299 NUTP=311.2 HTP=2880 PDI= 1.049

PDF= 0.968 ALFA=0.905 XTT= 0.38 WE= 16.3 FR= 0.87

	TMIX	RESL	RESG	P	PRL	PRG	VSL	VSG
INLET	71.70	3855	22810.0	17.4	6.51	0.710	1.03	82.48
OUTLET	96.51	5155	22021.9	16.4	4.81	0.707	1.04	91.56
MEAN	84.11	4505	22416.4	16.9	5.62	0.708	1.03	87.10

Z	RESL	VSG	TBULK	(TW-TB)	NUTP	HTP
2.0	3957	83.22	73.76	10.09	305.4	2786.0
4.5	4087	84.15	76.33	10.43	294.9	2699.0
7.5	4245	85.29	79.42	10.25	299.6	2754.0
11.0	4432	86.64	83.04	10.09	303.4	2802.0
16.5	4733	88.81	88.74	9.55	319.1	2970.0
21.0	4985	90.63	93.41	9.14	332.1	3110.0
22.5	5070	91.25	94.97	8.91	340.6	3196.0

TEST NO.: A1.10 FLOW PATTERN:ANNULAR-MIST

ML= 267 MG= 49.43 QFLUX= 28287 NUTP=344.0 HTP=3185 PDT= 1.278

PDF= 1.213 ALFA=0.924 XTT= 0.25 WE= 16.3 FR= 0.87

	TMIX	RESL	RESG	P	PRL	PRG	VSL	VSG
INLET	72.25	3882	37173.0	18.8	6.47	0.710	1.03	124.64
OUTLET	96.64	5162	35909.6	17.5	4.81	0.707	1.04	139.35
MEAN	84.45	4522	36541.3	18.2	5.59	0.708	1.03	132.11

Z	RESL	VSG	TBULK	(TW-TB)	NUTP	HTP
2.0	3983	125.83	74.27	8.38	367.3	3352.0
4.5	4111	127.33	76.80	9.02	340.8	3121.0
7.5	4267	129.16	79.84	9.10	337.0	3099.0
11.0	4451	131.34	83.39	9.22	331.7	3065.0
16.5	4747	134.87	89.00	8.84	344.8	3210.0
21.0	4995	137.84	93.59	8.52	356.3	3338.0
22.5	5079	138.85	95.13	8.25	367.7	3451.0

TEST NO.: A1.11 FLOW PATTERN:ANNULAR-MIST

ML= 267 MG= 72.81 QFLUX= 28311 NUTP=275.2 HTP=2543 PDT= 1.554

PDF= 1.498 ALFA=0.936 XTT= 0.19 WE= 16.3 FR= 0.87

	TMIX	RESL	RESG	P	PRL	PRG	VSL	VSG
INLET	71.66	3853	54801.0	20.7	6.52	0.710	1.03	166.97
OUTLET	95.59	5104	52970.4	19.1	4.87	0.707	1.03	187.95
MEAN	83.62	4478	53886.2	19.9	5.65	0.708	1.03	177.59

Z	RESL	VSG	TBULK	(TW-TB)	NUTP	HTP
2.0	3952	168.65	73.64	8.55	360.2	3286.0
4.5	4077	170.78	76.12	9.99	307.9	2818.0
7.5	4229	173.38	79.10	10.65	288.5	2651.0
11.0	4409	176.49	82.59	11.48	267.0	2465.0
16.5	4699	181.52	88.09	12.00	254.6	2367.0
21.0	4941	185.77	92.60	12.22	249.1	2330.0
22.5	5023	187.22	94.11	12.29	247.6	2320.0

TEST NO.: A1.12 FLOW PATTERN:ANNULAR-MIST

ML= 267 MG=200.18 QFLUX= 17844 NUTP=120.7 HTP=1105 PDT= 3.948

PDF= 3.910 ALFA=0.958 XTT= 0.09 WE= 16.1 FR= 0.86

	TMIX	RESL	RESG	P	PRL	PRG	VSL	VSG
INLET	70.40	3791	150950.0	32.5	6.68	0.710	1.03	291.50
OUTLET	84.03	4484	148016.4	28.5	5.61	0.708	1.03	338.67
MEAN	77.22	4137	149483.5	30.5	6.13	0.709	1.03	315.04

Z	RESL	VSG	TBULK	(TW-TB)	NUTP	HTP
2.0	3846	295.11	71.53	7.53	258.1	2347.0
4.5	3917	299.73	72.94	12.29	158.5	1444.0
7.5	4002	305.44	74.64	15.49	125.9	1149.0
11.0	4102	312.33	76.63	18.34	106.4	974.0
16.5	4263	323.71	79.76	20.25	96.2	884.0
21.0	4395	333.55	82.33	21.02	92.5	854.0
22.5	4440	336.95	83.18	20.94	92.8	857.0

TEST NO.: A2. 1 FLOW PATTERN:BUBBLE

ML= 882 MG= 0.08 QFLUX= 13239 NUTP=100.8 HTP= 919 PDT= 0.941

PDF= 0.144 ALFA=0.063 XTT=226.75 WE= 174.2 FR= 9.39

	TMIX	RESL	RESG	P	PRL	PRG	VSL	VSG
INLET	71.55	12687	63.2	17.1	6.61	0.710	3.41	0.23
OUTLET	75.17	13284	62.8	16.2	6.30	0.709	3.40	0.25
MEAN	73.36	12986	63.0	16.6	6.46	0.710	3.40	0.24

Z	RESL	VSG	TBULK	(TW-TB)	NUTP	HTP
2.0	12736	0.23	71.85	13.57	107.1	974.0
4.5	12798	0.24	72.23	14.18	102.5	933.0
7.5	12872	0.24	72.68	14.40	100.9	918.0
11.0	12959	0.24	73.21	14.51	100.1	912.0
16.5	13097	0.24	74.04	14.60	99.4	907.0
21.0	13209	0.25	74.72	14.53	99.8	911.0
22.5	13247	0.25	74.94	14.35	101.1	923.0

TEST NO.: A2. 2 FLOW PATTERN:BUBBLE

ML= 882 MG= 0.16 QFLUX= 14024 NUTP=108.1 HTP= 985 PDT= 0.917

PDF= 0.162 ALFA=0.113 XTT=124.12 WE= 174.2 FR= 9.39

	TMIX	RESL	RESG	P	PRL	PRG	VSL	VSG
INLET	71.42	12665	123.0	17.0	6.62	0.710	3.41	0.45
OUTLET	75.25	13298	122.3	16.1	6.30	0.709	3.40	0.48
MEAN	73.33	12981	122.7	16.5	6.46	0.710	3.40	0.47

Z	RESL	VSG	TBULK	(TW-TB)	NUTP	HTP
2.0	12717	0.46	71.74	13.57	113.4	1031.0
4.5	12783	0.46	72.14	14.13	108.9	991.0
7.5	12861	0.46	72.62	14.28	107.8	981.0
11.0	12954	0.47	73.17	14.31	107.5	979.0
16.5	13099	0.48	74.05	14.36	107.1	977.0
21.0	13218	0.48	74.77	14.23	108.0	986.0
22.5	13258	0.48	75.01	14.15	108.6	992.0

TEST NO.: A2. 3 FLOW PATTERN:BUBBLE

ML= 882 MG= 0.42 QFLUX= 21698 NUTP=141.1 HTP=1290 PDT= 0.853

PDF= 0.197 ALFA=0.229 XTT= 53.45 WE= 174.7 FR= 9.40

	TMIX	RESL	RESG	P	PRL	PRG	VSL	VSG
INLET	72.74	12883	312.2	17.1	6.49	0.710	3.41	1.16
OUTLET	78.67	13871	309.6	16.2	6.01	0.709	3.41	1.23
MEAN	75.71	13377	310.9	16.6	6.25	0.709	3.40	1.19

Z	RESL	VSG	TBULK	(TW-TB)	NUTP	HTP
2.0	12964	1.16	73.24	16.20	146.6	1336.0
4.5	13066	1.17	73.85	16.85	141.0	1286.0
7.5	13189	1.18	74.60	17.02	139.5	1274.0
11.0	13333	1.19	75.46	16.97	139.8	1278.0
16.5	13560	1.21	76.82	16.84	140.7	1289.0
21.0	13747	1.22	77.93	16.63	142.4	1306.0
22.5	13809	1.23	78.30	16.55	143.1	1313.0

TEST NO.: A2. 4 FLOW PATTERN:SLUG

ML= 882 MG= 0.71 QFLUX= 23785 NUTP=161.4 HTP=1477 PDT= 0.829

PDF= 0.250 ALFA=0.319 XTT= 32.88 WE= 174.9 FR= 9.40

	TMIX	RESL	RESG	P	PRL	PRG	VSL	VSG
INLET	73.09	12940	534.0	17.0	6.46	0.710	3.41	1.98
OUTLET	79.59	14027	529.0	16.2	5.94	0.709	3.41	2.11
MEAN	76.34	13484	531.5	16.6	6.19	0.709	3.40	2.05

Z	RESL	VSG	TBULK	(TW-TB)	NUTP	HTP
2.0	13030	1.99	73.63	15.64	166.3	1517.0
4.5	13142	2.01	74.31	16.16	161.0	1470.0
7.5	13276	2.02	75.12	16.33	159.3	1455.0
11.0	13434	2.04	76.07	16.20	160.4	1467.0
16.5	13684	2.07	77.56	16.07	161.6	1481.0
21.0	13890	2.10	78.78	15.91	163.0	1497.0
22.5	13959	2.10	79.19	15.91	163.0	1497.0

TEST NO.: A2. 5 FLOW PATTERN:SLUG

ML= 882 MG= 1.02 QFLUX= 25985 NUTP=182.0 HTP=1668 PDT= 0.829

PDF= 0.306 ALFA=0.385 XTT= 23.69 WE= 175.1 FR= 9.40

	TMIX	RESL	RESG	P	PRL	PRG	VSL	VSG
INLET	73.71	13042	765.0	17.0	6.40	0.709	3.41	2.86
OUTLET	80.81	14233	757.3	16.1	5.84	0.709	3.41	3.04
MEAN	77.26	13638	761.1	16.6	6.12	0.709	3.40	2.95

Z	RESL	VSG	TBULK	(TW-TB)	NUTP	HTP
2.0	13140	2.87	74.30	15.32	185.3	1692.0
4.5	13262	2.89	75.04	15.77	180.0	1645.0
7.5	13410	2.91	75.92	15.86	178.9	1637.0
11.0	13583	2.94	76.96	15.74	180.1	1650.0
16.5	13857	2.98	78.59	15.25	185.6	1704.0
21.0	14083	3.02	79.92	15.52	182.3	1676.0
22.5	14158	3.03	80.36	15.41	183.6	1689.0

TEST NO.: A2. 6 FLOW PATTERN:SLUG

ML= 882 MG= 1.39 QFLUX= 25994 NUTP=174.5 HTP=1599 PDT= 0.826

PDF= 0.352 ALFA=0.443 XTT= 17.82 WE= 175.1 FR= 9.40

	TMIX	RESL	RESG	P	PRL	PRG	VSL	VSG
INLET	73.70	13041	1046.0	16.9	6.40	0.709	3.41	3.93
OUTLET	80.80	14233	1035.5	16.0	5.84	0.709	3.41	4.18
MEAN	77.25	13637	1040.9	16.4	6.12	0.709	3.40	4.06

Z	RESL	VSG	TBULK	(TW-TB)	NUTP	HTP
2.0	13139	3.95	74.29	15.58	182.4	1665.0
4.5	13261	3.98	75.03	16.14	175.9	1607.0
7.5	13409	4.01	75.92	16.40	173.1	1583.0
11.0	13582	4.05	76.95	16.39	173.1	1586.0
16.5	13856	4.11	78.58	16.30	173.8	1596.0
21.0	14082	4.16	79.92	16.23	174.4	1604.0
22.5	14158	4.17	80.36	16.17	174.9	1610.0

TEST NO.: A2. 7 FLOW PATTERN:SLUG

ML= 882 MG= 1.76 QFLUX= 25989 NUTP=178.4 HTP=1635 PDT= 0.786

PDF= 0.348 ALFA=0.485 XTT= 14.41 WE= 175.1 FR= 9.40

	TMIX	RESL	RESG	P	PRL	PRG	VSL	VSG
INLET	73.74	13047	1322.0	16.8	6.39	0.709	3.41	4.99
OUTLET	80.84	14239	1309.1	16.0	5.84	0.709	3.41	5.29
MEAN	77.29	13643	1315.8	16.4	6.11	0.709	3.40	5.14

Z	RESL	VSG	TBULK	(TW-TB)	NUTP	HTP
2.0	13145	5.01	74.33	15.44	183.9	1679.0
4.5	13268	5.04	75.07	15.74	180.4	1648.0
7.5	13415	5.08	75.96	16.02	177.2	1621.0
11.0	13589	5.13	76.99	16.07	176.4	1616.0
16.5	13863	5.20	78.62	15.98	177.2	1627.0
21.0	14088	5.26	79.95	15.72	179.9	1655.0
22.5	14164	5.28	80.40	15.59	181.4	1670.0

TEST NO.: A2. 8 FLOW PATTERN:SLUG

ML= 882 MG= 2.49 QFLUX= 25987 NUTP=180.9 HTP=1658 PDT= 0.790

PDF= 0.401 ALFA=0.544 XTT= 10.58 WE= 175.1 FR= 9.40

	TMIX	RESL	RESG	P	PRL	PRG	VSL	VSG
INLET	73.86	13067	1866.0	16.8	6.38	0.709	3.41	7.03
OUTLET	80.96	14259	1847.5	16.1	5.83	0.709	3.41	7.46
MEAN	77.41	13663	1857.0	16.4	6.10	0.709	3.40	7.25

Z	RESL	VSG	TBULK	(TW-TB)	NUTP	HTP
2.0	13165	7.06	74.45	15.14	187.6	1712.0
4.5	13288	7.11	75.19	15.68	181.0	1654.0
7.5	13435	7.16	76.08	15.83	179.2	1639.0
11.0	13609	7.23	77.11	15.85	178.9	1639.0
16.5	13883	7.33	78.74	15.66	180.8	1660.0
21.0	14108	7.41	80.07	15.55	181.9	1673.0
22.5	14184	7.44	80.51	15.33	184.4	1698.0

TEST NO.: A2. 9 FLOW PATTERN:SLUG

ML= 882 MG= 2.82 QFLUX= 25977 NUTP=190.3 HTP=1745 PDT= 0.804

PDF= 0.432 ALFA=0.563 XTT= 9.46 WE= 175.2 FR= 9.40

	TMIX	RESL	RESG	P	PRL	PRG	VSL	VSG
INLET	73.99	13088	2112.0	16.9	6.37	0.709	3.41	7.95
OUTLET	81.08	14280	2091.5	16.1	5.82	0.709	3.41	8.44
MEAN	77.53	13684	2102.2	16.5	6.09	0.709	3.41	8.20

Z	RESL	VSG	TBULK	(TW-TB)	NUTP	HTP
2.0	13186	7.99	74.58	14.37	197.5	1803.0
4.5	13309	8.04	75.32	14.75	192.4	1759.0
7.5	13457	8.10	76.20	14.99	189.1	1731.0
11.0	13630	8.18	77.24	15.08	187.9	1722.0
16.5	13904	8.29	78.86	14.86	190.5	1749.0
21.0	14130	8.39	80.19	14.89	189.9	1747.0
22.5	14205	8.42	80.64	14.79	191.1	1759.0

TEST NO.: A2.10 FLOW PATTERN:SLUG-ANNULAR

ML= 882 MG= 4.98 QFLUX= 30877 NUTP=222.7 HTP=2044 PDT= 0.927

PDF= 0.625 ALFA=0.646 XTT= 5.71 WE= 175.3 FR= 9.40

	TMIX	RESL	RESG	P	PRL	PRG	VSL	VSG
INLET	73.96	13083	3737.0	17.3	6.37	0.709	3.41	13.74
OUTLET	82.38	14503	3692.1	16.3	5.72	0.708	3.41	14.72
MEAN	78.17	13793	3714.6	16.8	6.04	0.709	3.41	14.24

Z	RESL	VSG	TBULK	(TW-TB)	NUTP	HTP
2.0	13199	13.82	74.66	14.67	229.9	2099.0
4.5	13345	13.92	75.53	15.38	219.1	2004.0
7.5	13521	14.04	76.58	15.45	218.0	1996.0
11.0	13727	14.19	77.81	15.30	220.0	2017.0
16.5	14053	14.42	79.75	15.32	219.4	2017.0
21.0	14323	14.62	81.33	14.07	238.3	2196.0
22.5	14413	14.68	81.86	15.24	220.1	2030.0

TEST NO.: A2.11 FLOW PATTERN:ANNULAR

ML= 882 MG= 8.97 QFLUX= 33291 NUTP=259.1 HTP=2374 PDT= 1.289

PDF= 1.047 ALFA=0.716 XTT= 3.42 WE= 175.1 FR= 9.40

	TMIX	RESL	RESG	P	PRL	PRG	VSL	VSG
INLET	72.62	12863	6740.0	17.9	6.49	0.710	3.41	23.78
OUTLET	81.70	14386	6653.3	16.6	5.78	0.708	3.41	25.98
MEAN	77.16	13624	6697.1	17.3	6.13	0.709	3.40	24.90

Z	RESL	VSG	TBULK	(TW-TB)	NUTP	HTP
2.0	12987	23.95	73.38	13.55	268.7	2450.0
4.5	13144	24.18	74.32	13.77	264.4	2413.0
7.5	13332	24.45	75.46	14.26	255.1	2332.0
11.0	13553	24.78	76.78	14.07	258.2	2365.0
16.5	13903	25.31	78.86	14.25	254.7	2339.0
21.0	14192	25.75	80.56	13.84	261.8	2410.0
22.5	14289	25.90	81.13	13.69	264.4	2436.0

TEST NO.: A2.12 FLOW PATTERN:ANNULAR

ML= 882 MG= 13.23 QFLUX= 35581 NUTP=298.6 HTP=2738 PDT= 1.681

PDF= 1.473 ALFA=0.756 XTT= 2.43 WE= 175.2 FR= 9.40

	TMIX	RESL	RESG	P	PRL	PRG	VSL	VSG
INLET	72.92	12912	9941.0	18.5	6.46	0.710	3.41	33.94
OUTLET	82.61	14542	9803.7	16.8	5.71	0.708	3.41	37.87
MEAN	77.77	13727	9872.4	17.7	6.08	0.709	3.41	35.93

Z	RESL	VSG	TBULK	(TW-TB)	NUTP	HTP
2.0	13045	34.25	73.73	12.60	308.6	2814.0
4.5	13212	34.65	74.74	13.13	296.1	2704.0
7.5	13414	35.13	75.95	13.17	294.8	2697.0
11.0	13650	35.71	77.36	13.08	296.7	2720.0
16.5	14025	36.66	79.58	12.97	298.8	2747.0
21.0	14335	37.46	81.40	12.86	300.9	2773.0
22.5	14439	37.74	82.01	12.59	307.1	2833.0

TEST NO.: A2.13 FLOW PATTERN:ANNULAR

ML= 882 MG= 18.79 QFLUX= 40999 NUTP=341.1 HTP=3132 PDT= 1.908

PDF= 1.724 ALFA=0.785 XTT= 1.81 WE= 175.4 FR= 9.41

	TMIX	RESL	RESG	P	PRL	PRG	VSL	VSG
INLET	72.78	12889	14124.0	19.5	6.47	0.710	3.41	45.85
OUTLET	83.92	14768	13900.1	17.6	5.61	0.708	3.41	51.69
MEAN	78.35	13828	14012.3	18.5	6.03	0.709	3.41	48.79

Z	RESL	VSG	TBULK	(TW-TB)	NUTP	HTP
2.0	13041	46.31	73.71	12.88	347.9	3173.0
4.5	13234	46.89	74.86	13.33	336.0	3069.0
7.5	13465	47.61	76.26	13.42	333.3	3050.0
11.0	13738	48.47	77.88	13.16	339.4	3113.0
16.5	14171	49.87	80.44	13.00	343.0	3157.0
21.0	14529	51.07	82.53	12.78	348.3	3214.0
22.5	14649	51.48	83.23	12.60	353.0	3261.0

TEST NO.: A2.14 FLOW PATTERN:ANNULAR

ML= 882 MG= 24.00 QFLUX= 40973 NUTP=365.1 HTP=3351 PDT= 2.293

PDF= 2.125 ALFA=0.803 XTT= 1.49 WE= 175.4 FR= 9.41

	TMIX	RESL	RESG	P	PRL	PRG	VSL	VSG
INLET	72.69	12874	18035.0	20.4	6.48	0.710	3.41	55.75
OUTLET	83.81	14749	17749.3	18.1	5.62	0.708	3.41	63.82
MEAN	78.25	13812	17892.3	19.3	6.04	0.709	3.41	59.79

Z	RESL	VSG	TBULK	(TW-TB)	NUTP	HTP
2.0	13027	56.37	73.62	12.04	372.1	3393.0
4.5	13218	57.17	74.77	12.28	364.3	3328.0
7.5	13450	58.15	76.16	12.44	359.5	3290.0
11.0	13722	59.34	77.78	12.43	359.3	3295.0
16.5	14153	61.28	80.33	12.11	368.1	3388.0
21.0	14510	62.95	82.42	12.06	368.9	3404.0
22.5	14630	63.53	83.12	11.68	380.6	3515.0

TEST NO.: A2.15 FLOW PATTERN:ANNULAR

ML= 882 MG= 52.49 QFLUX= 49771 NUTP=416.4 HTP=3819 PDT= 3.874

PDF= 3.745 ALFA=0.850 XTT= 0.80 WE= 175.2 FR= 9.40

	TMIX	RESL	RESG	P	PRL	PRG	VSL	VSG
INLET	71.03	12601	39547.0	24.9	6.62	0.710	3.41	99.56
OUTLET	84.43	14856	38792.1	21.1	5.58	0.708	3.41	120.05
MEAN	77.73	13729	39169.9	23.0	6.09	0.709	3.41	109.68

Z	RESL	VSG	TBULK	(TW-TB)	NUTP	HTP
2.0	12784	101.07	72.14	11.88	458.1	4170.0
4.5	13013	103.02	73.53	12.72	427.7	3900.0
7.5	13291	105.46	75.21	12.93	420.3	3841.0
11.0	13617	108.42	77.16	13.22	410.6	3763.0
16.5	14137	113.39	80.24	13.25	408.9	3763.0
21.0	14568	117.76	82.76	13.31	406.3	3752.0
22.5	14713	119.28	83.60	13.08	413.1	3819.0

TEST NO.: A2.16 FLOW PATTERN:ANNULAR

ML= 882 MG= 90.80 QFLUX= 52782 NUTP=443.1 HTP=4068 PDT= 5.330

PDF= 5.221 ALFA=0.873 XTI= 0.55 WE= 175.4 FR= 9.41

	TMIX	RESL	RESG	P	PRL	PRG	VSL	VSG
INLET	71.51	12679	68362.0	31.2	6.57	0.710	3.41	137.84
OUTLET	85.58	15055	66994.4	25.9	5.50	0.708	3.41	169.42
MEAN	78.54	13867	67678.3	28.5	6.02	0.709	3.41	153.35

Z	RESL	VSG	TBULK	(TW-TB)	NUTP	HTP
2.0	12871	140.14	72.67	11.32	509.3	4639.0
4.5	13113	143.11	74.14	12.22	471.6	4304.0
7.5	13405	146.82	75.89	12.67	454.4	4157.0
11.0	13749	151.37	77.94	13.04	441.0	4045.0
16.5	14296	159.03	81.17	13.49	425.4	3920.0
21.0	14750	165.83	83.82	13.78	415.8	3845.0
22.5	14903	168.21	84.70	13.70	417.7	3867.0

TEST NO.: A2.17 FLOW PATTERN:ANNULAR-MIST

ML= 882 MG=154.36 QFLUX= 55279 NUTP=457.9 HTP=4203 PDT= 6.758

PDF= 6.661 ALFA=0.889 XTI= 0.39 WE= 175.4 FR= 9.41

	TMIX	RESL	RESG	P	PRL	PRG	VSL	VSG
INLET	71.33	12651	116241.0	41.9	6.59	0.710	3.41	174.22
OUTLET	85.82	15098	113847.1	35.2	5.48	0.708	3.41	211.91
MEAN	78.58	13874	115044.4	38.6	6.02	0.709	3.41	192.79

Z	RESL	VSG	TBULK	(TW-TB)	NUTP	HTP
2.0	12848	176.99	72.53	10.56	571.8	5207.0
4.5	13096	180.57	74.04	11.65	517.9	4726.0
7.5	13397	185.02	75.85	12.39	486.6	4451.0
11.0	13751	190.46	77.96	13.18	457.0	4192.0
16.5	14315	199.60	81.28	14.36	418.6	3858.0
21.0	14784	207.66	84.01	14.88	403.4	3731.0
22.5	14941	210.47	84.92	14.61	410.4	3800.0

TEST NO.: A2.18 FLOW PATTERN:ANNULAR-MIST

ML= 882 MG=210.55 QFLUX= 55325 NUTP=416.8 HTP=3823 PDT= 8.086

PDF= 7.996 ALFA=0.897 XTI= 0.33 WE= 175.4 FR= 9.41

	TMIX	RESL	RESG	P	PRL	PRG	VSL	VSG
INLET	71.26	12638	158578.0	51.0	6.60	0.710	3.41	195.45
OUTLET	85.55	15050	155354.5	42.9	5.50	0.708	3.41	236.96
MEAN	78.40	13844	156966.4	47.0	6.03	0.709	3.41	215.92

Z	RESL	VSG	TBULK	(TW-TB)	NUTP	HTP
2.0	12833	198.51	72.44	10.27	587.5	5350.0
4.5	13077	202.45	73.92	11.83	510.1	4655.0
7.5	13373	207.37	75.70	13.16	458.3	4192.0
11.0	13722	213.37	77.79	14.60	412.8	3786.0
16.5	14279	223.42	81.07	16.73	360.0	3316.0
21.0	14741	232.29	83.76	17.92	335.6	3102.0
22.5	14896	235.38	84.66	17.83	337.1	3120.0

TEST NO.: A3. 1 FLOW PATTERN:BUBBLE

ML=1799 MG= 0.40 QFLUX= 47252 NUTP=214.0 HTP=1976 PDT= 1.285

PDF= 0.545 ALFA=0.128 XTT=105.28 WE= 734.2 FR= 39.18

	TMIX	RESL	RESG	P	PRL	PRG	VSL	VSG
INLET	79.63	28625	296.9	17.8	5.90	0.709	6.95	1.08
OUTLET	85.95	30843	294.2	16.5	5.46	0.708	6.95	1.17
MEAN	82.79	29734	295.6	17.2	5.67	0.708	6.95	1.13

Z	RESL	VSG	TEULK	(TW-TB)	NUTP	HTP
2.0	28807	1.09	80.15	22.26	230.1	2117.0
4.5	29036	1.10	80.81	23.46	218.4	2011.0
7.5	29311	1.11	81.60	23.91	214.1	1974.0
11.0	29633	1.12	82.53	24.08	212.6	1962.0
16.5	30143	1.14	83.98	23.96	213.4	1973.0
21.0	30563	1.16	85.17	24.55	208.1	1928.0
22.5	30703	1.17	85.56	24.68	207.0	1918.0

TEST NO.: A3. 2 FLOW PATTERN:BUBBLE-SLUG

ML=1799 MG= 0.90 QFLUX= 47397 NUTP=243.5 HTP=2272 PDT= 1.337

PDF= 0.690 ALFA=0.237 XTT= 49.74 WE= 742.8 FR= 39.27

	TMIX	RESL	RESG	P	PRL	PRG	VSL	VSG
INLET	87.79	31495	664.1	17.9	5.30	0.708	6.95	2.46
OUTLET	94.13	33795	658.2	16.6	4.92	0.707	6.96	2.68
MEAN	90.96	32645	661.1	17.3	5.11	0.707	6.96	2.57

Z	RESL	VSG	TEULK	(TW-TB)	NUTP	HTP
2.0	31684	2.48	88.31	18.95	268.1	2494.0
4.5	31921	2.50	88.97	20.22	251.4	2340.0
7.5	32207	2.53	89.77	20.71	245.4	2287.0
11.0	32541	2.56	90.69	20.95	242.4	2262.0
16.5	33070	2.61	92.15	21.27	238.6	2230.0
21.0	33505	2.66	93.34	21.51	235.8	2207.0
22.5	33650	2.67	93.74	21.61	234.5	2197.0

TEST NO.: A3. 3 FLOW PATTERN:SLUG

ML=1799 MG= 1.21 QFLUX= 46546 NUTP=255.5 HTP=2396 PDT= 1.363

PDF= 0.758 ALFA=0.285 XTT= 37.90 WE= 746.6 FR= 39.32

	TMIX	RESL	RESG	P	PRL	PRG	VSL	VSG
INLET	91.38	32789	888.8	18.0	5.06	0.707	6.95	3.31
OUTLET	97.61	35079	881.2	16.6	4.72	0.706	6.97	3.61
MEAN	94.49	33934	885.0	17.3	4.89	0.707	6.96	3.47

Z	RESL	VSG	TEULK	(TW-TB)	NUTP	HTP
2.0	32978	3.34	91.90	17.50	283.7	2651.0
4.5	33214	3.37	92.54	18.74	265.1	2479.0
7.5	33498	3.40	93.32	19.23	258.3	2418.0
11.0	33831	3.45	94.23	19.58	253.6	2377.0
16.5	34357	3.52	95.66	19.91	249.2	2340.0
21.0	34790	3.58	96.83	20.01	247.7	2330.0
22.5	34935	3.60	97.22	20.15	245.9	2314.0

TEST NO.: A3. 4 FLOW PATTERN:SLUG

ML=1799 MG= 1.52 QFLUX= 45969 NUTP=268.8 HTP=2527 PDT= 1.407

PDF= 0.836 ALFA=0.325 XTT= 30.81 WE= 749.0 FR= 39.34

	TMIX	RESL	RESG	P	PRL	PRG	VSL	VSG
INLET	93.57	33590	1112.0	18.1	4.93	0.707	6.95	4.15
OUTLET	99.73	35870	1103.5	16.7	4.60	0.706	6.97	4.54
MEAN	96.65	34730	1108.3	17.4	4.76	0.707	6.97	4.35

Z	RESL	VSG	TBULK	(TW-TB)	NUTP	HTP
2.0	33777	4.18	94.09	16.30	300.1	2813.0
4.5	34012	4.22	94.73	17.49	279.7	2624.0
7.5	34296	4.27	95.50	17.90	273.2	2565.0
11.0	34627	4.33	96.39	18.32	266.8	2508.0
16.5	35151	4.42	97.81	18.70	261.3	2461.0
21.0	35583	4.50	98.96	18.87	258.7	2440.0
22.5	35727	4.53	99.35	18.87	258.7	2441.0

TEST NO.: A3. 5 FLOW PATTERN:SLUG

ML=1799 MG= 1.80 QFLUX= 45991 NUTP=279.7 HTP=2636 PDT= 1.455

PDF= 0.910 ALFA=0.354 XTT= 26.52 WE= 750.7 FR= 39.36

	TMIX	RESL	RESG	P	PRL	PRG	VSL	VSG
INLET	95.12	34157	1311.0	18.2	4.84	0.707	6.95	4.89
OUTLET	101.28	36452	1300.0	16.8	4.52	0.706	6.97	5.35
MEAN	98.20	35305	1305.5	17.5	4.68	0.706	6.97	5.12

Z	RESL	VSG	TBULK	(TW-TB)	NUTP	HTP
2.0	34346	4.92	95.63	15.59	313.1	2941.0
4.5	34582	4.97	96.27	16.61	294.1	2764.0
7.5	34867	5.03	97.04	17.38	280.9	2643.0
11.0	35201	5.10	97.94	17.68	276.2	2601.0
16.5	35729	5.21	99.35	17.82	273.7	2583.0
21.0	36163	5.30	100.51	18.10	269.3	2545.0
22.5	36308	5.34	100.89	18.13	268.7	2541.0

TEST NO.: A3. 6 FLOW PATTERN:SLUG

ML=1799 MG= 2.12 QFLUX= 46016 NUTP=294.4 HTP=2780 PDT= 1.523

PDF= 1.002 ALFA=0.384 XTT= 22.86 WE= 752.7 FR= 39.39

	TMIX	RESL	RESG	P	PRL	PRG	VSL	VSG
INLET	96.92	34822	1539.0	18.3	4.73	0.707	6.95	5.74
OUTLET	103.08	37134	1526.4	16.8	4.42	0.706	6.97	6.31
MEAN	100.00	35978	1532.9	17.6	4.58	0.706	6.97	6.03

Z	RESL	VSG	TBULK	(TW-TB)	NUTP	HTP
2.0	35012	5.79	97.43	14.69	331.8	3123.0
4.5	35250	5.85	98.07	15.80	308.5	2906.0
7.5	35537	5.91	98.84	16.34	298.3	2813.0
11.0	35874	6.00	99.74	16.71	291.5	2752.0
16.5	36405	6.14	101.15	17.02	286.1	2706.0
21.0	36842	6.25	102.31	17.21	282.7	2678.0
22.5	36989	6.29	102.70	17.21	282.7	2679.0

TEST NO.: A3. 7 FLOW PATTERN:SLUG

ML=1799 MG= 2.35 QFLUX= 46037 NUTP=301.2 HTP=2849 PDT= 1.567

PDF= 1.062 ALFA=0.402 XTT= 20.86 WE= 754.0 FR= 39.41

	TMIX	RESL	RESG	P	PRL	PRG	VSL	VSG
INLET	98.11	35266	1702.C	18.4	4.66	C.706	6.95	6.33
OUTLET	104.28	37590	1688.5	16.9	4.36	0.706	6.98	6.97
MEAN	101.20	36428	1695.6	17.7	4.51	C.706	6.97	6.65

Z	RESL	VSG	TEULK	(TW-TB)	NUTP	HTP
2.0	35457	6.38	98.63	14.28	340.9	3214.0
4.5	35697	6.45	99.27	15.46	315.1	2973.0
7.5	35986	6.53	100.04	15.98	304.7	2878.0
11.0	36324	6.62	100.94	16.40	296.9	2807.0
16.5	36858	6.77	102.35	16.60	292.9	2775.0
21.0	37297	6.90	103.51	16.69	291.2	2763.0
22.5	37444	6.95	103.89	16.68	291.2	2764.C

TEST NO.: A3. 8 FLOW PATTERN:SLUG

ML=1799 MG= 2.55 QFLUX= 45991 NUTP=310.6 HTP=2942 PDT= 1.630

PDF= 1.137 ALFA=0.416 XTT= 19.37 WE= 755.1 FR= 39.42

	TMIX	RESL	RESG	P	PRL	PRG	VSL	VSG
INLET	99.09	35632	1844.C	18.5	4.61	C.706	6.95	6.85
OUTLET	105.25	37962	1829.5	16.9	4.31	0.706	6.98	7.57
MEAN	102.17	36797	1837.3	17.7	4.46	C.706	6.97	7.21

Z	RESL	VSG	TEULK	(TW-TB)	NUTP	HTP
2.0	35824	6.91	99.61	14.14	343.6	3244.0
4.5	36064	6.98	100.25	15.08	322.2	3044.0
7.5	36354	7.07	101.02	15.57	312.1	2952.0
11.0	36693	7.17	101.91	15.83	306.8	2905.0
16.5	37228	7.35	103.33	15.87	305.7	2900.0
21.0	37669	7.49	104.48	16.13	300.5	2855.0
22.5	37816	7.54	104.87	16.12	300.8	2859.0

TEST NO.: A3. 9 FLOW PATTERN:SLUG-ANNULAR

ML=1799 MG= 6.40 QFLUX= 41426 NUTP=326.5 HTP=3064 PDT= 2.064

PDF= 1.696 ALFA=0.566 XTT= 8.79 WE= 747.2 FR= 39.32

	TMIX	RESL	RESG	P	PRL	PRG	VSL	VSG
INLET	92.29	33123	4675.C	19.6	5.01	C.707	6.95	16.04
OUTLET	97.84	35164	4639.9	17.6	4.70	C.706	6.97	18.04
MEAN	95.07	34143	4657.8	18.6	4.86	C.707	6.96	17.05

Z	RESL	VSG	TEULK	(TW-TB)	NUTP	HTP
2.0	33291	16.2C	92.76	11.99	368.5	3448.0
4.5	33501	16.40	93.33	13.12	336.8	3154.0
7.5	33755	16.64	94.03	13.32	331.5	3106.0
11.0	34052	16.93	94.83	13.75	321.1	3013.0
16.5	34521	17.41	96.11	13.78	320.1	3008.0
21.0	34907	17.83	97.15	13.94	316.3	2976.0
22.5	35036	17.97	97.49	14.05	313.8	2954.0

TEST NO.: A3.10 FLOW PATTERN:ANNULAR

ML=1799 MG= 8.92 QFLUX= 41450 NUTP=358.6 HTP=3375 PDT= 2.380

PDF= 2.051 ALFA=0.611 XIT= 6.62 WE= 749.6 FR= 39.35

	TMIX	RESL	RESG	P	PRL	PRG	VSL	VSG
INLET	94.45	33912	6499.0	20.5	4.88	0.707	6.95	21.48
OUTLET	100.00	35971	6450.2	18.1	4.58	0.706	6.97	24.43
MEAN	97.23	34941	6474.9	19.3	4.73	0.706	6.97	22.95

Z	RESL	VSG	TBULK	(TW-TB)	NUTP	HTP
2.0	34081	21.70	94.91	11.07	398.0	3734.0
4.5	34294	21.99	95.49	11.89	370.8	3481.0
7.5	34550	22.35	96.18	12.07	364.9	3430.0
11.0	34849	22.79	96.99	12.33	357.2	3361.0
16.5	35322	23.50	98.26	12.64	348.1	3281.0
21.0	35711	24.11	99.31	12.67	347.1	3276.0
22.5	35841	24.32	99.65	12.74	345.2	3259.0

TEST NO.: A3.11 FLOW PATTERN:ANNULAR

ML=1799 MG= 12.32 QFLUX= 41459 NUTP=394.3 HTP=3718 PDT= 2.892

PDF= 2.595 ALFA=0.649 XIT= 5.09 WE= 751.3 FR= 39.37

	TMIX	RESL	RESG	P	PRL	PRG	VSL	VSG
INLET	95.95	34464	8957.0	22.0	4.79	0.707	6.95	27.73
OUTLET	101.50	36534	8889.6	19.1	4.50	0.706	6.97	32.09
MEAN	98.72	35499	8923.6	20.6	4.65	0.706	6.97	29.90

Z	RESL	VSG	TBULK	(TW-TB)	NUTP	HTP
2.0	34635	28.06	96.41	10.16	433.1	4071.0
4.5	34849	28.49	96.99	10.93	402.5	3787.0
7.5	35106	29.01	97.68	11.17	393.8	3709.0
11.0	35407	29.65	98.49	11.28	389.8	3675.0
16.5	35883	30.70	99.76	11.29	389.1	3674.0
21.0	36274	31.61	100.80	11.31	388.2	3671.0
22.5	36405	31.93	101.15	11.32	387.6	3667.0

TEST NO.: A3.12 FLOW PATTERN:ANNULAR

ML=1799 MG= 14.81 QFLUX= 41751 NUTP=409.3 HTP=3863 PDT= 3.157

PDF= 2.876 ALFA=0.669 XIT= 4.38 WE= 752.0 FR= 39.38

	TMIX	RESL	RESG	P	PRL	PRG	VSL	VSG
INLET	96.61	34706	10762.0	22.9	4.75	0.707	6.95	32.10
OUTLET	102.19	36795	10680.3	19.7	4.47	0.706	6.97	37.42
MEAN	99.40	35751	10721.3	21.3	4.61	0.706	6.97	34.74

Z	RESL	VSG	TBULK	(TW-TB)	NUTP	HTP
2.0	34878	32.51	97.07	9.89	447.8	4214.0
4.5	35094	33.02	97.65	10.62	416.8	3925.0
7.5	35354	33.66	98.35	11.05	400.5	3775.0
11.0	35658	34.43	99.16	10.91	405.6	3827.0
16.5	36138	35.71	100.44	10.91	405.3	3830.0
21.0	36532	36.83	101.49	10.83	407.7	3858.0
22.5	36664	37.22	101.84	10.73	411.4	3895.0

TEST NO.: A3.13 FLOW PATTERN:ANNULAR

ML=1799 MG= 25.14 QFLUX= 41343 NUTP=434.5 HTP=4078 PDT= 4.288

PDF= 4.048 ALFA=0.718 XTT= 2.92 WE= 747.3 FR= 39.32

	TMIX	RESL	RESG	P	PRL	PRG	VSL	VSG
INLET	92.39	33158	18370.0	26.2	5.00	0.707	6.95	47.25
OUTLET	97.91	35190	18231.2	21.9	4.70	0.706	6.97	56.70
MEAN	95.15	34174	18301.1	24.1	4.85	0.707	6.96	51.90

Z	RESL	VSG	TEULK	(TW-TB)	NUTP	HTP
2.0	33325	47.94	92.85	9.07	486.3	4551.0
4.5	33535	48.84	93.42	9.85	447.7	4193.0
7.5	33787	49.95	94.11	10.08	437.1	4097.0
11.0	34083	51.32	94.92	10.28	428.4	4019.0
16.5	34550	53.61	96.18	10.31	427.1	4014.0
21.0	34934	55.63	97.22	10.44	421.4	3966.0
22.5	35062	56.34	97.57	10.31	426.4	4015.0

TEST NO.: A3.14 FLOW PATTERN:ANNULAR

ML=1799 MG= 45.52 QFLUX= 46828 NUTP=465.7 HTP=4377 PDT= 5.589

PDF= 5.389 ALFA=0.765 XTT= 1.85 WE= 748.4 FR= 39.34

	TMIX	RESL	RESG	P	PRL	PRG	VSL	VSG
INLET	93.04	33394	33238.0	31.0	4.96	0.707	6.95	72.45
OUTLET	99.27	35699	32954.1	25.4	4.63	0.706	6.97	88.76
MEAN	96.16	34547	33096.5	28.2	4.79	0.707	6.97	80.43

Z	RESL	VSG	TEULK	(TW-TB)	NUTP	HTP
2.0	33584	73.63	93.56	9.07	549.9	5150.0
4.5	33822	75.15	94.21	10.25	486.8	4563.0
7.5	34108	77.05	94.99	10.69	466.3	4376.0
11.0	34443	79.39	95.89	10.95	455.3	4278.0
16.5	34973	83.36	97.32	10.86	458.5	4316.0
21.0	35409	86.89	98.50	11.22	443.6	4182.0
22.5	35554	88.13	98.89	11.21	443.7	4185.0

TEST NO.: A3.15 FLOW PATTERN:ANNULAR

ML=1799 MG= 68.35 QFLUX= 46559 NUTP=473.0 HTP=4454 PDT= 6.923

PDF= 6.745 ALFA=0.790 XTT= 1.37 WE= 750.0 FR= 39.36

	TMIX	RESL	RESG	P	PRL	PRG	VSL	VSG
INLET	94.53	33939	49804.0	36.1	4.87	0.707	6.95	93.64
OUTLET	100.71	36237	49382.4	29.1	4.55	0.706	6.97	116.28
MEAN	97.62	35088	49593.2	32.6	4.71	0.706	6.97	104.68

Z	RESL	VSG	TEULK	(TW-TB)	NUTP	HTP
2.0	34128	95.25	95.04	8.77	564.3	5295.0
4.5	34365	97.34	95.68	9.92	499.0	4687.0
7.5	34650	99.97	96.46	10.34	478.5	4499.0
11.0	34985	103.20	97.36	10.68	463.0	4358.0
16.5	35513	108.71	98.77	10.82	456.7	4307.0
21.0	35947	113.65	99.93	10.90	453.1	4280.0
22.5	36092	115.39	100.32	10.99	449.3	4246.0

TEST NO.: A3.16 FLOW PATTERN:ANNULAR

ML=1799 MG= 92.68 QFLUX= 46698 NUTP=490.4 HTP=4624 PDT= 7.846

PDF= 7.682 ALFA=0.808 XTT= 1.10 WE= 751.1 FR= 39.37

	TMIX	RESL	RESG	P	PRL	PRG	VSL	VSG
INLET	95.53	34308	67432.0	40.5	4.81	0.707	6.95	113.33
OUTLET	101.71	36614	66862.8	32.6	4.49	0.706	6.97	141.04
MEAN	98.62	35461	67147.6	36.6	4.65	0.706	6.97	126.83

Z	RESL	VSG	TEULK	(TW-TB)	NUTP	HTP
2.0	34497	115.30	96.04	8.43	588.1	5526.0
4.5	34735	117.85	96.68	9.48	522.8	4917.0
7.5	35021	121.06	97.46	9.97	497.3	4682.0
11.0	35357	125.02	98.36	10.37	477.8	4503.0
16.5	35887	131.76	99.77	10.45	473.5	4471.0
21.0	36323	137.81	100.93	10.60	466.5	4412.0
22.5	36469	139.95	101.32	10.66	463.8	4389.0

TEST NO.: A3.17 FLOW PATTERN:ANNULAR

ML=1799 MG=110.98 QFLUX= 46688 NUTP=508.0 HTP=4789 PDT= 8.372

PDF= 8.212 ALFA=0.814 XTT= 0.99 WE= 751.1 FR= 39.37

	TMIX	RESL	RESG	P	PRL	PRG	VSL	VSG
INLET	95.52	34303	80754.0	45.1	4.81	0.707	6.95	121.82
OUTLET	101.68	36603	80074.0	36.7	4.50	0.706	6.97	150.13
MEAN	98.60	35453	80414.1	40.9	4.65	0.706	6.97	135.65

Z	RESL	VSG	TEULK	(TW-TB)	NUTP	HTP
2.0	34492	123.85	96.03	8.02	617.7	5805.0
4.5	34730	126.48	96.67	9.05	547.8	5152.0
7.5	35015	129.77	97.44	9.63	514.7	4845.0
11.0	35350	133.83	98.34	10.01	494.7	4662.0
16.5	35878	140.71	99.75	10.12	488.8	4616.0
21.0	36313	146.86	100.91	10.36	477.4	4515.0
22.5	36459	149.03	101.29	10.30	479.8	4540.0

TEST NO.: A3.18 FLOW PATTERN:ANNULAR

ML=1799 MG=188.77 QFLUX= 55172 NUTP=483.4 HTP=4514 PDT=10.570

PDF=10.427 ALFA=0.835 XTT= 0.72 WE= 743.2 FR= 39.28

	TMIX	RESL	RESG	P	PRL	PRG	VSL	VSG
INLET	87.76	31487	138850.0	59.2	5.30	0.708	6.95	155.63
OUTLET	94.97	34102	137461.1	48.6	4.87	0.707	6.96	190.58
MEAN	91.37	32794	138155.8	53.9	5.08	0.707	6.96	172.75

Z	RESL	VSG	TEULK	(TW-TB)	NUTP	HTP
2.0	31701	158.15	88.36	9.23	640.4	5957.0
4.5	31970	161.42	89.11	10.84	545.3	5078.0
7.5	32294	165.50	90.01	11.58	510.3	4758.0
11.0	32674	170.52	91.06	12.42	475.8	4441.0
16.5	33276	179.01	92.71	13.36	442.0	4135.0
21.0	33771	186.57	94.07	13.80	427.7	4009.0
22.5	33937	189.23	94.52	13.98	422.0	3958.0

TEST NO.: A4. 1 FLOW PATTERN:BUBBLE

ML=3598 MG= 0.33 QFLUX= 40942 NUTP=317.8 HTP=2949 PDI= 2.167

PDF= 1.368 ALFA=0.058 XTT=236.03 WE= 2952.0 FR=156.00

	TMIX	RESL	RESG	P	PRL	PRG	VSL	VSG
INLET	85.19	61135	243.5	19.0	5.49	0.708	13.89	0.85
OUTLET	87.93	63087	242.5	16.8	5.31	0.708	13.91	0.95
MEAN	86.56	62111	243.0	17.9	5.40	0.708	13.91	0.90

Z	RESL	VSG	TBULK	(TW-TB)	NUTP	HTP
2.0	61297	0.85	85.41	12.83	344.0	3187.0
4.5	61499	0.86	85.70	13.45	328.1	3041.0
7.5	61743	0.88	86.04	13.71	321.9	2985.0
11.0	62027	0.89	86.44	13.99	315.3	2925.0
16.5	62475	0.92	87.07	14.15	311.6	2893.0
21.0	62842	0.94	87.58	14.25	309.4	2875.0
22.5	62965	0.95	87.76	14.28	308.8	2870.0

TEST NO.: A4. 2 FLOW PATTERN:BUBBLE

ML=3598 MG= 0.74 QFLUX= 41041 NUTP=343.3 HTP=3207 PDI= 2.282

PDF= 1.534 ALFA=0.116 XTT=114.22 WE= 2973.0 FR=157.00

	TMIX	RESL	RESG	P	PRL	PRG	VSL	VSG
INLET	90.18	64706	538.8	19.2	5.15	0.707	13.89	1.87
OUTLET	92.93	66702	536.7	16.9	4.99	0.707	13.92	2.13
MEAN	91.55	65704	537.7	18.1	5.07	0.707	13.92	2.00

Z	RESL	VSG	TBULK	(TW-TB)	NUTP	HTP
2.0	64872	1.89	90.41	11.90	369.2	3443.0
4.5	65079	1.92	90.69	12.54	350.4	3270.0
7.5	65328	1.95	91.04	12.68	346.5	3235.0
11.0	65618	1.99	91.44	12.88	341.2	3186.0
16.5	66076	2.05	92.07	12.98	338.2	3162.0
21.0	66452	2.10	92.59	13.07	335.8	3141.0
22.5	66578	2.12	92.76	13.06	336.1	3145.0

TEST NO.: A4. 3 FLOW PATTERN:BUBBLE

ML=3598 MG= 1.23 QFLUX= 41051 NUTP=359.0 HTP=3358 PDI= 2.404

PDF= 1.702 ALFA=0.170 XTT= 73.13 WE= 2977.0 FR=157.00

	TMIX	RESL	RESG	P	PRL	PRG	VSL	VSG
INLET	91.17	65424	899.1	20.0	5.09	0.707	13.89	3.02
OUTLET	93.92	67428	895.7	17.6	4.93	0.707	13.92	3.44
MEAN	92.55	66426	897.4	18.8	5.01	0.707	13.92	3.23

Z	RESL	VSG	TBULK	(TW-TB)	NUTP	HTP
2.0	65591	3.05	91.40	11.45	383.5	3582.0
4.5	65798	3.09	91.69	12.03	364.9	3409.0
7.5	66048	3.14	92.03	12.32	356.4	3331.0
11.0	66340	3.20	92.43	12.24	358.5	3353.0
16.5	66800	3.31	93.06	12.35	355.3	3326.0
21.0	67177	3.39	93.58	12.36	354.7	3322.0
22.5	67303	3.42	93.75	12.41	353.3	3310.0

TEST NO.: A4. 4 FLOW PATTERN:BUBBLE-FROTH

ML=3598 MG= 1.52 QFLUX= 41062 NUTP=364.6 HTP=3413 PDT= 2.486

PDF= 1.806 ALFA=0.196 XTT= 60.82 WE= 2980.0 FR=157.00

	TMIX	RESL	RESG	P	PRL	PRG	VSL	VSG
INLET	91.82	65894	1113.0	20.4	5.05	0.707	13.89	3.67
OUTLET	94.57	67904	1109.2	17.9	4.89	0.707	13.93	4.18
MEAN	93.19	66899	1111.3	19.2	4.97	0.707	13.92	3.93

Z	RESL	VSG	TBULK	(TW-TB)	NUTP	HTP
2.0	66060	3.71	92.05	11.07	396.2	3703.0
4.5	66269	3.76	92.33	11.79	372.0	3479.0
7.5	66519	3.82	92.68	12.02	365.1	3415.0
11.0	66812	3.90	93.08	12.12	361.9	3388.0
16.5	67274	4.02	93.71	12.21	359.0	3363.0
21.0	67652	4.13	94.23	12.22	358.7	3363.0
22.5	67778	4.16	94.40	12.18	359.7	3373.0

TEST NO.: A4. 5 FLOW PATTERN:BUEBLE-FROTH

ML=3598 MG= 1.81 QFLUX= 40354 NUTP=370.0 HTP=3469 PDT= 2.546

PDF= 1.885 ALFA=0.220 XTT= 52.26 WE= 2985.0 FR=157.00

	TMIX	RESL	RESG	P	PRL	PRG	VSL	VSG
INLET	93.03	66774	1324.0	20.8	4.97	0.707	13.89	4.31
OUTLET	95.73	68758	1319.2	18.2	4.82	0.707	13.93	4.91
MEAN	94.38	67766	1321.7	19.5	4.90	0.707	13.93	4.61

Z	RESL	VSG	TBULK	(TW-TB)	NUTP	HTP
2.0	66938	4.35	93.25	10.63	404.9	3791.0
4.5	67144	4.41	93.53	11.41	377.4	3535.0
7.5	67391	4.49	93.87	11.57	371.9	3485.0
11.0	67680	4.57	94.26	11.67	368.7	3457.0
16.5	68136	4.72	94.88	11.80	364.5	3419.0
21.0	68509	4.85	95.39	11.94	360.1	3381.0
22.5	68634	4.89	95.56	11.95	359.8	3379.0

TEST NO.: A4. 6 FLOW PATTERN:BUBBLE-FROTH

ML=3598 MG= 2.08 QFLUX= 40527 NUTP=374.3 HTP=3511 PDT= 2.631

PDF= 1.987 ALFA=0.239 XTT= 46.39 WE= 2986.0 FR=157.00

	TMIX	RESL	RESG	P	PRL	PRG	VSL	VSG
INLET	93.33	66993	1518.0	21.0	4.95	0.707	13.89	4.89
OUTLET	96.04	68988	1513.1	18.4	4.80	0.707	13.93	5.59
MEAN	94.68	67990	1515.9	19.7	4.88	0.707	13.93	5.24

Z	RESL	VSG	TBULK	(TW-TB)	NUTP	HTP
2.0	67158	4.94	93.55	10.36	416.8	3904.0
4.5	67365	5.01	93.83	11.27	383.5	3594.0
7.5	67614	5.09	94.17	11.38	379.7	3559.0
11.0	67905	5.20	94.57	11.61	372.1	3489.0
16.5	68363	5.37	95.19	11.79	366.2	3437.0
21.0	68738	5.51	95.70	11.93	361.9	3399.0
22.5	68864	5.56	95.87	11.90	362.9	3409.0

TEST NO.: A4. 7 FLOW PATTERN:BUBBLE-FROTH

ML=3598 MG= 2.51 QFLUX= 40418 NUTP=381.3 HTP=3578 PDT= 2.741

PDF= 2.121 ALFA=0.267 XTT= 39.47 WE= 2988.0 FR=157.00

	TMIX	RESL	RESG	P	PRL	PRG	VSL	VSG
INLET	93.67	67243	1830.0	21.4	4.93	0.707	13.89	5.80
OUTLET	96.37	69235	1823.5	18.6	4.78	0.707	13.93	6.65
MEAN	95.02	68239	1826.9	20.0	4.86	0.707	13.93	6.23

Z	RESL	VSG	TBULK	(TW-TB)	NUTP	HTP
2.0	67408	5.86	93.89	10.13	425.2	3984.0
4.5	67615	5.95	94.17	10.89	395.4	3706.0
7.5	67863	6.05	94.51	11.09	388.3	3642.0
11.0	68154	6.18	94.91	11.50	374.4	3513.0
16.5	68611	6.38	95.53	11.64	369.8	3472.0
21.0	68986	6.56	96.04	11.51	373.9	3513.0
22.5	69111	6.62	96.21	11.49	374.6	3520.0

TEST NO.: A4. 8 FLOW PATTERN:BUBBLE-FROTH

ML=3598 MG= 2.80 QFLUX= 41095 NUTP=383.3 HTP=3597 PDT= 2.839

PDF= 2.233 ALFA=0.284 XTT= 35.96 WE= 2988.0 FR=157.00

	TMIX	RESL	RESG	P	PRL	PRG	VSL	VSG
INLET	93.67	67242	2045.0	21.7	4.93	0.707	13.89	6.38
OUTLET	96.42	69268	2037.8	18.8	4.78	0.707	13.93	7.35
MEAN	95.04	68255	2041.6	20.3	4.86	0.707	13.93	6.86

Z	RESL	VSG	TBULK	(TW-TB)	NUTP	HTP
2.0	67410	6.45	93.89	10.23	427.9	4010.0
4.5	67620	6.55	94.18	11.12	393.9	3692.0
7.5	67872	6.66	94.53	11.32	386.8	3628.0
11.0	68168	6.81	94.93	11.52	380.2	3567.0
16.5	68633	7.04	95.56	11.70	374.2	3514.0
21.0	69014	7.24	96.07	11.70	373.9	3513.0
22.5	69141	7.31	96.25	11.76	372.0	3496.0

TEST NO.: A4. 9 FLOW PATTERN:FROTH

ML=3598 MG= 6.36 QFLUX= 41458 NUTP=424.1 HTP=3979 PDT= 3.617

PDF= 3.117 ALFA=0.410 XTT= 18.20 WE= 2987.0 FR=157.00

	TMIX	RESL	RESG	P	PRL	PRG	VSL	VSG
INLET	93.52	67133	4643.0	24.5	4.94	0.707	13.89	12.81
OUTLET	96.29	69175	4626.0	20.9	4.79	0.707	13.93	15.02
MEAN	94.90	68154	4634.9	22.7	4.86	0.707	13.93	13.91

Z	RESL	VSG	TBULK	(TW-TB)	NUTP	HTP
2.0	67302	12.98	93.75	9.56	462.5	4333.0
4.5	67513	13.19	94.04	10.15	435.5	4082.0
7.5	67768	13.45	94.38	10.30	429.3	4025.0
11.0	68066	13.77	94.79	10.52	420.0	3940.0
16.5	68534	14.31	95.42	10.54	418.9	3933.0
21.0	68919	14.78	95.95	10.74	411.0	3862.0
22.5	69047	14.94	96.12	10.85	406.9	3824.0

TEST NO.: A4.10 FLOW PATTERN:FRCTH

ML=3598 MG= 8.77 QFLUX= 41459 NUTP=439.1 HTP=4122 PDT= 4.152

PDF= 3.692 ALFA=0.457 XTT= 14.06 WE= 2989.0 FR=157.0C

	TMIX	RESL	RESG	P	PRL	PRG	VSL	VSG
INLET	93.89	67407	6394.0	26.2	4.92	0.707	13.89	16.51
OUTLET	96.67	69452	6369.9	22.1	4.77	0.707	13.93	19.60
MEAN	95.28	68430	6382.1	24.1	4.84	0.707	13.93	18.04

Z	RESL	VSG	TBULK	(TW-TB)	NUTP	HTP
2.0	67577	16.74	94.12	9.12	484.4	4541.0
4.5	67789	17.03	94.41	9.75	453.0	4247.0
7.5	68044	17.40	94.76	9.95	443.9	4164.0
11.0	68342	17.85	95.16	10.16	434.9	4082.0
16.5	68811	18.59	95.80	10.20	432.8	4066.0
21.0	69196	19.25	96.32	10.41	424.0	3985.0
22.5	69324	19.48	96.49	10.53	419.2	3941.0

TEST NO.: A4.11 FLOW PATTERN:FROTH

ML=3598 MG= 10.60 QFLUX= 41460 NUTP=458.5 HTP=4307 PDT= 4.439

PDF= 4.002 ALFA=0.484 XTT= 12.05 WE= 2991.0 FR=157.0C

	TMIX	RESL	RESG	P	PRL	PRG	VSL	VSG
INLET	94.36	67748	7723.0	27.2	4.89	0.707	13.89	19.24
OUTLET	97.13	69796	7693.6	22.8	4.74	0.707	13.93	22.96
MEAN	95.74	68772	7708.4	25.0	4.81	0.707	13.93	21.07

Z	RESL	VSG	TBULK	(TW-TB)	NUTP	HTP
2.0	67918	19.51	94.59	8.80	501.6	4705.0
4.5	68130	19.86	94.88	9.37	471.1	4420.0
7.5	68385	20.30	95.22	9.54	462.8	4344.0
11.0	68684	20.84	95.63	9.73	453.5	4259.0
16.5	69154	21.74	96.26	9.76	452.2	4251.0
21.0	69540	22.54	96.78	9.87	446.7	4202.0
22.5	69668	22.82	96.96	9.98	441.9	4157.0

TEST NO.: A4.12 FLOW PATTERN:FROTH

ML=3598 MG= 12.19 QFLUX= 40223 NUTP=472.4 HTP=4441 PDT= 4.795

PDF= 4.373 ALFA=0.501 XTT= 10.85 WE= 2993.0 FR=157.0C

	TMIX	RESL	RESG	P	PRL	PRG	VSL	VSG
INLET	94.95	68186	8873.0	28.5	4.85	0.707	13.89	21.14
OUTLET	97.64	70177	8840.2	23.7	4.71	0.706	13.93	25.37
MEAN	96.30	69181	8856.6	26.1	4.78	0.707	13.93	23.22

Z	RESL	VSG	TBULK	(TW-TB)	NUTP	HTP
2.0	68351	21.45	95.18	8.19	522.6	4905.0
4.5	68557	21.85	95.46	8.71	491.6	4616.0
7.5	68805	22.34	95.79	9.00	475.5	4467.0
11.0	69095	22.95	96.18	9.11	469.7	4414.0
16.5	69552	23.98	96.80	9.34	457.9	4307.0
21.0	69927	24.89	97.31	9.29	460.5	4334.0
22.5	70052	25.21	97.48	9.18	465.7	4384.0

TEST NO.: A4.13 FLOW PATTERN:FROTH

ML=3598 MG= 14.73 QFLUX= 40671 NUTP=484.4 HTP=4554 PDT= 5.251

PDF= 4.851 ALFA=0.527 XTT= 9.32 WE= 2994.0 FR=157.00

	TMIX	RESL	RESG	P	PRL	PRG	VSL	VSG
INLET	95.07	68272	10722.0	29.8	4.85	0.707	13.89	24.48
OUTLET	97.79	70287	10682.7	24.5	4.70	0.706	13.93	29.66
MEAN	96.43	69280	10702.8	27.1	4.77	0.707	13.93	27.02

Z	RESL	VSG	TEULK	(TW-TB)	NUTP	HTP
2.0	68439	24.85	95.30	8.05	537.6	5046.0
4.5	68648	25.34	95.58	8.67	499.2	4688.0
7.5	68899	25.95	95.92	8.83	489.9	4603.0
11.0	69193	26.69	96.32	8.98	481.7	4528.0
16.5	69655	27.95	96.94	9.07	476.8	4486.0
21.0	70034	29.07	97.45	9.31	464.4	4371.0
22.5	70161	29.46	97.62	9.32	463.9	4369.0

TEST NO.: A4.14 FLOW PATTERN:FROTH

ML=3598 MG= 17.01 QFLUX= 40918 NUTP=482.1 HTP=4538 PDT= 5.618

PDF= 5.232 ALFA=0.544 XTT= 8.34 WE= 2998.0 FR=157.00

	TMIX	RESL	RESG	P	PRL	PRG	VSL	VSG
INLET	95.92	68900	12372.0	31.1	4.80	0.707	13.89	27.11
OUTLET	98.66	70933	12325.7	25.5	4.65	0.706	13.94	33.03
MEAN	97.29	69917	12348.9	28.3	4.73	0.706	13.93	30.01

Z	RESL	VSG	TEULK	(TW-TB)	NUTP	HTP
2.0	69069	27.54	96.15	8.09	537.5	5052.0
4.5	69280	28.09	96.43	8.70	500.1	4702.0
7.5	69533	28.78	96.78	8.91	488.1	4591.0
11.0	69829	29.63	97.17	9.06	479.6	4513.0
16.5	70296	31.07	97.80	9.26	469.2	4419.0
21.0	70678	32.35	98.32	9.34	465.0	4383.0
22.5	70806	32.80	98.49	9.30	467.3	4405.0

TEST NO.: A4.15 FLOW PATTERN:FROTH

ML=3598 MG= 19.41 QFLUX= 40989 NUTP=493.3 HTP=4647 PDT= 5.922

PDF= 5.550 ALFA=0.561 XTT= 7.53 WE= 3001.0 FR=157.00

	TMIX	RESL	RESG	P	PRL	PRG	VSL	VSG
INLET	96.64	69433	14101.0	32.2	4.76	0.707	13.89	29.90
OUTLET	99.38	71474	14048.4	26.3	4.61	0.706	13.94	36.56
MEAN	98.01	70453	14074.9	29.2	4.69	0.706	13.93	33.16

Z	RESL	VSG	TEULK	(TW-TB)	NUTP	HTP
2.0	69602	30.38	96.87	7.97	545.8	5134.0
4.5	69813	31.00	97.15	8.54	509.8	4798.0
7.5	70068	31.78	97.50	8.63	504.0	4745.0
11.0	70365	32.73	97.90	8.85	491.5	4630.0
16.5	70834	34.35	98.52	8.96	485.3	4575.0
21.0	71218	35.79	99.04	9.27	469.0	4424.0
22.5	71347	36.30	99.21	9.46	459.4	4335.0

TEST NO.: A4.16 FLOW PATTERN:FROTH

ML=3598 MG= 20.55 QFLUX= 41077 NUTP=486.6 HTP=4550 PDT= 6.150

PDF= 5.781 ALFA=0.566 XTT= 7.29 WE= 2976.0 FR=157.00

	TMIX	RESL	RESG	P	PRL	PRG	VSL	VSG
INLET	90.96	65271	15050.0	32.8	5.10	0.707	13.89	30.79
OUTLET	93.71	67272	14992.6	26.6	4.94	0.707	13.92	37.82
MEAN	92.33	66271	15021.3	29.7	5.02	0.707	13.92	34.22

Z	RESL	VSG	TEULK	(TW-TB)	NUTP	HTP
2.0	65437	31.30	91.19	8.03	546.9	5106.0
4.5	65644	31.95	91.47	8.64	508.3	4748.0
7.5	65893	32.76	91.82	8.91	492.9	4606.0
11.0	66185	33.77	92.22	9.12	481.5	4502.0
16.5	66644	35.48	92.85	9.19	478.0	4473.0
21.0	67021	37.01	93.36	9.49	462.7	4332.0
22.5	67147	37.54	93.54	9.51	461.8	4325.0

TEST NO.: A4.17 FLOW PATTERN:FROTH

ML=3598 MG= 22.59 QFLUX= 40995 NUTP=485.7 HTP=4550 PDT= 6.414

PDF= 6.054 ALFA=0.576 XTT= 6.78 WE= 2982.0 FR=157.00

	TMIX	RESL	RESG	P	PRL	PRG	VSL	VSG
INLET	92.25	66204	16512.0	33.9	5.02	0.707	13.89	32.82
OUTLET	94.99	68211	16449.6	27.5	4.86	0.707	13.93	40.38
MEAN	93.62	67208	16481.0	30.7	4.94	0.707	13.92	36.51

Z	RESL	VSG	TEULK	(TW-TB)	NUTP	HTP
2.0	66371	33.35	92.47	7.92	552.7	5169.0
4.5	66579	34.05	92.76	8.69	503.9	4715.0
7.5	66829	34.93	93.10	8.81	496.9	4652.0
11.0	67121	36.01	93.50	9.09	481.4	4508.0
16.5	67582	37.85	94.13	9.25	473.1	4435.0
21.0	67960	39.50	94.64	9.46	462.6	4339.0
22.5	68086	40.08	94.82	9.48	461.2	4327.0

FROTH FLOW PATTERN:TEST NO.: A4.18

ML=3598 MG= 24.83 QFLUX= 41013 NUTP=502.2 HTP=4710 PDT= 6.691

PDF= 6.340 ALFA=0.586 XTT= 6.32 WE= 2986.0 FR=157.00

	TMIX	RESL	RESG	P	PRL	PRG	VSL	VSG
INLET	93.27	66951	18121.0	35.0	4.96	0.707	13.89	34.98
OUTLET	96.01	68967	18052.7	28.3	4.80	0.707	13.93	43.14
MEAN	94.64	67959	18087.1	31.6	4.88	0.707	13.93	38.96

Z	RESL	VSG	TEULK	(TW-TB)	NUTP	HTP
2.0	67118	35.56	93.50	7.64	572.1	5358.0
4.5	67327	36.31	93.78	8.36	523.3	4903.0
7.5	67579	37.26	94.12	8.49	515.1	4828.0
11.0	67872	38.42	94.52	8.74	500.2	4691.0
16.5	68335	40.41	95.15	9.05	483.0	4533.0
21.0	68714	42.19	95.67	9.10	480.1	4510.0
22.5	68841	42.82	95.84	9.10	480.3	4512.0

TEST NO.: A4.19 FLOW PATTERN:FRCTH

ML=3598 MG= 33.38 QFLUX= 46276 NUTP=506.1 HTP=4774 PDT= 7.436

PDF= 7.113 ALFA=0.619 XTT= 5.01 WE= 3005.0 FR=157.00

	TMIX	RESL	RESG	P	PRL	PRG	VSL	VSG
INLET	97.44	70028	24227.0	38.2	4.71	0.706	13.89	43.43
OUTLET	100.53	72339	24124.7	30.8	4.55	0.706	13.94	53.82
MEAN	98.99	71183	24176.0	34.5	4.63	0.706	13.94	48.49

Z	RESL	VSG	TBULK	(TW-TB)	NUTP	HTP
2.0	70219	44.17	97.70	8.18	599.5	5646.0
4.5	70458	45.13	98.02	9.10	538.9	5077.0
7.5	70747	46.33	98.41	9.29	527.9	4976.0
11.0	71083	47.81	98.86	9.55	513.5	4843.0
16.5	71614	50.34	99.57	10.03	488.8	4614.0
21.0	72049	52.61	100.15	11.22	437.3	4132.0
22.5	72195	53.41	100.34	10.15	482.8	4562.0

TEST NO.: A4.20 FLOW PATTERN:FRCTH

ML=3598 MG= 49.77 QFLUX= 45999 NUTP=532.9 HTP=5036 PDT= 8.988

PDF= 8.695 ALFA=0.655 XTT= 3.75 WE= 3011.0 FR=157.00

	TMIX	RESL	RESG	P	PRL	PRG	VSL	VSG
INLET	98.84	71071	36049.0	44.5	4.63	0.706	13.89	55.71
OUTLET	101.91	73379	35898.1	35.5	4.48	0.706	13.94	69.65
MEAN	100.38	72225	35973.6	40.0	4.56	0.706	13.94	62.48

Z	RESL	VSG	TBULK	(TW-TB)	NUTP	HTP
2.0	71262	56.69	99.10	7.71	631.3	5956.0
4.5	71501	57.97	99.42	8.62	564.6	5329.0
7.5	71789	59.57	99.80	8.98	542.1	5119.0
11.0	72125	61.56	100.25	9.23	527.3	4982.0
16.5	72655	64.95	100.95	9.47	514.1	4862.0
21.0	73090	68.01	101.53	9.72	500.5	4737.0
22.5	73235	69.09	101.72	9.70	501.2	4745.0

TEST NO.: A4.21 FLOW PATTERN:FRCTH

ML=3598 MG= 63.94 QFLUX= 46375 NUTP=540.2 HTP=5109 PDT=10.083

PDF= 9.807 ALFA=0.675 XTT= 3.15 WE= 3014.0 FR=157.00

	TMIX	RESL	RESG	P	PRL	PRG	VSL	VSG
INLET	99.40	71487	46276.0	49.3	4.60	0.706	13.89	64.69
OUTLET	102.49	73816	46081.5	39.2	4.45	0.706	13.94	81.13
MEAN	100.94	72651	46179.1	44.2	4.53	0.706	13.94	72.66

Z	RESL	VSG	TBULK	(TW-TB)	NUTP	HTP
2.0	71680	65.84	99.66	7.58	646.8	6107.0
4.5	71921	67.34	99.98	8.56	572.8	5410.0
7.5	72211	69.23	100.36	8.96	547.4	5173.0
11.0	72551	71.57	100.81	9.23	531.4	5025.0
16.5	73085	75.57	101.52	9.33	525.4	4973.0
21.0	73524	79.19	102.10	9.69	505.6	4789.0
22.5	73671	80.47	102.30	9.77	501.6	4752.0

TEST NO.: A4.22 FLOW PATTERN:FRCTH

ML=3598 MG= 95.21 QFLUX= 46350 NUTP=559.6 HTP=5289 PDT=11.665

PDF=11.412 ALFA=0.704 XTT= 2.40 WE= 3012.0 FR=157.00

	TMIX	RESL	RESG	P	PRL	PRG	VSL	VSG
INLET	98.88	71097	68955.0	58.2	4.63	0.706	13.89	81.42
OUTLET	101.96	73415	68665.7	46.6	4.48	0.706	13.94	101.56
MEAN	100.42	72256	68810.8	52.4	4.55	0.706	13.94	91.21

Z	RESL	VSG	TEULK	(TW-TB)	NUTP	HTP
2.0	71289	82.84	99.13	7.26	675.9	6377.0
4.5	71529	84.68	99.45	8.24	595.3	5619.0
7.5	71818	87.01	99.84	8.53	574.8	5428.0
11.0	72156	89.88	100.29	8.88	552.5	5221.0
16.5	72688	94.78	101.00	9.18	534.1	5051.0
21.0	73125	99.20	101.58	9.35	524.3	4962.0
22.5	73270	100.76	101.77	9.35	523.9	4960.0

TEST NO.: A4.23 FLOW PATTERN:FRCTH

ML=3598 MG=105.37 QFLUX= 46213 NUTP=558.6 HTP=5276 PDT=12.379

PDF=12.132 ALFA=0.710 XTT= 2.24 WE= 3009.0 FR=157.00

	TMIX	RESL	RESG	P	PRL	PRG	VSL	VSG
INLET	98.30	70667	76375.0	61.2	4.66	0.706	13.89	85.71
OUTLET	101.37	72972	76054.4	48.8	4.51	0.706	13.94	107.19
MEAN	99.84	71819	76214.8	55.0	4.58	0.706	13.94	96.14

Z	RESL	VSG	TEULK	(TW-TB)	NUTP	HTP
2.0	70857	87.22	98.56	7.14	685.1	6459.0
4.5	71096	89.18	98.88	8.26	592.9	5593.0
7.5	71384	91.65	99.26	8.52	574.5	5422.0
11.0	71719	94.71	99.71	8.90	550.2	5195.0
16.5	72248	99.94	100.41	9.21	531.0	5018.0
21.0	72683	104.66	100.99	9.31	525.2	4967.0
22.5	72828	106.33	101.18	9.36	522.5	4943.0

TEST NO.: A5. 1 FLOW PATTERN:BUBBLE

ML=5397 MG= 0.41 QFLUX= 44522 NUTP=441.9 HTP=4145 PDT= 3.624

PDF= 2.815 ALFA=0.044 XTT=291.59 WE= 6719.0 FR=353.00

	TMIX	RESL	RESG	P	PRL	PRG	VSL	VSG
INLET	93.68	100880	299.6	22.0	4.93	0.707	20.84	0.92
OUTLET	95.67	103072	298.7	18.4	4.82	0.707	20.89	1.10
MEAN	94.68	101976	299.1	20.2	4.88	0.707	20.89	1.01

Z	RESL	VSG	TEULK	(TW-TB)	NUTP	HTP
2.0	101062	0.93	93.85	9.90	479.5	4493.0
4.5	101290	0.95	94.06	10.45	454.4	4259.0
7.5	101563	0.97	94.30	10.63	446.6	4187.0
11.0	101883	1.00	94.59	10.77	440.8	4134.0
16.5	102386	1.04	95.05	10.93	434.1	4074.0
21.0	102798	1.08	95.42	11.10	427.4	4013.0
22.5	102935	1.09	95.55	11.08	428.2	4021.0

TEST NO.: A5. 2 FLOW PATTERN:BUBBLE

ML=5397 MG= 1.38 QFLUX= 30491 NUTP=459.6 HTP=4322 PDT= 3.984

PDF= 3.242 ALFA=0.123 XTT=100.34 WE= 6738.0 FR=354.00

	TMIX	RESL	RESG	P	PRL	PRG	VSL	VSG
INLET	95.88	103299	1005.0	23.4	4.80	0.707	20.84	2.92
OUTLET	97.24	104811	1003.4	19.4	4.73	0.707	20.90	3.51
MEAN	96.56	104055	1004.3	21.4	4.77	0.707	20.90	3.21

Z	RESL	VSG	TBULK	(TW-TB)	NUTP	HTP
2.0	103425	2.97	95.99	6.61	490.4	4608.0
4.5	103582	3.02	96.13	7.09	457.4	4298.0
7.5	103771	3.09	96.30	7.15	453.4	4262.0
11.0	103991	3.18	96.50	7.10	456.6	4293.0
16.5	104338	3.32	96.81	7.03	461.3	4339.0
21.0	104622	3.44	97.07	7.08	458.0	4310.0
22.5	104717	3.49	97.15	7.10	456.8	4298.0

TEST NO.: A5. 3 FLOW PATTERN:BUBBLE

ML=5397 MG= 1.67 QFLUX= 30466 NUTP=478.9 HTP=4497 PDT= 4.087

PDF= 3.361 ALFA=0.141 XTT= 85.59 WE= 6727.0 FR=353.00

	TMIX	RESL	RESG	P	PRL	PRG	VSL	VSG
INLET	94.80	102108	1217.0	23.9	4.87	0.707	20.84	3.46
OUTLET	96.16	103613	1215.1	19.8	4.79	0.707	20.89	4.16
MEAN	95.48	102860	1216.2	21.9	4.83	0.707	20.89	3.80

Z	RESL	VSG	TBULK	(TW-TB)	NUTP	HTP
2.0	102233	3.51	94.91	6.28	516.9	4850.0
4.5	102390	3.57	95.05	6.57	494.0	4636.0
7.5	102577	3.66	95.22	6.69	484.8	4551.0
11.0	102797	3.76	95.42	6.82	475.6	4466.0
16.5	103142	3.93	95.73	6.93	468.1	4397.0
21.0	103424	4.08	95.99	6.94	467.6	4393.0
22.5	103519	4.13	96.07	6.86	472.6	4441.0

TEST NO.: A5. 4 FLOW PATTERN:BUBBLE

ML=5397 MG= 2.13 QFLUX= 30225 NUTP=484.1 HTP=4546 PDT= 4.251

PDF= 3.544 ALFA=0.164 XTT= 70.41 WE= 6727.0 FR=353.00

	TMIX	RESL	RESG	P	PRL	PRG	VSL	VSG
INLET	94.80	102106	1550.0	25.0	4.87	0.707	20.84	4.22
OUTLET	96.15	103599	1547.3	20.7	4.79	0.707	20.89	5.06
MEAN	95.47	102853	1548.7	22.8	4.83	0.707	20.89	4.63

Z	RESL	VSG	TBULK	(TW-TB)	NUTP	HTP
2.0	102230	4.28	94.91	6.25	515.1	4833.0
4.5	102385	4.36	95.05	6.49	496.2	4656.0
7.5	102572	4.45	95.22	6.52	493.7	4634.0
11.0	102789	4.58	95.42	6.68	481.8	4523.0
16.5	103132	4.78	95.73	6.77	475.3	4464.0
21.0	103412	4.96	95.98	6.82	471.6	4431.0
22.5	103506	5.03	96.06	6.83	470.9	4425.0

TEST NO.: A5. 5 FLOW PATTERN:BUBBLE

ML=5397 MG= 2.31 QFLUX= 30465 NUTP=486.6 HTP=4569 PDT= 4.333

PDF= 3.633 ALFA=0.173 XTT= 65.91 WE= 6728.0 FR=353.00

	TMIX	RESL	RESG	P	PRL	PRG	VSL	VSG
INLET	94.84	102153	1679.0	25.3	4.86	0.707	20.84	4.51
OUTLET	96.20	103658	1676.8	21.0	4.79	0.707	20.89	5.42
MEAN	95.52	102905	1678.4	23.1	4.83	0.707	20.89	4.95

Z	RESL	VSG	TEULK	(TW-TB)	NUTP	HTP
2.0	102278	4.57	94.95	6.26	518.5	4865.0
4.5	102435	4.66	95.09	6.51	498.7	4680.0
7.5	102622	4.77	95.26	6.67	486.2	4564.0
11.0	102842	4.90	95.46	6.72	483.0	4535.0
16.5	103187	5.12	95.77	6.71	483.4	4540.0
21.0	103470	5.31	96.03	6.81	476.1	4473.0
22.5	103564	5.38	96.12	6.82	475.4	4467.0

TEST NO.: A5. 6 FLOW PATTERN:BUBBLE-FROTH

ML=5397 MG= 4.88 QFLUX= 33646 NUTP=498.5 HTP=4687 PDT= 4.971

PDF= 4.348 ALFA=0.264 XTT= 35.85 WE= 6736.0 FR=353.00

	TMIX	RESL	RESG	P	PRL	PRG	VSL	VSG
INLET	95.65	103047	3552.0	29.0	4.82	0.707	20.84	8.34
OUTLET	97.15	104714	3545.1	24.0	4.74	0.707	20.90	10.03
MEAN	96.40	103881	3548.8	26.5	4.78	0.707	20.90	9.17

Z	RESL	VSG	TEULK	(TW-TB)	NUTP	HTP
2.0	103186	8.46	95.77	6.61	541.3	5084.0
4.5	103359	8.62	95.93	6.93	516.5	4853.0
7.5	103567	8.82	96.12	6.98	512.5	4816.0
11.0	103810	9.06	96.34	7.28	491.6	4622.0
16.5	104193	9.47	96.68	7.34	487.5	4584.0
21.0	104506	9.84	96.96	7.43	481.8	4533.0
22.5	104610	9.96	97.06	7.42	482.4	4539.0

TEST NO.: A5. 7 FLOW PATTERN:BUBBLE-FROTH

ML=5397 MG= 6.95 QFLUX= 33703 NUTP=500.1 HTP=4703 PDT= 5.508

PDF= 4.928 ALFA=0.315 XTT= 26.82 WE= 6740.0 FR=354.00

	TMIX	RESL	RESG	P	PRL	PRG	VSL	VSG
INLET	95.99	103421	5056.0	30.8	4.80	0.707	20.84	11.18
OUTLET	97.49	105093	5045.6	25.3	4.72	0.706	20.90	13.56
MEAN	96.74	104257	5050.9	28.1	4.76	0.707	20.90	12.34

Z	RESL	VSG	TEULK	(TW-TB)	NUTP	HTP
2.0	103560	11.35	96.11	6.45	555.6	5221.0
4.5	103733	11.57	96.27	6.95	515.3	4843.0
7.5	103942	11.85	96.46	7.02	510.5	4800.0
11.0	104186	12.19	96.68	7.25	494.1	4647.0
16.5	104569	12.77	97.02	7.34	487.9	4591.0
21.0	104884	13.28	97.30	7.39	485.0	4565.0
22.5	104989	13.46	97.40	7.41	483.6	4552.0

TEST NO.: A5. 8 FLOW PATTERN:FROTH

ML=5397 MG= 8.70 QFLUX= 33718 NUTP=514.2 HTP=4842 PDT= 5.948

PDF= 5.395 ALFA=0.347 XTT= 22.40 WE= 6749.0 FR=354.00

	TMIX	RESL	RESG	P	PRL	PRG	VSL	VSG
INLET	96.93	104465	6319.0	32.4	4.74	0.707	20.84	13.33
OUTLET	98.43	106144	6306.3	26.4	4.66	0.706	20.90	16.26
MEAN	97.68	105304	6312.8	29.4	4.70	0.706	20.90	14.76

Z	RESL	VSG	TEULK	(TW-TB)	NUTP	HTP
2.0	104604	13.54	97.05	6.18	579.1	5449.0
4.5	104779	13.81	97.21	6.82	524.8	4939.0
7.5	104988	14.16	97.40	7.04	509.0	4792.0
11.0	105233	14.58	97.62	7.06	507.4	4777.0
16.5	105618	15.29	97.96	6.97	513.7	4839.0
21.0	105934	15.92	98.24	7.20	497.2	4686.0
22.5	106039	16.15	98.34	7.15	500.8	4720.0

TEST NO.: A5. 9 FLOW PATTERN:FROTH

ML=5397 MG= 13.47 QFLUX= 33223 NUTP=514.9 HTP=4821 PDT= 6.932

PDF= 6.428 ALFA=0.405 XTT= 16.11 WE= 6705.0 FR=353.00

	TMIX	RESL	RESG	P	PRL	PRG	VSL	VSG
INLET	92.52	99609	9838.0	36.3	5.00	0.707	20.84	18.28
OUTLET	94.01	101234	9818.3	29.3	4.92	0.707	20.89	22.49
MEAN	93.26	100422	9828.4	32.8	4.96	0.707	20.88	20.33

Z	RESL	VSG	TEULK	(TW-TB)	NUTP	HTP
2.0	99744	18.58	92.65	5.88	603.6	5647.0
4.5	99913	18.97	92.80	6.68	530.9	4967.0
7.5	100116	19.46	92.99	6.81	521.4	4880.0
11.0	100353	20.06	93.20	6.92	513.0	4803.0
16.5	100725	21.08	93.54	7.07	502.1	4703.0
21.0	101031	22.00	93.82	7.28	487.2	4565.0
22.5	101133	22.32	93.91	7.27	487.7	4570.0

TEST NO.: A5.10 FLOW PATTERN:FROTH

ML=5397 MG= 19.14 QFLUX= 33255 NUTP=524.1 HTP=4918 PDT= 8.151

PDF= 7.683 ALFA=0.448 XTT= 12.40 WE= 6722.0 FR=353.00

	TMIX	RESL	RESG	P	PRL	PRG	VSL	VSG
INLET	94.24	101488	13948.0	40.9	4.90	0.707	20.84	23.09
OUTLET	95.72	103126	13919.8	32.8	4.82	0.707	20.89	28.68
MEAN	94.98	102307	13934.1	36.9	4.86	0.707	20.89	25.81

Z	RESL	VSG	TEULK	(TW-TB)	NUTP	HTP
2.0	101624	23.48	94.36	5.95	595.5	5584.0
4.5	101794	24.00	94.51	6.45	549.5	5153.0
7.5	101999	24.64	94.70	6.61	536.0	5028.0
11.0	102237	25.44	94.92	6.83	519.0	4870.0
16.5	102613	26.80	95.26	6.92	512.1	4807.0
21.0	102921	28.03	95.53	7.16	495.2	4650.0
22.5	103024	28.46	95.63	7.29	485.8	4562.0

TEST NO.: A5.11 FLOW PATTERN:FRCTH

ML=5397 MG= 27.20 QFLUX= 33215 NUTP=542.5 HTP=5096 PDT= 9.341

PDF= 8.908 ALFA=0.489 XTT= 9.60 WE= 6729.0 FR=353.00

	TMIX	RESL	RESG	P	PRL	PRG	VSL	VSG
INLET	94.95	102278	19809.0	46.4	4.86	0.707	20.84	29.00
OUTLET	96.43	103918	19768.8	37.1	4.78	0.707	20.90	36.13
MEAN	95.69	103098	19789.1	41.7	4.82	0.707	20.89	32.46

Z	RESL	VSG	TBULK	(TW-TB)	NUTP	HTP
2.0	102414	29.50	95.08	5.63	628.1	5895.0
4.5	102585	30.15	95.23	6.18	572.1	5371.0
7.5	102789	30.98	95.42	6.25	565.9	5313.0
11.0	103028	31.99	95.63	6.58	537.4	5047.0
16.5	103405	33.72	95.97	6.82	518.6	4873.0
21.0	103713	35.29	96.25	6.91	511.8	4811.0
22.5	103816	35.84	96.34	7.02	503.3	4731.0

TEST NO.: A5.12 FLOW PATTERN:FROTH

ML=5397 MG= 41.80 QFLUX= 33706 NUTP=555.5 HTP=5231 PDT=10.887

PDF=10.494 ALFA=0.536 XTT= 7.03 WE= 6749.0 FR=354.00

	TMIX	RESL	RESG	P	PRL	PRG	VSL	VSG
INLET	96.90	104437	30354.0	54.2	4.74	0.707	20.84	38.24
OUTLET	98.40	106113	30292.1	43.4	4.67	0.706	20.90	47.60
MEAN	97.65	105275	30323.4	48.8	4.71	0.706	20.90	42.79

Z	RESL	VSG	TBULK	(TW-TB)	NUTP	HTP
2.0	104576	38.90	97.03	5.39	664.4	6251.0
4.5	104751	39.76	97.18	6.09	587.5	5529.0
7.5	104960	40.84	97.37	6.30	567.8	5345.0
11.0	105204	42.17	97.59	6.54	547.6	5156.0
16.5	105588	44.45	97.93	6.66	537.4	5063.0
21.0	105903	46.51	98.22	6.91	517.8	4879.0
22.5	106008	47.23	98.31	6.85	522.4	4924.0

TEST NO.: A6. 1 FLOW PATTERN:BUBBLE

ML=7196 MG= 0.49 QFLUX= 33438 NUTP=518.4 HTP=4873 PDT= 5.441

PDF= 4.625 ALFA=0.034 XTT=350.16 WE= 11975.0 FR=629.00

	TMIX	RESL	RESG	P	PRL	PRG	VSL	VSG
INLET	95.84	137674	352.7	26.3	4.81	0.707	27.78	0.91
OUTLET	96.96	139331	352.2	20.9	4.75	0.707	27.86	1.14
MEAN	96.40	138502	352.4	23.6	4.78	0.707	27.86	1.02

Z	RESL	VSG	TBULK	(TW-TB)	NUTP	HTP
2.0	137811	0.93	95.93	6.17	576.5	5417.0
4.5	137984	0.95	96.05	6.76	526.4	4947.0
7.5	138191	0.98	96.19	6.72	529.1	4973.0
11.0	138432	1.01	96.35	6.88	516.6	4856.0
16.5	138812	1.07	96.61	7.00	507.8	4775.0
21.0	139124	1.12	96.82	7.11	500.3	4706.0
22.5	139228	1.14	96.89	7.13	498.6	4690.0

TEST NO.: A6. 2 FLOW PATTERN:BUBBLE

ML=7196 MG= 1.00 QFLUX= 33446 NUTP=538.6 HTP=5068 PDT= 5.752

PDF= 4.961 ALFA=0.064 XTT=185.93 WE= 11988.0 FR=629.00

	TMIX	RESL	RESG	P	PRL	PRG	VSL	VSG
INLET	96.52	138689	727.1	27.4	4.77	0.707	27.78	1.81
OUTLET	97.64	140351	726.0	21.7	4.71	0.706	27.87	2.27
MEAN	97.08	139520	726.6	24.6	4.74	0.707	27.86	2.03

Z	RESL	VSG	TBULK	(TW-TB)	NUTP	HTP
2.0	138827	1.84	96.62	6.10	582.4	5477.0
4.5	139000	1.88	96.73	6.57	540.7	5085.0
7.5	139208	1.94	96.87	6.63	535.8	5040.0
11.0	139450	2.00	97.04	6.61	537.8	5061.0
16.5	139831	2.11	97.29	6.58	540.2	5084.0
21.0	140143	2.22	97.50	6.78	524.3	4936.0
22.5	140247	2.26	97.57	6.82	520.8	4904.0

TEST NO.: A6. 3 FLOW PATTERN:BUBBLE

ML=7196 MG= 1.38 QFLUX= 33459 NUTP=542.2 HTP=5107 PDT= 5.902

PDF= 5.125 ALFA=0.081 XTT=143.48 WE= 12000.0 FR=629.00

	TMIX	RESL	RESG	P	PRL	PRG	VSL	VSG
INLET	97.21	139707	1002.0	29.1	4.73	0.706	27.78	2.35
OUTLET	98.33	141374	1000.5	23.2	4.67	0.706	27.87	2.93
MEAN	97.77	140540	1001.3	26.2	4.70	0.706	27.87	2.64

Z	RESL	VSG	TBULK	(TW-TB)	NUTP	HTP
2.0	139845	2.39	97.30	6.07	585.4	5510.0
4.5	140019	2.45	97.42	6.41	553.9	5214.0
7.5	140227	2.51	97.56	6.37	557.8	5252.0
11.0	140470	2.60	97.72	6.65	534.5	5034.0
16.5	140852	2.74	97.98	6.71	529.4	4988.0
21.0	141166	2.86	98.19	6.66	533.6	5028.0
22.5	141270	2.91	98.26	6.74	526.7	4963.0

TEST NO.: A6. 4 FLOW PATTERN:BUBBLE

ML=7196 MG= 1.76 QFLUX= 33471 NUTP=548.8 HTP=5174 PDT= 6.064

PDF= 5.302 ALFA=0.098 XTT=116.54 WE= 12012.0 FR=629.00

	TMIX	RESL	RESG	P	PRL	PRG	VSL	VSG
INLET	97.90	140726	1275.0	29.8	4.69	0.706	27.78	2.93
OUTLET	99.02	142398	1273.1	23.7	4.63	0.706	27.87	3.66
MEAN	98.46	141562	1274.1	26.8	4.66	0.706	27.87	3.29

Z	RESL	VSG	TBULK	(TW-TB)	NUTP	HTP
2.0	140865	2.98	97.99	5.85	607.3	5722.0
4.5	141039	3.05	98.11	6.31	563.1	5305.0
7.5	141248	3.13	98.25	6.33	560.5	5282.0
11.0	141492	3.24	98.41	6.48	548.3	5168.0
16.5	141875	3.41	98.67	6.70	529.6	4993.0
21.0	142189	3.57	98.88	6.65	533.7	5034.0
22.5	142294	3.63	98.95	6.57	540.2	5096.0

TEST NO.: A6. 5 FLOW PATTERN:BUBBLE-FROTH

ML=7196 MG= 2.13 QFLUX= 33487 NUTP=544.3 HTP=5136 PDT= 6.242

PDF= 5.493 ALFA=0.113 XTT= 98.97 WE= 12025.0 FR=629.00

	TMIX	RESL	RESG	P	PRL	PRG	VSL	VSG
INLET	98.62	141812	1545.0	30.5	4.65	0.706	27.78	3.48
OUTLET	99.75	143489	1543.1	24.3	4.59	0.706	27.88	4.34
MEAN	99.18	142650	1544.3	27.4	4.62	0.706	27.87	3.90

Z	RESL	VSG	TEULK	(TW-TB)	NUTP	HTP
2.0	141951	3.54	98.72	6.06	585.3	5520.0
4.5	142126	3.62	98.83	6.45	550.3	5190.0
7.5	142335	3.72	98.97	6.41	553.3	5219.0
11.0	142580	3.84	99.14	6.53	543.1	5124.0
16.5	142964	4.05	99.39	6.67	532.3	5024.0
21.0	143279	4.24	99.61	6.62	535.6	5057.0
22.5	143385	4.31	99.68	6.61	537.1	5071.0

TEST NO.: A6. 6 FLOW PATTERN:BUBBLE-FROTH

ML=7196 MG= 2.46 QFLUX= 33952 NUTP=561.9 HTP=5306 PDT= 6.404

PDF= 5.666 ALFA=0.125 XTT= 88.01 WE= 12034.0 FR=630.00

	TMIX	RESL	RESG	P	PRL	PRG	VSL	VSG
INLET	99.14	142579	1780.0	31.3	4.62	0.706	27.78	3.92
OUTLET	100.27	144283	1777.3	24.9	4.56	0.706	27.88	4.90
MEAN	99.71	143431	1778.7	28.1	4.59	0.706	27.88	4.40

Z	RESL	VSG	TEULK	(TW-TB)	NUTP	HTP
2.0	142720	3.99	99.23	5.95	604.6	5705.0
4.5	142898	4.08	99.35	6.28	572.6	5404.0
7.5	143110	4.19	99.49	6.33	568.4	5365.0
11.0	143359	4.33	99.66	6.45	557.1	5260.0
16.5	143750	4.57	99.92	6.49	554.1	5234.0
21.0	144070	4.78	100.13	6.54	550.0	5196.0
22.5	144177	4.86	100.20	6.52	551.6	5211.0

TEST NO.: A6. 7 FLOW PATTERN:FROTH

ML=7196 MG= 2.84 QFLUX= 34069 NUTP=565.1 HTP=5341 PDT= 6.570

PDF= 5.841 ALFA=0.137 XTT= 78.42 WE= 12047.0 FR=630.00

	TMIX	RESL	RESG	P	PRL	PRG	VSL	VSG
INLET	99.86	143668	2051.0	32.2	4.58	0.706	27.78	4.40
OUTLET	101.00	145383	2048.6	25.6	4.52	0.706	27.88	5.49
MEAN	100.43	144525	2050.2	28.9	4.55	0.706	27.88	4.93

Z	RESL	VSG	TEULK	(TW-TB)	NUTP	HTP
2.0	143810	4.47	99.96	5.94	606.3	5727.0
4.5	143989	4.57	100.08	6.18	583.1	5508.0
7.5	144203	4.70	100.22	6.26	575.8	5441.0
11.0	144453	4.86	100.39	6.40	563.4	5325.0
16.5	144846	5.12	100.65	6.52	552.6	5224.0
21.0	145168	5.36	100.86	6.56	549.4	5196.0
22.5	145276	5.45	100.93	6.68	539.9	5106.0

TEST NO.: A6. 8 FLOW PATTERN:FROTH

ML=7196 MG= 6.33 QFLUX= 33263 NUTP=577.7 HTP=5428 PDT= 7.606

PDF= 6.943 ALFA=0.217 XTT= 42.14 WE= 11968.0 FR=629.00

	TMIX	RESL	RESG	P	PRL	PRG	VSL	VSG
INLET	95.40	137020	4606.0	38.6	4.83	0.707	27.78	8.13
OUTLET	96.51	138666	4599.9	30.9	4.77	0.707	27.86	10.07
MEAN	95.95	137843	4603.4	34.8	4.80	0.707	27.86	9.07

Z	RESL	VSG	TBULK	(TW-TB)	NUTP	HTP
2.0	137157	8.26	95.49	5.56	636.6	5978.0
4.5	137328	8.44	95.60	5.91	599.2	5627.0
7.5	137534	8.66	95.74	6.10	580.8	5455.0
11.0	137774	8.94	95.91	6.15	575.2	5404.0
16.5	138151	9.41	96.16	6.26	565.8	5317.0
21.0	138460	9.84	96.37	6.33	559.0	5255.0
22.5	138563	9.99	96.44	6.36	556.8	5235.0

TEST NO.: A6. 9 FLOW PATTERN:FROTH

ML=7196 MG= 9.88 QFLUX= 33408 NUTP=592.0 HTP=5580 PDT= 8.490

PDF= 7.874 ALFA=0.272 XTT= 29.50 WE= 12009.0 FR=629.00

	TMIX	RESL	RESG	P	PRL	PRG	VSL	VSG
INLET	97.75	140510	7164.0	42.5	4.70	0.706	27.78	11.54
OUTLET	98.87	142177	7153.3	34.1	4.64	0.706	27.87	14.33
MEAN	98.31	141343	7158.8	38.3	4.67	0.706	27.87	12.90

Z	RESL	VSG	TBULK	(TW-TB)	NUTP	HTP
2.0	140648	11.74	97.84	5.30	668.4	6296.0
4.5	140822	11.99	97.96	5.76	615.0	5794.0
7.5	141030	12.31	98.10	5.89	602.1	5674.0
11.0	141273	12.71	98.26	6.10	580.9	5475.0
16.5	141655	13.39	98.52	6.12	578.8	5457.0
21.0	141969	14.01	98.73	6.19	572.9	5403.0
22.5	142073	14.22	98.80	6.25	566.8	5346.0

TEST NO.: A6.10 FLOW PATTERN:FROTH

ML=7196 MG= 15.97 QFLUX= 33333 NUTP=596.8 HTP=5635 PDT= 9.744

PDF= 9.182 ALFA=0.335 XTT= 20.28 WE= 12033.0 FR=630.00

	TMIX	RESL	RESG	P	PRL	PRG	VSL	VSG
INLET	99.11	142539	11562.0	48.1	4.62	0.706	27.78	16.54
OUTLET	100.23	144212	11544.9	38.4	4.57	0.706	27.88	20.62
MEAN	99.67	143376	11553.7	43.2	4.59	0.706	27.88	18.52

Z	RESL	VSG	TBULK	(TW-TB)	NUTP	HTP
2.0	142678	16.83	99.20	5.24	673.2	6352.0
4.5	142852	17.20	99.32	5.73	616.6	5819.0
7.5	143061	17.67	99.46	5.88	600.4	5667.0
11.0	143305	18.25	99.62	5.97	591.4	5584.0
16.5	143688	19.24	99.88	6.04	584.4	5519.0
21.0	144003	20.14	100.09	6.10	578.3	5463.0
22.5	144107	20.46	100.16	6.19	570.2	5387.0

TEST NO.: A6.11 FLOW PATTERN:FRCTH

ML=7196 MG= 20.78 QFLUX= 33285 NUTP=612.4 HTP=5784 PDT=10.480

PDF= 9.945 ALFA=0.368 XTT= 16.67 WE= 12038.0 FR=630.00

	TMIX	RESL	RESG	P	PRL	PRG	VSL	VSG
INLET	99.36	142913	15042.0	52.2	4.61	0.706	27.78	19.84
OUTLET	100.47	144584	15019.7	41.7	4.55	0.706	27.88	24.68
MEAN	99.92	143749	15031.1	47.0	4.58	0.706	27.88	22.20

Z	RESL	VSG	TBULK	(TW-TB)	NUTP	HTP
2.0	143052	20.18	99.45	5.24	672.5	6347.0
4.5	143226	20.63	99.57	5.47	644.2	6081.0
7.5	143435	21.19	99.71	5.66	623.0	5882.0
11.0	143678	21.88	99.87	5.78	609.9	5761.0
16.5	144061	23.05	100.13	5.90	597.1	5641.0
21.0	144375	24.12	100.34	6.05	582.6	5506.0
22.5	144480	24.49	100.41	6.03	584.3	5522.0

FROTH FLOW PATTERN:TEST NO.: A6.12

ML=7196 MG= 28.40 QFLUX= 33279 NUTP=621.7 HTP=5870 PDT=11.513

PDF=11.010 ALFA=0.405 XTT= 13.29 WE= 12034.0 FR=630.00

	TMIX	RESL	RESG	P	PRL	PRG	VSL	VSG
INLET	99.18	142643	20559.0	58.1	4.62	0.706	27.78	24.37
OUTLET	100.29	144312	20527.7	46.6	4.56	0.706	27.88	30.22
MEAN	99.74	143478	20543.4	52.3	4.59	0.706	27.88	27.21

Z	RESL	VSG	TBULK	(TW-TB)	NUTP	HTP
2.0	142782	24.78	99.27	4.98	707.6	6678.0
4.5	142955	25.32	99.39	5.40	652.8	6161.0
7.5	143164	25.99	99.53	5.43	649.2	6129.0
11.0	143407	26.83	99.69	5.66	622.2	5874.0
16.5	143790	28.25	99.95	5.99	588.6	5559.0
21.0	144104	29.53	100.15	5.99	588.5	5560.0
22.5	144208	29.99	100.22	5.91	596.4	5635.0

TEST NO.: A6.13 FLOW PATTERN:FRCTH

ML=7196 MG= 32.28 QFLUX= 33228 NUTP=613.5 HTP=5792 PDT=11.948

PDF=11.457 ALFA=0.421 XTT= 12.11 WE= 12033.0 FR=630.00

	TMIX	RESL	RESG	P	PRL	PRG	VSL	VSG
INLET	99.09	142508	23373.0	60.7	4.62	0.706	27.78	26.51
OUTLET	100.20	144174	23337.5	48.7	4.57	0.706	27.88	32.83
MEAN	99.65	143341	23355.3	54.7	4.59	0.706	27.88	29.59

Z	RESL	VSG	TBULK	(TW-TB)	NUTP	HTP
2.0	142647	26.96	99.18	5.07	693.4	6543.0
4.5	142820	27.54	99.30	5.44	646.7	6103.0
7.5	143028	28.27	99.44	5.58	631.2	5958.0
11.0	143271	29.17	99.60	5.73	614.3	5800.0
16.5	143653	30.71	99.85	6.00	586.5	5539.0
21.0	143966	32.10	100.06	6.05	581.3	5492.0
22.5	144070	32.58	100.13	6.01	585.0	5527.0

TEST NO.: A6.14 FLOW PATTERN:FROTH

ML=7196 MG= 53.07 QFLUX= 33310 NUTP=606.1 HTP=5715 PDT=14.636

PDF=14.187 ALFA=0.471 XTT= 8.65 WE= 12016.0 FR=629.00

	TMIX	RESL	RESG	P	PRL	PRG	VSL	VSG
INLET	98.13	141071	38479.0	75.4	4.68	C.706	27.78	35.03
OUTLET	99.24	142734	38420.3	60.7	4.62	C.706	27.87	43.23
MEAN	98.68	141903	38449.7	68.0	4.65	C.706	27.87	39.02

Z	RESL	VSG	TBULK	(TW-TB)	NUTP	HTP
2.0	141210	35.61	98.22	4.96	712.7	6717.0
4.5	141383	36.37	98.34	5.55	636.0	5995.0
7.5	141590	37.32	98.48	5.68	622.2	5865.0
11.0	141833	38.49	98.64	5.86	602.6	5682.0
16.5	142214	40.48	98.89	6.04	584.7	5515.0
21.0	142526	42.28	99.10	6.23	567.0	5349.0
22.5	142631	42.91	99.17	6.20	569.5	5373.0

TEST NO.: A6.15 FLOW PATTERN:FROTH

ML=7196 MG= 68.61 QFLUX= 33315 NUTP=591.7 HTP=5580 PDT=15.146

PDF=14.728 ALFA=0.507 XTT= 7.04 WE= 12017.0 FR=629.00

	TMIX	RESL	RESG	P	PRL	PRG	VSL	VSG
INLET	98.19	141168	49740.0	79.1	4.67	C.706	27.78	43.17
OUTLET	99.31	142831	49665.0	63.9	4.62	C.706	27.87	53.11
MEAN	98.75	141999	49702.9	71.5	4.64	0.706	27.87	48.02

Z	RESL	VSG	TBULK	(TW-TB)	NUTP	HTP
2.0	141306	43.88	98.29	5.02	704.0	6635.0
4.5	141479	44.80	98.40	5.64	626.7	5908.0
7.5	141687	45.95	98.54	5.75	614.4	5793.0
11.0	141929	47.37	98.70	6.04	585.0	5517.0
16.5	142311	49.79	98.96	6.26	564.4	5324.0
21.0	142623	51.96	99.17	6.37	554.1	5228.0
22.5	142727	52.72	99.24	6.43	549.3	5183.0

TEST NO.: A7. 1 FLOW PATTERN:BUBBLE

ML=8995 MG= 0.45 QFLUX= 74871 NUTP=601.0 HTP=5485 PDT= 8.154

PDF= 7.319 ALFA=0.019 XTT=551.96 WE= 18128.0 FR=977.00

	TMIX	RESL	RESG	P	PRL	PRG	VSL	VSG
INLET	73.02	131834	342.0	35.9	6.48	0.710	34.73	0.60
OUTLET	75.02	135221	341.0	27.7	6.31	C.709	34.72	0.78
MEAN	74.02	133528	341.5	31.8	6.40	C.709	34.71	0.69

Z	RESL	VSG	TBULK	(TW-TB)	NUTP	HTP
2.0	132115	0.61	73.18	13.08	627.1	5716.0
4.5	132467	0.63	73.39	13.44	610.5	5566.0
7.5	132889	0.65	73.64	13.59	603.9	5509.0
11.0	133383	0.67	73.94	13.67	600.3	5477.0
16.5	134160	0.72	74.40	13.80	594.2	5425.0
21.0	134797	0.75	74.77	13.87	591.0	5399.0
22.5	135010	0.77	74.90	13.65	600.4	5486.0

TEST NO.: A7. 2 FLOW PATTERN:BUBBLE

ML=8995 MG= 0.69 QFLUX= 77345 NUTP=600.4 HTP=5468 PDT= 8.050

PDF= 7.225 ALFA=0.031 XTT=360.67 WE= 18089.0 FR=976.00

	TMIX	RESL	RESG	P	PRL	PRG	VSL	VSG
INLET	71.38	129085	515.8	32.2	6.63	0.710	34.73	1.01
OUTLET	73.45	132560	514.2	24.1	6.45	0.710	34.71	1.34
MEAN	72.41	130822	515.0	28.1	6.54	0.710	34.71	1.16

Z	RESL	VSG	TBULK	(TW-TB)	NUTP	HTP
2.0	129373	1.03	71.55	13.64	622.7	5664.0
4.5	129734	1.06	71.76	13.98	607.6	5528.0
7.5	130167	1.10	72.02	14.03	605.3	5509.0
11.0	130674	1.14	72.33	14.16	599.9	5462.0
16.5	131471	1.22	72.80	14.34	592.3	5396.0
21.0	132125	1.30	73.19	14.29	594.1	5415.0
22.5	132343	1.32	73.32	14.17	599.0	5461.0

TEST NO.: A7. 3 FLOW PATTERN:BUBBLE

ML=8995 MG= 1.06 QFLUX= 77332 NUTP=609.1 HTP=5545 PDT= 8.281

PDF= 7.469 ALFA=0.046 XTT=247.39 WE= 18086.0 FR=976.00

	TMIX	RESL	RESG	P	PRL	PRG	VSL	VSG
INLET	71.29	128936	797.3	33.1	6.64	0.710	34.73	1.51
OUTLET	73.36	132410	794.9	24.8	6.46	0.710	34.71	2.01
MEAN	72.32	130673	796.1	29.0	6.55	0.710	34.71	1.75

Z	RESL	VSG	TBULK	(TW-TB)	NUTP	HTP
2.0	129225	1.55	71.46	13.49	629.9	5729.0
4.5	129585	1.59	71.68	13.81	614.9	5594.0
7.5	130018	1.64	71.93	13.88	612.1	5570.0
11.0	130524	1.71	72.24	13.92	610.2	5555.0
16.5	131321	1.83	72.71	14.07	603.3	5495.0
21.0	131975	1.94	73.10	14.14	600.2	5470.0
22.5	132193	1.98	73.23	13.99	606.5	5529.0

TEST NO.: A7. 4 FLOW PATTERN:BUBBLE

ML=8995 MG= 1.93 QFLUX= 77318 NUTP=617.4 HTP=5621 PDT= 8.714

PDF= 7.923 ALFA=0.071 XTT=152.93 WE= 18084.0 FR=976.00

	TMIX	RESL	RESG	P	PRL	PRG	VSL	VSG
INLET	71.20	128788	1453.0	37.0	6.65	0.710	34.73	2.47
OUTLET	73.27	132259	1449.2	28.3	6.47	0.710	34.71	3.22
MEAN	72.23	130523	1451.4	32.6	6.56	0.710	34.71	2.83

Z	RESL	VSG	TBULK	(TW-TB)	NUTP	HTP
2.0	129076	2.52	71.37	13.27	639.9	5819.0
4.5	129436	2.59	71.59	13.62	623.9	5675.0
7.5	129869	2.67	71.85	13.69	620.5	5646.0
11.0	130375	2.78	72.15	13.79	615.7	5605.0
16.5	131171	2.96	72.62	13.89	611.4	5569.0
21.0	131824	3.12	73.01	13.91	610.0	5560.0
22.5	132042	3.18	73.14	13.63	622.3	5672.0

TEST NO.: A7. 5 FLOW PATTERN:BUBBLE

ML=8995 MG= 2.45 QFLUX= 80316 NUTP=615.2 HTP=5606 PDT= 8.911

PDF= 8.132 ALFA=0.085 XTT=125.62 WE= 18102.0 FR=976.00

	TMIX	RESL	RESG	P	PRL	PRG	VSL	VSG
INLET	71.86	129900	1844.C	38.4	6.59	C.710	34.73	3.02
OUTLET	74.01	133516	1839.1	29.5	6.40	C.709	34.71	3.92
MEAN	72.94	131708	1842.C	34.0	6.49	C.710	34.71	3.45

Z	RESL	VSG	TBULK	(TW-TB)	NUTP	HTP
2.0	130200	3.09	72.04	13.81	638.4	5811.0
4.5	130575	3.16	72.27	14.15	623.0	5672.0
7.5	131026	3.27	72.54	14.25	618.4	5632.0
11.0	131553	3.39	72.85	14.37	613.4	5589.0
16.5	132383	3.61	73.34	14.46	609.3	5555.C
21.0	133063	3.81	73.75	14.49	607.8	5545.0
22.5	133290	3.88	73.88	14.36	613.4	5596.C

TEST NO.: A7. 6 FLOW PATTERN:BUBBLE-FROTH

ML=8995 MG= 3.21 QFLUX= 80328 NUTP=623.2 HTP=5682 PDT= 9.256

PDF= 8.491 ALFA=0.102 XTT=101.03 WE= 18113.0 FR=976.00

	TMIX	RESL	RESG	P	PRL	PRG	VSL	VSG
INLET	72.31	130642	2415.C	40.4	6.55	C.710	34.73	3.77
OUTLET	74.46	134266	2408.2	31.2	6.36	0.709	34.71	4.86
MEAN	73.38	132454	2412.C	35.8	6.45	C.710	34.71	4.30

Z	RESL	VSG	TBULK	(TW-TB)	NUTP	HTP
2.0	130942	3.84	72.49	13.62	646.9	5891.C
4.5	131319	3.94	72.71	13.97	630.6	5745.0
7.5	131770	4.06	72.98	14.06	626.8	5712.C
11.0	132299	4.22	73.29	14.15	622.6	5677.0
16.5	133130	4.49	73.79	14.32	614.8	5609.C
21.0	133812	4.73	74.19	14.26	617.3	5635.0
22.5	134039	4.82	74.32	14.12	623.6	5693.0

TEST NO.: A7. 7 FLOW PATTERN:FROTH

ML=8995 MG= 5.56 QFLUX= 80693 NUTP=628.3 HTP=5730 PDT= 9.806

PDF= 9.077 ALFA=0.144 XTT= 65.93 WE= 18115.0 FR=976.00

	TMIX	RESL	RESG	P	PRL	PRG	VSL	VSG
INLET	72.39	130789	4183.C	45.9	6.54	C.710	34.73	5.75
OUTLET	74.56	134431	4170.5	36.1	6.35	0.709	34.71	7.28
MEAN	73.48	132610	4177.C	41.0	6.45	C.710	34.71	6.49

Z	RESL	VSG	TBULK	(TW-TB)	NUTP	HTP
2.0	131092	5.86	72.57	13.70	646.1	5885.0
4.5	131470	6.00	72.80	14.06	629.5	5735.0
7.5	131924	6.17	73.07	14.19	623.9	5686.0
11.0	132455	6.39	73.39	14.28	619.9	5652.0
16.5	133290	6.76	73.88	14.40	614.5	5607.C
21.0	133976	7.10	74.29	14.42	613.5	5601.0
22.5	134204	7.22	74.42	10.81	815.9	7450.0

TEST NO.: A7. 8 FLOW PATTERN:FROTH

ML=8995 MG= 7.73 QFLUX= 84069 NUTP=646.3 HTP=5891 PDT=10.509

PDF= 9.806 ALFA=0.175 XTT= 50.94 WE= 18105.0 FR=976.00

	TMIX	RESL	RESG	P	PRL	PRG	VSL	VSG
INLET	71.95	130046	5816.0	49.4	6.58	0.710	34.73	7.42
OUTLET	74.20	133834	5797.1	38.9	6.39	0.709	34.71	9.39
MEAN	73.08	131940	5806.6	44.1	6.48	0.710	34.71	8.37

Z	RESL	VSG	TBULK	(TW-TB)	NUTP	HTP
2.0	130360	7.56	72.14	13.74	671.4	6112.0
4.5	130753	7.73	72.37	14.08	655.2	5966.0
7.5	131226	7.96	72.65	14.21	649.4	5915.0
11.0	131778	8.24	72.98	14.31	644.3	5872.0
16.5	132647	8.72	73.50	14.44	638.7	5825.0
21.0	133359	9.15	73.92	14.45	637.9	5821.0
22.5	133597	9.31	74.06	14.07	654.7	5975.0

TEST NO.: A7. 9 FLOW PATTERN:FROTH

ML=8995 MG= 16.84 QFLUX= 87868 NUTP=669.9 HTP=6099 PDT=12.735

PDF=12.104 ALFA=0.261 XTT= 27.96 WE= 18085.0 FR=976.00

	TMIX	RESL	RESG	P	PRL	PRG	VSL	VSG
INLET	71.11	128638	12686.0	60.2	6.66	0.710	34.73	13.24
OUTLET	73.46	132582	12642.7	47.4	6.45	0.710	34.71	16.73
MEAN	72.28	130610	12664.4	53.8	6.56	0.710	34.71	14.93

Z	RESL	VSG	TBULK	(TW-TB)	NUTP	HTP
2.0	128965	13.49	71.30	13.73	703.0	6392.0
4.5	129374	13.80	71.55	14.15	682.3	6206.0
7.5	129866	14.20	71.84	14.28	675.9	6150.0
11.0	130441	14.70	72.19	14.42	669.4	6093.0
16.5	131346	15.55	72.73	14.68	657.4	5989.0
21.0	132088	16.32	73.17	14.61	660.3	6019.0
22.5	132336	16.59	73.31	14.43	668.3	6093.0

TEST NO.: A7.10 FLOW PATTERN:FROTH

ML=8995 MG= 25.30 QFLUX= 92210 NUTP=677.8 HTP=6171 PDT=14.289

PDF=13.699 ALFA=0.309 XTT= 20.67 WE= 18085.0 FR=976.00

	TMIX	RESL	RESG	P	PRL	PRG	VSL	VSG
INLET	71.02	128495	19059.0	68.3	6.67	0.710	34.73	17.53
OUTLET	73.49	132633	18990.9	54.0	6.45	0.710	34.71	22.09
MEAN	72.26	130564	19025.1	61.1	6.56	0.710	34.71	19.74

Z	RESL	VSG	TBULK	(TW-TB)	NUTP	HTP
2.0	128838	17.85	71.23	14.04	721.4	6559.0
4.5	129267	18.26	71.49	14.57	695.2	6323.0
7.5	129783	18.79	71.79	14.72	688.0	6260.0
11.0	130386	19.43	72.15	14.91	679.5	6185.0
16.5	131335	20.54	72.72	15.45	655.3	5970.0
21.0	132114	21.55	73.18	15.15	668.1	6090.0
22.5	132374	21.91	73.34	14.97	675.8	6162.0

TEST NO.: A7.11 FLOW PATTERN:FRCTH

ML=8995 MG= 30.31 QFLUX= 95824 NUTP=680.5 HTP=6191 PDT=14.942

PDF=14.371 ALFA=0.331 XTI= 18.07 WE= 18073.0 FR=976.00

	TMIX	RESL	RESG	P	PRL	PRG	VSL	VSG
INLET	70.49	127615	22856.0	72.0	6.72	0.710	34.73	19.89
OUTLET	73.06	131905	22770.6	57.1	6.49	0.710	34.71	25.01
MEAN	71.78	129760	22813.3	64.6	6.60	0.710	34.71	22.38

Z	RESL	VSG	TEULK	(TW-TB)	NUTP	HTP
2.0	127970	20.25	70.71	14.45	728.8	6621.0
4.5	128415	20.72	70.97	15.07	699.0	6353.0
7.5	128950	21.30	71.30	15.26	690.2	6275.0
11.0	129575	22.03	71.67	15.46	681.1	6196.0
16.5	130560	23.28	72.26	15.98	659.1	6001.0
21.0	131367	24.41	72.74	15.76	667.9	6084.0
22.5	131637	24.81	72.90	15.48	679.6	6192.0

Table H.2 Helium-Water Data

TEST NO.:H1. 1 FLOW PATTERN:SLUG

ML= 267 MG= 0.15 QFLUX= 12082 NUTP= 86.6 HTP= 794 PDT= 0.344

PDF= 0.010 ALFA=0.607 XTT= 16.28 WE= 16.1 FR= 0.87

	TMIX	RESL	RESG	P	PRL	PRG	VSL	VSG
INLET	72.86	3913	103.4	15.9	6.46	0.691	1.03	3.24
OUTLET	83.74	4469	102.1	15.6	5.63	0.691	1.03	3.37
MEAN	78.30	4191	102.8	15.8	6.03	0.691	1.03	3.31

Z	RESL	VSG	TBULK	(TW-TB)	NUTP	HTP
2.0	3958	3.25	73.76	15.07	87.6	799.0
4.5	4015	3.26	74.90	15.29	86.3	788.0
7.5	4083	3.28	76.25	15.22	86.6	792.0
11.0	4164	3.30	77.84	15.14	86.9	797.0
16.5	4292	3.33	80.33	15.24	86.3	794.0
21.0	4398	3.36	82.38	15.27	85.9	793.0
22.5	4434	3.37	83.06	14.83	88.4	816.0

TEST NO.:H1. 2 FLOW PATTERN:SLUG

ML= 267 MG= 0.26 QFLUX= 12076 NUTP= 90.9 HTP= 834 PDT= 0.299

PDF= 0.030 ALFA=0.684 XTT= 9.83 WE= 16.1 FR= 0.87

	TMIX	RESL	RESG	P	PRL	PRG	VSL	VSG
INLET	72.94	3917	180.5	15.8	6.45	0.691	1.03	5.69
OUTLET	83.81	4473	178.3	15.5	5.62	0.691	1.03	5.91
MEAN	78.37	4195	179.4	15.7	6.03	0.691	1.03	5.81

Z	RESL	VSG	TBULK	(TW-TB)	NUTP	HTP
2.0	3962	5.71	73.85	14.25	92.6	844.0
4.5	4019	5.74	74.98	14.60	90.3	825.0
7.5	4087	5.76	76.33	14.79	89.1	815.0
11.0	4168	5.80	77.92	14.73	89.3	819.0
16.5	4296	5.85	80.41	14.44	91.0	837.0
21.0	4402	5.89	82.45	14.07	93.2	860.0
22.5	4437	5.91	83.13	13.35	98.1	906.0

TEST NO.:H1. 3 FLOW PATTERN:SLUG

ML= 267 MG= 0.38 QFLUX= 12078 NUTP= 91.0 HTP= 835 PDT= 0.332

PDF= 0.098 ALFA=0.726 XTT= 7.10 WE= 16.1 FR= 0.87

	TMIX	RESL	RESG	P	PRL	PRG	VSL	VSG
INLET	73.02	3921	261.1	16.1	6.45	0.691	1.03	8.11
OUTLET	83.88	4477	257.9	15.7	5.62	0.691	1.03	8.44
MEAN	78.45	4199	259.5	15.9	6.02	0.691	1.03	8.28

Z	RESL	VSG	TBULK	(TW-TB)	NUTP	HTP
2.0	3966	8.14	73.93	14.55	90.7	828.0
4.5	4023	8.17	75.06	15.14	87.1	796.0
7.5	4092	8.21	76.41	15.35	85.9	786.0
11.0	4172	8.26	78.00	13.31	98.8	906.0
16.5	4300	8.34	80.49	15.22	86.4	794.0
21.0	4406	8.41	82.53	13.96	93.9	866.0
22.5	4441	8.43	83.21	13.12	99.8	922.0

TEST NO.:H1. 4 FLOW PATTERN:SLUG

ML= 267 MG= 0.68 QFLUX= 15568 NUTP= 96.7 HTP= 882 PDT= 0.377

PDF= 0.194 ALFA=0.786 XTT= 4.20 WE= 16.0 FR= 0.86

	TMIX	RESL	RESG	P	PRL	PRG	VSL	VSG
INLET	66.61	3604	471.8	15.7	7.06	0.691	1.03	14.69
OUTLET	80.59	4305	464.5	15.4	5.88	0.691	1.03	15.42
MEAN	73.60	3955	468.1	15.5	6.45	0.691	1.03	15.07

Z	RESL	VSG	TBULK	(TW-TB)	NUTP	HTP
2.0	3661	14.75	67.77	17.11	100.2	906.0
4.5	3732	14.83	69.22	17.58	97.4	883.0
7.5	3818	14.92	70.97	17.98	95.2	864.0
11.0	3920	15.03	73.01	18.14	94.1	858.0
16.5	4082	15.21	76.22	17.72	96.1	880.0
21.0	4216	15.35	78.85	17.13	99.2	911.0
22.5	4261	15.40	79.72	16.37	103.7	953.0

TEST NO.:H1. 5 FLOW PATTERN:SLUG

ML= 267 MG= 0.82 QFLUX= 15561 NUTP=101.7 HTP= 928 PDT= 0.398

PDF= 0.229 ALFA=0.801 XTT= 3.56 WE= 16.0 FR= 0.86

	TMIX	RESL	RESG	P	PRL	PRG	VSL	VSG
INLET	66.79	3613	567.8	15.8	7.04	0.691	1.03	17.57
OUTLET	80.75	4314	559.0	15.4	5.86	0.691	1.03	18.48
MEAN	73.77	3963	563.4	15.6	6.44	0.691	1.03	18.04

Z	RESL	VSG	TBULK	(TW-TB)	NUTP	HTP
2.0	3670	17.65	67.95	16.88	101.5	918.0
4.5	3741	17.75	69.40	17.10	100.1	907.0
7.5	3827	17.86	71.14	17.19	99.4	903.0
11.0	3928	18.00	73.18	17.01	100.3	914.0
16.5	4090	18.21	76.38	16.65	102.2	935.0
21.0	4224	18.39	79.01	16.14	105.2	966.0
22.5	4269	18.45	79.88	15.51	109.4	1006.0

TEST NO.:H1. 6 FLOW PATTERN:SLUG

ML= 267 MG= 1.11 QFLUX= 18110 NUTP=118.3 HTP=1080 PDT= 0.431

PDF= 0.283 ALFA=0.826 XTT= 2.69 WE= 16.1 FR= 0.86

	TMIX	RESL	RESG	P	PRL	PRG	VSL	VSG
INLET	66.56	3602	773.4	15.9	7.06	0.691	1.03	23.90
OUTLET	82.79	4419	759.4	15.4	5.71	0.691	1.03	25.27
MEAN	74.67	4011	766.4	15.6	6.36	0.691	1.03	24.60

Z	RESL	VSG	TBULK	(TW-TB)	NUTP	HTP
2.0	3668	24.01	67.91	17.22	115.8	1048.0
4.5	3751	24.16	69.60	17.15	116.1	1053.0
7.5	3851	24.33	71.63	17.51	113.6	1033.0
11.0	3969	24.54	73.99	16.98	116.9	1066.0
16.5	4158	24.87	77.72	16.47	120.1	1101.0
21.0	4313	25.14	80.74	15.97	123.6	1137.0
22.5	4366	25.23	81.76	15.66	125.9	1160.0

TEST NO.:H1. 7 FLOW PATTERN:SLUG-ANNULAR

ML= 267 MG= 1.86 QFLUX= 19693 NUTP=149.2 HTP=1364 PDT= 0.494

PDF= 0.375 ALFA=0.861 XTT= 1.70 WE= 16.1 FR= 0.86

	TMIX	RESL	RESG	P	PRL	PRG	VSL	VSG
INLET	66.55	3602	1289.0	16.0	7.05	0.691	1.03	39.48
OUTLET	84.14	4490	1264.8	15.5	5.61	0.691	1.03	42.02
MEAN	75.35	4046	1277.4	15.8	6.30	0.691	1.03	40.79

Z	RESL	VSG	TBULK	(TW-TB)	NUTP	HTP
2.0	3673	39.70	68.01	15.63	138.6	1254.0
4.5	3763	39.96	69.84	15.82	136.8	1240.0
7.5	3872	40.29	72.04	16.43	131.5	1196.0
11.0	4000	40.66	74.60	15.90	135.6	1238.0
16.5	4205	41.27	78.63	11.42	187.7	1723.0
21.0	4376	41.77	81.94	15.18	141.2	1302.0
22.5	4433	41.94	83.05	14.66	146.1	1349.0

TEST NO.:H1. 8 FLOW PATTERN:SLUG-ANNULAR

ML= 267 MG= 2.37 QFLUX= 21709 NUTP=170.1 HTP=1564 PDT= 0.512

PDF= 0.406 ALFA=0.875 XTT= 1.36 WE= 16.2 FR= 0.87

	TMIX	RESL	RESG	P	PRL	PRG	VSL	VSG
INLET	69.80	3761	1636.0	16.0	6.72	0.691	1.03	50.57
OUTLET	89.14	4755	1602.1	15.5	5.26	0.691	1.03	54.03
MEAN	79.47	4258	1619.5	15.8	5.96	0.691	1.03	52.35

Z	RESL	VSG	TBULK	(TW-TB)	NUTP	HTP
2.0	3840	50.86	71.41	14.07	168.8	1535.0
4.5	3940	51.22	73.41	14.61	162.4	1481.0
7.5	4062	51.66	75.83	14.73	160.9	1471.0
11.0	4206	52.18	78.65	13.80	171.2	1572.0
16.5	4435	53.00	83.09	13.93	169.1	1562.0
21.0	4626	53.69	86.73	12.92	181.7	1686.0
22.5	4691	53.92	87.94	12.17	192.7	1791.0

TEST NO.:H1. 9 FLOW PATTERN:ANNULAR

ML= 267 MG= 5.61 QFLUX= 28277 NUTP=286.0 HTP=2639 PDT= 0.901

PDF= 0.828 ALFA=0.914 XTT= 0.64 WE= 16.2 FR= 0.87

	TMIX	RESL	RESG	P	PRL	PRG	VSL	VSG
INLET	69.53	3747	3877.0	17.0	6.72	0.691	1.03	112.65
OUTLET	94.33	5035	3772.2	16.1	4.94	0.691	1.03	124.14
MEAN	81.93	4391	3824.8	16.6	5.78	0.691	1.03	118.51

Z	RESL	VSG	TBULK	(TW-TB)	NUTP	HTP
2.0	3849	113.59	71.58	11.31	273.1	2484.0
4.5	3978	114.77	74.16	11.43	269.7	2462.0
7.5	4134	116.21	77.25	11.16	275.6	2526.0
11.0	4320	117.93	80.87	13.75	223.5	2058.0
16.5	4620	120.68	86.60	16.29	188.1	1746.0
21.0	4868	122.97	91.25	9.81	310.1	2895.0
22.5	4952	123.75	92.81	9.43	322.2	3015.0

TEST NO.:H1.10 FLOW PATTERN:ANNULAR

ML= 267 MG= 6.81 QFLUX= 28288 NUTP=263.4 HTP=2429 PDT= 1.043

PDF= 0.976 ALFA=0.921 XTT= 0.54 WE= 16.2 FR= 0.87

	TMIX	RESL	RESG	P	PRL	PRG	VSL	VSG
INLET	69.39	3741	4710.0	17.4	6.74	0.691	1.03	133.64
OUTLET	94.09	5022	4582.8	16.4	4.96	0.691	1.03	148.29
MEAN	81.74	4381	4646.4	16.9	5.80	0.691	1.03	141.09

Z	RESL	VSG	TBULK	(TW-TB)	NUTP	HTP
2.0	3842	134.83	71.44	11.14	277.4	2522.0
4.5	3970	136.33	74.00	11.60	266.0	2427.0
7.5	4125	138.16	77.07	11.70	263.2	2411.0
11.0	4310	140.34	80.67	11.70	262.4	2416.0
16.5	4606	143.84	86.34	11.82	258.7	2400.0
21.0	4855	146.79	91.00	11.61	262.5	2450.0
22.5	4939	147.79	92.55	11.13	273.5	2558.0

TEST NO.:H1.11 FLOW PATTERN:ANNULAR

ML= 267 MG= 7.24 QFLUX= 28238 NUTP=246.2 HTP=2260 PDT= 0.806

PDF= 0.741 ALFA=0.924 XTT= 0.51 WE= 16.1 FR= 0.87

	TMIX	RESL	RESG	P	PRL	PRG	VSL	VSG
INLET	65.63	3557	5029.0	16.7	7.12	0.691	1.03	147.18
OUTLET	90.24	4814	4893.7	15.9	5.20	0.691	1.03	161.41
MEAN	77.93	4185	4961.7	16.3	6.10	0.691	1.03	154.45

Z	RESL	VSG	TBULK	(TW-TB)	NUTP	HTP
2.0	3656	148.35	67.67	13.12	236.4	2138.0
4.5	3781	149.82	70.22	13.16	235.2	2135.0
7.5	3934	151.61	73.29	13.01	237.4	2164.0
11.0	4115	153.73	76.87	12.85	239.8	2196.0
16.5	4406	157.13	82.52	12.17	251.9	2325.0
21.0	4649	159.97	87.16	11.57	264.1	2452.0
22.5	4732	160.93	88.71	11.25	271.3	2524.0

TEST NO.:H1.12 FLOW PATTERN:ANNULAR

ML= 267 MG= 9.93 QFLUX= 29415 NUTP=198.2 HTP=1811 PDT= 1.064

PDF= 1.007 ALFA=0.934 XTT= 0.39 WE= 16.1 FR= 0.86

	TMIX	RESL	RESG	P	PRL	PRG	VSL	VSG
INLET	62.43	3403	6919.0	17.4	7.47	0.691	1.03	191.78
OUTLET	87.76	4681	6726.1	16.4	5.37	0.691	1.03	213.40
MEAN	75.09	4042	6822.6	16.9	6.36	0.691	1.03	202.77

Z	RESL	VSG	TBULK	(TW-TB)	NUTP	HTP
2.0	3504	193.53	64.53	15.62	207.6	1870.0
4.5	3631	195.75	67.15	16.07	201.4	1820.0
7.5	3786	198.45	70.31	16.22	199.1	1808.0
11.0	3970	201.66	74.00	16.35	196.9	1797.0
16.5	4265	206.83	79.81	16.36	196.1	1803.0
21.0	4514	211.18	84.59	16.29	196.2	1816.0
22.5	4598	212.65	86.18	16.21	196.9	1826.0

TEST NO.:H1.13 FLOW PATTERN:ANNULAR-MIST

ML= 267 MG= 12.11 QFLUX= 25966 NUTP=176.7 HTP=1616 PDT= 1.363

PDF= 1.311 ALFA=0.938 XTT= 0.33 WE= 16.1 FR= 0.86

	TMIX	RESL	RESG	P	PRL	PRG	VSL	VSG
INLET	64.64	3509	8414.0	18.4	7.24	0.691	1.03	222.07
OUTLET	86.79	4630	8209.3	17.1	5.43	0.691	1.03	248.99
MEAN	75.71	4069	8312.1	17.8	6.29	0.691	1.03	235.71

Z	RESL	VSG	TBUIK	(TW-TB)	NUTP	HTP
2.0	3598	224.23	66.47	13.50	211.4	1909.0
4.5	3710	226.97	68.77	14.92	191.1	1731.0
7.5	3846	230.31	71.53	15.69	181.4	1649.0
11.0	4008	234.29	74.76	16.19	175.4	1602.0
16.5	4267	240.74	79.84	16.85	168.0	1545.0
21.0	4484	246.20	84.02	17.26	163.6	1513.0
22.5	4557	248.05	85.41	17.23	163.7	1516.0

TEST NO.:H1.14 FLOW PATTERN:ANNULAR-MIST

ML= 267 MG= 19.05 QFLUX= 23796 NUTP=154.5 HTP=1413 PDT= 1.496

PDF= 1.453 ALFA=0.949 XTT= 0.23 WE= 16.1 FR= 0.86

	TMIX	RESL	RESG	P	PRL	PRG	VSL	VSG
INLET	66.46	3597	13214.0	20.4	7.05	0.691	1.03	317.00
OUTLET	86.15	4596	12927.7	18.9	5.47	0.691	1.03	353.63
MEAN	76.31	4097	13071.3	19.7	6.23	0.691	1.03	335.56

Z	RESL	VSG	TBUIK	(TW-TB)	NUTP	HTP
2.0	3677	319.94	68.09	12.15	214.6	1942.0
4.5	3777	323.67	70.13	14.08	185.1	1680.0
7.5	3899	328.21	72.58	15.51	167.9	1529.0
11.0	4043	333.64	75.45	16.98	153.2	1400.0
16.5	4274	342.41	79.98	19.12	135.8	1249.0
21.0	4467	349.83	83.69	20.52	126.3	1167.0
22.5	4532	352.36	84.93	20.09	128.8	1193.0

TEST NO.:H1.15 FLOW PATTERN:ANNULAR-MIST

ML= 267 MG= 33.57 QFLUX= 20674 NUTP=119.0 HTP=1080 PDT= 2.092

PDF= 2.055 ALFA=0.958 XTT= 0.16 WE= 16.0 FR= 0.86

	TMIX	RESL	RESG	P	PRL	PRG	VSL	VSG
INLET	63.23	3441	23368.0	24.9	7.43	0.691	1.03	455.71
OUTLET	79.34	4241	22949.6	22.8	5.98	0.691	1.03	510.98
MEAN	71.28	3841	23158.9	23.8	6.68	0.691	1.03	483.63

Z	RESL	VSG	TBUIK	(TW-TB)	NUTP	HTP
2.0	3505	460.10	64.56	12.02	189.3	1705.0
4.5	3586	465.67	66.22	14.79	153.9	1389.0
7.5	3684	472.50	68.23	17.29	131.6	1192.0
11.0	3799	480.66	70.58	19.63	115.9	1052.0
16.5	3984	493.92	74.28	23.08	98.5	899.0
21.0	4138	505.20	77.32	25.20	90.1	826.0
22.5	4190	509.04	78.34	25.43	89.3	819.0

TEST NO.:H2. 1 FLOW PATTERN:BUBBLE

ML= 882 MG= 0.02 QFLUX= 17841 NUTP=109.6 HTP=1001 PDT= 0.931

PDF= 0.169 ALFA=0.103 XTT=297.49 WE= 174.6 FR= 9.40

	TMIX	RESL	RESG	P	PRL	PRG	VSL	VSG
INLET	72.70	12876	14.0	17.1	6.50	0.691	3.41	0.41
OUTLET	77.58	13687	13.9	16.2	6.10	0.691	3.40	0.44
MEAN	75.14	13282	14.0	16.6	6.30	0.691	3.40	0.42

Z	RESL	VSG	TBULK	(TW-TB)	NUTP	HTP
2.0	12943	0.41	73.11	17.06	114.5	1043.0
4.5	13027	0.41	73.62	17.74	110.1	1004.0
7.5	13128	0.42	74.23	17.97	108.7	992.0
11.0	13246	0.42	74.94	17.98	108.6	992.0
16.5	13432	0.43	76.05	17.87	109.2	999.0
21.0	13585	0.43	76.97	17.76	109.8	1005.0
22.5	13636	0.44	77.27	17.58	110.8	1015.0

TEST NO.:H2. 2 FLOW PATTERN:BUBBLE

ML= 882 MG= 0.08 QFLUX= 21686 NUTP=148.0 HTP=1354 PDT= 0.847

PDF= 0.243 ALFA=0.289 XTT= 83.84 WE= 174.7 FR= 9.40

	TMIX	RESL	RESG	P	PRL	PRG	VSL	VSG
INLET	72.65	12868	57.3	17.1	6.50	0.691	3.41	1.67
OUTLET	78.58	13855	56.9	16.2	6.02	0.691	3.41	1.78
MEAN	75.61	13361	57.1	16.6	6.26	0.691	3.40	1.73

Z	RESL	VSG	TBULK	(TW-TB)	NUTP	HTP
2.0	12949	1.68	73.15	15.47	153.5	1399.0
4.5	13051	1.69	73.76	16.05	147.9	1349.0
7.5	13173	1.71	74.50	16.21	146.4	1336.0
11.0	13317	1.72	75.37	16.15	146.9	1342.0
16.5	13544	1.75	76.72	16.04	147.7	1352.0
21.0	13731	1.77	77.84	15.83	149.5	1371.0
22.5	13793	1.77	78.21	15.76	150.1	1377.0

TEST NO.:H2. 3 FLOW PATTERN:BUBBLE

ML= 882 MG= 0.12 QFLUX= 28294 NUTP=181.8 HTP=1665 PDT= 0.848

PDF= 0.300 ALFA=0.355 XTT= 60.27 WE= 175.0 FR= 9.40

	TMIX	RESL	RESG	P	PRL	PRG	VSL	VSG
INLET	72.91	12910	81.7	16.8	6.47	0.691	3.41	2.43
OUTLET	80.64	14205	81.0	16.0	5.86	0.691	3.41	2.59
MEAN	76.78	13558	81.3	16.4	6.16	0.691	3.40	2.51

Z	RESL	VSG	TBULK	(TW-TB)	NUTP	HTP
2.0	13017	2.44	73.56	16.42	188.4	1718.0
4.5	13150	2.45	74.36	16.99	182.1	1663.0
7.5	13310	2.48	75.33	17.20	179.8	1644.0
11.0	13498	2.50	76.45	17.15	180.1	1649.0
16.5	13796	2.54	78.23	17.01	181.3	1664.0
21.0	14042	2.57	79.68	16.80	183.4	1686.0
22.5	14124	2.58	80.16	16.62	185.4	1705.0

TEST NO.:H2. 4 FLOW PATTERN:BUBBLE-SIUG

ML= 882 MG= 0.16 QFLUX= 25956 NUTP=192.0 HTP=1757 PDT= 0.849

PDF= 0.346 ALFA=0.409 XTT= 46.00 WE= 174.9 FR= 9.40

	TMIX	RESL	RESG	P	PRL	PRG	VSL	VSG
INLET	72.82	12895	111.1	17.0	6.48	0.691	3.41	3.26
OUTLET	79.91	14081	110.3	16.2	5.91	0.691	3.41	3.47
MEAN	76.36	13488	110.7	16.6	6.19	0.691	3.40	3.37

Z	RESL	VSG	TBULK	(TW-TB)	NUTP	HTP
2.0	12992	3.28	73.41	14.42	196.9	1795.0
4.5	13114	3.30	74.15	14.83	191.4	1747.0
7.5	13261	3.32	75.03	14.97	189.6	1733.0
11.0	13434	3.36	76.07	14.90	190.3	1741.0
16.5	13706	3.41	77.69	14.72	192.4	1764.0
21.0	13931	3.45	79.02	14.59	193.9	1781.0
22.5	14006	3.46	79.47	14.43	195.9	1801.0

TEST NO.:H2. 5 FLOW PATTERN:BUBBLE-SIUG

ML= 882 MG= 0.24 QFLUX= 25963 NUTP=182.1 HTP=1666 PDT= 0.854

PDF= 0.414 ALFA=0.482 XTT= 32.01 WE= 174.8 FR= 9.40

	TMIX	RESL	RESG	P	PRL	PRG	VSL	VSG
INLET	72.46	12835	166.1	16.9	6.51	0.691	3.41	4.89
OUTLET	79.55	14019	164.8	16.1	5.94	0.691	3.41	5.20
MEAN	76.00	13427	165.5	16.5	6.22	0.691	3.40	5.05

Z	RESL	VSG	TBULK	(TW-TB)	NUTP	HTP
2.0	12932	4.91	73.05	14.77	192.4	1754.0
4.5	13054	4.95	73.78	15.40	184.5	1683.0
7.5	13201	4.98	74.67	15.62	181.8	1660.0
11.0	13373	5.03	75.70	15.71	180.7	1652.0
16.5	13645	5.11	77.33	15.71	180.4	1653.0
21.0	13870	5.17	78.66	15.67	180.8	1660.0
22.5	13945	5.19	79.10	15.45	183.3	1683.0

TEST NO.:H2. 6 FLOW PATTERN:SLUG

ML= 882 MG= 0.36 QFLUX= 25970 NUTP=182.8 HTP=1673 PDT= 0.797

PDF= 0.413 ALFA=0.549 XTT= 22.46 WE= 174.9 FR= 9.40

	TMIX	RESL	RESG	P	PRL	PRG	VSL	VSG
INLET	72.93	12913	245.4	16.9	6.47	0.691	3.41	7.26
OUTLET	80.02	14100	243.5	16.1	5.90	0.691	3.41	7.71
MEAN	76.47	13506	244.4	16.5	6.18	0.691	3.40	7.49

Z	RESL	VSG	TBULK	(TW-TB)	NUTP	HTP
2.0	13010	7.30	73.52	14.85	191.3	1744.0
4.5	13132	7.35	74.25	15.39	184.6	1684.0
7.5	13279	7.40	75.14	15.82	179.5	1640.0
11.0	13452	7.47	76.17	15.61	181.8	1663.0
16.5	13725	7.58	77.80	15.54	182.4	1672.0
21.0	13949	7.66	79.13	15.44	183.3	1684.0
22.5	14025	7.69	79.58	15.51	182.4	1677.0

TEST NO.:H2. 7 FLOW PATTERN:SLUG

ML= 882 MG= 0.53 QFLUX= 28273 NUTP=202.9 HTP=1859 PDT= 0.851

PDF= 0.518 ALFA=0.609 XTT= 15.82 WE= 175.1 FR= 9.40

	TMIX	RESL	RESG	P	PRL	PRG	VSL	VSG
INLET	73.44	12997	362.7	17.0	6.42	0.691	3.41	10.66
OUTLET	81.15	14293	359.6	16.2	5.82	0.691	3.41	11.36
MEAN	77.29	13645	361.2	16.6	6.11	0.691	3.40	11.02

Z	RESL	VSG	TEULK	(TW-TB)	NUTP	HTP
2.0	13103	10.72	74.08	14.71	210.1	1917.0
4.5	13236	10.79	74.88	15.25	202.6	1851.0
7.5	13397	10.88	75.84	15.29	201.9	1847.0
11.0	13585	10.98	76.97	15.54	198.6	1819.0
16.5	13883	11.15	78.74	15.16	203.2	1866.0
21.0	14129	11.29	80.19	14.90	206.5	1900.0
22.5	14211	11.33	80.67	15.03	204.6	1884.0

TEST NO.:H2. 8 FLOW PATTERN:SLUG

ML= 882 MG= 0.63 QFLUX= 30642 NUTP=204.3 HTP=1873 PDT= 0.903

PDF= 0.594 ALFA=0.637 XTT= 13.31 WE= 175.1 FR= 9.40

	TMIX	RESL	RESG	P	PRL	PRG	VSL	VSG
INLET	73.07	12936	436.7	16.8	6.45	0.691	3.41	12.96
OUTLET	81.43	14340	432.6	15.9	5.80	0.691	3.41	13.88
MEAN	77.25	13638	434.7	16.4	6.12	0.691	3.40	13.43

Z	RESL	VSG	TEULK	(TW-TB)	NUTP	HTP
2.0	13051	13.03	73.76	15.79	212.1	1935.0
4.5	13195	13.13	74.63	16.50	203.0	1854.0
7.5	13369	13.24	75.68	16.53	202.5	1852.0
11.0	13573	13.38	76.90	16.56	202.0	1850.0
16.5	13896	13.60	78.82	16.25	205.5	1887.0
21.0	14162	13.78	80.39	16.22	205.5	1892.0
22.5	14252	13.85	80.91	16.17	206.2	1899.0

TEST NO.:H2. 9 FLOW PATTERN:SLUG

ML= 882 MG= 0.73 QFLUX= 30640 NUTP=207.3 HTP=1900 PDT= 0.953

PDF= 0.660 ALFA=0.656 XTT= 11.74 WE= 175.1 FR= 9.40

	TMIX	RESL	RESG	P	PRL	PRG	VSL	VSG
INLET	73.23	12963	502.3	16.9	6.44	0.691	3.41	14.86
OUTLET	81.59	14368	497.7	15.9	5.78	0.691	3.41	15.95
MEAN	77.41	13666	500.0	16.4	6.10	0.691	3.40	15.41

Z	RESL	VSG	TEULK	(TW-TB)	NUTP	HTP
2.0	13078	14.94	73.93	15.50	216.0	1971.0
4.5	13223	15.06	74.80	16.06	208.4	1904.0
7.5	13396	15.20	75.84	16.24	206.1	1885.0
11.0	13601	15.36	77.06	16.22	206.1	1888.0
16.5	13924	15.62	78.98	16.21	205.9	1891.0
21.0	14190	15.84	80.55	16.08	207.3	1908.0
22.5	14279	15.92	81.07	15.78	211.1	1945.0

TEST NO.:H2.10 FLOW PATTERN:SLUG

ML= 882 MG= 0.85 QFLUX= 30636 NUTP=212.1 HTP=1945 PDT= 1.058

PDF= 0.782 ALFA=0.675 XTT= 10.28 WE= 175.2 FR= 9.40

	TMIX	RESL	RESG	P	PRL	PRG	VSL	VSG
INLET	73.44	12997	584.9	17.1	6.42	0.691	3.41	17.10
OUTLET	81.80	14403	579.4	16.0	5.77	0.691	3.41	18.47
MEAN	77.62	13700	582.1	16.6	6.09	0.691	3.41	17.80

Z	RESL	VSG	TBULK	(TW-TB)	NUTP	HTP
2.0	13112	17.21	74.13	15.06	222.3	2028.0
4.5	13257	17.36	75.00	15.68	213.5	1950.0
7.5	13431	17.53	76.05	15.95	209.8	1919.0
11.0	13635	17.73	77.27	15.94	209.6	1921.0
16.5	13958	18.06	79.19	15.77	211.5	1944.0
21.0	14225	18.33	80.76	15.69	212.4	1956.0
22.5	14314	18.43	81.28	15.39	216.5	1995.0

TEST NO.:H2.11 FLOW PATTERN:SLUG

ML= 882 MG= 0.96 QFLUX= 30631 NUTP=217.1 HTP=1991 PDT= 1.115

PDF= 0.851 ALFA=0.689 XTT= 9.23 WE= 175.2 FR= 9.40

	TMIX	RESL	RESG	P	PRL	PRG	VSL	VSG
INLET	73.51	13010	659.2	17.1	6.41	0.691	3.41	19.23
OUTLET	81.87	14415	653.1	16.0	5.76	0.691	3.41	20.83
MEAN	77.69	13713	656.1	16.6	6.08	0.691	3.41	20.04

Z	RESL	VSG	TBULK	(TW-TB)	NUTP	HTP
2.0	13125	19.36	74.21	14.84	225.6	2059.0
4.5	13269	19.52	75.08	15.40	217.3	1985.0
7.5	13443	19.72	76.12	15.63	214.0	1958.0
11.0	13647	19.96	77.34	15.60	214.1	1963.0
16.5	13971	20.34	79.26	15.34	217.4	1998.0
21.0	14237	20.67	80.83	15.18	219.5	2021.0
22.5	14327	20.78	81.35	15.09	220.7	2033.0

TEST NO.:H2.12 FLOW PATTERN:SLUG-ANNULAR

ML= 882 MG= 1.12 QFLUX= 30633 NUTP=219.6 HTP=2015 PDT= 1.206

PDF= 0.957 ALFA=0.706 XTT= 8.09 WE= 175.3 FR= 9.40

	TMIX	RESL	RESG	P	PRL	PRG	VSL	VSG
INLET	73.85	13065	768.0	17.4	6.38	0.691	3.41	22.10
OUTLET	82.20	14473	760.9	16.2	5.74	0.691	3.41	24.05
MEAN	78.03	13769	764.4	16.8	6.05	0.691	3.41	23.09

Z	RESL	VSG	TBULK	(TW-TB)	NUTP	HTP
2.0	13180	22.26	74.54	14.63	228.7	2088.0
4.5	13325	22.46	75.41	15.28	218.9	2001.0
7.5	13499	22.70	76.46	15.33	218.0	1995.0
11.0	13704	22.99	77.68	15.27	218.7	2006.0
16.5	14027	23.46	79.59	15.26	218.5	2009.0
21.0	14294	23.85	81.16	15.06	221.2	2037.0
22.5	14384	23.98	81.68	15.02	221.6	2043.0

TEST NO.:H2.13 FLOW PATTERN:SLUG-ANNULAR

ML= 882 MG= 1.57 QFLUX= 33087 NUTP=235.8 HTP=2165 PDT= 1.468

PDF= 1.249 ALFA=0.743 XTT= 5.98 WE= 175.4 FR= 9.41

	TMIX	RESL	RESG	P	PRL	PRG	VSL	VSG
INLET	73.80	13057	1079.0	17.7	6.38	0.691	3.41	30.54
OUTLET	82.82	14578	1069.0	16.2	5.69	0.691	3.41	33.75
MEAN	78.31	13817	1074.4	17.0	6.03	0.691	3.41	32.16

Z	RESL	VSG	TBULK	(TW-TB)	NUTP	HTP
2.0	13181	30.79	74.55	14.72	245.5	2241.0
4.5	13337	31.12	75.49	15.60	231.6	2117.0
7.5	13525	31.52	76.61	15.85	227.8	2086.0
11.0	13746	31.99	77.93	15.41	234.1	2147.0
16.5	14096	32.76	80.00	15.28	235.6	2168.0
21.0	14385	33.42	81.69	15.32	234.7	2164.0
22.5	14481	33.64	82.25	12.54	286.1	2640.0

TEST NO.:H2.14 FLOW PATTERN:ANNULAR

ML= 882 MG= 2.35 QFLUX= 38335 NUTP=250.9 HTP=2305 PDT= 1.835

PDF= 1.647 ALFA=0.780 XTT= 4.22 WE= 175.5 FR= 9.41

	TMIX	RESL	RESG	P	PRL	PRG	VSL	VSG
INLET	73.50	13007	1615.0	18.4	6.40	0.691	3.41	43.92
OUTLET	83.94	14771	1596.9	16.6	5.61	0.691	3.41	49.54
MEAN	78.72	13889	1606.2	17.5	6.00	0.691	3.41	46.74

Z	RESL	VSG	TBULK	(TW-TB)	NUTP	HTP
2.0	13151	44.36	74.37	15.68	266.8	2436.0
4.5	13331	44.92	75.45	16.44	254.4	2326.0
7.5	13549	45.60	76.76	16.55	252.6	2313.0
11.0	13805	46.43	78.28	16.70	250.0	2294.0
16.5	14211	47.78	80.67	16.25	256.4	2361.0
21.0	14546	48.94	82.63	18.14	229.7	2120.0
22.5	14659	49.34	83.29	16.06	258.9	2392.0

TEST NO.:H2.15 FLOW PATTERN:ANNULAR

ML= 882 MG= 3.31 QFLUX= 41100 NUTP=272.4 HTP=2503 PDT= 2.256

PDF= 2.092 ALFA=0.808 XTT= 3.13 WE= 175.6 FR= 9.41

	TMIX	RESL	RESG	P	PRL	PRG	VSL	VSG
INLET	73.54	13013	2278.0	19.1	6.40	0.691	3.41	59.76
OUTLET	84.71	14904	2250.3	16.8	5.56	0.691	3.41	68.87
MEAN	79.12	13959	2264.4	17.9	5.97	0.691	3.41	64.32

Z	RESL	VSG	TBULK	(TW-TB)	NUTP	HTP
2.0	13167	60.46	74.46	15.74	285.0	2602.0
4.5	13360	61.36	75.63	16.34	274.4	2510.0
7.5	13594	62.46	77.02	16.62	269.5	2469.0
11.0	13868	63.80	78.65	16.70	267.9	2460.0
16.5	14303	65.99	81.21	16.35	273.1	2516.0
21.0	14663	67.89	83.32	16.39	272.0	2513.0
22.5	14784	68.54	84.02	15.85	281.1	2600.0

TEST NO.:H2.16 FLOW PATTERN:ANNULAR

ML= 882 MG= 4.62 QFLUX= 41072 NUTP=293.8 HTP=2700 PDT= 2.693

PDF= 2.549 ALFA=0.830 XTT= 2.37 WE= 175.6 FR= 9.41

	TMIX	RESL	RESG	P	PRL	PRG	VSL	VSG
INLET	73.63	13028	3179.0	20.0	6.39	0.691	3.41	79.33
OUTLET	84.77	14915	3139.9	17.4	5.55	0.691	3.41	93.05
MEAN	79.20	13972	3159.4	18.7	5.96	0.691	3.41	86.15

Z	RESL	VSG	TBULK	(TW-TB)	NUTP	HTP
2.0	13182	80.37	74.55	14.38	311.7	2846.0
4.5	13374	81.70	75.71	15.19	295.0	2698.0
7.5	13607	83.35	77.10	15.21	294.2	2696.0
11.0	13881	85.35	78.73	15.37	290.8	2671.0
16.5	14315	88.66	81.29	15.22	293.1	2701.0
21.0	14675	91.55	83.38	15.33	290.6	2685.0
22.5	14795	92.55	84.08	15.25	292.1	2701.0

TEST NO.:H2.17 FLOW PATTERN:ANNULAR

ML= 882 MG= 6.85 QFLUX= 43945 NUTP=322.1 HTP=2964 PDT= 3.245

PDF= 3.120 ALFA=0.853 XTT= 1.71 WE= 175.8 FR= 9.41

	TMIX	RESL	RESG	P	PRL	PRG	VSL	VSG
INLET	74.10	13106	4709.0	21.5	6.34	0.691	3.41	109.76
OUTLET	85.99	15126	4648.0	18.3	5.47	0.691	3.41	131.34
MEAN	80.04	14116	4678.9	19.9	5.89	0.691	3.41	120.43

Z	RESL	VSG	TBULK	(TW-TB)	NUTP	HTP
2.0	13270	111.36	75.09	13.79	347.5	3176.0
4.5	13477	113.43	76.32	14.67	326.3	2987.0
7.5	13726	115.99	77.81	14.83	322.6	2959.0
11.0	14018	119.12	79.54	14.96	319.5	2937.0
16.5	14484	124.35	82.27	14.97	318.6	2939.0
21.0	14869	128.93	84.50	15.01	317.2	2935.0
22.5	14998	130.53	85.25	14.77	322.1	2984.0

TEST NO.:H2.18 FLOW PATTERN:ANNULAR

ML= 882 MG= 9.70 QFLUX= 43919 NUTP=334.3 HTP=3073 PDT= 3.766

PDF= 3.656 ALFA=0.871 XTT= 1.29 WE= 175.7 FR= 9.41

	TMIX	RESL	RESG	P	PRL	PRG	VSL	VSG
INLET	73.72	13044	6672.0	23.1	6.38	0.691	3.41	144.52
OUTLET	85.56	15051	6584.9	19.3	5.50	0.691	3.41	175.33
MEAN	79.64	14047	6628.5	21.2	5.93	0.691	3.41	159.69

Z	RESL	VSG	TBULK	(TW-TB)	NUTP	HTP
2.0	13207	146.78	74.70	14.22	337.1	3079.0
4.5	13411	149.70	75.93	13.70	349.5	3197.0
7.5	13659	153.33	77.41	14.02	341.1	3127.0
11.0	13950	157.78	79.14	14.39	331.9	3050.0
16.5	14412	165.25	81.85	14.50	328.9	3033.0
21.0	14795	171.85	84.08	14.62	325.8	3013.0
22.5	14923	174.15	84.82	14.53	327.6	3033.0

TEST NO.:H3. 1 FLOW PATTERN:BUBBLE

ML=3598 MG= 0.03 QFLUX= 48354 NUTP=324.9 HTP=2972 PDT= 2.261

PDF= 1.444 ALFA=0.039 XTT=769.59 WE= 2908.0 FR=156.00

	TMIX	RESL	RESG	P	PRI	PRG	VSL	VSG
INLET	74.26	53571	20.5	18.8	6.36	0.691	13.89	0.55
OUTLET	77.49	55776	20.5	16.6	6.10	0.691	13.89	0.62
MEAN	75.87	54673	20.5	17.7	6.23	0.691	13.89	0.58

Z	RESL	VSG	TEULK	(TW-TB)	NUTP	HTP
2.0	53753	0.55	74.52	15.47	341.7	3120.0
4.5	53982	0.56	74.86	16.14	327.7	2994.0
7.5	54257	0.57	75.27	16.25	325.3	2973.0
11.0	54578	0.58	75.74	16.40	322.3	2948.0
16.5	55084	0.60	76.48	16.29	324.3	2969.0
21.0	55499	0.61	77.09	16.44	321.3	2944.0
22.5	55638	0.62	77.29	16.53	319.4	2928.0

TEST NO.:H3. 2 FLOW PATTERN:BUBBLE

ML=3598 MG= 0.07 QFLUX= 48383 NUTP=325.0 HTP=2977 PDT= 2.307

PDF= 1.526 ALFA=0.081 XTT=370.15 WE= 2912.0 FR=156.00

	TMIX	RESL	RESG	P	PRI	PRG	VSL	VSG
INLET	75.23	54229	46.5	19.1	6.28	0.691	13.89	1.22
OUTLET	78.47	56444	46.3	16.8	6.02	0.691	13.89	1.39
MEAN	76.85	55337	46.4	17.9	6.15	0.691	13.89	1.31

Z	RESL	VSG	TEULK	(TW-TB)	NUTP	HTP
2.0	54412	1.24	75.50	15.59	338.9	3099.0
4.5	54642	1.25	75.83	16.15	327.3	2994.0
7.5	54918	1.27	76.24	16.27	324.7	2971.0
11.0	55240	1.30	76.71	16.37	322.6	2954.0
16.5	55749	1.34	77.45	16.24	325.0	2979.0
21.0	56166	1.38	78.06	16.38	322.0	2955.0
22.5	56306	1.39	78.26	16.37	322.2	2957.0

TEST NO.:H3. 3 FLOW PATTERN:BUBBLE

ML=3598 MG= 0.12 QFLUX= 49759 NUTP=373.5 HTP=3416 PDT= 2.454

PDF= 1.715 ALFA=0.131 XTT=220.16 WE= 2907.0 FR=156.00

	TMIX	RESL	RESG	P	PRI	PRG	VSL	VSG
INLET	74.12	53479	84.9	19.8	6.37	0.691	13.89	2.14
OUTLET	77.45	55748	84.5	17.4	6.11	0.691	13.89	2.45
MEAN	75.79	54614	84.7	18.6	6.24	0.691	13.89	2.30

Z	RESL	VSG	TEULK	(TW-TB)	NUTP	HTP
2.0	53667	2.16	74.40	13.81	394.1	3598.0
4.5	53902	2.19	74.74	14.35	379.3	3464.0
7.5	54185	2.23	75.16	14.53	374.5	3422.0
11.0	54515	2.28	75.65	14.60	372.6	3407.0
16.5	55036	2.35	76.41	14.85	366.3	3353.0
21.0	55463	2.41	77.04	14.61	371.9	3407.0
22.5	55606	2.44	77.24	14.53	373.8	3426.0

TEST NO.:H3. 4 FLOW PATTERN:BUBBLE

ML=3598 MG= 0.28 QFLUX= 55461 NUTP=400.4 HTP=3668 PDT= 2.769

PDF= 2.113 ALFA=0.229 XTT=109.14 WE= 2912.0 FR=156.00

	TMIX	RESL	RESG	P	PRL	PRG	VSL	VSG
INLET	75.18	54195	190.7	21.2	6.28	0.691	13.89	4.52
OUTLET	78.89	56736	189.9	18.4	5.99	0.691	13.89	5.21
MEAN	77.03	55466	190.3	19.8	6.13	0.691	13.89	4.87

Z	RESL	VSG	TBULK	(TW-TB)	NUTP	HTP
2.0	54405	4.57	75.49	14.20	426.5	3900.0
4.5	54668	4.64	75.87	14.87	407.4	3727.0
7.5	54985	4.73	76.34	15.15	399.7	3659.0
11.0	55355	4.82	76.88	15.13	400.1	3665.0
16.5	55938	4.99	77.73	15.37	393.5	3609.0
21.0	56417	5.14	78.43	15.27	396.0	3635.0
22.5	56577	5.19	78.66	15.18	398.3	3658.0

TEST NO.:H3. 5 FLOW PATTERN:BUBBLE-FROTH

ML=3598 MG= 0.80 QFLUX= 62377 NUTP=475.3 HTP=4352 PDT= 3.517

PDF= 2.997 ALFA=0.389 XTT= 44.95 WE= 2910.0 FR=156.00

	TMIX	RESL	RESG	P	PRL	PRG	VSL	VSG
INLET	74.28	53589	549.8	24.2	6.36	0.691	13.89	11.36
OUTLET	78.46	56439	547.2	20.7	6.02	0.691	13.89	13.32
MEAN	76.37	55014	548.5	22.5	6.19	0.691	13.89	12.34

Z	RESL	VSG	TBULK	(TW-TB)	NUTP	HTP
2.0	53824	11.51	74.63	13.54	503.6	4600.0
4.5	54119	11.70	75.06	14.03	485.9	4441.0
7.5	54473	11.93	75.59	14.20	479.9	4389.0
11.0	54888	12.22	76.19	14.37	474.1	4340.0
16.5	55543	12.69	77.15	14.69	463.5	4247.0
21.0	56080	13.11	77.94	14.47	470.3	4314.0
22.5	56260	13.25	78.20	14.30	475.9	4368.0

TEST NO.:H3. 6 FLOW PATTERN:FROTH

ML=3598 MG= 2.39 QFLUX= 66877 NUTP=476.5 HTP=4367 PDT= 6.033

PDF= 5.644 ALFA=0.543 XTT= 18.73 WE= 2913.0 FR=156.00

	TMIX	RESL	RESG	P	PRL	PRG	VSL	VSG
INLET	74.96	54051	1640.0	31.1	6.30	0.691	13.89	26.46
OUTLET	79.44	57115	1632.7	25.1	5.94	0.691	13.90	32.85
MEAN	77.20	55583	1636.8	28.1	6.12	0.691	13.89	29.57

Z	RESL	VSG	TBULK	(TW-TB)	NUTP	HTP
2.0	54303	26.92	75.34	14.46	505.0	4617.0
4.5	54620	27.51	75.80	15.05	485.3	4439.0
7.5	55001	28.24	76.36	15.20	480.3	4396.0
11.0	55447	29.16	77.01	15.37	474.9	4351.0
16.5	56151	30.71	78.04	15.65	465.9	4275.0
21.0	56730	32.10	78.88	15.45	471.8	4333.0
22.5	56923	32.60	79.16	15.16	480.6	4416.0

TEST NO.:H3. 7 FLOW PATTERN:FROTH

ML=3598 MG= 3.29 QFLUX= 73356 NUTP=505.4 HTP=4636 PDT= 6.826

PDF= 6.470 ALFA=0.581 XTT= 14.58 WE= 2915.0 FR=156.00

	TMIX	RESL	RESG	P	PRL	PRG	VSL	VSG
INLET	75.31	54284	2260.0	33.8	6.26	0.691	13.89	33.59
OUTLET	80.21	57652	2248.6	27.0	5.88	0.691	13.90	42.13
MEAN	77.76	55968	2254.8	30.4	6.07	0.691	13.89	37.74

Z	RESL	VSG	TBULK	(TW-TB)	NUTP	HTP
2.0	54562	34.19	75.72	14.82	540.1	4940.0
4.5	54910	34.97	76.23	15.50	516.5	4727.0
7.5	55329	35.96	76.84	15.70	509.6	4668.0
11.0	55819	37.17	77.56	15.93	502.2	4604.0
16.5	56593	39.25	78.68	16.18	494.2	4538.0
21.0	57229	41.12	79.60	16.02	498.5	4583.0
22.5	57441	41.79	79.91	15.60	511.7	4707.0

TEST NO.:H3. 8 FLOW PATTERN:FROTH

ML=3598 MG= 4.24 QFLUX= 73294 NUTP=524.4 HTP=4804 PDT= 7.574

PDF= 7.242 ALFA=0.609 XTT= 12.02 WE= 2912.0 FR=156.00

	TMIX	RESL	RESG	P	PRL	PRG	VSL	VSG
INLET	74.46	53711	2917.0	36.3	6.34	0.691	13.89	40.26
OUTLET	79.36	57063	2901.8	28.8	5.95	0.691	13.90	50.90
MEAN	76.91	55387	2909.8	32.6	6.14	0.691	13.89	45.42

Z	RESL	VSG	TBULK	(TW-TB)	NUTP	HTP
2.0	53987	41.01	74.87	14.22	563.1	5145.0
4.5	54334	41.98	75.38	14.92	536.6	4906.0
7.5	54750	43.19	75.99	15.19	526.9	4821.0
11.0	55238	44.71	76.71	15.40	519.6	4759.0
16.5	56008	47.30	77.83	15.55	514.3	4717.0
21.0	56641	49.65	78.75	15.43	517.8	4756.0
22.5	56853	50.48	79.06	15.20	525.6	4829.0

TEST NO.:H3. 9 FLOW PATTERN:FROTH

ML=3598 MG= 5.67 QFLUX= 69764 NUTP=545.4 HTP=5002 PDT= 8.481

PDF= 8.173 ALFA=0.638 XTT= 9.66 WE= 2915.0 FR=156.00

	TMIX	RESL	RESG	P	PRL	PRG	VSL	VSG
INLET	75.24	54237	3895.0	39.8	6.27	0.691	13.89	49.20
OUTLET	79.90	57435	3874.8	31.3	5.91	0.691	13.90	62.54
MEAN	77.57	55836	3884.9	35.6	6.09	0.691	13.89	55.65

Z	RESL	VSG	TBULK	(TW-TB)	NUTP	HTP
2.0	54501	50.13	75.63	12.83	593.2	5425.0
4.5	54832	51.34	76.11	13.67	557.0	5097.0
7.5	55229	52.86	76.69	13.90	547.8	5017.0
11.0	55695	54.75	77.37	14.08	540.6	4955.0
16.5	56429	58.00	78.44	14.17	536.7	4927.0
21.0	57033	60.95	79.32	14.21	534.7	4915.0
22.5	57235	62.00	79.61	13.97	543.7	4999.0

TEST NO.:H3.10 FLOW PATTERN:FROTH

ML=3598 MG= 8.09 QFLUX= 69756 NUTP=552.4 HTP=5066 PDT= 9.795

PDF= 9.514 ALFA=0.670 XTT= 7.47 WE= 2915.0 FR=156.00

	TMIX	RESL	RESG	P	PRL	PRG	VSL	VSG
INLET	75.30	54280	5552.0	45.1	6.26	0.691	13.89	61.90
OUTLET	79.96	57476	5523.3	35.3	5.90	0.691	13.90	79.07
MEAN	77.63	55878	5537.7	40.2	6.08	0.691	13.89	70.20

Z	RESL	VSG	TBULK	(TW-TB)	NUTP	HTP
2.0	54544	63.09	75.69	12.35	616.4	5638.0
4.5	54874	64.64	76.17	13.34	570.6	5222.0
7.5	55271	66.60	76.76	13.70	555.7	5090.0
11.0	55736	69.03	77.44	13.94	545.7	5003.0
16.5	56470	73.21	78.50	14.20	535.4	4915.0
21.0	57074	77.02	79.38	13.98	543.4	4994.0
22.5	57276	78.38	79.67	13.70	554.3	5097.0

TEST NO.:H3.11 FLOW PATTERN:FROTH

ML=3598 MG= 9.72 QFLUX= 73290 NUTP=558.3 HTP=5121 PDT=10.180

PDF= 9.912 ALFA=0.685 XTT= 6.54 WE= 2916.0 FR=156.00

	TMIX	RESL	RESG	P	PRL	PRG	VSL	VSG
INLET	75.41	54351	6674.0	48.1	6.25	0.691	13.89	69.79
OUTLET	80.30	57710	6637.9	37.9	5.88	0.691	13.90	88.59
MEAN	77.85	56031	6656.0	43.0	6.06	0.691	13.89	78.89

Z	RESL	VSG	TBULK	(TW-TB)	NUTP	HTP
2.0	54628	71.10	75.81	12.74	627.3	5739.0
4.5	54975	72.80	76.32	13.86	576.9	5281.0
7.5	55393	74.95	76.93	14.24	561.4	5144.0
11.0	55882	77.62	77.65	14.43	553.9	5079.0
16.5	56653	82.20	78.77	14.81	539.3	4953.0
21.0	57288	86.35	79.69	14.59	547.0	5030.0
22.5	57500	87.83	79.99	14.23	560.6	5157.0

TEST NO.:H4. 1 FLOW PATTERN:BUBBLE

ML=8995 MG= 0.12 QFLUX= 91716 NUTP=585.6 HTP=5301 PDT= 7.977

PDF= 7.158 ALFA=0.038 XTT=647.16 WE= 17983.0 FR=975.00

	TMIX	RESL	RESG	P	PRL	PRG	VSL	VSG
INLET	66.84	121577	82.9	32.2	7.09	0.691	34.73	1.26
OUTLET	69.29	125621	82.6	24.3	6.85	0.691	34.70	1.66
MEAN	68.06	123599	82.8	28.2	6.97	0.691	34.69	1.45

Z	RESL	VSG	TBULK	(TW-TB)	NUTP	HTP
2.0	121912	1.29	67.04	16.73	605.9	5477.0
4.5	122332	1.32	67.30	17.10	592.6	5359.0
7.5	122836	1.37	67.60	17.19	589.5	5333.0
11.0	123425	1.43	67.96	17.34	584.1	5287.0
16.5	124353	1.52	68.53	17.48	579.2	5246.0
21.0	125114	1.61	68.99	17.49	578.8	5246.0
22.5	125368	1.65	69.14	17.23	587.3	5325.0

TEST NO.:H4. 2 FLOW PATTERN:BUBBLE

ML=8995 MG= 0.15 QFLUX= 87720 NUTP=587.8 HTP=5317 PDT= 8.204

PDF= 7.391 ALFA=0.046 XTT=536.05 WE= 17966.0 FR=975.00

	TMIX	RESL	RESG	P	PRL	PRG	VSL	VSG
INLET	66.21	120555	103.9	33.1	7.16	0.691	34.73	1.54
OUTLET	68.56	124411	103.6	24.9	6.93	0.691	34.69	2.03
MEAN	67.39	122483	103.8	29.0	7.04	0.691	34.69	1.77

Z	RESL	VSG	TBULK	(TW-TB)	NUTP	HTP
2.0	120874	1.57	66.41	15.93	608.9	5499.0
4.5	121274	1.61	66.65	16.24	597.2	5395.0
7.5	121755	1.67	66.94	16.37	592.6	5356.0
11.0	122317	1.74	67.29	16.53	586.7	5306.0
16.5	123202	1.86	67.83	16.69	580.9	5256.0
21.0	123928	1.97	68.27	16.71	580.1	5252.0
22.5	124170	2.01	68.41	16.64	582.5	5275.0

TEST NO.:H4. 3 FLOW PATTERN:BUBBLE

ML=8995 MG= 0.28 QFLUX= 91675 NUTP=596.9 HTP=5401 PDT= 8.594

PDF= 7.804 ALFA=0.074 XTT=322.95 WE= 17973.0 FR=975.00

	TMIX	RESL	RESG	P	PRL	PRG	VSL	VSG
INLET	66.43	120919	195.8	37.3	7.13	0.691	34.73	2.57
OUTLET	68.89	124954	195.3	28.7	6.90	0.691	34.69	3.33
MEAN	67.66	122936	195.6	33.0	7.01	0.691	34.69	2.94

Z	RESL	VSG	TBULK	(TW-TB)	NUTP	HTP
2.0	121253	2.62	66.64	16.42	617.1	5576.0
4.5	121672	2.69	66.89	16.81	603.0	5450.0
7.5	122175	2.78	67.20	16.90	599.7	5423.0
11.0	122763	2.88	67.56	16.99	596.4	5395.0
16.5	123689	3.07	68.12	17.14	590.8	5349.0
21.0	124448	3.24	68.58	17.15	590.4	5348.0
22.5	124702	3.30	68.74	16.91	598.5	5423.0

TEST NO.:H4. 4 FLOW PATTERN:FROTH

ML=8995 MG= 0.42 QFLUX= 95717 NUTP=606.3 HTP=5487 PDT= 9.022

PDF= 8.255 ALFA=0.100 XTT=231.31 WE= 17978.0 FR=975.00

	TMIX	RESL	RESG	P	PRL	PRG	VSL	VSG
INLET	66.61	121210	291.9	39.3	7.11	0.691	34.73	3.64
OUTLET	69.18	125427	291.1	30.2	6.87	0.691	34.70	4.71
MEAN	67.89	123319	291.5	34.7	6.99	0.691	34.69	4.15

Z	RESL	VSG	TBULK	(TW-TB)	NUTP	HTP
2.0	121560	3.72	66.83	16.91	625.4	5652.0
4.5	121997	3.81	67.09	17.28	612.3	5535.0
7.5	122523	3.93	67.41	17.34	609.9	5516.0
11.0	123137	4.08	67.79	17.47	605.3	5478.0
16.5	124105	4.34	68.37	17.59	601.1	5444.0
21.0	124899	4.58	68.86	17.65	598.8	5427.0
22.5	125164	4.66	69.02	17.43	606.0	5493.0

TEST NO.:H4. 5 FLOW PATTERN:FROTH

ML=8995 MG= 0.54 QFLUX= 95715 NUTP=612.1 HTP=5541 PDT= 9.374

PDF= 8.622 ALFA=0.118 XTT=188.34 WE= 17982.0 FR=975.CC

	TMIX	RESL	RESG	P	PRL	PRG	VSL	VSG
INLET	66.75	121429	377.0	41.2	7.10	0.691	34.73	4.48
OUTLET	69.31	125648	375.9	31.8	6.85	0.691	34.70	5.78
MEAN	68.03	123539	376.4	36.5	6.98	0.691	34.69	5.10

Z	RESL	VSG	TBULK	(TW-TB)	NUTP	HTP
2.0	121779	4.57	66.96	16.73	632.3	5715.0
4.5	122216	4.69	67.23	17.09	618.9	5596.0
7.5	122742	4.83	67.55	17.20	614.9	5562.0
11.0	123357	5.02	67.92	17.30	611.0	5530.0
16.5	124325	5.33	68.51	17.43	606.3	5492.0
21.0	125120	5.62	68.99	17.45	605.5	5488.0
22.5	125385	5.72	69.15	17.24	612.8	5556.0

TEST NO.:H4. 6 FLOW PATTERN:FROTH

ML=8995 MG= 0.73 QFLUX= 95712 NUTP=619.0 HTP=5605 PDT= 9.695

PDF= 8.961 ALFA=0.138 XTT=152.45 WE= 17985.0 FR=975.CC

	TMIX	RESL	RESG	P	PRL	PRG	VSL	VSG
INLET	66.88	121648	503.8	45.2	7.09	0.691	34.73	5.46
OUTLET	69.44	125869	502.4	35.5	6.84	0.691	34.70	6.93
MEAN	68.16	123758	503.1	40.4	6.96	0.691	34.69	6.17

Z	RESL	VSG	TBULK	(TW-TB)	NUTP	HTP
2.0	121998	5.56	67.09	16.54	639.3	5780.0
4.5	122435	5.70	67.36	16.89	626.0	5661.0
7.5	122962	5.86	67.68	17.02	621.1	5620.0
11.0	123577	6.07	68.05	17.10	618.3	5597.0
16.5	124545	6.43	68.64	17.22	613.5	5558.0
21.0	125340	6.75	69.12	17.24	612.6	5554.0
22.5	125606	6.87	69.28	17.10	617.5	5599.0

TEST NO.:H4. 7 FLOW PATTERN:FROTH

ML=8995 MG= 0.99 QFLUX= 99837 NUTP=633.4 HTP=5737 PDT=10.243

PDF= 9.533 ALFA=0.167 XTT=119.10 WE= 17992.0 FR=975.CC

	TMIX	RESL	RESG	P	PRL	PRG	VSL	VSG
INLET	67.10	122013	688.0	48.4	7.06	0.691	34.73	6.98
OUTLET	69.78	126421	685.9	38.1	6.81	0.691	34.70	8.82
MEAN	68.44	124217	687.0	43.2	6.93	0.691	34.69	7.87

Z	RESL	VSG	TBULK	(TW-TB)	NUTP	HTP
2.0	122378	7.11	67.32	16.80	656.4	5936.0
4.5	122835	7.27	67.60	17.18	641.8	5806.0
7.5	123384	7.48	67.94	17.27	638.2	5776.0
11.0	124027	7.75	68.33	17.43	632.4	5727.0
16.5	125038	8.20	68.94	17.58	626.7	5680.0
21.0	125869	8.60	69.44	17.67	623.3	5653.0
22.5	126146	8.75	69.61	17.39	633.2	5744.0

TEST NO.:H4. 8 FLOW PATTERN:FROTH

ML=8995 MG= 1.31 QFLUX=110672 NUTP=664.7 HTP=6026 PDT=10.869

PDF=10.184 ALFA=0.196 XTT= 95.65 WE= 18008.0 FR=976.00

	TMIX	RESL	RESG	P	PRL	PRG	VSL	VSG
INLET	67.64	122890	903.9	51.2	7.00	0.691	34.73	8.67
OUTLET	70.60	127792	900.9	40.3	6.73	0.691	34.70	10.98
MEAN	69.12	125341	902.4	45.8	6.86	0.691	34.70	9.79

Z	RESL	VSG	TBULK	(TW-TB)	NUTP	HTP
2.0	123296	8.83	67.88	17.66	691.4	6257.0
4.5	123804	9.04	68.19	18.13	673.6	6099.0
7.5	124414	9.31	68.56	18.19	671.4	6082.0
11.0	125128	9.63	68.99	18.28	667.6	6051.0
16.5	126254	10.19	69.67	18.84	647.8	5877.0
21.0	127177	10.70	70.23	18.46	660.6	5998.0
22.5	127485	10.89	70.42	18.18	670.6	6090.0

TEST NO.:H4. 9 FLOW PATTERN:FROTH

ML=8995 MG= 2.23 QFLUX= 99839 NUTP=668.2 HTP=6061 PDT=13.164

PDF=12.529 ALFA=0.254 XTT= 63.78 WE= 18015.0 FR=976.00

	TMIX	RESL	RESG	P	PRL	PRG	VSL	VSG
INLET	68.08	123622	1540.0	59.8	6.96	0.691	34.73	12.66
OUTLET	70.76	128049	1535.7	46.7	6.71	0.691	34.70	16.18
MEAN	69.42	125835	1538.0	53.3	6.83	0.691	34.70	14.36

Z	RESL	VSG	TBULK	(TW-TB)	NUTP	HTP
2.0	123989	12.91	68.30	15.68	702.2	6359.0
4.5	124448	13.22	68.58	16.20	679.7	6157.0
7.5	124999	13.62	68.92	16.39	671.8	6088.0
11.0	125644	14.12	69.31	16.48	667.9	6057.0
16.5	126660	14.97	69.92	16.69	659.5	5985.0
21.0	127494	15.75	70.42	16.79	655.2	5951.0
22.5	127772	16.03	70.59	16.49	666.7	6056.0

Table H.3 Freon-Water Data

TEST NO.:F1. 1 FLOW PATTERN:BUBBLE-SLUG

ML= 267 MG= 1.86 QFLUX= 13921 NUTP=107.8 HTP= 991 PDT= 0.528

PDF= 0.065 ALFA=0.457 XTT= 9.90 WE= 16.2 FR= 0.87

	TMIX	RESL	RESG	P	PRL	PRG	VSL	VSG
INLET	73.70	3955	1924.0	16.4	6.38	0.770	1.03	1.27
OUTLET	86.23	4600	1862.9	15.9	5.45	0.769	1.03	1.34
MEAN	79.96	4277	1893.6	16.2	5.90	0.770	1.03	1.31

Z	RESL	VSG	TEULK	(TW-TB)	NUTP	HTP
2.0	4007	1.27	74.74	13.50	112.5	1027.0
4.5	4073	1.28	76.04	13.85	109.6	1002.0
7.5	4152	1.29	77.61	13.98	108.4	994.0
11.0	4246	1.30	79.43	14.00	108.1	993.0
16.5	4394	1.32	82.31	14.19	106.5	982.0
21.0	4517	1.33	84.66	14.23	106.0	981.0
22.5	4559	1.34	85.45	14.36	105.0	972.0

TEST NO.:F1. 2 FLOW PATTERN:SLUG

ML= 267 MG= 2.45 QFLUX= 12373 NUTP= 93.7 HTP= 861 PDT= 0.488

PDF= 0.067 ALFA=0.507 XTT= 7.71 WE= 16.1 FR= 0.87

	TMIX	RESL	RESG	P	PRL	PRG	VSL	VSG
INLET	73.52	3945	2530.0	16.2	6.40	0.770	1.03	1.69
OUTLET	84.64	4517	2458.2	15.7	5.56	0.769	1.03	1.78
MEAN	79.08	4231	2494.2	16.0	5.97	0.770	1.03	1.73

Z	RESL	VSG	TEULK	(TW-TB)	NUTP	HTP
2.0	3992	1.69	74.44	13.35	101.1	923.0
4.5	4050	1.70	75.60	13.77	98.0	896.0
7.5	4121	1.72	76.99	14.09	95.7	876.0
11.0	4204	1.73	78.61	14.36	93.8	861.0
16.5	4335	1.75	81.16	14.79	90.9	837.0
21.0	4444	1.77	83.26	14.90	90.1	832.0
22.5	4480	1.77	83.95	14.84	90.4	836.0

TEST NO.:F1. 3 FLOW PATTERN:SLUG

ML= 267 MG= 3.08 QFLUX= 12678 NUTP= 88.2 HTP= 809 PDT= 0.405

PDF= 0.017 ALFA=0.546 XTT= 6.28 WE= 16.1 FR= 0.87

	TMIX	RESL	RESG	P	PRL	PRG	VSL	VSG
INLET	72.76	3908	3188.0	16.2	6.47	0.770	1.03	2.13
OUTLET	84.16	4491	3095.3	15.8	5.60	0.769	1.03	2.23
MEAN	78.46	4199	3141.9	15.9	6.02	0.770	1.03	2.18

Z	RESL	VSG	TEULK	(TW-TB)	NUTP	HTP
2.0	3955	2.14	73.70	15.07	91.9	838.0
4.5	4015	2.15	74.89	15.36	90.1	823.0
7.5	4086	2.16	76.31	15.78	87.6	802.0
11.0	4171	2.18	77.97	15.87	87.1	798.0
16.5	4305	2.20	80.59	15.58	88.5	814.0
21.0	4417	2.22	82.73	15.89	86.7	800.0
22.5	4454	2.23	83.45	15.56	88.4	817.0

TEST NO.:F1. 4 FLOW PATTERN:SLUG

ML= 267 MG= 4.03 QFLUX= 12682 NUTP= 87.1 HTP= 800 PDI= 0.365

PDF= 0.014 ALFA=0.590 XTT= 4.91 WE= 16.1 FR= 0.87

	TMIX	RESL	RESG	P	PRL	PRG	VSL	VSG
INLET	73.23	3931	4173.0	16.1	6.42	0.770	1.03	2.81
OUTLET	84.63	4516	4052.1	15.7	5.56	0.769	1.03	2.94
MEAN	78.93	4223	4113.0	15.9	5.98	0.770	1.03	2.87

Z	RESL	VSG	TEULK	(TW-TB)	NUTP	HTP
2.0	3979	2.82	74.18	15.42	89.8	819.0
4.5	4038	2.83	75.36	15.80	87.6	800.0
7.5	4110	2.85	76.79	15.93	86.8	795.0
11.0	4195	2.87	78.45	16.08	85.9	788.0
16.5	4330	2.90	81.06	15.81	87.2	803.0
21.0	4441	2.92	83.21	15.85	86.8	802.0
22.5	4479	2.93	83.92	15.19	90.5	837.0

TEST NO.:F1. 5 FLOW PATTERN:SLUG

ML= 267 MG= 4.97 QFLUX= 12080 NUTP= 87.5 HTP= 803 PDI= 0.340

PDF= 0.016 ALFA=0.622 XTT= 4.07 WE= 16.1 FR= 0.87

	TMIX	RESL	RESG	P	PRL	PRG	VSL	VSG
INLET	72.95	3917	5148.0	16.0	6.45	0.770	1.03	3.47
OUTLET	83.80	4473	5005.4	15.7	5.62	0.769	1.03	3.62
MEAN	78.38	4195	5077.1	15.9	6.03	0.770	1.03	3.54

Z	RESL	VSG	TEULK	(TW-TB)	NUTP	HTP
2.0	3962	3.48	73.85	14.35	92.0	839.0
4.5	4019	3.50	74.98	15.05	87.7	801.0
7.5	4088	3.52	76.34	15.81	83.4	763.0
11.0	4168	3.54	77.92	15.10	87.2	799.0
16.5	4296	3.57	80.41	15.10	87.0	800.0
21.0	4402	3.60	82.45	14.67	89.4	825.0
22.5	4437	3.61	83.13	13.87	94.5	872.0

TEST NO.:F1. 6 FLOW PATTERN:SLUG

ML= 267 MG= 5.54 QFLUX= 12077 NUTP= 88.5 HTP= 812 PDI= 0.328

PDF= 0.017 ALFA=0.638 XTT= 3.68 WE= 16.1 FR= 0.87

	TMIX	RESL	RESG	P	PRL	PRG	VSL	VSG
INLET	72.86	3913	5740.0	16.0	6.46	0.770	1.03	3.88
OUTLET	83.70	4467	5581.2	15.6	5.63	0.769	1.03	4.04
MEAN	78.28	4190	5661.0	15.8	6.04	0.770	1.03	3.96

Z	RESL	VSG	TEULK	(TW-TB)	NUTP	HTP
2.0	3958	3.89	73.76	14.12	93.4	852.0
4.5	4014	3.91	74.89	14.85	88.8	811.0
7.5	4083	3.93	76.24	15.12	87.2	798.0
11.0	4163	3.95	77.82	15.08	87.3	800.0
16.5	4291	3.99	80.31	15.20	86.4	795.0
21.0	4397	4.02	82.35	14.40	91.1	840.0
22.5	4432	4.03	83.03	13.61	96.3	889.0

TEST NO.:F1. 7 FLOW PATTERN:SLUG-ANNULAR

ML= 267 MG= 11.16 QFLUX= 14300 NUTP=112.0 HTP=1030 PDT= 0.334

PDF= 0.098 ALFA=0.726 XTT= 1.97 WE= 16.2 FR= 0.87

	TMIX	RESL	RESG	P	PRL	PRG	VSL	VSG
INLET	73.09	3924	11555.0	16.1	6.43	0.770	1.03	7.73
OUTLET	85.89	4582	11178.1	15.8	5.48	0.769	1.03	8.09
MEAN	79.49	4253	11366.8	16.0	5.94	0.770	1.03	7.91

Z	RESL	VSG	TBULK	(TW-TB)	NUTP	HTP
2.0	3978	7.76	74.16	12.96	120.4	1098.0
4.5	4045	7.80	75.49	13.44	116.0	1061.0
7.5	4126	7.84	77.08	13.89	112.2	1028.0
11.0	4221	7.90	78.95	14.03	110.9	1018.0
16.5	4373	7.98	81.89	14.10	110.1	1015.0
21.0	4498	8.05	84.29	14.07	110.2	1019.0
22.5	4540	8.07	85.10	14.09	109.9	1018.0

TEST NO.:F1. 8 FLOW PATTERN:SLUG-ANNULAR

ML= 267 MG= 15.86 QFLUX= 15619 NUTP=134.7 HTP=1239 PDT= 0.379

PDF= 0.176 ALFA=0.765 XTT= 1.43 WE= 16.2 FR= 0.87

	TMIX	RESL	RESG	P	PRL	PRG	VSL	VSG
INLET	73.20	3930	16421.0	16.2	6.42	0.770	1.03	10.97
OUTLET	87.15	4649	15839.2	15.8	5.39	0.769	1.03	11.53
MEAN	80.18	4289	16130.4	16.0	5.89	0.770	1.03	11.26

Z	RESL	VSG	TBULK	(TW-TB)	NUTP	HTP
2.0	3988	11.01	74.36	12.30	138.5	1264.0
4.5	4061	11.07	75.81	12.57	135.4	1238.0
7.5	4149	11.15	77.55	12.62	134.7	1235.0
11.0	4254	11.23	79.58	12.62	134.5	1236.0
16.5	4419	11.37	82.78	12.65	133.9	1236.0
21.0	4557	11.48	85.41	12.59	134.3	1244.0
22.5	4603	11.52	86.28	12.57	134.4	1246.0

TEST NO.:F1. 9 FLOW PATTERN:ANNULAR

ML= 267 MG= 25.10 QFLUX= 18544 NUTP=181.2 HTP=1671 PDT= 0.039

PDF=-0.128 ALFA=0.807 XTT= 0.95 WE= 16.2 FR= 0.87

	TMIX	RESL	RESG	P	PRL	PRG	VSL	VSG
INLET	73.59	3949	25957.0	16.3	6.37	0.770	1.03	17.20
OUTLET	90.07	4805	24878.1	16.3	5.20	0.769	1.03	17.80
MEAN	81.83	4377	25418.1	16.3	5.76	0.769	1.03	17.51

Z	RESL	VSG	TBULK	(TW-TB)	NUTP	HTP
2.0	4018	17.25	74.96	11.24	179.8	1643.0
4.5	4105	17.32	76.67	11.40	177.1	1622.0
7.5	4210	17.40	78.73	11.29	178.5	1639.0
11.0	4333	17.49	81.13	11.16	180.3	1661.0
16.5	4531	17.63	84.91	10.99	182.4	1689.0
21.0	4695	17.74	88.01	10.75	186.1	1730.0
22.5	4750	17.78	89.05	10.61	188.5	1755.0

TEST NO.:F1.10 FLOW PATTERN:ANNULAR

MI= 267 MG= 35.85 QFLUX= 20702 NUTP=212.0 HTP=1957 PDT= 0.546

PDF= 0.403 ALFA=0.836 XTT= 0.69 WE= 16.2 FR= 0.87

	TMIX	RESL	RESG	P	PRL	PRG	VSL	VSG
INLET	73.33	3936	37092.0	16.7	6.39	0.770	1.03	24.02
OUTLET	91.62	4888	35386.9	16.1	5.10	0.769	1.03	25.72
MEAN	82.47	4412	36239.9	16.4	5.72	0.769	1.03	24.89

Z	RESL	VSG	TEULK	(TW-TB)	NUTP	HTP
2.0	4012	24.16	74.85	10.58	213.1	1946.0
4.5	4108	24.34	76.74	10.81	208.3	1907.0
7.5	4225	24.56	79.03	10.82	207.9	1909.0
11.0	4362	24.81	81.69	10.74	208.9	1926.0
16.5	4582	25.22	85.89	10.41	214.9	1992.0
21.0	4765	25.55	89.33	10.27	217.3	2023.0
22.5	4827	25.66	90.48	10.14	219.7	2049.0

TEST NO.:F1.11 FLOW PATTERN:ANNULAR

MI= 267 MG= 43.84 QFLUX= 21699 NUTP=240.0 HTP=2217 PDT= 0.658

PDF= 0.527 ALFA=0.851 XTT= 0.58 WE= 16.2 FR= 0.87

	TMIX	RESL	RESG	P	PRL	PRG	VSL	VSG
INLET	73.16	3928	45386.0	17.1	6.40	0.770	1.03	28.67
OUTLET	92.24	4922	43211.1	16.4	5.06	0.769	1.03	30.92
MEAN	82.70	4425	44298.7	16.8	5.70	0.769	1.03	29.82

Z	RESL	VSG	TEULK	(TW-TB)	NUTP	HTP
2.0	4007	28.85	74.74	9.86	239.6	2188.0
4.5	4107	29.09	76.72	10.05	234.9	2152.0
7.5	4229	29.38	79.10	10.07	234.0	2150.0
11.0	4372	29.71	81.88	9.96	236.0	2177.0
16.5	4602	30.25	86.27	9.63	243.3	2256.0
21.0	4793	30.70	89.86	9.39	249.0	2321.0
22.5	4858	30.85	91.06	9.26	252.1	2353.0

TEST NO.:F1.12 FLOW PATTERN:ANNULAR

MI= 267 MG= 48.77 QFLUX= 22733 NUTP=256.4 HTP=2369 PDT= 0.734

PDF= 0.609 ALFA=0.858 XTT= 0.53 WE= 16.2 FR= 0.87

	TMIX	RESL	RESG	P	PRL	PRG	VSL	VSG
INLET	73.15	3927	50487.0	17.4	6.40	0.770	1.03	31.36
OUTLET	93.10	4968	47965.0	16.6	5.01	0.769	1.03	34.02
MEAN	83.13	4448	49226.3	17.0	5.67	0.769	1.03	32.72

Z	RESL	VSG	TEULK	(TW-TB)	NUTP	HTP
2.0	4010	31.58	74.81	9.63	257.1	2349.0
4.5	4115	31.86	76.88	9.85	251.0	2299.0
7.5	4242	32.19	79.37	9.80	251.8	2314.0
11.0	4393	32.59	82.27	9.75	252.6	2331.0
16.5	4633	33.22	86.85	9.47	259.0	2404.0
21.0	4833	33.75	90.60	9.27	263.9	2462.0
22.5	4901	33.93	91.86	9.07	269.4	2517.0

TEST NO.:F1.13 FLOW PATTERN:ANNULAR

ML= 267 MG= 85.32 QFLUX= 25969 NUTP=315.0 HTP=2911 PDT= 1.123

PDF= 1.025 ALFA=0.890 XTT= 0.34 WE= 16.2 FR= 0.87

	TMIX	RESL	RESG	P	PRL	PRG	VSL	VSG
INLET	71.78	3859	88650.0	19.1	6.52	0.770	1.03	49.51
OUTLET	94.13	5024	83699.6	18.0	4.95	0.769	1.03	54.92
MEAN	82.95	4441	86175.1	18.6	5.69	0.769	1.03	52.27

Z	RESL	VSG	TBULK	(TW-TB)	NUTP	HTP
2.0	3951	49.96	73.63	9.04	313.2	2856.0
4.5	4068	50.51	75.95	9.24	305.8	2798.0
7.5	4210	51.19	78.73	9.23	305.6	2807.0
11.0	4378	52.00	81.99	9.08	310.0	2859.0
16.5	4647	53.29	87.12	8.79	319.0	2963.0
21.0	4873	54.37	91.33	8.47	330.0	3081.0
22.5	4949	54.74	92.74	8.31	336.0	3143.0

TEST NO.:F1.14 FLOW PATTERN:ANNULAR

ML= 267 MG=122.37 QFLUX= 28266 NUTP=372.8 HTP=3449 PDT= 1.624

PDF= 1.540 ALFA=0.907 XTT= 0.26 WE= 16.3 FR= 0.87

	TMIX	RESL	RESG	P	PRL	PRG	VSL	VSG
INLET	71.96	3868	127084.0	21.2	6.49	0.770	1.03	63.81
OUTLET	95.82	5117	119538.2	19.6	4.85	0.768	1.03	72.39
MEAN	83.89	4492	123311.5	20.4	5.63	0.769	1.03	68.16

Z	RESL	VSG	TBULK	(TW-TB)	NUTP	HTP
2.0	3966	64.50	73.93	8.10	380.0	3467.0
4.5	4091	65.37	76.41	8.46	363.2	3325.0
7.5	4243	66.44	79.38	8.52	360.0	3309.0
11.0	4423	67.71	82.86	8.45	361.8	3341.0
16.5	4712	69.76	88.34	8.08	377.2	3509.0
21.0	4954	71.50	92.84	7.72	393.3	3680.0
22.5	5036	72.09	94.34	7.49	404.7	3794.0

TEST NO.:F1.15 FLOW PATTERN:ANNULAR

ML= 267 MG=206.59 QFLUX= 30586 NUTP=363.4 HTP=3351 PDT= 2.447

PDF= 2.386 ALFA=0.934 XTT= 0.16 WE= 16.2 FR= 0.87

	TMIX	RESL	RESG	P	PRL	PRG	VSL	VSG
INLET	69.22	3732	216119.0	21.1	6.75	0.770	1.03	107.64
OUTLET	93.98	5016	202744.7	18.7	4.97	0.769	1.03	127.73
MEAN	81.60	4374	209432.0	19.9	5.81	0.769	1.03	117.70

Z	RESL	VSG	TBULK	(TW-TB)	NUTP	HTP
2.0	3833	109.19	71.27	8.09	412.8	3753.0
4.5	3962	111.17	73.84	8.88	375.7	3428.0
7.5	4117	113.62	76.92	9.21	361.6	3312.0
11.0	4302	116.56	80.53	9.42	352.7	3247.0
16.5	4599	121.40	86.21	9.37	352.9	3274.0
21.0	4848	125.57	90.88	9.04	364.6	3403.0
22.5	4932	127.01	92.44	8.80	374.2	3499.0

TEST NO.:F2. 1 FLOW PATTERN:BUBBLE

ML= 882 MG= 1.03 QFLUX= 19720 NUTP=123.1 HTP=1125 PDT= 0.894

PDF= 0.176 ALFA=0.157 XTT= 50.50 WE= 174.7 FR= 9.40

	TMIX	RESL	RESG	P	PRL	PRG	VSL	VSG
INLET	72.75	12883	1073.0	17.2	6.49	0.770	3.41	0.67
OUTLET	78.13	13781	1058.0	16.3	6.05	0.770	3.41	0.72
MEAN	75.44	13332	1065.5	16.7	6.27	0.770	3.40	0.70

Z	RESL	VSG	TEULK	(TW-TB)	NUTP	HTP
2.0	12957	0.68	73.20	16.80	128.5	1171.0
4.5	13050	0.68	73.76	17.58	122.8	1120.0
7.5	13161	0.69	74.43	17.79	121.3	1107.0
11.0	13292	0.69	75.22	17.73	121.7	1112.0
16.5	13498	0.70	76.45	17.55	122.8	1124.0
21.0	13668	0.71	77.46	17.26	124.7	1143.0
22.5	13724	0.72	77.80	17.14	125.6	1152.0

TEST NO.:F2. 2 FLOW PATTERN:BUBBLE

ML= 882 MG= 1.49 QFLUX= 19711 NUTP=132.0 HTP=1208 PDT= 0.873

PDF= 0.196 ALFA=0.206 XTT= 36.33 WE= 174.8 FR= 9.40

	TMIX	RESL	RESG	P	PRL	PRG	VSL	VSG
INLET	73.14	12949	1544.0	17.2	6.46	0.770	3.41	0.97
OUTLET	78.53	13847	1523.0	16.3	6.02	0.770	3.41	1.03
MEAN	75.84	13398	1533.8	16.7	6.24	0.770	3.40	1.00

Z	RESL	VSG	TEULK	(TW-TB)	NUTP	HTP
2.0	13023	0.98	73.59	15.76	136.9	1248.0
4.5	13115	0.98	74.15	16.38	131.7	1202.0
7.5	13227	0.99	74.83	16.51	130.6	1193.0
11.0	13358	1.00	75.61	16.47	130.8	1196.0
16.5	13564	1.01	76.85	16.32	131.9	1208.0
21.0	13734	1.03	77.86	16.14	133.3	1222.0
22.5	13791	1.03	78.19	16.00	134.4	1233.0

TEST NO.:F2. 3 FLOW PATTERN:BUBBLE

ML= 882 MG= 2.38 QFLUX= 21688 NUTP=149.7 HTP=1369 PDT= 0.841

PDF= 0.228 ALFA=0.280 XTT= 23.78 WE= 174.8 FR= 9.40

	TMIX	RESL	RESG	P	PRL	PRG	VSL	VSG
INLET	72.92	12912	2468.0	17.1	6.47	0.770	3.41	1.56
OUTLET	78.84	13900	2430.8	16.2	6.00	0.770	3.41	1.66
MEAN	75.88	13406	2449.8	16.7	6.23	0.770	3.40	1.61

Z	RESL	VSG	TEULK	(TW-TB)	NUTP	HTP
2.0	12993	1.56	73.41	15.47	153.5	1399.0
4.5	13095	1.58	74.03	15.96	148.8	1357.0
7.5	13218	1.59	74.77	16.04	147.9	1351.0
11.0	13361	1.60	75.63	16.04	147.8	1351.0
16.5	13589	1.63	76.99	15.81	149.8	1372.0
21.0	13776	1.65	78.10	15.49	152.7	1401.0
22.5	13838	1.65	78.47	15.48	152.8	1402.0

TEST NO.:F2. 4 FLOW PATTERN:BUBBLE-SLUG

ML= 882 MG= 3.34 QFLUX= 23769 NUTP=166.1 HTP=1519 PDT= 0.832

PDF= 0.269 ALFA=0.340 XTT= 17.51 WE= 174.7 FR= 9.40

	TMIX	RESL	RESG	P	PRL	PRG	VSL	VSG
INLET	72.43	12831	3467.0	17.0	6.52	0.770	3.41	2.19
OUTLET	78.92	13913	3409.3	16.2	5.99	0.770	3.41	2.33
MEAN	75.67	13372	3438.5	16.6	6.25	0.770	3.40	2.26

Z	RESL	VSG	TEULK	(TW-TB)	NUTP	HTP
2.0	12920	2.20	72.97	15.29	170.2	1551.0
4.5	13031	2.22	73.65	15.76	165.1	1506.0
7.5	13166	2.24	74.46	15.90	163.5	1493.0
11.0	13323	2.26	75.40	15.74	165.1	1509.0
16.5	13572	2.29	76.89	15.61	166.3	1523.0
21.0	13777	2.32	78.11	15.41	168.3	1544.0
22.5	13845	2.33	78.52	15.34	169.0	1551.0

TEST NO.:F2. 5 FLOW PATTERN:BUBBLE-SLUG

ML= 882 MG= 4.89 QFLUX= 28267 NUTP=194.0 HTP=1776 PDT= 0.842

PDF= 0.338 ALFA=0.410 XTT= 12.43 WE= 174.9 FR= 9.40

	TMIX	RESL	RESG	P	PRL	PRG	VSL	VSG
INLET	72.38	12823	5067.0	17.0	6.52	0.770	3.41	3.20
OUTLET	80.10	14113	4966.7	16.2	5.90	0.770	3.41	3.42
MEAN	76.24	13468	5017.3	16.6	6.20	0.770	3.40	3.31

Z	RESL	VSG	TEULK	(TW-TB)	NUTP	HTP
2.0	12928	3.22	73.02	15.48	199.9	1821.0
4.5	13061	3.24	73.82	16.00	193.3	1763.0
7.5	13221	3.27	74.79	16.14	191.5	1749.0
11.0	13408	3.30	75.91	16.06	192.3	1759.0
16.5	13705	3.35	77.68	15.89	194.1	1780.0
21.0	13949	3.40	79.13	15.68	196.4	1805.0
22.5	14031	3.41	79.62	15.58	197.6	1817.0

TEST NO.:F2. 6 FLOW PATTERN:BUBBLE-SLUG

ML= 882 MG= 5.46 QFLUX= 28263 NUTP=202.3 HTP=1853 PDT= 0.857

PDF= 0.370 ALFA=0.430 XTT= 11.25 WE= 175.0 FR= 9.40

	TMIX	RESL	RESG	P	PRL	PRG	VSL	VSG
INLET	72.82	12895	5656.0	17.1	6.48	0.770	3.41	3.57
OUTLET	80.53	14187	5543.8	16.2	5.87	0.770	3.41	3.81
MEAN	76.68	13541	5600.2	16.6	6.17	0.770	3.40	3.69

Z	RESL	VSG	TEULK	(TW-TB)	NUTP	HTP
2.0	13001	3.59	73.46	14.88	207.8	1895.0
4.5	13134	3.62	74.27	15.33	201.7	1841.0
7.5	13294	3.65	75.23	15.41	200.4	1832.0
11.0	13482	3.68	76.35	15.41	200.3	1833.0
16.5	13779	3.74	78.12	15.17	203.1	1864.0
21.0	14024	3.79	79.57	15.12	203.7	1872.0
22.5	14106	3.81	80.06	15.00	205.1	1887.0

TEST NO.:F2. 7 FLOW PATTERN:SLUG

MI= 882 MG= 7.63 QFLUX= 28268 NUTP=194.6 HTP=1782 PDT= 0.851

PDF= 0.415 ALFA=0.490 XTT= 8.32 WE= 174.9 FR= 9.40

	TMIX	RESL	RESG	P	PRL	PRG	VSL	VSG
INLET	72.55	12850	7909.0	17.0	6.50	0.770	3.41	5.00
OUTLET	80.26	14141	7751.8	16.2	5.89	0.770	3.41	5.34
MEAN	76.40	13496	7830.7	16.6	6.19	0.770	3.40	5.18

Z	RESL	VSG	TEULK	(TW-TB)	NUTP	HTP
2.0	12956	5.03	73.19	14.78	209.3	1908.0
4.5	13089	5.06	73.99	15.16	203.9	1860.0
7.5	13249	5.11	74.95	15.61	197.9	1808.0
11.0	13436	5.16	76.08	15.95	193.6	1771.0
16.5	13733	5.24	77.85	16.23	190.0	1743.0
21.0	13977	5.31	79.30	16.47	187.1	1719.0
22.5	14059	5.33	79.78	16.26	189.4	1742.0

SLUG-ANNULAR FLOW PATTERN:TEST NO.:F2. 8

MI= 882 MG= 14.96 QFLUX= 30609 NUTP=217.7 HTP=1993 PDT= 0.928

PDF= 0.584 ALFA=0.600 XTT= 4.56 WE= 174.9 FR= 9.40

	TMIX	RESL	RESG	P	PRL	PRG	VSL	VSG
INLET	72.30	12810	15522.0	17.2	6.52	0.770	3.41	9.69
OUTLET	80.64	14206	15187.4	16.3	5.86	0.770	3.41	10.41
MEAN	76.47	13508	15354.8	16.7	6.18	0.770	3.40	10.06

Z	RESL	VSG	TEULK	(TW-TB)	NUTP	HTP
2.0	12924	9.75	73.00	15.12	221.6	2019.0
4.5	13067	9.82	73.86	15.42	217.2	1982.0
7.5	13240	9.91	74.91	15.54	215.4	1967.0
11.0	13443	10.02	76.12	15.44	216.6	1982.0
16.5	13764	10.19	78.04	15.33	217.8	1998.0
21.0	14029	10.33	79.60	15.17	219.9	2021.0
22.5	14118	10.38	80.12	15.08	221.0	2033.0

TEST NO.:F2. 9 FLOW PATTERN:ANNULAR

MI= 882 MG= 26.65 QFLUX= 35589 NUTP=268.1 HTP=2455 PDT= 1.134

PDF= 0.857 ALFA=0.678 XTT= 2.74 WE= 175.0 FR= 9.40

	TMIX	RESL	RESG	P	PRL	PRG	VSL	VSG
INLET	71.78	12724	27690.0	17.7	6.57	0.770	3.41	16.79
OUTLET	81.46	14344	26999.2	16.5	5.80	0.769	3.41	18.27
MEAN	76.62	13534	27345.0	17.1	6.17	0.770	3.40	17.54

Z	RESL	VSG	TEULK	(TW-TB)	NUTP	HTP
2.0	12856	16.91	72.58	14.43	270.1	2460.0
4.5	13022	17.06	73.59	14.74	264.3	2410.0
7.5	13222	17.25	74.80	14.71	264.6	2417.0
11.0	13458	17.47	76.21	14.62	265.9	2433.0
16.5	13830	17.82	78.43	14.39	269.6	2475.0
21.0	14139	18.12	80.25	14.19	273.1	2513.0
22.5	14242	18.22	80.85	13.93	278.0	2560.0

TEST NO.:F2.10 FLOW PATTERN:ANNULAR

ML= 882 MG= 36.89 QFLUX= 41013 NUTP=310.1 HTP=2843 PDT= 1.368

PDF= 1.123 ALFA=0.715 XTT= 2.07 WE= 175.2 FR= 9.40

	TMIX	RESL	RESG	P	PRL	PRG	VSL	VSG
INLET	72.00	12761	38303.0	18.3	6.54	0.770	3.41	22.46
OUTLET	83.14	14633	37207.1	16.9	5.67	0.769	3.41	24.80
MEAN	77.57	13697	37755.1	17.6	6.10	0.770	3.41	23.65

Z	RESL	VSG	TEULK	(TW-TB)	NUTP	HTP
2.0	12913	22.65	72.93	14.42	311.2	2836.0
4.5	13105	22.89	74.09	14.75	304.1	2775.0
7.5	13336	23.18	75.48	14.68	305.1	2790.0
11.0	13607	23.53	77.10	14.57	307.0	2813.0
16.5	14038	24.09	79.66	14.32	311.8	2866.0
21.0	14395	24.56	81.75	13.98	318.9	2940.0
22.5	14514	24.72	82.45	13.79	323.1	2982.0

TEST NO.:F2.11 FLOW PATTERN:ANNULAR

ML= 882 MG= 45.53 QFLUX= 40983 NUTP=337.5 HTP=3095 PDT= 1.603

PDF= 1.375 ALFA=0.736 XTT= 1.74 WE= 175.2 FR= 9.40

	TMIX	RESL	RESG	P	PRL	PRG	VSL	VSG
INLET	71.99	12758	47278.0	18.9	6.54	0.770	3.41	26.69
OUTLET	83.10	14626	45928.4	17.4	5.68	0.769	3.41	29.78
MEAN	77.54	13692	46603.4	18.1	6.10	0.770	3.41	28.25

Z	RESL	VSG	TEULK	(TW-TB)	NUTP	HTP
2.0	12910	26.93	72.91	13.27	338.0	3080.0
4.5	13101	27.24	74.07	13.54	331.0	3021.0
7.5	13332	27.63	75.45	13.53	330.8	3025.0
11.0	13603	28.09	77.07	13.41	333.5	3056.0
16.5	14033	28.82	79.62	13.06	341.6	3141.0
21.0	14388	29.46	81.71	12.87	346.1	3191.0
22.5	14508	29.67	82.41	12.63	352.4	3253.0

TEST NO.:F2.12 FLOW PATTERN:ANNULAR

ML= 882 MG= 48.88 QFLUX= 40976 NUTP=347.1 HTP=3183 PDT= 1.685

PDF= 1.463 ALFA=0.743 XTT= 1.64 WE= 175.2 FR= 9.40

	TMIX	RESL	RESG	P	PRL	PRG	VSL	VSG
INLET	72.07	12772	50747.0	19.2	6.53	0.770	3.41	28.27
OUTLET	83.17	14639	49299.7	17.5	5.67	0.769	3.41	31.66
MEAN	77.62	13706	50023.5	18.4	6.09	0.770	3.41	29.98

Z	RESL	VSG	TEULK	(TW-TB)	NUTP	HTP
2.0	12924	28.54	72.99	12.90	347.4	3165.0
4.5	13115	28.88	74.15	13.15	340.5	3108.0
7.5	13345	29.30	75.54	13.11	341.4	3122.0
11.0	13616	29.80	77.15	12.99	343.9	3152.0
16.5	14046	30.61	79.70	12.75	349.9	3217.0
21.0	14401	31.30	81.79	12.51	356.0	3283.0
22.5	14521	31.54	82.48	12.36	360.0	3322.0

TEST NO.:F2.13 FLOW PATTERN:ANNULAR

ML= 882 MG= 57.65 QFLUX= 40969 NUTP=351.8 HTP=3226 PDT= 1.772

PDF= 1.564 ALFA=0.760 XTT= 1.42 WE= 175.2 FR= 9.40

	TMIX	RESL	RESG	P	PRL	PRG	VSL	VSG
INLET	72.01	12762	59858.0	19.4	6.54	0.770	3.41	32.90
OUTLET	83.09	14625	58153.4	17.7	5.68	0.769	3.41	36.98
MEAN	77.55	13694	59006.1	18.6	6.10	0.770	3.41	34.96

Z	RESL	VSG	TBULK	(TW-TB)	NUTP	HTP
2.0	12913	33.23	72.93	12.80	350.3	3192.0
4.5	13104	33.64	74.08	12.95	345.8	3156.0
7.5	13334	34.14	75.47	12.99	344.4	3149.0
11.0	13604	34.74	77.08	12.82	348.6	3194.0
16.5	14033	35.72	79.63	12.56	355.2	3266.0
21.0	14388	36.55	81.71	12.33	361.1	3329.0
22.5	14507	36.84	82.40	12.08	368.3	3399.0

TEST NO.:F2.14 FLOW PATTERN:ANNULAR

ML= 882 MG=111.39 QFLUX= 49821 NUTP=440.4 HTP=4053 PDT= 2.972

PDF= 2.808 ALFA=0.812 XTT= 0.83 WE= 175.8 FR= 9.41

	TMIX	RESL	RESG	P	PRL	PRG	VSL	VSG
INLET	73.45	13000	115225.0	22.5	6.40	0.770	3.41	54.77
OUTLET	86.82	15271	111305.9	19.6	5.41	0.769	3.41	64.74
MEAN	80.13	14135	113265.6	21.1	5.89	0.770	3.41	59.73

Z	RESL	VSG	TBULK	(TW-TB)	NUTP	HTP
2.0	13183	55.52	74.56	12.38	439.1	4010.0
4.5	13415	56.49	75.95	12.64	429.8	3932.0
7.5	13694	57.70	77.62	12.61	430.1	3943.0
11.0	14023	59.15	79.57	12.47	434.5	3995.0
16.5	14546	61.56	82.63	12.12	445.8	4116.0
21.0	14980	63.65	85.15	11.84	455.6	4220.0
22.5	15126	64.38	85.99	11.60	464.5	4307.0

TEST NO.:F2.15 FLOW PATTERN:ANNULAR

ML= 882 MG=156.76 QFLUX= 52517 NUTP=472.3 HTP=4344 PDT= 3.805

PDF= 3.657 ALFA=0.832 XTT= 0.65 WE= 175.7 FR= 9.41

	TMIX	RESL	RESG	P	PRL	PRG	VSL	VSG
INLET	72.74	12881	162473.0	25.7	6.46	0.770	3.41	67.17
OUTLET	86.72	15254	156688.8	21.9	5.42	0.769	3.41	81.10
MEAN	79.73	14068	159581.1	23.8	5.92	0.770	3.41	74.07

Z	RESL	VSG	TBULK	(TW-TB)	NUTP	HTP
2.0	13073	68.21	73.90	11.86	483.3	4409.0
4.5	13314	69.55	75.35	12.31	465.5	4256.0
7.5	13606	71.21	77.10	12.30	465.1	4262.0
11.0	13950	73.24	79.13	12.25	466.5	4287.0
16.5	14496	76.60	82.34	12.02	473.9	4373.0
21.0	14950	79.55	84.97	11.78	482.6	4469.0
22.5	15102	80.58	85.85	11.55	492.0	4562.0

TEST NO.:F3. 1 FLOW PATTERN:BUBBLE

ML=3598 MG= 0.84 QFLUX= 46797 NUTP=346.9 HTP=3174 PDT= 2.338

PDF= 1.518 ALFA=0.035 XTT=226.51 WE= 2909.0 FR=156.00

	TMIX	RESL	RESG	P	PRL	PRG	VSL	VSG
INLET	74.52	53751	863.0	19.4	6.34	0.770	13.89	0.48
OUTLET	77.65	55886	856.0	17.1	6.09	0.770	13.89	0.55
MEAN	76.09	54818	859.5	18.3	6.21	0.770	13.89	0.51

Z	RESL	VSG	TEULK	(TW-TB)	NUTP	HTP
2.0	53927	0.49	74.78	14.37	356.0	3252.0
4.5	54149	0.49	75.11	13.70	373.2	3410.0
7.5	54415	0.50	75.50	14.93	342.8	3134.0
11.0	54726	0.51	75.96	14.99	341.1	3121.0
16.5	55216	0.53	76.67	14.95	341.9	3131.0
21.0	55618	0.54	77.26	14.97	341.3	3128.0
22.5	55753	0.55	77.46	14.85	344.0	3154.0

TEST NO.:F3. 2 FLOW PATTERN:BUBBLE

ML=3598 MG= 1.32 QFLUX= 50217 NUTP=350.2 HTP=3202 PDT= 2.361

PDF= 1.556 ALFA=0.053 XTT=151.11 WE= 2906.0 FR=156.00

	TMIX	RESL	RESG	P	PRL	PRG	VSL	VSG
INLET	73.86	53302	1366.0	19.7	6.40	0.770	13.89	0.75
OUTLET	77.22	55588	1354.9	17.3	6.13	0.770	13.89	0.86
MEAN	75.54	54445	1360.9	18.5	6.26	0.770	13.89	0.80

Z	RESL	VSG	TEULK	(TW-TB)	NUTP	HTP
2.0	53491	0.76	74.14	14.99	366.5	3345.0
4.5	53728	0.77	74.49	15.53	353.9	3231.0
7.5	54013	0.78	74.91	15.67	350.5	3202.0
11.0	54346	0.80	75.40	15.79	347.8	3180.0
16.5	54870	0.82	76.17	15.79	347.6	3181.0
21.0	55301	0.85	76.80	15.78	347.7	3185.0
22.5	55445	0.85	77.01	15.65	350.4	3211.0

TEST NO.:F3. 3 FLOW PATTERN:BUBBLE

ML=3598 MG= 2.05 QFLUX= 52504 NUTP=355.3 HTP=3248 PDT= 2.425

PDF= 1.640 ALFA=0.079 XTT=102.40 WE= 2905.0 FR=156.00

	TMIX	RESL	RESG	P	PRL	PRG	VSL	VSG
INLET	73.50	53063	2119.0	19.8	6.43	0.770	13.89	1.15
OUTLET	77.02	55450	2099.8	17.4	6.14	0.770	13.89	1.32
MEAN	75.26	54257	2109.5	18.6	6.29	0.770	13.89	1.23

Z	RESL	VSG	TEULK	(TW-TB)	NUTP	HTP
2.0	53260	1.16	73.79	15.29	375.7	3427.0
4.5	53507	1.18	74.16	15.95	360.3	3288.0
7.5	53805	1.20	74.60	16.17	355.3	3244.0
11.0	54152	1.22	75.11	16.25	353.5	3231.0
16.5	54701	1.26	75.92	16.34	351.3	3214.0
21.0	55151	1.30	76.58	16.28	352.3	3226.0
22.5	55301	1.31	76.80	16.23	353.4	3237.0

TEST NO.:F3. 4 FLOW PATTERN:BUBBLE-FROTH

MI=3598 MG= 2.91 QFLUX= 52773 NUTP=365.1 HTP=3338 PDT= 2.488

PDF= 1.726 ALFA=0.104 XTT= 75.51 WE= 2906.0 FR=156.00

	TMIX	RESL	RESG	P	PRL	PRG	VSL	VSG
INLET	73.63	53152	3004.0	20.2	6.42	0.770	13.89	1.60
OUTLET	77.17	55553	2976.5	17.8	6.13	0.770	13.89	1.83
MEAN	75.40	54352	2990.4	19.0	6.27	0.770	13.89	1.71

Z	RESL	VSG	TEULK	(TW-TB)	NUTP	HTP
2.0	53350	1.61	73.93	14.54	397.1	3623.0
4.5	53599	1.64	74.30	15.45	373.8	3412.0
7.5	53898	1.67	74.74	15.72	367.2	3354.0
11.0	54247	1.70	75.25	15.91	362.8	3316.0
16.5	54799	1.76	76.06	16.14	357.5	3271.0
21.0	55252	1.81	76.73	16.03	359.8	3295.0
22.5	55403	1.82	76.95	16.16	356.9	3269.0

TEST NO.:F3. 5 FLOW PATTERN:FROTH

MI=3598 MG= 3.58 QFLUX= 52512 NUTP=366.9 HTP=3357 PDT= 2.513

PDF= 1.766 ALFA=0.123 XTT= 63.00 WE= 2908.0 FR=156.00

	TMIX	RESL	RESG	P	PRL	PRG	VSL	VSG
INLET	74.21	53539	3691.0	20.5	6.37	0.770	13.89	1.94
OUTLET	77.72	55935	3658.0	18.0	6.08	0.770	13.89	2.23
MEAN	75.97	54737	3674.9	19.3	6.22	0.770	13.89	2.08

Z	RESL	VSG	TEULK	(TW-TB)	NUTP	HTP
2.0	53737	1.96	74.50	14.17	405.0	3698.0
4.5	53985	1.99	74.87	15.16	378.7	3460.0
7.5	54284	2.02	75.31	15.54	369.4	3376.0
11.0	54632	2.07	75.82	15.76	364.1	3330.0
16.5	55183	2.13	76.63	16.06	357.3	3271.0
21.0	55634	2.19	77.29	15.90	360.7	3306.0
22.5	55785	2.21	77.51	16.06	357.0	3273.0

TEST NO.:F3. 6 FLOW PATTERN:FROTH

MI=3598 MG= 4.11 QFLUX= 52510 NUTP=371.3 HTP=3397 PDT= 2.581

PDF= 1.846 ALFA=0.136 XTT= 55.94 WE= 2909.0 FR=156.00

	TMIX	RESL	RESG	P	PRL	PRG	VSL	VSG
INLET	74.34	53629	4244.0	20.8	6.35	0.770	13.89	2.20
OUTLET	77.86	56025	4205.5	18.2	6.07	0.770	13.89	2.52
MEAN	76.10	54827	4224.9	19.5	6.21	0.770	13.89	2.36

Z	RESL	VSG	TEULK	(TW-TB)	NUTP	HTP
2.0	53827	2.22	74.63	13.99	410.3	3747.0
4.5	54075	2.26	75.00	14.92	384.6	3515.0
7.5	54373	2.30	75.44	15.31	374.8	3426.0
11.0	54722	2.34	75.95	15.52	369.6	3381.0
16.5	55273	2.42	76.76	15.90	360.6	3303.0
21.0	55725	2.49	77.42	15.83	362.2	3320.0
22.5	55875	2.51	77.64	15.96	359.2	3294.0

TEST NO.:F3. 7 FLOW PATTERN:FROTH

ML=3598 MG= 4.82 QFLUX= 55310 NUTP=374.1 HTP=3425 PDT= 2.610

PDF= 1.890 ALFA=0.154 XTT= 48.62 WE= 2910.0 FR=156.00

	TMIX	RESL	RESG	P	PRL	PRG	VSL	VSG
INLET	74.56	53778	4974.0	21.0	6.33	0.770	13.89	2.56
OUTLET	78.26	56305	4926.1	18.4	6.04	0.770	13.89	2.94
MEAN	76.41	55042	4950.1	19.7	6.19	0.770	13.89	2.75

Z	RESL	VSG	TBULK	(TW-TB)	NUTP	HTP
2.0	53987	2.59	74.87	14.52	416.0	3801.0
4.5	54248	2.63	75.25	15.58	387.8	3545.0
7.5	54563	2.67	75.72	15.97	378.3	3460.0
11.0	54931	2.73	76.26	16.29	370.8	3394.0
16.5	55512	2.82	77.11	16.53	365.3	3347.0
21.0	55988	2.90	77.80	16.67	362.1	3321.0
22.5	56147	2.93	78.03	16.66	362.2	3323.0

TEST NO.:F3. 8 FLOW PATTERN:FROTH

ML=3598 MG= 5.44 QFLUX= 55291 NUTP=379.1 HTP=3469 PDT= 2.647

PDF= 1.938 ALFA=0.167 XTT= 43.84 WE= 2909.0 FR=156.00

	TMIX	RESL	RESG	P	PRL	PRG	VSL	VSG
INLET	74.38	53658	5612.0	21.2	6.35	0.770	13.89	2.86
OUTLET	78.09	56183	5558.5	18.5	6.05	0.770	13.89	3.29
MEAN	76.23	54920	5585.5	19.9	6.20	0.770	13.89	3.07

Z	RESL	VSG	TBULK	(TW-TB)	NUTP	HTP
2.0	53867	2.89	74.69	14.32	421.7	3852.0
4.5	54128	2.93	75.08	15.30	394.9	3608.0
7.5	54442	2.98	75.54	15.69	385.0	3521.0
11.0	54810	3.05	76.08	16.10	375.3	3434.0
16.5	55390	3.15	76.93	16.38	368.7	3377.0
21.0	55865	3.24	77.62	16.46	366.7	3363.0
22.5	56024	3.27	77.86	16.50	365.7	3355.0

TEST NO.:F3. 9 FLOW PATTERN:FROTH

ML=3598 MG= 17.76 QFLUX= 58099 NUTP=395.1 HTP=3614 PDT= 3.243

PDF= 2.678 ALFA=0.338 XTT= 15.92 WE= 2908.0 FR=156.00

	TMIX	RESL	RESG	P	PRL	PRG	VSL	VSG
INLET	73.89	53323	18351.0	23.5	6.39	0.770	13.89	8.36
OUTLET	77.78	55970	18166.1	20.3	6.08	0.770	13.89	9.77
MEAN	75.83	54646	18259.0	21.9	6.24	0.770	13.89	9.06

Z	RESL	VSG	TBULK	(TW-TB)	NUTP	HTP
2.0	53541	8.46	74.21	14.65	433.6	3957.0
4.5	53815	8.60	74.62	15.52	409.5	3740.0
7.5	54145	8.77	75.10	15.88	400.0	3656.0
11.0	54530	8.97	75.67	16.30	389.6	3563.0
16.5	55138	9.31	76.56	16.36	388.0	3553.0
21.0	55637	9.61	77.29	16.61	382.1	3502.0
22.5	55804	9.71	77.53	16.30	389.2	3568.0

TEST NO.:F3.10 FLOW PATTERN:FROTH

ML=3598 MG= 22.38 QFLUX= 58089 NUTP=413.3 HTP=3782 PDT= 3.494

PDF= 2.959 ALFA=0.374 XTT= 13.16 WE= 2909.0 FR=156.00

	TMIX	RESL	RESG	P	PRL	PRG	VSL	VSG
INLET	74.28	53589	23105.0	24.5	6.36	0.770	13.89	10.12
OUTLET	78.17	56240	22872.2	21.0	6.05	0.770	13.89	11.89
MEAN	76.23	54915	22989.0	22.7	6.20	0.770	13.89	11.00

Z	RESL	VSG	TEULK	(TW-TB)	NUTP	HTP
2.0	53808	10.25	74.61	14.18	447.6	4088.0
4.5	54082	10.42	75.01	14.92	425.6	3889.0
7.5	54412	10.63	75.50	15.21	417.4	3816.0
11.0	54798	10.89	76.06	15.49	409.9	3751.0
16.5	55407	11.32	76.95	15.66	405.1	3711.0
21.0	55907	11.70	77.68	15.74	402.9	3695.0
22.5	56074	11.83	77.93	15.49	409.1	3753.0

TEST NO.:F3.11 FLOW PATTERN:FROTH

ML=3598 MG= 32.71 QFLUX= 60932 NUTP=442.6 HTP=4049 PDT= 4.036

PDF= 3.547 ALFA=0.428 XTT= 9.75 WE= 2908.0 FR=156.00

	TMIX	RESL	RESG	P	PRL	PRG	VSL	VSG
INLET	73.84	53287	33807.0	26.6	6.40	0.770	13.89	13.53
OUTLET	77.91	56062	33448.6	22.6	6.07	0.770	13.89	16.09
MEAN	75.87	54675	33628.0	24.6	6.23	0.770	13.89	14.80

Z	RESL	VSG	TEULK	(TW-TB)	NUTP	HTP
2.0	53516	13.73	74.17	14.10	472.5	4312.0
4.5	53803	13.97	74.60	14.73	452.6	4133.0
7.5	54149	14.27	75.11	15.04	443.1	4050.0
11.0	54553	14.64	75.70	15.15	439.8	4022.0
16.5	55190	15.26	76.64	15.25	436.6	3998.0
21.0	55713	15.81	77.40	15.29	435.2	3989.0
22.5	55888	15.99	77.66	15.09	440.9	4043.0

TEST NO.:F3.12 FLOW PATTERN:FROTH

ML=3598 MG= 40.03 QFLUX= 63878 NUTP=460.9 HTP=4221 PDT= 4.425

PDF= 3.959 ALFA=0.456 XTT= 8.33 WE= 2910.0 FR=156.00

	TMIX	RESL	RESG	P	PRL	PRG	VSL	VSG
INLET	74.40	53672	41302.0	28.1	6.35	0.770	13.89	15.69
OUTLET	78.67	56588	40843.7	23.7	6.01	0.770	13.89	18.80
MEAN	76.54	55130	41073.0	25.9	6.18	0.770	13.89	17.23

Z	RESL	VSG	TEULK	(TW-TB)	NUTP	HTP
2.0	53913	15.92	74.76	14.20	491.6	4490.0
4.5	54214	16.22	75.20	14.81	471.3	4308.0
7.5	54577	16.59	75.74	15.08	462.9	4234.0
11.0	55002	17.04	76.36	15.24	457.8	4191.0
16.5	55671	17.79	77.34	15.35	454.3	4164.0
21.0	56222	18.45	78.14	15.39	452.7	4154.0
22.5	56406	18.68	78.41	15.20	458.3	4207.0

TEST NO.:F3.13 FLOW PATTERN:FRCTH

ML=3598 MG= 45.44 QFLUX= 63861 NUTP=467.6 HTP=4281 PDT= 4.671

PDF= 4.218 ALFA=0.472 XTT= 7.60 WE= 2910.0 FR=156.00

	TMIX	RESL	RESG	P	PRL	PRG	VSL	VSG
INLET	74.18	53520	46916.0	29.3	6.37	0.770	13.89	17.04
OUTLET	78.45	56433	46395.4	24.6	6.02	0.770	13.89	20.48
MEAN	76.31	54977	46655.8	26.9	6.19	0.770	13.89	18.74

Z	RESL	VSG	TEULK	(TW-TB)	NUTP	HTP
2.0	53761	17.30	74.54	13.98	499.4	4561.0
4.5	54062	17.62	74.98	14.62	477.5	4363.0
7.5	54424	18.03	75.51	14.92	467.9	4278.0
11.0	54848	18.52	76.14	15.03	464.2	4249.0
16.5	55517	19.36	77.12	15.06	462.9	4241.0
21.0	56067	20.09	77.92	15.19	458.6	4207.0
22.5	56250	20.35	78.18	14.96	465.7	4274.0

TEST NO.:F3.14 FLOW PATTERN:FRCTH

ML=3598 MG= 49.79 QFLUX= 63865 NUTP=472.4 HTP=4326 PDT= 4.922

PDF= 4.479 ALFA=0.483 XTT= 7.10 WE= 2911.0 FR=156.00

	TMIX	RESL	RESG	P	PRL	PRG	VSL	VSG
INLET	74.44	53698	51369.0	30.2	6.34	0.770	13.89	18.08
OUTLET	78.71	56613	50800.0	25.3	6.00	0.770	13.89	21.82
MEAN	76.58	55156	51084.9	27.8	6.17	0.770	13.89	19.92

Z	RESL	VSG	TEULK	(TW-TB)	NUTP	HTP
2.0	53939	18.36	74.80	13.82	504.9	4613.0
4.5	54240	18.71	75.24	14.47	482.2	4407.0
7.5	54603	19.15	75.78	14.71	474.4	4339.0
11.0	55027	19.69	76.40	14.91	467.6	4281.0
16.5	55697	20.60	77.38	14.94	466.6	4277.0
21.0	56247	21.40	78.18	14.98	464.9	4266.0
22.5	56431	21.68	78.45	14.81	470.1	4316.0

APPENDIX I

DERIVATION OF PRESSURE DROP AND HOLDUP EQUATIONS FOR HORIZONTAL STRATIFIED FLOW

I.1 Derivation of the Turbulent-Turbulent Flow Equations

Equating V_{G1} (Eq. (8.3)) and V_{G2} (Eq. (8.4)) at the position of maximum gas velocity gives (see Fig. 8.1)

$$a^{1/7}\left(\frac{\tau_{WG}}{\tau_{WL}}\right)^{4/7} - b^{1/7}\left(\frac{\tau_i}{\tau_{WL}}\right)^{4/7} = \delta^{1/7}\left(\frac{\nu_G}{\nu_L}\right)^{1/7}\left(\frac{\rho_G}{\rho_L}\right)^{4/7} \tag{I.1}$$

From Eqs. (8.2) and (8.5) one obtains

$$a^{8/7}\left(\frac{\tau_{WG}}{\tau_{WL}}\right)^{4/7} + b^{8/7}\left(\frac{\tau_i}{\tau_{WL}}\right)^{4/7} = \delta^{8/7}\left(\frac{\nu_G}{\nu_L}\right)^{1/7}\left(\frac{\rho_G}{\rho_L}\right)^{4/7}\left[\frac{Q_G}{Q_L} - \frac{8}{7}\frac{b}{\delta}\right] \tag{I.2}$$

Solving Eqs. (I.1) and (I.2) for the ratios of the shear stresses yields

$$\left(\frac{\tau_{WG}}{\tau_{WL}}\right)^{4/7} = \frac{1}{\gamma}\left(\frac{\delta}{a}\right)^{1/7}\left(\frac{\nu_G}{\nu_L}\right)^{1/7}\left(\frac{\rho_G}{\rho_L}\right)^{4/7}\left[\delta\frac{Q_G}{Q_L} - \frac{b}{7}\right] \tag{I.3}$$

and

$$\left(\frac{\tau_i}{\tau_{WL}}\right)^{4/7} = \frac{1}{\gamma}\left(\frac{\delta}{b}\right)^{1/7}\left(\frac{\nu_G}{\nu_L}\right)^{1/7}\left(\frac{\rho_G}{\rho_L}\right)^{4/7}\left[\delta\frac{Q_G}{Q_L} - \frac{b}{7} - \gamma\right] \tag{I.4}$$

from which

$$\left(\frac{\tau_i}{\tau_{WG}}\right)^{4/7}\left(\frac{b}{a}\right)^{1/7} = 1 - \frac{\gamma}{\delta}\frac{Q_L}{Q_G}\Big/\left[1 - \frac{b}{7\delta}\frac{Q_L}{Q_G}\right] \tag{I.5}$$

In the second term in the square bracket above, b/δ is of the order of $\alpha/2(1-\alpha)$ with $[Q_L/Q_G][\alpha/(1-\alpha)]$ being the inverse of the slip ratio which is of the order of 0.05; this would make the maximum value of this term $\sim$ 0.0035, i.e. $<<$ 1,

and therefore would be neglected here (this term is 14 times smaller than terms neglected subsequently). Equation (I.5) may therefore be approximated extremely closely by

$$\left(\frac{\tau_i}{\tau_{WG}}\right)^{4/7} \left(\frac{b}{a}\right)^{1/7} \simeq 1 - \frac{\gamma}{\delta}\left(\frac{Q_L}{Q_G}\right) \qquad (I.6)$$

A force balance on each individual phase and both phases together yields

$$\left(\frac{\Delta P}{\Delta L}\right)_{TPF} = (\tau_{WL} - \tau_i)/\delta \qquad (I.7)$$

$$= (\tau_{WG} + \tau_i)/\gamma \qquad (I.8)$$

$$= (\tau_{WG} + \tau_{WL})/H \qquad (I.9)$$

Also a force balance in the gas phase between the upper wall and the position of maximum velocity, and between the interface and the position of maximum velocity yields

$$\left(\frac{\Delta P}{\Delta L}\right)_{TPF} = \tau_i/b = \tau_{WG}/a \qquad (I.10)$$

From the above equations it follows that

$$\frac{\gamma}{H} = \frac{\tau_i}{\tau_{WL}} + \frac{\delta}{h}\frac{\tau_{WG}}{\tau_{WL}} \qquad (I.11)$$

and

$$(\tau_i/\tau_{WG}) = b/a \qquad (I.12)$$

Equations (I.6) and (I.12) together with $a+b = \gamma$ can now be solved for a and b to give

$$a = \gamma/\left[1 + \left(1 - \frac{\gamma}{\delta}\frac{Q_L}{Q_G}\right)^{7/5}\right] \qquad (I.13)$$

and

$$b = \gamma\left(1 - \frac{\gamma}{\delta}\frac{Q_L}{Q_G}\right)^{7/5} / \left[1 + \left(1 - \frac{\gamma}{\delta}\frac{Q_L}{Q_G}\right)^{7/5}\right] \qquad (I.14)$$

The ratio τ_{WG}/τ_{WL} in Eq. (I.3) and $\frac{\gamma}{H}$ in Eq. (I.11) can therefore be rewritten as

$$\frac{\tau_{WG}}{\tau_{WL}} = \left(\frac{\delta}{\gamma}\right)^{1/4}\left(\frac{\rho_G}{\rho_L}\right)\left(\frac{\nu_G}{\nu_L}\right)^{1/4}\left(\frac{Q_G}{Q_L}\right)^{7/4}\left[1 + \left(1 - \frac{\gamma}{\delta}\frac{Q_L}{Q_G}\right)^{7/5}\right]^{1/4} \times \left[\frac{\delta}{\gamma} - \frac{1}{7}\frac{Q_L}{Q_G}\frac{\left(1 - \frac{\gamma}{\delta}\frac{Q_L}{Q_G}\right)^{7/5}}{1 + \left(1 - \frac{\gamma}{\delta}\frac{Q_L}{Q_G}\right)^{7/5}}\right]^{7/4} \qquad (I.15)$$

and

$$\frac{\gamma}{H} = \left(\frac{\tau_{WG}}{\tau_{WL}}\right)\left[\frac{\delta}{H} + \left(1 - \frac{\gamma}{\delta}\frac{Q_L}{Q_G}\right)^{7/5}\right] \qquad (I.16)$$

Using Eq. (I.8) the two-phase pressure drop can now be written as follows

$$\left(\frac{\Delta P}{\Delta L}\right)_{TPF} = \tau_{WL}\frac{1}{\gamma}\left(\frac{\tau_{WG}}{\tau_{WL}}\right)\left[1 + \left(1 - \frac{\gamma}{\delta}\frac{Q_L}{Q_G}\right)^{7/5}\right] \qquad (I.17)$$

For single-phase flow, the assumption of the 1/7th power-law velocity profile allows the pressure gradient to be derived as

$$\left(\frac{\Delta P}{\Delta L}\right)_{SPF} = 0.06817\ \rho\ \nu^{1/4}\ Q^{7/4}/H^3 \qquad (I.18)$$

The Lockhart-Martinelli parameter X^2 which is defined as the ratio of the pressure drop of the liquid phase to that of the gas phase when each phase flows alone in the channel

is therefore given by

$$X_{tt}^2 = (\Delta P_{SPF})_L / (\Delta P_{SPF})_G$$

$$= \left(\frac{\rho_L}{\rho_G}\right) \left(\frac{\nu_L}{\nu_G}\right)^{1/4} \left(\frac{Q_L}{Q_G}\right)^{7/4} \qquad \text{(I.19)}$$

Now, noting that $\alpha = \gamma/h$ and $(1-\alpha) = \delta/h$, Eqs. (I.15) and (I.16) are combined to give the relation between the void fraction α and X_{tt}; this is Eq. (8.6) in Chapter 8. Equations (8.2) and (I.15) are used to substitute for τ_L and (τ_{WG}/τ_{WL}) in Eq. (I.17) and the result is divided by Eq. (I.18) for the appropriate phase; the expressions for the two-phase pressure drop ratios ϕ_L^2 (the ratio of the two-phase pressure drop to the pressure drop as if the liquid phase alone were flowing) and ϕ_G^2 (the ratio of the two-phase pressure drop to the pressure drop as if the gas phase alone were flowing) thus obtained are Eqs. (8.7) and (8.8) in Chapter 8.

I.2 Derivation of the Laminar-Turbulent Flow Equations

Starting with Eqs. (8.10) and (8.11) in Chapter 8 and using the force-balance equations (Eqs. (I.7) to (I.9) yields the interfacial velocity V_i and Q_L as

$$V_i = \frac{1}{2\mu_L} \frac{(\delta + 2b)}{b} \delta \tau_i \qquad \text{(I.20)}$$

and

$$Q_L = \frac{1}{6\mu_L} \frac{(2\delta + 3b)}{(\delta + b)} \delta^2 \tau_{WL}$$

$$= \frac{1}{6\mu_L} (2\delta + 3b) \frac{\delta^2}{b} \tau_i \qquad \text{(I.21)}$$

Equating Eqs. (8.3) and (8.4) at the position of maximum gas velocity, with V_i substituted from Eq. (I.20) gives

$$a^{1/7}\left(\frac{\tau_{OG}}{\tau_i}\right)^{4/7} - b^{1/7}\,\frac{1}{\tau_i^{3/7}} = 0.05747\,\left(\frac{1}{\mu_L}\right)\rho_G^{4/7}\,\nu_G^{1/7}\,\frac{\delta\,(\delta+2b)}{b} \tag{I.22}$$

Equation (8.12) is divided by Eq. (I.21) and the result is rearranged to yield

$$a^{8/7}\left(\frac{\tau_{WG}}{\tau_i}\right)^{4/7} + b^{8/7}\,\frac{1}{\tau_i^{3/7}} = 0.02189\,\frac{1}{\mu_L}\,\rho_G^{4/7}\,\nu_G^{1/7} \times \frac{\delta^2(2\delta+3b)}{b}\left[\frac{Q_G}{Q_L} - 3\,\frac{b}{\delta}\left(\frac{\delta+2b}{2\delta+3b}\right)\right] \tag{I.23}$$

Equations (I.22) and (I.23) may be manipulated to yield

$$\tau_{WG}^{4/7}/\tau_i = \frac{1}{\mu_L}\,\rho_G^{4/7}\,\nu_G^{1/7}\,\left(\frac{\delta}{\gamma}\right)(1/b\,a^{1/7}) \times [0.02189\,\delta(2\delta+3b)\,\frac{Q_G}{Q_L} - 0.0082\,b(\delta+2b)] \tag{I.24}$$

and

$$\tau_i^{-3/7} = \frac{1}{\mu_L}\,\rho_G^{4/7}\,\nu_G^{1/7}\,\left(\frac{\delta}{\gamma}\right)\,(1/b^{8/7}) \times [0.02189\,\delta(2\delta+3b)\frac{Q_G}{Q_L} - 0.06567\,b(\delta+2b) - 0.0575\,a(\delta+2b)] \tag{I.25}$$

From the last two equations, it follows that

$$\left(\frac{\tau_i}{\tau_{WG}}\right)^{4/7}\left(\frac{b}{a}\right)^{1/7} = 1 - \frac{21}{8}\,\left(\frac{Q_L}{Q_G}\right)\left(\frac{\gamma}{\delta}\right)\left(\frac{\delta+2b}{2\delta+3b}\right)/\left[1 - \frac{3}{8}\,\frac{Q_L}{Q_G}\left(\frac{b}{\delta}\right)\left(\frac{\delta+2b}{2\delta+3b}\right)\right] \tag{I.26}$$

The form of Eq. (I.26) is not appropriate to solve (with $a+b=\gamma$) for a and b; a reasonable approximation is therefore necessary to obtain expression for a and b such as

those obtained for the turbulent-turbulent case. In the second term in the square bracket above, b/δ is of the order of $\alpha/2(1-\alpha)$ and $(\delta+2b)/(2\delta+3b)$ is of the order of $2/(4-\alpha)$ with $[Q_L/Q_G][\alpha/(1-\alpha)]$ being the inverse of the slip ratio, this term would be of the order of 1/8 of the inverse of the slip ratio and its maximum value would be $\sim$ 0.0075, i.e. << 1. Neglecting this term would closely approximate Eq. (I.26) by

$$\left(\frac{\tau_i}{\tau_{WG}}\right)^{4/7} \left(\frac{b}{a}\right)^{1/7} \simeq 1 - \frac{21}{4} \left(\frac{Q_L}{Q_G}\right) \frac{\alpha}{(1-\alpha)(4-\alpha)} \qquad (I.27)$$

or

$$\tau_i/\tau_{CG} = b/a \simeq \left[1 - 5.25 \left(\frac{Q_L}{Q_G}\right) \frac{\alpha}{(1-\alpha)(4-\alpha)}\right]^{7/5} = B_2 \qquad (I.28)$$

Therefore,

$$a = \gamma/(1 + B_2) \qquad \text{and} \qquad b = \gamma B_2/(1+B_2) \qquad (I.29)$$

Now, the two-phase pressure gradient and the single-phase pressure gradients are given by

$$\left(\frac{\Delta P}{\Delta L}\right)_{TPF} = 6 \mu_L Q_L/\delta^2 (2\delta + 3b) \qquad (I.30)$$

$$(\Delta P_{SPF}/\Delta L)_L = 12 \mu_L Q_L/H^3 \qquad (I.31)$$

and

$$(\Delta P_{SPF}/\Delta L)_G = 0.06817 \rho_G \nu_G^{1/4} Q_G^{7/4}/H^3 \qquad (I.32)$$

Therefore,

$$X_{\ell t}^2 = 176.0 \frac{\mu_L \, Q_L}{\rho_G \, \nu_G^{1/4} \, Q_G^{7/4}} \qquad (I.33)$$

Finally, the relation between α and $X_{\ell t}^2$ (Eq. (8.13) in Chapter 8) is obtained using Eqs. (I.11), (I.21), (I.25), (I.28) and (I.33). The two-phase pressure drop ratio Φ_L^2 is obtained by dividing Eq. (I.30) and (I.31); this is Eq. (8.15) in Chapter 8.

TABLE I.1

PRESSURE DROP RATIOS AND HOLDUP

CALCULATED FROM THE PRESENT THEORY

Turbulent - Turbulent				Laminar - Turbulent			
X	$1-\alpha$	ϕ_G	ϕ_L	X	$1-\alpha$	ϕ_G	ϕ_L
13.08	0.80	11.18	0.85	17.44	0.80	11.18	0.64
6.06	0.70	6.09	1.00	8.19	0.70	6.09	0.74
3.27	0.60	3.95	1.21	4.50	0.60	3.95	0.88
1.89	0.50	2.83	1.50	2.65	0.50	2.83	1.07
1.11	0.40	2.15	1.94	1.59	0.40	2.15	1.36
0.64	0.30	1.71	2.68	0.93	0.30	1.71	1.83
0.33	0.20	1.40	4.19	0.50	0.20	1.40	2.80
0.13	0.10	1.17	8.74	0.21	0.10	1.17	5.68
0.12	0.09	1.15	9.76	0.18	0.09	1.15	6.32
0.10	0.08	1.13	11.03	0.16	0.08	1.13	7.17
0.09	0.07	1.12	12.67	0.14	0.07	1.12	8.15
0.07	0.06	1.10	14.85	0.12	0.06	1.10	9.53
0.06	0.05	1.08	17.90	0.09	0.05	1.08	11.45